Bioprospecting with Marine Halophilic Eubacteria and Haloarchaea for Bioactives

A thesis submitted to Goa University for the award of degree of

DOCTOR OF PHILOSOPHY

IN

MICROBIOLOGY

BY

JYOTHI JUDITH ALVARES M.Sc.

Research Guide

Prof. Irene Furtado

DEPARTMENT OF MICROBIOLOGY
GOA UNIVERSITY

May 2019

Certificate

This is to certify that this thesis entitled **"Bioprospecting with Marine Halophilic Eubacteria and Haloarchaea for Bioactives"**, submitted by **Jyothi Judith Alvares** for the award of the degree of **Doctor of Philosophy** in **Microbiology**, is a record of the original and independent work carried out under my guidance and supervision. The thesis or any part thereof has not been previously submitted to form the basis for the award of any degree or diploma to any University or Institution in India or abroad.

Prof. Irene Furtado

Research Guide
Department of Microbiology,
Goa University.

Declaration

As required by the Goa University ordinance O.B.9 and as per UGC 2009 regulations, I, Jyothi Judith Alvares, hereby state that the work presented in the thesis entitled **"Bioprospecting with Marine Halophilic Eubacteria and Haloarchaea for Bioactives"** is my original contribution and the same has not been previously submitted in full or part thereof, to form the basis for the award of any degree or diploma to any University or Institution. To the best of my knowledge the present study is the first comprehensive work of its kind from the study area. The literature related to the problem investigated has been cited. Due acknowledgements have been made wherever facilities and suggestions have been availed.

Jyothi Judith Alvares

Ph.D Research Scholar
Department of Microbiology,
Goa University.

Acknowledgement

To God be the glory and thanks, for giving me the opportunity, good health, strength, for His grace and wisdom to complete this research study in time. To Mother Mary, all praise, for Her presence and guidance along the way.

I would like to extend my sincere gratitude to the many people, who contributed in many ways to the successful completion of this thesis

With a grateful heart, I would like thank my guide and supervisor, Professor Irene Furtado for consenting to carry out the PhD program under her guidance and supervision, for suggesting the PhD topic, for so willingly giving me the opportunity to tap into her immense academic knowledge, for the timely guidance and lucid discussions, for her time and patience, for being very accommodating to my timings (since I have a full time job) and most importantly for making me an independent thinker.

My profound gratitude goes to my Vice Chancellors (VC) nominee, Dr. Maria Judith Gonsalves; Scientist, NIO, Dona Paula for consistently being there during the entire tenure of my PhD program, for her willing help and suggestions during the Faculty Research Committee (FRC) presentations. Many thanks to the Present Dean of Faculty of Life Science and Environment, Goa University; Prof. PK Sharma and the former Dean's; Prof. Janarthanam, Prof. Saroj Bhonsle and Prof G.N Nayak for all their suggestions during the FRC presentations and the entire tenure of my research.

I owe my sincere thanks to the Department of Microbiology, Goa University; Present HOD; Prof Sandeep Garg, Former HODs; Prof. S.K. Dubey, Prof Sarita Nazareth, Prof. Saroj Bhonsle and the teaching faculty; Dr. Lakshangi Chari, Dr. Priya D'Costa, Dr. Milind Naik, Dr. Varada Damre and Dr. Trelita Lobo and Dr. Shyamalina Haldar.

I am hugely appreciative of the help rendered by the non-teaching staff of Department of Microbiology, Goa University; Saraswati, Veena, Prathana, Shashikant, Deepashree, Dominic, Budhaji, Narayan, Rajesh and Gajanan.

I am grateful to Department of Chemistry Goa University, for the permission to use the Vibrating sample Magnetometer, Fourier Transform – Infra Red instrument and the Rotavap instrument.

I also thank the University Science Instrumentation Centre (USIC), Goa University for the SEM-EDX facility.

I thankfully acknowledge Prof. S.K. Shyama, Department of Zoology, Goa University for providing the facilities required to carry out the comet assay.

I am also obliged to the Director of National Institute of Oceanography, Indian Institute of Technology Bombay and Malaviya National Institute of Technology, Jaipur for extending the instrumentation facilities required for the research work.

I also oblige the willingness extended by Prof. Judith Braganca from BITS Pilani, Goa campus to help with the molecular biology analysis. I am also grateful to her concern all along the tenure of my PhD work.

It is also of great pleasure to extend my thanks to all the research scholars (past and present) from the Department of Microbiology: Dr. Neha Prabhu, Dr. Amrita Kharangate Lad, Dr. Akshaya Bicholkar, Cristabel Pinto, Sulochana Shet, Divya Vaigankar, Sajiya Mujawir. Many thanks to my senior lab mates from the Haloarchaeal research group: Dr. Subhojit Basu, Dr. Sherryanne Velho-Pereira, Dr. Sanika Naik and Dr. Sushama Patil.

I gratefully acknowledge the help rendered by Perantho Dias from Department of Biotechnology, Goa University, for his help on solvent fractionation, Dr Santosh Shetgaoankar from Deccan Chemicals and Manali Jadhav from IIT, Bombay.

I sincerely place on record my sincere thanks to my good friend Dr. Avelyno D'Costa for always being there, for all his ever willing help with statistics and the comet assay.

Many thanks to my dear co-lab mates, Sanket Gaonkar and Alisha Malik for all their help and cooperation with experimental work during the PhD tenure. Many thanks to Sanket for the late night company and for the yummy black tea.

I owe a great deal of appreciation and gratitude to all the research scholars from Department of Chemistry, Goa University, who helped me in carrying out analysis in their Department; Chandan Naik, Rahul Kerkar, Ketan Mandrekar, Abijit Shetgaonkar, Daniel Coutinho and Pratik Asogekar.

I also sincerely thank Dr. Savio Rodrigues, Prof and HOD Department of Microbiology, Goa Medical College and Dr. Maria Jose Rodrigues, Associate Professor, Department of Microbiology, Goa Medical College for providing me with the ATCC strain of *Ps. aeruginosa* and also for their concern all along during my PhD tenure.

Finally, my deep and sincere gratitude to my family and all my friends, (including my friends from Goa Medical College and Dr. Laura), for their continuous and unparalleled love, ever willing help and support all along and till the completion of my thesis.

Thank you all and God bless.

Jyothi Judith Alvares

'Come forth into the light of things, Let nature be your teacher'

William Wordsworth (1770-1850)

To,

My parents; thanks to you **dad**, for encouraging me into higher studies. The completion of this thesis is an evidence of your prayers and intangible help from up above. I miss your presence as I submit my thesis. Thanks to you **mom**, for an unbelievable support, the unconditional love, patience and understanding, for all your untiring help, sleepless nights keeping me company until the completion of this thesis. Thank you both for making me what I am today.

My siblings; Nirmal and Vidya, together with their families; your support, love and help have been a source of motivation to me. Thank you all very much for the long distance calls and whatsapp messages that constantly re instilled confidence and hope when things were wary.

My best friend and mentor, Dr. Fatima De Souza, thank you for the reminders that hard work faced with perseverance and diligence bring a much deeper reward than may be realized on the surface. If I have completed my thesis today, it's because six years ago, you realised I could do it, even as a part time student.

You all are the most important people in my world and I dedicate this thesis to you

To,

My beloved dad,

Philip John Alvares

(1947-2016)

…with love

Table of Contents Page No

Chapter I: Biotechnological Potential of Marine Extremely Halophilic Eubacteria and Haloarchaea - Advancement in Bioprospecting

Chapter II: Bioprospects of Extremely Halophilic Eubacteria and Haloarchaea as Producers of Bioactives

---

Chapter IV: Chemical Profiling of *Haloferax alexandrinus* GUSF-1 (KF796625)

Chapter V: Biosynthesis of Nanoparticles by Extremely Halophilic *Chromohalobacter salexegines* GUVFFM-3 (JF330126) and Haloarchaeon *Haloferax alexandrinus* GUSF-1 (KF796625)

List of Abbreviations and Symbols

Ag	Silver
AHL	Acyl-homoserine lactones
ANOVA	Analysis of Variance
As(III)	Arsenic ions
ATCC	American Type Culture Collection
AU	Arbitrary Units
BABR	Bisanhydrobacterioruberin
BLAST	Basic Local Alignment Search Tool
bp	Base pair(s)
BR	Bacterioruberin
BSA	Bovine Serum Albumin
CFU	Colony forming unit
CFS	Cell Free Supernatant
cm	Centimeter
d	Day/ s
DAD	Diode Array Detector
DMSO	Dimethyl Sulfoxide
DW	Distilled Water
DDW	Double Distilled Water
DNA	Deoxyribonucleic acid
EDTA	Ethylene Diamine Tetra Acetic acid
EDS	Energy Dispersive Spectroscopy
EPS	Exopolysaccharide
ESI MS	Electro Spray Ionisation Mass Spectroscopy
GDEM	Glycerol Diether Moities
(F)	Forward primer
FT-IR	Fourier Transform Infra Red
g	Gram
g/l	Gram per Litre
h	Hour
HL	Human Lymphocytes
HRLC-MS/MS	High Resolution Liquid Chromatography- Mass spectroscopy
Kb	Kilo bytes
kDa	Kilo Dalton
Kg	Kilo Gram
Km	Kilo Meter
LI	Lugols iodine
LMPA	Low Melting point agar
m	Meter
M	Molar
MABR	Monoanhydrobacterioruberin
MALDI – TOF	Matrix-Assisted Laser Desorption Ionization / Time-of-Flight

MEGA	Molecular Evolutionary Genetics Analysis
µg	Microgram
mg	Milligram
min	Minute
µl	Microlitre
ml	MilliLitre
µm	Micrometer
mm	millimeter
µM	Micro molar
mM	Millimolar
Mn	Manganese
MUSCLE	Multiple Sequence Comparison by Log-Expectation
MWCO	Molecular Weight Cut Off
m/z	Mass to charge ratio
NADH	Micotinamide adenine dinucleotide
NCBI	National Centre for Biotechnology Information
ng	Nanogram
NGSM	NaCl Glucose Synthetic Medium
NHE	Na^+ H^+ Exchanger
NJ	Neighbour Joining
nm	Nano meter
NMPA	Normal melting point agar
NPs	Nanoparticles
NR	Nitrate Reductase
NSM	NaCl Synthetic Medium
NTYE	NaCl Tryptone Yeast Extract
OD	Optical Density
PAGE	Poly Acryl Amide Gel Electrophoresis
PBS	Phosphate buffer saline
PCR	Polymerase Chain Reaction
PHA	Polyhydroxyalkanoates
PE	Polyethylene
PEG	Polyethylene glycol
PG	Phosphatidyl Glycerol
PUFA	Polyunsaturated Fatty Acid
Psig	pounds per square inch gauge
QS	Quorum Sensing
(R)	Reverse primer
RBC	Red blood Corpuscles
RDP	Ribosomal Database Project
R_f	Retention Factor
rpm	Revolutions Per Minute
RT	Room Temperature

R_t	Retention time
RNA	Ribo Nucleic Acid
rRNA	ribosomal RNA
SAED	Selective Area Electron Diffraction
SD	Standard deviation
S-DGD	Sulfated Diglycosyl Diether
Se	Selenium
sec	second
SEM	Scanning Electron Microscopy
SeNP	Selenium nanoparticles
sp.	Species
SPR	Surface Plasmon Resonance
SPSS	Statistical package for the social sciences
S-TeGD	Sulfated Tetraglycosyl Diglycosyl Diether
TACK	*Thaumarchaeota Aigarchaeota Crenarchaeota Korarchaeota*
TLC	Thin Layer Chromatography
Tris HCL	Tris hydrochloride
Te	Tellurium
TEM	Transmission Electron Microscopy
UPGMA	Unweighted Pair Group Method with Arithmetic Mean
U	Unit
UV	Ultraviolet
Vis	Visible
v/v	Volume by Volume
VSM	Vibrating sample magnetometer
WHO	World Health Organisation
w/v	Weight by Volume
XRD	X-Ray Diffraction
YE	Yeast Extract
œ	alpha
ß	Beta
€	Extinction coefficient
%	Percentage
λ	Wavelength
°C	Degree centigrade

Chapter I

Biotechnological Potential of Marine Extremely Halophilic Eubacteria and Haloarchaea - Advancement in Bioprospecting

1.1 BIOPROSPECTING IN MARINE EXTREMELY HALOPHILIC EUBACTERIA AND HALOARCHAEA

Bioprospecting in microorganisms is the systematic search for and development of new biological resources which may also have commercial value (Nader and Hill, 1999). It includes whole organisms (Tamayo *et al*., 1997), genes (Reid *et al*., 1993), chemical compounds (Ehrlich and Raven, 1964), extracts from microorganisms (Tamayo *et al*., 1997). These resources may be used in food production, pest control, for the development of new drugs and for other related biotechnological applications. The goals of bioprospecting include the sustainable use of biological resources through biotechnology and the scientific and socioeconomic development of source countries and local communities. As a systematic search for valuable chemical and genetic constituents of biological diversity, bioprospecting activities continue to be associated with the identification and collection of active compounds existing in nature for purposes of commercial use (Wink, 1993). Informal bioprospecting began when prehistoric people noticed that one plant root tasted better than another, or that some plants could be used as medicines. Much later scientists have been able to identify the active ingredients in these plants and their extract or replicate that ingredient for widespread use. Alexander Fleming's discovery of penicillin was accidental bioprospecting and hence we can see that potential rewards from bioprospecting are significant (Mateos *et al*., 2001). The underlying aim of bioprospecting is to find new resources and products from nature that can be used by humans. Improving human health, through both medicine and better nutrition are key focal areas. Bioprospecting incorporates two fundamental goals, (i) the sustainable use through biotechnology of biological resources and their conservation, and (ii) the scientific and socioeconomic development of source countries and local communities (Sittenfeld, 1996).

Bioprospecting can be broadly classified into (i) Traditional bioprospecting and (ii) Modern bioprospecting. Traditional bioprospecting is the search for and utilization of biological resources is as old as humankind and has been the key to the survival, adaptation and evolution of the human species (Tamayo *et al*., 1997). Modern bioprospecting uses the three important resources from living nature, namely;

chemicals, genes, and designs; modern bio prospecting can be differentiated into (a) chemical, (b) gene and (c) bionic prospect (Tamayo *et al*., 1997).

1.2 EXTREMOPHILES AND THEIR HABITATS

Extremophiles (*extremus* meaning extreme and *philia* meaning love) are a group of organisms that survive in the most deleterious geochemical and physical conditions, often difficult for the otherwise mesophilic organisms to cope (MacElroy, 1974). They include members of all three domains of life, i.e., Eubacteria, Archaea, and Eukarya (Madigan and Mars, 1997). Extremophiles may be divided into two broad categories: extremophilic organisms which require one or more extreme conditions in order to grow and extremotolerant organisms which can tolerate extreme values of one or more physicochemical parameters though growing optimally at "normal" conditions. Extremophiles are taxonomically widely distributed and are a functionally diverse group.

They are further classified according to the conditions in which they grow:
(i) Thermophiles and hyperthermophiles (organisms growing at high or very high temperatures, respectively), (ii) Psychrophiles (organisms that grow best at low temperatures), (iii) Acidophiles and alkaliphiles (organisms optimally adapted to acidic or basic pH values, respectively) (iv) Barophiles (organisms that grow best under pressure) and (v) Halophiles (organisms that require NaCl for growth) (Madigan and Mars, 1997).

1.2.1 Hypersaline environments and microbial halophiles

Hypersaline environments like solar salterns, wet land estuarines and mangroves have salinities far more than the normal seawater salinities and hence such environments are inhabited by halophiles - the salt loving organisms. Based on the mineral composition, the hypersaline water bodies are divided into thalasohaline and athalasohaline. Thalasohaline environments have mineral composition similar to marine environments with sodium and chloride being dominant element and the pH may vary from neutral to slightly alkaline (DasSarma and Arora, 2001). In contrast, athalasohaline environments have magnesium and potassium as dominant ions with trace amounts of carbonate, chloride and sulfate. Their ionic strength is in complete

contrast with the sea water and they contain high amount of organic carbon, nitrogen and phosphate compounds (DasSarma and Arora, 2001). Examples of athalasohaline environments include Dead Sea, soda lakes and alkaline soil (Oren, 2002). Halophiles include Eukaryotes, Prokaryotes and Archaea. Halophiles are distributed in hypersaline environments all over the world, mainly in natural hypersaline brines, coastal and deep sea locations as well as in artificial salterns also called the solar salterns (Oren, 2000).

Halophiles survive in a range of salinity as low as 2% and to as high as 37%. Halophiles are categorised based on the salinity requirements into four broad categories, namely: (i) halotolerant microorganisms that do not show an absolute requirement for salt for growth but grow well upto very high salt concentrations (considered extremely halotolerant if the growth range extends above 2.5 M (15%, w/v) NaCl; (ii) moderate halophiles, growing in media containing 0.5–2.5 M (3-15%, w/v) NaCl; (iii) borderline extreme halophiles, growing in media containing 1.5–4.0 M (7-20%, w/v) NaCl and (iv) extreme halophiles, growing best in media containing 2.5–5.2 M (15-25%, w/v) NaCl (Kushner and Kamekura, 1988).

1.2.2 Extremely halophilic Eubacteria

The Domain Bacteria contains many types of halophilic and halotolerant microorganisms, spread over a large number of phylogenetic subgroups. The different branches of the Proteobacteria contain halophilic representatives. Halophiles are also found among the cyanobacteria. Within the lineages of the Gram - positive bacteria (Firmicutes), halophiles are found both within the aerobic branches (*Bacillus* and related organisms) and within the anaerobic branches. There is even an order, the *Halanaerobiales,* consisting of two families (the Halanaerobiaceae and the *Halobacteroidaceae* that consists solely of halophilic anaerobic microorganisms. (Oren, 2002; Kushner and Kamekura, 1988).

1.2.3 Haloarchaea - the extremely halophilic members of the Domain Archaea

It was sometime in the late 1970s the non-monolithic nature of prokaryotes, and the distinctiveness of “Archaeabacteria” was first recognized (Balch *et al*., 1977; Fox *et al*., 1977; Woese and Fox, 1977). Ribosomal RNA (rRNA)-based analyses further

supported these findings and this uniqueness was eventually formalized with the establishment of the three domains of Life: Eukarya, Bacteria and Archaea (Woese *et al*., 1990). The Archaeal branch of the Tree of Life was sparsely populated, and sub-divided into *Euryarchaeota* and *Crenarchaeota* (Woese *et al*., 1990). They included only cultured representatives, all of which originating from extreme environments. Advances in cultivation-independent techniques and particularly the use of metagenomics and single amplified genomes (SAGs) revealed several novel phylogenetic groups, which are quickly reshaping view of the Archaea (Eme and Doolittle, 2015). A flurry of ongoing additions of new archaeal phyla, has led to the creation of two superphyla (**Fig 1.1**), commonly referred to as TACK (Guy and Ettema, 2011) and DPANN (Rinke *et al*. 2013). The TACK superphylum includes *Thaumarchaeota* (Brochier-Armanet *et al*., 2008), *Aigarchaeota* (Nunoura *et al*., 2010), *Crenaerchaeota* (Woese *et al*., 1990), *Korarchaeota* (Barns *et al*., 1996) and (Guy and Ettema, 2011) and the DPANN superphylum includes Diapherotrites, Parvarchaeota, Aenigmarchaeota, Nanohaloarchaeota, and Nanoarchaeota (Rinke *et al*., 2013).

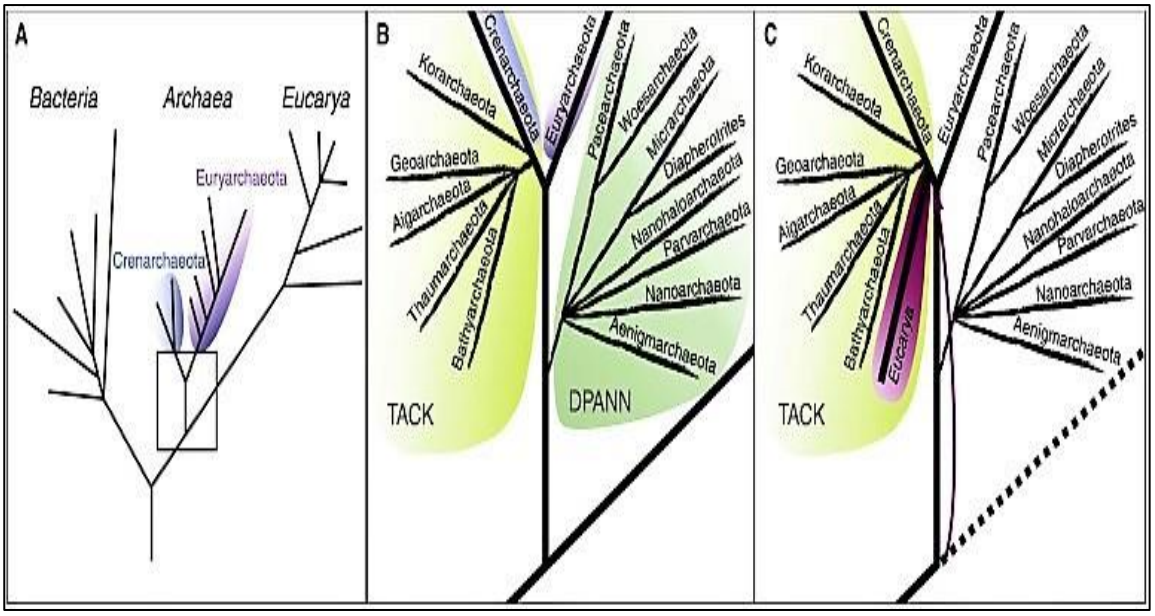

Fig. 1.1 A: The three Domain Tree of Life, as conceived by Woese and colleagues (Woose *et al*., 1990) Area in square is expanded in panel **B**: Archaeal phyla and superphyla by Castelle *et al*. (2015); **C:** Traditional placement of the branch leading to eukaryotes as shown in a dotted line indicates that eukaryotes may instead emerge from within or at the base of the archaeal TACK superphylum (Williams *et al*., 2014)

Haloarchaea are traditionally associated with the members of the class *Halobacteria* belonging to Phylum E*uryarchaeota*. This class is divided into three orders: (1) the *Halobacteriales* with families *Halobacteriaceae, Haloarculaceae* and *Halococcaceae*; (2) the *Haloferacales* with families *Haloferacaceae* and *Halorubraceae*; and (3) the *Natrialbales* with family *Natrialbaceae*. The class *Halobacteria* currently includes 177 species with validly published names, placed in 58 genera (LSPN; List of Prokaryotic Names with Standing in nomenclature version 2.1, updated 19 July 2018).

Haloarchaeal cultures can be clearly distinguished from other extremely halophilic prokaryotes by the presence of diether core lipids that forms the basis for most polar lipid structures present in the family *Halobacteriaceae* known as 2,3-di-O-phytanyl-*sn* glycerol (C_{20}, C_{20}), also called archaeol (Kates, 1978) and detectable by procedures of Ross et al., 1985. These core ether lipids are completely absent in eubacteria and

eukarya. The polar lipids and the non-polar or neutral lipids make up the total membrane lipids of these microbes.

Neutral lipids account for approximately 10% of the total lipid content of the halophilic Archaea of the family *Halobacteriaceae* (Kamekura and Kates, 1988); they consist almost exclusively of C_{20}–C_{50} isoprenoids and isoprenoid-derived compounds. The diphytanylglycerol diether lipid core is considered as one of the most useful chemotaxonomic markers of the domain "Archaea". A great variety of polar lipids is encountered in the different representatives of the *Halobacteriaceae*, including phospholipids, sulfolipids and glycolipids. Haloarchaea are also known for its insensitivity towards many antibiotics especially cell wall and protein synthesis inhibitors. Bile salt such as Difco's bacto peptone has been known to cause lysis of halobacteria due to presence of high concentration of taurine conjugates of cholic acid (Purdy *et al*., 2004). Proteins of haloarchaea are either resistant to high salt concentration and/ or require salts for activity. As a group, they contain an excess ratio of acidic to basic amino acids, a feature likely to be required for activity at high salinity. Surface negative charges are thought to be important for solvation of halophilic proteins, and to prevent the denaturation, aggregation and precipitation that usually results when non halophilic proteins are exposed to high salt concentrations (Dym *et al*., 1995). A unique feature of haloarchaea is the purple membrane, specialized regions of the cell membrane that contain a two-dimensional crystalline lattice of a chromoprotein, bacteriorhodopsin. Bacteriorhodopsin contains a protein moiety (bacterioopsin) and a covalently bound chromophore (retinal) and acts as a light-dependent transmembrane proton pump (Krebs and Khorana, 1993). Halobacteria produce buoyant gas vesicles, like many aquatic bacteria (DasSarma and Arora, 1997). Gas vesicles are hollow proteinaceous structures surrounding a gasfilled space. The function of gas vesicles for haloarchaea, whose primary metabolism is aerobic and that live in concentrated brines in which the solubility of molecular oxygen is low (especially at high temperatures), is to enable the cells to float to the more oxygenated surface layers. This also increases the availability of light for purple membrane-mediated photophosphorylation.

Haloarchaea produce large quantities of red-orange carotenoids. Carotenoids have been shown to be necessary for stimulating an active photo repair system for repair of

thymine dimers resulting from ultraviolet radiation. The most abundant carotenoids are C_{50} bacterioruberin, although smaller amounts of biosynthetic intermediates such as ß-carotene and lycopene are also present. Several retinal proteins, in addition to bacteriorhodopsin, are also produced by haloarchaea, including halorhodopsin, which is an inwardly directed light-driven chloride pump and two sensory rhodopsins, which mediate the phototactic response (towards green light and away from blue and ultraviolet light) (Spudich, 1993).

While the rest of the microbes maintain a cytoplasm that is osmotically at least equivalent to the saline medium outside the cell, the ways in which osmotic equilibrium is achieved in haloarchaea differs (Kushner and Kamekura, 1988) and is listed as below;

i. They balance the salt outside with high ionic concentrations, mainly KCl within the cytoplasm and their intracellular enzymatic machinery is adapted to function in high salt.

ii. Some exclude salt from their cytoplasm to a large extent and instead accumulate organic osmotic solutes also called as compatible solutes. They provide osmotic balance without interfering with the metabolic functions of the cell. Examples of compatible solutes include amino acids such as proline; glycine betaine or its precursor – choline; ectoine and hydroxyectoine.

1.3 MICROBES – OVERCOMERS OF STRESS

Throughout history, humans have had an intimate relationship with nature, most obviously depending on it for sustenance and production. As modern society emerged and the human population increased into urban areas, industrialization has helped generating the growth needed for further increases in human development, which is seen as the bottom-line output (Fuller *et al*., 2007). In last century, medical science has made incredible advances with an overall decrease in mortality rate and an increase in life expectancy with the discovery of new life saving drugs (Sen and Chakrabovty, 2017). Industrialization coupled with technological advancement has continued to affect the environment in a negative way (**Fig. 1.2**). Industrial benefits resulting from technological adaptation in major activities has indirectly contributed

towards higher living standards though bad part on technology manifest more (Ausubel and Langford, 1997).

The development of modern technology has resulted in negative effects including:
i) Air pollution ii) Global warming iii) Destruction of natural environment iv) Water pollution v) Soil pollution and vi) Solid wastes (Ausubel and Langford, 1997).

Since industrialization and use of chemical technology has begun to impact human health lives in a negative manner, it is important to harness the prospects and potentials of a microbial system that works normally or is adapted to function under stressful conditions in order to restore the balance between stressors and health. Hence we focused on the bioprospects of extremophiles which thrive normally under extreme conditions for potential bioactives.

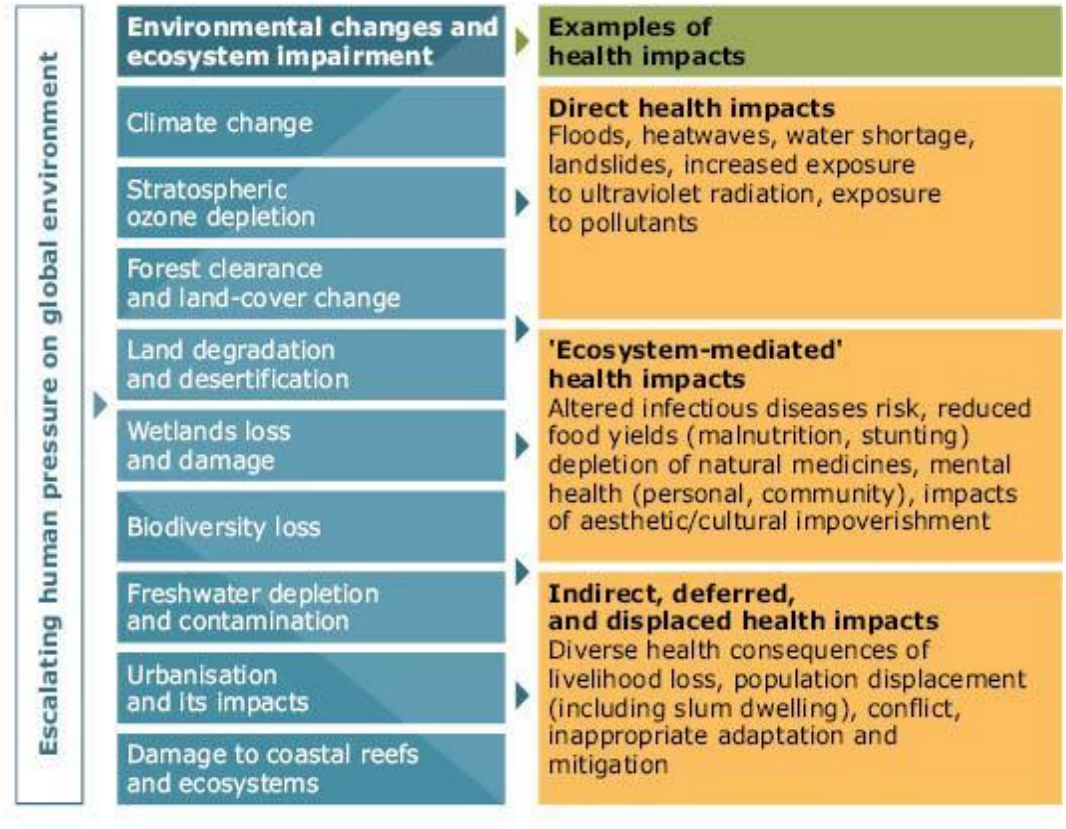

Fig. 1.2 Harmful effects of ecosystem change on human health (Barton and Grant, 2006)

1.4 BIOPROSPECTS OF HALOARCHAEA

Due to the high saline environments that the halophiles thrive in, they have evolved physiological and genetic characteristics within them for adaption to such environment. These characteristics include internal compatible solutes, efficient ion pumps, UV absorbing pigments and acidic proteins, which help them to resist osmotic stress and the denaturing effects of salts, as well as the accompanying intense solar radiation. Many of the same characteristics which help them to counteract the deleterious effects of their environment also constitute valuable resources for biotechnology and nanotechnology. Applications of halophilic microorganisms are varied and represent significant commercial opportunities in the chemical, environmental, biofuel, medical industries. Although currently established applications of haloarchaea are limited, many other novel applications are under development. Haloarchaea are envisaged to be potent producers of bioactives secondary metabolites (Bernan and Maiese, 1997) and hence are targets for bioprospecting for antimicrobials such as halocins (O'Connor and Shand, 2002), novel biosynthesis of enzymes (Kakhki *et al*., 2011), compatible solutes, poly hydroxyl alkanoates (Braganca and Furtado, 2004; Salgaonkar *et al*., 2017), antioxidants (Hou and Cui, 2018), bioremediation of hydrocarbons and environmental pollutants (Fathepure and Nicholson, 2004). Haloarchaeal cultures with potential for different bioactives such as amylases, chitinases, lipases, proteases, cellulose, bioremediation of hydrocarbons and metals, uptake of heavy metals such as arsenic and cadmium and biosynthesis of nanomaterials have been also reported from solar salts and estuarine sediments from Goa - India (Fernandes, 1999; Alvares, 2000; Braganca, 2002; Raghavan and Furtado, 2005; Fernandes, 2006; Naik and Furtado, 2014; Patil and Furtado, 2014; Goankar and Furtado, 2018a; Goankar and Furtado, 2018b; Malik and Furtado, 2018).

1.4.1 Antioxidant production

1.4.1.1 Effects of oxidative stress

Free radicals are atoms, molecules or ions with unpaired electrons that are highly unstable and active towards chemical reactions with other molecules. They derive from three elements: oxygen, nitrogen and sulfur, thus creating reactive oxygen

species (ROS), reactive nitrogen species (RNS) and reactive sulfur species (RSS). Internally, free radicals are produced as a normal part of metabolism within the mitochondria, through xanthine oxidase, peroxisomes, inflammation processes, phagocytosis, arachidonate pathways, ischemia and physical exercise. External factors that help to promote the production of free radicals are smoking, environmental pollutants, radiation, drugs, pesticides, industrial solvents and ozone. It is ironic that these elements, essential to life (especially oxygen) have deleterious effects on the human body through these reactive species (Lobo *et al*., 2010). The balance between the production and neutralization of ROS by antioxidants is very delicate, and if this balance tends to the overproduction of ROS, the cells start to suffer the consequences of oxidative stress (Wiernsperger, 2003). It is estimated that every day a human cell is targeted by the hydroxyl radical and other such species and average of 105 times inducing oxidative stress (Valko *et al*., 2004). The main targets of ROS, RNS and RSS are proteins, DNA (deoxyribonucleic acid) and RNA (ribonucleic acid) molecules, sugars and lipids (Halliwel and Chirico, 1993; Lobo *et al*., 2010) **(Fig. 1.3)**. These reactions lead to the production of ROS, RNS and RSS whom have been linked to many severe diseases like cancer, cardiovascular diseases including atherosclerosis and stroke, neurological disorders, renal disorders, liver disorders, hypertension, rheumatoid arthritis, adult respiratory distress syndrome, auto-immune deficiency diseases, inflammation, degenerative disorders associated with aging, diabetes mellitus, diabetic complications, cataracts, obesity, autism, Alzheimer's, Parkinson's and Huntington's diseases, vasculitis, glomerulonephritis, lupus erythematous, gastric ulcers, hemochromatosis and preeclampsia, among others (Lobo *et al*., 2010; Lü *et al*., 2010).

1.4.1.2 Antioxidants and prooxidants

Halliwell and Gutteridge, (1995), defined antioxidants as "any substance that, when present at low concentrations compared with that of an oxidizable substrate, significantly delays or inhibits oxidation of that substrate". Another property that a compound should have to be considered an antioxidant is the ability, after scavenging the radical, to form a new radical that is stable through intramolecular hydrogen bonding on further oxidation (Halliwell, 1990; Halliwell, 2007; Khlebnikov *et al*., 2007). A living system maintains a balance between free radicals and oxidative stress.

The antioxidant activity can be effective through various ways: as inhibitors of free radical oxidation reactions (preventive oxidants) by inhibiting formation of free lipid radicals; by interrupting the propagation of the autoxidation chain reaction (chain breaking antioxidants); as singlet oxygen quenchers; as reducing agents which convert hydroperoxides into stable compounds; as metal chelators that convert metal pro-oxidants (iron and copper derivatives) into stable products; and finally as inhibitors of pro-oxidative enzymes (lipooxigenases) (Darmanyan *et al*., 1998; Heim *et al*., 2002; Min and Boff, 2002; Pokorny, 2007; Kancheva, 2009). Antioxidants may be of great benefit in improving the quality of life by preventing or postponing the onset of degenerative diseases.

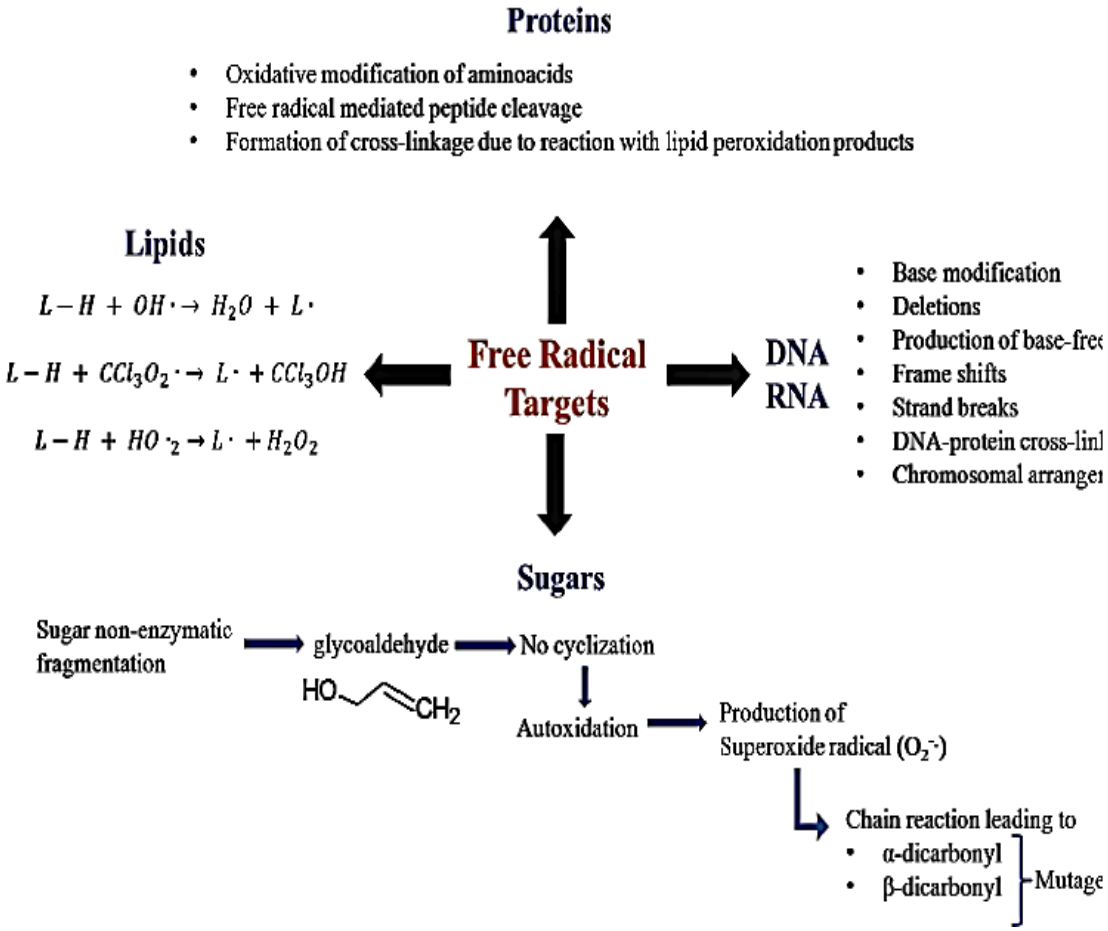

Fig. 1.3 Targets of free radicals (Halliwel and Chirico, 1993; Lobo *et al*., 2010)

1.4.1.3 Antioxidant production in haloarchaea

The first report of hydroxyl scavenging ability of bacterioruberin with a scavenging capacity higher than ß carotene was reported by Saito *et al*., 1994. Later in a study carried out by Mandelli *et al*., 2012, carotenoids from *Halococcus morrhuae* and *Halobacterium salinarium* were extracted, identified as bacterioruberin, bisanhydrobacterioruberin and trisanhydrobacterioruberin were found to possess antioxidant potential. Pathak and Sardar, 2012, reported the presence of antioxidant activity of carotenoid extracts of a haloarchaeal isolate, *Halorubrum* sp. from solar salterns of Mumbai. Similarly carotenoid extracts from the halophilic Archaea, *Halobacterium halobium* were found to have potent antiradical scavenging activity and antiproliferative activity (Abbes *et al*., 2013). The invitro scavenging capacity of a C_{50} carotenoid, bacterioruberin, extracted from *Haloarcula japonica* cells against 1, 1-diphenyl-2-picrylhydrazyl ($DPPH^{\bullet}$) radicals was evaluated and the antioxidant capacity of bacterioruberin was found to be much higher than that of β-carotene (Yatsunami *et al*., 2014). The production of carotenoid pigment with a high degree of $DPPH^{\bullet}$ scavenging activity by an extremely halophilic archaeon, *Haloferax* sp. BKW301 (NCBI Accession No. KT240044) is reported to be isolated from multi-pond solar saltern of West Bengal, India (Biswas *et al*., 2016). For the first time Squillaci *et al*. (2017) identified seven geometric isomers of bacterioruberin derivatives and 30 different carotenoids with antioxidant activity were identified in a haloarchaeon *Haloterrigena turkmenica*. The antioxidant capacities of carotenoid determined by $DPPH^{\bullet}$ radical scavenging assay produced by halophilic archaeal strains *Halogeometricum rufum, Halogeometricum limi, Haladaptatus litoreus, Haloplanus vescus, Halopelagius inordinatus, Halogranum rubrum, and Haloferax volcanii* have been assessed and reported in another study carried out by Hou and Cui, 2018. The antioxidant capacities of the carotenoids from these strains were reported to be significantly higher than β-carotene. Antioxidant potential of marine halophilic and archaeal bacterial bionts from several dominant marine invertebrates (sponges, corals and bivalve) has been reported by Velho Pereira *et al*. (2015).

1.4.2 Antibacterial compounds and halocins

The vast majority of antibacterial compounds have come from non-extreme, terrestrial microorganisms. However, while these microorganisms continue to be studied extensively, the rate of discovery of novel metabolites from terrestrial microorganisms is decreasing (Behal *et al*., 2003). Resistance to the available antibiotics is of great concern because of rapid spread of multi drug resistant clones causing havoc in the health sector (Tenover, 2006). Microorganism frequently cohabitating saline econiches, foster the production of bioproducts or metabolites that is used to encounter the predator or the co-competitor so as to thrive in such environments. Many of the times, these same metabolites which help them counteract the deleterious effects of toxic products in their environment also constitute valuable resources for biotechnology. Discovery and identification of new sources of natural products such as the solar salterns, therefore, plays an important role in uncovering of novel drugs and bioproducts. Bacteria in marine environments are often under extreme conditions of pressure, temperature, salinity and depletion of micronutrients, with survival and proliferation often depending on the ability to produce biologically active compounds. The function or importance of these compounds to the organism's development is usually of ecological nature as they serve as defence against predators/ as competitive weapons used against other bacteria, fungi, amoebae, plants, insects, large animals for interspecies competition and hence antagonistic in nature (Demain and Fang, 2000). It has been reported that haloarchaea have been shown to extracellularly produce molecules with antimicrobial qualities termed as halocins and microhalocins. They were for the first time reported in the genus *Halobacterium* in 1982 (Rodriguez-Valera *et al*., 1982). These molecules lyse sensitive cells, liberating the content and enriching the environment and then when nutrients become abundant again, the halocin producing organism gets an advantage of this nutrient influx and thrives, thus reducing competition for survival (Reeves, 1972; Kis-Papo and Oren, 2000). These molecules are proteinaceous in nature and secreted extracellularly, with a particular characteristic of being active or having antagonistic activity against microorganisms closely related to the producer (O'Connor and Shand, 2002).

Like bacteriocin and Eukaryocins which are produced in Eubacteria and Eukaryota, halocins are diverse in size, consisting of proteins as large as 35 kDa (kilo Dalton) and

peptide ‘‘microhalocins’’ as small as 7435 Da. They are salt dependent, thermolabile and most showing a broad spectrum of activity except for a few (O’Connor and Shand, 2002). Information on only a handful of halocins is available and detailed in **Table 1.1**. The purified halocins include **H1** (Platas *et al*., 2002), **H4** (Meseguer and Rodriguez-Valera, 1985; Cheung *et al*., 1997), **H6** (Torreblanca *et al*., 1989). Though halocins H2, H3 and H5 are reported, not much is known about these biomolecules (Rodriguez-Valera *et al*., 1982). The microhalocins as included in **Table 1.1b:** S8 (Price and Shand, 2000) and R1 (Rdest and Strum, 1987; O’Connor and Shand, 2002). Halocins **H4**, **H6** and **R1** are characterised at the protein level (Shand *et al*., 1998) whereas, halocin **H4** has been characterised at the gene and mRNA levels (Cheung *et al*., 1997). Platas *et al*., 1996 and his team found that in a co-culture of *Haloferax mediterranei* (a halocin producer) and *Halobacterium salinarum* (a non-producer) that was devoid of any nutrients, *Haloferax mediterranei* was able to grow at the expense of *Halobacterium salinarum* (presumably through release of cellular constituents from *Halobacterium salinarum.* Hence they presumed that one of ecological implication of halocin production is that it provides the species producing them, means to avoid competition by other species that have the same environmental requirements. Pasic *et al*. (2008) reported the isolation of an extremely haloarchaeon Sech7a producing a halocin, which is stable over a wide range of pH and found it to be thermolabile over 80ºC (Pasic *et al*., 2008).

In the Indian scenario, there have been a few reports on the discovery of such antagonistic substances with a potential for clinical trials. Halocin production among Goan salt pans isolates was first reported by Bansal and Furtado, 2004. In a later study carried out by Salgaonkar *et al*., 2012, cell free supernatants of 24 isolates belonging to *Haloferax*, *Haloarcula* and *Halorubrum* from salt pans of Goa were reported for antagonistic activity. Kavitha *et al*. (2011) reported an archaeon *Halferax volcanii* KPS1 growing at 25% NaCl at 40^{o}C, from Kovalam in Kanyakumari, India, which was found to produce a halocin KPS1. It was found to have a broad spectrum of activity and stable over a wide range of pH, proteinaceous in nature, which they proposed could be beneficial in the development of an antimicrobial peptide. A halocin (SH10) has been reported to be produced by an extremely halophilic archaeon *Natrinema* sp. BTSH10 from a salt pan in Kanyakumari, Tamil Nadu, India, at 42°C, pH 8.0 after 104 hours of incubation (Karthikeyan *et al*., 2013). Sujatha and Jasmine,

2017, focused on production of halocin, a peptide antibiotic in five strains (*Haloarcula hispanica*, *Haloarcula marismortui*, *Haloarcula vallismortis*, *Halobacterium salinarum* and *Haloferax larseni*) isolated from Parangipettai saltpans against *Haloarcula vallismortis*. They found that *Haloarcula hispanica* showed the highest antagonistic activity. *Haloferax larsenii* strain HA1 isolated from Pachpadra salt lake, Rajasthan, India, was found to be halocidal against indicator strain *Haloferax larsenii* HA10. The molecular weight of halocin HA1 was found to be ~14 kDa (Kumar *et al*., 2016).

In addition to having antimicrobial properties, halocin H6 can inhibit the Na^+/H^+ exchanger (NHE) in mammalian cells. This property can protect tissues including the myocardium from damage caused when blood returns after ischemic conditions. Currently, halocin H6 is the only known biological molecule that exerts a specific inhibitory effect on the Na^+/ H^+ exchanger of mammalian cells (Mirabet *et al*., 2002; Alberola *et al*., 1988). Both halocin, H6, from *Haloferax gibbonsii* (Ma2.39) and microhalocin S8 were found to retain ~50% activity at temperatures close to 100°C (Torreblanca *et al*., 1989). These proteins have promising applications for the future of antimicrobial and pharmaceutical product development especially in the canning and food industry. Besides the ability to possess antimicrobial activity against gram positive and gram negative human pathogens, the role of halocins in prevention of halophilic bacterial damage on brine cured hides is reported (Birbir *et al*., 2004; Kavitha *et al*., 2011)

Table 1.1 Characteristics of halocins

Halocin	Producer (source)	Size	Thermal Stability	Salt dependancy	Activity spectrum	Mechanism	References
A4	Haloarchaeon TuA4	7,435 Da	ND	no	broad	cytocidal	Haseltine *et al*. 2001 Duncan, 2004
C8	*Hbt.* strain AS7092,	7,427 Da	at 100 ˚C	no	broad	Cytocidal with primary target at the cell wall	Li *et al*., 2003
G1	*Hbt.* strain GRB	ND	ND	ND	Broad	ND	Soppa and Oesterhelt, 1989
H1	*Hfx. mediterranei* M2a, previously Xia3	31 kDa	< 50C	yes	broad	Alters membrane permeability.	Rodrıguez-Valera *et al*., 1982 Platas *et al*., 1996 Platas *et al*., 2002
H2	Haloarchaeon Gla2.2	ND	ND	Broad	ND	ND	Rodriguez-Valera *et al*., 1982
H3	Haloarchaeon GAA12	ND	ND	Broad	ND	ND	Rodriguez-Valera *et al*., 1982
H4	*Hbt mediterranei* R4	34.9 kDa	< 60C	Partially	Broad	ND	Rodriguez-Valera *et al*., 1982 Meseguer and Rodriguez-Valera, 1986 Cheung *et al*., 1997
H5	Haloarchaeon Ma 2.20	ND	ND	ND	Narrow	ND	Rodriguez-Valera *et al*., 1982
H6	*Hfx. gibbonsii* Ma2.39	3 kDa	≤ 90 ˚C	No	Broad	Na^+/H^+ antiporter inhibitor	Rodriguez-Valera *et al*., 1982 Torreblanca *et al*.,1989
HA1	*Hfx larsenii* HA1	≈14 kDa	ND	ND	ND	ND	Kumar *et al*., 2016
KPS1	*Hfx. volcanii* KPS1	ND	>80°C	ND	broad	ND	Kavitha *et al*., 2008
S8	Haloarchaeon S8a	≈3.58 kDa	≤ 90°C	No	broad	ND	Price and Shand, 2000
R1	*Hbt.* sp. GNlOl	3.8 kDa	60°C	No	broad	cytostatic	Rdest and Sturm, 1987
SH10	*Natrinema sp.* BTSH10	ND	ND	ND	ND	ND	Karthikeyan *et al*., 2013
-	*Haloarchaeon Sech* 7a	ND	>80°C	ND	ND	ND	Pasic *et al*., 2008
-	*Hfx., Har.,Hrb* sp.	ND	ND	ND	ND	ND	Salogaonkar *et al*., 2013
-	*Hfx., Har., Hbt* sp.	ND	ND	ND	ND	ND	Sujatha and Jasmine, 2017

*ND – Not determine

1.4.3 Bacteriorhodopsin and retinal pigments

The ability to convert light to chemical energy in a nonchlorophyll system was first discovered in the haloarchaea (Oesterhelt and Stoeckenius, 1971). The apoprotein, bacterio-opsin, is combined with a retinal protein to make bacteriorhodopsin which is then organized into a two-dimensional crystalline array in the purple membrane of haloarchaea. Bacteriorhodopsin has several qualities that make it useful in an industrial setting: it is functional at 45°C and pH values (1–11), its reactions are self-regenerative and can be manipulated chemically, genetically, or immunologically (Racker and Stoeckenius, 1974). Bacteriorhodopsin from *Halobacterium* species is being marketed for light sensors, nonlinear optics, and optical data processing (Hampp *et al*., 1991; Hampp *et al*., 1992).

1.4.4 Extremozymes

Halophilic enzymes are of particular interest because they are active in environments with low water activity. They have a predominance of negatively charged residues on the solvent-exposed surfaces of the protein. These negative charges attract water molecules and thereby keep the proteins hydrated so that they do not precipitate. It has also been shown that the hydrogen bonds formed between the negative side chains and the water molecules lead to the formation of a stable hydration shell (Balasubramanian *et al*., 2002). The increase in negative charges also results in an increase in ion-pair networks in halophilic enzymes (Dym *et al*., 1995) Other proposed adaptations of halophilic enzymes are the reduction of hydrophobic surfaces and the unusually high number of ordered side chains (Britton *et al*., 2006). Extremoenzymes from halophilic microorganism are not only are extremely high salt tolerant but also they are thermotolerant because of the specific environment they live. These kinds of enzymes have catalytic function in the condition of low water activity, the situation that is common in the presence of organic solvents (Marhuenda-Egea and Bonete, 2002), which is a better environment for some enzymatic reactions (Serdakowski and Dordick, 2008). Enzymes from extreme halophiles are expected to show optimal activities in extreme conditions like, low water activity, presence of organic solvents and relatively high temperature and pH, thus the possibility to have a

wide variety of extreme halophiles (Haloarchaea) producing extracellular hydrolytic enzymes will be of valuable importance for biotechnological applications.

1.4.4.1 Natural polymers

Amylase is an enzyme involved in breakdown of starch. There are three types of amylases; α-amylase, β-amylase and γ-amylase. α- amylase (E.C.3.2.1.1) is an endo-hydrolase enzyme that catalyses the hydrolysis of internal α-1, 4-glycosidic linkages in starch to yield products like glucose and maltose (Gupta *et al*., 2003). Hence, terminal glucose residues and α-1, 6-linkages cannot be cleaved by α-amylase. The substrate that α-amylase acts upon is starch. Starch is a polysaccharide composed of two types of polymers; amylose and amylopectin. Amylose constitutes 20-25% of the starch molecule. It is a linear chain consisting of repetitive glucose units linked by α-1, 4-glycosidic linkage. Amylopectin constitutes 75-80% of starch and is characterized by branched chains of glucose units. The linear successive glucose units are linked by α-1, 4-glycosidic linkage while branching occurs every 15-45 glucose units where α-1, 6 glycosidic bonds are present (Leveque *et al*., 2000b; Bertoldo and Antranikian, 2002). These amylases represent approximately 30% of the worldwide industrial enzyme production, the starch hydrolysis being considered to be the main way of their use (Van der Kaaij *et al*., 2002).

β-amylase (EC 3.2.1.2) is an exo-hydrolase enzyme that acts from the nonreducing end of a polysaccharide chain by hydrolysis of α-1, 4-glucan linkages to yield successive maltose units. Since it is unable to cleave branched linkages in branched polysaccharides such as glycogen or amylopectin, the hydrolysis is incomplete and dextrin units remain. Primary sources of β-Amylase are the seeds of higher plants and sweet potatoes. It can be used for structural studies of starch and glycogen molecules produced by various methods. In the industry it is used for fermentation in brewing and distilling industry. Also, it is used to produce high maltose syrups (Sivaramakrishnan *et al*., 2006).

γ-amylase (EC 3.2.1.3) cleaves α (1-6) glycosidic linkages, in addition to cleaving the last α (1-4) glycosidic linkages at the non-reducing end of amylose and amylopectin, unlike the other forms of amylase, yielding glucose. γ- amylase is most efficient in acidic environments and has an optimum pH of 3 (Sivaramakrishnan *et al*., 2006).

Lipases as a class of hydrolytic enzymes (EC 3.1.1.1) hydrolyse triglycerides to fatty acids and glycerol, and under certain conditions catalyse the reverse reaction (Teo *et al*., 2003). Lipases act mostly on long chain acyl glycerol and are able to catalyze transesterification and enantio selective hydrolysis reactions (Matsumoto *et al*., 2004). Other diverse applications include the modification of biologically active molecules, the enhancement of flavor or nutraceutical properties in foods and the resolution of racemic mixtures remarkably in the presence of some organic solvents; they perform esterification, amidation, and polymerisation reactions (Bornscheuer and Kaslauskas, 1999; Jaeger and Eggert, 2002; Schmid and Verger, 1998; Sharma *et al*., 2001). These enzymes have experienced the greatest market increase during the last few years with their wide and diverse applications ranging from detergents to food industry (Gandol *et al*., 2000; Tamerler *et al*., 2001; Teo *et al*., 2003). A few studies have been carried out concerning the production of extracellular enzymes from haloarchaea as predominant microbiota of these extreme environments. Lizama *et al*. (2001) during the study on haloarchaeal strains isolated from salt lake in Chile showed their isolates produced amylase and lipase. Elevi *et al*. (2004) studied the production of amylase and lipase in haloarchaea. Ozcan *et al*. (2007) and Birbir *et al*. (2007) have reported the presence of amylase and lipase activity in haloarchaeal strains screened in their studies. *Haloarcula valismortui*, *H. saccharovorum* are known to utilise carbon sources as diverse as sugars such as fructose, glucose and even some are known to grow on hydrocarbons (Wijaya and Rangaswamy, 1992).

Halophilic proteases are widely used in the detergent and food industries. They are also used in the baking, dairy, and leather industry as well as in the manufacture of soy products and in the production of aspartame. Proteolytic activity with potential industrial application has been characterized in *Halobacterium* sp. (Norberg and Hofsten, 1969; Izotova *et al*., 1983), *Haloferax* mediteranei (Kamekura *et al*., 1996*)*, *Natrialba asiatica* (Kamekura and Seno, 1990), *Natrialba* magadii (Gimenez *et al*., 2000), *Natronococcus occultus* (Studdert *et al*., 1997; Elsztein *et al*., 2001) and *Natronomonas pharaonis* (Stan-Lotter *et al*., 1999).

1.4.4.2 Hydrocarbons

Huge volumes of oily wastewater are generated during oil rigging and production activities. Produced waters display a wide range of salinities, ranging from low to high and transporting of this spilled brine to land, inhibits plant growth, leading to increased erosion and loss of topsoil and contamination of groundwater by both salt and hydrocarbons (Fathepure and Nicholson, 2004). In the last few decades, extensive urbanization and rapid industrialization has resulted in the addition of a large number of xenobiotic compounds into the environment. The chemical properties and quantities of the xenobiotic compounds determine their toxicity and persistence in the environment. Organic (aromatic/ non-aromatic) compounds constitute a major group of environmental pollutants (Dagley, 1986). These compounds are highly persistent in the environment due to their thermodynamic stability (Diaz *et al*., 2002). Many of these compounds have been reported to be toxic to the living organisms (Diaz, 2004). Bioremediation, which utilizes the microbial metabolic potential of the degrading microorganisms, has come up as an efficient and cost-effective means of large scale removal of these compounds in comparison to the physico-chemical means of bioremediation.

Oxygenases belong to the oxidoreductive group of enzymes (EC 1.13), which oxidize the substrates by transferring oxygen from molecular oxygen (O_2) and utilize FAD/NADH/NADPH as the co-substrate. They play a key role in the metabolism of organic compounds by increasing their reactivity or water solubility or bringing about cleavage of the aromatic ring (Arora *et al*., 2009). Oxygenases can further be grouped into two categories; Monooxygenases which catalyse the incorporation of one atom of O_2 into the organic substrate and the other atom is reduced to water and dioxygenases in which both atoms from a single molecule of O_2 are incorporated into the organic substrates (Ullrich and Hofrichter, 2005). Dioxygenases include two major classes: haem-dependent iron sulphur dioxygenases and Rieske iron-sulphur non-haem dioxygenases the majority of which are NADH dependent (Burton, 2003). Benzoate has been widely used as a model compound for the study of the bacterial catabolism of aromatic compounds (Gibson and Harwood, 2002). Benzoate is the simplest aromatic salt and is an intermediate of the biodegradation of many aromatic compounds, such as mandelate and toluene (Harwood and Parales, 1996; Wackett,

2002). It has also been reported to be an intermediate during the anaerobic biodegradation of benzene (Caldwell and Suflita, 2000). The biodegradation of benzoate has been well documented, and a two-stage degradation pathway is generally accepted (Harwood and Parales, 1996). Benzoate is converted by the aromatic dioxygenases to dihydroxylated compounds aromatic ring cleavage substrates such as catechol, gentsate, protocatechuate and their derivatives by hydroxylation of the aromatic nucleus brought about by oxygenases and dehydrogenases (Van der Meer *et al*., 1992), followed by catechol ring cleavage and subsequent reactions leading to the Krebs cycle intermediates (**Fig. 1.6**). Other than benzoate, many aromatic compounds such as benzene, phenol, and salicylate are also converted to catechol during the first degradation stage (Harwood and Parales, 1996; Wackett, 2002). A culture from a Goan salt pan, *Halobacterium* strain R1 MTCC 3265 was able to tolerate and transform many hydrocarbons such as crude oil, petrol, diesel, kerosene, hexane, cyclohexane, benzene, toluene, xylene and sodium benzoate during growth (Aguiar, 1994; Prabhu, 2002 Raghavan and Furtado, 2005).

However, further conversion of these intermediates into tricarboxylic acid (TCA) cycle intermediates was found to be highly diverged (divergent mode), they then undergo ring cleavage reactions producing non-cyclic molecules which are in turn converted into species that can enter in the citric acid cycle. Ring cleavage reactions are catalyzed by extradiol-cleaving dioxygenases (ECDs) via the ortho cleavage or the intradiol cleaving dioxygenases (ICDs) via the meta- cleavage pathway (Kukor and Olsen, 1991; Hamzah and Albaharna, 1994).

Table 1.2 Extremozymes produced by haloarchaea

Extremozyme	Producer cultures	Optimal Activity	Reference
β-Galactosidase	*Haloferax lucentense*	23% NaCl	Holmes *et al*., 1997
Amylase	*Halorubrum xinjiangense*	23% NaCl	Moshfegh *et al*., 2013
Amylase	*Haloferax mediterranei*	17% NaCl	Pérez-Pomares *et al*., 2003
Amylase	*Natronococcus amylolyticus*	15% NaCl	Kobayashi *et al*., 1994
Amyloglucosidase	*Halorubrum sodomense*	7.5% NaCl	Oren, 1983 Chaga *et al*., 1993
Class I fructose aldolase	*Haloarcula vallismortis*	20% KCl	Krishnan and Altekar, 1991
Lipase	*Natronococcus sp.*	23% NaCl	Boutaiba *et al*., 2006
Protease	*Haloferax mediterranei*	-	Stepanov *et al*., 1992
Protease	*Halobacterium salinarum*	23% NaCl	Ryu *et al*., 1994
Serine protease	*Halobacterium salinarum*	-	Izotova *et al*., 1983
Serine protease	*Natrialba asiatica*	10−15% NaCl	Kamekura and Seno, 1990 Kamekura *et al*., 1992
α-Amylase	*Haloferax* sp. HA10	18% NaCl	Bajpai *et al*., 2015
α-Amylase	*Haloarcula* sp. strain S-1	25% NaCl	Fukushima *et al*., 2005
Lipase	Haloarchaeal strains A43, B53, E7, A138 and B49	20-25% NaCl	Ozcan *et al*., 2009
Esterase	Haloarchaeal strains A43, B53, E7, A138 and B49	20-25% NaCl	Ozcan *et al*., 2009
Lipase	*Haloarcula marismortui*	30% NaCl	Camacho *et al*., 2009
Protease and Lipase	*Halococcoccus agarlyticus* GUGFAWS-3 *Haloferax* ATCC 645	25% NaCl	Goankar and Furtado, 2018a Goankar and Furtado, 2018b
Cellulase and xylanase	*Halococcoccus saccharolyticus* strain $GUFF_{70}$ *Halorubrum sacchorovorum* strain GUMFSA1	25% NaCl	Malik and Furtado, 2018

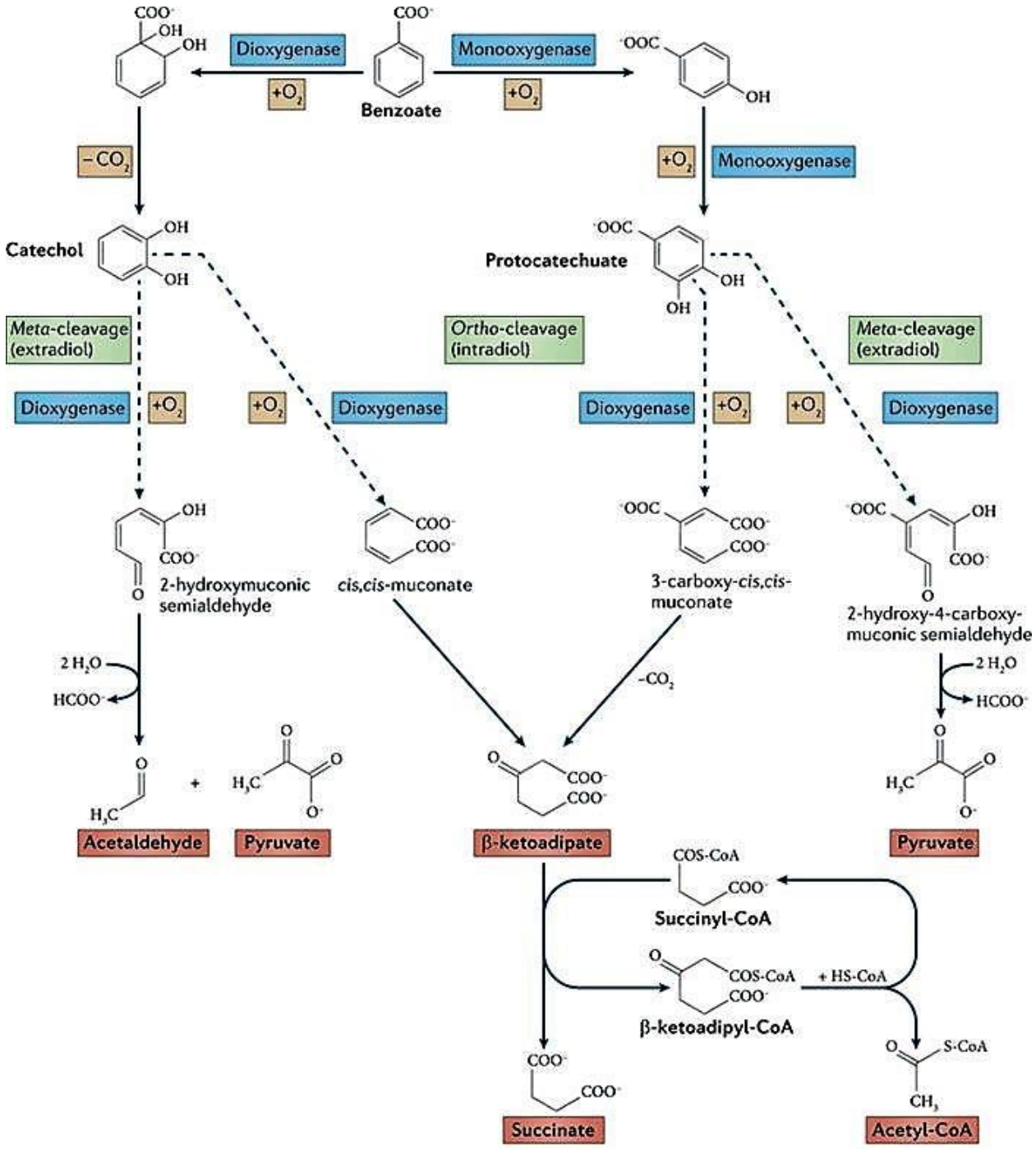

Fig. 1.6 Microbial degradation of benzoate (Fuchs *et al*., 2011)

Since conventional microbiological treatment processes do not function at high salt concentrations, bioremediation i.e. utilizing the metabolic activities of microorganisms to transform organic contaminants into non-hazardous forms, of oilfield brine can be accomplished only by using consortium of extremely halophilic microorganisms capable of degrading petroleum compounds or through bioaugmentation (the addition of known degrading organisms to a site) (Fathepure and Nicholson, 2004). The only field study known to us on the degradation of hydrocarbons at high salt concentrations was performed in the Great Salt Lake, Utah (Ward and Brock, 1978). In a study carried out by Bertrand *et al*., (1990) the halobacterial strain EH4, isolated from a salt-marsh in the south of France, was found to biodegrade alkanes (tetradecane, hexadecane, eicosane, heneicosane and pristane) and aromatic hydrocarbons (acenaphtene, phenaphtrene, anthracene and 9-methyl-anthracene). The metabolic potential of the halophilic archaeabaeteria such as *Halobacterium, Haloferax, Haloarcula* under aerobic conditions, is limited due to the restricted range of compounds that have been tested as potential substrates (Oren *et al*., 1992). Emerson *et al*. (1994) isolated a pink-pigmented halophilic *Haloferax* sp. D1227, a halophilic archaeon capable of using aromatic substrates (e.g., benzoate, cinnamate and phenylpropanoate) as sole carbon and energy sources for growth. Al-Mailem *et al*. (2010) in their study carried out on the hypersaline coasts of the Arabian Gulf isolated two extreme halophilic *Haloferax* strains and one strain each of *Halobacterium* and *Halococcus* on a mineral salt medium with crude oil vapor as a sole source of carbon and energy. These archaea grew best in the presence of 4 M NaCl and needed at least 1 M NaCl for growth. Cuadros-Orellana *et al*. (2006) enriched and isolated 10 halophilic archaea from Dead Sea water samples on the basis of their ability to aerobically grow on p-hydroxybenzoic acid (pHBA) as the sole carbon and energy source. A work carried out by Tapilatu *et al*. (2010) in Camargue, France showed for the first time the potential role of halophilic archaea belonging to the genera *Haloarcula* and *Haloferax* in the degradation of hydrocarbons in both pristine and hydrocarbon-contaminated hypersaline environment. Erdoğmuş *et al*. (2013) reported that halophilic Archaea isolated from Çamaltı Saltern, Turkey, namely *Halobacterium piscisalsi, Halorubrum ezzemoulense, Halobacterium salinarium, Haloarcula hispanica, Haloferax* sp., *Halorubrum* sp. and *Haloarcula* sp. at 20% NaCl was able degrade aromatic hydrocarbons (namely, p-hydroxybenzoic

acid, naphthalene, phenanthrene and pyrene). Activity of catechol 1, 2 dioxygenase and protocatechuate 3, 4 dioxygenase enzymes was demonstrated.

1.4.5 Mycosporines, mycosporine-like amino acids (MAAs) and compatible solutes

Mycosporines and mycosporine-like amino acids (MAAs) are low-molecular weight water-soluble molecules absorbing UV radiation in the wavelength range 310–365 nm. They are composed of either an amino cyclohexenone or an amino cycloheximine ring, carrying nitrogen or imino alcohol substituents. When substituted with amino acid residues, they are designated as mycosporine-like amino acids (MAAs). They are accumulated by a wide range of microorganisms, prokaryotic (cyanobacteria) as well as eukaryotic (microalgae, yeasts and fungi) and a variety of marine macroalgae, corals and other marine life forms. The role that MAAs play as sunscreen compounds to protect against damage by harmful levels of UV radiation is well established (Dunlap and Yamamoto, 1995). Compatible solutes are small organic osmolytes used by cells of numerous water-stressed organisms and tissues to maintain cell volume. Similar compounds are accumulated by some organisms in anhydrobiotic, thermal and possibly pressure stresses. These solutes are amino acids and derivatives, polyols and sugars, methylamines, methylsulfonium compounds and urea. Except for urea, they are often called ‘compatible solutes’, a term indicating lack of perturbing effects on cellular macromolecules and implying interchangeability (Brown and Simpson, 1972; Yancey *et al*., 1982). Ectoine and its derivatives have been patented as moisturizers in cosmetics and as stabilizers in polymerase chain reactions (Montitsche *et al*., 2002). Glycine betaine, a common osmolyte, has been proposed as a feed additive. Glycerol, as an emulsifier softener, protective medium, and as nutrient and nutrient supplements among other applications (Ben-Amotz *et al*., 1982).

1.4.6 Polyhydroxyalkanoates

Halophilic archaea produce large quantities of polyhydroxyalkanoates (PHA) which have been utilized for their application as biodegradable plastics. They show features of biocompatability and resistance to water. Therefore, they are of interest to the medical and pharmaceutical community for use in surgical sutures, bone replacement,

and delayed release medications (Lafferty *et al*., 1988). Braganca and Furtado, (2004), reported the production of PHA among *Halobacterium*, *Haloarcula* and *Haloferax* species from Goan salt pans and Fish jetty samples. Salgaonkar and Bragança, (2017) investigated *Halogeometricum borinquense*, a new haloarchael PHA producer growing on hydrolyzed sugarcane bagasse exhibited a superior performance in terms of PHA productivity (Salgaonkar and Braganca, 2017). Accumulation of PHA in the extremely halophilic archaeon *Natrinema ajinwuensis* RM-G10 has been reported by Mahansaria *et al*. (2018).

1.4.7 Synthesis of nanoparticles by haloarchaea

Natural and anthropogenic activities such as erosion and mining have resulted in deposition of toxic heavy metals and their derivatives in soils, rivers and oceans (Alvarenga *et al*., 2013). The use of microbial-based bioremediation attracts considerable interest and research on the use of halophiles for metal bioremediation is flourishing (Bini, 2010). Naik and Furtado, (2014) reported metal ion adsorption using dried cells of haloarchaeon *Halobacterium* sp. GUSF (MTCC3265) which adsorbed 99% Mn^{2+} in 60 min at pH 6.8 and 30ºC on contact with 109.54 mg Mn^{2+} per liter in saline solution whereas Salgaonkar *et al*. (2016) reported for the first time the resistance of halophilic archaea to zinc oxide nanoparticles (ZnO NPs). Braganca and Furtado, (2017) reported the use of *Halobacterium* strain R1 MTCC 3265 in removal of cadmium ions upto 18 ppm in saline and upto 63% in non-saline environments. Such metals resistance in halophilic archaea also makes them possible candidates for the green synthesis of metal nanoparticles (NPs) which can be employed in various fields.

Silver nanoparticles (AgNPs) synthesized by *Halococcus salifodinae* BK3 are reported to have anti-bacterial activity against both Gram-positive (*S. aureus* and *M. luteus*) and Gram-negative (*E. coli* and *P. aeruginosa*) bacteria (Srivastava *et al*., 2013). Patil and Furtado, (2014) reported the use of cells of a haloarchaeon, *Haloferax alexandrinus* for the green synthesis of silver nanoparticles which exhibited broad spectrum antimicrobial activity against human and mammalian pathogens, in the order of *Ps. aeruginosa* ATCC 9027 > *B. bronchiseptica* ATCC 4617 > *B. subtilis* ATCC 6633 > *S. aureus* ATCC 6538P > *S. epidermidis* ATCC 12228 > *E. coli* ATCC

8739 > *S. typhimurium* ATCC 14028. Selenium nanoparticles (SeNPs) synthesized by *Halococcus salifodinae* BK18 are reported to stop the proliferation of cancerous HeLa cell lines when studied *in vitro* (Srivastava *et al*., 2014). The haloarcheon has also been reported to synthesize tellurium nanoparticles with anti-bacterial potential (Srivastava *et al*., 2015).

1.4.8 Arsenic toxicity and antigenotocity

Human health hazards due to As(III) and As(V) contamination of water have been reported globally (Nriagu, 2007; Smedley and Kinniburgh, 2002). The current drinking water standard, or Maximum Contaminant Level (MCL) for arsenic from the U.S. Environmental Protection Agency (EPA) is 0.010 mg L^{-1} or parts per million (ppm) (Nigra *et al*., 2017). Arsenic can get into the human body through drinking water as well as eating food that has been contaminated with the metalloid.

Arsenic induced disorders range from skin cancers, internal cancers (bladder, kidney, and lung) and diseases of the blood vessels of the legs and feet, diabetes, increased blood pressure, and reproductive disorders (Hughes, 2002). In human beings, inorganic arsenic has been reported to (i) modulate expression and/or DNA-binding activities of several key transcription factors (Simeonova, 2000) (ii) damage and distort zinc finger domains participate in protein-nucleic acid and protein-protein interactions in many groups of proteins involved in DNA repair (Witkiewicz-Kucharczyk and Bal, 2006) (iii) inhibit the nucleotide excision repair (NER) and base excision repair (BER) (De Boer and Hoeijmakers, 2000).

Arsenic content of the coastal waters and estuarine waters around Goa as early as Fondekar and Reddy, (1974) and Fondekar and Reddy, (1976) as a part of a general pollution study of the impact of fertilizer plants and other industrial activity on the coast of Goa on the west coast of India. According to a study carried out by Zingde *et al*. (1976a) elevated levels of arsenic (25 ppm) have been reported among crustaseans from the shores of Goa. Zingde *et al*., (1976b) has also reported mortality among fish with high levels of arsenic from a bay in South Goa which was reported to be recipient to effluent discharge from a fertilizer factory in the vicinity.

Formation of stress granules (SGs) and a class of proteins called metallothioneins (MTs) have been reported as the cellular response of eukaryotic cells in defense against trivalent arsenic (Lee and Weinfeld, 2004; Anderson and Kedersha, 2009). Resistance to As (III) toxicity in mammalian cells correlated with higher levels of enzymatic antioxidants such as reduced glutathione (GSH) and GSH-related enzymes has been reported (Ventura-Lima *et al*., 2011). In recent years, efforts are underway to avert, suppress and ameliorate cellular damage induced by As(III) through biomolecules. And microbes living under extreme pH, osmotic pressure and salinity (Haloarchaea) are expected to harbour self protective biomolecules which would have antigenotoxic property. Resistance to As(III) and As(V) has been studied in several haloarchaeal cultures of genera *Halobacterium*, *Haloferax* and *Halococcus*, isolated from Goan solar salts and estuarine sediments and the conversion of toxic As(III) to As(V) has also been reported (Braganca, 2002).

1.5 TECHNIQUES EMPLOYED FOR SCREENING AND CHARACTERIZATION OF BIOACTIVES

1.5.1 Enzyme Production

Presence of hydrolytic enzymes among haloarchaea are checked by conventional agar plate methods, which employs mineral medium with 20% NaCl and the specific substrate as a single source of carbon. Zones of decolourisation or precipitation are then measured with a scale. Examples of different enzymes screened include amylase activity (Amoozegar *et al*., 2003), cellulase (CMCase) (Zhou and Li, 2004), chitinase activity (Park *et al*., 2000), DNase activity (Onishi *et al*., 1983), lipase activity (Samad *et al*., 1989) and pectinolytic activity (Soares *et al*., 1999), protease activity (Amoozegar *et al*., 2008), pullulanase activity (Ruben *et al*., 1993), xylanase activity (Wejse and Ingvorsen, 2003).

1.5.2 Antioxidants

Preliminary screening for antioxidant production can be achieved using the filter paper method (Takao *et al*., 1994) or the Agar- DPPH$^{\bullet}$ method (Alvares and Furtado, 2018). In the filter paper method, a sterile whatman filter paper is placed on top of fully grown colonies on a solid agar for a few hours till the replica of the individual

colonies is obtained. The filter paper is then sprayed with specific reagents (eg. $DPPH^{\bullet}$) to check for decolourization, based on which colonies can be scored as positive or negative for activity. In the Agar-$DPPH^{\bullet}$ method, the $DPPH^{\bullet}$ reagent is directly layered on the solid agar which has the fully grown colonies and then incubated in the dark for 30 minutes. The colonies positive for the activity shows zones of decolourization around it. Different *in vitro* and *in vivo* assays for quantification and assessing different types of antioxidant activity are available (Alam *et al*., 2013) and known antioxidant compounds are used as positive controls and for comparison. Solvent extracts from fully grown cells or cellular components are used for the assay.

1.5.2.1 *In vitro* methods

In vitro antioxidant tests use free radical traps and are relatively straightforward to perform. Among free radical scavenging methods listed below in **Table 1.3**, $DPPH^{\bullet}$ free radical scavenging assay is rapid, simple and inexpensive in comparison to other available assays (Brand-Williams *et al*., 1995).

1.5.2.2 *In vivo* models

For all *in vivo* methods the samples that are to be tested are usually administered to the testing animals (mice, rats, etc.) at a definite dosage regimen as described by the respective method. After a specified period of time, the animals are usually sacrificed and blood or tissues are used for the assay. The in vivo methods are listed in **Table 1.3**

Table 1.3 List of antioxidant assays

	Assay	Reference
In vitro	Cupric ion reducing antioxidant capacity (CUPRAC) method	Apak *et al*., 2008
	1, 1-diphenyl-2-picrylhydrazyl ($DPPH^{\bullet}$) assay	Brand-Williams *et al*., 1995
	DMPD (N,N-dimethyl-p-phenylene diamine dihydrochloride) method	Fogliano *et al*., 1999
	Ferric reducing-antioxidant power (FRAP) assay	Benzie and Strain, 1999
	Ferric thiocyanate (FTC) method	Kikuzaki *et al*., 1991
	Hydrogen peroxide scavenging (H_2O_2) assay	Ruch *et al*., 1989
	Hydroxyl radical averting capacity (HORAC)	Ou *et al*., 2002
	Hydroxyl radical scavenging activity	Kunchandy and Rao, 1990
	Oxygen radical absorbance capacity (ORAC)	Prior *et al*., 2003
	Peroxynitrite radical scavenging activity	Kooy *et al*., 1994
	Phosphomolybdenum method	Prieto *et al*., 1999
	Reducing power method (RP)	Oyaizu, 1986
	ß-carotene linoleic acid method/conjugated diene assay	Kabouche *et al*., 2007
	Superoxide radical scavenging activity (SOD)	Meyer and Isaksen, 1995
	Thiobarbituric acid (TBA) method	Ottolenghi, 1959
	Total radical-trapping antioxidant parameter (TRAP) method	Ghiselli *et al*., 1995
	Trolox equivalent antioxidant capacity (TEAC) method	Seeram *et al*., 2006
	Xanthine oxidase method	Noro *et al*., 1983
In vivo	Catalase (CAT)	Aebi, 1984
	Ferric reducing ability of plasma	Umesh *et al*., 2010
	Glutathione peroxidase (GSHPx) estimation	Wood, 1970
	LDL assay	Buege and Aust, 1978
	Lipid peroxidation (LPO) assay	Ohkawa, 1979
	Reduced glutathione (GSH) estimation	Sapakal *et al*., 2008
	Superoxide dismutase (SOD)	Mccord and Fridovich, 1969

1.5.3 Production of antagonism; purification and characterization

Screening of antibacterial activity is achieved by using spread plate or the agar well technique. Pathogens are spread plate on the solidified media and allowed to dry, the producer cultures are spotted or loaded in the wells, incubated at 37°C and checked for zones of clearing. Halocin production is detected by a double layered technique (Meseguer *et al*., 1986), which could be agar overlay method, which involves overlaying soft agar medium, maintained at 50°C seeded with indicator strain over a base agar. 20 µl of producers strain being tested for production of halocins is spotted onto these plates and incubated to check for zones of clearing which is an indicator of the kill effect. This double layered technique can be modified wherein wells cut out on such plates are filled with either producer cultures or cell free supernatant of producer cultures. A general procedure for purifying a halocin includes (i) generation of cell-free supernatants by centrifugation, (ii) concentration of the cell free by filtration through a series of filters with progressively smaller NMWCO (Nominal Molecular weight cut-off) filters; The retentate with the highest activity is used for subsequent steps, (iii) heat and acetone precipitation of contaminated proteins which are removed by filtration, (iv) Concentration of the heat – treated, acetone precipitated supernatant using smaller NMWCO filters, (v) chromatographic techniques such as Gel filtration column chromatography and HPLC, (vi) SDS-PAGE in order to visualize the purity of the halocin (Shand, 2007).

1.5.4 Hydrocabon degradation

Cultures are grown in mineral medium with the appropriate hydrocarbon/ pollutant and checked for growth. Mono and dioxygenases responsible for breakdown of the aromatic benzene ring and the type of ring cleavage is also assessed using specific enzyme assays and test (Garcia *et al*., 2005).

1.5.5 Biosynthesis of nanoparticles and characterization techniques

Biogenic synthesis of nanoparticles can be achieved (i) during growth, (ii) culture supernatant, (iii) whole cells, (iv) cell lysate and (v) cellular parts.

Spectroscopy based techniques such as UV-Vis, Dyanamic Light Scaterring, X-Ray Diffraction analysis, Energy-dispersive X-ray spectroscopy, Fourier Transform-Infra

Red spectroscopy, and Raman Spectroscopy are considered indirect methods of determining data related to composition, structure, crystal phase and properties of nanoparticles. Wavelengths between 300 and 800 nm are generally used for characterizing metallic nanoparticles ranging in size from 2 nm up to around 100 nm (Poinern, 2014). DLS spectroscopy can be used to determine size distribution and quantify the surface charge of nanoparticles suspended in a liquid (Poinern, 2014; Jiang *et al*., 2009). The elemental composition of nanoparticles can be determined via EDS mapping. Whereas XRD examination produces a diffraction pattern that is subsequently compared with data contained in a standard crystallographic database to determine structural information. Analysis of the XRD data identifies crystallite size, structure, preferred crystal orientation, and phases present in samples (Klug and Alexander, 1974). FT-IR spectroscopy can be used to investigate surface chemistry and identify surface residues such as functional groups like carbonyls and hydroxyls moieties that attach to the surface during nanoparticle synthesis. Raman spectroscopy is useful in detecting vibrational modes of molecules and can be used to identify vibrational signals of a variety of chemical species that are attached to the surface of nanoparticles during synthesis (Poinern, 2014). Some of the microscopic techniques routinely used include atomic force microscopy (AFM), transmission electron microscopy (TEM), scanning electron microscopy (SEM), Microscopic based techniques such as AFM, SEM and TEM are considered direct methods of obtaining data from images taken of the nanoparticles. In particular, both SEM and TEM have been extensively used to determine size and morphological features of nanoparticles (Cao, 2011; Feldheim and Foss, 2002).

1.6 RECENT TRENDS IN BIOPROSPECTING - METAGENOME-BASED BIOPROSPECTING

Since the culture-dependent methods only catch a very limited fraction of the total diversity of a given sample, metagenomic methods for bioprospecting can be highly valuable. Although these methods do not require cultivation, they may be restrained by the amount and quality of DNA obtainable from the environment or community of interest. The metagenomic approach can either be i) sequence based, involving high-throughput sequencing and bioinformatics analysis, or ii) function based, aimed at

functional expression of metagenomic libraries to identify genes or gene clusters of interest (**Fig. 1.7**).

1.6.1 Sequence-based metagenomics

The sequence-based approach includes screening for genes by hybridization with labeled DNA probes or by PCR, both of which are based on sequences of known genes (Aakvik *et al*., 2011; Simon and Daniel, 2011; Lee and Lee, 2013). Since the price for direct high-throughput sequencing of metagenomic DNA has reached a level affordable for many laboratories (de Pascale *et al*., 2012; Hunter *et al*., 2012), this is now the standard technology for gene discovery (Ekkers *et al*., 2012). As outlined in **Fig. 1.7**, the sequence-based approach consists of three main steps: (1) the sequencing itself (2) bioinformatic analyses including functional annotation of genes and finally (3) the heterologous expression of identified genes to document activity.

The outcome of the sequencing and bioinformatics pipeline is typically a long list of genes of interest, which has to be investigated further to choose the best candidates for expression. Only 2.8% of more than 20 million proteins in the UniProt database have had their existence confirmed at either the protein or transcript level (Temperton and Giovannoni, 2012), indicating that a significant part of the annotated genes might not be expressed in the laboratory or at a too low level in nature to be detected. Nevertheless, a prioritized list of expression targets can be made from analyses of properties of similar proteins, signal peptides, degree of novelty, etc., and the sequence information can be used for codon optimization and choice of expression organism.

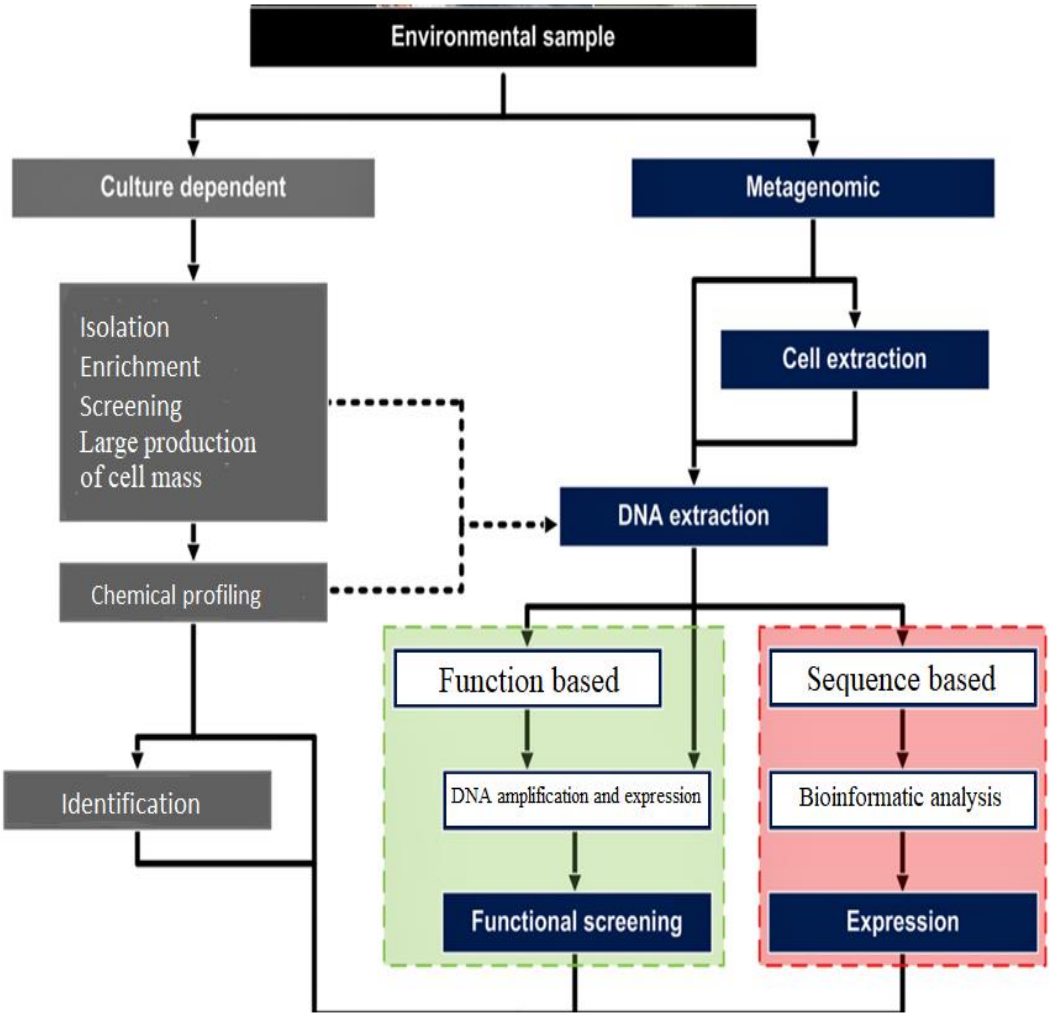

Fig.1.7 General overview of culture-dependent and metagenomic methods for bioprospecting.

1.6.2 Function-based metagenomics

Functional metagenomics is the study of a metagenome by expression in a foreign host. This approach involves critical decisions regarding DNA fragment size, vectors and expression hosts (Ekkers *et al*., 2012). As for the sequence based approach, the starting point is DNA (or cDNA). This has to be of good quality in terms of purity and fragment length. If the concentration of the purified DNA is too low for cloning, as is often the case for extreme environments, the DNA can be amplified by multiple displacement amplification (MDA) (Taupp *et al*., 2011).

1.7 CHEMICAL PROFILING

Hydrophobically associated cellular components may be extracted with relatively non-polar solvents such as ethyl ether, chloroform or benzene. However, membrane-associated polar lipids require polar solvents such as ethanol or methanol to disrupt the hydrogen bonding or electrostatic forces between the lipids and the protein. One or two dimensional thin layer chromatography (TLC) is one of the most effective and versatile techniques for separation of intact complex lipids (phospholipids, glycolipids, etc.) and their lipid moieties, as well as for neutral lipids; it offers many advantages that make it the method of choice in most instances: rapidity, detectability of all organic compounds by charring and preparative-scale operation. Furthermore mass spectrometry techniques are powerful analytical methods in studies of structural characterization of cellular components such as lipid mixtures, isolated lipid components or chemical degradation products of these lipids. High performance liquid chromatography (HPLC) and thin layer chromatography (TLC) are the most common methods used with hydrocarbons, such as carotenoids (Khachick *et al*., 1986).

Carotenoids are highly non polar compounds. Rverse Phase (RP) - HPLC is commonly used to elute hydrophobic compounds, as with a non-polar stationary phase and polar mobile phase, polar compounds are eluted first, removing them from the system. RP- HPLC also gives better resolution of non-polar compounds (Bakalyar *et al*., 1977). Each carotenoid has a distinct visible spectrum and as such it is possible to distinguish them based on their absorbance patterns (Britton *et al*., 1995). In order to do this it is necessary to use a photo diode array to scan a range of visible wavelengths as the sample moves past it. This allows a spectrum to be obtained for each peak on the chromatogram, thus aiding in the identification.

1.8 GENERAL FEATURES OF THE TWO EXTREMELY HALOPHILIC *Haloferax alexandrinus AND Chromohalobacter salexigenes* UNDER STUDY

1.8.1 *Haloferax alexandrinus*

Haloferax alexandrinus belongs to the genus *Haloferax* from the domain Archaea, phylum *Euryarchaeota*, class *Halobacteria*, order *Halobacteriales* family *Halobacteriaceae*. Cell of *Haloferax alexandrinus* are rod-shaped with dimensions

that vary from 1.1 to 1.5 μm, 1.6-2.0 μm in size. The major phospholipids produced are phosphatidylglycerophosphate-methyl ester (PGP-Me) and phosphatidylglycerol (PG). This genus also contained two glycolipids, unsulfated diglycosyl diether, and sulfated diglycosyl diether. Analysis of the non polar lipids showed the presence of 3-hydroxyechinenone, ß-carotene, gamma-carotene, lycopene, cis-astaxanthin, trisanhydrobacterioruberin, bacterioruberin isomer, and canthaxanthin. Canthaxanthin is the unique C_{50} red carotenoid produced in *Haloferax alexandrinus* (Asker *et al*., 2002). *Haloferax alexandrinus* is also reported to biosynthesize silver nanoparticles (Patil and Furtado, 2014). Other species in the genus *Haloferax* are reported for their use in degradation of pollutants (Al-Mailem *et al*., 2010; Tapilatu *et al*., 2010), production of carotenoids (Biswas *et al*., 2016), enzymes (Bajpai *et al*., 2015; Stepanov *et al*., 1992), production of halocins (Torreblanca *et al*., 1989)

1.8.2 *Chromohalobacter salexigenes*

Chromohalobacter salexigenes belongs to gamma-Proteobacterium of the Domain Bacteria, Phylum *Proteobacteria*, Class *Gammaproteobacteria*, Order *Oceanospirillales* and Family *Halomonadaceae*, shows a broad salinity range for growth. Cells are gram-negative, straight or sometimes slightly curved, rods (0.6–1.2 × 1.5–4.2 μm), cells occur singly, in pairs, and in short chains. Motile by polar or peritrichous flagella. Spores are not formed. Moderately halophilic in nature Salt is required for growth. The optimum salt concentration for growth is between 8 and 10%. Cells sometimes grow at salt concentrations up to 30%. The broader ranges of temperature and pH observed for growth are 5–45°C (optimal 30-37°C) and pH 5.0-10.0 (optimal pH 7.5), respectively. Cells are catalase positive and oxidase negative. Most strains reduce nitrates. Phenylalanine deaminase test is negative. Gelatin, starch, Tween 80, esculin, DNA, and tyrosine are not hydrolyzed. Acid is produced aerobically from D-glucose and other sugars. Carbohydrates, amino acids, and some polyols can serve as sole carbon sources. Colonies are cream to brown-yellow pigmented. The mol% G + C of the DNA is: 62–66. Osmoprotection is achieved by the accumulation of compatible solutes either by transport (betaine, choline) or synthesis (mainly ectoine and hydroxyectoine). Ectoines can play additional roles as nutrients and in the case of hydroxyectoine, in thermotolerance. A supplementary solute, trehalose, not present in cells grown at 37°C, is accumulated at higher

temperatures, suggesting its involvement in the response to heat stress (Vargas *et al*., 2018). Biogenic approach for the synthesis of titanium dioxide nanoparticles using a *Chromohalobacter salexigens* Strain PMT-1 has been investigated (Tharanya *et al*., 2015).

Studies carried out by Velho-Pereira and Furtado, (2012) showed that cultures belonging to the genus *Chromohalobacter* were seen to show maximum antimicrobial activity. Further, the evaluation of antioxidants produced by halophilic bionts from marine sponges, coral and bivalves revealed that *Chromohalobacter israelensis* (JX839255) was an excellent scavenger of free radical and the antioxidant compound was identified as a peptide (Velho-Pereira *et al*., 2015).

Not many reports are available on studies devoted to bioprospecting with marine extremely halophilic eubacteria and haloarchaea using live cultures (Behal, 2003). As against in silico, pure cultures may be the only way to comprehensive characterization of physiological properties and full assessment of application potential of individual microbial species (Vartoukian, 2010).

Globally, solar salt plays an important role in all forms of life (Aral *et al*., 2004). Goa situated on the west coast of India, is engaged in natural salt production through green process of salt farming for the past 1500 years (Furtado and Fernandes, 2009). These salt pans in Goa are mostly situated inside the sea coast bordering four talukas of Goa, namely Pernem, Bardez, Tiswadi and Salcete. This solar salt is widely used in moderate quantities as fertiliser and soil conditioner in Goa (Mani *et al*., 2012).

The Goan estuarine ecosystems such as solar salterns and mangroves are inundated with riverian waters and are subjected to influx of nutrients; hence it is possible that these ecosystems harbour extremely halophilic microrganisms that have the potential to produce bioactives of biotechnological importance.

1.9 Aim and scope of the study

In light of the above, the present research study to be submitted to Goa University, as a **Thesis, for evaluation and award of the Doctor of Philosophy degree in the subject of Microbiology,** was directed at evaluating the bioprospects of extremely halophilic eubacteria and haloarchaea associated with solar salts, estuarine sediments of Goa- India and two of the representative cultures, namely the haloarchaeon *Haloferax alexandrinus* GUSF-1 (KF796625) and the extremely halophilic eubacterial *Chromohalobacter salexigenes* GUVFFM-3 (JF330126) in the fields of : i) Extremozymes such as amylases, lipases and aromatic oxygenases; ii) Antagonism against human pathogens and against haloarchaeal members of the same domain and Protogonism in terms of promotion of microbial growth, antigenotxicity and antioxidants; iii) Chemical characterization of structural and functional biomolecules and iv) Biosynthesis of nanoparticles of selenium, tellurium and manganese oxide. The observations, experimental results of this study, the inferences and conclusions derived thereof, are put together as a thesis entitled,

"Bioprospecting with Marine Halophilic Eubacteria and Haloarchaea for Bioactives"

Chapter II

Bioprospects of Extremely Halophilic Eubacteria and Haloarchaea as Producers of Bioactives

The estuarine ecosystem experience varying salinities and therefore the microflora that thrive in these regions are expected to survive under conditions of varying salinities and produce bioactives which are active at various salinities. Despite advances in understanding the diversity and systematics of extreme halophiles, studying their hydrolytic enzymes have received less attention. Survival and proliferation of marine bacteria subjected to extreme conditions often depends on the ability to produce biologically active compounds which inhibits growth of co-members and also helps self to tide over adverse conditions of the milieu. Thus, an econiche member, in order to thrive or gain dominance, over co-members of the econiche, either belonging to the same phylotype as itself or different phylotype/s, belonging to the same Domain produces metabolites, that antagonize co-inhabitating or transient microbial members. Although such antagonistic/ protogonistic activities are well documented among terrestrial microorganisms, studies devoted to these aspects are in their infancy among marine microbes.

In the last 3 decades marine microbes are evaluated for their bioactive potential. Most studies are focused on use of marine microbes requiring salt levels of 2.5 %. There is very little information on bioactives from extremely halophilic eubacteria and Archaea (Haloarchaea) which require NaCl above 15% The Goan estuarine ecosystems such as solar salterns and mangroves are inundated with riverian waters and are subjected to influx of nutrients, hence it is possible that these ecosystems harbour extremely halophilic microrganisms that have the potential to produce bioactives of biotechnological importance.

This chapter deals with the screening and sorting of diversity of cultures from coastal solar salts and sediments from estuarine areas of Goa-India, available with my research guide, Prof. Irene Furtado (Sequeira and Furtado, 1992; Fernandes, 1999; Fernandes and Furtado, 2005; Braganca and Furtado, 2009; Velho - Pereira and Furtado, 2014) pertaining to: **I) Production of hydrolytic extremozymes:-** (a) Amylase (b) Lipase and (ii) Aromatic oxygenases; **II) Antagonism:-** (i) Antimicrobial activity (v/s human pathogens) and (ii) Antagonism (halocin production) (v/s haloarchaea); **III) Protogonism** (i) Enhanced growth of human pathogens and (ii) Alleviation of genotoxicity. The chapter also includes taxonomic characterization of GUIF2 and GUIF4 exhibiting multiple bioactivities.

2.1 METHODOLOGY

2.1.1 MICROBIAL CULTURES

2.1.1.1 Extremely halophilic eubacteria and haloarchaeal cultures

A total of 117 cultures from the Haloarchaeal Repository, Department of Microbiology, Goa University were used in the screening for different bioactives. Of these, 101 were isolated from six different solar salts pans (Sequeira, 1992; Fernandes and Furtado, 2005; Braganca and Furtado, 2009), 15 cultures were isolated from sediments of Mandovi estuary (Braganca and Furtado, 2009) and 1 culture (bacterial biont) from the sponge *Fasciospongia cavernosa*, an inhabitant of Mandapam -India (Velho-Pereira and Furtado, 2014). These cultures are listed in **Table 2.1**. These cultures are coded as **GU** - **G**oa **U**niversity; **BF** - **B**raganca and **F**urtado, FLF - **F**ernandes **L**obo and **F**urtado, FF - **F**ernandes and **F**urtado, **IF** - **I**rene **F**urtado, **SF** - **S**equeira and **F**urtado and **VFFM-3** - **V**elho-Pereira **F**urtado ***Fasciospongia cavernosa*** **M**andapam.

2.1.1.2 Human bacterial and fungal pathogens

Human bacterial pathogens such as *S. epidermidis* ATCC 12228, *S. aureus* ATCC 6538P, *B.subtilis* ATCC 6633, *E. coli* ATCC 8739, *S. typhimurium* ATCC 14028, *S. abony* ATCC 6017, *Ps. aeruginosa* ATCC 9027 and the fungal pathogen *C. albicans* ATCC 10231 were used in this study.

2.1.2 MAINTAINANCE AND MEDIA

2.1.2.1 Extremely halophilic eubacteria and haloarchaeal cultures

Extremely halophilic cultures were maintained on 1.5% agar slopes of either NSM (20 % NaCl Synthetic Medium) with 2% glucose (NGSM), pH 7 (Aguiar and Furtado, 1996; Raghavan and Furtado, 2004; ***Appendix I***) or 15% TYE (Tryptone Yeast Extract)/ NTYE (25% NaCI Tryptone Yeast Extract) medium, pH 7.0 (Aguiar and Furtado, 1996; ***Appendix I***) at ambient room temperature (28 ± 2ºC) and regularly subcultured.

2.1.2.2 Human bacterial and fungal pathogens

Human bacterial pathogens were maintained on nutrient agar slopes at 4ºC and regularly subcultured. A loopful was pregrown separately in 5 ml nutrient broth to A_{480} =1 at 480 nm at 37ºC for 24 h before use. The fungal pathogen was maintained on Czapex dox agar slope at 4ºC and regularly subcultured. A loopful was pre grown separately in 5 ml of Czapex dox broth to A_{480} =1 at 37ºC for 24 h before use.

2.1.3 SCREENING FOR DEGRADATIVE EXTREMOZYMES

2.1.3.1 Demonstration of extracellular lipase and amylase in extremely halophilic eubacteria and haloarchaea

The ability to produce amylase and lipase was tested qualitatively among 117 extremely halophilic and haloarchaeal cultures. The screening for amylase and lipase production was carried out using the conventional agar plate technique. Production of amylase and/ or lipase was done on agar with appropriate substrate. Each of the 117 cultures from the NTYE agar slopes were spot inoculated onto NSM containing 0.5% soluble starch/ 0.5% tween 80, using a template (**Fig. 2.1**). The plates were incubated for a week at 37ºC till full growth of colonies was seen. The starch plates with growth were then flooded with Lugol's iodine (LI, ***Appendix I***) prepared in 15% NaCl, and checked for zones of clearing around the colony after draining off the LI. Those cultures surrounded by colourless zones were scored as amylase producers. A positive reaction for the lipolytic enzyme was indicated by the formation of opaque zone around the colony growing on NSM 0.5% tween 80.

2.1.3.2 Prospecting for production of aromatic oxygenases

The ability to degrade sodium benzoate and produce aromatic oxygenases was checked by growing the cultures in sodium benzoate as sole source of carbon. Each of the 117 cultures from NTYE agar slopes were inoculated into 3 ml of NSM containing 0.1% sodium benzoate and incubated at room temperature. Growth was monitored at 600 nm using the UV-Visible spectrophotometer (UV-1601, Shimadzu, Kyoto, Japan) against uninoculated medium as blank.

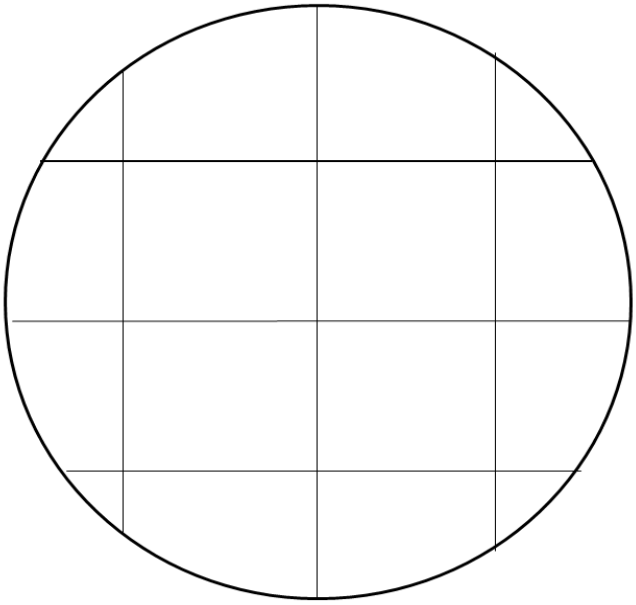

Fig. 2.1 Template used for screening of extremely halophilic and haloarchaeal cultures for production of extremozymes, antimicrobial activity, antagonistic activity (halocin production) and protogonostic activity

2.1.4 SCREENING FOR ANTAGONISTIC ACTIVITY

2.1.4.1 Screening of haloarchaeal cultures for antimicrobial activity against human pathogens

Antibacterial/ antifungal activity was tested by agar well diffusion assay in which 0.1 ml aliquot of individual pathogens pre-grown in Nutrient broth/ Czapex broth were surface plated onto Mueller-Hinton agar, in separate petri plates to obtain lawn growth. After half hour standing, wells were bored into the agar with a sterile 10 mm diameter cork borer and 100 µl of each of the pre-grown haloarchaeal cultures were separately added. Entire experimental set up was carried out aseptically. All plates were incubated at 37ºC and monitored for growth and for zones of inhibition of growth around the well, if any, for a period of 2 d. Zone sizes were calculated as total zone size - diameter of the well bore (5 mm). The experiment was performed three times for each culture and the final values were presented as the mean ± SD. Controls were maintained for each test pathogen.

2.1.4.2 Screening for antagonism (halocin production) among haloarchaeal cultures

Production of antagonism (halocin production) among haloarchaeal cultures was assayed by monitoring inhibition of growth by one haloarchaeon on another using the agar overlay method, wherein each of the cultures was spotted over cultures layered in the solidified medium. Each of the 30 cultures were grown in 25 ml of NGSM + YE, in a 100 ml flask, at 42ºC and shaker conditions (REMI CIS-24 PLUS India) at 150 rpm. 3 ml of each of the culture (A_{600} = 2.0) were mixed with 25 ml of molten NGSM+ YE and plated onto the surface of a 150 mm plate containing the same medium already solidified; this culture was termed as the indicator culture. 20 µl of each of the cultures were spotted onto these plates (termed as producer) using a replica **(Fig. 2.1)**. Inhibitory activity was considered positive in those cultures with clear inhibition zones. The experiment was performed three times for each culture and the final values were presented as the mean ± SD.

2.1.5 SCREENING FOR PROTOGONISTIC ACTIVITY

2.1.5.1 Enhanced growth of human pathogens

Protogonism among haloarchaeal cultures against human bacterial and fungal cultures was tested by agar well diffusion assay in which 0.1 ml aliquot of individual pathogens, pre-grown in nutrient broth/ czapex broth were surface plated onto Mueller-Hinton agar, in separate petri plates to obtain lawn growth. After half hour standing, wells were bored into the agar, with a sterile 5mm diameter cork borer and 100 µl of each of the pre-grown haloarchaeal cultures were separately added. Entire experimental set up was carried out aseptically. All plates were incubated at 37ºC and monitored for growth and for zones of exhibition of growth around the well, if any, for a period of 2 d. Zone sizes were calculated as total zone size - diameter of the well bore (5 mm). Assay was carried out in triplicates and mean was recorded. Controls were maintained for each test pathogen.

2.1.5.2 Alleviation of Arsenic(As)(III) induced genotoxicity

2.1.5.2.1 Preparation of Human lymphocytes (HL)

Human lymphocytes (HL) were obtained from the blood of a 30 years old female (non-smoker) donor with her health status compatible with the WHO guidelines required for a blood donor. Blood collected in a heparinized tube was centrifuged at 3000 rpm for 15 min and the whitish layer of lymphocytes, lying just below the upper plasma layer was collected, washed with equal volumes of 0.85% NH_4Cl (w/v, g 100 ml^{-1}) to remove contaminant RBCs and re suspended in 0.1 M Phosphate Buffer Saline (PBS), pH 7.4, checked for viability by 0.5 % tryptan blue exclusion test (Strober, 2015**)**. HL were adjusted to 10^7 cells ml^{-1} using a haemocytometer and stored at 4°C, till further use.

2.1.5.2.2 Whole cells of *Haloferax alexandrinus* GUSF-1(KF796625) and preparation of methanolic extract (*Hfx*E)

Whole cells of *Haloferax alexandrinus* GUSF-1(KF796625) grown in NTYE medium containing 25% NaCl, 37ºC, pH 7 and at shaker conditions were harvested on the sixth day, at 10000 rpm, 4ºC for 10 min in high speed centrifuge (Eppendorf centrifuge 5804 R). Cells were washed with 15% NaCl and treated with methanol, at 4 ºC in the dark, overnight. The methanolic extract recovered by centrifuging (Eppendorf centrifuge 5804 R) at 10000 rpm, for 10 min, termed as '*Hfx*E', was concentrated to dryness under vacuum using rotary evaporator (Buchi Rotavapor, R-201) and re - dissolved in methanol to give a concentration of 1 mg ml^{-1}.

2.1.5.2.3 Selenium nanoparticles (SeNPs)

SeNPs used in this study for evaluation of its antigenotoxicity, have been biosynthesized by the same culture, *Haloferax alexandrinus* GUSF-1 (KF796625), the characterization of the same SeNPs is described in the following **Chapter V**.

2.1.5.2.4 As(III) genotoxicity assay and antigenotoxicity with *Hfx*E and SeNPs

Aliquots of 20 µl of HL were added to six sets of three wells each of a 96 well micro titre plate. In the first set of wells, lymphocytes suspended in PBS pH 7.4 were mixed

with 10 µM of As(III). The second and third set up consisted of lymphocytes mixed with 10 µM of As(III) and 25/50 µg ml^{-1} of *Hfx*E. The fourth set consisted of lymphocytes mixed with 10 µM of As(III) and 50 µg ml^{-1} SeNPs. Untreated lymphocytes and lymphocytes with methanol serving as negative control made up the fifth and sixth set. The total volume of each of the wells was made to 100 µl with 0.1 M PBS pH 7.4. Thereafter, the plate was incubated at 37ºC for 2 h.

2.1.5.2.5 Assessment of As(III) genotoxicity in HL and antigenotoxicity of *Hfx*E and SeNPs by comet assay

All the steps were carried out in dim light to prevent photo degradation of DNA. The procedure of Dhawan *et al*. (2001) was followed**.** Freshly prepared 400 µl of 1% normal melting point agarose (NMPA, w/v, g 100 ml^{-1}; ***Appendix I***), in 0.1 M PBS, pH 7.4, and poured on a fully frosted glass slides and covered with a cover slip and allowed to stand at room temperature (RT). After removing the coverslip 80 µl of 0.5% low melting point agarose (LMPA, w/v, g 100 ml^{-1}; ***Appendix I***) in 0.1 M PBS, pH 7.4 and 20 µl of either i) HL; ii) HL exposed to methanol; iii) HL exposed to As(III); iv) HL exposed to As(III) and 25 ml^{-1} µg of *Hfx*E v) HL exposed to As(III) and 50 µg ml^{-1} of *Hfx*E vi) HL exposed to As(III) and 50 µg ml^{-1} SeNPs were individually mixed and layered over separate NMPA slides. A third layer of 100 µl LMPA was then added over the second layer and on solidifying was covered with a coverslip. The slides were then placed in freshly prepared, cold lysis solution (pH 10, ***Appendix I*)**, in a petri dish at 4°C for 16 h. Each slide was immersed in a horizontal electrophoresis tank containing buffer (pH 13.5**;** ***Appendix I***) and allowed to stand for 20 min at RT to allow unwinding of DNA. Electrophoresis was run at 18 V and 300 mA for 30 min. Each slide was placed in chilled neutralization buffer (pH 7.5; *Appendix I*) for 10 min, rinsed with distilled water and stained with 80 µl of 15 µg ml^{-1} ethidium bromide (***Appendix I***). A cover slip was placed over the gel on diffusion of ethidium bromide and viewed using a fluorescence microscope (BX53 Olympus fluorescence microscope - Japan) at 200X magnification and a green filter. Images of individual slides were captured using ProgRes®Capture Pro 2.7. Each of the captured image was analyzed using CASP image analysis software for DNA content in terms of its percentage damage (Konca *et al*., 2003). All the experiments were carried out in triplicates. Using IBM-SPSS 23 software a one-way analysis of variance (ANOVA)

was performed to assess the overall variation in DNA damage between HL exposed to 10 µm As(III) only and 10 µm As(III) plus *Hfx*E at 25 µg ml^{-1} and 50 µg ml^{-1} concentrations. Further the inter-individual differences of DNA damage between each of the concentrations of *Hfx*E and HL exposed to 10 µm As(III) was compared using Dunnett's multiple comparison post hoc test. A level of probability of $p < 0.05$ was considered statistically significant data. A students *t* test was also used to assess differences in % mean tail DNA between each of the concentrations of *Hfx*E and SeNPs.

2.1.6 STATISTICAL ANALYSIS

All experiments were carried out in triplicates and results averaged. The experimental data was analyzed using IBM-SPSS 23 statistical software. Analysis of variance and significant differences between means of different cultures were performed with one-way analysis of variance (ANOVA).

2.1.7 QUANTIFICATION OF BIOACTIVITY

Quantification of individual bioactivity was assessed using the earlier reported quantification procedures (Velho-Pereira and Furtado, 2012) to obtain:

2.1.7.1 Percent Overall Screening Efficiency Score (POSES)

POSES was calculated =

$$\frac{\text{TPA (total number of producers of amylase/ lipase/ aromatic oxygenase/ Antagonistic/ protogonistic activity)}}{\text{TS (Total number of cultures)}} \times 100$$

2.1.7.2 Percent Overall Inhibition Efficiency Score (POIES)

$$\text{POIES was calculated} = \frac{\text{TNIS (total number of pathogens)}}{\text{TNTS (total number of pathogens used in the study)}} \times 100$$

2.1.8 TAXONOMIC IDENTIFICATION OF GUIF2 AND GUIF4

The culture GUIF2 was seen to show maximum growth in the presence of sodium benzoate hence it was selected as a promising culture for production of aromatic

oxygenase enzyme. The culture GUIF4 was seen to show maximum zone or precipitation when grown on mineral medium and tween 80; hence we envisaged it to be a potential producer for lipase production.

2.1.8.1 Morphological Characterization

2.1.8.1.1 Gram staining

GUIF2 and GUIF4 was gram stained using modified gram staining method for halophiles (Dussault, 1955). A single colony of GUIF2 and GUIF4 was picked from a NTYE plate and a suspension was made in sterile NSM. A smear was prepared from the suspension, air-dried and fixed with 2% acetic acid for 3 min. The slide was then flooded with 2% aqueous crystal violet and allowed to stain for 1 min followed by 1 % Gram's iodine solution for 1 min. Excess stain was discarded and then decolourized with 70% ethanol. The slide was then treated with 0.5% safranine for 2 min washed, air dried and observed under oil immersion objective of 100x and total magnification of 1000, using a phase contrast microscope (Olympus model BX 40).

2.1.8.1.2 Scanning Electron Microscopy

Cells of GUIF2 and GUIF4 were harvested during the stationary phase on day 6 (10000 rpm, 10 min, 4ºC), washed with 15% NaCl and then fixed with (2% v/v) gluteraldehyde prepared in 15% NaCl for 24 h. The cells were dehydrated for 30 mins each with different concentrations of acetone; 30, 50, 70, 90 and 100%. The coverslips were then coated and mounted on to gold stubs and observed under scanning electron microscope coupled with energy dispersive X-ray spectrometer (SEM-EDX) (JEOL JSM-5800LV).

2.1.8.2 Chemotaxonomic characterization

2.1.8.2.1 Glycerol diether moieties (GDEM)

A simple method of distinguishing archaebacterial halophilic taxa from eubacterial halophilic taxa, using TLC patterns of glycerol diether moieties (GDEM) from whole organism methanolysates, was followed to establish the haloarchaeal nature of the isolates (Ross *et al*., 1965**)**. GUIF2 and GUIF4 were grown in NTYE medium at 37 ºC. Cultures were harvested by centrifugation (10000 rpm) after 5 d of growth.

Wet cells (100 mg) were mixed with methanol (3 ml), toluene (3 ml) and conc. H_2SO_4 (0.1 ml) and heated at 50°C for 18 h. The long-chain components were extracted from this mixture by adding 1.5 ml hexane. Hexane extracts were spotted on to TLC silica gel GF254 plate (Merck, Darmstadt, Germany). The chromatograms were resolved using solvent system consisting of petroleum ether (60-80°C): diethyl ether (85:15, v/v). GDEM were revealed by drying the TLC plates after spraying with 10% dodecaphosphomolybdic acid in absolute ethanol and heating for 15 min at 150°C. A positive control was also maintained. The spots at R_f 0.2 of GUIF2 and GUIF4 were scrapped from the TLC plate and hexane was added to the silica gel with the hydrolysis product. The FT- IR spectrum of the spot at R_f 0.2 obtained by preparative TLC was recorded on a Fourier Transform IR spectrometer (FT-IR) (Shimadzu IR Prestige-21). The sample was ground with IR grade KBr to form a pellet and analyzed in the 4000 to 400 cm^{-1} spectral region at a resolution of 4.0 cm^{-1}.

2.1.8.2.2 Response to antibiotics

The cultures were studied for its resistance/ sensitivity to 700 U of penicillin. The culture was spread plated on NTYE agar plates and the disc loaded with penicillin was placed aseptically on the plate. The plate was incubated at 37°C and growth monitored visually.

2.1.8.2.3 Tolerance to bile salts

Bile salt such as difco's bacto peptone has been known to cause lysis of halobacteria due to presence of high concentration of taurine conjugates of cholic acid. A loopful of GUIF2 and GUIF4 was spot inoculated onto 25% MacConkeys agar and incubated at 37°C for a week. Absence of growth indicated lysis of the cells and hence sensitivity to bile salts.

2.1.8.2.4 Pigment characteristics

Cells of GUIF2 and GUIF4 growing in NTYE were harvested by centrifuging at 10000 rpm using a cooling centrifuge (REMI, India), at 4°C, for 20 min. Pellet was washed twice with 15% NaC1 and acetone was added to the pellet, vortexed and the coloured supernatant separated from the cell debris. The acetone fraction containing

the pigments was scanned between 300 nm and 600 nm using a UV-Visible spectrophotometer (UV-1601, Shimadzu, Kyoto, Japan) (Raghavan and Furtado, 2005).

2.1.8.3 Biochemical characterization

Tentative identification of the cultures, GUIF2 and GUIF4 was done based on biochemical characteristics following Bergey's Manual of Systematic Bacteriology Volume I (2nd edition), The Prokaryotes: Volume IV (2nd edition) (Tindall, 1992) and (Hezayen *et al*., 2001) up to genus level.

2.1.8.4 Molecular characterization

2.1.8.4.1 PCR amplification of genomic DNA

A single colony each of GUIF2 and GUIF4 of was grown in NTYE medium for 6 d and cells were harvested by centrifuging at 10000 rpm at 4ºC for 10 min. Genomic DNA was extracted by suspending the cell pellet in distilled water and boiling at 60ºC for 10 min, 60ºC, followed by centrifugation. Genomic DNA was amplified using archaeal primers A109(F) AC(G/T)GCTCAGTAACACGT and 1510(R) GGTTACCTTGTTACGACTT. PCR was performed using a 100 µl microfuge tube. Each of the PCR reaction contained mixtures containing 10X *Taq* buffer, 2 mM $MgCl_2$, 10 mM of dNTPs (Sigma, India), 10 µM of each primer (IDT technologies, Singapore), 2 U *Taq* Polymerase and 10 ng template DNA. Final volume was made up to 50 µl with ultrapure distilled water. The PCR was performed in a thermal cycler (Applied Biosystems, USA) using following conditions: Initial denaturation at 94 °C for 5 min, followed by 30 cycles of denaturation at 94°C for 30 sec, annealing at 53.5°C for 30 sec and strand extension at 68°C for 1 min and final extension at 68°C for 10 min. The PCR products were verified on a 1% agarose gel through submerged DNA electrophoresis and was visualised over a UV illuminator (Bio-Rad, USA) after staining with ethidium bromide. Intact amplified PCR products were eluted from the gel and purified with gel elution kit (Chromous Biotech Pvt. Ltd.,India), according to manufacturer's instruction (Salgaonkar and Braganca, 2015b).

2.1.8.4.2 DNA sequencing

The 16S rDNA amplicon corresponding to 1.4 kb was bidirectionally sequenced using the Big Dye terminator sequence method (BigDye® Terminator v3.1 Cycle Sequencing Kit, Applied Biosystems) in India. The reactions were analyzed through automated DNA sequencer (Applied Biosystems) and electrograms were reported in Chromas – pro version 2.6.4. The sequences obtained were manually curated to remove flashing sequences.

2.1.8.4.3 Phylogenetic analysis of 16S rRNA gene sequence

The phylogenetic position of both the cultures was determined based on the 16S rRNA gene sequence obtained. The sequences were subjected to homology search with the available nucleotide database in National Center for Biotechnology Information (NCBI, Bethesda, MD, USA) BLAST (Basic Local Alignment Search Tool) search program (Altschul *et al*., 1997), inorder to identify the closest homologues for the 16S rRNA gene sequence of GUIF2 and GUIF4 and also submitted to the NCBI GenBank using SEQUIN program at the NCBI site (www.ncbi.nlm.nih.gov) to obtain an accession number for the sequences. The sequences of identified phylogenetic neighbours were retrieved from the NCBI GenBank database and aligned with the sequences of the cultures using Multiple sequence alignment feature of MEGA version 7.0 Clustal W analysis. The phylogenetic tree was reconstructed with Neighbour-Joining (NJ) (Saitou and Nei, 1987) algorithm using MEGA v7.0 (Tamura *et al*., 2011). The evolutionary distances were computed using the Tamura 3- parameter method (Tamura, 1992). Percentage support values were obtained using a bootstrap procedure with 1000 resampling (Felsenstein, 1985).

2.1.9 DIVERSITY STUDIES

The generic level occurrence and diversity of the extremely halophilic eubacteria and haloarchaea associated with solar salt sample/ estuarine sediment / sponge sample and which were positive for production of extremozymes, was calculated as:

Shannon-Weiner's diversity index 'H' (Shannon and Weaver, 1949)

The generic diversity in community was carried out by Shannon-Weiner's diversity index H' by using the generalization:

$H' = \Sigma [(n/N)\ln(n/N)]$;

Where n=number of individual isolates; N= total number of all cultures.

2.1.10 GROWTH STUDIES OF GUIF2 IN HYDROCARBONS

2.1.10.1 Effect of benzene, petrol, engine oil (Castrol) and insecticide (Lindane) on growth and pigmentation of GUIF2

5% of GUIF2 (A_{600} = 1) grown in NTYE was centrifuged and wet pellet was inoculated into NTYE and NSM containing 0.1% of benzene/ commercial insecticide as sole source of carbon. The flasks were incubated at 37^{o}C for 15 d at 150 rpm. Growth was monitored by taking out aliquot of culture broth and measuring the absorbance at A_{600} nm against uninnoculated medium using UV-Visible spectrophotometer (UV-1601, Shimadzu, Kyoto, Japan). Appropriate negative controls of medium with benzene/ commercial insecticides were maintained. Growth of culture in NTYE and NSM with 0.1% glucose was also monitored. The experiment was performed in triplicates and results averaged. Development of pigmentation of GUIF2 was also monitored. Pigment was extracted from wet cells with acetone and scanned against acetone as detailed in **2.1.8.2.4.**

2.1.10.2 Growth and pigmentation of GUIF2 in sodium benzoate

GUVFFM-3, GUSF-1 and GUIF2 were inoculated to a final concentration of into NSM/ with 0.1% sodium benzoate (SBNSM). The flasks were incubated at 37^{o}C, at 150 rpm and monitored for growth at A_{600} nm over a period of 15 d against uninoculated medium using the UV-Vis spectrophotometer (UV-1601, Shimadzu, Kyoto, Japan). Pigment was extracted from wet cells with acetone and scanned against acetone as detailed in **2.1.8.2.4**.

2.1.10.3 Degradation of sodium benzoate by GUIF2

2.1.10.3.1 Preparation of cell lysate/ crude enzyme

GUIF2 was grown in NSM with 0.1% sodium benzoate. The cells were harvested by centrifugation at 10000 rpm, 4^{o}C and for 10 min. The clear supernatant obtained after centrifugation was used for detection of catechol. The cells were washed thrice using 15% NaCl and centrifuged after each washing under the same conditions. Crude enzyme was prepared by suspending the cells in sterile distilled water and sonicating the cells which were maintained on ice. The suspensions were centrifuged at 10000 for 10 min at 4°C and the cell lysate was used to evaluate Rothera's test for cleavage of the aromatic ring and for the enzyme assay. Total protein content of the crude extract was determined by Folin Lowry Method using Bovine serum albumin (BSA) as a standard solution (Lowry, 1951) ***(Appendix II)***.

2.1.10.3.2 Detection of catechol by Arnows test

Detection of catechol was done using the method of Arnow (Arnow, 1937). A set of two tubes was used for the tests, 1 tube had 1 ml of culture supernatant and the other tube had l ml of NSM with 0.1% sodium benzoate medium which served as blank control. To each of these tubes, l ml of 0.5 M HC1 was added and thoroughly shaken; to this, l ml of nitrite molybdate reagent (***Appendix I***) was added. Finally, l ml of 1 M NaOH was added to the above and mixed well, development of a pink colour denoted the presence of catechol which was spectrophotometrically read at 505 nm. A standard curve was prepared from a stock solution of 1 g ml $^{-1}$ of catechol (***Appendix II***).

2.1.0.3.3 Rotheras test for cleavage

The presence of ring cleavage dioxygenase activity was identified visually in crude enzyme by Rothera reactions (Ottow and Zolg, 1974). For this reaction, 2 ml of crude enzyme was incubated with 2.5 ml of 4 mM catechol as substrate. Appropriate control tube with distilled water was maintained. The tubes were shaken for about 30 sec and kept standing at RT (28 ± 2ºC) for 10 min. The tubes were checked for a green-yellow color developing within 3 min which would indicate a positive meta-cleavage (muconic acid semi-aldehyde; the extradiol cleavage product). The tubes were further

incubated for 18 h at 28°C. 1 g of ammonium sulphate, five drops of a freshly prepared aqueous 1% sodium nitroprusside solution, as well as 0.5 ml of concentrated ammonia was added. Development of a deep purple color within 3 min, determined visually is indicative of an ortho-cleavage of the substrate (in this case, catechol).

2.1.10.3.4 Enzyme assay for Catechol 1, 2-dioxygenase enzyme

The enzyme assay for detection of catechol 1, 2-dioxygenase activity was carried out according to Garcia *et al*. (2005). The reaction mixtures for the enzyme assay of catechol 1, 2-dioxygenase contained 1 ml of 0.8 mM catechol, 0.8 ml of 50 mM Tris-HCl buffer (pH 8.0), 0.2 ml of 0.1 mM 2-mercaptoetanol and 1 ml of crude enzyme. After the addition of the crude enzyme, the reaction mixture was incubated at 30°C in a water-bath. At specified time intervals, aliquots were used to monitored increase in absorbance at 260 nm, corresponding to the formation of *cis, cis* - muconic acid, using UV-Vis spectrophotometer (UV–1601, Shimadzu, Kyoto, Japan). The enzyme assay was carried out in triplicates. Extinction coefficient of the oxidation product of catechol was determined as $€_{260\ nm}$ = 16800/ mol cm. One unit of enzyme activity is defined as the amount of enzymes required to generate µmol of cis cis muconic acid produced per min at 30°C.

2.1 RESULTS

All the observations and results using marine extremely halophilic eubacterial and haloarchaeal cultures which are listed in **Table 2.1** are compiled and presented **under three main sections namely,**

SECTION A: Bioprospecting for production of extremozymes in extremely halophilic eubacteria and haloarchaea
A: Amylase; **B:** Lipase and **C:** Aromatic oxygenase

SECTION B: Bioprospecting for production of antagonism among haloarchaea
A: Antimicrobial activity v/s human pathogens; **B:** Antagonism (halocin production) v/s haloarchaea

SECTION C: Bioprospecting for production of protogonism

A: Enhanced growth of human pathogens; **B:** Alleviation of genotoxicity

Table 2.1 Identity of marine extremely halophilic eubacterial and haloarchaeal cultures used in this study

	Sampling site	Culture designation	Identity
Solar salt	**Arambol (A)**	$GUFF_{9}$	*Halobacterium* sp.
		$GUFF_{41}$	*Haloferax* sp
		$GUFF_{42}$	*Haloferax sp*
		$GUFF_{43}$	*Haloferax sp*
		$GUFF_{44}$	*Haloferax sp*
		$GUFF_{54}$	*Halococcus* sp
		$GUFF_{55}$	*Halobacterium* sp
		$GUFF_{95}$	*Gluconobacter* sp
		$GUFF_{96}$	*Natrialba* sp.
		$GUFF_{180}$	*Halococcus* sp.
	Agarwada (Ag)	$GUFF_{20}$	*Haloferax* sp.
		$GUFF_{34}$	*Haloarcula* sp.
		$GUFF_{35}$	*Halobacterium* sp.
		$GUFF_{37}$	*Natrialba* sp.
		$GUFF_{38}$	*Haloferax* sp.
		$GUFF_{39}$	*Halococcus* sp.
		$GUFF_{58}$	*Halococcus* sp.
		$GUFF_{59}$	*Halococcus* sp.
		$GUFF_{88}$	*Halobacterium* sp.
		$GUFF_{90}$	*Halorubrum* sp.
		$GUFF_{146}$	*Alteromonas* sp.
		$GUFF_{148}$	*Halobacterium* sp.
		$GUFF_{186}$	*Haloarcula* sp.
		$GUFF_{187}$	*Haloarcula* sp.
		$GUFF_{188}$	*Haloarcula* sp.
		$GUFF_{189}$	*Haloarcula* sp.
	Arpora (Ar)	$GUFF_{19}$	*Halobacterium* sp.
		$GUFF_{22}$	*Haloferax* sp
		$GUFF_{25}$	*Natrialba* sp.
		$GUFF_{26}$	*Halococcus* sp.
		$GUFF_{51}$	*Halococcus* sp.
		$GUFF_{53}$	*Halococcus* sp
		$GUFF_{98}$	*Halococcus* sp.
		$GUFF_{99}$	*Halococcus* sp.
		$GUFF_{102}$	*Halococcus* sp.
		$GUFF_{137}$	*Haloarcula* sp.
		$GUFF_{179}$	*Halococcus* sp.
		$GUFF_{199}$	*Haloarcula* sp.
		$GUFF_{201}$	*Halococcus* sp.
		$GUFF_{205}$	*Halococcus* sp.

	Sampling site	Culture designation	Identity
Solar salt	**Nerul (N)**	$GUFF_{28}$	*Halococcus* sp.
		$GUFF_{33}$	*Natrinema* sp.
		$GUFF_{56}$	*Halococcus* sp.
		$GUFF_{69}$	*Halococcus* sp.
		$GUFF_{82}$	*Natrinema* sp.
		$GUFF_{83}$	*Gluconobacter* sp.
		$GUFF_{84}$	*Gluconobacter* sp.
		$GUFF_{116}$	*Halococcus* sp.
		$GUFF_{117}$	*Halococcus* sp.
		$GUFF_{141}$	*Alteromonas* sp.
		$GUFF_{145}$	*Alteromonas* sp.
		$GUFF_{182}$	*Halococcus* sp.
		$GUFF_{185}$	*Haloarcula* sp.
		$GUFF_{202}$	*Halococcus* sp.
	Ribandar (R)	$GUBF_{1}$	*Haloferax* sp.
		$GUBF_{2}$	*Haloferax* ATCC BAA 645
		$GUBF_{3}$	*Haloferax* ATCC BAA 646
		$GUBF_{7}$	*Haloarcula* sp.
		$GUBF_{19}$	*Halobacterium* sp.
		$GUBF_{20}$	*Halobacterium* sp.
		$GUFF_{2}$	*Halococcus* sp
		$GUFF_{3}$	*Haloarcula* sp
		$GUFF_{45}$	*Halococcus* sp.
		$GUFF_{46}$	*Halococcus* sp.
		$GUFF_{47}$	*Halococcus* sp.
		$GUFF_{60}$	*Halobacterium* sp.
		$GUFF_{61}$	*Halobacterium* sp.
		$GUFF_{70}$	*Halococcus* sp.
		$GUFF_{72}$	*Halorubrum* sp.
		$GUFF_{120}$	*Halococcus* sp.
		$GUFF_{168}$	*Halococcus* sp.
		$GUFF_{170}$	*Halococcus* sp.
		$GUFF_{172}$	*Halococcus* sp.
		$GUFF_{204}$	*Halococcus* sp.
	Siridao (S)	$GUBF_{18}$	*Halobacterium* sp.
		$GUFF_{6}$	*Halococcus* sp.
		$GUFF_{10}$	*Haloferax* sp.
		$GUFF_{12}$	*Natrialba* sp.
		$GUFF_{14}$	*Halococcus* sp.
		$GUFF_{16}$	*Haloarcula* sp.
		$GUFF_{24}$	*Haloferax* sp.
		$GUFF_{36}$	*Haloarcula* sp.
		$GUFF_{49}$	*Halococcus* sp.
		$GUFF_{50}$	*Halococcus* sp.
		$GUFF_{63}$	*Halococcus* sp.
		$GUFF_{64}$	*Halococcus* sp.
		$GUFF_{65}$	*Halococcus* sp.
		$GUFF_{66}$	*Halococcus* sp.

	Sampling Site	Culture Designation	Identity
Solar salt	**Siridao (S)**	$GUFF_{76}$	*Gluconobacter* sp.
		$GUFF_{113}$	*Halococcus* sp.
		$GUFF_{198}$	*Halococcus* sp.
		$GUFF_{209}$	*Halococcus* sp.
		$GUFF_{225}$	*Natrialba* sp.
		$GUFF_{226}$	*Natrialba* sp.
		$GUFF_{229}$	*Natronomonas* sp.
		$GUFF_{227}$	*Haloferax* sp.
		$GUFF_{230}$	*Natronocccus* sp.
		$GUFF_{231}$	*Natrialba* sp.
		$GUFF_{233}$	*Natronocccus* sp.
		GUSF	*Halobacterium* strain R_1
		GUSF-1	*Haloferax alexandrinus* (KF796625)
Estuarine Sediment	**Baiguinim (B)**	$GUBF_9$	*Haloarcula* ATCC BAA 652
	Betim Jetty (BJ)	$GUBF_{10}$	*Halobacterium* ATCC BAA 653
		$GUFLF_3$	*Haloferax* sp.
		$GUFLF_8$	*Haloferax* sp.
		$GUFLF_{14}$	*Haloferax* sp.
		$GUFLF_{16}$	*Haloferax* sp.
		$GUFLF_{18}$	*Haloterrigena* sp.
		GUIF2	Unidentified Haloarchaea
		GUIF3	*Haloferax* sp.
		GUIF4	Unidentified Haloarchaea
		GUIF5	*Halobacterium* sp.
	Captain of Ports (CP)	$GUBF_{15}$	*Haloarcula* sp.
	Dona Paula (DP)	$GUBF_{12}$	*Halobacterium* ATCC BAA 655
	Panjim Jetty (PJ)	$GUBF_5$	*Halobacterium* ATCC BAA 647
	Ribandar Patto (RP)	$GUBF_{11}$	*Halobacterium* ATCC BAA 654
Sponge	***Fasciospongia cavernosa* (FC)**; an inhabitant of Mandapam –India	GUVFFM-3	*Chromohalobacter salexegines* (JF330126)

SECTION A

BIOPROSPECTING FOR PRODUCTION OF EXTREMOZYMES IN EXTREMELY HALOPHILIC EUBACTERIA AND HALOARCHAEA

2.2.1 AMYLASE PRODUCTION

2.2.1.1 Production of extracellular amylase among extremely halophilic eubacteria and haloarchaea

Of the 117 cultures screened for their ability to degrade starch, 33 cultures (28%) produced extracellular amylase with clear zones around colonies after flooding with LI (**Fig. 2.2)**.

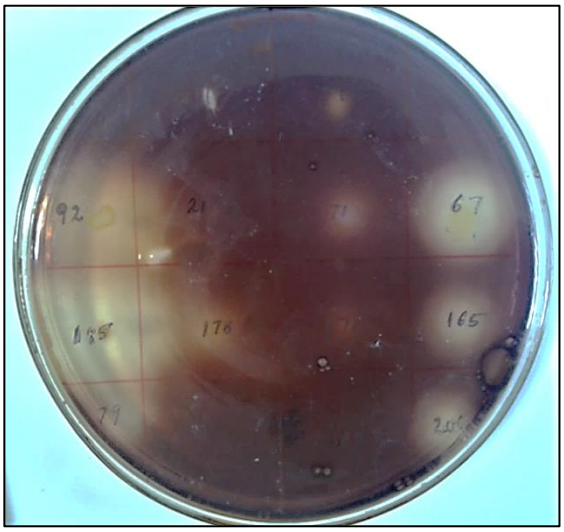

Fig. 2.2 Growth on 20% NSM agar with 0.5% starch and subsequent flooding with LI reveal amylase producing cultures with clear zones around it against a blue stained background

As recorded in **Fig. 2.3**, the zone size ranged from a minimum of 5 ± 0.22/ 0.14 exhibited by $GUFF_{34}$ and $GUBF_{10}$ to a maximum of 24 ± 0.21/0.09 exhibited by the euryhaline biont GUVFFM-3. The zone sizes which were ≤ 10 mm were shown by $GUBF_{1}$, $GUBF_{10}$, $GUBF_{18}$, $GUFF_{2}$, $GUFF_{34}$, $GUFF_{72}$ $GUFF_{88}$, $GUFF_{90}$ and

$GUFF_{141}$. The zone sizes which were ≤ 20 mm were shown by $GUBF_2$, $GUBF_3$, $GUBF_5$, $GUBF_7$, $GUBF_9$, $GUBF_{11}$, $GUBF_{12}$, $GUBF_{15}$, $GUBF_{19}$, $GUBF_{20}$, GUSF, $GUFF_2$, $GUFF_{45}$, $GUFF_{50}$, $GUFF_{117}$, GUFLF3, $GUFLF_{14}$, $GUFLF_{16}$, $GUFLF_{18}$, GUIF3, GUIF5, $GUFF_{113}$ and $GUFF_{137}$ showed zone sizes 21 and 22 mm respectively.

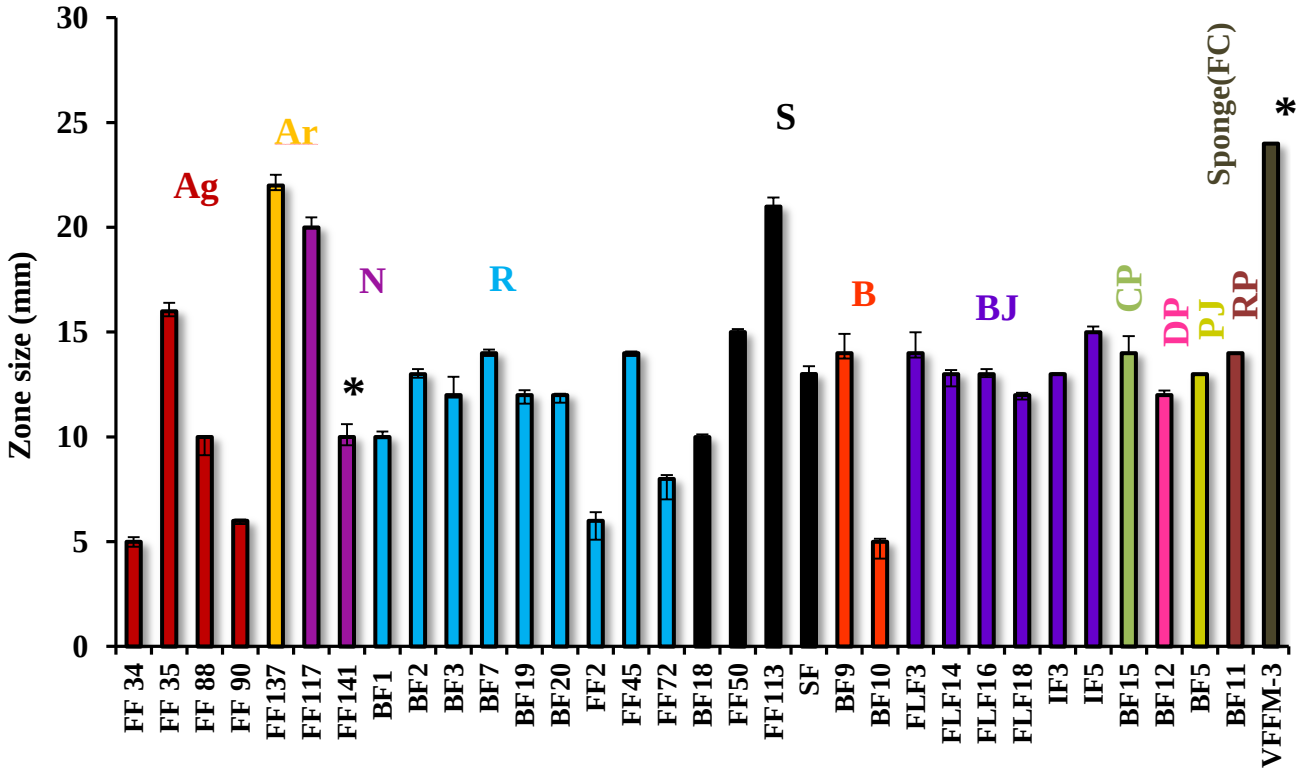

Fig. 2.3: Amylase production among extremely halophilic eubacteria and haloarchaeal cultures from different solar salts, estuarine sediments and sponge. Cultures are coded as **GU-Goa University; BF** (**B**raganca and **F**urtado**); FLF** (**F**ernandes **L**obo and **F**urtado)**; FF** (**F**ernandes and **F**urtado)**; IF** (**I**rene **F**urtado)**; SF** (**S**equeira and **F**urtado) and **VFFM** (**V**elho **F**urtado *Fasciospongia cavernosa* **M**andapam), but for convenience, the code of the culture in the figure is written only as BF, FLF, FF, IF SF and VFFM. The cultures marked with an asterix* are eubacteria, the rest of the cultures are haloarchaea.

The percent overall screening efficiency score for amylase production exhibited by cultures and computed by scoring amylase producers and no producers score against the total cultures screened from different solar salts, estuarine sediments and sponge is depicted in **Fig. 2.4.** The highest activity score of 100% was obtained for the cultures from the estuarine sediments of Baigiunim, Captain of Ports, Dona Paula, Panjim Jetty, Ribandar Jetty and the sponge, while, the lowest score of 7% was obtained for cultures from solar salts of Arpora. Cultures from the solar salts of Nerul, Siridao, Agarwada and Ribandar gave an equal score of 14%, 15%, 25% and 45% respectively.

A highly significant variation ($F = 28.429$; $p<0.001$) of zone sizes was observed within cultures positive for extracellular production of amylase from different sampling sites as per the one-way ANOVA obtained using the IBM SPSS software.

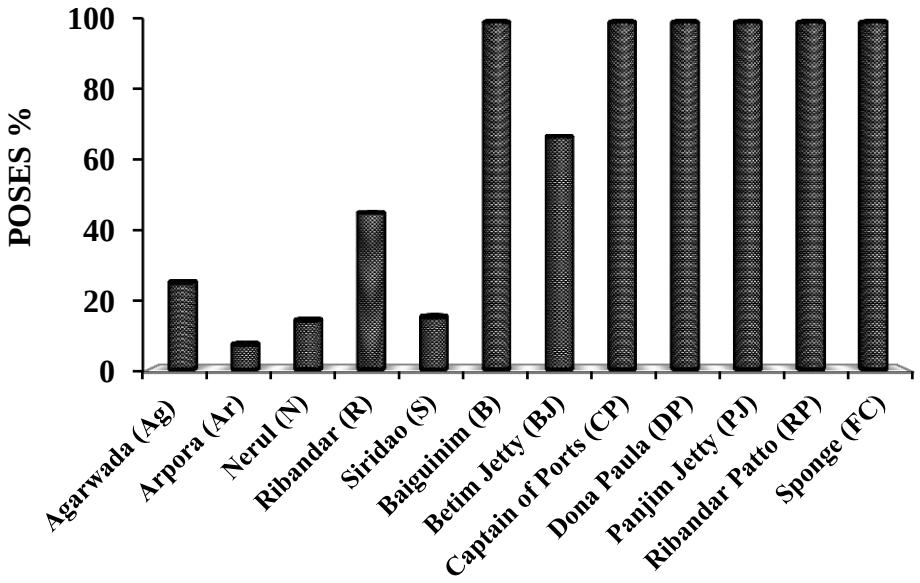

Fig. 2.4 Percent overall screening efficiency score (POSES %) for amylase production among extremely halophilic eubacteria and haloarchaeal cultures from different solar salts, estuarine sediments and sponge

2.2.1.2 Diversity of amylase producing extremely halophilic eubacterial and haloarchaeal genera from solar salts, estuarine sediments and from sponge

The eubacterial genera present were *Alteromonas* and *Chromohalobacter* while the haloarchaeal amylase producing genera present were *Halobacterium*, *Haloarcula*, *Halorubrum*, *Halococcus* and *Haloferax* **(Fig. 2.5)**. The ocurrence of amylase producing members was in the order, *Halobacterium* > *Haloferax* > *Haloarcula* = *Halococcus* > *Halorubrum* > *Alteronomonas* = *Chromohalobacter*.

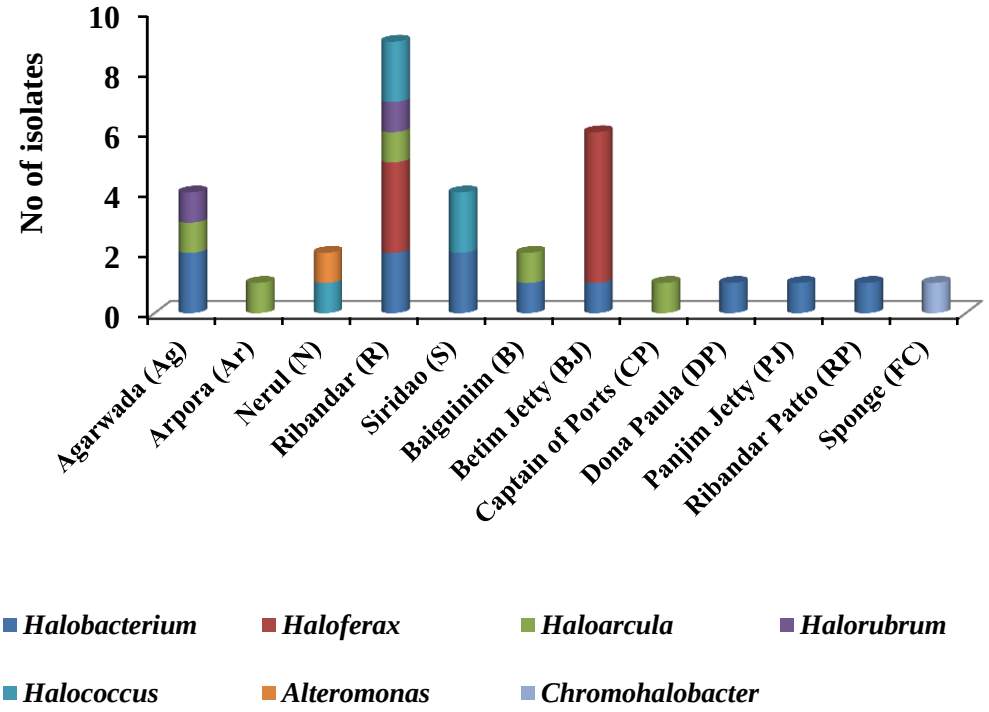

Fig. 2.5 Amylase producing extremely halophilic eubacterial and haloarchaeal genera present in different solar salts, estuarine sediments and sponge

The Shannon-Wei**n**er Diversity Index 'H' calculated for amylase producers was 1.71, 0.98, 0.67, 0.53, 0.51 for Ribandar, Agarwada, Siridao, Baiguinuim and Betim Jetty respectively. An index for of 0.21 was obtained for Arpora, Nerul and Captain of Ports while a value of 0.32 was calculated for Dona Paula, Panjim Jetty and Ribandar Patto **(Fig. 2.6)**.

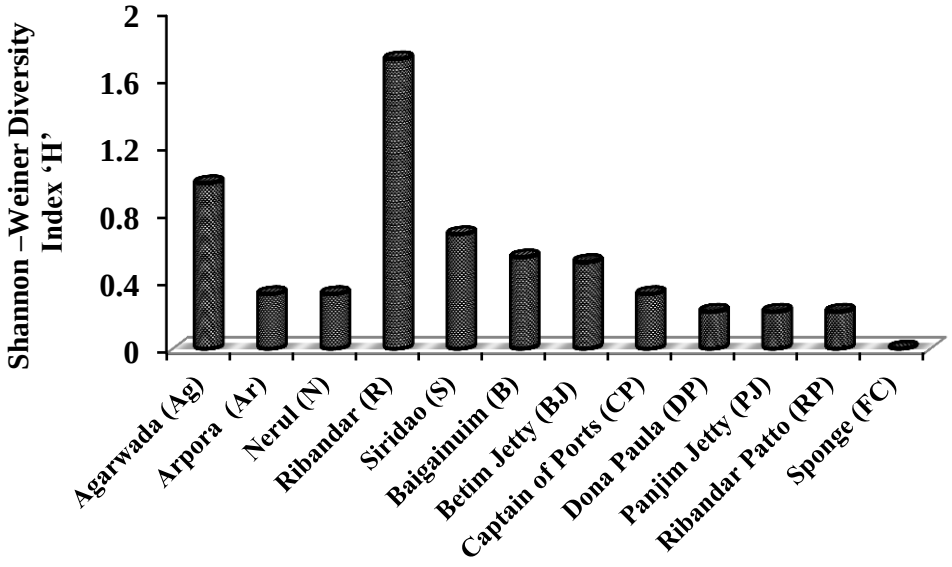

Fig. 2.6 Shannon-Weiner Diversity Index "H" of amylase producing extremely halophilic eubacterial and haloarchaeal genera in different solar salts, estuarine sediments and sponge

2.2.2 LIPASE PRODUCTION

2.2.2.1 Production of extracellular lipase among extremely halophilic eubacteria and haloarchaea

The presence of lipolytic enzymes was demonstrated by the formation of conspicuous halos **(Fig. 2.7)**. From a total of 117 cultures, 33(28%) were positive for Lipase production.

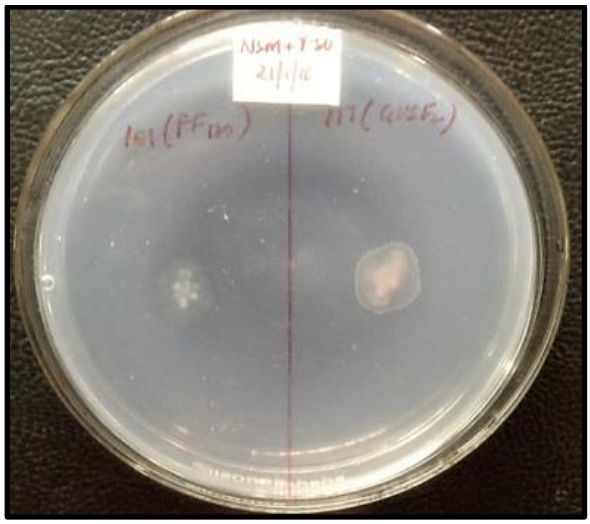

Fig. 2.7 Growth of cultures on 20% NSM agar with 0.1% tween 80 showing zones of precipitation around the colony which is an indicator of lipase production

As recorded in **Fig. 2.8**, the degree of the zone of precipitation around growth varied in cultures from different solar salts, estuarine sediments and sponge. The zone size ranged from a minimum of 5 ± 0.24/0.1 85/ 0.156/0.24 exhibited by the cultures $GUFF_{47/65/66}$ and GUSF-1, to a maximum of 15 ± 0.08 exhibited by GUIF4. The zone sizes which were ≤ 10 mm were shown by $GUBF_5$, $GUBF_7$ $GUBF_{12}$, $GUBF_{18}$, GUIF2, $GUFF_{12,}$ $GUFF_{34}$, $GUFF_{35}$, $GUFF_{54}$, $GUFF_{53}$, $GUFF_{72}$, $GUFF_{113}$, $GUFF_{137}$, $GUFF_{141}$, $GUFF_{145}$, $GUFF_{146}$, $GUFF_{180}$, $GUFF_{201}$, $GUFF_{205}$, $GUFF_{229}$, $GUFF_{231}$ and GUSF. The zone sizes which were ≤ 20 mm were shown by $GUFF_{16,}$ $GUFF_{41,}$ $GUFF_{44}$, $GUFF_{226}$, GUIF4 and GUIF5.

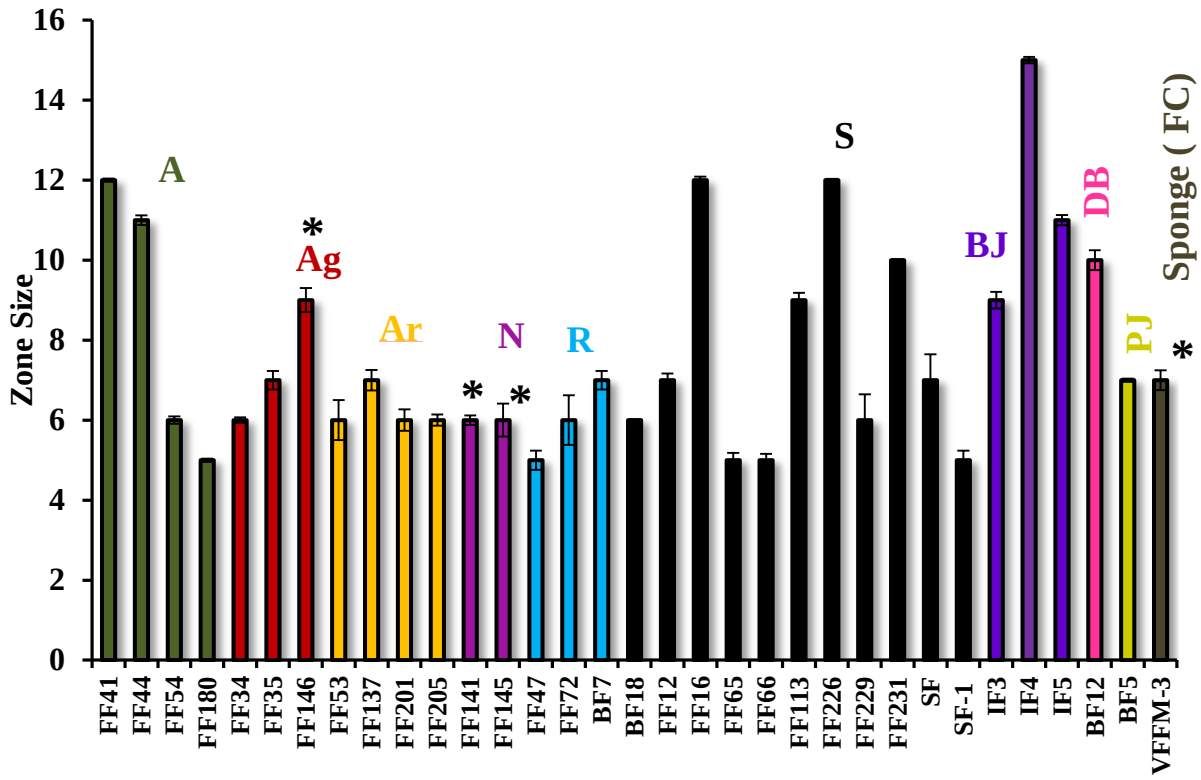

Fig. 2.8 Lipase production among extremely halophilic eubacterial and haloarchaeal cultures in different solar salts: estuarine sediments and sponge. The cultures marked with an asterix* are eubacteria, the rest of the cultures are haloarchaea

The percent overall screening efficiency score for lipase production exhibited by cultures and computed by scoring lipase producers and no producers score against the total cultures screened from different solar salts, estuarine sediments and sponge is depicted in **Fig. 2.9.** The highest activity score of 100% was obtained for the cultures from estuarine sediments of Dona Paula and Panjim Jetty and sponge, while, the lowest score of 10% was obtained for cultures from the solar salt of Ribandar. A score of 44 %/ 40%/ 33%/ 29%/ 19% and 14% was obtained for the cultures from the solar salts of Siridao/ Arambol, estuarine sediments from Betim Jetty and solar salts from Arpora/ Agarwada/ Nerul respectively.

A highly significant variation ($F = 3.044$; $p<0.001$) of zone sizes was observed within cultures positive for extra cellular production of lipase from different sampling sites as per the one-way ANOVA obtained using the IBM SPSS software.

Based on highest zone size produced by the culture GUIF4, it was found to be the most potential culture among the lipase producers and hence further studies to identify it were undertaken.

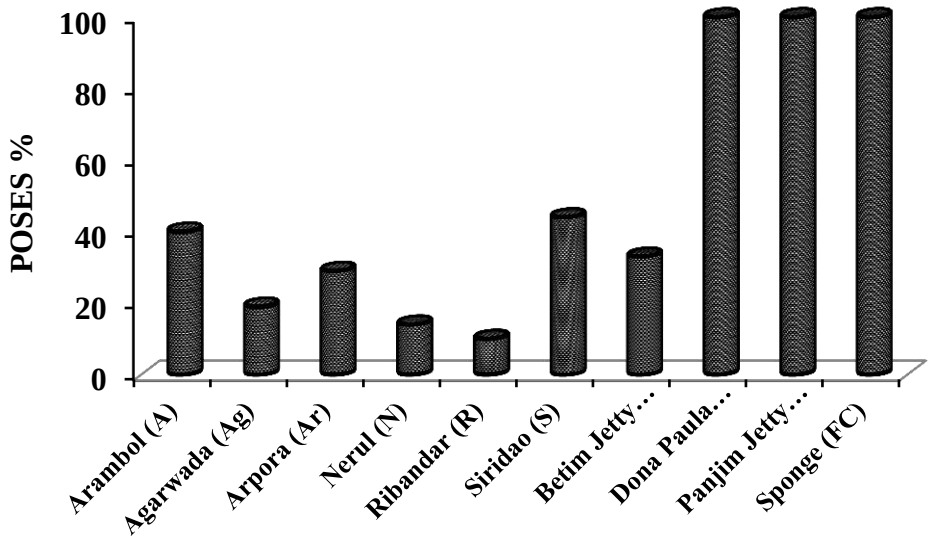

Fig. 2.9 Percent overall screening efficiency score (POSES %) for lipase production among extremely halophilic eubacteria and haloarchaeal cultures from different solar salts, estuarine sediments and from sponge

2.2.2.2 Identification of GUIF4

2.2.2.2.1 Evaluation of Morphological characteristics

Cells of GUIF4 stained negative to the Gram reaction and under scanning electron microscope were seen as cup shaped **(Fig. 2.10)**.

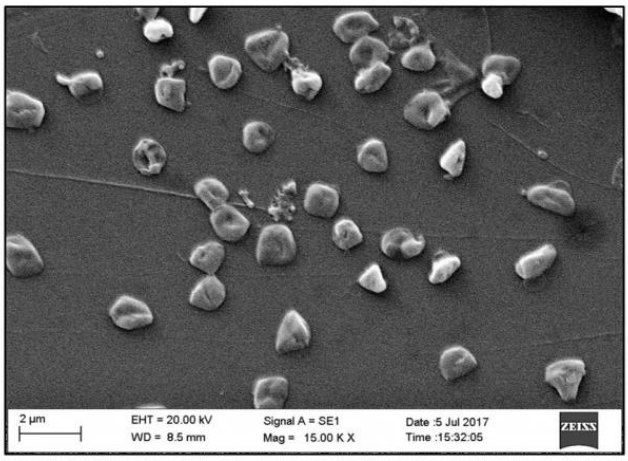

Fig. 2.10 Scanning electron micrograph of GUIF4 cells

2.2.2.2.2 Chemotaxonomic characteristics of GUIF4

2.2.2.2.2.1 Pigment characteristics

GUIF4 when grown on NTYE was seen to produce an orange red pigment as seen in **Fig. 2.11 A.** The pigment extracted in acetone showed characteristic absorptions of carotenoids at 369 and 387 465, 491 and 524 **(Fig. 2.11 B)**.

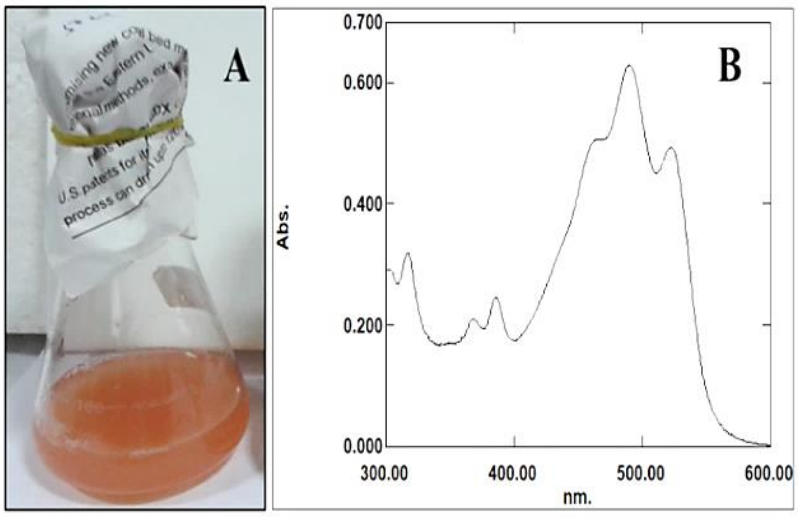

Fig. 2.11 A: Growth of GUIF4 in NTYE with orange pigment **B:** Visible absorption spectra of pigment extracts of GUIF4

2.2.2.2.2.2 Glycerol Diether moieties

The TLC plates separated using petroleum ether (60-80°C): diethyl ether (85:15, v/v) on spraying with 10% dodecaphosphomolybdic acid in absolute ethanol and heating for 15 min at 150°C gave a spot with R_f values of 0.2 for control *Haloferax* sp. and GUIF4. The FT- IR spectrum of the sample at spot at R_f value 0.2 revealed a peak at 1076 for control *Haloferax* sp. and for GUIF4 **(Fig. 2.12)**

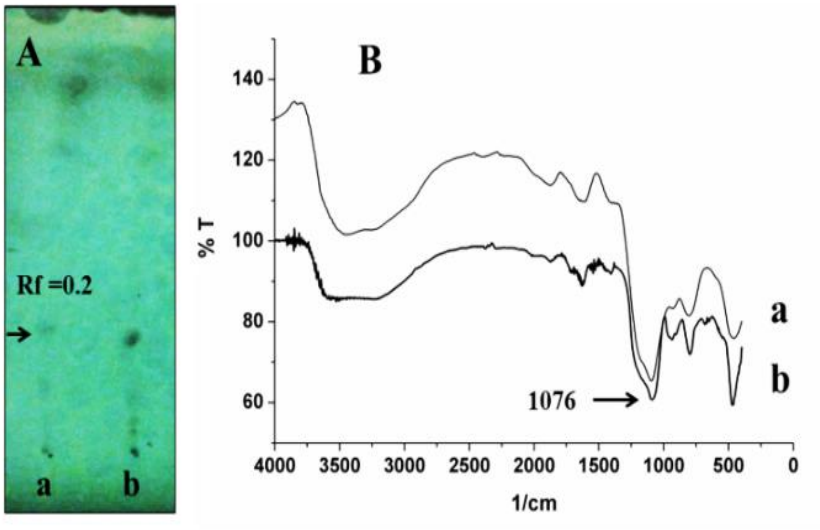

Fig. 2.12 A: TLC profile of methanolysates of **a.** positive control *Haloferax* sp.; **b.** GUIF4 developed in petroleum ether (60-80°C): diethyl ether (85:15, v/v) on staining with 10% dodecaphosphomolybdic acid **B:** FTIR of spot at R_f 0.2 obtained at **a** and **b** in **A**

2.2.2.2.2.3 Salt tolerance, response to antibiotics and bile salts

GUIF4 did not grow without salt, but grew in 15% and 20% NaCl. It also failed to grow on MacConkey's agar, with and without 700 U of penicillin.

2.2.2.2.3 Biochemical characterization of GUIF4

The major biochemical characteristics of GUIF4 are shown in **Table 2.2**.

Table 2.2 Biochemical characteristics of GUIF4

Biochemical Test	**GUIF4**
Glucose	+
Sucrose	+
Fructose	-
Galactose	+
Xylose	+
Mannose	-
Maltose	+
Lactose	+
Sorbitol	+
Mannitol	+
Indole	+
Nitrate	+
MR	+
VP	-
Citrate	+
TSI	+
Urease	+
Catalase	+
Tween 80	+
Starch	-
Motility	Non motile
Growth on 0% NaCl	-
Growth on 15% NaCl	+
Growth on 25% NaCl	+
Lysis in 0% NaCl	+
Optimum pH	7
	Growth on pH 7> pH 9>pH>5
Bile salts	No growth (sensitive)
Penicillin-G (700U)	Growth (insensitive)
Tentative classification	***Haloferax* sp.**

2.2.2.2.4 Phylogenetic characterization of GUIF4

The extracted DNA was checked for it's purity on 0.8 % agarose gel **(Fig. 2.13 A)**. The genomic DNA of GUIF4 was seen as a discrete band below the well in which it was loaded. The PCR amplification of genomic DNA resulted in 1.4 kb PCR product **(Fig. 2.13 B)**. The 16S ribosomal RNA gene sequence thus obtained is listed in **Table 2.3**. BLASTn search of the 16S rRNA gene sequence on the NCBI website revealed that GUIF4 belonged to the *Haloferax* genera. The culture GUIF4 was found to be related with 99% similarity to *Haloferax gibbonsii* strain ARA6 with accession number CP011947 isolated from sea salt in South Korea **(Fig. 2.14)**. The GenBank accession number for the 16S rRNA gene sequence for GUIF4 was MG199078. The phylogenetic tree was constructed with Neighbour-Joining (NJ) algorithm using MEGA v 7.0 and the outgroup used was *Methanococcus voltae* PS (NR104985) belonging to phylum *Crenarchaeota* of the Archaeal Domain. The biochemicals of GUIF4 were compared with that of *Haloferax gibbonsii* strain ARA6 (CP011947).

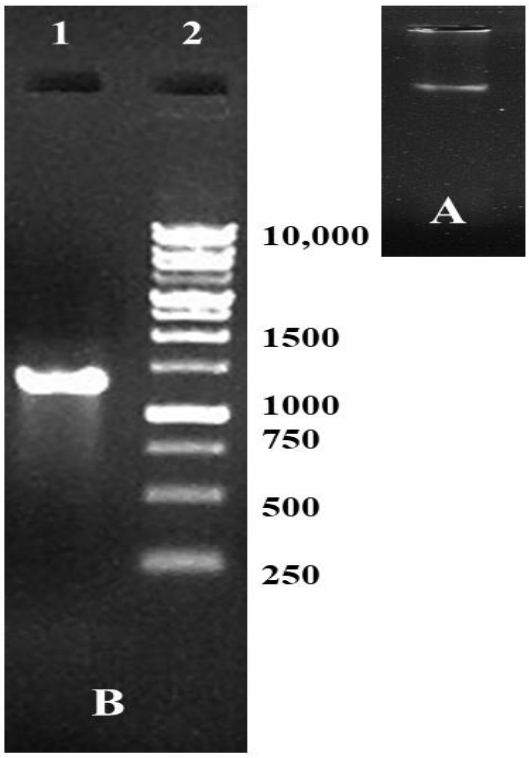

Fig. 2.13 Agarose gel electrophoreis of the PCR product of GUIF4

Table 2.3 16S ribosomal RNA gene sequence of GUIF4

Culture	16S ribosomal RNA partial gene sequence	Generic identification	Accession No.
GUIF 4	TACTCAGGAGACGATACCTCGGGAACTGAGGCTAATAGTTCATAGGGGAGTCGCGCTGGAAATGC CGACTCCCCCAAACGCTCCGGCGCCGTAGGATGTGTCTGCGGCCGATTAGGTAGACGGTGGGGTAA CGGCCCACCGTGCCGATAATCGGTACGGGTTGTGAGAGCAAGAGCCCGGAGACGGAATCTGAGAC AAGATTCCGGGCCCTACGGGGCGCAGCAGGCGCGAAACCTTTACACTGCACGCAAGTGCGATAAG GGGACCCCAAGTGCGAGGGCATATAGTCCTCGCTTTTCTCGACTGTAAGGCGGTCGAGGAATAAGA GCTGGGCAAGACCGGTGCCAGCCGCCGCGGTAATACCGGCAGCTCAAGTGATGACCGATATTATT GGGCCTAAAGCGTCCGTAGCCGGCCATGAAGGTTCATCGGGAAATCCGCCAGCTCAACTGGCGGG CGTCCGGTGAAAACCACATGGCTTGGGACCGGAAGGCTCGAGGGGTACGTCCGGGGTAGGAGTGA AATCCCGTAATCCTGGACGGACCACCGATGGCGAAAGCACCTCGAGAAGACGGATCCGACGGTGA GGGACGAAAGCTAGGGTCTCGAACCGGATTAGATACCCGGGTAGTCCTAGCTGTAAACGATGCTC GCTAGGTGTGACACAGGCTACGAGCCTGTGTTGTGCCGTAGGGAAGCCGAGAAGCGAGCCGCCTG GGAAGTACGTCCGCAAGGATGAAACTTAAAGGAATTGGCGGGGGAGCACTACAACCGGAGGAGC CTGCGGTTTAATTGGACTCAACGCCGGACATCTCACCAGCTCCGACTACAGTGATGACGATCAGGT TGATGACCTTATCACGACGCTGTAGAGAGGAGGTGCATGGCCGCCGTCAGCTCGTACCGTGAGGCG TCCTGTTAAGTCAGGCAACGAGCGAGACCCGCACTTCTAATTGCCAGCAGCAGTTTCGACTGGCTG GGTACATTAGAAGGACTGCCGCTGCTAAAGCGGAGGAAGGAACGGGCAACGGTAGTCAGTATGCC CGAATGAGCTGGGCTACACGCGGCTACATGTCGAGACATGGGTTGCTATCTCGGAAGAGACGCTAT CTCTAACTCGATCGTAGTCGATGAGGGCTGAACCTCGCCCTCAT	***Haloferax gibbonsii* strain GUIF4**	**MG199078**

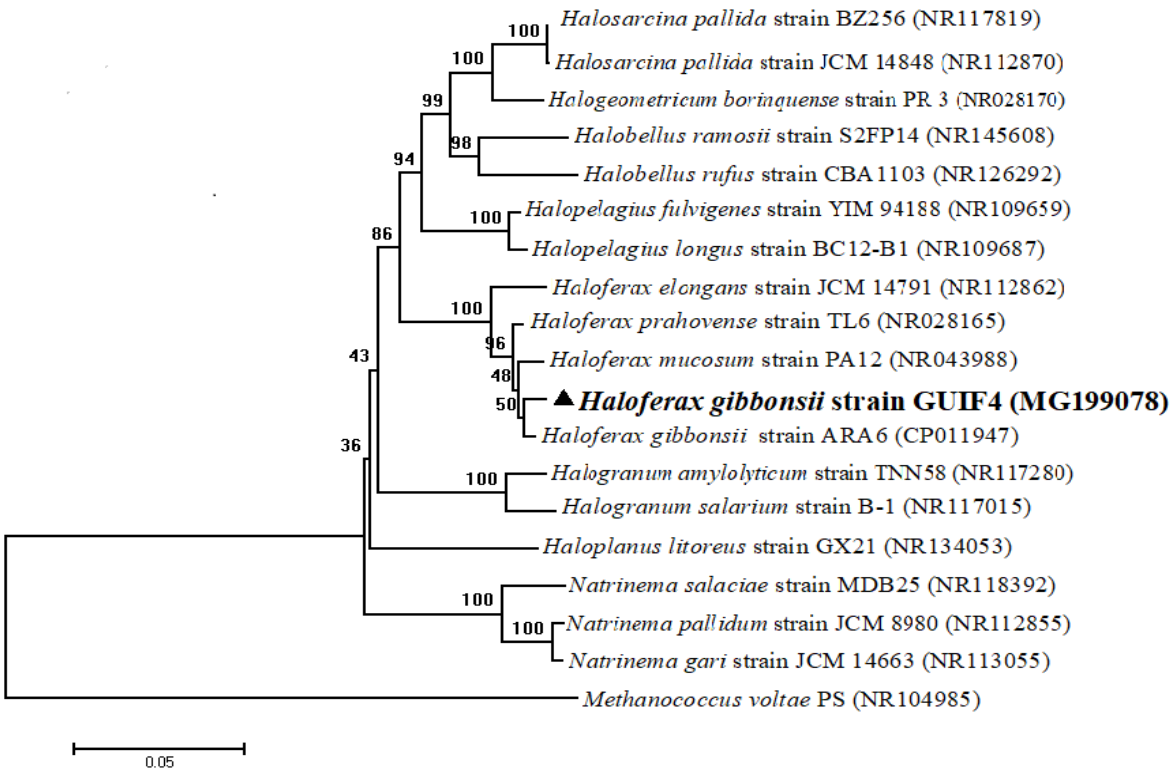

Fig. 2.14 The phylogenetic position of GUIF4 was inferred using the Neighbor-Joining method. The optimal tree with the sum of branch length = 0.70470728 is shown. The percentage of replicate trees in which the associated taxa clustered together in the bootstrap test (1000 replicates) is shown above the branches. The evolutionary distances were computed using the Tamura 3-parameter method and are in the units of the number of base substitutions per site. The analysis involved 19 nucleotide sequences. Codon positions included were 1st+2nd+3rd+Noncoding. All ambiguous positions were removed for each sequence pair. There were a total of 1496 positions in the final dataset. Evolutionary analyses were conducted in MEGA7. The outgroup used is *Methanococcus voltae* PS (NR104985) belonging to phylum *Crenarchaeota*

2.2.2.2.5 Diversity of lipase producing extremely halophilic eubacterial and haloarchaeal genera in solar salts, estuarine sediments and sponge

The eubacterial genera present was *Alteromonas* and *Chromohalobacter*, while the haloarchaeal lipase producing genera in solar salts were *Halobacterium*, *Haloferax*, *Haloarcula*, *Halorubrum*, *Halococcus*, *Natrialba* and *Natronomonas* **(Fig. 2.15)**.

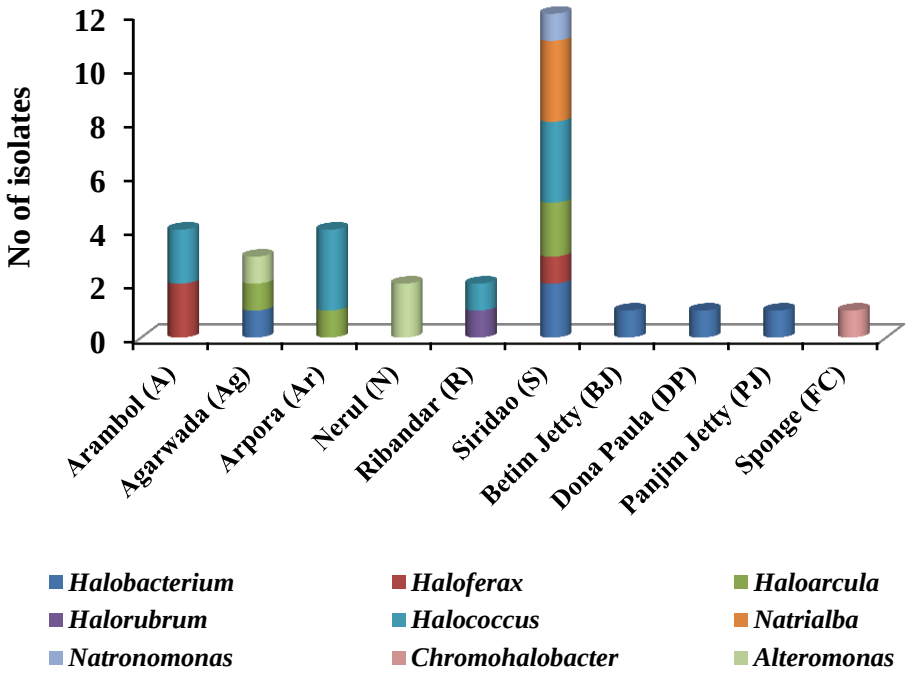

Fig. 2.15 Lipase producing extremely halophilic eubacterial and haloarchaeal genera from different solar salts, estuarine sediments and from sponge

The overall ocurrence of lipase producing members were in the order, *Halococcus*>*Halobacterium* > *Haloarcula* > *Haloferax* > *Natrialba* > *Alteronomonas* > *Halorubrum* = *Natronomonas* = *Chromohalobacter*. The Shannon-Weiner Diversity Index 'H' calculated for lipase producers were 1.3, 0.87, 0.7, 0.68 and 0.66 for Siridao, Agarwada, Arambol, Arpora and Betim Jetty respectively. An index of 0.29 was obtained for lipase producers from Dona Paula and Panjim Jetty while a value of 0.23 was calculated for lipase producers from Ribandar Patto **(Fig. 2.16)**.

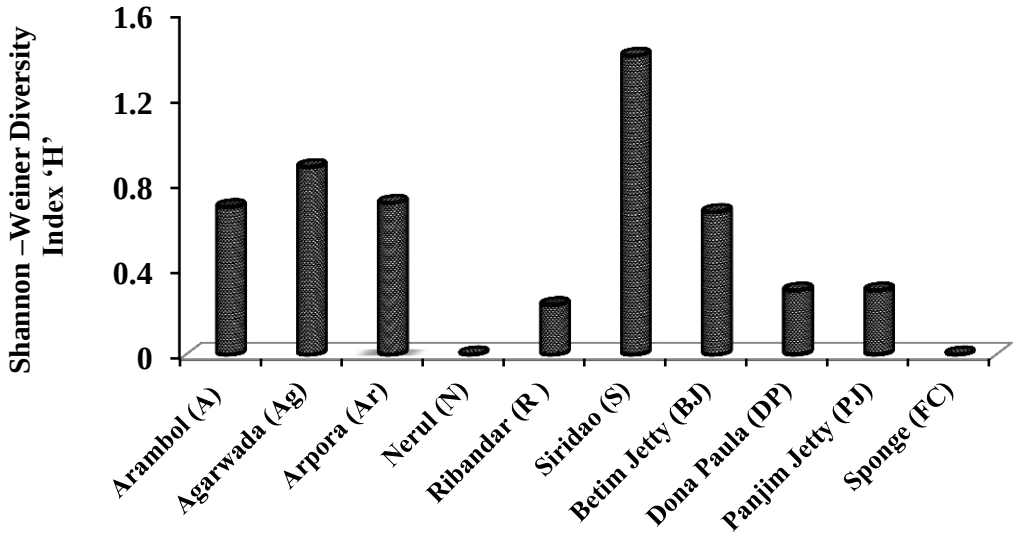

Fig. 2.16 Shannon-Weiner Diversity Index "H" for lipase producing extremely halophilic eubacterial and haloarchaeal genera from different solar salts, estuarine sediments from sponge

2.2.3 AROMATIC OXYGENASES

2.2.3.1` Production of aromatic oxygenases among extremely halophilic eubacteria and haloarchaea

As recorded in **Fig. 2.17 A**, growth measured at A_{600} varied in cultures among different solar salt from a minimum of 0.06 ± 0.01 for the culture $GUFF_{141}$ to a maximum of 1.364 ± 0.08 exhibited by $GUFF_{66}$. Absorbances of > 1 were obtained for $GUFF_{22}$, $GUFF_{35}$, $GUFF_{58}$, $GUFF_{66,}$ $GUFF_{69,}$ $GUBF_1$ and $GUBF_2$. **Fig. 2.17 B** depicts the growth variation of cultures among the estuarine sediments and sponge. A minimum of absorbance of 0.123 ± 0.01 for the isolate $GUFLF_3$ to a maximum of 1.441 ± 0.08 by GUIF2 was obtained.

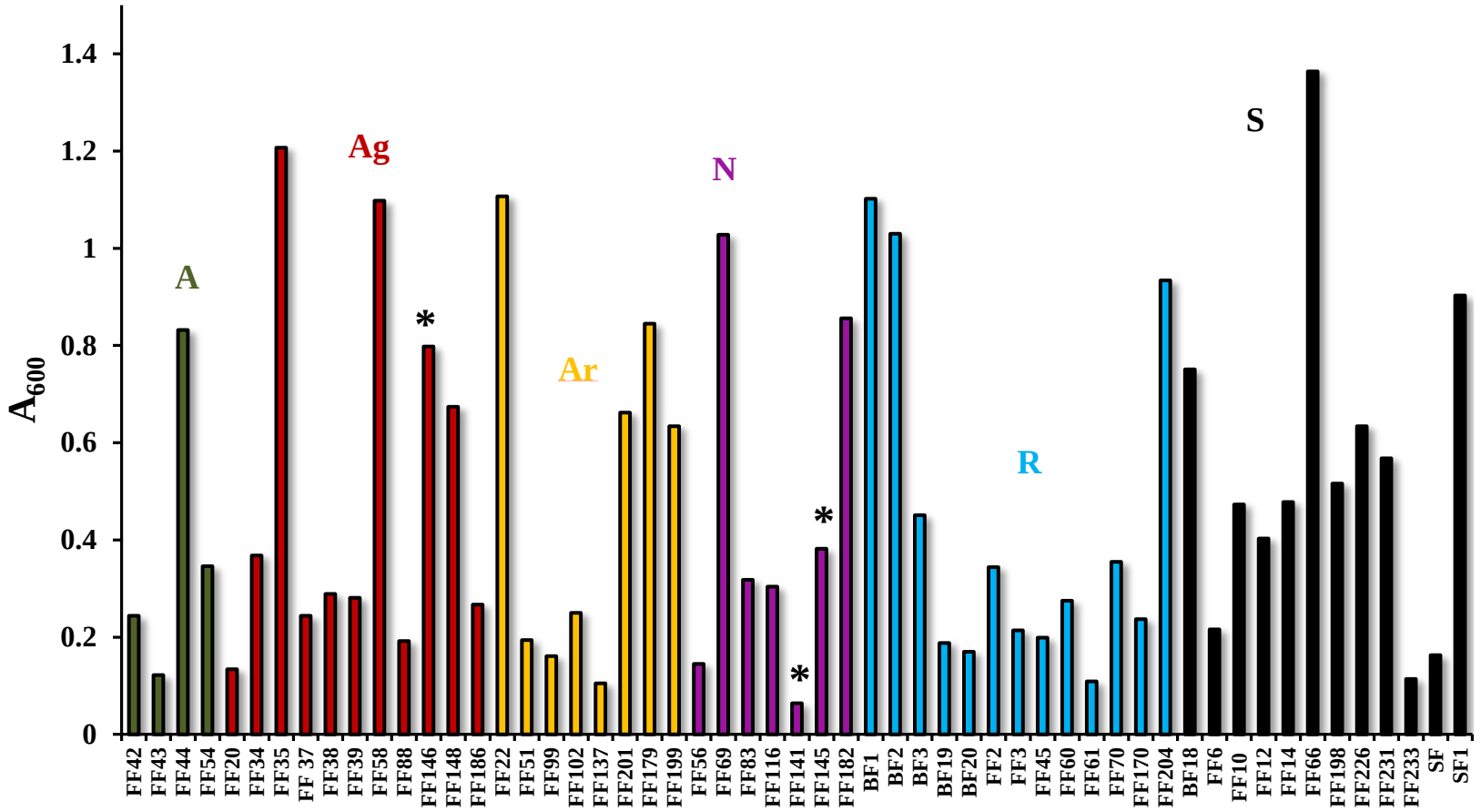

Fig. 2.17 A: Aromatic oxygenase production among extremely halophilic eubacteria and haloarchaeal cultures from different solar salts. The cultures marked with an asterix* are eubacteria, the rest of the cultures are haloarchaea

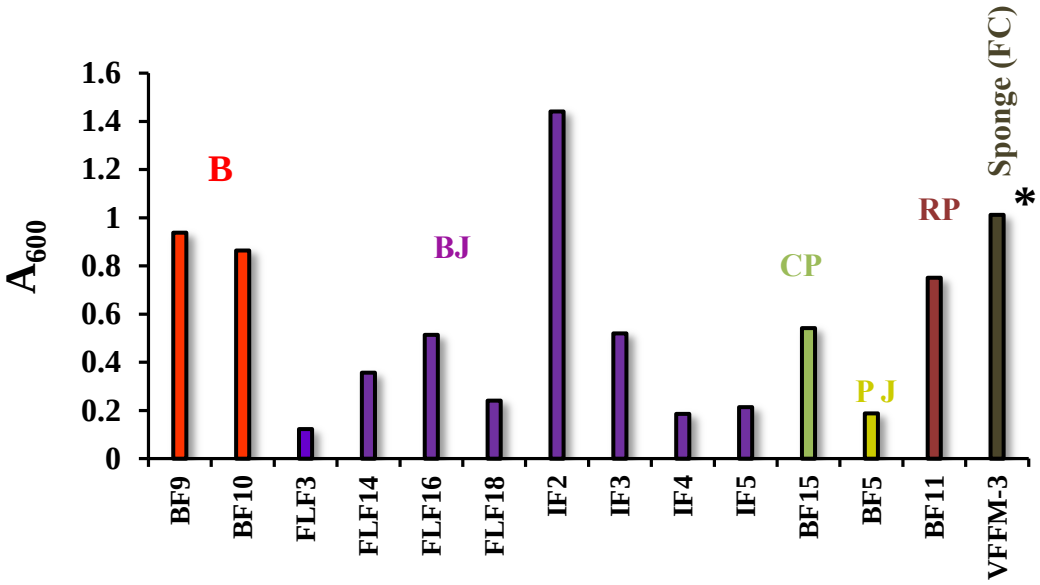

Fig. 2.17 B: Aromatic oxygenase production among extremely halophilic eubacteria and haloarchaeal cultures from estuarine sediments and from sponge**.** The cultures marked with an asterix* are eubacteria, the rest of the cultures are haloarchaea

The percent overall screening efficiency score for aromatic oxygenase production exhibited by cultures and computed by scoring aromatic oxygenase producers and no producers score against the total cultures screened from different solar salts, estuarine sediments and sponge is depicted in **Fig. 2.18**. The highest activity score of 100 % was obtained for the cultures from estuarine sediments of Baiguinim, Captain of Ports, Dona Paula, Panjim Jetty, Ribandar Patto and the sponge, while the lowest score of 40 % was obtained for the cultures from Arambol solar salt. A score of 69%/ 65%/ 57%/ 50% and 45% was obtained for the cultures from the solar salts of Agarwada/ Ribandar/ Arpora/ Nerul and Siridao solar salt respectively.

A highly significant variation ($F = 159.918$; $p<0.001$) among growth was observed within cultures positive for production of aromatic oxygenases, from different sampling sites, as per the one-way ANOVA obtained using the IBM SPSS software.

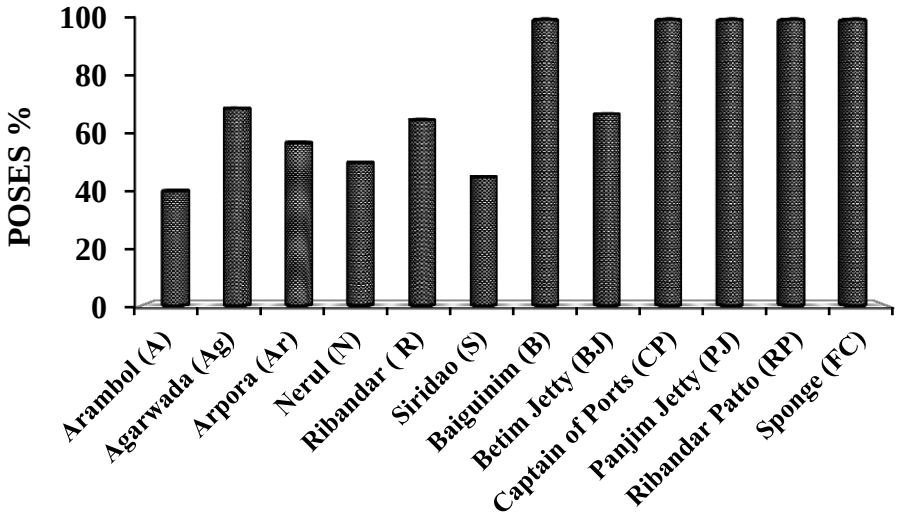

Fig. 2.18 Percent overall screening efficiency score (POSES %) for aromatic oxygenase production among extremely halophilic eubacteria and haloarchaeal cultures from different solar salts, estuarine sediments and sponge.

2.2.3.2 Identification of GUIF2

2.2.3.2.1 Evaluation of Morphological characteristics

Cells of GUIF2 stained negative to the Gram reaction and under scanning electron microscope were cup shaped **(Fig. 2.19)**.

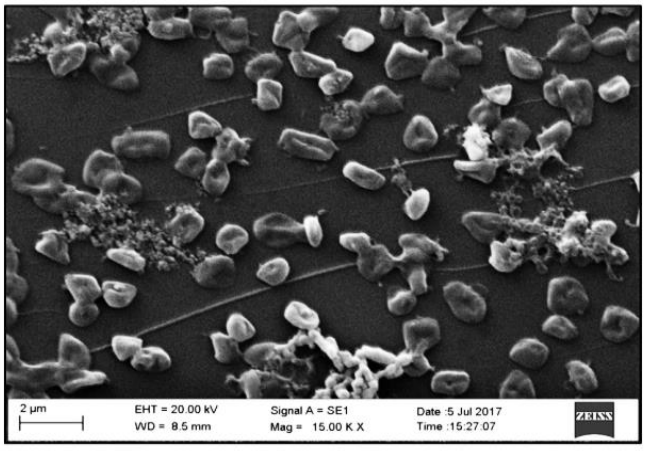

Fig. 2.19 Scanning electron micrograph of GUIF2 cells

2.2.3.2.2 Chemotaxonomic characteristics of GUIF2

2.2.3.2.2.1 Pigment characteristics

GUIF2 when grown on NTYE was seen to produce an orange red pigment as seen in **Fig. 2.20 A.** The pigment extracted in acetone showed characteristic absorptions of carotenoids at 369, 387, 465, 491 and 524 **(Fig. 2.20 B)**.

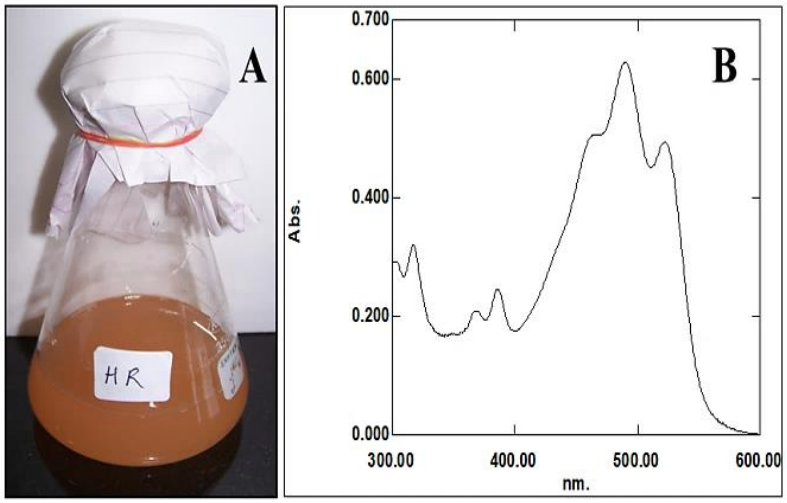

Fig. 2.20 A: Growth of GUIF2 in NTYE with orange pigmentation

B: Visible absorption spectra of pigment extracts of GUIF2

2.2.3.2.2.2 Glycerol Diether Moieties

The TLC plates separated using petroleum ether (60-80°C): diethyl ether (85:15, v/v) on spraying with 10% dodecaphosphomolybdic acid in absolute ethanol and heating for 15 min at 150°C gave a spot with R_f values of 0.2 for control *Haloferax* sp. and GUIF2. The FT- IR spectrum of the sample at spot with R_f value of 0.2 revealed a peak at 1076 for control *Haloferax* sp. and GUIF2 **(Fig. 2.21)**.

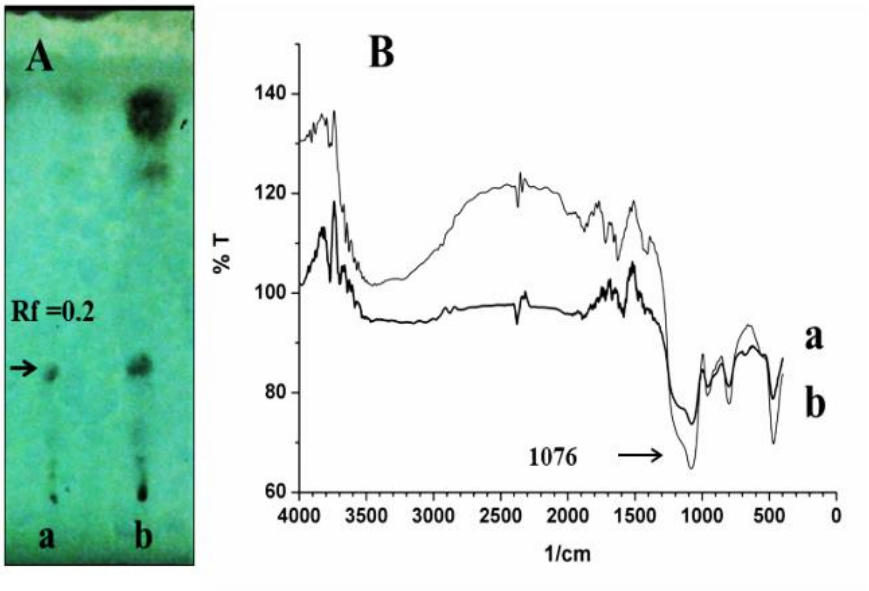

Fig. 2.21 A: TLC profile of methanolysates of **a:** positive control *Haloferax* sp.; **b:** GUIF2 developed in petroleum ether (60-80°C): diethyl ether (85:15, v/v) on staining with 10 % dodecaphosphomolybdic acid **B:** FTIR of spot at R_f 0.2 obtained at **a** and **b** in **A**

2.2.3.2.2.3 Salt tolerance, response to antibiotics and bile salts

GUIF2 did not grow without salt, but grew in 15% and 20% NaCl. It also failed to grow on Macconkey's agar, with and without 700 U of Penicillin.

2.2.3.2.3 Biochemical characterization of GUIF2

The major biochemical characteristics of GUIF2 are shown in **Table 2.4.**

Table 2.4 Biochemical characterization of GUIF2

Biochemical Test	**GUIF2**
Glucose	+
Sucrose	+
Fructose	+
Galactose	+
Xylose	+
Mannose	+
Maltose	+
Lactose	+
Sorbitol	+
Mannitol	+
Indole	+
Nitrate	+
MR	+
VP	-
Citrate	+
TSI	-
Urease	+
Catalase	+
Tween 80	-
Starch	-
Motility	Non motile
Growth on 0% NaCl	-
Growth on 15% NaCl	+
Growth on 25% NaCl	+
Lysis in 0% NaCl	+
Optimum pH	7
	Growth on pH 7 > pH 9 > pH 5
Bile salts	No growth (sensitive)
Penicillin-G (700U)	Growth (insensitive)
Tentative classification	***Haloferax* sp.**

2.2.3.2.4 Phylogenetic characterization of GUIF2

The extracted DNA was checked for it's purity on 0.8 % agarose gel **(Fig. 2.22 A)**. The genomic DNA of GUIF2 was seen as a discrete band below the wells they were loaded. The PCR amplification of genomic DNA resulted in 1.4 kb PCR product **(Fig. 2.22 B)**. The 16S ribosomal RNA gene sequence obtained is listed in **Table 2.5**. BLASTn search on the NCBI site of the 16S rRNA gene sequence revealed that GUIF2 belonged to the *Haloferax* genera. The culture GUIF2 was found to be related with 99% similarity to *Haloferax volcanii* strain DS2 with accession number NR028203 and had evolutionary similarity between 95-98% to several available type strains of the genus *Haloferax* **(Fig. 2.23)**. The GenBank accession number for the 16S rRNA gene sequence for GUIF2 was MH169338. The phylogenetic tree was constructed with Neighbour-Joining (NJ) algorithm using MEGA v7.0 and the outgroup used was *Methanococcus voltae* PS (NR104985) belonging to *Crenarchaeota* form the Domain Archaea. The biochemicals of GUIF2 were compared with that of *Haloferax volcanii* strain DS2 (NR028203).

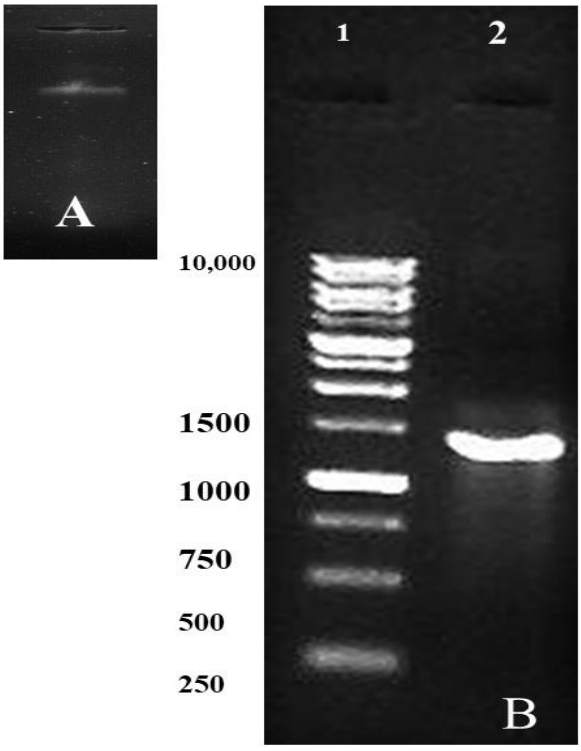

Fig. 2.22 Agarose gel electrophoresis of the PCR product of GUIF2

Table 2.5 16S ribosomal RNA gene sequence of GUIF2

Culture	16S ribosomal RNA gene partial sequence	Generic Identification	Accession No
GUIF 2	ACTTCGAGACGATACCTCGGGAACTGAGGCTAATAGTTCATACGGGAGTCATGCTGGAATGCCG ACTCCCCGAACGCTCAGGCGCTGTAGGATGTGGCTGCGGCCGATTAGGTAGACGGTGGGGTAAC GGCCCACCGTGCCGATATCGGTACGGGTTGTGAGAGCAAGAGCCCGGAGACGGAATCTGAGACA AGATTCCGGGCCCTACGGGGCGCAGCAGGCGCGAAACCTTTACACTGCACGCAAGTGCGATAAG GGGACCCCAAGTGCGAGGGCATATAGTCCTCGCTTTTCACGACTGTAAGGCGGTCGTGGAATAAG AGCTGGGCAAGACCGGTGCCAGCCGCCGCGGTAATACCGGCAGCTCAAGTGATGACCGATATTA TTGGGCCTAAAGCGTCCGTAGCCGGCCACGAAGGTTCATCGGGAAATCCGCCAGCTCAACTGGC GGGCGTCCGGTGAAAACCACGTGGCTTGGGACCGGAAGGCTCGAGGGGTACGTCCGGGGTAGGA GTGAAATCCCGTAATCCTGGACGGACCACCGATGGCGAAAGCACCTCGAGAAGACGGATCCGAC GGTGAGGGACGAAAGCTAGGGTCTCGAACCGGATTAGATACCCGGGTAGTCCTAGCTGTAAACG ATGCTCGCTAGGTGTGACACAGGCTACGAGCCTGTGTTGTGCCGTAGGGAAGCCGAGAAGCGAG CCGCCTGGGAAGTACGTCCGCAAGGATGAAACTTAAAGGAATTGGCGGGGGAGCACTACAACCG GAGGAGCCTGCGGTTTAATTGGACTCAACGCCGGACATCTCACCAGCTCCGACTACAGTGATGAC GATCAGGTTGATGACCTTATCACGACGCTGTAGAGAGGAGGTGCATGGCCGCCGTCAGCTCGTAC CGTGAGGCGTCCTGTTAAGTCAGGCAACGAGCGAGACCCGCACTTCTAATTGCCAGCAGCAGTTT CGACTGGCTGGGTACATTAGAAGGACTGCCGCTGCTAAAGCGGAGGAAGGAACGGGCAACGGTA GGTCAGTATGCCCCGAATGAGCTGGGCTACACGCGGGCTACAATGGTCGAGACAATGGGTTGCT ATCTCGAAAGAGAACGCTAATCTCCTAAACTCGATCGTAGTTCGGATTGAGGGCTGAAACTCGCC CTCATGAAGCTGGATTCGGTAGTAATCGCATTTCAATAGAGTGCGGTGAATACGTCCCTGCTCCT TGCACACACCGCCCGTCAAAGCACCCGAGTGAGGTCCGGATGAGGCCACCACACGGTGGTCGAA TCTGCCCTG	***Haloferax* sp. strain GUIF2**	**MH169338**

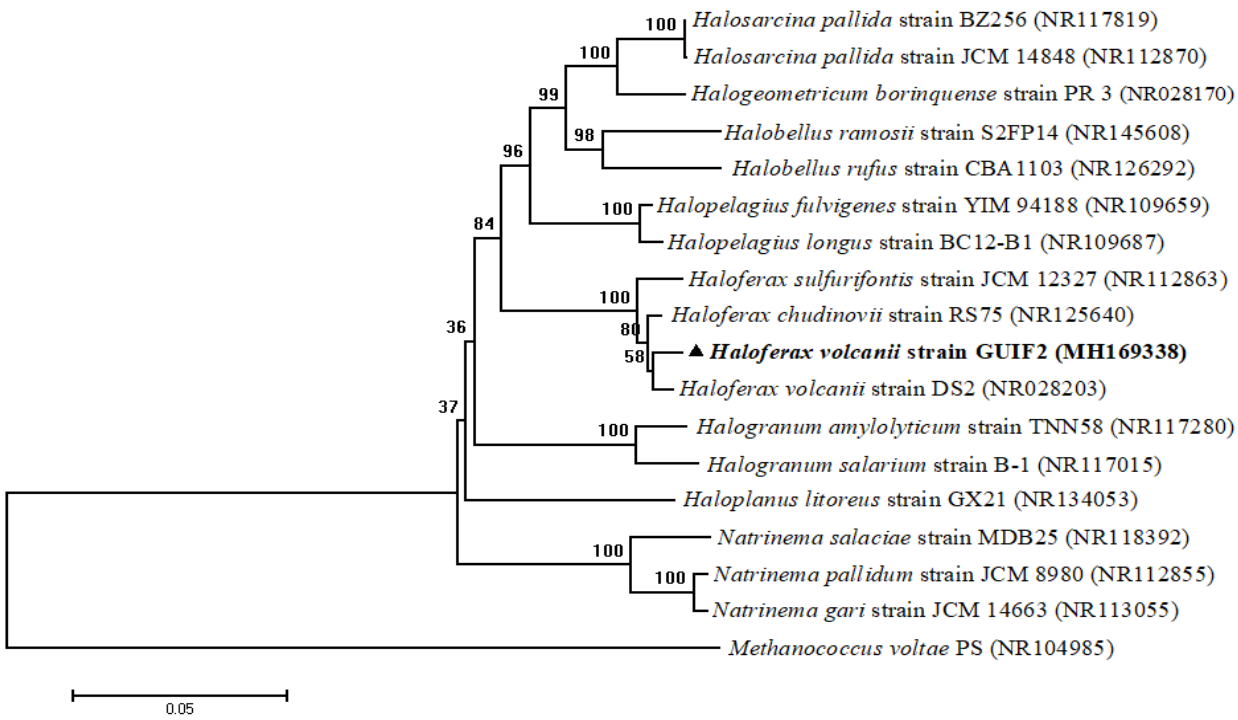

Fig. 2.23 The phylogenetic position of GUIF2 was inferred using the Neighbor-Joining method. The optimal tree with the sum of branch length = 0.69328512 is shown. The percentage of replicate trees in which the associated taxa clustered together in the bootstrap test (1000 replicates) are shown above the branches. The evolutionary distances were computed using the Tamura 3-parameter method and are in the units of the number of base substitutions per site. The analysis involved 18 nucleotide sequences. Codon positions included were 1st+2nd+3rd+Noncoding. All ambiguous positions were removed for each sequence pair. There were a total of 1496 positions in the final dataset. Evolutionary analyses were conducted in MEGA7. The outgroup used is *Methanococcus voltae* PS (NR104985) belonging to phylum *Crenarchaeota*

2.2.3.3 Diversity of aromatic oxygenase producing extremely halophilic eubacterial and haloarchaeal genera retrieved from solar salts, estuarine sediments and from sponge

The eubacterial genera present were *Alteromonas*, *Gluconobacter* and *Chromohalobacter*, while haloarchaeal genera in solar salts were *Halobacterium*, *Haloferax*, *Haloarcula*, *Halorubrum*, *Halococcus*, *Natrialba*, *Natrinema* and *Natronomonas* **(Fig. 2.24)**.

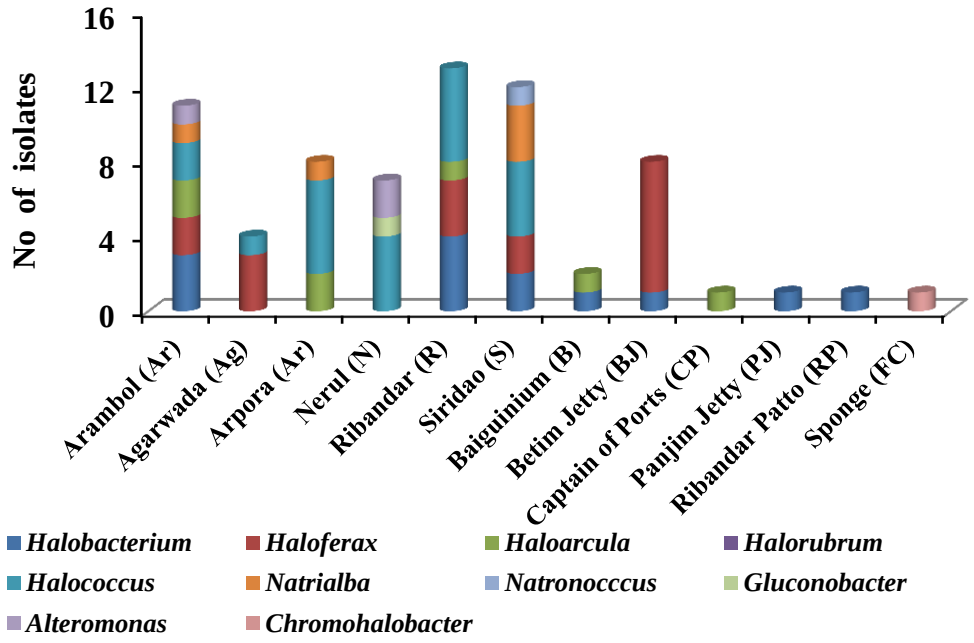

Fig. 2.24 Aromatic oxygenase producing extremely halophilic eubacterial and haloarchaeal genera present in different solar salts, estuarine sediments and from sponge

The overall occurrence of aromatic oxygenase producing members was in the order, *Halococcus* >*Halobacterium* > *Haloarcula* > *Haloferax* > *Natrialba* > *Alteronomonas* > *Halorubrum* = *Natronomonas* = *Natrinema* = *Chromohalobacter*. The Shannon - Weiner Diversity Index 'H' calculated for aromatic oxygenase producing genera was found to 1.86, 1.28, 1.16, 1.02, 0.58, 0.56, 0.47, 0.45 and 0.27

for Agarwada, Ribandar, Siridao, Arpora, Nerul, Betim Jetty, Baiginuim, Arambol, Captain of Ports. A value of 0.197 was calculated for aromatic oxygenase producing genera for Panjim Jetty and Ribandar Patto **(Fig. 2.25)**.

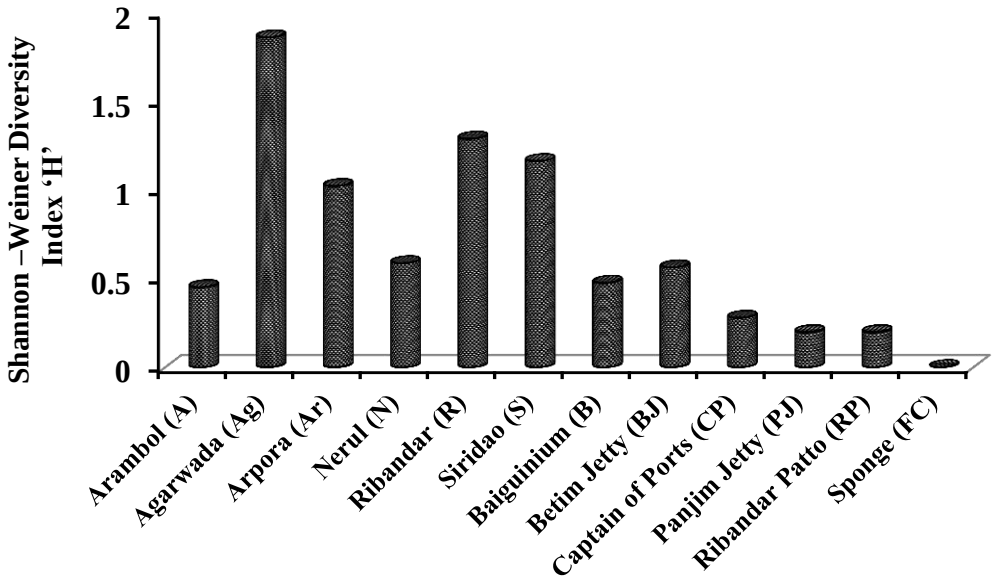

Fig. 2.25 Shannon-Weiner Diversity Index "H" for aromatic oxygenase producing extremely halophilic eubacterial and haloarchaeal genera present in different solar salts: estuarine sediments and sponge

2.2.4 HYDROLYTIC ENZYME PROFILE OF CULTURES

Multiple enzyme activity was detected in many cultures. From a total of 117 cultures screened for the production of extremozymes, 84 produced at least 1 enzyme and 33 produced none. Nine cultures from 117 showed the production of all 3 enzymes **(Table 2.6**). Of the 9 cultures, 7 were haloarchaeal while 2 belonged to eubacteria. The haloarchaeal cultures belonged to only two haloarchaeal genera with *Halobacterium* as the predominant genera followed by *Haloarcula*. The eubacterial cultures $GUFF_{141}$ and GUVVFM-3 showing multi enzyme activity belonged to *Alteromonas* and *Chromohalobacter*. Thirty one isolates from a total of 117 were positive for any 2 enzymes (**Table 2.6**) of which 2 cultures were eubacteria and 29

were haloarchaeal cultures. Both the eubacterial genera belonged to *Alteromonas* and the haloarchaeal genera were a total of 6 in the order *Haloferax* (9 cultures) > *Halobacterium* (7 cultures) > *Halococcus* (6 cultures) > *Haloarcula* (3 cultures) = *Natrialba* (3 cultures) > *Halorubrum* (1 culture). Four cultures showed the combined production of amylase and lipase enzymes. Fifteen cultures showed the combined production of amylase and aromatic oxygenase enzyme while 12 cultures showed the combined production of lipase and aromatic oxygenase enzyme (**Fig. 2.26 A, B, C & D**).

Table 2.6 Extremely halophilic eubacteria and haloarchaeal cultures with multienzyme activity

Culture	Identity	Amylase	Lipase	Aromatic Oxygenase
Production of all 3 extremozymes				
$GUFF_{141}$	*Alteromonas* sp.	+	+	+
GUVFFM-3	*Chromohalobacter salexigenes* (JF330126)	+	+	+
$GUBF_{5}$	*Halobacterium* ATCC BAA 647	+	+	+
$GUBF_{18}$	*Halobacterium* sp.	+	+	+
$GUFF_{35}$	*Halobacterium* sp	+	+	+
GUSF	*Halobacterium* sp. MTCC 3265	+	+	+
GUIF5	*Halobacterium* sp.	+	+	+
$GUFF_{34}$	*Haloarcula* sp	+	+	+
$GUFF_{137}$	*Haloarcula* sp.	+	+	+
Production of any 2 extremozymes				
$GUFF_{145}$	*Alteromonas* sp.	-	+	+
$GUFF_{146}$	*Alteromonas* sp.	-	+	+
$GUBF_{1}$	*Haloferax* ATCC BAA 644	+	-	+
$GUFF_{44}$	*Haloferax* sp.	-	+	+
$GUFLF_{3}$	*Haloferax* sp.	+	-	+
$GUFLF_{14}$	*Haloferax* sp.	+	-	+
$GUFLF_{16}$	*Haloferax* sp.	+	-	+

GUIF2	*Haloferax* sp.	-	+	+
GUIF3	*Haloferax* sp.	+	-	+
GUIF4	*Haloferax* sp.	-	+	+
GUSF-1	*Haloferax alexandrines* (KF796625)	-	+	+
$GUBF_{10}$	*Halobacterium* ATCC BAA 653	+	-	+
$GUBF_{11}$	*Halobacterium* ATCC BAA 654	+	-	+
$GUBF_{12}$	*Halobacterium* ATCC BAA 655	+	+	-
$GUBF_{19}$	*Halobacterium* sp.	+	-	+
$GUBF_{20}$	*Halobacterium* sp.	+	-	+
$GUFF_{88}$	*Halobacterium* sp.	+	-	+
$GUFLF_{18}$	*Halobacterium* sp.	+	-	+
$GUFF_{2}$	*Halococcus* sp.	+	-	+
$GUFF_{45}$	*Halococcus* sp.	+	-	+
$GUFF_{54}$	*Halococcus* sp.	-	+	+
$GUFF_{66}$	*Halococcus* sp.	-	+	+
$GUFF_{113}$	*Halococcus* sp.	+	+	-
$GUFF_{201}$	*Halococcus* sp.	-	+	+
$GUBF_{7}$	*Haloarcula* ATCC BAA 650	+	+	-
$GUBF_{9}$	*Haloarcula* ATCC BAA 652	+	-	+
$GUBF_{15}$	*Haloarcula* sp.	+	-	+
$GUFF_{12}$	*Natrialba* sp.	-	+	+
$GUFF_{226}$	*Natrialba* sp.	-	+	+
$GUFF_{231}$	*Natrialba* sp.	-	+	+
$GUFF_{72}$	*Halorubrum* sp.	+	+	-

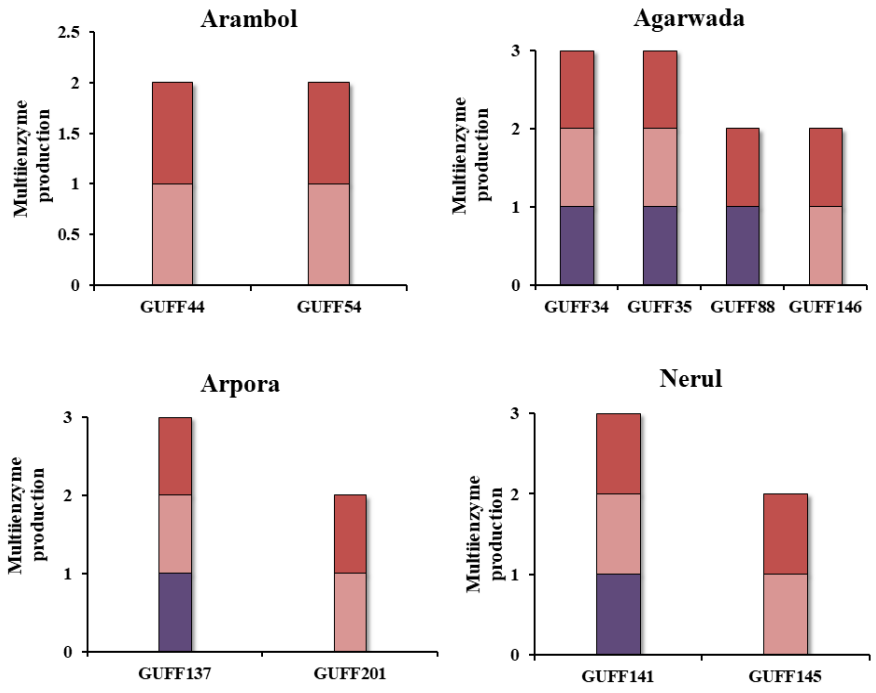

Fig. 2.26 A: Multienzyme production; amylase lipase aromatic oxygenases in different sampling sites

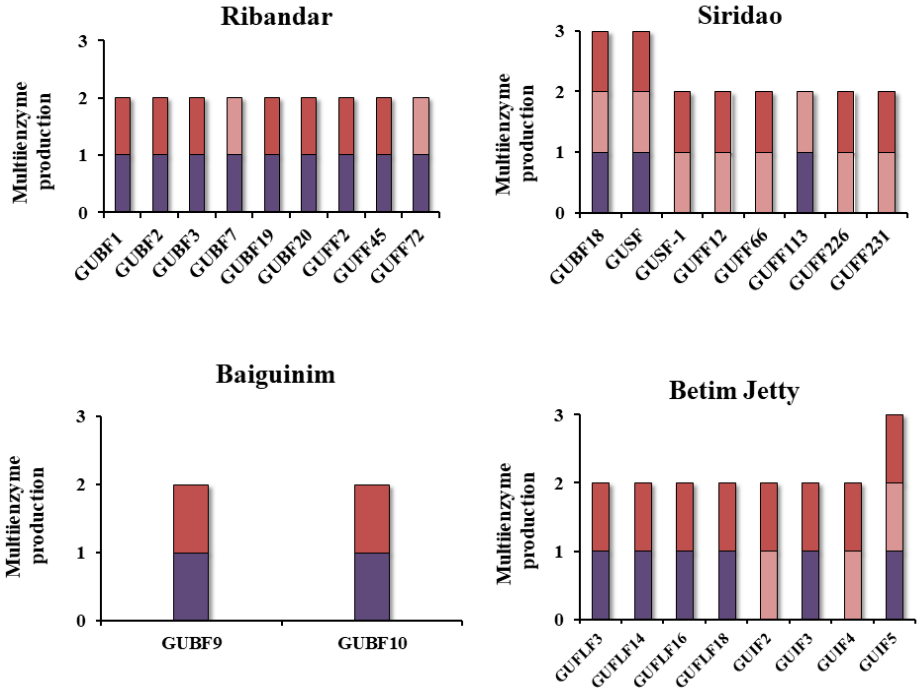

Fig. 2.26 B: Multienzyme production; amylase lipase aromatic oxygenases in different sampling sites

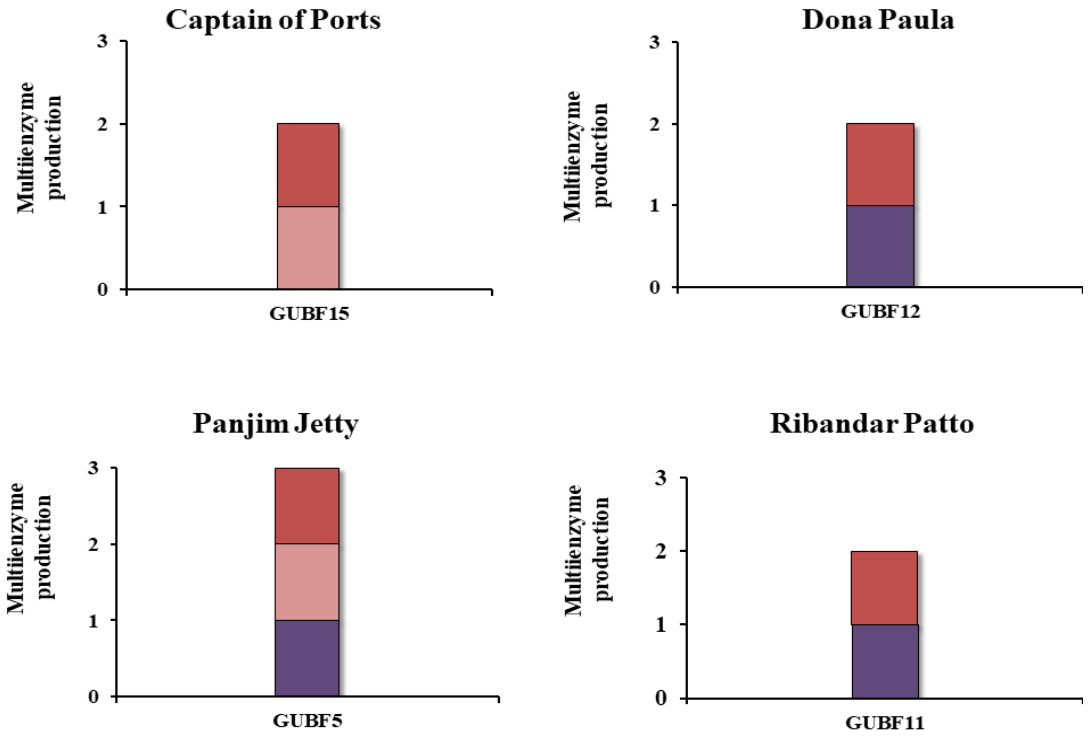

Fig. 2.26 C: Multienzyme production; amylase lipase aromatic oxygenases in different sampling sites

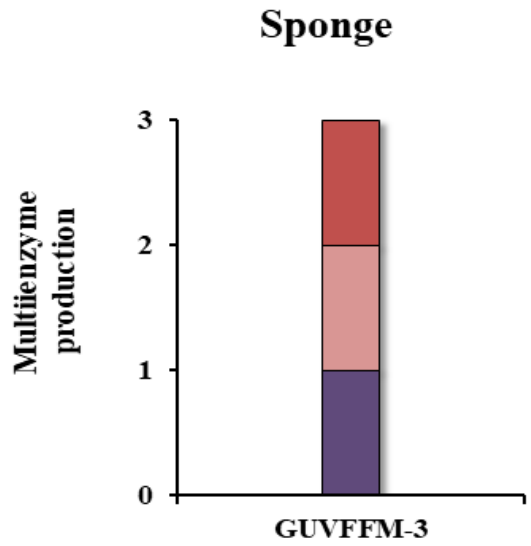

Fig. 2.26 D: Multienzyme production; amylase lipase aromatic oxygenase in sponge culture

2.2.5 GROWTH STUDIES OF *Haloferax volcanii* GUIF2 (MH169338) IN HYDROCARBONS

2.2.5.1 Growth and pigmentation in hydrocarbons

As seen in **Fig. 2.27 A**, the culture grew in NTYE without lag phase, and reached an exponential phase in 10 d, attaining an absorbance of 2.2 after which it reached the stationary phase. The culture had a light orange coloration by day 3 and which deepened to a bright orange red on further incubation. Similarly, in presence of 0.1 % of petrol, benzene and engine oil in NTYE, the culture reached the stationary phase on day 11, attaining an absorbance of 2.015, 2.145 and 2.144 respectively. Maximum growth in the presence of lindane was 2.005 on day 10 and then attained stationary phase. When grown in NTYE, the pigment extract of GUIF2 showed absorption peaks at 316, 367, 385, 459, 489 and 522nm. Some of these peaks were shifted or abolished when the culture was grown in NTYE with the different hydrocarbons. The pigment profile of the culture grown in the presence of petrol showed peaks at 317, 368, 385, 465, 489, 521 nm. The pigment profile of the culture grown in the presence of lindane showed peaks at 317, 368, 386, 492, 524 nm. The pigment profile of the culture grown in the presence of castrol showed peaks at 316, 364, 385, 492, 523 nm. The pigment profile of the culture grown in the presence of benzene showed peaks at 317, 368, 385, 465, 489, and 521 nm **(Fig. 2.27 B)**.

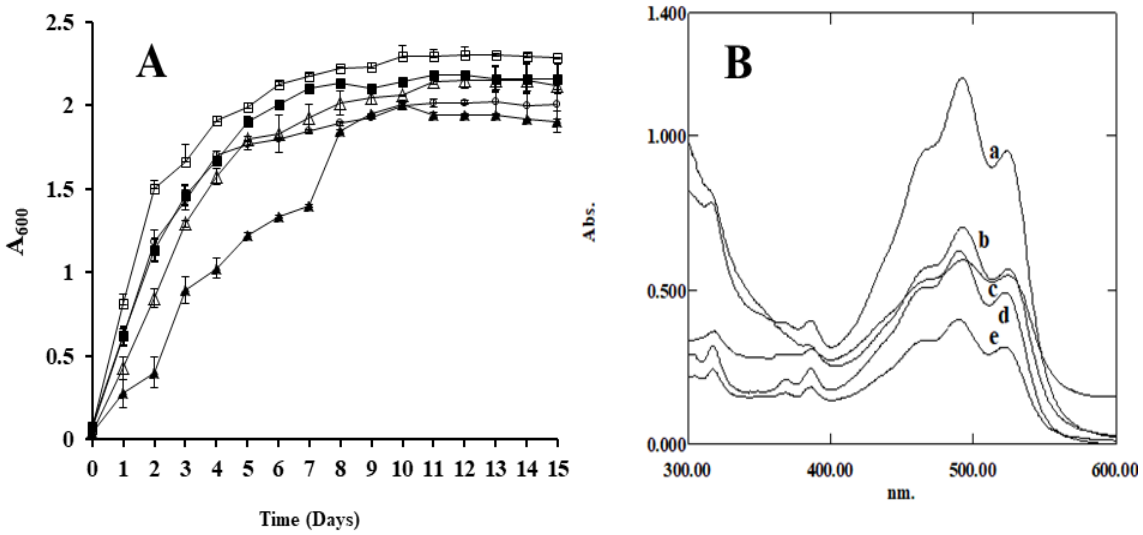

Fig. 2.27 A: Growth profile of *Haloferax volcanii* GUIF2 (MH169338) inNTYE —□— NTYE + 0.1% petrol —○—; NTYE + 0.1% benzene —■—NTYE + 0.1% lindane —▲— and NTYE + 0.1% Castrol —△— **B:** Pigment profile of GUIF2 in **a:** NTYE and NTYE with different hydrocarbons; **b:** petrol; **c:** lindane **d:** castrol **e:** benzene

When grown with glucose as sole source of carbon and energy, it steadily grew with a maximum OD of 0.75 till day 8 after which growth remained steady (**Fig. 2.28 A)**. When grown in mineral medium with crude oil, the OD increased till 0.16 in the first two days after which there was no further rise in absorbance. Similar growth pattern was seen when grown in mineral medium with hydrocarbons like benzene, engine oil and lindane. The pigment of the culture grown in mineral medium with NSM with 0.1% glucose, showed peaks at 364, 386, 491 and 523. No peaks were seen in the absorption spectrum of pigment of the culture when grown in NSM with 0.1% petrol. When grown in NSM with 0.1% lindane, peaks were seen at 340, 468, 496 and 529 nm. When grown in NSM with 0.1% castrol, all peaks were seen to be abolished from 300 to 600 nm. The pigment profile of the culture when grown in NSM with 0.1 % benzene peaks showed the presence of only one peak at 514 nm (**Fig. 2.28 B)**.

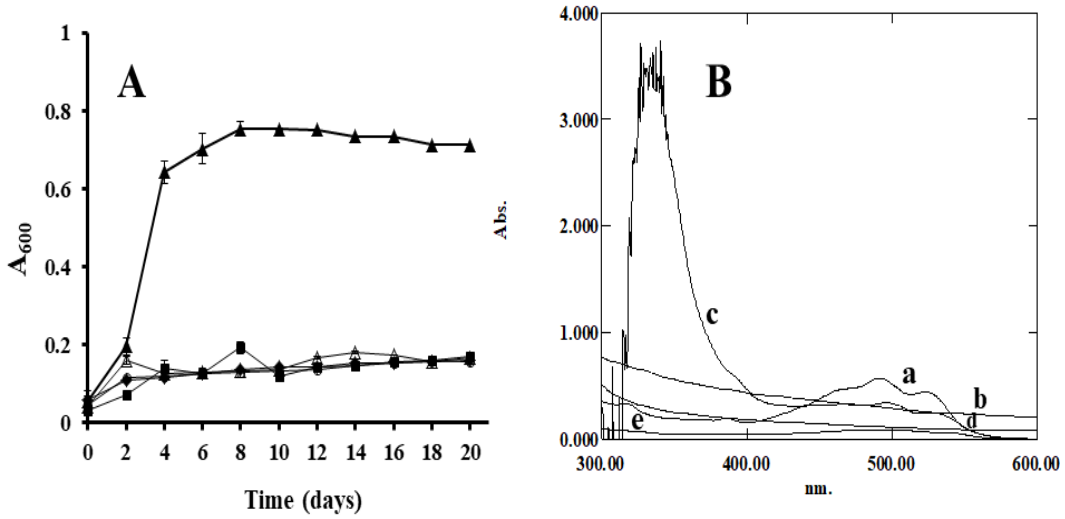

Fig. 2.28 A: Growth profile of *Haloferax volcanii* GUIF2 (MH169338) in NSM with; NSM + 0.1% glucose —▲—; NSM + 0.1% petrol —△—; NSM + 0.1% benzene —○— NSM + 0.1% Castrol —■— ; NSM + 0.1 % lindane —▲— ; **B:** Pigment profile of GUIF2 in **a:** NSM and 0.1% glucose and NSM with different hydrocarbons; **b:** petrol **c:** lindane **d:** castrol **e:** benzene

2.2.5.2 Effect of sodium benzoate on growth and pigmentation of *Haloferax volcanii* GUIF2 (MH169338)

As depicted in **Fig. 2.29 A**, the culture reached maximum growth on the seventh day with absorbance of 1.23 in NSM with 0.1% glucose, while in SBNSM, it reached maximum growth on the eight day with absorbance of 1.123. Growth in SBNSM was accompanied by formation of a brown coloration in the medium from day 2 of incubation, while the culture growing in NSM with 0.1% glucose showed a pink colouration **(Fig. 2.29 B)**. The pigment of the cells grown in NSM with 0.1% glucose, showed peaks at 317, 368, 364, 385, 465, 489 and while the pigment scan of cells grown in SBNSM showed only the presence of peak at 346 **(Fig. 2.29 C)**.

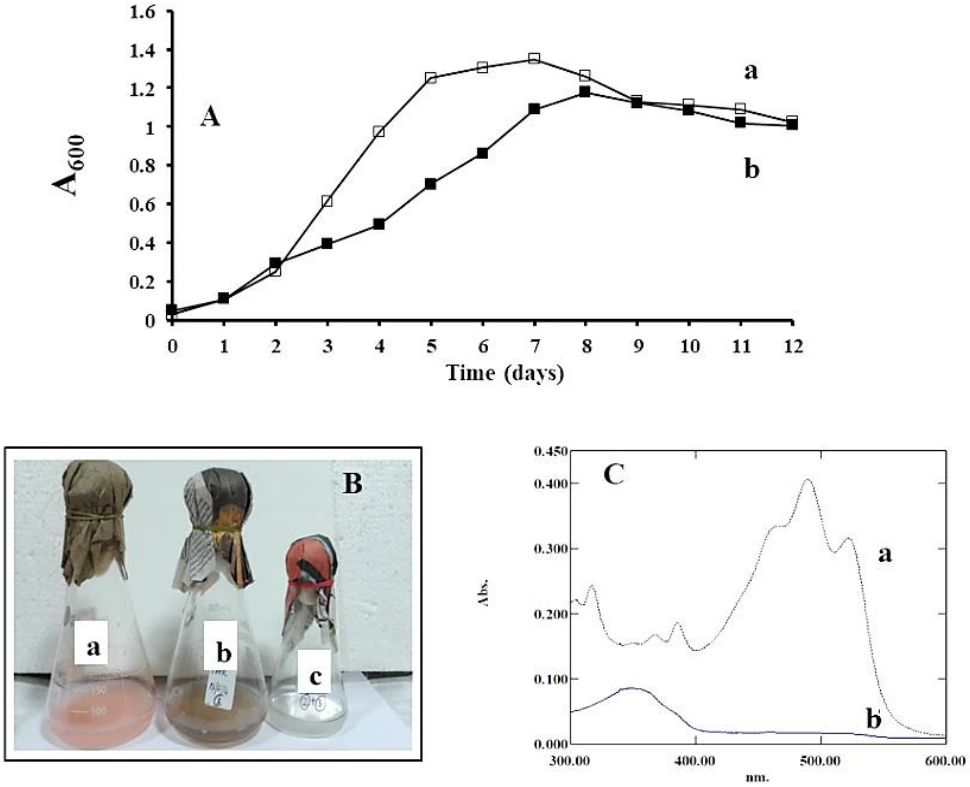

Fig. 2.29 A: Growth of *Haloferax volcanii* GUIF2 (MH169338) in **a:** NSM with 0.1% glucose; **b:** SBNSM **B:** Pigmentation developing during growth of *Haloferax volcanii* GUIF2 (MH169338) in **a:** NSM with 0.1% glucose; **b:** SBNSM; **c:** control flask of SBNSM **C:** Pigment scan of *Haloferax volcanii* GUIF2 (MH169338) grown in **a:** NSM with 0.1% glucose; **b:** grown in SBNSM

2.2.5.3 Sodium benzoate degradation by *Haloferax volcanii* GUIF2 (MH169338)

The cell lysate of *Haloferax volcanii* GUIF2 (MH169338) gave a pink colouration with nitrite molybdate reagent indicating that sodium benzoate was degrading to catechol (163 µg ml^{-1}). On further incubation with ammonium sulphate, sodium nitroprusside and ammonia the development of purple colour indicates a positive ortho cleavage. There was no purple colour developed in the control tube on addition on ammonium sulphate, sodium nitroprusside and ammonia **(Fig. 2.30 A)**

Rothera test results showed that *Haloferax volcanii* GUIF2 (MH169338) could degrade catechol by the ortho cleavage of the β- ketoadipate pathway because it gave a purple colour. Therefore, after determining the presence of the enzymes by using Rothera test, the activity of the enzyme Catechol 1, 2-dioxygenase was spectrophotometrically monitored for 100 min by tracking the formation of the product at 260 nm. The activity of catechol 1, 2 dioxygenase enzyme in the cell free extract increased linearly till 60 min after which it remained steady till 100 min of reaction time indicating degradation through the ortho cleavage pathway **(Fig. 2.30 B)**. The protein concentration of the cell lysate was found to be 813 µg ml^{-1}.

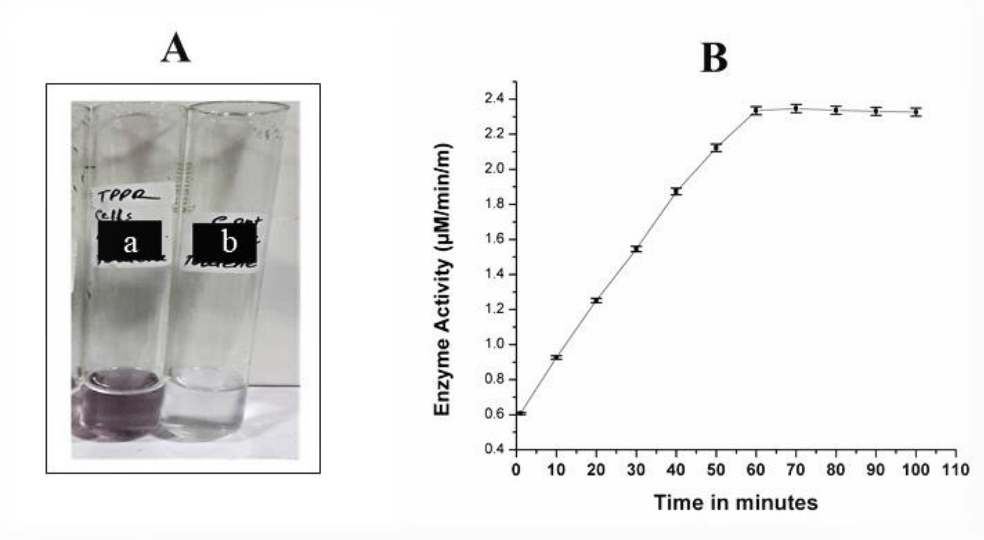

Fig. 2.30 Sodium degradation in *Haloferax volcanii* GUIF2 (MH169338)**; A:** Rothera's test with cells grown in **a:** SBNSM **b:** control; **B:** Catechol 1, 2 Dioxygenase enzyme assay in 50 mM Tris- HCl buffer (pH 8.0) with cell lysate of *Haloferax volcanii* GUIF2 (MH169338) grown in SBNSM of 7 d

SECTION B: BIOPROSPECTING FOR PRODUCTION OF ANTAGONISM AMONG HALOARCHAEA

2.2.6 ANTIMICROBIAL ACTIVITY OF HALOARCHAEA V/S HUMAN PATHOGENS

Of the 30 cultures screened for antimicrobial activity, only 6 cultures were positive for antimicrobial activity as seen by clearing observed around the wells which was loaded with culture broth of the haloarchaeal cultures **(Fig. 2.31)**.

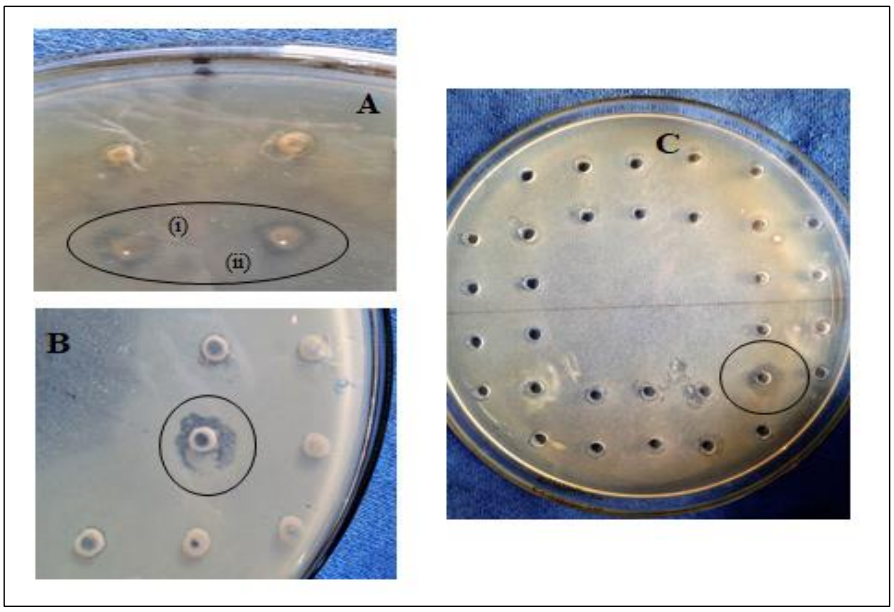

Fig. 2.31 A: Clearing seen around the well as a indication of antibacterial activity **i.** GUIF2 and **ii.** GUIF4 v/s *C. albicans* 10231 **B:** $GUFF_{82}$ against *S. typhimurium* ATCC 14028 and **C:** $GUBF_5$ v/s *C. albicans* 10231

Antibacterial activity in terms of zone of inhibition against ATCC pathogens is depicted in **Fig. 2.32**. Of the 30 haloarchaeal cultures screened for antimicrobial activity, only 6 cultures were positive for activity (**Table 2.7**). Of the eight pathogens tested *S. epidermidis* ATCC 12228, *B. subtilis* ATCC 6633, *E. coli* ATCC 8739, *Ps. aeruginosa* ATCC 9027 were not inhibited by any of the cultures. The sizes of zone of inhibition observed were 8-12 mm. $GUFF_{82}$ inhibited *S. typhimurium* ATCC 14028 with a zone size of 11 mm while $GUFF_{231}$ inhibited *S. aureus* ATCC 6538 with a

zone size of 9 mm, respectively. GUIF2 inhibited the growth of *S. abony* ATCC 6017 with a zone size of 12, whereas GUIF4 and GUIF5 and $GUBF_5$ inhibited *C. albicans* with a zone size of 12, 8 and 13 mm respectively.

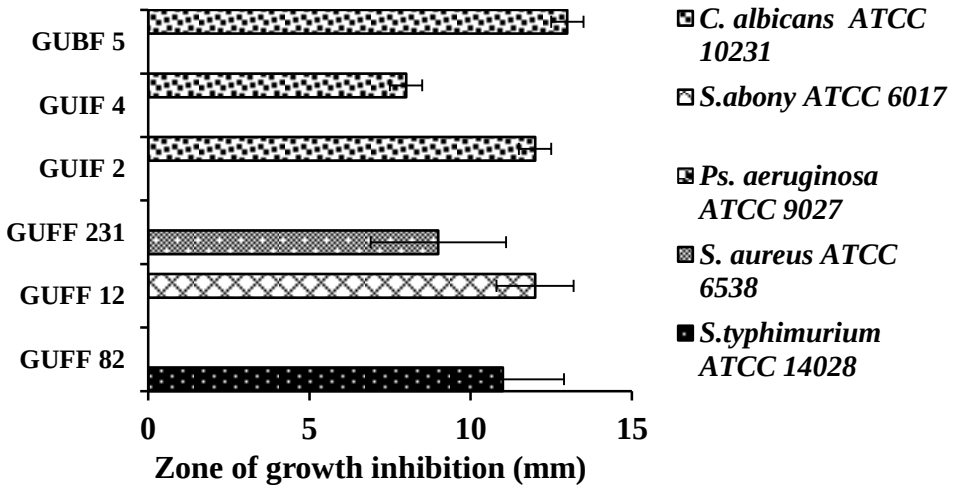

Fig. 2.32 Inhibition of growth of human pathogens by haloarchaeal cultures

The calculated POISES indicated that 25% of pathogens were inhibited by haloarchaeal cultures from solar salt of Siridao and estuarine sediments of Betim Jetty while a score of 13% of pathogens were inhibited by cultures from the solar salt sample of Nerul and estuarine sediment of Panjim Jetty (**Fig. 2.33)**. Further, the Percent overall screening efficiency score of the antimicrobial assay (POSES) was computed for all sampling sites with cultures showing antimicrobial activity. A 100% score was obtained for the cultures from the estuarine sediments of Panjim Jetty followed by 50% for cultures from solar salt of Nerul, 40% for the cultures from solar salt of Siridao and 25% for cultures from the estuarine sediments of Betim Jetty **(Fig. 2.33)**.

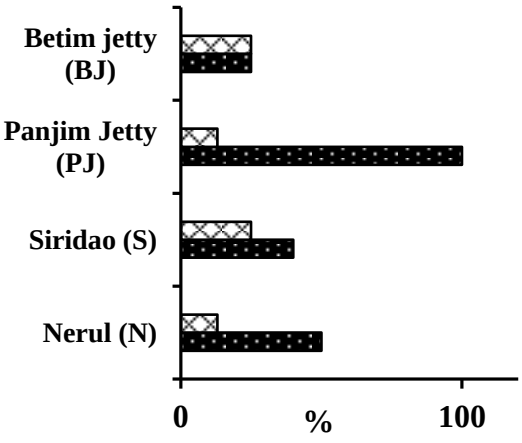

Fig. 2.33 Percent Overall Inhibition Screening Efficiency Score (▨ POISES) and Percent Overall Screening Efficiency Score (■ POSES) for antibacterial activity present in solar salts and estuarine sediments

Table 2.7 Haloarchaeal cultures from solar salts and estuarine sediments inhibiting growth of human pathogens

Culture Designation	*S.typhimurium* ATCC 14028	*S. aureus* ATCC 6538	*B. subtilis* ATCC 6633	*E. coli* ATCC 8739	*Ps. aeruginosa* ATCC 9027	*S. abony* ATCC 6017	*S. epidermidis* ATCC 12228	*C. albicans* ATCC 10231
$GUBF_1$	-	-	-	-	-	-	-	-
$GUBF_2$	-	-	-	-	-	-	-	-
$GUBF_3$	-	-	-	-	-	-	-	-
$GUBF_5$	-	-	-	-	-	-	-	13 mm
$GUBF_{10}$	-	-	-	-	-	-	-	-
$GUBF_{11}$	-	-	-	-	-	-	-	-
$GUBF_{15}$	-	-	-	-	-	-	-	-
$GUBF_{20}$	-	-	-	-	-	-	-	-
GUSF-1	-	-	-	-	-	-	-	-
GUSF	-	-	-	-	-	-	-	-
$GUFLF_3$	-	-	-	-	-	-	-	-
$GUFLF_{14}$	-	-	-	-	-	-	-	-
$GUFLF_{16}$	-	-	-	-	-	-	-	-
$GUFLF_{18}$	-	-	-	-	-	-	-	-
$GUFF_{10}$	-	-	-	-	-	-	-	-
$GUFF_{12}$	-	-	-	-	-	12 mm	-	-
$GUFF_{34}$	-	-	-	-	-	-	-	-
$GUFF_{41}$	-	-	-	-	-	-	-	-
$GUFF_{58}$	-	-	-	-	-	-	-	-
$GUFF_{72}$	-	-	-	-	-	-	-	-
$GUFF_{82}$	11 mm	-	-	-	-	-	-	-
$GUFF_{88}$	-	-	-	-	-	-	-	-
$GUFF_{148}$	-	-	-	-	-	-	-	-
$GUFF_{188}$	-	-	-	-	-	-	-	-
$GUFF_{231}$	-	9 mm	-	-	-	-	-	-
$GUFF_{233}$	-	-	-	-	-	-	-	
$GUIF_5$	-	-	-	-	-	-	-	-
$GUIF_2$	-	-	-	-	-	-	-	12 mm
$GUIF_3$	-		-	-	-	-	-	-
$GUIF_4$	-	-	-	-	-	-	-	8 mm

2.2.7 Antagonism (halocin production) v/s haloarchaeal cultures

We studied production of halocin among 30 haloarchaeal cultures using the agar overlay method. The culture that produce the kill effect was termed as **Producers**, while the culture that was killed due to the antagonistic effect was termed as **Indicators**. Twenty two (73%) cultures were seen to be antagonistic as seen by the appearance of a clearing around the spotted culture **(Fig. 2.34)**. The remaining 8 (28%) cultures did not produce any inhibitory activity. The diameters of the inhibitory zones varied from a minimum of 7 mm, produced by $GUFF_{82}$ against $GUFLF_{18}$ to a maximum of 36 mm produced by $GUBF_{10}$ against culture GUIF4 **(Table 2.8; Fig. 2.35 A & B).** Fourteen of the cultures were sensitive to the inhibitory substance produced by the producers while 16 cultures were not sensitive to any of the inhibitory substance produced. Eight cultures neither produced any inhibition nor were sensitive to any of the produced antagonistic molecules. The culture $GUBF_{10}$ was seen to kill 7 indicators; ($GUBF_{20}$, $GUBF_3$, $GUBF_5$, $GUBF_2$, $GUIF_3$, $GUFF_{188}$ and GUIF4), with zone sizes varying from 16-36 mm, followed by GUSF-1 and $GUFLF_{14}$, both targeting 5 indicator cultures ($GUBF_3$, $GUBF_5$, $GUBF_{20}$, $GUFF_{82}$, $GUFLF_3$,) and ($GUBF_3$, $GUBF_5$, $GUBF_{20}$, $GUFF_{82}$, GUIF4) with zone sizes from 14-34 mm. The remaining producers were seen to target 4, 3, 2 and 1 indicator cultures. The cultures GUIF4 and $GUBF_3$ was targeted by 10 different producers ($GUBF_1$, $GUBF_2$, $GUBF_3$, $GUBF_5$, $GUBF_{10}$, $GUBF_{15}$, $GUBF_{20}$, $GUFLF_{14}$, $GUFLF_{18}$, $GUIF_3$) and ($GUBF_1$, $GUBF_2$, $GUBF_5$, $GUBF_{10}$, $GUBF_{15}$, GUSF-1, $GUFLF_{14}$, $GUFLF_{16}$, $GUIF_3$, $GUIF_4$). The growth of culture $GUBF_5$ was inhibited by 8 different producers ($GUBF_2$, $GUBF_{10}$, $GUBF_{15}$, GUSF-1, $GUFLF_{14}$, $GUFLF_{16}$, $GUFLF_{18}$ and GUIF3), while the culture $GUFF_{188}$ was inhibited by 6 different producers ($GUBF_{10}$, $GUBF_{11}$, $GUFF_{12}$, $GUFF_{41}$, $GUFF_{82}$, $GUFF_{233}$ and $GUIF_4$). The other indicator cultures were targeted by 1, 2, 3, 4 and 5 producers respectively. The producers were from solar salts; Arambol, Agarwada, Nerul, Ribandar, Siridao and estuarine sediments; Baiguimin, Betim Jetty, Captain of ports, Panjim Jetty, Ribandar Patto and belonged to *Haloferax*, *Halobacterium*, *Haloarcula*, *Halorubrum*, *Natrinema*, *Natronococcus* and *Natrialba* genera. The indicators were from solar salts; Agarwada (Ag), Nerul (N) Ribandar (R) Siridao (S) and estuarine sediments; Betim Jetty (BJ) and Panjim Jetty (PJ) and belonged to *Haloferax*, *Halobacterium*, *Haloarcula* and *Natrinema* genera.

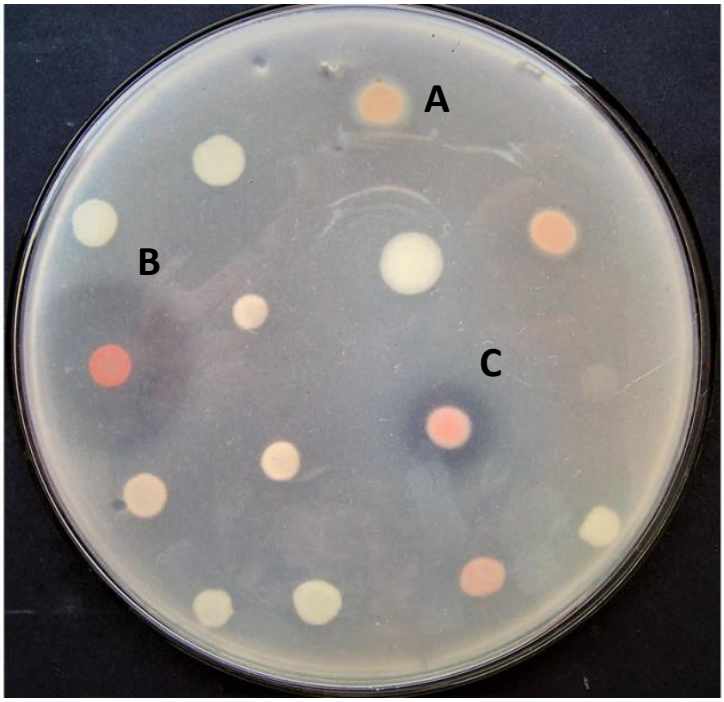

Fig. 2.34 Zone of clearing seen an indication of antagonism (halocin production). The indicator used is GUIF4 and cultures **A:** $GUBF_3$ **B:** $GUBF_{10}$ and **C:** $GUBF_5$ producers of antagonism indicated by the clearing around the spotted colony

Table 2.8 Haloarchaeal cultures (producers) from solar salts and estuarine sediments inhibiting growth of haloarchaeal cultures (indicators) from solar salts and estuarine sediments

		PRODUCERS CULTURES																				
INDICATOR CULTURES ↓		A	Ag		N	R					S			B	BJ						CP	PJ	RP
		GUFF$_{41}$	**GUFF$_{148}$**	**GUFF$_{188}$**	**GUFF$_{82}$**	**GUBF$_{1}$**	**GUBF$_{1}$**	**GUBF$_{3}$**	**GUBF$_{20}$**	**GUFF $_{72}$**	**GUSF-1**	**GUFF$_{12}$**	**GUFF$_{233}$**	**GUBF$_{10}$**	**GUFLF$_{3}$**	**GUFLF$_{14}$**	**GUFLF$_{16}$**	**GUFLF$_{18}$**	**GUIF$_{3}$**	**GUIF$_{4}$**	**GUB$_{15}$**	**GUBF$_{5}$**	**GUBF$_{11}$**
Ag	**GUFF$_{188}$**	19			20							22	19	25						17			12
	GUFF$_{82}$										17					14							
	GUFF$_{88}$		17																				
	GUBF$_{2}$								33					20					20			10	11
	GUBF$_{3}$					24	29				34			18		25	32		35	26	25	23	
	GUBF$_{20}$					21					21			16		19							
	GUSF-1				12		22	12															
	GUFLF$_{3}$										33												
	GUFLF$_{14}$											17											
	GUFLF$_{16}$	12								17		13											
	GUFLF$_{18}$			12	7										16								
BJ	**GUIF$_{3}$**													23							25		
	GUIF$_{4}$					26	22	13	31					**36**		30		18	23		35	14	
PJ	**GUBF$_{5}$**						17				16			18		17	21	16	22		21		

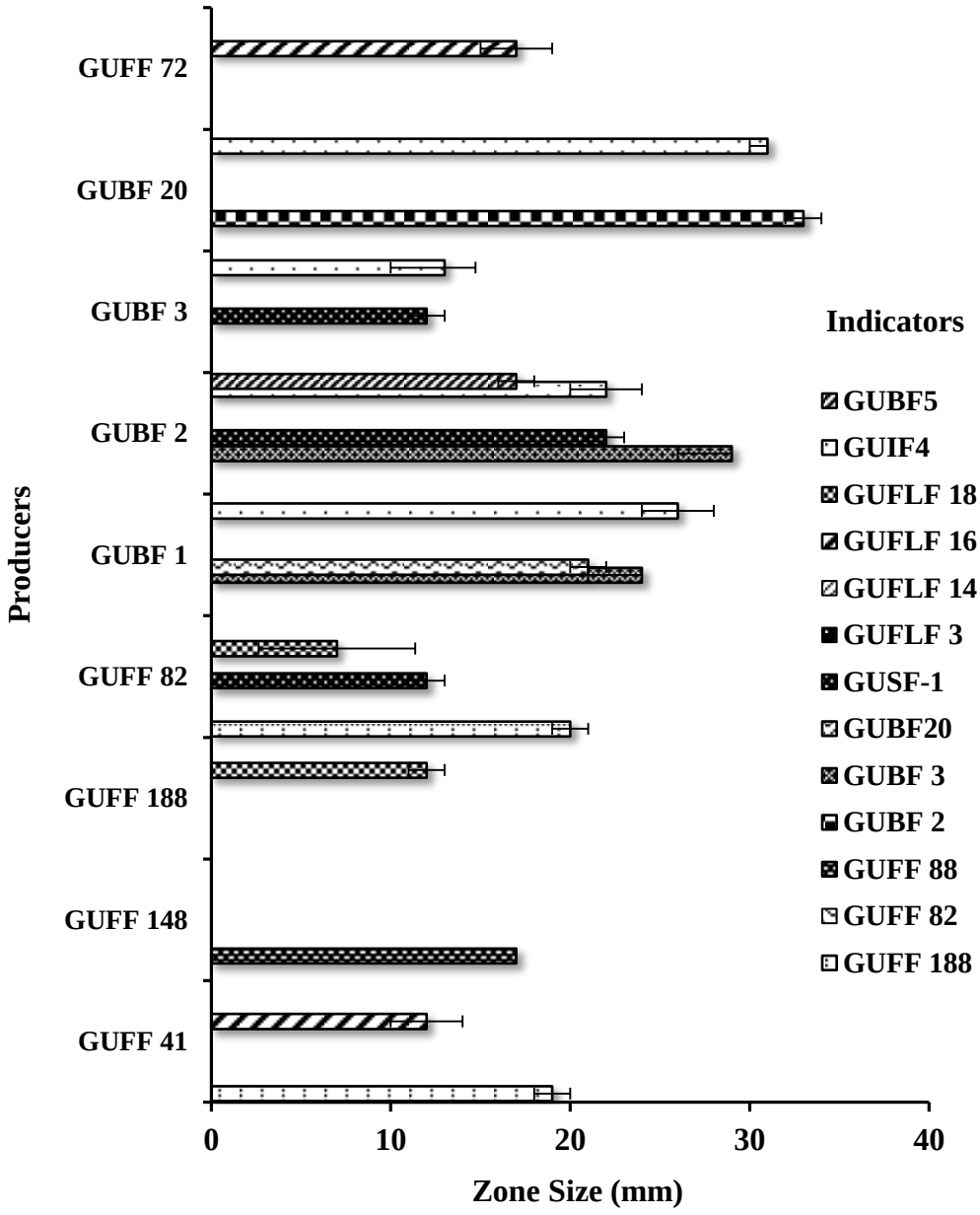

Fig. 2.35 A: Range of zone sizes (mean ± SD) produced by the producers v/s indicators, obtained from the zones of clearing seen around the producer cultures using the agar overlay method

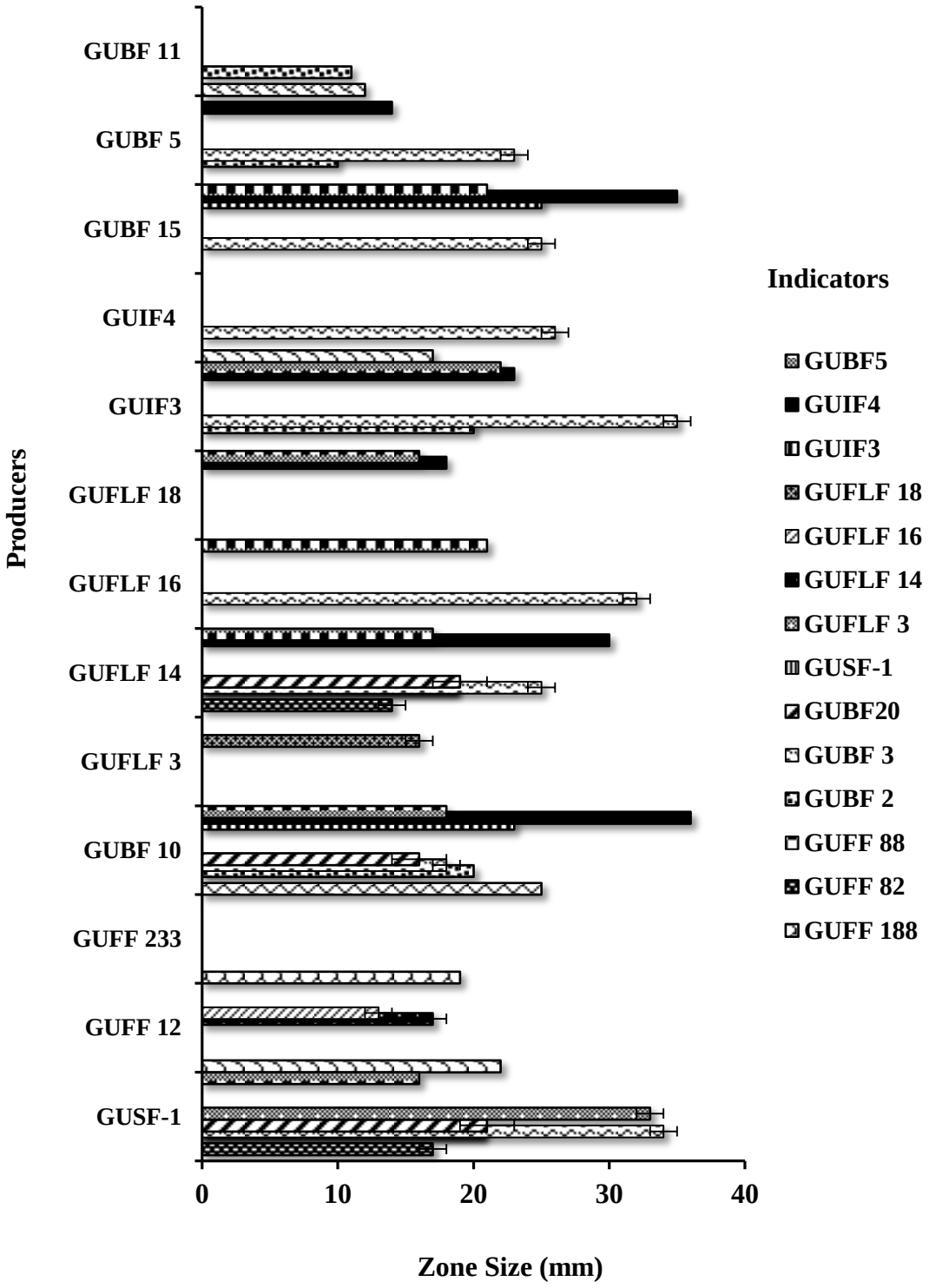

Fig. 2.35 B: Range of zone sizes (mean ± SD) produced by the producers v/s indicators, obtained from the zones of clearing seen around the producer colonies using the agar overlay method

Except for the culture $GUFF_{41}$ from the Arpora sampling site which neither produced any inhibition nor was sensitive to any of the produced inhibitory substance, all other cultures from the remaining 10 sampling sites interacted with cultures from their own sampling sites as well with cultures from any one of the other 9 sampling sites. There were a total of 60 interactions among the cultures, with 19 interactions between cultures belonging to *Haloferax* and 4 interactions between cultures belonging to *Halobacterium*. The highest POSES score of 100 % was obtained for the cultures from Arambol and Ribandar solar salts and estuarine sediments of Baiguinim, Captain of Ports, Panjim Jetty and Ribandar Patto. Cultures from solar salts of Agarwada and Siridao gave an equal score of 67%. Score of 50% was obtained for cultures from solar salt of Nerul. Cultures from the estuarine sediment sample of Betim Jetty gave a score of 75%. The POIES score indicated that 100% of haloarchaeal cultures were inhibited by the isolates from the solar salt sample of Nerul, Siridao and Panjim Jetty and 75% of haloarchaeal cultures were inhibited by the cultures from estuarine sediment sample of Betim Jetty. The cultures from the solar salt sample of Ribandar and Agarwada inhibited 50% and 33% respectively of haloarchaeal cultures respectively (**Fig. 2.36**).

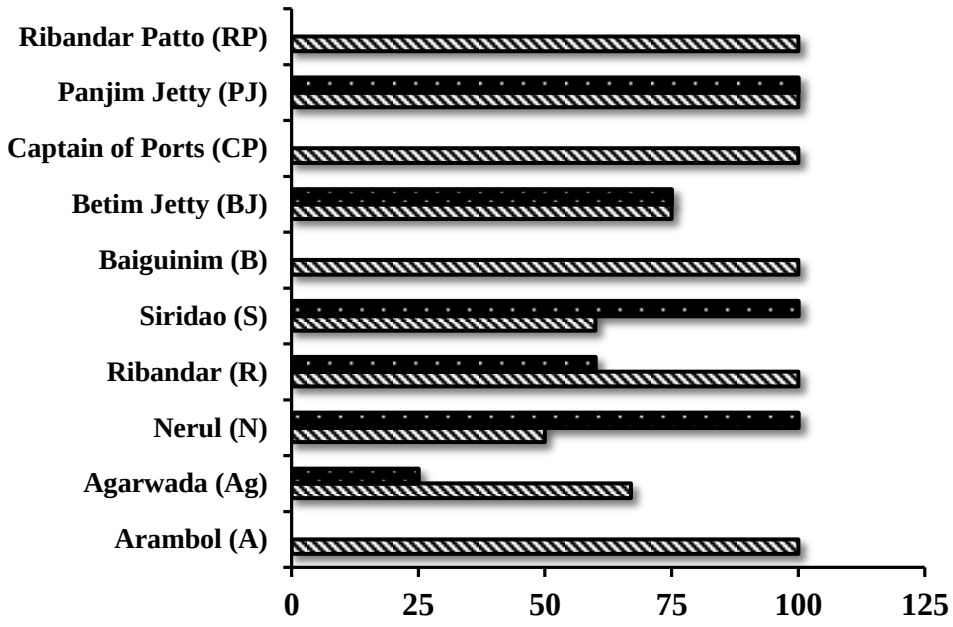

Fig. 2.36 Percent Overall Inhibition Efficiency Score (▨ POIES) and the Percent Overall Screening Efficiency Score (■ POSES) exhibited by cultures

Presence of halocin producing cultures belonging to different genera differed among samples from different sampling sites **(Fig. 2.37)**. The maximum of 2 genera were found in Arambol, Agarwada, Ribandar, Siridao, Captain of Ports, while a single genera was found in solar salt sample of Nerul and in sediments from Betim Jetty, Baiguinim, Panjim Jetty and Ribandar Patto. Ocurrence of cultures with antagonistic activity was: *Haloferax* > *Halobacterium* > *Haloarcula*> *Halorubrum* = *Natrialba* = *Natrinema* = *Natronococcus*

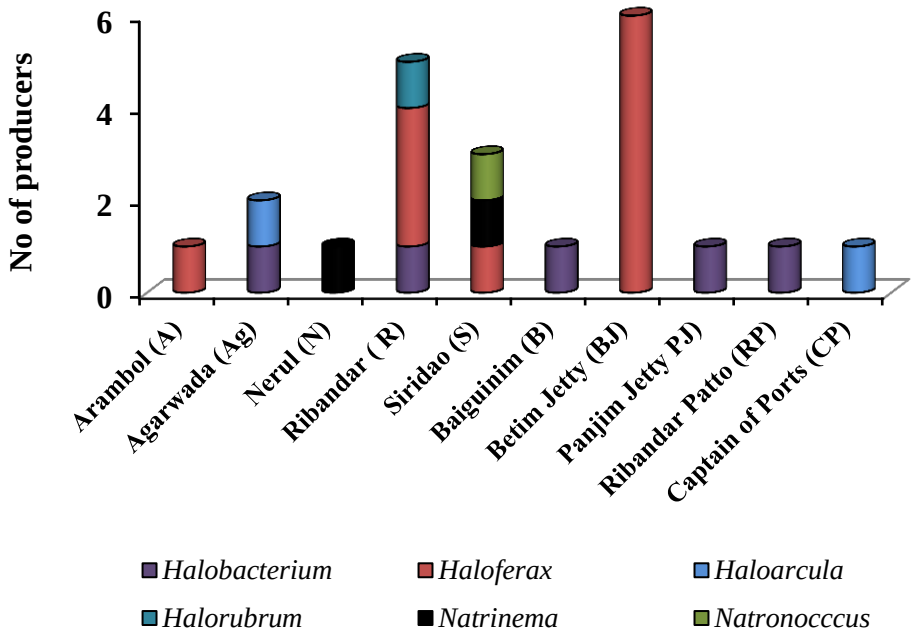

Fig. 2.37 Antagonism (halocin production) producing genera present in different solar salts and estuarine sediments

SECTION C: BIOPROSPECTING FOR PRODUCTION OF PROTOGONISM

2.2.8 Enhanced growth of human pathogens in the presence of haloarchaeal cultures

Protogonistic activity in terms of zone of exhibition against ATCC human pathogens is depicted in **Fig. 2.38**. A total of 27 cultures were positive for protogonistic activity towards two pathogens as seen by increased growth zones around the wells which were loaded with culture broth of the haloarchaeal cultures. Of the eight pathogens tested, only the growth of *E. coli* ATCC 8739 and *S.abony* ATCC 6017 was seen to be exhibited. Zones of exhibition ranged from 7- 25 mm. From the 30 cultures screened for protogonistic activity, 22 cultures were found to be showing zones of growth exhibition against *E.coli* ATCC 8739 and 27 cultures showed zones of growth exhibition against *S. abony* ATCC 6017. To rule out the possibility that NTYE medium would promote growth of the human pathogens, *E. coli* ATCC 8739 and *S.abony* ATCC 6017, they were separately inoculated in NTYE and grown at 37°C, but they failed to grow **(Fig. 2.38).**

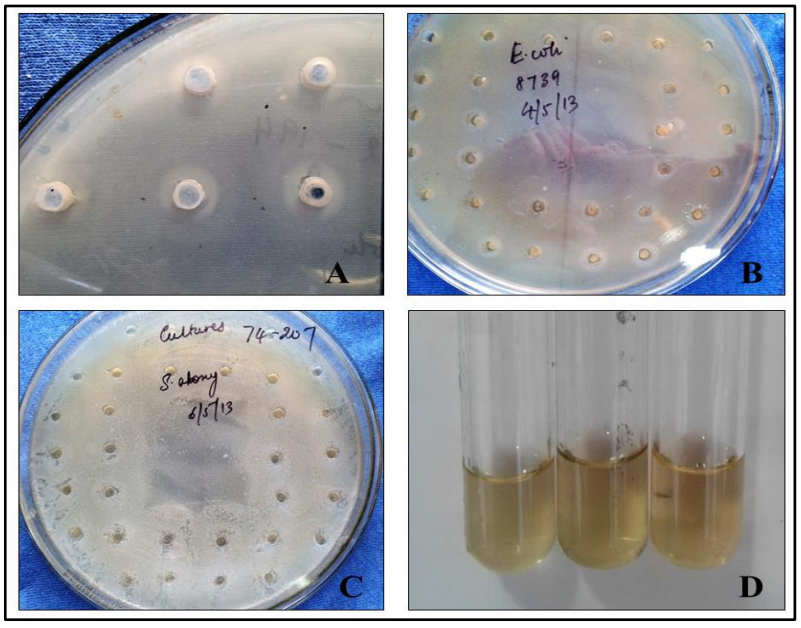

Fig. 2.38 Protogonistic activity of haloarchaeal cultures towards **A** and **B:** *E. coli* ATCC 8739 and **C:** *S.abony* ATCC 6017 **D:** Control of NTYE and *E. coli* ATCC 8739 and *S.abony* ATCC 6017 growing in NTYE respectively

The zones of growth exhibition against *E.coli* ATCC 8739 varied from a minimum of 7 mm exhibited by GUSF and GUSF-1 to a maximum of 12 mm by $GUFLF_3$, $GUFLF_{14}$, $GUFLF_{18}$ and $GUFF_{12}$ respectively. The zones of growth exhibition against *S. abony* ATCC 6017 varied from a minimum of 7 mm exhibited by $GUBF_{11}$, $GUBF_{15}$, GUSF and $GUFLF_3$ to a maximum of 25 mm $GUFF_{88}$ and $GUBF_5$ respectively **(Table 2.9; Fig. 2.39).**

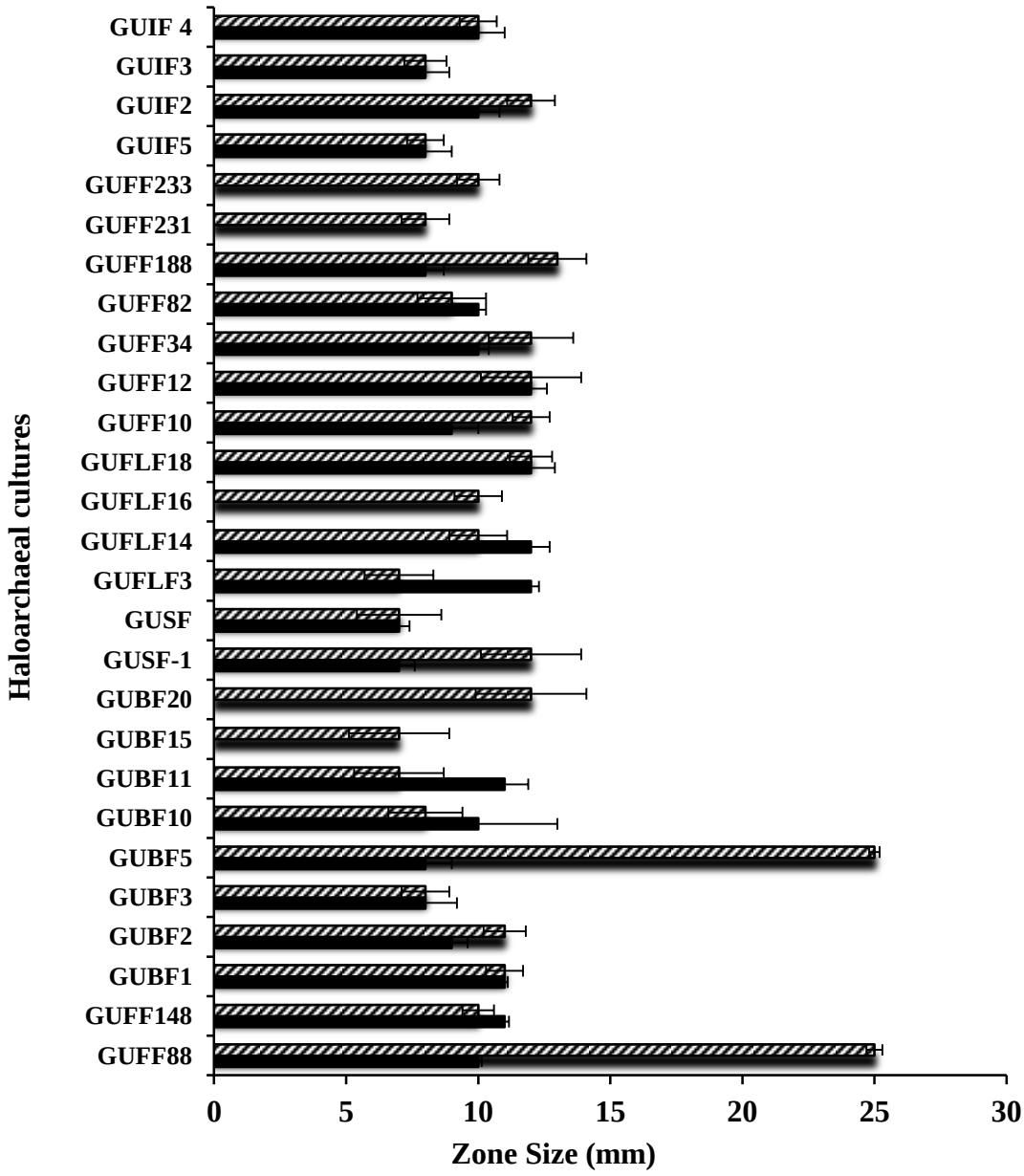

Fig. 2.39 Haloarchaeal cultures exhibiting protogonistic activity present in solar salts and estuarine sediments towards human pathogens; *S. abony* ATCC 6017 ▨ and *E. coli* ATCC 8739 ■

Table 2.9 Haloarchaeal cultures from solar salts and estuarine sediments exhibiting growth of human pathogens

Culture Designation	*S.typhimurium* ATCC 14028	*S. aureus* ATCC 6538	*B. subtilis* ATCC 6633	*E. coli* ATCC 8739	*Ps. aeruginosa* ATCC 9027	*S.abony* ATCC 6017	*S.epidermidis* ATCC 12228	*C. albicans* ATCC 10231
$GUFF_{148}$	-	-	-	11	-	10	-	-
$GUBF_{1}$	-	-	-	11	-	11	-	-
$GUBF_{2}$	-	-	-	9	-	11	-	-
$GUBF_{3}$	-	-	-	8	-	8	-	-
$GUBF_{5}$	-	-	-	8	-	25	-	-
$GUBF_{10}$	-	-	-	10	-	8	-	-
$GUBF_{11}$	-	-	-	11	-	7	-	-
$GUBF_{15}$	-	-	-	-	-	7	-	-
$GUBF_{20}$	-	-	-	-	-	12	-	-
GUSF-1	-	-	-	7	-	12	-	-
GUSF	-	-	-	7	-	7	-	-
$GUFLF_{3}$	-	-	-	12	-	7	-	-
$GUFLF_{14}$	-	-	-	12	-	10	-	-
$GUFLF_{16}$	-	-	-	-	-	10	-	-
$GUFLF_{18}$	-	-	-	12	-	12	-	-
$GUFF_{10}$	-	-	-	9	-	12	-	-
$GUFF_{12}$	-	-	-	12	-	12	-	-
$GUFF_{34}$	-	-	-	10	-	12	-	-
$GUFF_{41}$	-	-	-	-	-	-	-	-
$GUFF_{58}$	-	-	-	-	-	-	-	-
$GUFF_{72}$	-	-	-	-	-	-	-	-
$GUFF_{82}$	-	-	-	10	-	9	-	-
$GUFF_{88}$	-	-	-	10	-	25	-	-
$GUFF_{148}$	-	-	-	11	-	10	-	-
$GUFF_{188}$	-	-	-	8	-	13	-	-
$GUFF_{231}$	-	-	-	-	-	8	-	-
$GUFF_{233}$	-	-	-	-	-	10	-	-
GUIF2	-	-	-	10	-	12	-	-
GUIF3	-	-	-	8	-	8	-	-
GUIF4	-	-	-	10	-	10	-	-
GUIF5	-	-	-	8	-	8	-	-

Percent overall screening efficiency score of the protagonistic activity was computed for all the cultures from all sampling sites showing exhibition of growth. A 100% score was obtained for the cultures from estuarine sediments of Baiginuim, Captain of Ports, Panjim Jetty and Ribandar Patto, followed by 60% for solar salt sample of Siridao and Ribandar, 50% for cultures from Nerul solar salt sample **(Fig. 2.40)**.

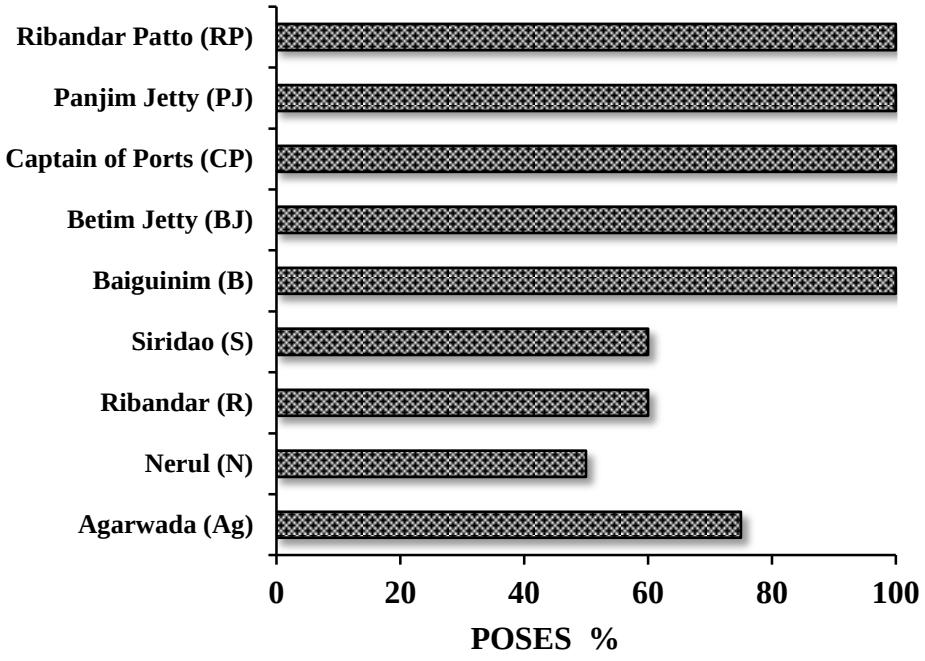

Fig. 2.40 Percent Overall Screening Efficiency Score (POSES) for protogonistic activity present in solar salts and estuarine sediments

2.2.9 EVALUATING THE ROLE OF METHANOLIC EXTRACT '*Hfx*E' OF *Haloferax alexndrinus.* GUSF-(KF796625) IN ALLEVIATION OF ARSENIC As(III) GENOTOXICITY

2.2.9.1 Single strand breaks in human lymphocytes and antigenotoxicity of *Hfx*E

Human lymphocytes, obtained from a healthy donor as per WHO guidelines, showed 90% viability by the trypan blue exclusion test. These HL as well as HL exposed to methanol when viewed under fluorescent microscope clearly showed intact DNA. By the end of 2 h of exposure to 10 µM As(III), the initial number of 10^7 HL was reduced to 65%, indicating the genotoxic effect of 10 µm As(III), resulting in comet like images due to the damage to DNA of HL by 10 µM As (III). HL exposed to 10 µM of As(III) showed mean % tail DNA of 82.43% ± 9.57. Addition of 25 µg ml^{-1} of *Hfx*E reduced the adverse effect of As(III) on viability of HL with accompaning decrease in size of the tail corresponding to reduction in the DNA damage by 68% with the mean % tail DNA of 26.06% ± 10.58. Increase of *Hfx*E to 50 µg ml^{-1}, further increased the viability of the cells to 76% and decreased the DNA damage by an additional 24% with a mean % tail DNA of 6.196 ± 2.80. Presence of same quantity of SeNPs instead of *Hfx*E, during exposure of HL to As(III) also exerted a protective effect and decreased the DNA damage by only 42% with % mean tail DNA of 47.84 ± 0.823 and increased the viable counts to 72% (**Fig. 2.41; Fig. 2.42**). Further, as seen in **Fig. 2.42**, the one-way ANOVA the *Hfx*E exerted protection with a highly significant variation of $F = 43.666$; $p<0.001$. Additionally, the Dunnets multi comparison post hoc analysis clearly ascertained that *Hfx*E exerted dose dependent protection to HL from As(III) and decreased the genotoxocity to HL by $p< 0.001$. Although a highly significant difference of $p<0.001$was observed between the % mean tail DNA of 25 µg ml^{-1} of *Hfx*E and SeNPs by the *t* test, the difference in % mean tail DNA between 50 µg ml^{-1} of *Hfx*E and SeNPs was statistically insignificant at $p > 0.1728$.

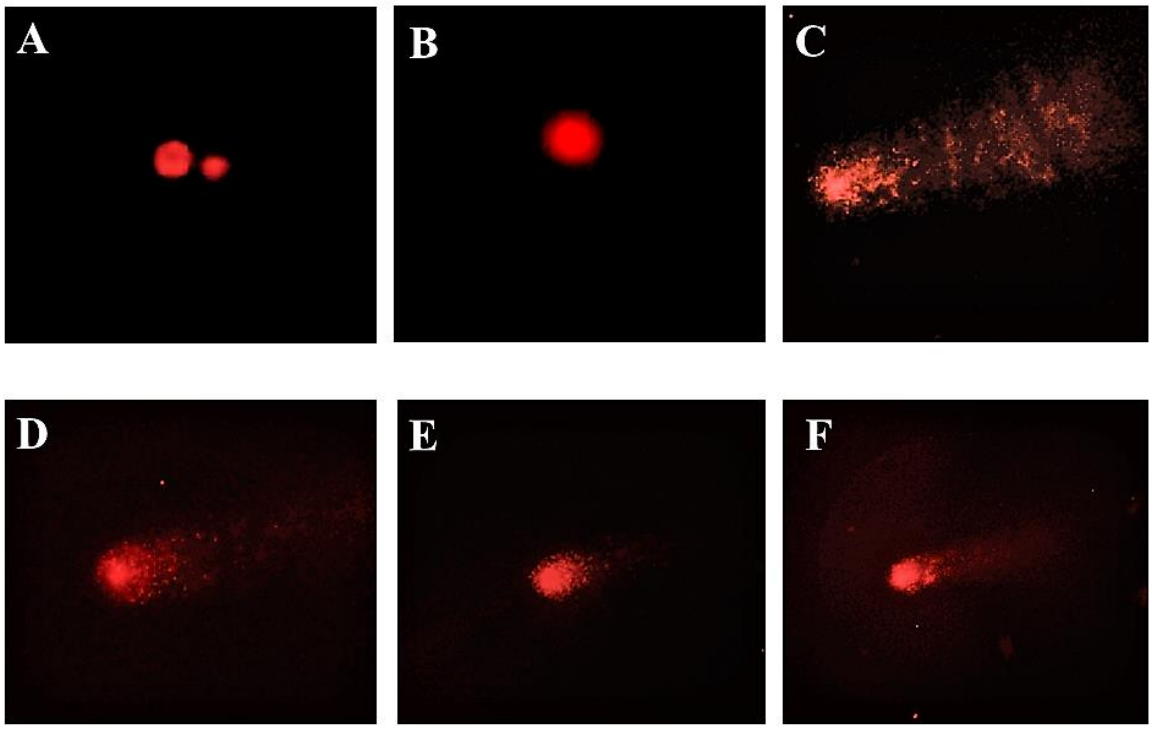

Fig. 2.41 Fluorescent micrographs of ethidium bromide stained agarose slides of human lymphocytes (HL) exposed to As(III), *Hfx*E and SeNPs. A. HL; HL exposed to: B. methanol; C. 10 µM As(III); D. 10 µM As(III) and 25 µg ml^{-1} of *Hfx*E; E. 10 µM As(III) and 50 µg ml^{-1} of *Hfx*E; F. 10 µM As(III) and 50 µg ml^{-1} of SeNPs

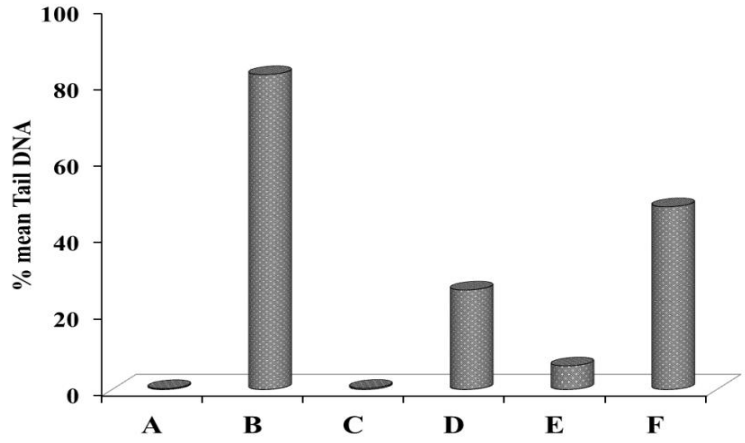

Fig. 2.42 Supression of As(III) DNA damage by *Hfx*E and SeNPs **A:** HL; **B:** 10 µM As(III); **C:** Methanol; **D:** 10 µM As(III) and 25 µg ml^{-1} of *Hfx*E; **E:** 10 µM As (III) and 50 µg ml^{-1} of *Hfx*E; **F:** 10 µM As(III) and 50 µg ml^{-1} of SeNPs. The DNA damage was evaluated by comet assay and expressed as % mean tail DNA

2.2.8.2 Spectral analysis and Thin Layer Chromatography of *Hfx*E

As seen in **Fig. 2.43 A**, the absorption spectra of *Hfx*E showed three fingered peaks at 464, 490 and 524 nm and two cis peaks at 368 and 386. The absorption spectra of *Hfx*E, recovered after incubation with HL and 10 µM As(III) revealed decrease in the intensity of the peaks at 464, 490 and 524 nm, while peaks from 300-400 nm were completely abolished as seen in **Fig. 2.43 B**.

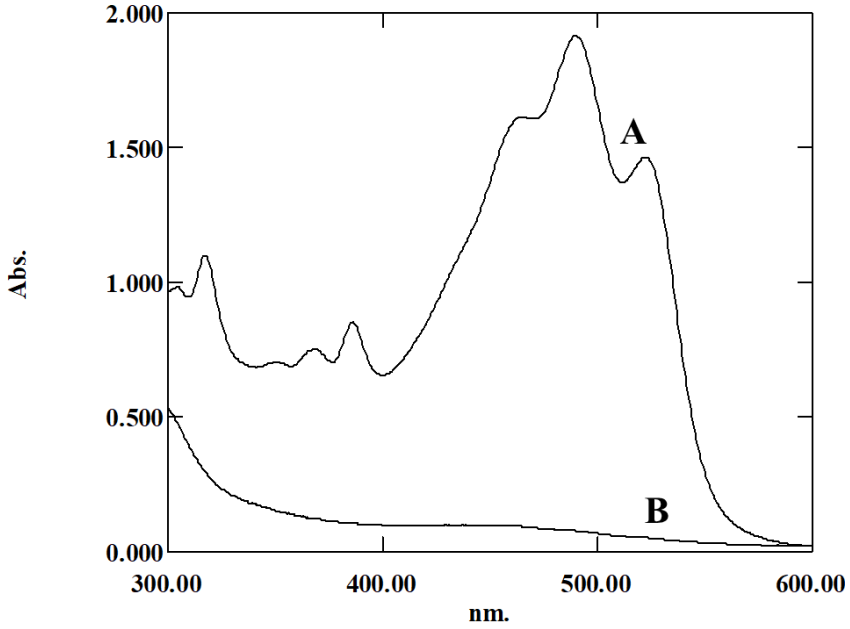

Fig. 2.43 Absorption scan of **A**: *Hfx*E and **B:** *Hfx*E recovered after 2 h of incubation with HL and 10 µM of As(III)

Thin layer chromatography analysis of *Hfx*E resolved to give four self coloured spots: **i**. pink, at R_f 0.4; **ii**. dark pink at R_f 0.55; **iii**. pink orange at R_f 0.69 and **iv**. light pink at R_f 0.75 as depicted in **Fig. 2.44 A**. *Hfx*E recovered on incubation with As(III), on TLC, showed only a single light orange spot at R_f 0.55 wherein, in the un interacted *Hfx*E, the spot at R_f 0.55 was dark pink in colour (**Fig. 2.44 B**). The spots at R_f 0.4 (pink), 0.69 (dark pink) and 0.75 (pink orange) failed to show up in the chromatogram of *Hfx*E recovered on interacting with As(III) for 2 h and developed in benzene: acetone (2:1 v/v) (**Fig. 2.44 C)**. The spot at R_f 0.4, 0.55, 0.69 and 0.75 on elution with methanol revealed peaks at 368,385,463,490 and 522 nm (**Fig. 2.45 A**); 458, 482 and 516 (**Fig. 2.45 B**); 447, 478 and 509 (**Fig. 2.45 C**); 421 and 438 nm (**Fig. 2.45 D).**

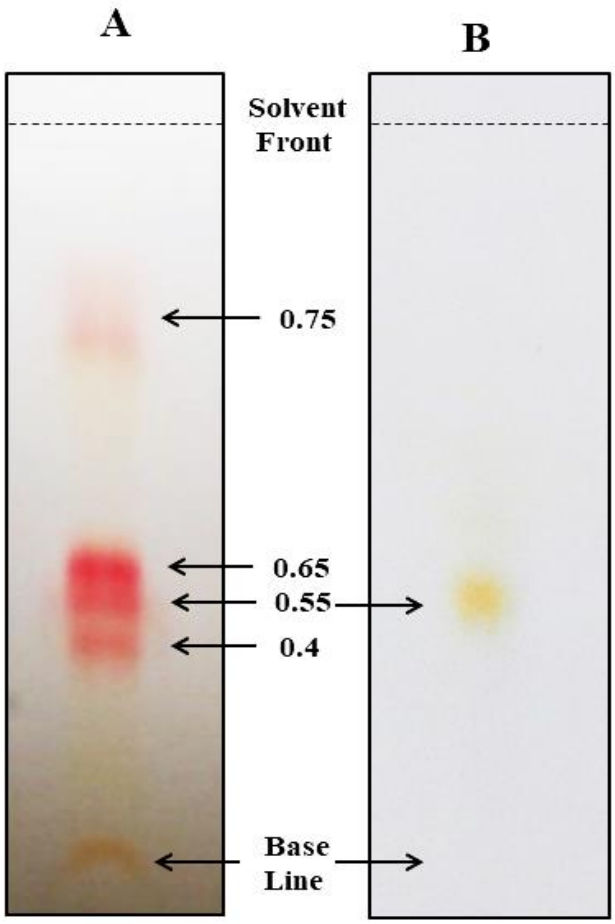

Fig. 2.44 Thin layer chromatogram developed in benzene: acetone (2:1 v: v) of **A:** *Hfx*E; **B:** *Hfx*E recovered after 2 h of incubation with 10 µM of As(III). BL – Base line; SF – Solvent front

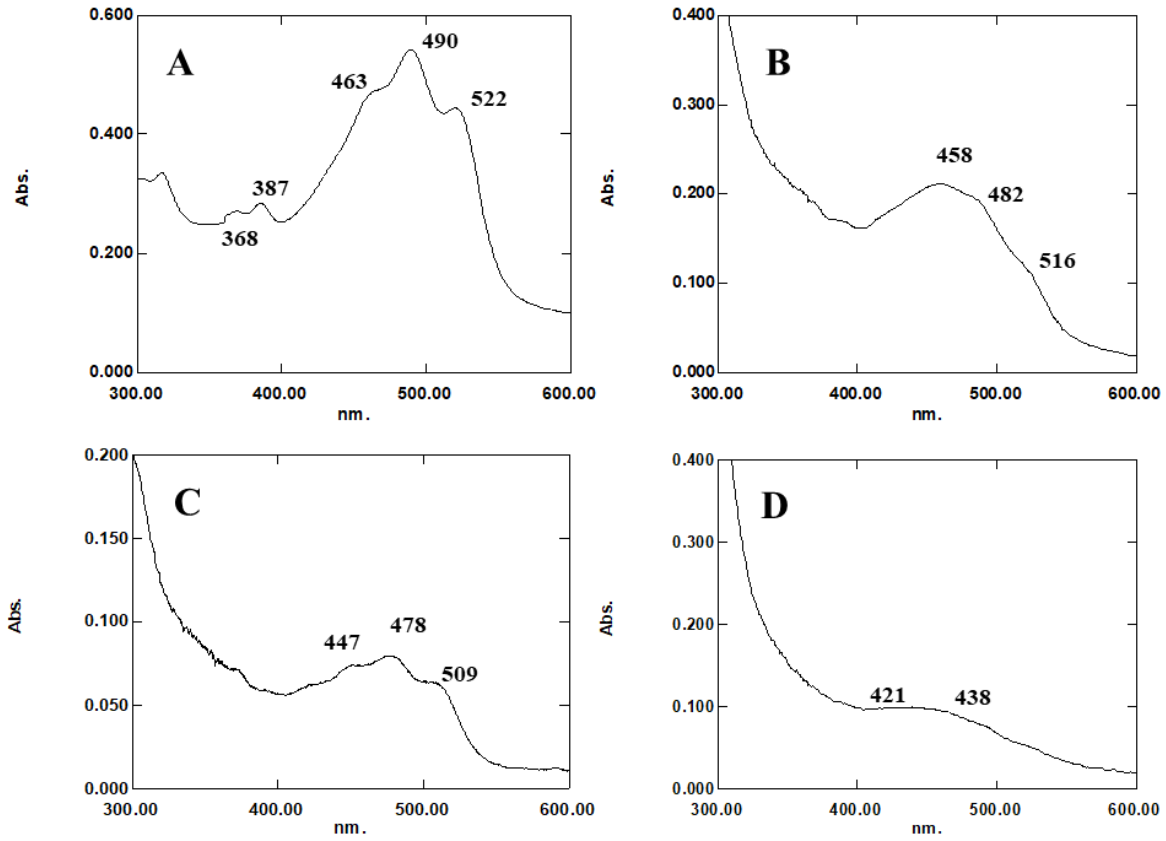

Fig. 2.45 Absorption scan of components of *Hfx*E resolved on silica gel TLC in benzene: acetone (2:1) and individually eluted in methanol according to their R_f; **A:** 0.4; **B:** 0.55, **C:** 0.69, **D:** 0.75

2.3 DISCUSSION

The observations and results obtained on production of extremozymes, antagonism, protogonism and antigenotoxic studies are discussed under three sections;

Section A: Bioprospecting for production of extremozymes in extremely halophilic eubacteria and haloarchaea

Halophilic extremozymes are extremely salt-tolerant; they are capable of retaining stability at ambient temperatures for prolonged periods and are often considerably thermotolerant. Furthermore, given that halophilic enzymes possess salt-enriched solvation shells because of which they retain enzyme activity in environments of low water activity, such as in the presence of high levels of organic solvents (Madern *et al*., 2000). The commercial utilization of starch is dependent on the conversion of an insoluble material into simple sugars. The hydrolysis of starch to low molecular products is widely used in the sugar, textile industries and in brewing (Yankov and Dobreba, 1986).

The ability to produce amylase and lipase extremozymes was qualitatively screened among 117 marine halophilic extreme halophilic and haloarchaeal cultures isolated from six solar salts, six estuarine regions and the isolate from the sponge sample. For amylase and lipase screening, the conventional plate techniques were used. The plates were flooded with Lugols iodine and zones of decolourization around a fully grown colony were considered as amylase producers. In the case of lipase production, zone of precipitation around a fully grown colony was considered positive. This is due to the formation of precipitates of calcium laurate, palmitate, stearate or oleate around the zones of bacterial growth (Gutierrez and Gonzalez, 1970). **33 cultures were found to be positive for amylase and lipase production**. In an early study, Gonzalez and Gutierrez, (1970) demonstrated the production of extracellular lipases by haloarchaea; they detected lipolytic activity in 66% of their isolates. Lizama *et al*. (2001) during the study on haloarchaeal strains isolated from salt lake in Chile showed that their isolates produced amylase and lipase. Elevi *et al*. (2004) studied the production of amylase and lipase in haloarchaea which showed high rate of amylase production but neither produced any lipase activity. More recently, Bhatnagar *et al*.

(2005) screened an Algerian culture collection for lipolytic activity and reported the detection of lipolytic activity in 35 haloarchaea. Ozcan *et al*. (2006) and Birbir *et al*. (2007) also demonstrated amylase and lipase activity in the haloarchaeal strains, respectively. A clear dominance of haloarchaea is detected in our study, although a population of eubacteria is also present. The results of this study support the result of previous studies on production of hydrolytic enzymes in cultures isolated from other hyper saline habitats.

In oil production and exploration operations spills are inevitable. Large volumes of crude oil spills occur during transportation, due to leaks from underground storage tanks and due to poor management. Several accidental oil spills in the marine environment results in the release of toxic and carcinogenic compounds such as BTEX (Benzene, Toluene, Ethylbenzene and Xylene) that are detrimental to human health and the environment. Since salt pans of Goa and the estuaries are situated along the coastline of the Arabian sea, they receive water which is obviously pollution by crude oil, grease and other hydrocarbons due to the heavy trawlers and barge activity in the Arabian Sea. Benzene, one of the BTEX compounds, is of particular concern. This priority pollutant, as listed by the United States Environmental Protection Agency, is highly stable, water soluble and a known human carcinogen and poses special concern for rapid contamination of subsurface and drinking water (Brusa *et al*., 2001; Margesin and Schinner, 2001). Keeping this in mind, we screened the 117 cultures from solar salts and estuarine sediments for presence of aromatic oxygenases responsible for the cleavage of the benzene ring. The screening technique for aromatic oxygenases which brings about cleavage of the benzene ring was carried out using growth measurement at A_{600} of each of the cultures grown in NSM with 0.1 % sodium benzoate. A total of **69 cultures were able to produce aromatic oxygenases**.

GUIF2 and GUIF4 which were found to be good producers of lipase and aromatic oxygenase were characterized using poyphasic taxonomy and molecular ribotyping techniques. Cells of GUIF2 and GUIF4 were seen to be cup shaped which is a typical distinguishing feature of *Haloferax* sp. Further GUIF2 and GUIF4 were found to be resistant to penicillin G, which is known to inhibit bacteria and eubacteria, but not Archaea. Haloarchaea are known for its resistance towards many antibiotics especially those of cell wall and protein synthesis (Purdy *et al*., 2004). Further the

absolute requirements of NaCl for growth, extreme sensitivity to bile salts affirmed that the cultures belonged to haloarchaea of Domain Archaea. Bile salts such as difco's bactopeptone has been known to cause lysis of haloarchaea due to it's presence of high concentration of taurine conjugates of cholic acid (Purdy *et al*., 2004). Core lipids are completely absent in eubacteria and eukarya. The presence of GDEM at R_f 0.2 in the TLC profile of the methanolysate of GUIF2 and GUIF4 and the IR peak of the spot at Rf 0.2 at 1076 which is indicative of the ether; C-O-C functional group. This is the main key for assigning affiliation of Domains to cultures (Purdy *et al*., 2004), hence both the cultures, GUIF2 and GUIF4 were assigned to the Domain Archaea. These were considered as extreme halophiles as the culture could grow in NaCl upto 25 % salt and was lysed in distilled water and hence were referred to Phylum *Euryarchaeata*, class *Halobacteria*, order *Halobacteriales*. The peaks present in the visible scan of the pigment extracted in acetone, indicated the presence of red carotenoids. The phenotypic test used were in accordance to minimal standards proposed for describing and assigning taxa in the order *Halobacteriales* (Oren *et al*., 1997). Based on cellular morphology showing cup shaped cells, requirement of pH and Mg^{+2} ions and the biochemical characteristics, further identification of GUIF2 and GUIF4 to the genus level was carried out using Bergey's Manual of Systematic Bacteriology Volume I (2nd edition), The Prokaryotes: Volume IV (2nd edition), the culture GUIF2 and GUIF4 was found to belong to the genus *Haloferax*. The extracted genomic DNA of GUIF2 and GUIF4 when subjected to agarose gel electrophoresis was seen as a discrete band indicating the purity of the genomic material. The PCR amplification of this genomic DNA resulted in an approximately 1.4 kb PCR product. GenBank accession number obtained for GUIF2 using the NCBI GenBank software was MH169338. BLASTn search and phylogenetic analysis of the 16S ribosomal RNA gene sequence of **GUIF2 was related with 99% similarity to *Haloferax volcanii* strain DS2** with accession number NR028203. GenBank accession number obtained for GUIF4 using the NCBI GenBank software was MG199078. BLASTn search and phylogenetic analysis of the 16S ribosomal RNA gene sequence of **GUIF4 was related with 99% similarity to *Haloferax gibbonsii* strain ARA6** with accession number CP011947 isolated from sea salt in South Korea.

Benzene rings are found throughout nature, hence the ubiquity of aromatic rings in nature allows for the exposure of these compounds to microorganisms despite any lack of environmental contamination. This prior exposure to aromatics may allow the hypersaline organisms to carry the genes necessary for the degradation of pollutants if they are ever exposed to them. Therefore, it is important to survey naturally occurring hypersaline environments to try to understand the ability of native organisms in pristine hypersaline environments to degrade hydrocarbons, such as BTEX. These organisms could be used in bioremediation projects where the environment is co-contaminated with hydrocarbons since non-halophiles would not be able to survive in hypersaline conditions. However reports on organisms that possess the ability to degrade these rings, especially in hypersaline environments have remained elusive.

Of the 69 isolates found to be positive for production of aromatic oxygenases, 4 were extremely halophilic eubacteria belonging to the *Alteromonas*, *Gluconobacter* and *Chromohalobacter*. The ring cleaving aromatic oxygenase producing haloarchaeal genera were *Halobacterium*, *Haloferax, Haloarcula*, *Halorubrum*, *Halococcus*, *Natrialba, Natrinema* and *Natronomonas*. The highest occurrence of lipase producing genera was in the solar salt of Agarwada, who also had the highest Shannon-Weiner Diversity Index 'H' of 1.86. Even though organisms belonging to various genera have been shown to degrade hydrocarbons, members of the genera *Halomonas*, , *Haloferax, Haloarcula* and *Halobacterium* dominate among the published literature. Among eubacteria, *Halomonas* sp. has been frequently reported for their ability to degrade phenolics and benzoates (Olajire and Essien, 2014). Garcia *et al*. (2004) and Garcia *et al*. (2005) have reported several strains of *Halomonas* sp. including the *Halomonas organivorans* from water and sediment of salterns and hypersalines oils collected in different part of the Southern Spain. These isolates are reported to degrade a wide range of aromatic compounds including benzoic acid, p-hydroxy benzoic acid, phenol, salicylic acid, p-aminosalicylic acid, phenylacetic acid, phenylpropionic acid, cinnamic acid, ferulic acid, and *p*-coumaric acid as the sole sources of carbon. Much of the BTEX degradation activity has been reported among *Pseudomonas* sp. (Gibson *et al*., 1975; Zamanian and Mason, 1987; Reardon *et al*., 2000; You *et al.*, 2013). Kim *et al*. (2008) has reported the presence of *Chromohalobacter* sp. strain HS-2 from salted fermented clams that degrade benzoate and p-hydroxybenzoate as the sole carbon and energy sources. *Gluconobacter* are

characterized by their acid tolerance, ability to grow in low-nutrient conditions and their resistance to benzoic and sorbic acids (Eyles and Warth, 1989). *Gluconobacter* can cause off flavours in ready to drink beverages (Sand, 1975). **Our strain GUFF$_{83}$ (*Gluconobacter* sp.) was seen to grow and tolerate 0.1 % sodium benzoate**. This indicated the importance of studying resistance of extremely halophilic eubacteria in canned and fish fermentation products to sodium benzoate, when used as a preservative in the food industry. Studies have also documented aerobic degradation of benzoates by extremely halophilic archaea growing in near-saturated brines (>30 % NaCl). For example, Emerson *et al*. (1994) isolated a *Haloferax* sp. D1227 from an oil-brine soil near Grand Rapids, Michigan which was able to degrade benzoic acid, 3-hydroxybenzoic acid, 3-phenylpropionic acid and cinnamic acid as the sole sources of carbon at salt concentration ranging from 5 to 30% NaCl. When grown on ^{14}C-benzoate, strain D1227 converted 70% of the substrate to $^{14}CO_2$ and assimilated 19 % of the ^{14}C-label into cell biomass. These compounds were degraded via a gentisate pathway (Fu and Oriel, 1999). Fairley *et al*. (2002) reported a novel halophilic archaeon, *Haloarcula* sp. D1 from a high salt enrichment culture degrading *p*-hydroxybenzoic acid as the sole source of carbon. Cuadros-Orellana *et al*. (2012) have isolated 44 archaeal strains belonging to four groups in the Halobacteriaceae family from five geographically different saline environments; the Uyuni salt marsh in Bolivia, solar saltern in Chile, solar saltern in Puerto Rico, Dead Sea near Jordan and sabkhas in Saudi Arabia. Analysis of lipid composition and restriction analysis of 16S rDNA-gene places all the strain in. These strains degraded *p*-hydroxybenzoic acid as the sole carbon source in the presence of 20% NaCl. Similarly, Bonfá *et al*. (2011) have also reported the presence of 10 halophilic archaea, all belonging to the genus *Haloferax* utilizing *p*-hydroxybenzoic acid. These strains were also able to degrade a mixture of *p*-hydroxybenzoic acid, benzoic acid and salicylic acid as growth substrates in a medium containing 20% NaCl. Recently, Cuadros-Orellana *et al*. (2012) have reported the isolation of 10 halophilic archaea from Dead Sea that degrade *p*-hydroxybenzoic acid as the sole carbon and energy source of which one strain was found to degrade benzoic acid to gentisate. Erdogmuş *et al*. (2013) reported the ability of many archaeal strains belonging to *Halobacterium*, *Haloferax*, *Halorubrum* and *Haloarcula* group to degrade *p*-hydroxybenzoic acid in a medium containing 20% NaCl. These studies clearly

demonstrate that archaea metabolizing *p*-hydroxybenzoic is widespread in the environment.

Some reports indicate increased salinity has negative impact on the biodegradation of petroleum hydrocarbons (Ward and Brock, 1978, Mille *et al*., 1991, Rhykerd *et al*., 1995). It has been proposed that the salt contamination first be removed before further remediation takes place (Rhykerd *et al*., 1995). However, this type of activity is costly and damaging to the environment. The use of halotolerant and halophilic organisms in the cleanup of organic contaminants in saline environments would prevent costly remediation strategies that reduce or remove salt by dilution methods, reverse osmosis, ion exchange, or electrodialysis before biological treatment begins (Margesin and Schinner, 2001).

The growth profile of *Haloferax volcanii* GUIF2 (MH169338) when grown in NTYE, NTYE + petrol/ benzene/ castrol/ lindane showed slight variations in growth when compared with the control NTYE. Also the pigment peaks when compared to the control were slightly shifted. In view of the tolerance shown by the organism to hydrocarbons and recalcitrant compounds, it was desired to study the ability of the culture to utilize these hydrocarbons as a single source of carbon and energy.

Growth in mineral medium with the respective hydrocarbon was seen to be largely affected as seen by the absorbance values when compared to the control flask. The pigment of *Haloferax volcanii* GUIF2 (MH169338) grown in mineral medium with NSM with 0.1% glucose, showed peaks indicating the presence of red carotenoids, which were either shifted or completely abolished when grown in NSM with hydrocarbon. When grown in NSM with 0.1% castrol engine oil and 0.1% petrol, all peaks were seen to be abolished, in NSM with 0.1% benzene peaks showed the presence of only one peak and in the presence of the insecticide, all peaks were shifted when compared with the control. The inability of haloarchaeal cultures to develop the characteristic orange-red pigmentation during growth in the presence of aniline has been reported in a study carried out by Raghavan and Furtado, 2005). Growth was obtained even on addition of petrol/ benzene/ castrol/ lindane as a sole source of carbon suggesting that the organism had a high ability to tolerate different aliphatic and aromatic hydrocarbons.

The most straightforward approach to characterize degradation pathways is to analyze the catabolic enzymes (Cao *et al*., 2008). In nature, many compounds are transformed into common degradation intermediates before they are further degraded. This process of funneling compounds allows for common pathways in organisms that break down these substrates. For instance, many aromatic compounds are oxidized by the incorporation of oxygen into the ring. This can be accomplished via mono or dioxygenases, which introduce one or two oxygen atoms, respectively, into the benzene ring. It is more common for organisms to employ dioxygenases to incorporate the entire oxygen molecule into benzene to form a *cis*-diol, which is then rapidly transformed (Bouwer and Zehnder, 1993). Major breakdown intermediates of aromatic ring compounds are catechol or protocatechuate, (Harwood and Parales, 1996). Catechol is the most common intermediate of aerobic benzene degradation. Once catechol is formed, the ring can be cleaved and broken into fragments that can be further degraded (Dagley, 1975). This oxidation can occur through *ortho*-fission (between the hydroxyl groups) or *meta*-fission (adjacent to one of the hydroxyl groups) (Cerniglia, 1984). The ortho cleavage of catechol is catalyzed by catechol 1, 2-dioxygenase and generates *cis, cis*-muconic acid (Hayaishi *et al*., 1957) which can enter the citric acid cycle. Meta cleavage of catechol is catalyzed by catechol 2, 3-dioxygenase (C23O) and produces 2-hydroxymuconic semialdehyde (Bartilson and Shingler, 1989), which is eventually broken into acetaldehyde and pyruvate. **Using Arnow's test, a pink colouration detected in the cell lysate of *Haloferax volcanii* GUIF2 (MH169338). This indicated that sodium benzoate was degraded to catechol**. Rothera test results showed that *Haloferax volcanii* GUIF2 (MH169338) could **degrade catechol by the ortho cleavage of the β-ketoadipate pathway because there was no development of a yellow meta cleavage product**. Therefore, after determining the presence of the enzymes by using Rothera test, the activity of the enzyme was spectrophotometrically monitored for 100 minutes by measuring the product formed at 260 nm. Activity of catechol 1, 2 dioxygenase enzyme of the ortho cleavage pathway could be detected. **Spectrophotometric enzyme assays confirmed the results of the Rothera tests.**

It is interesting to note that multiple enzyme activity was also detected in many cultures. **Nine cultures showed presence of all 3 enzyme activity and 19 cultures were positive for any 2 enzymes**. Out of 117 cultures screened for production of the

three extremozymes; amylase, lipase and aromatic oxygenases, **84 produced at least 1 enzyme and 33 cultures produced none**. 33 cultures (28%) from among the 117 cultures were seen to produce amylase and lipase respectively. Fifteen cultures (13%) produced amylase and aromatic oxygenase and 12 cultures (10%) produced lipase and aromatic oxygenase respectively.

Section B: Bioprospecting for production of antagonism (halocin production) among haloarchaea

The resistance of numerous pathogenic bacteria to commonly used bioactive secondary metabolites is presently an urgent focus of research, and new antibacterial molecules are necessary to combat these pathogens. Screening of resources from the terrestial environement has been exploited and harnessed, so now the focus on posssible bioactives from the marine environment is the goal of medical reserach. **Our screens revealed antomicrobial activity of 6 cultures against 4 human pathogens *S. aureus* ATCC 6538, *S. typhimurium* ATCC 14028, *S. abony* ATCC 6017 and *C. albicans* 10231** with zone sizes of inhibition ranging from 8-12 mm. Thiocoraline, with strong antimicrobial activity against Gram-positive microorganisms has been reported from marine *Micromonospora* (Romero *et al*., 1997), while *Myxobacteria* are often reported to produce compounds that are synthesized both by polyketide synthesis and by polypeptidases (epothilons) (Běhal, 2003).

Solar salterns, in Goa which are used for salt production present an environment with increasing salt concentrations, from seawater to NaCl saturation. Studies pertaining to prospects of finding haloarchaea with potential of halocin production are limited. Halocins are proteinaceous antagonistic compounds secreted extracellularly and are reported to kill closely related species among haloarchaea (Rodriguez-Valera *et al*., 1982). Screening of 30 cultures for halocin production, revealed a great diversity in antagonistic activity. Our study revealed that **22 cultures were found to produce inhibitory activity as seen as a clearing around the producer**. The varying sizes of the zones of inhibitions were an indication that the halocins produced could be structurally and functionally different. Similar findings have been reported in the past, where a large set of haloarchaeal and extreme halophilic strains have been tested

against each other, halocin producers were found to be highly abundant and were seen to be inhibiting strains belonging to different phylogenetic groups and also across Domains, hence can be concluded that halocin production is a common phenomenon reported in earlier studies (Rodrıguez-Valera *et al*., 1982; Meseguer *et al*., 1986; Torreblanca *et al*., 1994). Halocins have also been screened for among cultures of Goan origin as early as 2004 and reported in studies (Bansal and Furtado, 2004) Salgaonkar *et al*., 2012). From our group of 30 cultures, 73% were identified as antagonistic producers and around 28% as non-antagonistic producers. These cultures not participating in this study might inhibit other strains, not included in this study. 40% of the cultures were not sensitive to any of the antagonistic biofactor produced here. Our study reported the involvement of *Natronococcus* isolated from the solar salt sample of Siridao which has not been reported before. Solar salterns are reported to have limited nutrients with limited organic and inorganic nutrients, thus, the secretion of halocins by which other haloarchaeal cultures are lysed can be an adaptive strategy employed by the producer halophilic archaea for survival during nutrient limiting conditions. Cell lysis leads to release of intracellular material thus enriching a nutrient starving environment (OConnor and Shand, 2002). It has been demonstrated in *Haloferax volcanii* that the extracellular DNA produced as a result of lysis of the cell can serve as a source of phosphorous (Chimileski *et al*., 2014). The role of halocins in prevention of halophilic bacterial damage on brine cured hides is also reported (Birbir *et al*., 2004). This screening effort reveals the ability of haloarchaeal cultures from solar salts and estuarine sediments of Goa to produce antibacterial compounds and halocins.

Section C: Bioprospecting for production of protogonism

Production of growth enhancing substances against human pathogens against *E.coli* ATCC 8739 and *S. abony* ATCC 6017 by 27 haloarchaeal cultures was observed by the presence of zones of exhibition around the wells. The zones of growth exhibition could be due to the secretion of some metabolites which would have promoted the growth of the indicator strains. The production of N-acyl-homoserine lactone (AHL), a quorum sensing molecule has been reported in *Haloterrigena hispanica* and *Natronocoocus occults* (Tommonaro *et al*., 2012; Abed *et al*., 2013). The presence of this low molecular weight compound or similar

biomolecules secreted in the environment increases cell density and hence could be factor attributed to zones of growth exhibition of *E.coli* ATCC 8739 and *S.typhi* ATCC 6017 by the 27 different haloarchaeal cultures that ranged from 7-25 mm. Haloarchaeal cultures are reported to produce exopolysacharides (EPS) which is composed mainly of biomolecules, polysaacharides, extracellular DNA (eDNA) and polypeptides which we envisage could be nourishing and providing nutrition to the pathogens (Sutherland *et al*., 2001; Squillaci *et al*., 2016;).

Elevated levels of arsenic in the coastal waters, the estuarine waters around the state of Goa and among crustaseans from the shores of Goa have been reported (Fondekar and Reddy, 1974; Fondekar and Reddy, 1976; Zingde *et al*., 1976(b)). Human lymphocytes from a healthy donor obtained as per WHO guidelines showed 90 % viability, when checked by the trypan blue exclusion test. These HL were used to check the genotoxicity of As (III) and the whole experiment was performed under dim light to prevent photo degradation of DNA. This HL when viewed under fluorescent microscope clearly showed intact DNA which was disrupted in the presence of 10 µm As (III) indicating the genotoxic effect of 10 µm As (III). The appearance of comet like images was due to the damage to DNA of HL by 10 µm As (III). Such damage is related to strand breaks which caused spreading of the fluorescence (Kumaravel *et al*., 2009). Our findings were also consistent with other reports of DNA strand breaks in lymphocytes exposed to arsenic (Prasad and Selvaraj, 2014). Haloarchaeal cultures isolated from salt pans of Goa are reported to grow in the presence of As(III) (Braganca, 2002). **Methanolic extract from the whole cells of *Haloferax alexandrinus* GUSF-1(KF796625) (*Hfx*E) at a concentration of 50 µg ml^{-1} was very effective and reduced DNA damage by As(III) by 92% increasing the viability of HL cells** and consequent decrease in size of the tail thus reducing the DNA damage. It was noteworthy that protection from *Hfx*E was twice that afforded by an equal amount of SeNPs. The role of defensive nutrients in modifying arsenic induced toxicity was initially proposed in the early 1930's by Mayer and Sulzberger, 1931, who suggested that adequate levels of ascorbic acid, in the diet prevented or reduced occurrence of arsenic induced anaphylaxis and the same was demonstrated in a study carried out in laboratory rats exposed to arsenic (Singh and Rana, 2007). L-ascorbic acid is a primary defensive nutrient because it can scavenge free radicals (Hume *et al*., 1991). Curcurmin at 50 µM and 80 mg of Diallyl trisulphide, the active

constituent of medicinal herb *Curcuma longa Linn* and *Allium sativum* was seen to reduce DNA damage of HL by As (III) by 50% and near 100% respectively (Mukherjee *et al*., 2007, Miltonprabu and Sumedha 2014). *Hfx*E at 50 µg ml^{-1} afforded a much higher protection (50% more) than 50 µg ml^{-1} SeNPs biosynthesized using *Haloferax alexandrinus* GUSF-1 (KF796625) and discussed in **Chapter V**, against cell death and DNA damage caused by As(III). Protection was also reported for biologically synthesized SeNPs at 1mg ml^{-1} by Prasad and Selvaraj, 2014. Although, Se was reported to protect against genotoxic As(III), adverse effects of Se itself are being unveiled and recorded (Mal *et al*., 2017). ***Hfx*E, offers benefits over SeNPs** and therefore is worthy of further investigation for unveiling of the antigenotoxic component.

The preliminary analysis pertaining to absorption spectra of the *Hfx*E revealed the characteristics three finger peaks, which are in good agreement with those reported for red carotenoids present in haloarchaea (Raghavan and Furtado, 2005; Naziri *et al*., 2014). Most carotenoids absorb maximally at three wavelengths (Britton *et al*., 1995). These peaks were seen to be abolished in *Hfx*E interacting with As(III). The effect was also reflected in the TLC profile of reaction mixture of *Hfx*E and As(III). Incubation of *Hfx*E with As(III) showed that *Hfx*E reacted with As(III) as reflected in the absorption spectrum and TLC profile of the reaction mixture. The chromatogram of *Hfx*E which was developed in benzene: acetone (2:1 v/v) and viewed by the naked eye revealed 4 spots with different R_f values. In comparison to the TLC profile of *Hfx*E, spots at R_f 0.4, 0.69 and 0.75 were absent in the reaction mixture, while the spot at R_f 0.55 changed from pink to light orange respectively suggested that it had interacted, but not to the extent that it could change its mobility. Each of the resolved spots on the chromatogram of *Hfx*E were eluted in methanol and analyzed. Comparing the absorption spectrum of each of them with published data, identification was possible. The spot at R_f 0.4 was confirmed as **bacterioruberin** (Asker *et al*., 2002). The spot at R_f 0.55 was confirmed as **bisanhydrobacterioruberin** (Squillaci *et al*., 2017), whereas peaks of the spot at R_f 0.69 revealed it to be **lycopene** (Asker *et al*., 2002). Spot 4 which was also a carotenoid as seen from the absorption spectrum couldn't be identified.

Occurrence of bisanhydrobacterioruberin and lycopene are reported as intermediates of the carotenoid biosynthetic pathway in genus *Haloferax* (Asker *et al*., 2002). Bacterioruberin of *H. salinarium* indicated scavenging of free radicals and reduced DNA strand-breaks induced on exposure to ionizing radiation and hence exhibited protective role against lethal effects to oxidative DNA-damaging agents (Shahmohammadi *et al*., 1998). Lycopene is used for increasing the rejoining of DNA strand breaks and reducing the cell death induced by oxidative stress (Torbergsen and Collins, 2000; Seo *et al*., 2009). This present study shows that there are three constituents of *Hfx*E that are involved in interaction with As(III), thereby reducing and suppressing the genotoxicity of As(III) to HL present in the methanolic extract of haloarcheon *Haloferax alexandrinus* GUSF-1 (KF796625) isolated from a solar saltern in Goa- India. These constituents mitigate arsenic-induced reactive oxidative DNA damage in human lymphocytes as demonstrated through the alkaline comet assay. This detailed study of antigenotoxicity of *Hfx*E and the mechanism of its action is a desired research effort.

In conclusion, **this study clearly reveals the presence of** (i) extreme halophilic eubacterial and haloarchaeal cultures isolated from solar salts, estuarine sediments and from sponge with **extremozyme producing potential** (ii) **The production of antimicrobial and antagonistic compounds in haloarchaea** and (iii) **Growth promoting substances produced by haloarchaea** evident by the zones of growth exhibition of *E.coli* ATCC 8739 and *S.typhi* ATCC 6017 and the **production of red carotenoids with antigenotoxic property** in *Haloferax alexandrinus* GUSF-1 (KF796625).

Chapter III

Antioxidant Production in Extremely Halophilic Eubacterial and Haloarchaeal Cultures

Globally, solar salt plays an important role in all forms of life (Aral *et al*., 2004). Goa situated on the west coast of India, is engaged in natural salt production through green process of salt farming for the past 1500 years (Furtado and Fernandes, 2009). These salt pans in Goa are mostly situated inside the sea coast bordering four talukas of Goa, namely Pernem, Bardez, Tiswadi and Salcete. This solar salt is widely used in moderate quantities as fertiliser and soil conditioner in Goa and in south Asian countries (Mani *et al*., 2012; Magat, 2000). A diverse group of halophiles; euryhaline, moderate and extreme halophiles have been known to be associated with salt pans. Eubacterial members belonging to genera *Aeromonas, Pseudomonas, Gluconobacter, Halomonas* and *Chromohalobacter* are predominantly associated with salt flakes (Fernandes and Furtado, 2005), whereas haloarchaeal genera like *Haloarcula, Halobacterium, Haloferax, Halococcus* have been associated with the salterns of Goa (Fernandes and Furtado, 2005; Sequeira 1992; Fernandes, 1999; Braganca and Furtado, 2009). Both in biota as well as in environment, oxidation reactions produce free radicals which are atoms, molecules or ions with unpaired electrons that are highly unstable and charged (Lü *et al*., 2010). These free radicals react with the first available oxidisable substrate causing damage and in case of cells, death. This process is however, averted by antioxidant molecules which scavenge free radicals as
(i) preventers: by preventing formation of free radicals; (ii) scavengers: by removing radicals and halting further propagation of chain reactions and (iii) repairers: which ameliorate oxidative damage to a cell (Lü *et al*., 2010). In recent years, researchers are keen to unveil antioxidant substances from plants, animals and microbes and natural substances with an ability to fight oxidative stress (Yevgenia *et al*., 2013). These marine halophilic microbes are reported to thrive and dominate salt crystals through production of osmolytes such as ectoine, betaines, mycosporine like amino acids (Oren and Gunde-Cimerman 2007) and carotenoid type of pigments (Shahmohammadi 1998) and antioxidant molecules like carotenoids (Hou and Cui 2018).

This chapter under **SECTION A**, details the assessment of the free radical scavenging potential of Goan solar salt and associated microbial cultures together with other extremely halophilic cultures from estuarine regions and from sponge. While **SECTION B** describes: the parameters inducing maximum free radical scavenging activity; antioxidant production in *Haloferax alexandrinus* GUSF-1 (KF796625) one

of the solar - salt associated culture; the extractability of antioxidant *Hfx*A from cells; Characterization and kinetics of *Hfx*A using the DPPH$^{\bullet}$ scavenging.

3.1 METHODOLOGY

SECTION A

FREE RADICAL SCAVENGING ACTIVITY BY EXTREMELY HALOPHILIC EUBACTERIA AND HALOARCHAEA

3.1.1 FREE RADICAL SCAVENGING ACTIVITY OF SOLAR SALT

3.1.1.1 Preparation of 1, 1-diphenyl-2-picrylhydrazyl (DPPH$^{\bullet}$) reagent

Various concentrations DPPH$^{\bullet}$ reagent were freshly prepared in methanol and stored in amber coloured bottles and at 4°C while not in use.

3.1.1.2 Evaluation of stability and linearity of DPPH$^{\bullet}$

Stability of DPPH$^{\bullet}$, was checked by monitoring absorbance of 0.1 mM and 0.2 mM stock solution, at 517 nm using the UV-Visible dual beam spectrophotometer (Shimadzu UV- 1800, Japan), every 5 min for over 40 min against methanol as blank. Compliance of 0.02, 0.04, 0.06, 0.08, 0.1, 0.12, 0.14, 0.16, 0.18 and 0.2 mM DPPH$^{\bullet}$ prepared from a stock solution of 0.2 mM DPPH$^{\bullet}$ to Beer Lambert's law was done by monitoring the absorbance at 517 nm (***Appendix II***).

3.1.1.3 Free radical scavenging activity of solar salt

Super saturated solutions of solar salt was prepared by gradually adding sterile ultrafiltered deionised water such that at each addition of water to 40 g of solar salt a super saturation state was maintained throughout the preparation. Each of the saturated solutions were individually filtered through whatman No 1 filter paper and analyzed separately for its ability to decolourize DPPH$^{\bullet}$. Salt solutions of $MgSO_2.7H_2O$, $MgCl_2$, NaCl, $CaCl_2.2H_2O$ prepared separately were also individually analyzed for DPPH$^{\bullet}$ decolourization as described in **3.1.1.4 below**.

3.1.1.4 DPPH$^{\bullet}$ decolourization assay

The DPPH$^{\bullet}$ decolourization was assayed by a method previously described but slightly modified (Brand-Williams *et al*., 1995). 0.5 ml of individual solutions of solar salt and other salts were added to 1 ml of 0.1 mM methanolic DPPH$^{\bullet}$ reagent, mixed vigorously with minimum light exposure, incubated in the dark at room temperature (28 ± 2ºC), for 30 min and monitored at 517 nm, using the UV-Visible spectrophotometer (UV-1601, Shimadzu, Kyoto, Japan) against methanol as blank. The stability of the DPPH$^{\bullet}$ solutions was also monitored separately by checking the absorbance of 0.1 mM methanolic solution of DPPH$^{\bullet}$, every 5 min, at 517 nm, for over an hour. Ascorbic acid (0.1%) was used as the positive control and also as the standard for the calibration curve. Results were averaged and expressed as % radical scavenging activity (% DPPH$^{\bullet}$ RSA) as detailed below in **3.1.1.5**. Results were also expressed as ascorbic acid equivalent (AAE) µg g^{-1} cells ± SD by constructing a standard curve from a 100 µg ml^{-1} stock solution of ascorbic acid (***Appendix II***).

3.1.1.5 Computation of % radical scavenging activity (% DPPH$^{\bullet}$ RSA)

% DPPH$^{\bullet}$ RSA was computed using the generalization;

% DPPH$^{\bullet}$ RSA = $(A_{control}–A_{test})/A_{control}) \times 100$,

where $A_{control}$ is the absorbance of control and A_{test} is the absorbance of the crude MEC. Results were expressed as mean ± SD of % DPPH$^{\bullet}$ RSA.

3.1.1.6 Growth of microbes from crude solar salt

A super saturated aqueous solution of crude solar salt was prepared by adding sterile distilled water to crude solar salt till a super saturation state was reached. An aliquote of 0.1 ml was spread plated onto NTYE agar plates and incubated at 37ºC in light, till well developed colonies were formed.

3.1.1.7 Development of Agar-growth-DPPH$^{\bullet}$ method

The fully formed colonies on NTYE agar were very carefully exposed to freshly prepared 0.1, 0.2 and 0.5 mM methanolic DPPH$^{\bullet}$ by layering the DPPH$^{\bullet}$ solution just to cover the surface of the agar and the colonies on it. Plates were incubated in the dark for 40 min at room temperature (28 ± 2^{o}C), and those colonies surrounded by

clear colourless/ straw colour haloes against a purple stained background were scored and recorded as positive free radical scavengers.

3.1.2 DEMONSTRATION OF FREE RADICAL SCAVENGING ABILITY OF EXTREMELY HALOPHILIC CULTURES

A total of 117 extremely halophilic cultures from **solar salts, estuarine sediments and from sponge** were spot inoculated onto NTYE agar using a template allowed to grow at 37ºC for a period of 7 d and then subjected to Agar-growth-DPPH$^{\bullet}$ method.

3.1.2.1 Culturing and preparation of methanolic extract of cells (MEC)

Each of the 100 cultures testing positive in the Agar-growth-DPPH$^{\bullet}$ method were individually inoculated into a set of three large sterile tubes with 5 ml of sterile NTYE broth. All tubes were incubated at 150 rpm on the orbital shaker (REMI CIS-24 PLUS - India) at 37ºC. After 6 d, cells were harvested at 10000 rpm, 4ºC for 10 min by using an Eppendorf centrifuge 5804 R. Cells washed with 15% NaCl and adjusted to a wet weight of 100 mg. 1 ml of methanol was added to the wet cells, the mixture kept standing overnight at 4ºC in the dark and the cell extract recovered by centrifuging at 10000 rpm, for 10 min. The resulting MEC was stored in the dark at 4°C until further use.

3.1.2.2 Evaluation of free radical scavenging efficiency of MEC

Evaluation of free radical scavenging activity of MEC was carried by DPPH$^{\bullet}$ decolourization method using 0.2 mM and expressed as % DPPH$^{\bullet}$ RSA.

3.1.3 QUANTIFICATION OF FREE RADICAL SCAVENGING ACTIVITY

3.1.3.1 Percent Overall Screening Efficiency Score (POSES) =

$$\frac{\text{TPA (total number of free radical scavengers in each solar salt / estuarine sediment/ sponge)}}{\text{TS (Total number of cultures)}} \times 100$$

3.1.4 DIVERSITY STUDIES

The occurrence of free radical scavengers and the genera level of diversity of extremely halophilic eubacteria and haloarchaea from solar salt sample estuarine sediments and sponge were calculated as:-

Shannon-Weiner's diversity index 'H' (Shannon and Weaver, 1949)

The generic diversity in community was carried out by Shannon-Weiner's diversity index H' by using the generalization:

$H' = \Sigma [(n/N) \ln(n/N)];$

Where n = number of individual cultures; N = total number of all cultures.

3.1.5 TOTAL ANTIOXIDANT CAPACITY AND TOTAL PHENOLIC CONTENT OF SELECT HALOARCHAEAL GENERA

Six cultures were selected for further analysis. MEC was obtained using the protocol detailed in **3.1.2.1**, from a wet weight of 0.5 g and was used to evaluate total antioxidant capacity and phenolic content. The total antioxidant capacity was quantitatively assessed by the spectrophotometric method of Prieto *et al*. (1999). 1 ml of MEC of each of the 6 cultures was individually mixed with 1 ml of phosphomolybdenum reagent solution (***Appendix I***). Blank consisted of 1 ml of methanol and 1 ml of reagent solution. The tubes were capped and incubated for 90 min at 95°C. After the tubes had cooled to room temperature, absorbance was measured at 695 nm using the UV-Visible spectrophotometer (UV-1601, Shimadzu, Kyoto, Japan). Ascorbic acid was used as a positive control ($r^2 = 0.96$). Results were also expressed as mg Ascorbic Acid Equivalent (AAE) g^{-1} of cells. Standard curve was constructed using a 100 mg ml^{-1} stock solution of ascorbic acid (***Appendix II***). The total phenolic content was determined spectrophotometrically using the Singleton and Rossi, (1965) method. The reaction mixture was prepared by mixing 0.5 ml of MEC, 2.5 ml of freshly prepared 10% Folin-Ciocalteu's reagent and 2.5 ml of 7.5% Na_2CO_3. Blank was concomitantly prepared, containing 0.5 ml of methanol, 2.5 ml 10% Folin-Ciocalteu's reagent dissolved in water (freshly prepared) and 2.5 ml of 7.5% of Na_2HCO_3. The reaction mixture was mixed thoroughly and allowed to stand for 90 min at room temperature. The absorbance was determined using the spectrophotometer at λmax = 765 nm. The samples were prepared in triplicate for

each analysis and the mean value of absorbance was obtained. Gallic acid was used as a positive control (r^2 = 0.99). The phenolic content was expressed in terms of mg of Gallic Acid Equivalent GAE g^{-1} of cells. Standard curve was constructed using a 100 µg ml^{-1} stock solution of gallic acid (***Appendix II***).

3.1.6 SPECTROSCOPIC ANALYSIS OF MEC OF SELECT HALOARCHAEAL CULTURES

Spectroscopic analysis of the MEC of each of the select haloarchaeal cultures was determined using an UV-Visible dual beam spectrophotometer (Shimadzu UV-1800, Japan) by scanning in the wavelength region of 190 - 800 nm.

3.1.7 STATISTICAL ANALYSIS

Statistical analysis was carried out using IBM-SPSS 23 statistical software. Analysis of variance and significant differences among means of different cultures were performed with one-way analysis of variance (ANOVA).

SECTION B

ANTIOXIDANT PRODUCTION BY *Haloferax alexandrinus* GUSF-1 (KF796625)

3.1.8 GROWTH AND FREE RADICAL SCAVENGING ACTIVITY OF *Haloferax alexandrinus* GUSF-1 (KF796625)

For growth and free radical scavenging activity, 5% of *Haloferax alexandrinus* GUSF-1 (KF796625) v/v was inoculated aseptically into a 3 sets of flasks having 100 ml of sterile NTYE broth in a 250 ml of Erlenmeyer flask incubated at 150 rpm and at 37 ºC. 5 ml of growing cells were aseptically withdrawn at regular time intervals and analyzed for growth and free radical scavenging activity. Growth was monitored as biomass and determined as dry weight g l^{-1}. Methanolic extract of cells was prepared from cells as detailed in **3.1.2.1** and was referred to as *Hfx*E. The free radical scavenging activity of *Hfx*E was carried out as detailed in **3.1.1.4** and expressed as in

3.1.1.5. This activity in *Hfx*E was capable of DPPH$^{\bullet}$ decolourization was termed as *Hfx*A.

3.1.9 FREE RADICAL SCAVENGING EXTRACTION CAPACITY OF SOLVENTS

To several cell pellets of *Haloferax alexandrinus* GUSF-1 (KF796625), 0.5 ml of each of the following solvents; hexane, petroleum ether (60-80ºC), chloroform, ethyl acetate, acetone, ethanol, methanol, and water were added separately and kept standing overnight. Extract of cell pellets were recovered by centrifuging at 10000 rpm, for 10 min with minimum exposure to light. Each of the crude extract was checked for free radical scavenging activity as detailed in **3.1.1.4 & 3.1.1.5**.

3.1.10 OPTIMIZATION OF PARAMETERS FOR MAXIMUM FREE RADICAL SCAVENGING ACTIVITY

Various paramaters including NaCl concentration, incubation temperature and initial pH of the growth medium were optimised for maximum growth and free radical scavenging activity. For growth of initial inoculum, 5% of *Haloferax alexandrinus* GUSF-1 (KF796625) was inoculated aseptically into a flask having 50 ml of sterile NTYE broth and grown at 37ºC till culture reached A_{600}=1. The optimal cultural conditions for growth and antioxidant production was carried out by inoculating 5 % of *Haloferax alexandrinus* GUSF-1 (KF796625) (A_{600} = 1) in eight flask, each having 100 ml of NTYE broth and different NaCl concentration; 5, 10, 15, 20, 25, 30, 35 and 40 %, incubating the flasks at different temperatures; 25°C, RT (28 ± 2°C), 37°C and 42°C and by growing the culture in medium with pH 5, 6, 7, 8 and 9, adjusted accordingly with 1N HCl or 1N NaOH. Respective flasks were incubated at 37 °C for 6 d and checked for free radical scavenging activity as detailed in **3.1.1.4 & 3.1.1.5**. Under optimised conditions, time course of antioxidant production and growth of *Haloferax alexandrinus* GUSF-1 (KF796625) was also studied.

3.1.11 KINETIC STUDIES OF FREE RADICAL SCAVENGING ACTIVITY OF *Hfx*A

*Hfx*A was concentrated to dryness under vacuum using rotary evaporator (Buchi Rotavapor, R-201) and was re dissolved in methanol to give a stock solution of 1 mg ml^{-1} and used for kinetic studies of free radical scavenging activity. Ascorbic acid was used as the positive control and for comparison studies.

3.1.11.1 Free radical scavenging effectiveness

Scavenging reaction between $DPPH^{\bullet}$ and *Hfx*A at different concentration (0.2-40 µg ml^{-1}) was followed as decrease in absorbance over period of time. Methanol was used as the reference solution and $DPPH^{\bullet}$ in methanol as control. The conversion of $DPPH^{\bullet}$ to DPPH-H is dependent on the relative concentrations of the reactants, but since the concentration of the $DPPH^{\bullet}$ is fixed at 0.2 mM and the concentration of *Hfx*A varies; the reaction rate for EC_{50} of *Hfx*A was calculated using the following equation:

$\ln (DPPH^{\bullet})_{t = 15} = \ln (DPPH^{\bullet})_{t = 1} - kt$; where, $(DPPH^{\bullet})_{t = 1}$ was the concentration of radical at initial time, 1 min and $(DPPH^{\bullet})_{t = 15}$ is the concentration of radical at steady time t = 15;

k is the first order rate constant obtained for fixed reaction incubation time (Mishra *et al*., 2012).The first order rate constant was also calculated at steady state for different concentrations of *Hfx*A used.

Half life ($t_{1/2}$) which is the time required for the concentration of a reactant to decrease to half of it's initial concentration at $t_{1/2} = [A] = 1/2\ [A]_0$; for 1^{st} order reaction was calculated using the equation; t = 0.693/ k for each of the concentration used.

3.1.11.2 Potency and kinetics of *Hfx*A

The potency and kinetics of *Hfx*A was deduced by obtaining the efficient/ effective concentration (EC_{50}) and TEC_{50}. The EC_{50} and TEC_{50} were further used to calculate the anti-radical power (ARP) expressed as the inverse of EC_{50}, antiradical efficiency (ARE), antioxidant index (AAI) and the stoichiometry of reactant.

3.1.11.3 Effective concentration (EC_{50})

The effective concentrationEC_{50}/ IC_{50} value, which is the concentration of substrate that causes 50% loss of the initial $DPPH^{\bullet}$ concentrations, was estimated using concentrations; 0-40 µg ml^{-1}. The experiment was performed three times and results averaged.

3.1.11.4 Time to attain the steady (TEC_{50})

The decrease in absorbance at 517 nm of $DPPH^{\bullet}$ radical till steady state (TEC_{50}) was also monitored for the EC_{50} concentration.

3.1.11.5 Antiradical power (ARP)

The antiradical power (ARP) defined as the reciprocal of EC_{50} was calculated using the formula ARP = 1/ EC_{50} (Mishra *et al*., 2012).

3.1.11.6 Antiradical efficiency (ARE)

The antiradical efficiency (ARE) = ARP/ TEC_{50} of *Hfx*A was estimated according to Sanchez et al. (1998).

3.1.11.7 Antioxidant activity index (AAI)

The antioxidant activity index (AAI) was determined using the following equation AAI = Cf/ EC_{50}; where Cf is the final concentration of $DPPH^{\bullet}$ solution in mg ml^{-1} and EC_{50} is the concentration providing 50% inhibition (Scherer and Godoy, 2009).

3.1.11.8 Stoichiometry of reactions

The stoichiometry value of *Hfx*A was expressed as the amount of antioxidant required to reduce 100 % $DPPH^{\bullet}$ radicals, deduced and calculated as $EC_{50} \times 2$ (Brand-Williams *et al*., 1995).

3.1.12 ISOLATION AND CHEMICAL CHARACTERIZATION OF ANTIOXIDANTS

3.1.12.1 Growth of *Haloferax alexandrinus* GUSF-1 (KF796625)

Haloferax alexandrinus GUSF-1 (KF796625) was inoculated into 500 ml of NTYE, pH 7 and grown under optimized conditions. Supernatant obtained from centrifuging culture broth was used to prepare extracts of supernatant using the protocol of Del Gallo and Haegi, 1990**.** The supernatant was first passed through a 0.2 μm filter and filtrates were precipitated overnight with the equal volume of cold ethanol at −20°C. The precipitated supernatant was centrifuged at 10000 for 30 min at 4°C and the pellet dispersed in sterile distilled water.

3.1.12.2 Preparation of hydroxylated methanolysates from wet cells

Wet cells of *Haloferax alexandrinus* GUSF-1 (KF796625) (100 mg) were mixed with methanol (3 ml), toluene (3 ml) and conc.H_2SO_4 (0.1 ml) and heated at 50°C for 18 h. The long-chain components were extracted from this mixture by adding 1.5 ml hexane (Ross *et al*., 1965)

3.1.12.3 Preparation of methanolic extract of cells with antioxidant capacity - (*Hfx*A)

*Hfx*A was prepared from washed wet cells as detailed in **3.1.2.1** and was concentrated to dryness under vacuum using rotary evaporator (Buchi Rotavapor, R-201) and stored at –20°C till use.

3.1.12.4 Separation of antioxidant components from *Hfx*A

*Hfx*A was separated into two layers by adding hexane and distilled water. The upper hexane layer was subjected to cold acetone precipitation by addition of cold acetone in small volumes. The precipitate was separated out, re dissolved in methanol and stored at -20 ^{o}C till further use. This extract has been termed as Acetone Precipitated Material (APM). The hexane layer left behind is termed as Hexane Extract (HE). HE was concentrated to dryness using liquid nitrogen and stored at -20 °C till use **(Fig 3.1).**

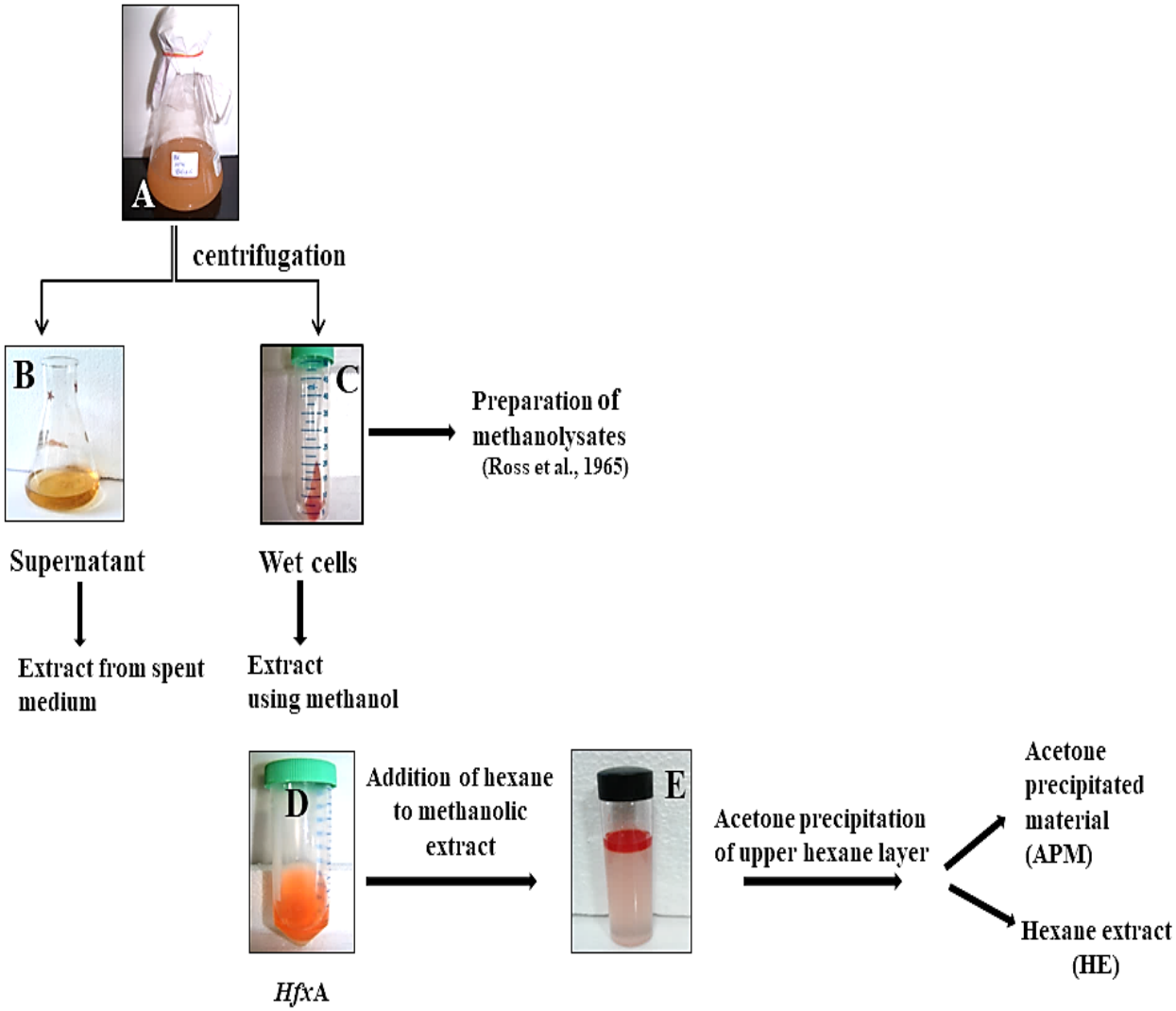

Fig. 3.1 Extraction steps followed for separation of free radical scavengers

A: Growth of *Haloferax alexandrinus* GUSF-1 (KF796625) under optimized conditions; **B:** Supernatant used for extraction; **C;** Wet cells obtained on centrifuging the culture broth used for methanolic extraction; **D:** Methanolic extract from wet cells with the antioxidant capacity *Hfx*A; **E:** Addition of hexane to *Hfx*A and acetone precipitation of the upper hexane layer

3.1.13 DETECTION OF FREE RADICAL SCAVENGING ACTIVITY OF CHEMICALLY SEPARATED COMPONENTS

3.1.13.1 Free radical scavenging assay

The free radical scavenging activity of extracts of supernatant, hydroxylated methanolysates, *Hfx*A, HE and APM and was assessed using the DPPH$^{\bullet}$ Assay. The DPPH$^{\bullet}$ Assay of each of the extracts was individually evaluated using 0.2mM DPPH$^{\bullet}$ prepared in methanol or hexane as detailed in **3.1.1.4 & 3.1.1.5.**

0.1 mM of DPPH$^{\bullet}$ prepared in methanol and hexane was also added to *Hfx*A or HE or APM and the reaction mixture was scanned at regular intervals using the UV-Vis spectrophotometer (UV-1601, Shimadzu, Kyoto, Japan).

3.1.13.2 Demonstration of free radical scavenging activity by Thin Layer Chromatography

3.1.13.2.1 Thin layer chromatography of hydroxylated methanolysates

The hydroxylated methanolysates were chromatographed on four different sheets. Hydroxylated methanolysates were spotted on to TLC silica gel GF254 plate (Merck, Darmstadt, Germany). The chromatograms were resolved using solvent system consisting of petroleum ether (60-80 °C): diethyl ether (85:15, v/v) and air dried in the dark. The 1st chromatogram was sprayed with 10% dodecaphosphomolybdic acid in absolute ethanol and heated for 15 min at 150 °C. The 2nd chromatogram was placed in an iodine chamber to detect colourless spots. The 3rd chromatogram was used to detect free radical scavenging activity by spraying with DPPH$^{\bullet}$ reagent. The 4th chromatogram was not treated. The spot corresponding to the R_f 0.2 obtained on the 1st chromatogram on spraying with 10 % dodecaphosphomolybdic acid was scrapped out from the 4th chromatogram. The sample was ground with IR grade KBr to form a pellet and further analyzed using a Fourier Transform- Infra Red spectrometer (FT-IR) (Shimadzu IR Prestige-21) in the 4000 to 400 cm^{-1} spectral region at a resolution of 4.0 cm^{-1}.

3.1.13.2.2 Thin layer chromatography of *Hfx*A

50 µl of *Hfx*A was spotted individually and in triplicate on a TLC silica gel GF254 plate (Merck, Darmstadt, Germany) and the chromatogram was developed in benzene: acetone (2:1). The resolved spots if any were viewed by naked eye. The 2nd chromatogram was sprayed with 0.2mM $DPPH^{\bullet}$ prepared in methanol, and further incubated in the dark for 30 min. White bands if any, appearing against a purple background was noted.

3.1.13.2.3 Thin layer chromatography of HE and characterization of spots positive for FRSA

50 µl of HE was spotted individually and in duplicate on several TLC silica gel GF254 plate (Merck, Darmstadt, Germany). The chromatograms were resolved using different solvent system (each in triplicates) (A) Acetone-petroleum ether (20:80; v/v) (Asker *et al*., 2002) (B) Methanol-chloroform (7:93; v/v) for bacterioruberin and monoanhydrobacterioruberin (Kushwaha *et al*., 1975) (C) n-heptane: benzene (9:1; v/v) for vitamin MK-8, squalene and its derivatives (Tornabene, 1969) (D) Acetone: hexane (1:1) for haloxanthin (Ronnekleiv *et al*., 1995). After developing in the respective solvent systems, the TLC plates were air dried in the dark. R_f of coloured spots were visualized. The 1st plate was placed in an iodine chamber to visualize spots (Kushwaha *et al*., 1974). The 2nd plate was used to detect free radical scavenging activity by spraying with 0.2 mM $DPPH^{\bullet}$ prepared in methanol. Select spots from respective chromatogram, positive for $DPPH^{\bullet}$ activity were scrapped off from the 3rd Chromatogram, redissolved in methanol and spectroscopic analysis was carried out using an UV-Visible dual beam spectrophotometer (Shimadzu UV-1800, Japan) by scanning in the wavelength of 190-800 nm using methanol as reference solution.

3.1.13.2.4 Thin layer chromatography of APM

APM was chromatographed on a TLC silica gel GF254 plate (Merck, Darmstadt, Germany). The chromatograms were resolved using solvent system consisting of chloroform: methanol: acetic acid: water (85:22.5:10:4, v/v). The chromatograms was air dried at RT in the dark and placed in an iodine chamber to detect colourless spots (Kushwaha *et al*., 1974).

3.1.14 CHEMICAL CHARACTERIZATION OF FREE RADICAL SCAVENGING MOLECULES

3.1.14.1 Spectroscopic analysis of extracts from culture supernatant and cells

A stock of 1mg/ ml of each of the extracts was individually prepared in the respective solvent; distilled water/ methanol/ hexane and acetone. Spectroscopic analysis of extracts from culture supernatant, methanol extracts of cells and solvent fractionation samples i.e *Hfx*A, HE and APM was determined using an UV-Visible dual beam spectrophotometer (Shimadzu UV-1800, Japan) by scanning in the wavelength region of 190-800 nm.

3.1.14.2 Fourier Transform-Infra Red Spectroscopic analysis of extracts of culture supernatant and cells

FT- IR analysis of concentrated extracts of culture supernatant, methanol extracts of cells and solvent fractionation samples i.e *Hfx*A, HE, APM was determined using a Fourier Transform-Infra Red spectrometer (Shimadzu IR Prestige-21) as detailed in **3.1.13.2.1.**

3.1.14.3 Qualitative chemical evaluation of cell extracts

Presence of secondary metabolites such phenolic compound, terpenoids, glycosides and saponin in *Hfx*A was done by spot test. Methanol was used as a control.

3.1.14.3.1 Phenolic compounds (Singleton *et al*., 1965)

0.5 ml of *Hfx*A, 2.5 ml of 10 % Folin-Ciocalteu's reagent dissolved in water (freshly prepared) and 2.5 ml of 7.5 % Na_2CO_3. Formation of bluish green coloration indicates presence of phenolic content.

3.1.14.3.2 Saponins (Harborne, 1998)

2 ml *Hfx*A was shaken well with 2 ml of distilled water. Production of persistent stable foam indicated presence of saponins.

3.1.14.3.3 Glycosides (Harborne, 1998)

2 ml of *Hfx*A was treated with 2 ml of glacial acetic acid and a drop of 5 % (w/v) $FeCl_3$. Formation of a brown ring is indicative of glycone.

3.2 RESULTS

SECTION A

FREE RADICAL SCAVENGING ACTIVITY BY EXTREMELY HALOPHILIC EUBACTERIA AND HALOARCHAEA

Solar salt is recovered merely by evaporation of sea water, through use of renewable energy sources of wind and sunlight. This solar salt, besides the main component of NaCl, has other elements enforcing health benefits such as Mg^{2+}, Ca^{2+}, K^{1+}, S trace elements of Cu^{2+}, Zn^{2+}, Fe^{3+}, Mn^{2+} and minute amounts of I_2. It is traditionally used by Goan farmers as annual application to fruiting trees mixed with manure.

3.2.1 STABILITY AND LINEARITY OF DPPH$^{\bullet}$

With different increasing concentrations of DPPH$^{\bullet}$, a very good linearity of absorbance versus concentration (R^2 = 0.9983) was obtained confirming to Beer Lambert's law (***Appendix II*****).** It was also observed that there was no significant differences in absorbance for 0.2 mM concentrations over different time intervals from 0 to 40 min.

3.2.2 ANTIOXIDANT ACTIVITY OF SOLAR SALT

Solar salts from six different salt pans, namely Arambol (A), Agarwada (Ag), Arpora (Ar), Nerul (N), Ribandar (R) and Siridao (S) could be categorized visually by the naked eye into: white with greyish tinge and the other white with brownish tinge (**Fig. 3.2)**. Saturated solutions of brownish solar salt and the greyish solar salt with a methanolic solution of $DPPH^{\bullet}$ resulted in decolourization of the purple colour of $DPPH^{\bullet}$ with a corresponding drop in absorbance at 517 nm. A drop in absorbance at 517 nm observed for the solar salt with the greyish tinge was 0.063 nm corresponding to 0.0793 µg AAE g^{-1}, whereas the drop in absorbance at 517 nm for the solar salt with a brownish tinge was 0.083 nm corresponding to 0.145 µg AAE g^{-1} when compared to the $DPPH^{\bullet}$ solution whose absorbance did not decline over a period of 1 h.

Fig. 3.2 Two varieties of solar salt **A:** white with greyish tinge **B:** white with brownish tinge

3.2.3 FREE RADICAL SCAVENGING ACTIVITY BY MICROBES IN SOLAR SALT

Aliquots of saturated solutions of solar salt when spread out onto nutrient rich agar with 25 % NaCl and incubated at 37 ^{o}C, developed into colonies in 8 d. As recorded in **Fig. 3.3 A**, a variety of colonies grew ranging from pin heads to 1-1.5 mm in size, butyrous to dry, with even and uneven margins, colourless and others having yellow, orange and red pigmentation, grew within a week on NTYE, but none on TYE agar which did not have any NaCl. Careful exposure of these bacterial colonies to methanolic DPPH$^{\bullet}$ directly, while still on agar resulted in some of the colonies exhibiting a light yellow halo around themselves, against a purple colour of DPPH$^{\bullet}$ retained by the agar thus indicating the ability of some colonies to decolourize DPPH$^{\bullet}$ and others not. This method, herein was referred by us as 'Agar-growth- DPPH$^{\bullet}$ method' (**Fig. 3.3 B**).

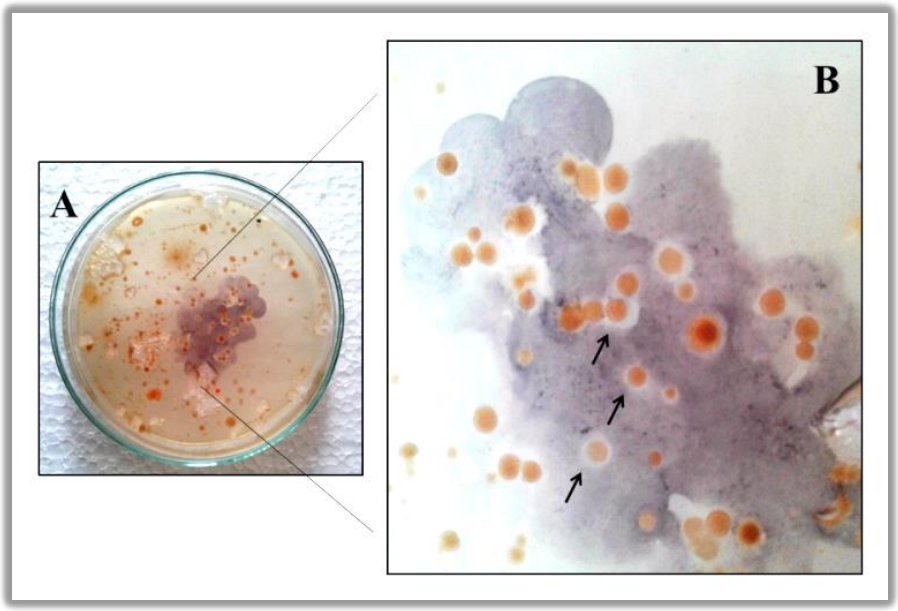

Fig. 3.3 A: Growth on NTYE agar on plating aliquot of saturated solution of solar salt and flooded with 0.1 mM DPPH$^{\bullet}$ **B:** Arrows indicating colonies showing free radical scavenging activity with a halo around it, against a purple stained NTYE plate

3.2.4 FREE RADICAL SCAVENGING ACTIVITY AMONG EXTREMELY HALOPHILIC CULTURES

Having established that the free radical scavenging ability of solar salt is associated with microbes growing in nutrient rich medium with 25 % NaCl, we screened out 117 extremely halophilic microbes retrieved from different solar salts, estuarine sediments and from sponge during earlier studies, for their ability to scavenge free radicals. One hundred of these cultures gave white-yellow zones around their colonies, by the 'Agar-growth-DPPH' method and were recorded as free radical scavengers.

Analysis of methanolic extract of cells (MEC) of each of these 100 extremely halophilic cultures which were positive for $DPPH^{\bullet}$ decolourization by the 'Agar-growth-DPPH' method, further confirmed their ability to decolourize the purple coloured solution of $DPPH^{\bullet}$ to varying shades of purple, with a corresponding decrease in absorbance at 517 nm. As recorded in **Fig. 3.4 A & 3.4 B**, the degree of $DPPH^{\bullet}$ decolourization, varied in cultures retrieved from different solar salts. Further as recorded in **Fig. 3.4 A & B**, the % $DPPH^{\bullet}$ RSA ranged from a minimum of 6.06 ± 0.19 exhibited by $GUFF_3$ to a maximum of 31.5 ± 0.43 shown by GUSF-1 and was followed by $GUFF_{188}$, $GUFF_{179}$, $GUFF_{66}$, and $GUFF_{72}$ respectively. A low activity of less than 10% was shown by 7 ($GUFF_{20, 35, 88, 90, 146, 148, 187}$), 5 ($GUBF_{2, 3}$, $GUFF_{3, 61, 168}$), 4 ($GUFF_{28, 56, 82, 83}$), 3 ($GUFF_{26, 98, 51}$), 2 ($GUFF_{36, 76}$) and 1 ($GUFF_{95}$) cultures respectively. All of the 15 cultures from the estuarine sediments and the culture from sponge also decolourized the purple coloured solution of $DPPH^{\bullet}$ to varying shades of purple, with a corresponding decrease in absorbance at 517 nm. As seen in **Fig. 3.4 C**, the degree of $DPPH^{\bullet}$ decolourization varied in cultures retrieved from different estuarine sediments including the culture from sponge. Further as recorded in **Fig 3.4 C**, the % $DPPH^{\bullet}$ RSA ranged from a minimum of 6.82 ± 0.07 exhibited by the culture coded as $GUFLF_{18}$, to a maximum of 29.37 ± 0.25 shown by $GUBF_5$ which gave the highest activity and was followed by GUIF3 and GUIF4. A low activity of less than 10 % was shown by 3 cultures; $GUFLF_{14}$, $GUFLF_{18}$ and GUVFFM-3 respectively. The Ascorbic Acid Equivalence (AAE) of the cultures positive for FRSA is mentioned in **Table No 3.1** and **3.2.**

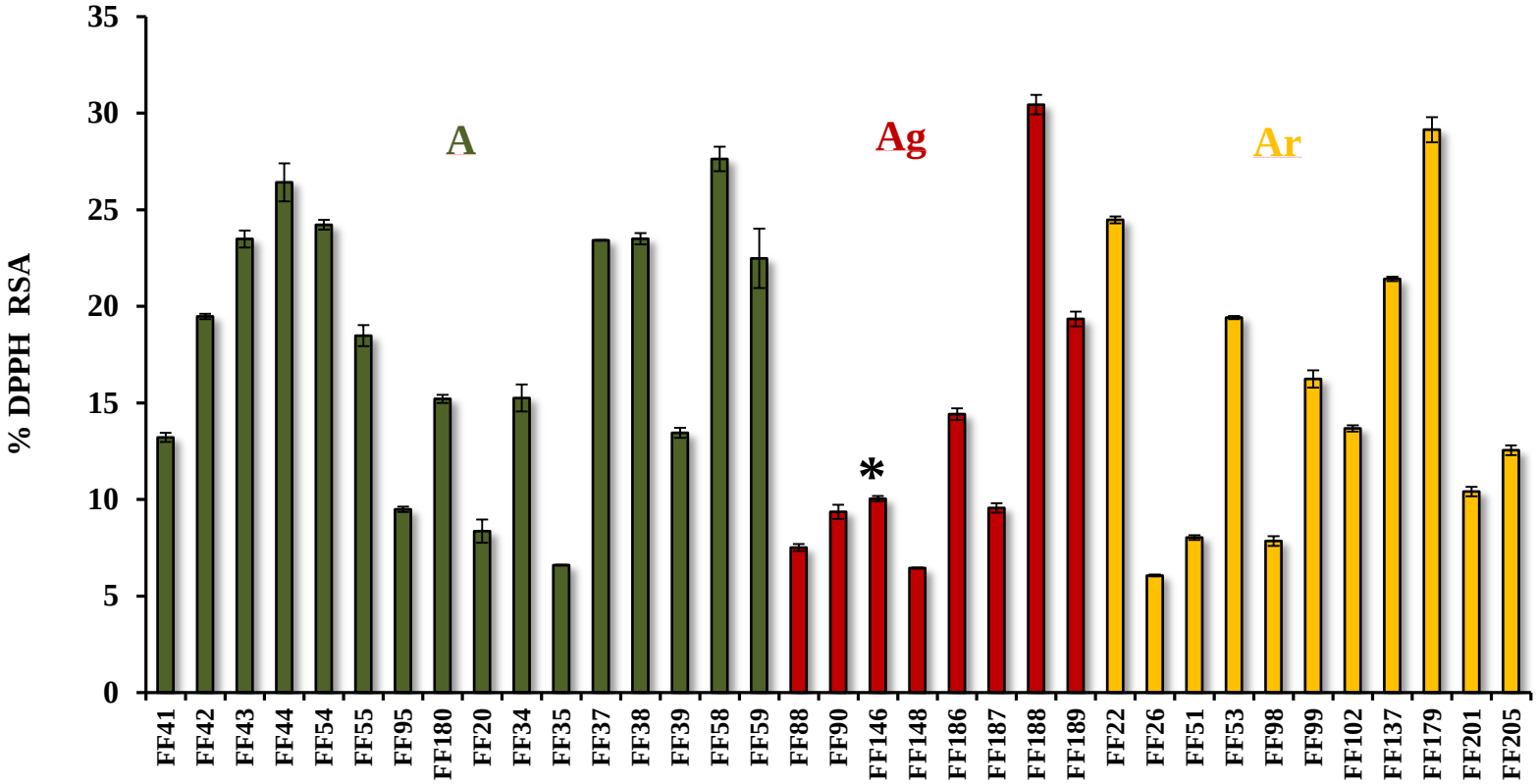

Fig. 3.4 A: Decolourization of DPPH$^{\bullet}$ by methanolic extracts of individual extremely halophilic eubacteria and haloarchaeal cultures from different solar salts. The culture marked with an asterix* is eubacteria, the rest of the cultures are haloarchaea.

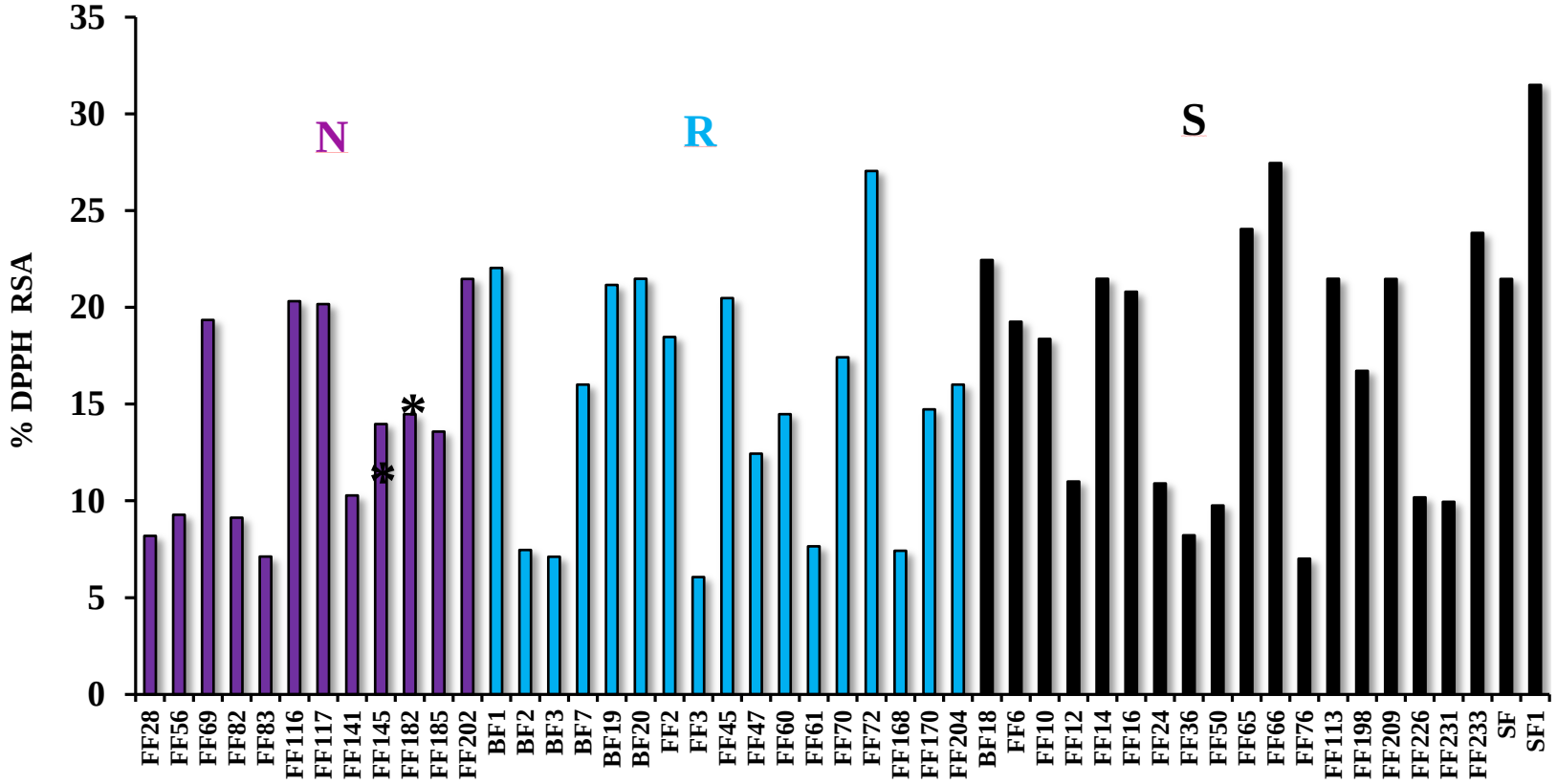

Fig. 3.4 B: Decolourization of DPPH$^{\bullet}$ by methanolic extracts of individual extremely halophilic eubacteria and haloarchaeal cultures from different solar salts. The cultures marked with an asterix* are eubacteria, the rest of the cultures are haloarchaea.

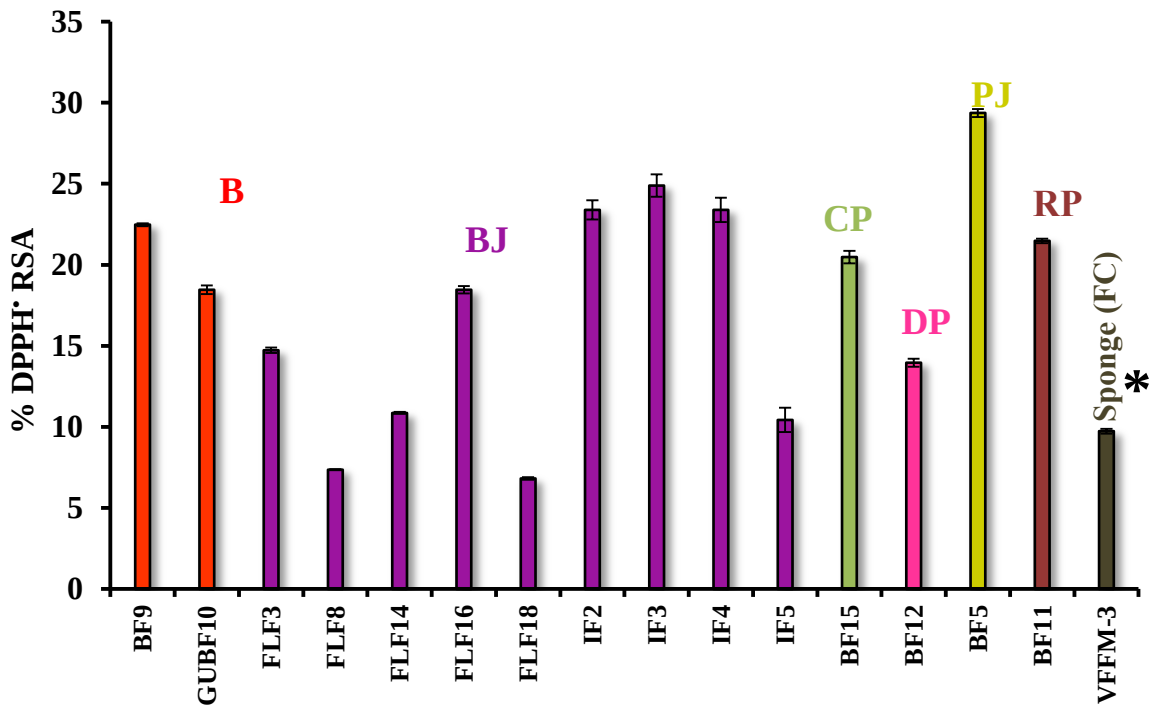

Fig. 3.4 C: Decolourization of DPPH• by methanolic extracts of individual extremely halophilic eubacteria and haloarchaeal cultures from estuarine sediments and the culture from sponge. The culture marked with an asterix* is eubacteria, the rest of the cultures are haloarchaea.

Table 3.1 Ascorbic Acid Equivalence of free radical scavenging activity of extremely halophilic and haloarchaeal cultures from solar salts

Solar Salt sample	Cultures (GU)	Free radical scavenging activity	Solar Salt sample	Cultures (GU)	Free radical scavenging activity	Solar Salt sample	Cultures (GU)	Free radical scavenging activity	Solar Salt sample	Cultures (GU)	Free radical scavenging activity	Solar Salt sample	Cultures (GU)	Free radical scavenging activity	Solar Salt sample	Cultures (GU)	Free radical scavenging activity
		µg AAE g^{-1}cells			µg AAE g^{-1}cells			µg AAE g^{-1}cells			µg AAE g^{-1}cells			µg AAE g^{-1}cells			µg AAE g^{-1}cells
A	FF_{41}	105.8 ± 0.18	**Ar**	FF_{22}	196 ± 0.36	**Ag**	FF_{20}	64.2 ± 0.64	**R**	BF_{1}	176.5 ± 0.16	**N**	FF_{28}	65.6 ± 0.26	**S**	BF_{18}	211.8 ± 1.24
	FF_{42}	156.0 ± 0.24		FF_{26}	48.5 ± 0.04		FF_{34}	122 ± 0.04		BF_{2}	59.6 ± 0.1		FF_{56}	74.3 ± 0.09		FF_{6}	154.2 ± 0.14
	FF_{43}	188.1 ± 0.3		FF_{51}	64.3 ± 0.1		FF_{35}	52.8 ± 0.016		BF_{3}	56.8 ± 0.02		FF_{69}	156 ± 0.6		FF_{10}	147 ± 0.14
	FF_{44}	211.6 ± 0.28		FF_{53}	155.5 ± 0.16		FF_{37}	187.5 ± 0.36		BF_{7}	130.3 ± 0.12		FF_{82}	36.5 ± 0.02		FF_{12}	88.2 ± 0.57
	FF_{54}	193.8 ± 0.2		FF_{98}	62.8 ± 0.2		FF_{38}	188 ± 0.56		BF_{19}	193.4 ± 0.08		FF_{83}	57 ± 0.02		FF_{14}	172 ± 0.3
	FF_{55}	148.0 ± 0.48		FF_{99}	130.1 ± 0.36		FF_{39}	107.6 ± 0.2		BF_{20}	172 ± 0.82		FF_{116}	183.5 ± 0.14		FF_{16}	166.6 ± 0.6
	FF_{95}	76 ± 0.008		FF_{102}	109.5 ± 0.12		FF_{58}	221.2 ± 0.5		FF_{2}	148 ± 0.16		FF_{117}	161.5 ± 0.06		FF_{24}	87.2 ± 0.4
	FF_{180}	121.8 ± 0.16		FF_{137}	171.5 ± 0.24		FF_{59}	180 ± 1.2		FF_{3}	48.5 ± 0.08		FF_{141}	82.3 ± 0.24		FF_{36}	65.8 ± 0.52
				FF_{179}	233.4 ± 0.52		FF_{88}	60 ± 0.14		FF_{45}	164 ± 0.08		FF_{145}	111.9 ± 0.19		FF_{50}	78 ± 0.54
				FF_{201}	83.3 ± 0.5		FF_{90}	74.4 ± 0.28		FF_{47}	99.6 ± 0.06		FF_{182}	115.9 ± 0.16		FF_{65}	192.6 ± 0.34
				FF_{205}	100.5 ± 0.2		FF_{146}	80.4 ± 0.62		FF_{60}	115.9 ± 0.34		FF_{185}	108.7 ± 0.15		FF_{66}	219.8 ± 0.016
							FF_{148}	51.6 ± 0.02		FF_{61}	61.2 ± 0.074		FF_{202}	182.5 ± 0.64		FF_{76}	56.16 ± 0.16
							FF_{186}	115.4 ± 0.42		FF_{70}	139.5 ± 1.32					FF_{113}	172 ± 0.52
							FF_{187}	76.4 ± 0.18		FF_{72}	56.4 ± 0.12					FF_{198}	133.9 ± 0.26
							FF_{188}	243.8 ± 0.4		FF_{168}	59.4 ± 1.3					FF_{209}	171.8 ± 0.22
							FF_{189}	155 ± 0.14		FF_{170}	118 ± 0.02					FF_{226}	81.5 ± 0.08
										FF_{204}	111.8 ± 0.08					FF_{231}	79.6 ± 0.12
																FF_{233}	191 ± 0.12
																SF	180 ± 0.36
																SF_{1}	**252.4 ±1.14**

Solar salts:
A- Arambol,
Ag- Agarwada, Ar- Arpora,
N- Nerul, R-Ribandar,
S- Siridao.
µg AAE g^{-1}cells – Ascorbic acid equivalence of 1 g of cells

Table 3.2 Ascorbic Acid Equivalence of free radical scavenging activity of extremely halophilic and haloarchaeal cultures from estuarine sediments and from sponge

Estuarine sediment	Cultures (GU)	Free radical scavenging activity	Estuarine sediment	Cultures (GU)	Free radical scavenging activity	Estuarine sediment	Cultures (GU)	Free radical scavenging activity	Estuarine sediment	Cultures (GU)	Free radical scavenging activity	Estuarine sediment	Cultures (GU)	Free radical scavenging activity	Estuarine sediment	Cultures (GU)	Free radical scavenging activity	Sponge	Cultures (GU)	Free radical scavenging activity
		µg AAE g $^{-1}$cells			**µg AAE g $^{-1}$cells**			**µg AAE g $^{-1}$cells**			**µg AAE g $^{-1}$cells**			**µg AAE g $^{-1}$cells**			**µg AAE g $^{-1}$cells**			**µgAAE g $^{-1}$cells**
B	BF_9	180.05 ± 0.09	**BJ**	FLF_3	117.98 ± 0.213	**CP**	BF_{15}	164.03 ± 0.321	**DP**	BF_{12}	111.81 ± 0.432	**PJ**	**BF_5**	**235.24 ± 0.231**	**PP**	BF_{11}	172.0465 ± 0.124	**FC**	VFFM-3	76 ± 0.22
	BF_{10}	147.85 ± 0.27		FLF_8	58.95 ± 0.112															
				FLF_{14}	86.98 ± 0.143															
				FLF_{16}	147.85 ± 0.32															
				FLF_{18}	54.62 ± 0.211															
				IF2	187.34 ± 0.132															
				IF3	199.35 ± 0.112															
				IF4	187.34 ± 0.108															
				IF5	83.54 ± 0.176															

Estuarine sediments: B- Baiguinim, BJ - Betim jetty, CP- Captain of Ports, DP- Dona Paula Bay , PJ - Panjim Jetty , RP – Ribandar Patto; Sponge FC - *Fasciospongia cavernosa*. µg AAE g $^{-1}$cells: Ascorbic acid equivalence of 1 g of cells.

The Percent Overall Screening Efficiency Score for free radical scavenging activity (POSES), exhibited by cultures and computed by scoring DPPH$^{\bullet}$ decolourization and no decolourization score against the total cultures screened from different solar salts, estuarine sediments and sponge is depicted in **Fig. 3.5**. The highest activity score of 100 % was obtained for the cultures from Agarwada solar salts, while, the lowest score of 74 % was obtained for cultures from solar salts of Siridao. Cultures from the solar salts of Nerul and Ribandar gave an equal score of 85 %, whereas cultures from the solar salts of Arambol and Arpora gave a score of 80 % and 79 %, respectively. The Percent Overall Screening Efficiency Score (POSES) for the cultures from the estuarine sediments was found to be 100 %. A highly significant variation (p<0.001) of free radical scavenging activity was observed within the free radical scavengers from different salt samples, estuarine sediments and from sponge as per the one-way ANOVA obtained using the IBM SPSS software.

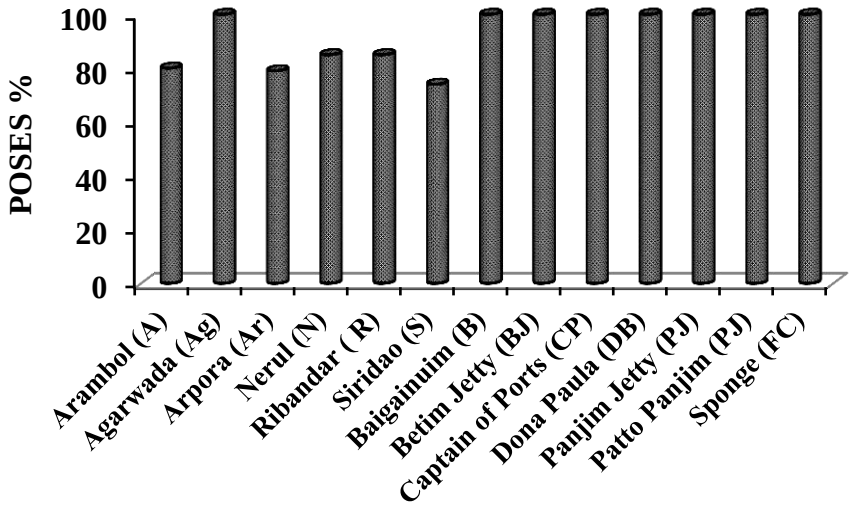

Fig. 3.5 Percent overall screening efficiency score for free radical scavenging activity among cultures from different solar salts, estuarine sediments and from sponge

3.2.5 DIVERSITY STUDIES OF FREE RADICAL SCAVENGING EXTREMELY HALOPHILIC EUBACTERIAL AND HALOARCHAEAL GENERA

Occurrence of free radical scavenging haloarchaea belonging to different genera differed among solar salts, estuarine sediments and from sponge (**Fig. 3.6**). A maximum of 6 genera were found in Agarwada, while a minimum of three haloarchaeal genera were found in Arambol, Arpora and Nerul. None of the solar salts had cultures belonging to all the 8 retrieved genera. Members of genus *Natrialba* were found in Agarwada and Siridao solar salts while *Natrinema* in Nerul and *Natronococcus* in Siridao. The frequency of occurrence of free radical scavenging members was: *Halococcus* > *Haloarcula* = *Haloferax* > *Halobacterium* > *Halorubrum* = *Natrialba* > *Natrinema* = *Natronococcus*.

Eubacteria although retrieved were 10 times less than that of haloarchaea and were restricted to genus *Gluconobacter* and *Alteromonas*. Further, as accounted in **Fig. 3.6**, the distribution of these two genera in Goan solar salts was very unequal. In the Nerul solar salt, members of *Gluconobacter* was 50 % of *Alteromonas*. Siridao and Arambol solar salt had only *Gluconobacter*, whereas Agarwada solar salt showed the presence of only *Alteromonas*. In estuarine sediments the free radical scavenging haloarchaeal genera present were *Haloarcula*, *Haloferax*, *Haloterigenna* and *Halobacterium* genera. None of estuarine sediments had cultures belonging to all the 4 retrieved genera. A maximum of 2 genera were found in the Betim jetty sample and the Baiguinim sample, while just one of haloarchaeal genera was found in Captain of Ports, Dona Paula, Panjim Jetty, Ribandar Patto. Members of *Haloarcula* and *Halobacterium* were found in the estuarine sediment samples from Baiguinim whereas members of *Haloferax* and *Halobacterium* was found in Betim Jetty. A member of *Haloarcula* was retrieved from Captain of Ports whereas a member of *Halobacterium* from Dona Paula, Panjim Jetty and Ribandar Patto estuarine sediments. The ocurrence of free radical scavenging members was: *Haloferax* = *Halobacterium* > *Haloarcula*.

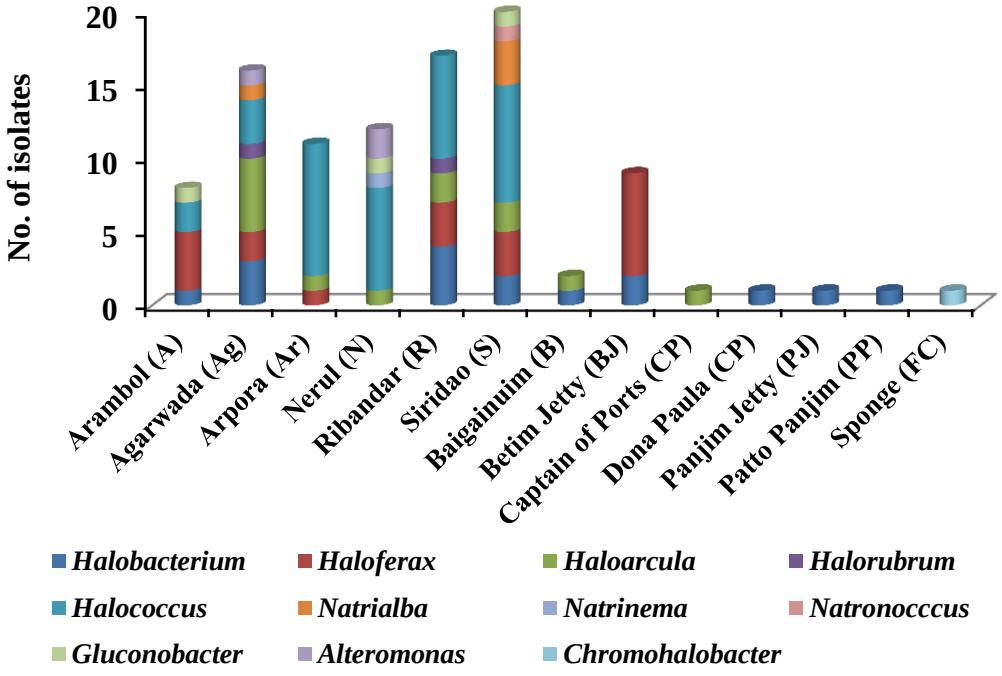

Fig. 3.6 Free radical scavenging by extremely halophilic eubacterial and haloarchaeal genera from different solar salts, estuarine sediments and sponge

The Shannon-Weiner Diversity Index 'H' calculated for free radical scavengers was 2.16, 1.75, 1.58, 1.39, 1.015, 0.7, 0.61, 0.37 and 0.16 for Agarwada, Siridao, Ribandar, Nerul, Arambol, Arpora, Betim Jetty and Baiguinuim respectively. An index of 0.61 was obtained for Captain of Ports, Dona Paula, Panjim Jetty, Ribandar Patto and sponge respectively **(Fig. 3.7)**.

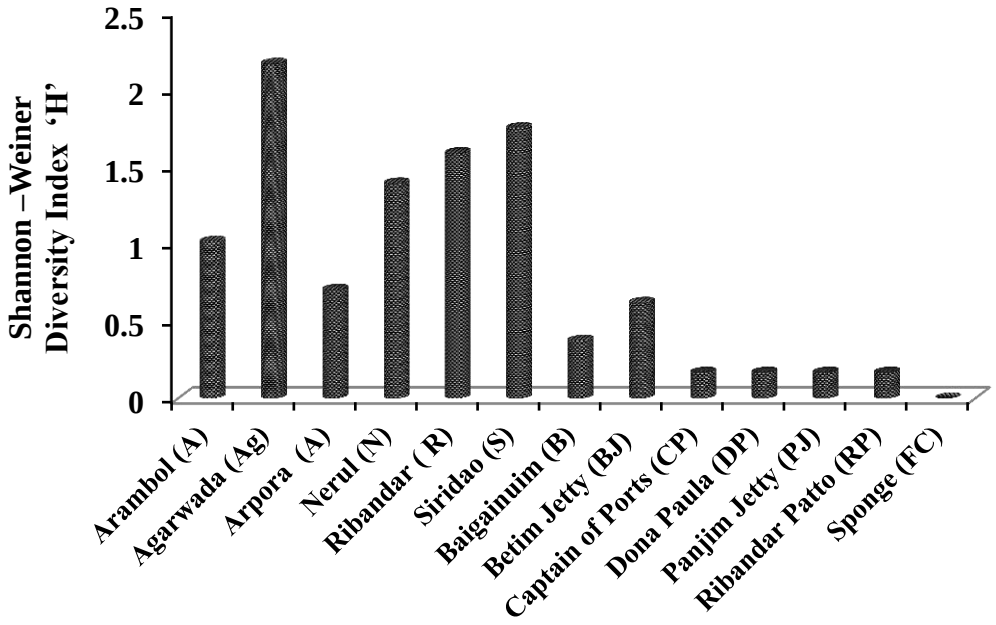

Fig. 3.7 Shannon-Weiner Diversity Index "H" for free radical scavengers from different solar salts, estuarine sediments and sponge

3.2.6 SPECTROCOSCOPIC ANALYSIS OF METHANOLIC EXTRACTS OF CELLS

Absorption spectrum between 300 - 600 nm revealed peaks for GUSF-1 at 522, 490, 464, 386, 368, 350, 317 and 304 nm (**Fig. 3.8 a**), while peaks for $GUFF_{188}$ were at 523, 490, 465, 386, 367 and 316 nm (**Fig. 3.8 b**). $GUFF_{179}$ showed peaks at 525, 492, 466, 406, 387, 368, 348 and 318 nm (**Fig. 3.8 c**). The peaks for $GUFF_{233}$ were present at 520, 488, 462, 384 and 316 nm while peaks for $GUFF_{72}$ were at 525, 490, 465, 384, 367 and 314 nm (**Fig. 3.8 d & e**). The peaks for $GUBF_5$ were at 522, 490, 464, 386, 368, 350, 317 and 304 nm (**Fig. 3.8 f**). Common peaks at 522 nm were seen for GUSF-1 and $GUFF_{72}$, similarly the peak at 490 nm was common for GUSF-1 and $GUFF_{188}$. The peak at 464 nm was common for GUSF-1 and $GUFF_{72}$ whereas the peak at 386 nm was common for the methanolic extract of GUSF-1 and $GUFF_{188}$. The peak at 317 nm was seen for both GUSF-1 and $GUFF_{72}$.

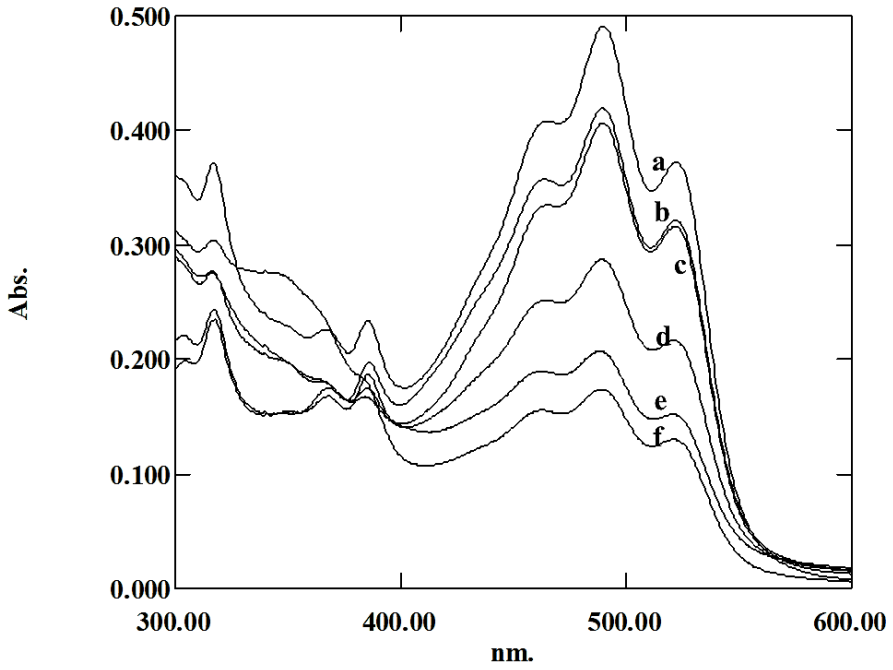

Fig. 3.8 Absorption spectrum of select haloarchaeal cultures

3.2.7 TOTAL ANTIOXIDANT CAPACITY OF SELECT HALOARCHAEAL GENERA

As recorded in **Fig. 3.9 A**, the total antioxidant capacity varied among the six different cultures belonging to select haloarchaeal genera. GUSF-1; *Haloferax alexandrinus* (KF796625) gave the maximum of 1.176 ± 0.75 mg AAE g^{-1} cells, whereas $GUFF_{72}$; *Halorubrum* sp. gave a minimum of 0.167 ± 0.001 mg AAE g^{-1} cells, which was nearly 10 times less. The order of antioxidant capacity was GUSF-1 *Haloferax alexandrinus* (KF796625) > $GUBF_5$ *Halobacterium* ATCC BAA 647 = $GUFF_{188}$ *Haloarcula* sp > $GUFF_{233}$ *Natronocccus* sp. > $GUFF_{179}$ *Halococcus* sp. > $GUFF_{72}$ *Halorubrum* sp. The reaction mixture consisting of MEC and the phosphomolybdenum reagent on scanning revealed that the peaks between 300-600 nm were abolished (**Fig. 3.9 B**).

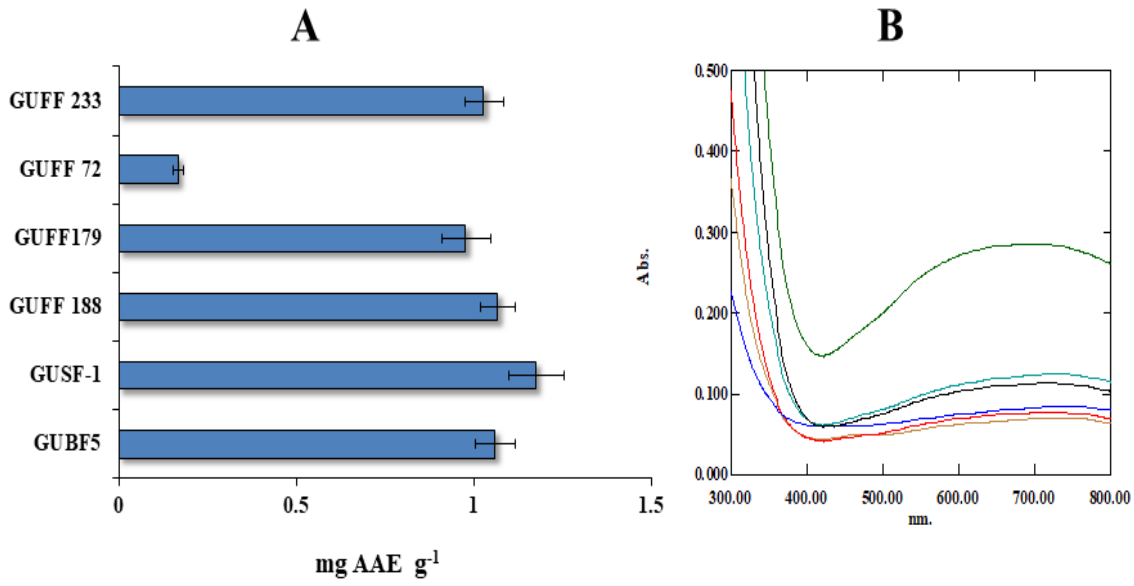

Fig. 3.9 A: Total antioxidant capacity of select haloarchaeal cultures and **B:** Interaction of MEC with phosphomolybdenum reagent

3.2.8 TOTAL PHENOLIC CONTENT OF SELECT RETRIEVED HALOARCHAEAL GENERA

Addition of FC reagent to the MEC developed blue colour which gave an absorption maximum at 765 nm. GUSF-1; *Haloferax alexandrinus* (KF796625) gave highest value of phenolic content of 0.784 ± 0.004 mg GAE g^{-1} cells (**Fig. 3.10**). This was followed by $GUFF_{179}$; *Halococcus* sp. > $GUFF_{188}$; *Haloarcula* sp. > $GUFF_{233}$; *Natronococcus* sp. The MEC of $GUFF_{72}$; *Halorubrum* sp. showed the minimum content of 0.135 ± 0.001 mg GAE g^{-1} cells. A positive correlation was also observed between phenolic content and total antioxidant capacity (R = 0.89, $p < 0.001$).

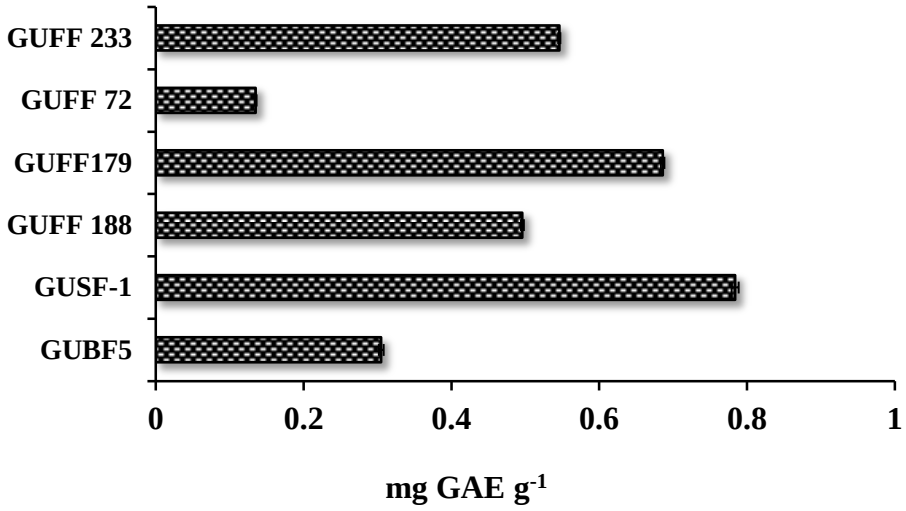

Fig. 3.10 Total phenolic content of select haloarchaeal cultures

SECTION B

ANTIOXIDANT PRODUCTION BY *Haloferax alexandrinus* GUSF-1 (KF796625)

Much attention has been given to potentials of natural antioxidant producers from marine environment because of their efficient ability as radical scavengers due to their redox properties. This section delves with antioxidant production in a relatively less explored haloarchaeal member of the Domain Archaea.

3.2.9 GROWTH AND PRODUCTION OF FREE RADICAL SCAVENGING ACTIVITY OF *Haloferax alexandrinus* GUSF-1 (KF796625)

Haloferax alexandrinus GUSF-1 (KF796625) started to grow with almost no lag phase and within 24 h reached the exponential phase in NTYE medium. Absorbance on day 0 was 0.24 and reached a maximum of 2.67 with biomass of 14.6 g l^{-1} by day 6. Stationary phase was observed by end of 6 d of incubation. Free scavenging activity increased steadily through all days of incubation upto 6 d as seen in **Fig. 3.11** and highest free scavenging activity was also found to be % DPPH$^{\bullet}$ RSA of 32.06 % (AAE was 15.96 µg ml^{-1}), after which a slight decrease in both growth and free scavenging activity was observed. Free scavenging activity was seen to be dependent on growth (p<0.001).

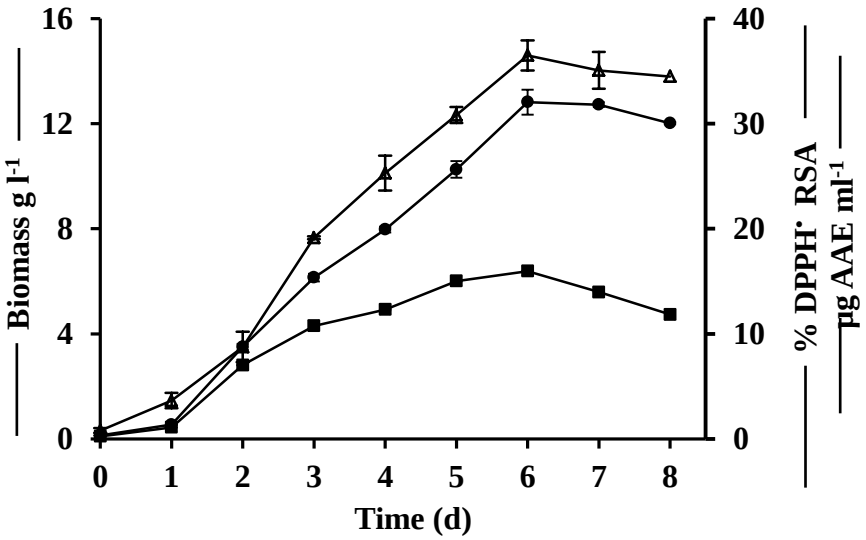

Fig. 3.11 Growth and free radical scavenging activity of *Haloferax alexandrinus* GUSF-1 (KF796625) with time; Biomass g l^{-1} —△—; free radical scavenging activity (% DPPH$^{\bullet}$ RSA) —●— ; Ascorbic Acid Equivalence —■—

3.2.10 EVALUATING THE FREE RADICAL SCAVENGING EXTRACTING CAPACITY OF DIFFERENT SOLVENTS

The extracting capacity of different solvents of different polarity of maximum free radical scavenging activity was assessed. Each extract was analyzed for DPPH$^{\bullet}$ decolourization (**Fig. 3.12**). Methanol extracts showed higher levels of scavenging

activity of 37.29 %, while lowest activity was expressed in hexane extract 4.358 %. Other solvents employed for extraction gave a DPPH$^{\bullet}$ decolourization in the following order; acetone 29.28 % > ethanol 23.3 % > ethyl acetate 15.74 % > water 12.31 % > chloroform 10.45 % > petroleum ether 8.883 % respectively.

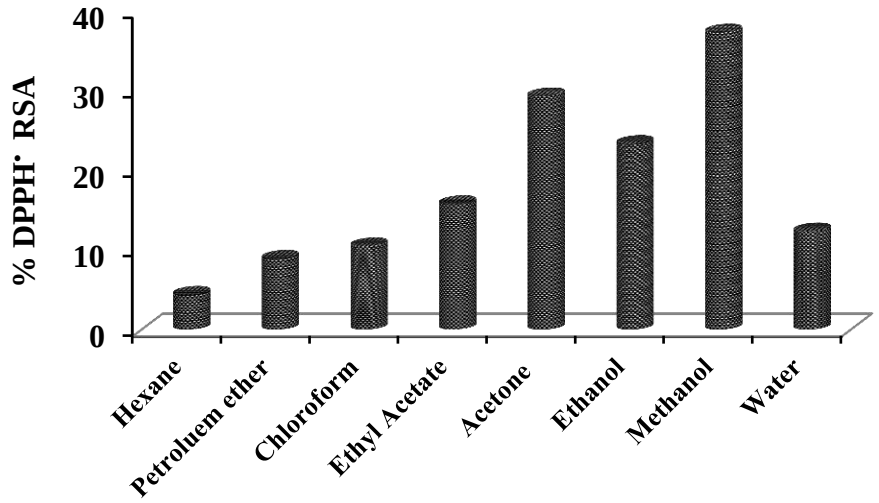

Fig. 3.12 Capacity of different solvents to extract free radical scavenger molecules from cells of *Haloferax alexandrinus* GUSF-1 (KF796625)

3.2.11 OPTIMIZATION OF PARAMATERS FOR MAXIMUM GROWTH AND FREE RADICAL SCAVENGING ACTIVITY

Maximum free radical scavenging activity of 34.21 % was seen in 25 % NaCl followed by 33.29, 27.43, 23.21, 17.42, 8.42, 6.893, 6.5 in 20 %, 30 %, 15 %, 35 %, 5 % and 40 % of NaCl concentration (**Fig. 3.13**). Free radical scavenging activity varied with temperature was found to be maximum in 42ºC, followed by 37ºC (33.09 %), RT (22.1 %), and 25ºC (10.52 %) (**Fig. 3.14**). When incubated in NTYE medium with different pH range; 5, 6, 7, 8 and 9, maximum free radical scavenging activity occurred at pH 7, i.e. % DPPH$^{\bullet}$ RSA of 38.05%, free radical scavenging activity was 27.95, 28.02, 11.47 and 4.21 % DPPH$^{\bullet}$ RSA in cells grown at pH 6, 8, 5 and pH 9 respectively (**Fig. 3.15**). Free radical scavenging activity was ≈ 50 % less in cells grown in dark conditions (**Fig. 3.16**). Thus 25 % NaCl in nutrient rich NTYE

medium, 42ºC, pH 7 and 150 rpm aeration are conducive for the maximum production of antioxidants in cells of *Haloferax alexandrinus* GUSF-1 (KF796625) (**Fig. 3.17**).

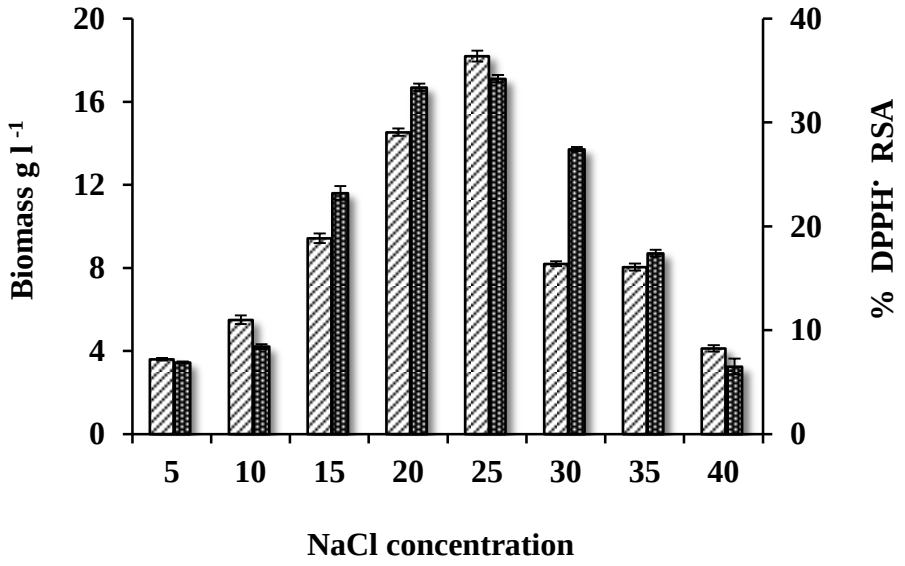

Fig. 3.13 Effect of NaCl concentration of growth medium on ▨ biomass g l $^{-1}$ and ▩ Free radical scavenging activity (% DPPH$^{\bullet}$ RSA)

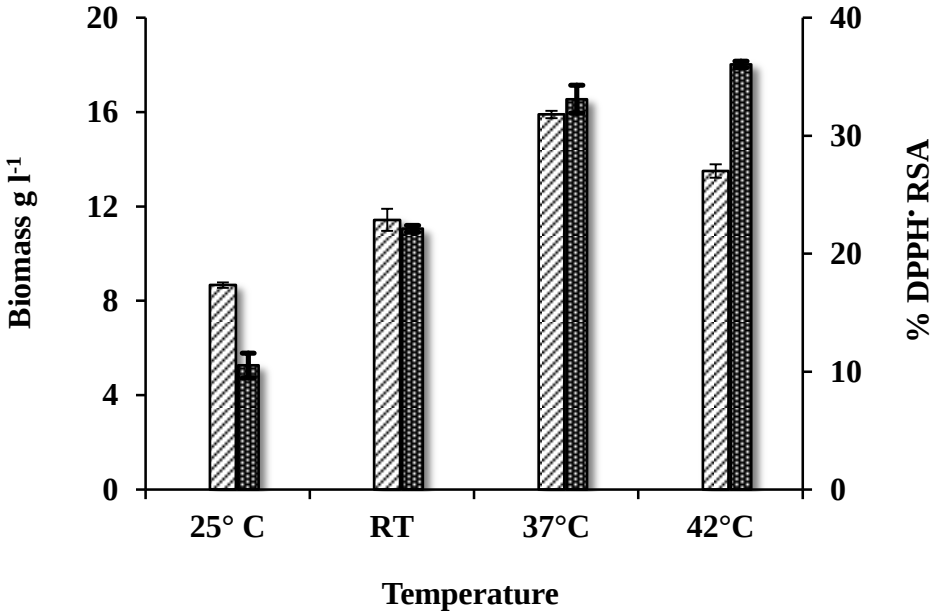

Fig. 3.14 Effect of temperature of incubation on growth medium on ▨ biomass g l^{-1} and ▩ free radical scavenging activity (% DPPH$^{\bullet}$ RSA)

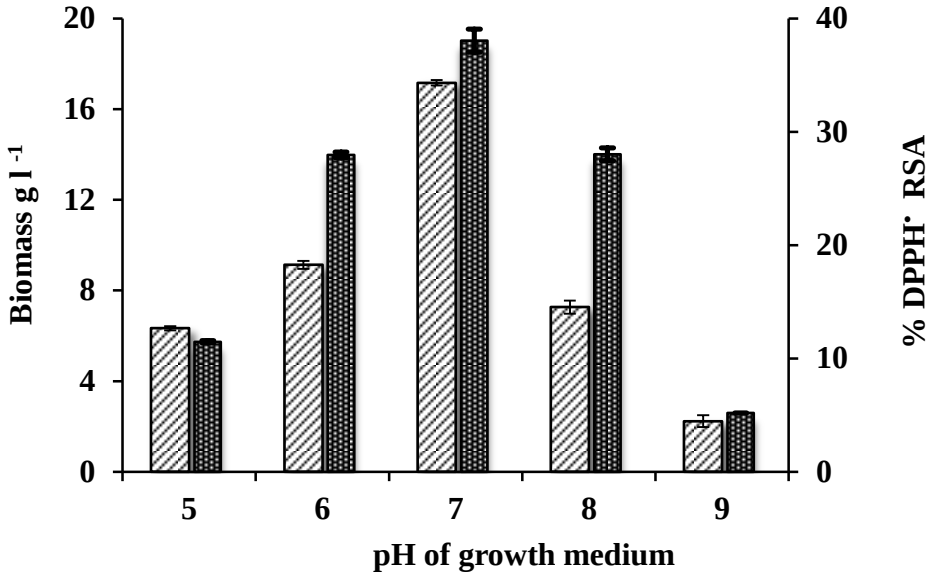

Fig. 3.15 Effect of pH of growth medium on growth on ▨ biomass g l^{-1} and ▩ free radical scavenging activity (% DPPH• RSA)

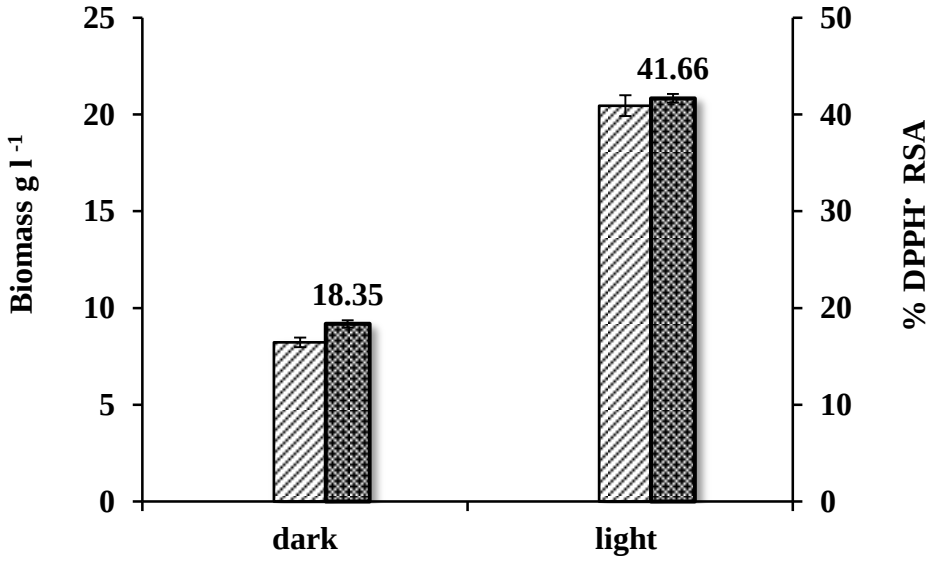

Fig. 3.16 Effect of dark and light during incubation on growth medium on biomass g ▨ l^{-1} and ▩ Free radical scavenging activity (% DPPH• RSA)

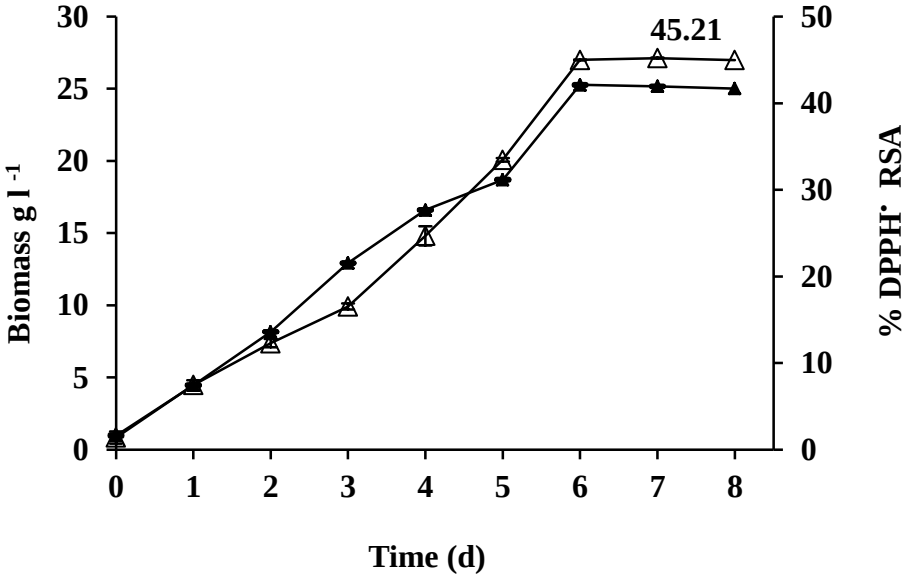

Fig. 3.17 Free radical scavenging activity % DPPH• RSA △and growth of cells ▲ at ambient light, 25 % NaCl, 42ºC, pH 7 and 150 rpm

3.2.12 KINETIC STUDIES OF FREE RADICAL SCAVENGING ACTIVITY OF *Hfx*A

3.2.12.1 Free radical scavenging effectiveness

The spectra of pure DPPH• in methanol showed two peaks, one at 517nm and the other at 327 nm (**Fig. 3.18 Aa**). Incubation of 0.1 mM DPPH• with *Hfx*A for 30 min decreased the absorbance of DPPH• at 517 nm from 0.548 to 0.108 and almost abolished the DPPH• peak at 517 nm (**Fig. 3.18 Ab**). The antioxidant molecules in *Hfx*A also interacted with the peak at 327 nm and decreased it from 0.919 to 0.575. The purple colour of DPPH• was simultaneously reduced to a serous yellow colour as seen in **Fig. 3.18 Ba** and **Bb**.

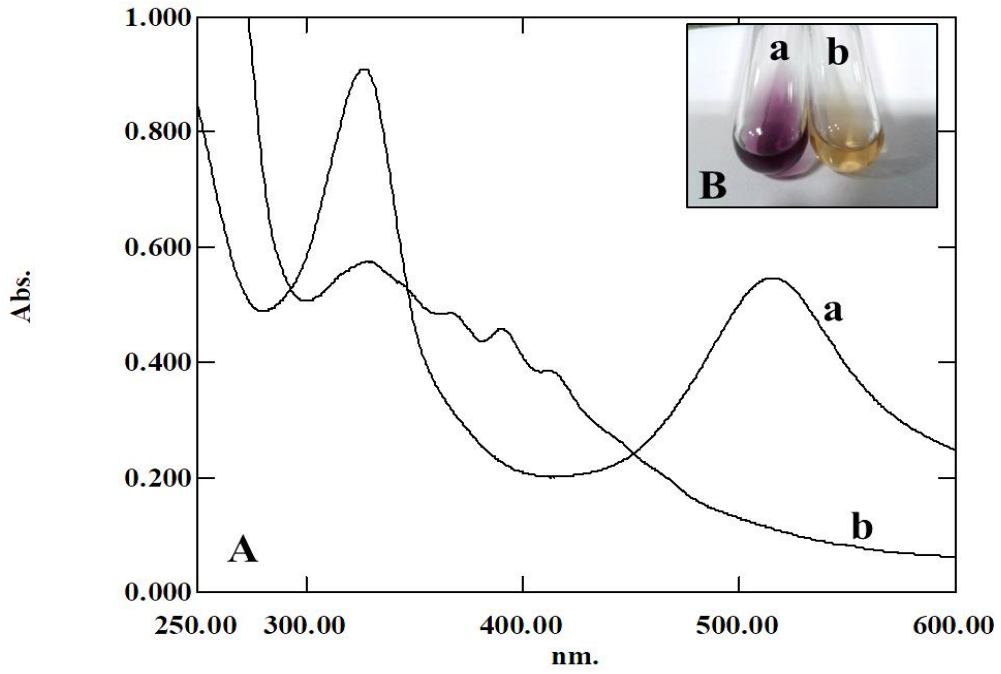

Fig. 3.18 Aa: Absorption spectrum of 0.1 mM DPPH$^{\bullet}$ and **Ab:** Mixture of 50 µg ml^{-1} of *Hfx*A and 0.1 mM DPPH$^{\bullet}$ for 30 min; **Bb:** Colour of DPPH$^{\bullet}$ in the reaction mixture decolorized as compared to control tube **Ba**

Free radical scavenging activity of *Hfx*A was also monitored as a function of time (**Fig. 3.19**). Addition of *Hfx*A to 0.2 mM DPPH$^{\bullet}$ decreased it's absorbance at 517 nm, in dark and at ambient temperature (28 ± 30ºC) while the absorbance of control DPPH$^{\bullet}$ at 517 nm was stable for experiments carried for over 30 min (**Fig. 3.19 A**). In the presence of 12 µg ml^{-1} of *Hfx*A, the purple colour of DPPH$^{\bullet}$ was changed to yellow and the absorbance at 517 nm decreased from 1.133 to 0.935 and remained steady at 0.935 from 15 min onwards (**Fig. 3.19 B**).

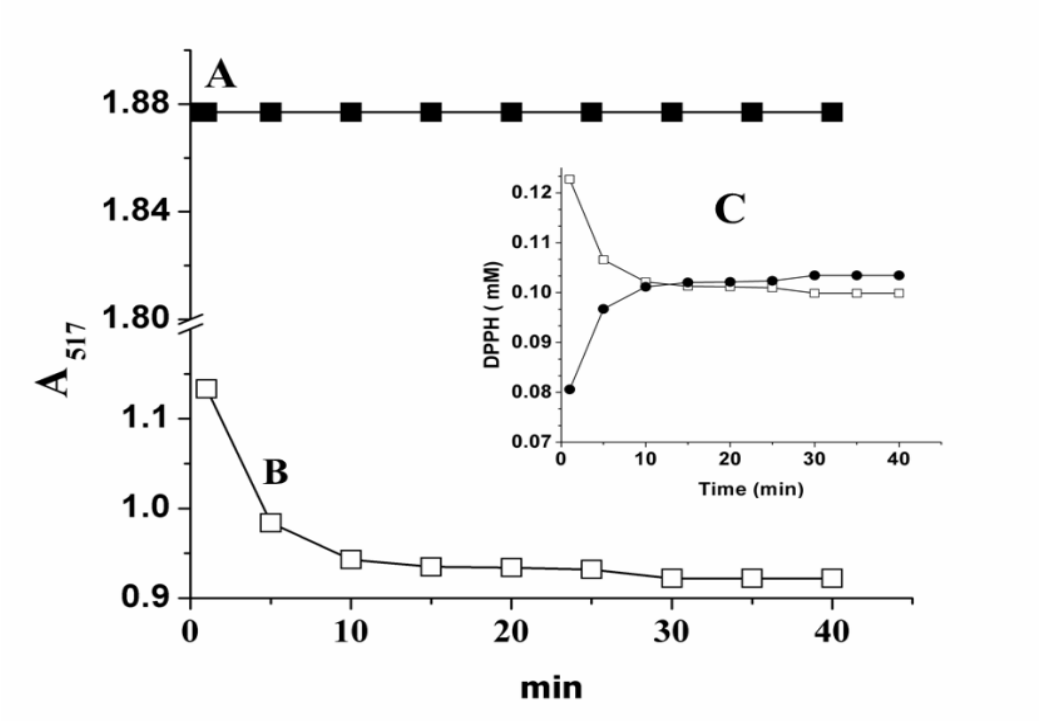

Fig. 3.19 Absorbance of **A:** 0.2mM DPPH$^{\bullet}$ at 517 nm —■—; **B:** 0.2 mM DPPH$^{\bullet}$ in the presence of 12 µg ml^{-1} of *Hfx*A at 517 nm —□—; **C:** Conc of DPPH$^{\bullet}$ monitored at A_{517} in the presence of *Hfx*A, residual DPPH$^{\bullet}$ —○— and scavenged DPPH$^{\bullet}$ —●—

As seen in **Fig. 3.19 C**, the DPPH$^{\bullet}$ is converted to DPPH$^{\bullet}$ molecule at a rate inversely proportional to the decay of radical till steady state. It may be noted that the rate of this decrease in the 1st 60 sec was very fast, sharp and corresponded to 120 × 10 $^{-4}$ sec^{-1} and an amount of 0.08 DPPH$^{\bullet}$ was converted to DPPH-H. The further conversion and formation of DPPH stable molecule from 60 sec to 5 min was 5.2 × 10 $^{-4}$ sec $^{-1}$ while that from 5 min to 10 min was 3.4 × 10 $^{-4}$ sec $^{-1}$.

3.2.12.2 Monitoring the reaction at various concentration of *Hfx*A

As depicted in **Fig. 3.20 A**, the amount of DPPH$^{\bullet}$ remaining decreased linearly with increasing concentration of *Hfx*A from 0.2 upto 20 µg ml^{-1} and levelled off thereafter. The effectiveness of *Hfx*A in scavenging free radicals was therefore taken as 4.68 µg ml^{-1} that caused 50 % decrease in initial DPPH$^{\bullet}$ concentration (**Fig. 3.20 B)**.

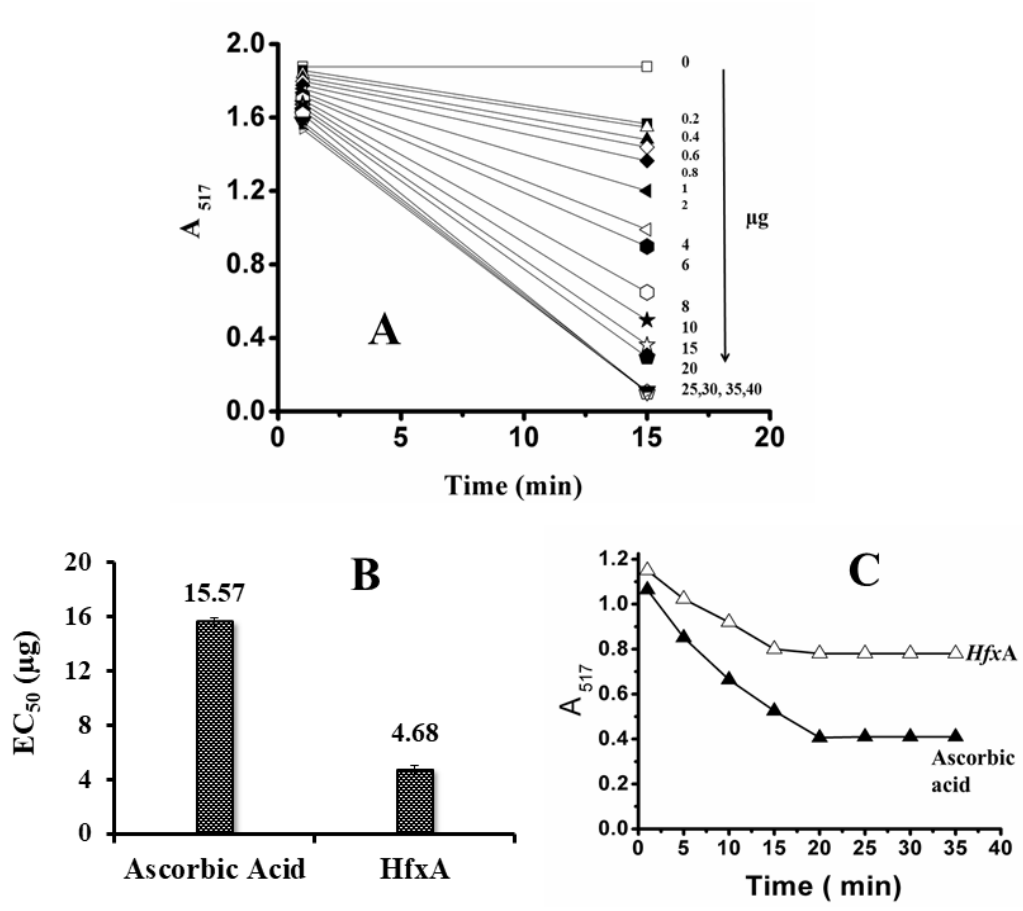

Fig. 3.20 A: The dependence of absorbance at 517 nm (A_C and A_T) on time of incubation; at t =1 min and t= time to reach final state (15 min), of different concentration of *Hfx*A from 0 to 40 µg ml^{-1} in the reaction mixture of DPPH (0.2 mM) in methanol medium; **B:** EC_{50} of *Hfx*A and ascorbic acid and **C:** TEC_{50} of *Hfx*A and ascorbic acid

Further since the $DPPH^{\bullet}$ decolourization progressed steadily at 517 nm till it reached a steady state saturation i.e. maximum decrease in $DPPH^{\bullet}$ in 15 min for EC_{50} of *Hfx*A and in 20 min for ascorbic acid, the TEC_{50} for *Hfx*A was fixed at 15 min (**Fig. 3.20 C)**. From the initial concentration (Cf) of $DPPH^{\bullet}$ and EC_{50} values of *Hfx*A and ascorbic acid, the AAI for *Hfx*A calculated as Cf/ EC_{50}, was 1.685 and the AAI of ascorbic acid was 0.506 units. The antiradical power (ARP) of 213 for *Hfx*A was calculated from the EC_{50} and was nearly 3.5 times that of ascorbic acid whose value was 64. *Hfx*A had an antiradical efficiency of 14237×10^{-3} which was 5 times more than 3210×10^{-3} for ascorbic acid. The stoichiometry value of antioxidant *Hfx*A

theoretically required to reduce 100 % of DPPH$^{\bullet}$ and ascorbic acid deduced accordingly to Brand-Williams *et al*. (1995), worked out to be 9.364 µg ml^{-1} which was three times less than the stoichiometry value of ascorbic acid respectively.

The radical scavenging by *Hfx*A at all concentration tested and the EC_{50}, resulted in progressive reduction of the available DPPH$^{\bullet}$ radical. The conversion of DPPH$^{\bullet}$ to DPPH-H is dependent on the relative concentrations of the reactants, but since the concentration of the DPPH$^{\bullet}$ is fixed at 0.2 mM and the concentration of *Hfx*A varies, the reaction follows first order (Mishra *et al*., 2012) with rate constant k calculated at t = 1 and t = 15 min for all concentration tested and the EC_{50} concentration of *Hfx*A and t = 20 min for ascorbic acid. The rate constant k for EC_{50} concentration was found to be 7 × 10^{-4} s^{-1} for *Hfx*A and 4 × 10^{-4} s^{-1} for ascorbic acid.

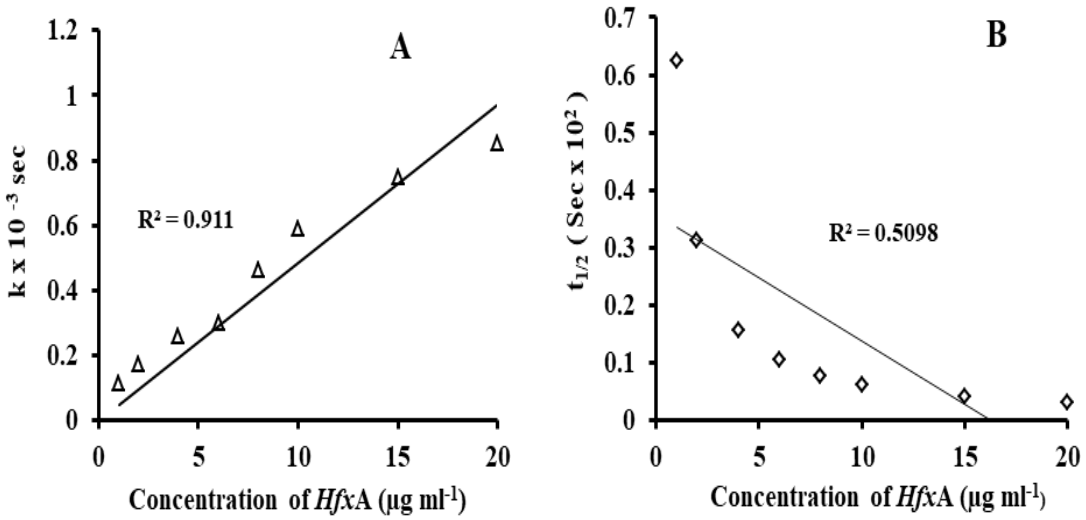

Fig. 3.21 A: Plot of rate constant k (sec) v/s concentration of *Hfx*A (µg) v/s and **B:** Plot of half life t1/2 v/s (sec) v/s concentration of *Hfx*A

Overall *Hfx*A, the antioxidant of *Haloferax alexandrinus* GUSF-1 (KF796625) decayed DPPH$^{\bullet}$ at k = 7 × 10^{-4} s^{-1} with EC_{50} of 4.68 µg ml^{-1}, TEC_{50} at 15 min, AAI of 1.685, ARP of 213, ARE of 14237 × 10^{-3}.

3.2.13 DETECTION, SEPARATION AND LOCALISATION OF FREE RADIAL SCAVENGING ACTIVITY

A total of 1 g of wet weight of *Haloferax alexandrinus* GUSF-1 (KF796625) cells were obtained by centrifuging 7 d of growth in NTYE **(Fig. 3.1 A)**. The supernatant was subjected to cold ethanol which resulted in a white precipitate **(Fig. 3.1 B)**. The wet cells were used to prepare hydroxylated methanolysates and also used to prepare methanolic extract with antioxidant capacity (*Hfx*A) which was orange in colour (**Fig. 3.1 C & D**). The addition of hexane to *Hfx*A results in separation into two phases; upper hexane layer and lower methanol. The hexane layer was separated out and further the addition of cold acetone to this hexane layer resulted in precipitation. This precipitate which is insoluble in acetone and contains polar components was termed as Acetone Precipitated Material (APM) and hexane extract, containing non polar components, that was left behind was termed as Hexane soluble Extract (HE) (**Fig. 3.1 E, F & G)**.

3.2.13.1 Extracts of culture supernatant of *Haloferax alexandrinus* GUSF-1 (KF796625)

The % DPPH$^{\bullet}$ RSA of culture supernatant of *Haloferax alexandrinus* GUSF-1 (KF796625) was found to be 20 %. The UV spectra of the EPS revealed the presence of one peak at 193 nm (**Fig. 3.22**).

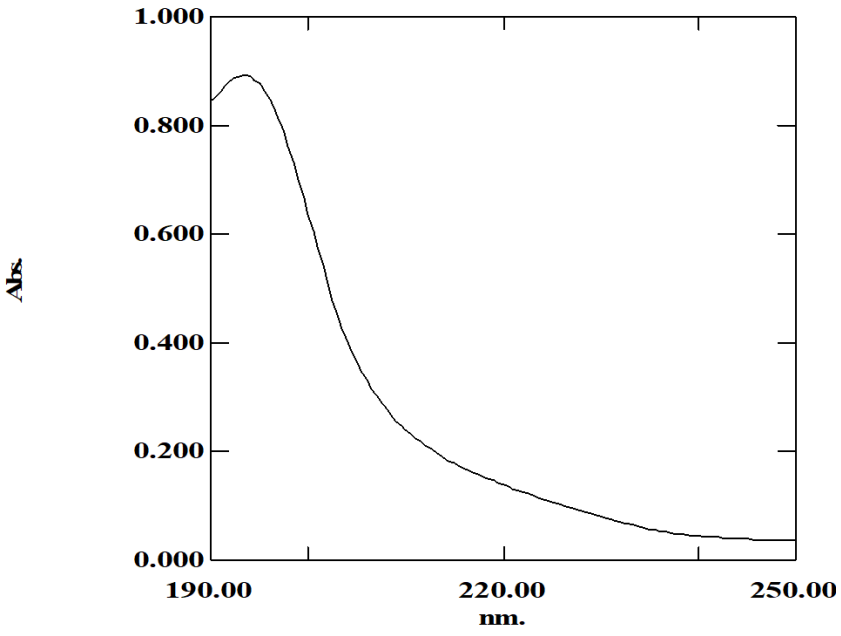

Fig. 3.22
UV scan of extract of culture supernatant of *Haloferax alexandrinus* GUSF-1 (KF796625)

FT-IR analysis of the EPS of *Haloferax alexandrinus* GUSF-1 (KF796625) revealed a range of peaks from 3900 cm^{-1} to 500 cm^{-1} (**Fig. 3.23**). Characteristic broad peak was observed around 3317 cm^{-1} in the stretching vibration region around 2912 cm^{-1}, a stretching band at 1625 cm^{-1} was seen, a broad stretch at 1041 cm^{-1} and an intense peak at 1124 cm^{-1}.

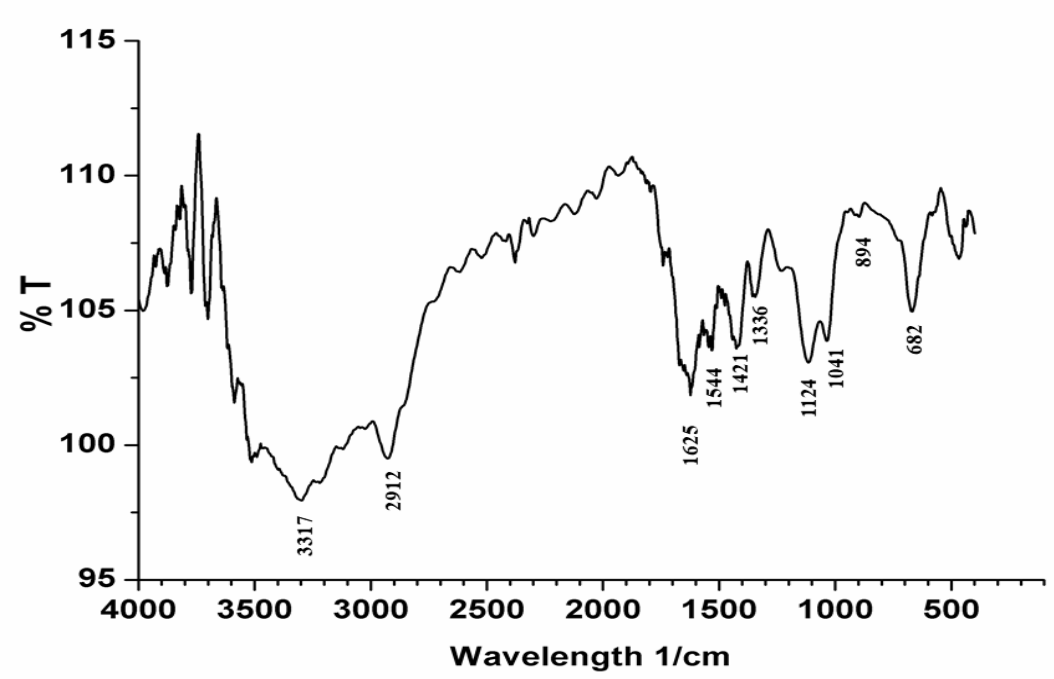

Fig. 3.23 FT-IR spectra of extract of culture supernatant *Haloferax alexandrinus* GUSF-1 (KF796625)

3.2.13.2 Extracts of cells of *Haloferax alexandrinus* GUSF-1 (KF796625)

3.2.13.2.1 Characterisation of hydroxylated methanolysates

The hydroxylated methanolysate extract was yellowish in colour and was of an oily consistency. The chromatogram plates developed in petroleum ether: diethyl ether (85: 15; v/v) revealed the presence of 6 spots in iodine chamber at R_f 0.2, 0.3, 0.48, 0.59, 0.78 and 0.89 (**Fig. 3.24 A**). On spraying the chromatogram with 10 % dodecaphosphomolybdic acid in absolute ethanol, a blue spot appeared around R_f 0.2 (**Fig. 3.24 B**). The chromatogram when sprayed with methanolic $DPPH^{\bullet}$ the purple colour was decolourized around the spot at R_f 0.2 (**Fig. 3.24 C**). The spot at the same position was scrapped from a resolved TLC plate which was not subjected to any treatment and dissolved in hexane. 50 µl of this extract was mixed with 50 µl of hexanic $DPPH^{\bullet}$ and on incubating for 30 min in the dark, $DPPH^{\bullet}$ was seen to be

decolourized (**Fig. 3.24 Db**). A DPPH$^{\bullet}$ control was also maintained (**Fig. 3.24Da**). The FT- IR spectral analysis of the hydroxylated methanolysate revealed an intense absorption peaks at 1076 cm^{-1} (**Fig. 3.25**).

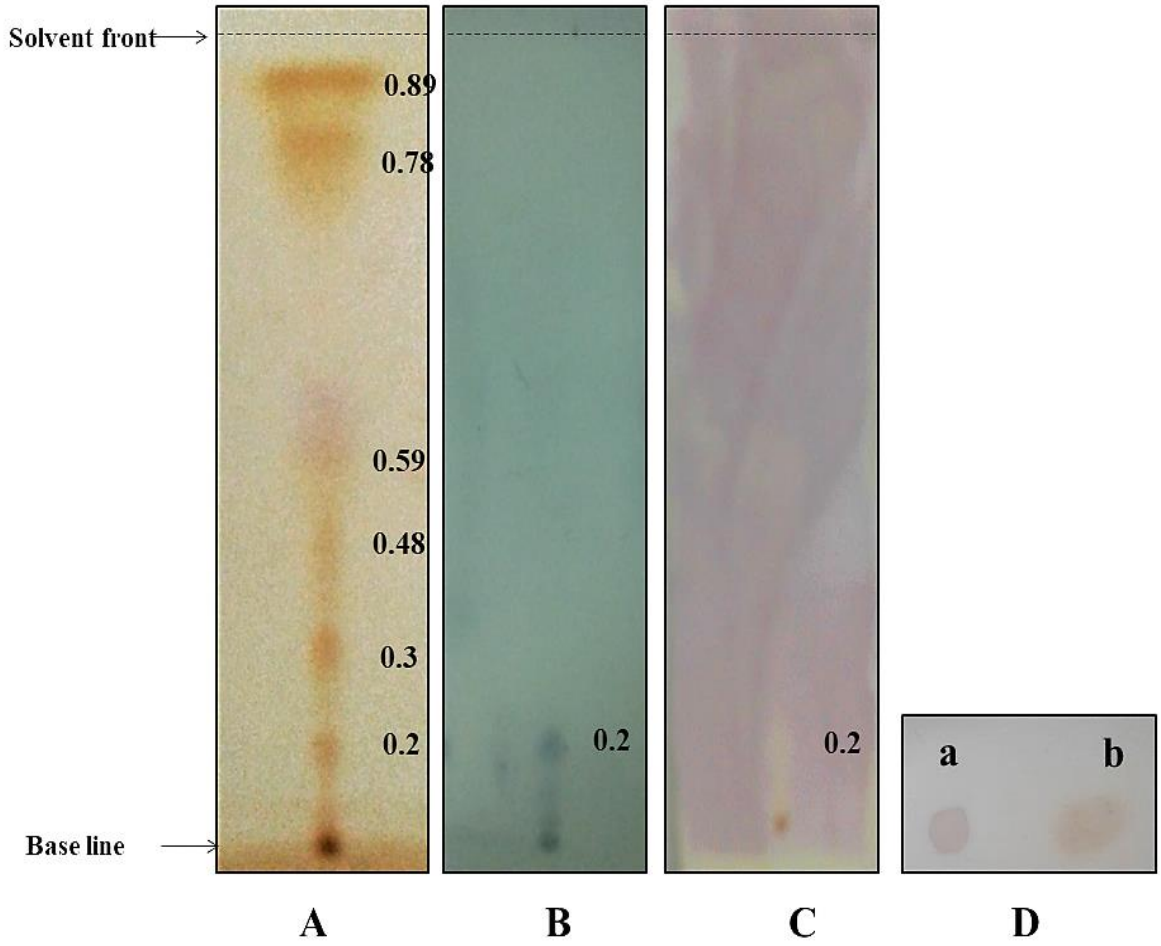

Fig. 3.24 TLC profile of hydroxylated methanolysates resolved in petroleum ether (40-60 °C): diethyl ether (85:15, v/v). **A:** Chromatogram developed with iodine vapours; **B:** Chromatogram sprayed with 10 % dodecaphosphomolybdic acid in absolute ethanol and heated at 150°C; **C:** Chromatogram sprayed with hexanic DPPH$^{\bullet}$ solution. **D:** Spot at approximately R_f 0.2 scrapped from resolved TLC plate, redissolved in hexane; **a:** hexanic DPPH$^{\bullet}$ used as a control **b:** DPPH$^{\bullet}$ spot assay carried out using the hexane extract

Fig. 3.25 FT- IR spectra of hydroxylated methanolysate of *Haloferax alexandrinus* GUSF-1 (KF796625)

3.2.13.2.2 Characterization of *Hfx*A

3.2.13.2.2.1 Spectroscopic analysis of *Hfx*A

*Hfx*A when scanned between 190 - 800 nm showed peaks at 214, 223, 265, and 287 nm in the UV region and at 304, 317, 350, 368, 386, 465, 486, 490 and 522 nm in the visible region (**Fig. 3.26)**.

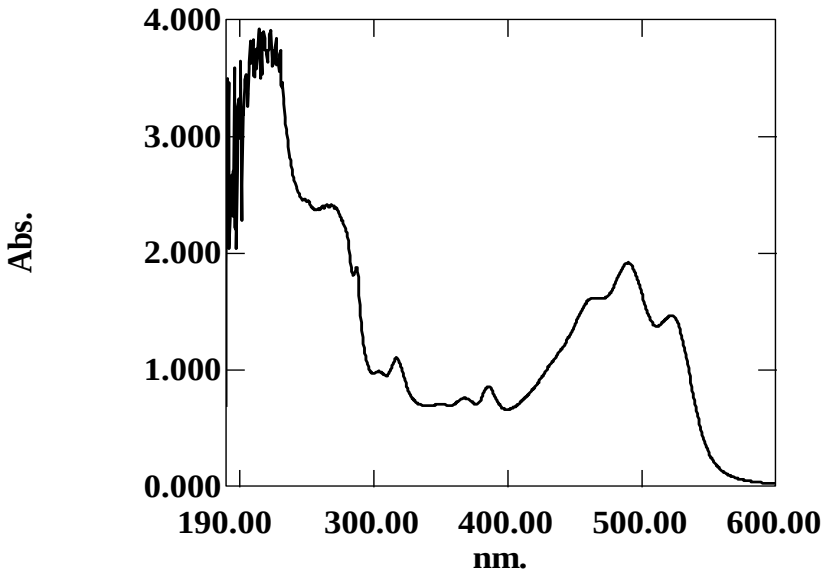

Fig. 3.26 UV-Vis absorption spectrum of *Hfx*A

3.2.13.2.2.2 Demonstration of radical scavenging activity of methanolic extracts (*Hfx*A) by thin layer chromatography

The radical scavenging activity of *Hfx*A was 41 %**.** After development of the chromatogram in benzene: acetone (2:1), 4 spots were visible to the naked eye with R_f of 0.4 (pink), 0.55 (pink), 0.69 (dark pink) and 0.75 (pink orange). On spraying with methanolic DPPH$^{\bullet}$, purple colour was decolourised and white zones were formed around each of the 4 spots (**Fig. 3.27)**. The spot at R_f 0.4, 0.55, 0.69 and 0.75 on elution with methanol revealed peaks at 368, 385, 463, 490 and 522 nm ; 458, 482 and 516 ; 447, 478 and 509; 421 and 438 nm respectively (**Fig. 3.28 A-D**).

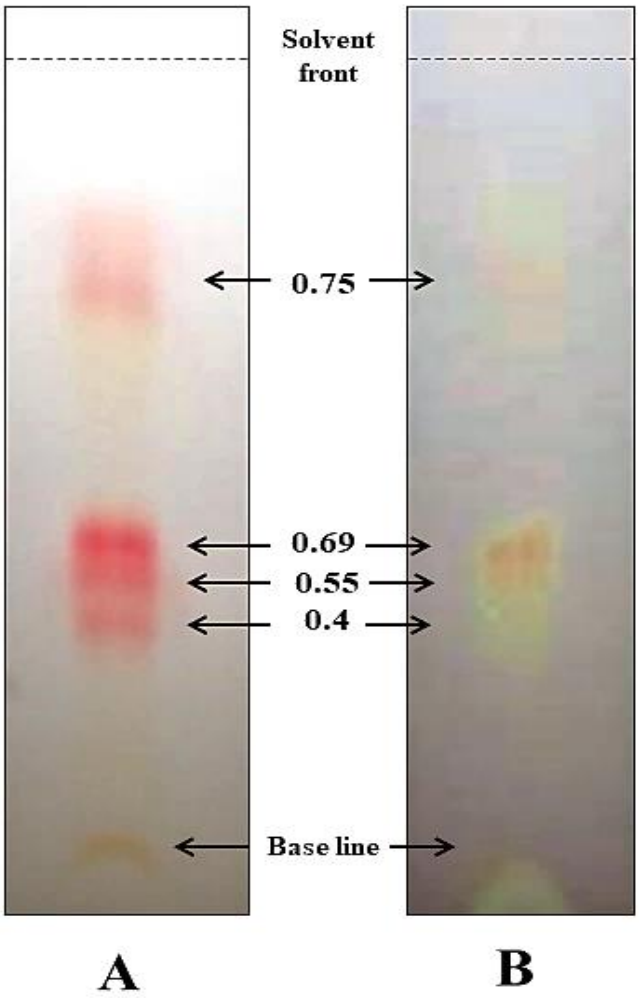

Fig. 3.27 A
TLC profile of *Hfx*A in benzene: acetone (2:1) **A:** Chromatogram viewed by naked eye; not subjected to DPPH$^{\bullet}$**; B:** Decolourization of DPPH$^{\bullet}$ by the different spots obtained on resolving *Hfx*A in benzene: acetone (2:1)

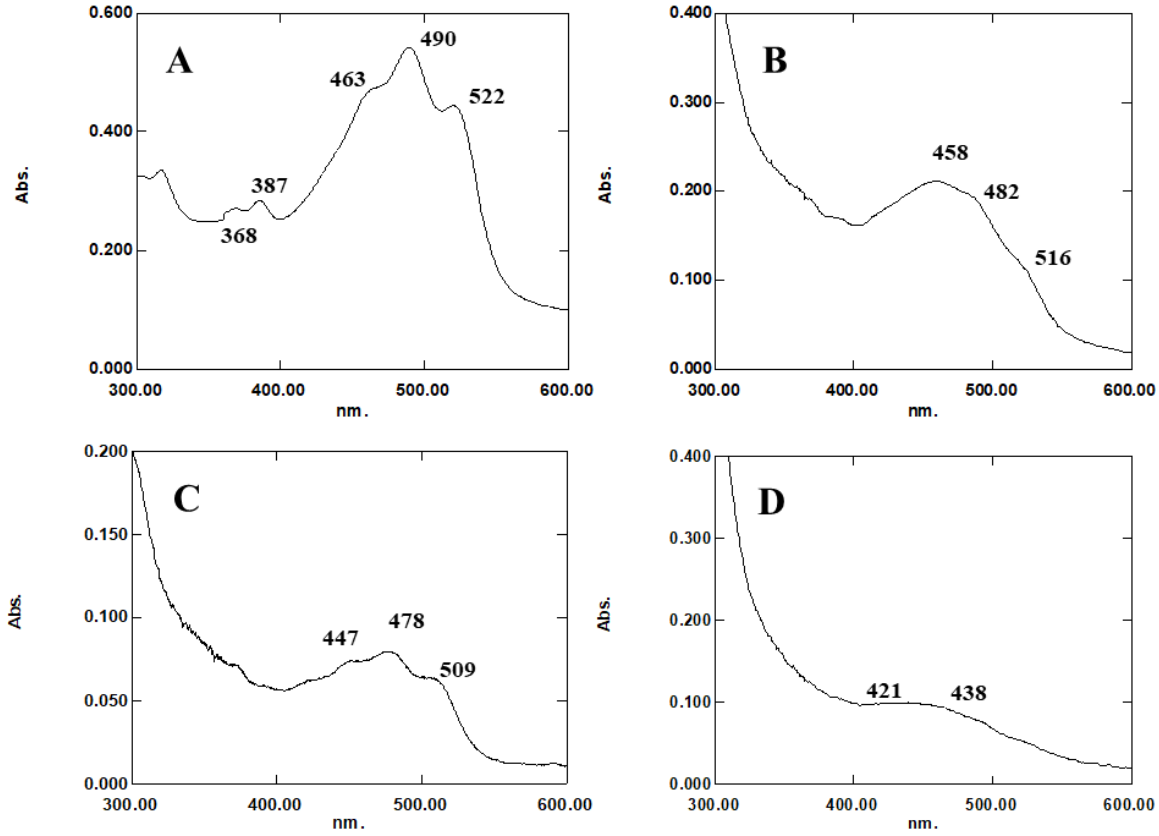

Fig. 3.28 Visible absorption spectrum of spots at **A:** R_f 0.4; **B:** R_f 0.55; **C:** R_f 0.69 and **D:** R_f 0.75

3.2.13.2.2.3 Preliminary characterization of *Hfx*A using chemical spot test

Alkaline Folin ceolcalteu's gave a bluish green colour when added to *Hfx*A. A faint brown ring on addition of glacial acetic acid and 5 % $FeCl_3$ was obtained at the interphase indicating the presence of glycones. The methanolic extract of *Haloferax alexandrinus* GUSF-1 (KF796625) was vigorously agitated with distilled water and even on standing for 10 min the foam did not persist but was lasting, hence indication of saponins.

3.2.13.2.2.4 FT- IR of *Hfx*A

The FT- IR spectral analysis of *Hfx*A revealed intense absorption peaks at 3400-3600 cm^{-1}. The stretching vibrations were observed at 2850 cm^{-1}, absorption peaks were observed at 1660 cm^{-1}. Peaks were seen at 1525 cm^{-1}, 1145cm^{-1} and around 965–960 cm^{-1} **(Fig. 3.29)**.

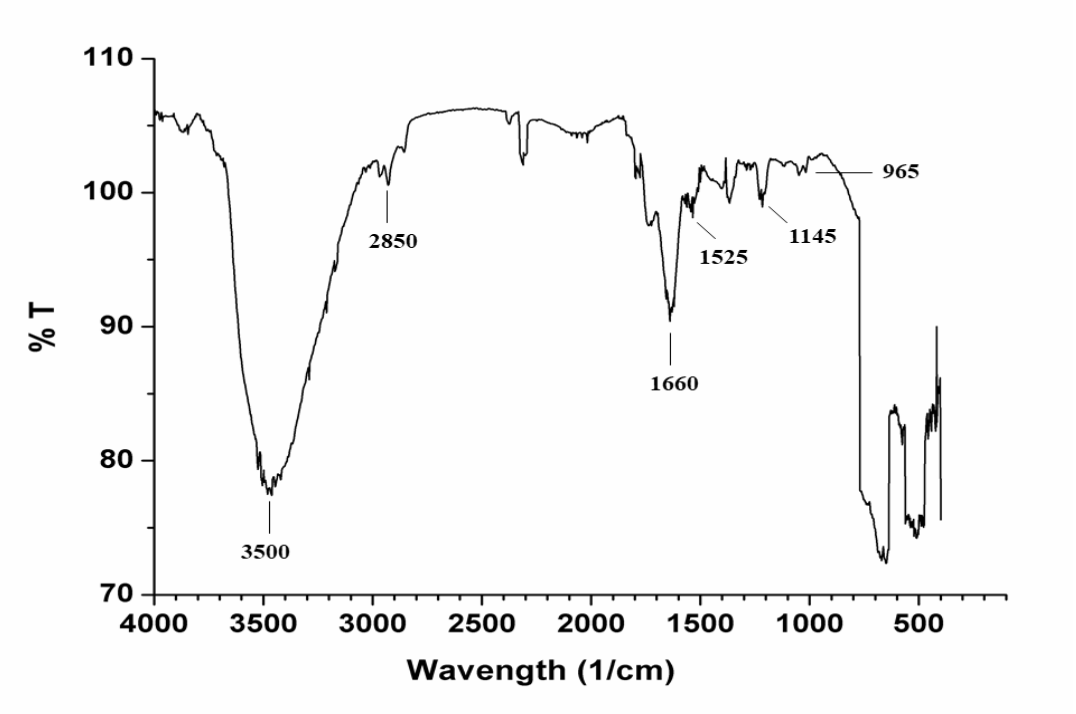

Fig. 3.29 FT- IR spectra of *Hfx*A

3.2.13.2.3 Characterization of Hexane extract (HE)

On addition of hexane to *Hfx*A, it separated out into two phases, an upper coloured hexane phase and a lower off white methanolic phase. We proceeded with the hexane phase which was further subjected to acetone precipitation by addition of cold acetone to precipitate out the polar lipids, the remaining hexane fraction termed as hexane extract (HE) was also further characterized.

3.2.13.2.3.1 Spectroscopic analysis of HE

HE when scanned between 190- 800 nm showed peaks at 195, 210 and 237 nm in the UV region and at 306, 372, 390, 465, 496 and 527 nm in the visible region (**Fig. 3.30**).

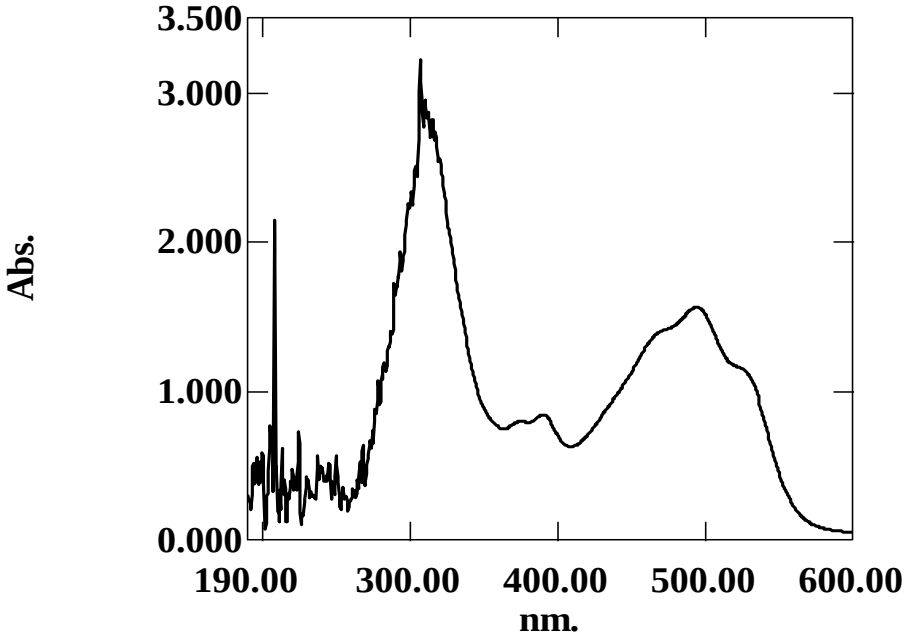

Fig. 3.30 UV-Vis absorption spectrum of HE

HE when added to methanolic DPPH$^{\bullet}$ solution phased out into two separate layer (**Fig. 3.31 A**), so inorder to check whether the extract was capable of reducing DPPH$^{\bullet}$, a 0.2 mM DPPH$^{\bullet}$ was prepared by dissolved in hexane (**Fig. 3.31 B**). On addition of HE to hexanic 0.2 mM DPPH$^{\bullet}$, a % DPPH$^{\bullet}$ RSA of 51 % was obtained. This reaction mixture when scanned revealed that both the peaks of hexanic DPPH$^{\bullet}$ seen at 509 nm and 321 nm were abolished as seen in **Fig. 3.31 C**.

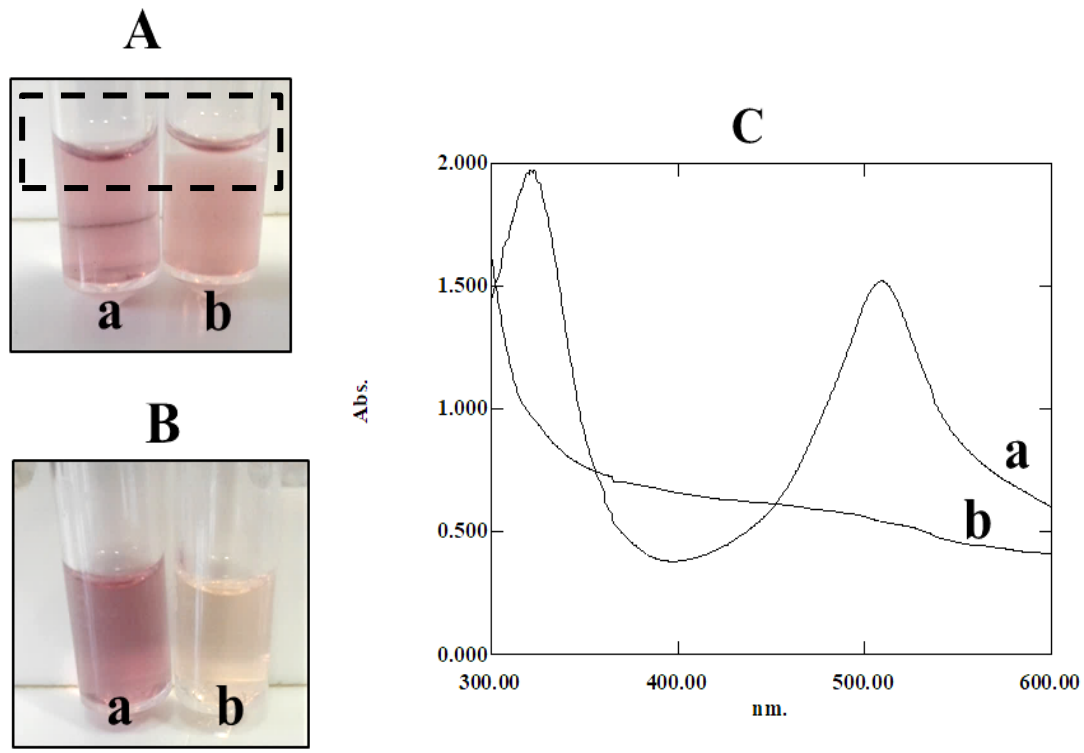

Fig. 3.31 DPPH$^{\bullet}$ decolourization of HE

Aa. Methanolic DPPH$^{\bullet}$; **Ab:** methanolic DPPH$^{\bullet}$ plus hexane extract ; **Ba.** Hexanic DPPH$^{\bullet}$; **Bb:** Hexanic DPPH$^{\bullet}$ plus hexane extract ; **C:** Spectra**: a:** hexanic DPPH$^{\bullet}$; **b:** hexanic DPPH$^{\bullet}$ plus hexane extract (HE)

3.2.13.2.3.2 Demonstration of radical scavenging activity of Hexane extract (HE) by Thin layer chromatography

The chromatogram developed in acetone-petroleum ether (20: 80; v/v) revealed 6 spots in iodine chamber at R_f 0.14, 0.4, 0.51, 0.53, 0.63 and 0.95 **(Fig 3.32A)**, whereas with naked eye 5 spots could be seen at R_f 0.14, 0.36, 0.40, 0.51 and 0.63 respectively (**Fig. 3.32 Ba**). On spraying the TLC plates with hexanic DPPH$^{\bullet}$, the purple colour was decolourized and white zones were formed around each of these spots and also spots at R_f position 0.47 and 0.72 (**Fig. 3.32Bb)**.

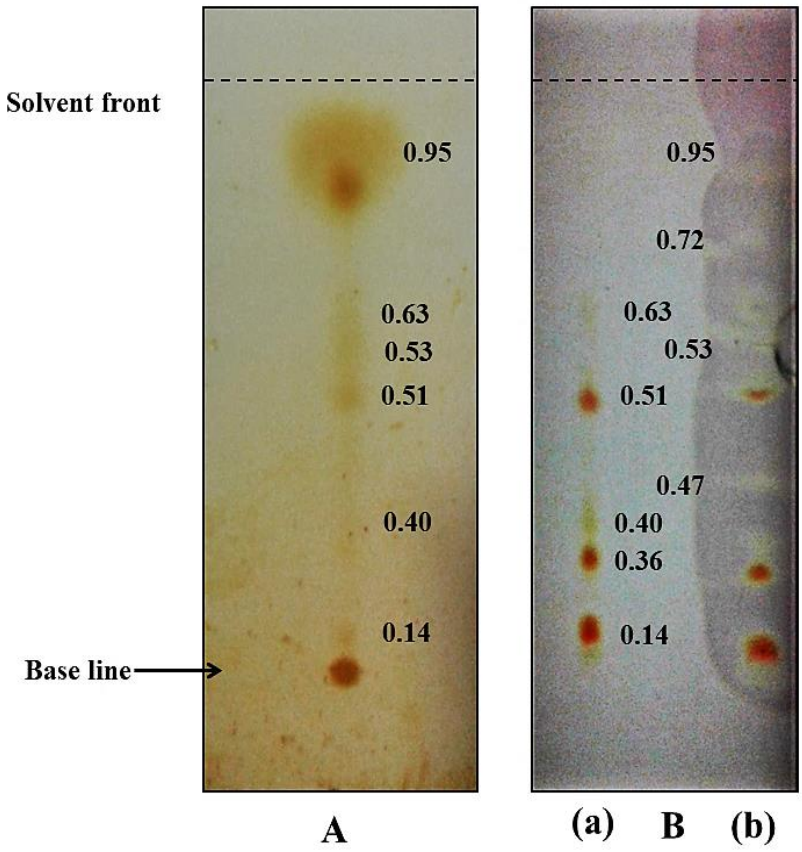

Fig. 3.32 TLC profile of HE developed in acetone-petroleum ether (20:80; v/v)
A: Chromatogram developed with iodine vapours; **Ba:** Chromatogram viewed by the naked eye; not subjected to DPPH$^{\bullet}$; **Bb:** Decolourization of DPPH$^{\bullet}$ by the different spots obtained on resolving HE in acetone-petroleum ether (20:80; v/v)

The spot at R_f 0.14 was scrapped from the TLC plate and redissolved in methanol. The UV-Vis absorption of this spot showed peaks at 368, 387, 463, 492 and 525 nm (**Fig. 3.33**).

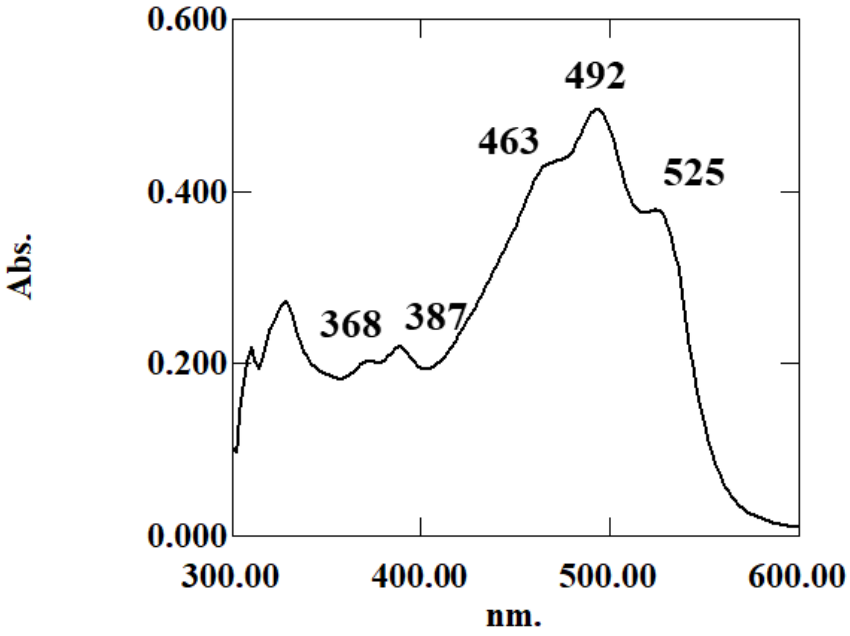

Fig. 3.33 Visible absorption **s**pectra of spot at R_f 0.14 resolved in acetone: petroleum ether (20:80; v/v)

The chromatogram developed in methanol: chloroform (7:93; v/v) revealed 6 spots in iodine chamber at R_f 0.9 (**Fig. 3.34 A**), whereas when viewed with the naked eye 5 spots could be seen at 0.24, 0.29 0.43 and 0.71 (**Fig. 3.34 Ba)**. On spraying with DPPH$^{\bullet}$, the purple colour was decolourized and white bands were seen around spots at R_f 0.24, 0.29, 0.43, and 0.71 respectively (**Fig. 3.34 Bb**).

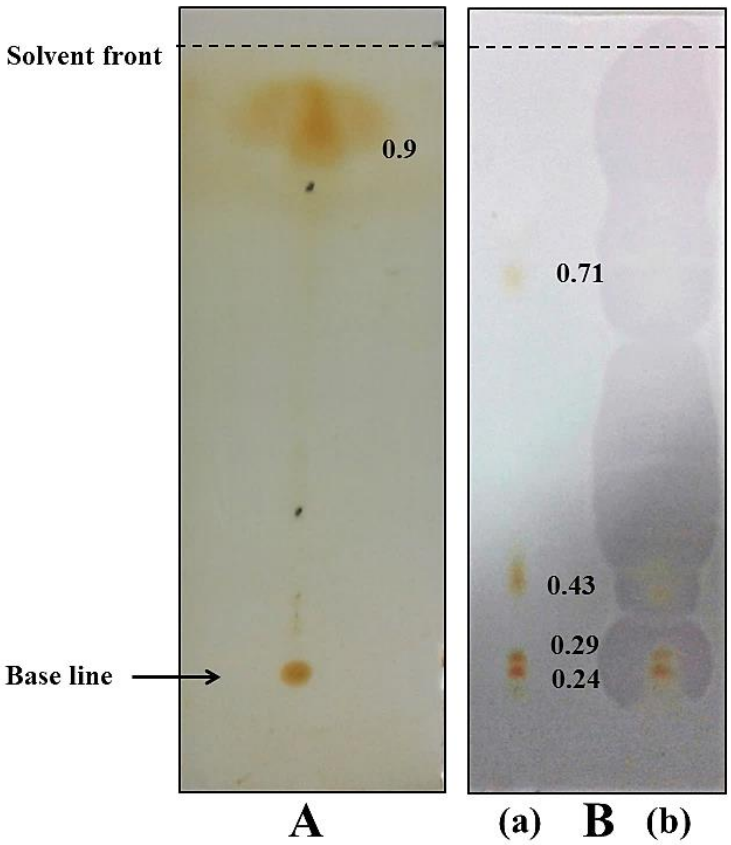

Fig. 3.34 TLC profile of HE developed in methanol: chloroform (7:93; v/v)
A: Chromatogram developed with iodine vapours; **Ba:** Chromatogram viewed by the naked eye; not subjected to DPPH$^{\bullet}$; **Bb:** Decolourization of DPPH$^{\bullet}$ by the different spots obtained on resolving HE in methanol: chloroform (7:93; v/v)

The UV- Vis absorption of spots at R_f 0.29 and R_f 0.43 revealed peaks at 368, 387, 464, 489, 522 nm and 389, 389, 464, 490, 522 nm respectively **(Fig. 3.35 & 3.36)**.

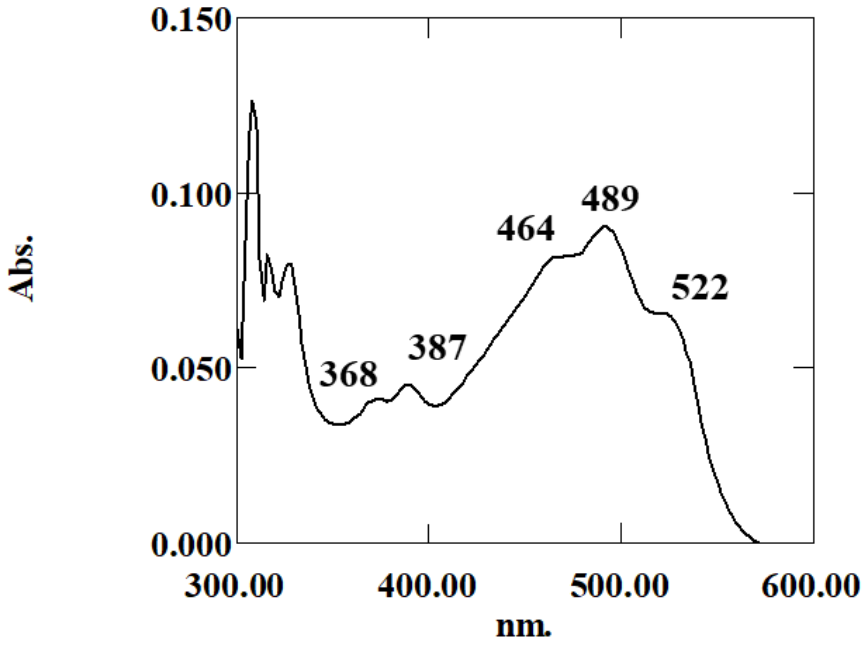

Fig. 3.35 Visible absorption **s**pectra of spot at R_f 0.29 resolved in methanol: chloroform (7:93; v/v)

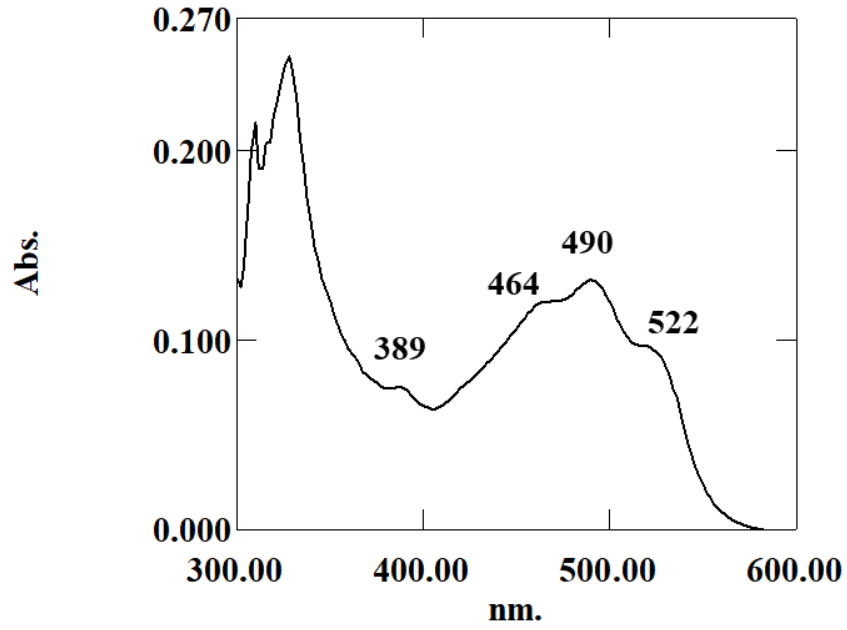

Fig. 3.36 Visible absorption **s**pectra of spot at R_f 0.43 resolved in methanol: chloroform (7:93; v/v)

After development of the chromatogram in acetone: hexane (1:1; v/v), 3 spots were visible to the naked eye having with R_f of 0.46, 0.58 and 0.77. On spraying with methanolic DPPH$^{\bullet}$, purple colour was decolourized and white zones were formed around each of the 3 spots (**Fig. 3.37)**.

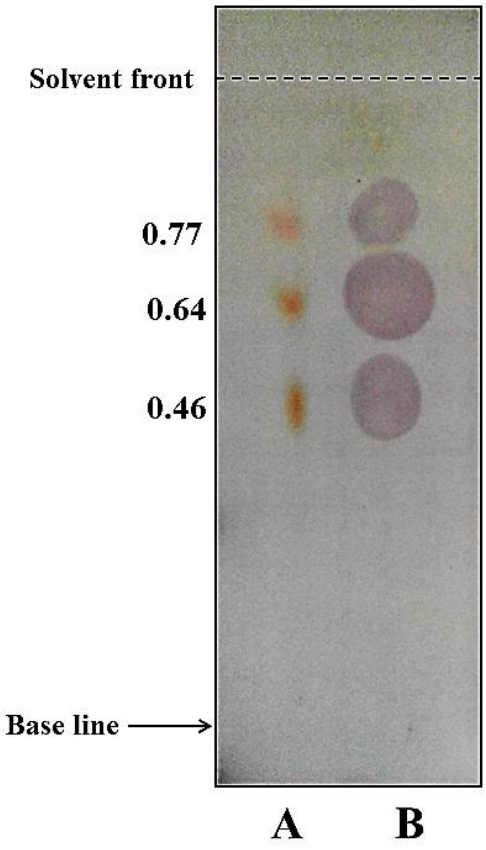

Fig. 3.37 TLC profile of HE in acetone: hexane (1:1; v/v)

A: Chromatogram viewed by the naked eye; not subjected to DPPH$^{\bullet}$**;**

B: Decolourization of DPPH$^{\bullet}$ by the different spots obtained on resolving HE in acetone: hexane (1:1; v/v)

The chromatogram developed in n-heptane: benzene (9:1; v/v) showed no spots visible to the naked eye (**Fig. 3.38 Aa**). On spraying with DPPH$^{\bullet}$, the purple colour was decolourized and white bands were seen around spot at R_f 0.9 (**Fig. 3.38Ab**). The chromatogram revealed 1 spot in the iodine chamber at R_f 0.9 (**Fig. 3.38 B**).

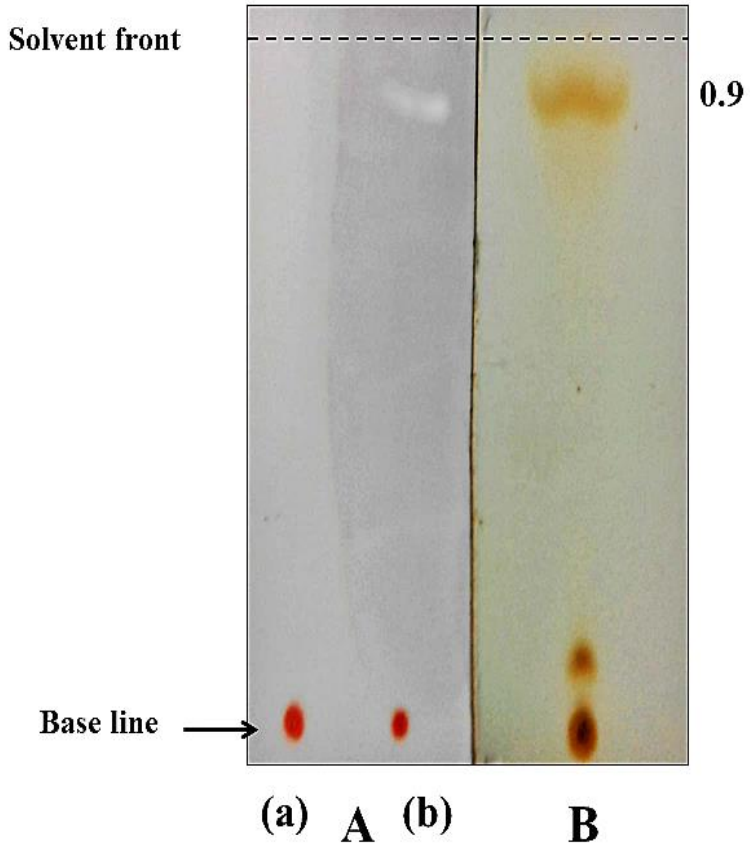

Fig. 3.38 TLC profile of HE developed in n-heptane: benzene (9:1, v/v)

Aa: Chromatogram viewed by the naked eye; not subjected to DPPH$^{\bullet}$; **Ab:** Decolourization of DPPH$^{\bullet}$ by the different spots obtained on resolving HE in n-heptane: benzene (9:1, v/v)**; B:** Chromatogram developed with iodine vapours

3.2.13. 2.3.3 FT-IR of Hexane extract (HE)

The FT- IR spectral analysis of HE revealed intense absorption peaks at 3462 cm^{-1}, Stretching vibrations were observed at 2924 cm^{-1}. Absorption bands were observed at 1735 cm^{-1}, 1637 cm^{-1}, 1220 cm^{-1} and 990 cm^{-1} (**Fig. 3.39)**.

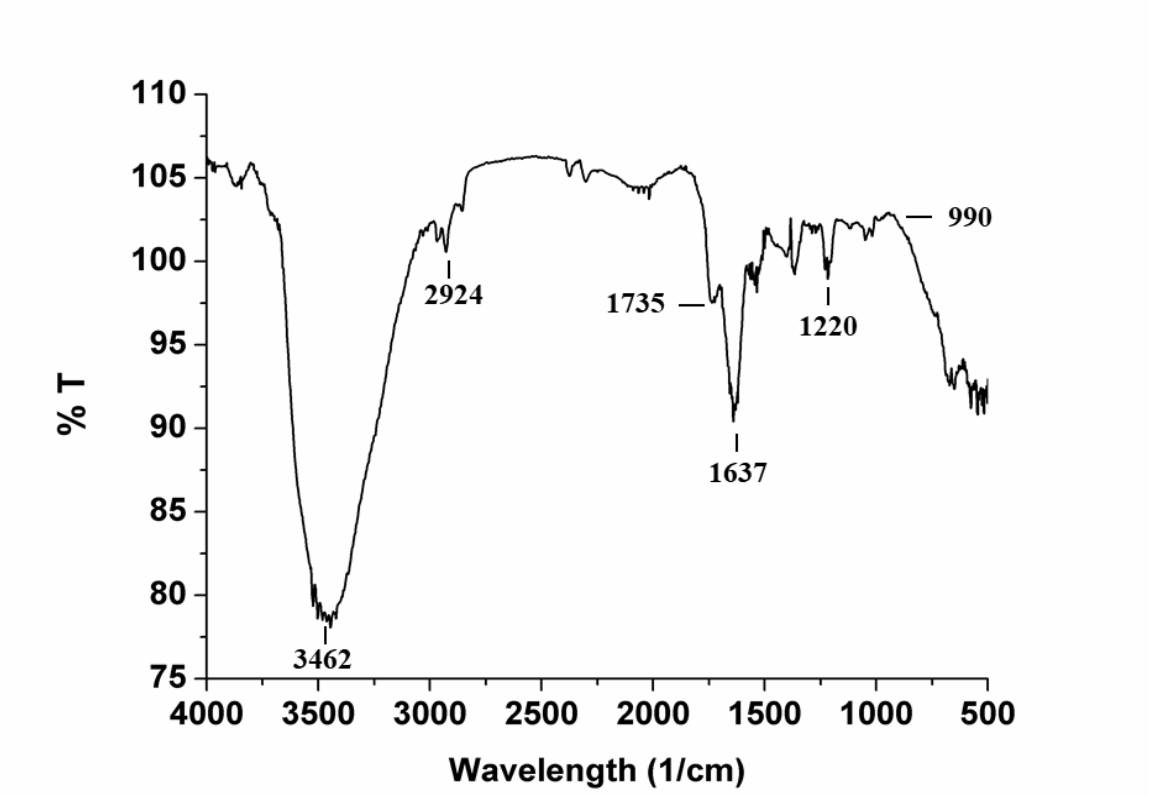

Fig. 3.39 FT-IR spectra of HE

3.2.13.2.4 Characterization of Acetone Precipitated Material (APM)

The precipitate left after acetone extraction had a faint off white texture. This was re dissolved in methanol and further analyzed.

3.2.13.2.4.1 Spectroscopic analysis of APM

The UV-Vis spectra of APM of revealed peaks only at 246, 256, 263, 270 nm. All peaks were in the UV region (**Fig. 3.40**) and no peaks were seen in the visible region.

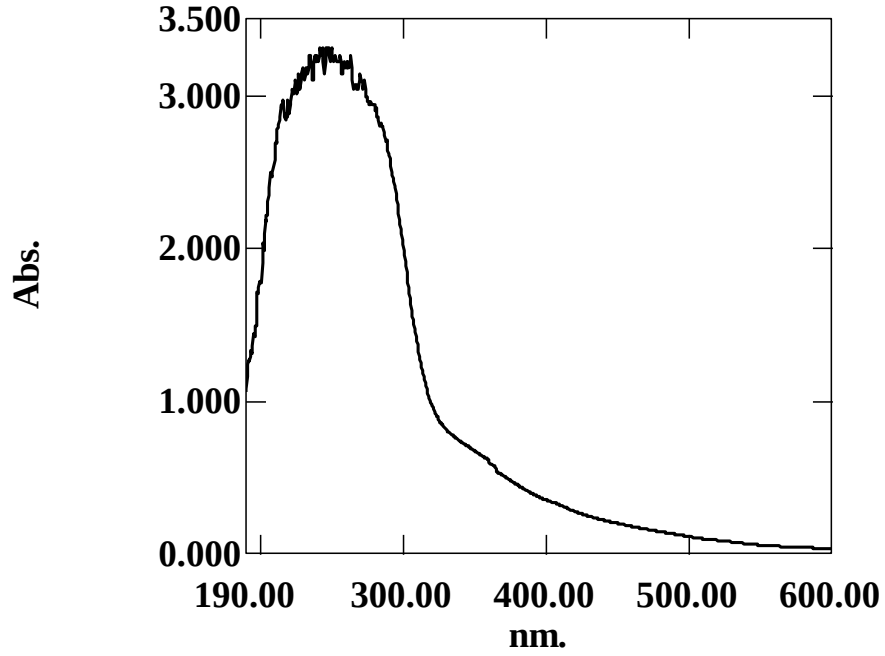

Fig. 3.40 UV-Visible absorption spectrum of APM

3.2.13.2.4.2 DPPH$^{\bullet}$ decolourization by APM

The addition of APM to methanolic DPPH$^{\bullet}$ gave % DPPH$^{\bullet}$ RSA of 38 %. The spectra of pure DPPH$^{\bullet}$ in hexane was deep purple in colour and showed two peaks, one at 517 nm and the other at 327 nm (**Fig. 3.41 Aa & Ab**). Incubation of DPPH$^{\bullet}$ with APM for 30 min, rendered the DPPH radical to yellow and decreased the absorbance of DPPH$^{\bullet}$ at 517 nm from 0.548 to 0.098 and almost abolished the DPPH$^{\bullet}$ peak at 327 nm (**Fig. 3.41 Ba & Bb)**.

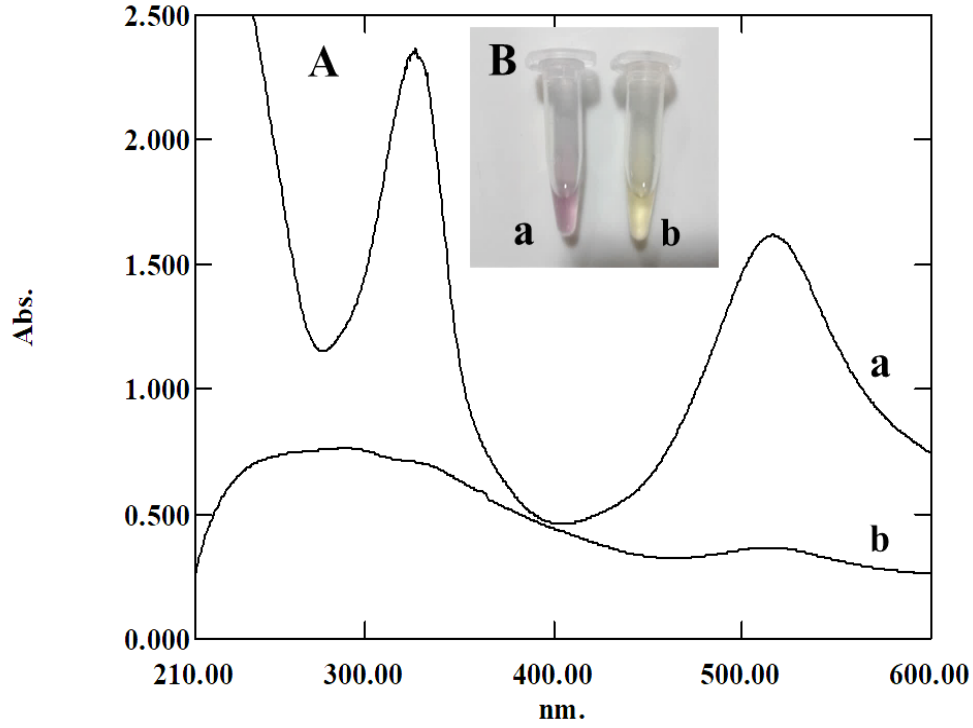

Fig. 3.41 DPPH$^{\bullet}$ decolourization of APM ; **A** Spectra: **a.** methanolic DPPH$^{\bullet}$; **b.** methanolic DPPH$^{\bullet}$ + APM **Ba:** methanolic DPPH$^{\bullet}$; **Bb:** methanolic DPPH$^{\bullet}$ + APM

3.2.13.2.4.3 Thin layer chromatography of APM

The chromatogram when resolved with solvent system of chloroform: methanol: acetic acid: water (85:22.5:10:4; v/v) revealed 3 spots in the iodine chamber at R_f 0.38, 0.51 and 0.64. When viewed with the naked eye no spots could be seen (**Fig. 3.42**).

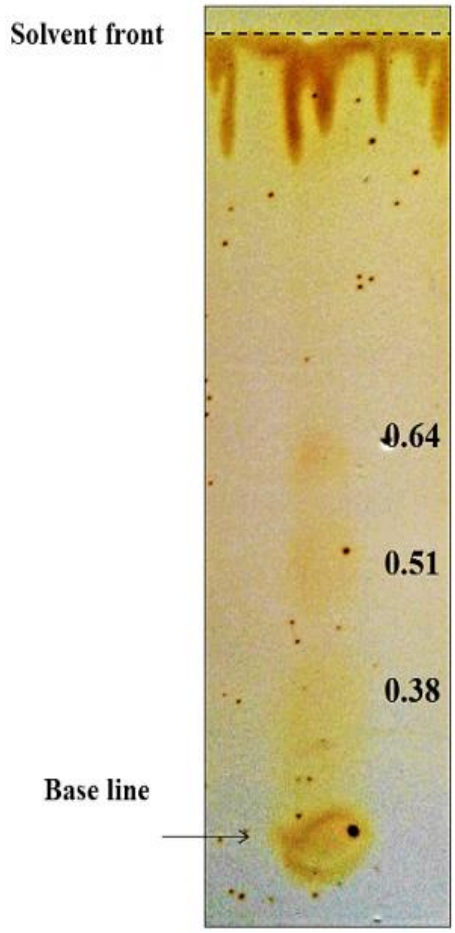

Fig. 3.42 TLC profile of APM resolved using solvent system chloroform: methanol: acetic acid: water (85:22.5:10:4; v/v)

3.2.13.2.4.4 FT-IR of APM

The FT-IR spectral analysis of APM revealed intense absorption bands 3262 cm^{-1}. Stretching vibrations were observed at 2850 -3000 cm^{-1}. Absorption bands were observed at 1735 cm^{-1}, 1365 cm^{-1} and 1217 cm^{-1} respectively (**Fig. 3.43**).

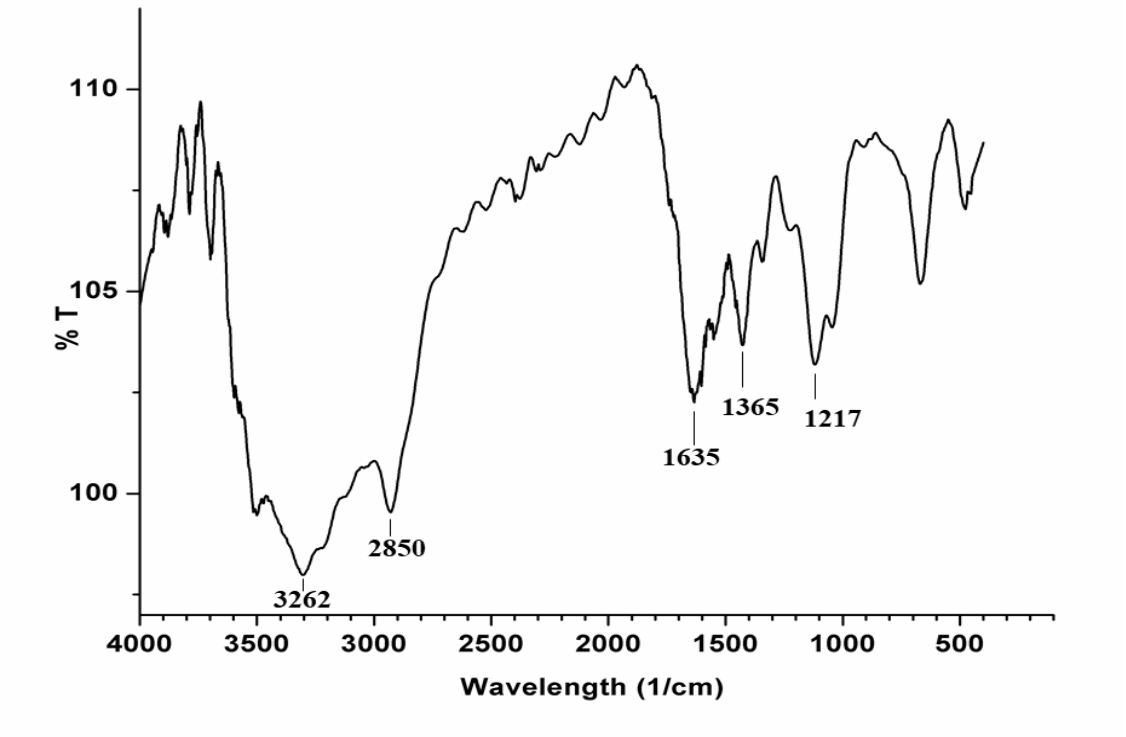

Fig. 3.43 FT- IR spectra of APM

3.3 DISCUSSION

Variation of colour between the 2 varieties of solar salt was merely due to the colour of the soil of evaporation pans, wherein sea water is allowed to stagnate during solar salt crystallization stage. The conventional, well tested and highly employed method of 1, 1-diphenyl-2-picrylhydrazyl ($DPPH^{\bullet}$) was used to quantify the antioxidant ability of solar salt and the extremely halophilic microbes retrieved from it. As the Goan crude solar salt is prepared through natural fractional crystallisation it essentially consists of NaCl with traces of $MgCl_2$ (Mani *et al*., 2012). Individual

solutions of however failed to decolourise DPPH$^{\bullet}$ reagent. This clearly indicated that **solar salt had ability to scavenge free radicals and hence possessed antioxidant activity**. This is the **first time free radical scavenging activity is checked and reported directly using solar salt**.

The absolute requirement of high concentration of NaCl for growth suggested that growth was either of members of heterotrophic halobacteria or of marine halophilic eubacteria, known to dominate hypersaline econiches having salts upto saturation concentration (Grant and Larsen, 1989). Such microbial growth has been reported from solar salts of Goa (Sequeira, 1992; Aguiar and Furtado, 1996; Khandavilli *et al*., 1999; Fernandes and Furtado, 2005; Braganca and Furtado, 2009). Such DPPH$^{\bullet}$ decolourization by microbial cultures has been conventionally evaluated in cultures, by spraying with DPPH$^{\bullet}$, a whatman filter paper, having the replicate of growth from agar plate (Velho-Pereira and Furtado, 2012). **The decolourization of DPPH$^{\bullet}$, herein observed by us of colonies on agar is taken as an indicator of free radical scavenging potential and a measure of antioxidant activity of the corresponding colony, similar to that observed with the filter paper replicates (Alvares and Furtado, 2018). This method, herein referred by us as 'Agar-growth-DPPH$^{\bullet}$ method', is direct, easy and gives easy reproducible antioxidant scoring efficiency.** Hence the antioxidant potential of solar salt was not an attribute of its chemical constituents, but of the microbes associated with it. These results support and confirm our presumption that tons of locally produced Goan solar salt, used as soil conditioner and fertilizer carried the free radical scavenging potential. The antioxidant potential of extremely eubacteria and haloarchaea associated with Goan solar salt is a reflection of constant exposure of these cultures to sunlight and radiations which is reported to trigger the formation of free radicals and reactive oxygen species (Mandelli *et al*., 2012; Abbes *et al*., 2013; Sikkandar *et al*., 2013; Rodrigo-Baños *et al*., 2015). Pathak and Sardar, (2012) have reported the antioxidant activity from *Halorubrum* sp. isolated from brine samples of solar salterns of Mumbai also evaluated through the DPPH$^{\bullet}$ assay.

Addition of methanolic extract of cells (MEC) (with absorption peaks between 300-600 nm) of each of the 6 cultures to phosphomolybdenum reagent, resulted in development of a bluish greenish colouration readable at 695 nm and was

accompanied by the disappearance of MEC absorption peaks between 300-600 nm, thus confirming the involvement of MEC in free radical scavenging through reduction of Mo (VI) to Mo (V) and formation of the bluish green phosphate complex, under acidic conditions. The formation of blue colour on addition of FC to MEC is attributed to an oxido - reduction reaction occurring between MEC and FC reagent, wherein phenolic moieties of the MEC are oxidised with simultaneous reduction of the alkaline FC. The extract of each of the 6 cultures **showed presence of phenolic content capable of reacting with the alkaline FC**.

The occurrence of non-pathogenic haloarchaea and marine halophilic eubacteria in Goan solar salts with an ability to scavenge free radicals adds value and promotes the traditional use of natural solar salt, in moderation, as conditioner and fertiliser to soils bearing trees such as *Cocos nucifera*, *Mangifera indica*, *Artocarpus heterophyllus* and others. The presence of phenolic moieties in these cells ensures their involvement in free radical scavenging of metals and hydrocarbons which are on increase as pollutants in coastal soils (Utkina *et al*., 2004). Based on high % $DPPH^{\bullet}$ RSA value, total antioxidant capacity and total phenolic content, *Haloferax alexandrinus* GUSF-1 (KF796625) was selected for further studies on antioxidant production.

Dissolution of $DPPH^{\bullet}$ in methanol resulted in formation of stable $DPPH^{\bullet}$ radicals and attained a deep purple colour with absorbance at 517 nm and as in Fig. 1, the intensity of colour increased linearly with increased concentration of $DPPH^{\bullet}$ thus indicating a goodness of fit of R = 0.988. In earlier preliminary study, growing colonies of *Haloferax alexandrinus* GUSF-1 (KF796625) on agar, as well as methanolic extracts of whole cells showed a visible decolourization of the deep purple colour of $DPPH^{\bullet}$ to mauve to yellow attributed to free radicals scavenging activity of cells and their extract.

The purpose of employing different organic solvents to extract free radical scavengers from the cells of *Haloferax alexandrinus* GUSF-1 (KF796625) was to ensure the complete extraction of wide polarity range of compounds, to avoid extraction errors and to ensure the complete solubilization of the bio molecules. The $DPPH^{\bullet}$ decolourization on receiving an electron or a H^{+} from a donor molecule in this case from individual extracts, changed the deep purple colour to yellow and consequently

decreased the absorbance at 517 nm and indicated the antioxidant nature of extract. The extent of change in colour corresponded to the H^+ received from the donor molecule, and was therefore, employed for detecting donor molecules such as antioxidants in the cell extracts and also the amount of antiradicals, therein. It is important to note that the other polar solvent such as ethanol, acetone, and ethyl acetate which is of intermediate polarity was found to be efficient in extraction of the antioxidant as compared to non- polar solvents used. Water even though lyses the haloarchaeal cells, was not found to be a suitable choice as a solvent. Methanol has been reported as a choice of solvent for extraction of bioactives. It denatures proteins which is important for further analysis. Moreover methanol among all the alcohols has low boiling point of just 65 °C, so concentration of bioactive compounds is easy by using the rotavapour. Since the methanolic extract from cells of *Haloferax alexandrinus* GUSF-1 (KF796625) showed maximum ability to scavenge molecules, we termed this extract as *Hfx*E and used it for all further studies. **As *Hfx*E had maximum free radical scavenging capacity and reflected presence of antioxidant component in *Hfx*E which hereafter we referred as *Hfx*A.**

In developing an optimal process for biological production, the effect of environment conditions is usually considered for improvement. The primary purpose of optimisation experiments is to select important main effects from less important ones. Maximum growth and free radical scavenging activity of *Hfx*A at different salt concentration of growth was optimized by growing the haloarchaeon *Haloferax alexandrinus* $GUSF_1$ (KF796625) culture in NTYE medium with different NaCl, temperarure, pH and aeration. **Thus 25% NaCl in nutrient rich NTYE medium, 42ºC, pH 7 and 150 rpm aeration are conducive for the maximum production of antioxidants in cells of *Haloferax alexandrinus* GUSF-1 (KF796625)**. Salt dependent growth is a common feature of extreme halophiles as reported by several authors (Fernandes and Furtado, 2005, Sequeira, 1992). Temperature is one of the most important environmental factors affecting the growth of microrganisms. It is known to influence many biosynthetic pathways. Biological properties such as antioxidant and antiproliferative of haloarchaea have been demonstrated in methanolic cell extracts *Haloterrigena turkmenica* (Squillaci *et al*., 2017) and ethanolic extracts of cells of *Halobacterium halobium* against human hepatoma cell lines (HepG2) (Abbes *et al*., 2013). Such biological activity among these extreme

halophiles can be interpreted as an adaptive feature of halophiles to such high salinity. Isolates belonging to the genus *Haloferax* are aerobic and hence shaker condition and light conditions during growth also influenced growth and free radical scavenging activity.

The extent of change in colour or absorbance at 517 nm corresponded to the residual amount of $DPPH^{\bullet}$ radical remaining in the reaction mixture and reflected the amount of H^+ donated by the antiradical biomolecule/ s in *Hfx*A and also the amount of antiradical, thereof. The antioxidant-$DPPH^{\bullet}$ reaction involved the transfer of H^+ via the HAT radical mechanism, wherein the H^+ is abstracted from the antioxidant molecule. Scavenging by the antioxidant in *Hfx*A was therefore considered to be mainly due to e^- transfer and negligible amount of H^+ atom transfer. This resulted in different EC_{50} values and the subsequent slower rate pointed to the role of secondary slow reactions, possibly involving dimerization of phenol derived radicals. Cells of *Haloferax alexandrinus* GUSF-1 (KF796625) possess phenolic moities content detectable by Folin Ceocalteu reagent (FC) at 765 nm due to the oxido reduction reaction wherein phenolic moieties of *Hfx*A are oxidised with simultaneous reduction of the alkaline FC (Alvares and Furtado, 2018).

The reaction of *Hfx*A is a multi-component system. The reversible conversion of DPPH-H to $DPPH^{\bullet}$ reaction also contributed towards the total capacity of the antioxidant in *Hfx*A. This dynamic behaviour of the reactants resulted in different EC_{50}/ IC_{50} values. The dependence of absorbance of $A_{c\ (517\ nm)}$ and $A_{s\ (517\ nm)\ (t\ =\ x)}$ on time is therefore exponential and a power function,

Hence, $Ac_{\ (517\ nm)} - A_{s\ (517\ nm)\ (t\ =\ x)} = a.t^{\ b}$;

the power of a and b, obtained by non-linear regression analysis. We assumed that the reaction occurs via the HAT radical mechanism wherein, the H atom abstracted from antioxidant molecule *Hfx*A as in, ArOH + $DPPH^{\bullet}$ = ArO + DPPH-H proceeded at highest initial rate in non-polar solvents, similar to the kinetic method for the reactivity of the antioxidant present in multicomponent system of plant extracts towards $DPPH^{\bullet}$ (Thaipong *et al*., 2006). Our observations suggested that the influence of sequential loss of proton and electron transfer (SPLET) mechanism is not completely suppressed in the reaction with $DPPH^{\bullet}$, hence we made no attempts to exclude it. Further, the study carried out analysis of the kinetics of the reactions

between antioxidants *Hfx*A and DPPH$^{\bullet}$ radical and interpret the kinetic data. We assumed the concentration of *Hfx*A to correspond to the concentration of *Hfx*E, used. Now in order to determine the kinetics of the relationship between antioxidant and DPPH$^{\bullet}$, kinetic curves were recorded using different concentration of *Hfx*E. As in Mishra *et al*., 2012, we used the scavenging of DPPH$^{\bullet}$ to estimate the effective concentration **EC_{50} of *Hfx*A which was four times more than the reference ascorbic acid.**

Natural antioxidants are in high demand for application as nutraceuticals, in preparation of cosmetics and as well as food additive because of consumer preferences. Oxidative stress and DNA damage are related to various diseases and pathological conditions such as carcinogenesis, atherosclerosis, cardiovascular, neurodegenerative disease as well as inflammation and ageing (Bonomoni *et al*., 2008; Klaunig *et al*., 2004; Laviano *et al*., 2007). The cold ethanol extracts of culture supernatants showed a modest capacity for scavenging DPPH$^{\bullet}$ (20% DPPH$^{\bullet}$ RSA) at a concentration of 1mg ml^{-1}. Antioxidants activities of EPS have been reported in haloarchaeon *Haloterrigena turkmenica* whose value was 3 times lower than our activity at the same concentration assayed (Squillaci *et al*., 2016). The FT-IR spectrum of cold ethanol extracts of culture supernatants revealed major peaks attributed as the hydroxyl groups, presence of alkenes, amide and carboxyl group. The peaks between 2000-1000 was indicative of the C-OH side groups and the C-O-C glycosidic band vibrations (Zhang *et al*., 2011), which suggested polysaccharide since this was obtained from culture broth after removing cells we record it as extracellular polysaccharide, the EPS. Exopolysaccharide is an extracellular biopolymer excreted by microorganism during growth. Little is reported about EPSs production from halophilic Archaea with Antón *et al*., (1988) firstly reporting the production of EPS by a halophilic archaeon, *Haloferax mediterranei* (ATCC 33500) as a producer of an extracellular polymer. Thus, under our experimental conditions, the haloarchaeon could be exploited for production of EPS as well as for other cellular bioactives at the same time. EPSs have also received an increasing pharmaceutical interest as antitumor, antiviral, immune-stimulatory and anti-inflammatory agents (Arena *et al*., 2006; Arena *et al*., 2009). The antioxidant power of the EPSs has also been pointed out by several authors (Sun *et al*., 2014) and EPSs having antioxidant activity could

be used as food supplements or as protective agents in pharmaceutics (Guo *et al*., 2010).

The **hydroxylated methanolysate obtained from cells was seen as a blue spot at R_f 0.2** after staining with 10 % dodecaphosphomolybdic acid in absolute ethanol which **was attributed to glycerol diether moieties (GDEM)** (Ross *et al*., 1985). The main lipid core of archaeal extreme halophiles, which represents the hydrophobic portion of complex polar membrane lipids, is usually obtained from archaeal lipids by strong-acid methanolysis or acetolysis to remove polar groups such as phosphate esters or sugars (Kates, 1986). The FT- IR spectral analysis of the hydroxylated methanolysate revealed an intense absorption peaks at 1076 cm^{-1} indicative of the C-O-C group. This configuration of archaeal diether phospholipids protects the extreme halophiles against hydrolysis of their membrane phospholipids by stereospecific phospholipases excreted by other organisms, thus helping these microorganisms to survive in competitive environments (Kates, 1986**)**.

The methanolic extract *Hfx*E was termed as *Hfx*A since it had antioxidant capacity. Methanol is often the best choice of solvents for extracting bioactives. The extract was bright orange in colour and was positive for free radical scavenging activity evaluated by the $DPPH^{\bullet}$ assay and showed clear distinct peaks between the UV and visible region. The unique, clear and distinct signals in an absorbance pattern in a visible spectrum of coloured extracts is attributed to their structure and presence of conjugated double bonds if any, which absorb light at specific frequencies (Britton *et al*., 1995). In the case of carotenoids the patterns produced are a distinctive three peak structure in the visible spectrum. The absorption spectrum revealed the characteristic pattern of red carotenoids. Britton *et al*., (1995) described that bacterioruberin and its derivatives exhibited the characteristic spectral peaks of red carotenoids at around 467, 493 and 527 nm for three fingered speaks and at 370 and 385 nm for two cis peaks very similar to those recorded in our spectrum. The crude *Hfx*A resolved into 4 distinct spots when developed in benzene: acetone (2:1) and on spraying with methanolic $DPPH^{\bullet}$, decolourization in the form of white bands around all the 4 spots could be seen, here by suggesting the involvement of more than one metabolite in scavenging of the $DPPH^{\bullet}$ radical. The spot at R_f 0.4, 0.55 and 0.69 separated on TLC in benzene: acetone (2:1) on elution with methanol revealed peaks

corresponding to bacterioruberin, bisanhydrobacterioruberin and lycopene respectively (Asker *et al*., 2002; Squillaci *et al*., 2017).

Spot test were carried out with *Hfx*A in order to qualitatively identify the presence of the phenols and glycosides. The addition of alkaline Folin Ceocalteau reagent resulted in a bluish green colouration indicating **presence of phenolic component in *Hfx*A** comparable to that reported by Singleton and Rossi (1965). Further the formation of a **brown ring and a long lasting lather indicated the presence of glycosidic linkages and saponins in the crude extract** (Harborne, 1998). This result confirms the presence of exopolymeric substances that could have been attached to the cell and was not detached in the washing process of the cells with 15 % NaCl. **The FTIR spectroscopic study of *Hfx*A confirmed that the presence of -OH, methylene group, C=O of a carbonyl group and CH=CH trans unsaturation.** Similar reports are available on purified carotenoid pigments obtained from *Haloferax* sp. BKW301 (Biswas *et al*., 2016), isolated from Indian solar salterns.

Hexane fraction (HE) when scanned between 190-800 nm showed peaks between 300-600 nm which were **indicative of the presence of red carotenoids** and it's derivatives in the hexane fraction. The free radical scavenging activity of the hexane fraction obtained was checked by the DPPH$^{\bullet}$ assay using methanolic DPPH$^{\bullet}$. The hexane extract owing to its polarity was seen to be separating out into two layers in the methanolic DPPH$^{\bullet}$, and a false negative test was obtained, therefore a 0.2 mM of DPPH$^{\bullet}$ in hexane was prepared and used for the assay. **The spectra of DPPH$^{\bullet}$ in methanol was found to show two peaks at 517 and 327 nm, which were shifted to 508 and 321nm when dissolved in hexane**. This reaction mixture when scanned revealed that both the peaks of DPPH$^{\bullet}$ seen at 508 nm and 321 nm were abolished indicating it's involvement in the decolourization of the purple coloured DPPH$^{\bullet}$ reagent. To further confirm the identity and the role as free radical scavengers, thin layer chromatography of the hexane extracts was performed using different solvent combination so as to achieve maximum separation and to assist in the identification process. The chromatograms after resolving in the respective solvent systems were sprayed with 0.2 mM hexanic DPPH$^{\bullet}$ solution, incubated in the dark for 30 minutes and checked for any decolourization around the resolved spots. When developed in acetone: petroleum ether (20:80, v/v), a total of **9 spots** were seen as detected with

iodine vapour and by naked eye. **All 9 were positive for DPPH$^{\bullet}$ decolourization as purple colour turned colourless around the spots after spraying with 0.2 mM hexanic DPPH$^{\bullet}$ with the concomitant disappearance of the resolved spots**. The spots at R_f 0.14 corresponded to **bacterioruberin,** the spot at R_f at 0.36 corresponded to **3-hydroxy echinone**, and the spots at R_f 0.53 corresponded to **canthaxanthin** as these had the same R_f as that reported by Asker *et al*. (2002). The UV- Vis scan of spot at R_f 0.14 matched with the peaks of bacterioruberin reported by Squillaci *et al*. (2017).

When hexane extract was resolved with solvent system of methanol and chloroform a total of 5 spots were viewed and DPPH$^{\bullet}$ decolourization was seen only around 4 spots at R_f 0.24, 0.29, 0.43 and 0.71. The spots at R_f 0.24 is attributed to **bacterioruberin**, the spot at R_f 0.29 was identified as **monoanhydrobacterioruberin** and the spot at R_f 0.43 revealed it to be **bisanhydrobacterioruberin** as confirmed with the R_f reported by Asker *et al*., (2002) and Kushwaha *et al*. (1975). The peaks in the UV-Vis scan of the spots at R_f 0.29 and 0.43 matched with data confirming the spot as monoanhydrobacterioruberin and bisanhydrobacterioruberin (Squillaci *et al*., 2017). The spot at Rf 0.46 obtained on resolving the hexane extract in acetone: hexane (1:1) and which decolourized DPPH$^{\bullet}$ was attributed to **haloxanthin** in the hexane extract as reported by Ronnekleiv *et al*. (1995). The spot at R_f 0.9 obtained on resolving the hexane extract in n-heptane: benzene (9:1, v/v) and which decolourized DPPH$^{\bullet}$ was attributed to **tetrahydrosqualene** since it matched the R_f reported by Tornabene *et al*. 1969**.** The FT-IR spectral analysis of hexane extract of *Haloferax alexandrinus* GUSF-1 (KF796625) revealed intense absorption peaks at different wave numbers indicating the presence of an alcohol, alkanes, carbonyl group, amide I (C=O) and amide II (N=H) bands, phosphate groups (P=O and P-O of the C-PO_3^{2-}) moiety and trans unsaturation (CH=CH). **The carotenoid pigments of halobacteria are reported to serve a function of the repair of DNA by photoreactivation and may protect the cells against damage by photosensitized oxidation** (Kates and Kushwaha, 1978; Kushner and Kamekura, 1988). The predominant C_{50} carotenoid, **bacterioruberin is reported to contain 13 pairs of conjugated double carbon bonds with four terminal hydroxyl groups** (Rodriguez-Amaya and Kimur, 2004), endowing biological tissues possessing it with effective protection against free radical species such as reactive nitrogen species such as DPPH$^{\bullet}$ (Squillaci *et al*., 2017) and

hydroxyl free-radicals (Saito *et al*., 1997). Carotenoids from halophiles are reported to have a very good antioxidant capacity mainly because of its singular chemical structure (Mandelli *et al*., 2012). The antioxidant capacity is reported to be **related to both the length of the conjugated double bond (cdb) system and presence of functional groups.** The antioxidant capacity of the carotenoids **increases with the increased extension and maximum overlap of the conjugated double bond molecular orbitals** (Miller *et al*., 1996; Albrecht *et al*., 2000; Tian *et al*., 2007). **The halophilic microorganism has the all trans BR as the major carotenoid, which has an extensive system of 13 cdb, two acyclic ψ end groups, four OH at the positions C-1, C-1´, C-3´´, C-3´´´**(Mandelli *et al*., 2012). This pigment protects Halobacteria from fatal injuries under direct intense sunlight and confers the halobacteria with resistance to oxidative DNA damage from radiography, UV-irradiation and H_2O_2 exposure (Mandelli *et al*., 2012; Shahmohammadi *et al*., 1998). Furthermore the branched isoprenoid chains would also ensure that the membrane lipids are in the liquid-crystalline phase at all ambient temperatures (Lindsey *et al*., 1979).

All peaks seen in the absorption spectrum of Acetone Precipitated Material (APM) were in the UV range. These peaks were abolished on reacting with DPPH$^{\bullet}$ and so was the characteristics peaks of pure DPPH$^{\bullet}$ at 517 and 327 nm which were missing in the scan of the reaction mixture. The FTIR spectral analysis of Acetone Precipitated Material revealed intense absorption bands at various wave numbers that were indicative of an -OH group arising from a alcohol, stretching vibrations of C-H of methylene group belonging to alkanes, characteristic of C=O of a carbonyl group, -C-H of an alkane, C-C belonging to a carbonyl group. **The FTIR spectroscopic study of APM confirmed that the presence of -OH from alcohol, methylene group, C=O of a carbonyl group, -C-H of an alkane and C-C belonging to a carbonyl group.**

Overall the study confirms the production of antioxidants by the extreme halophilic and haloarchaeal cultures isolated from solar salts, estuarine sediments and sponge. The antioxidant activity of the haloarchaeon *Haloferax alexandrinus* GUSF-1 (KF796625) is **attributed to red carotenoids, glycerol di ether moieties and lipids produced by the cells as well as the extracellular EPS secreted by the culture**.

Chapter IV

Chemical profiling of
Haloferax alexandrinus GUSF-(KF796625)

The haloarchaeon *Haloferax alexandrinus* GUSF-1 (KF796625) is envisaged to hold a promise in biotechnology because of the results obtained during earlier studies as well as those recorded in the preceding chapter pertaining to: production of lipase and aromatic oxygenase extremozymes, halocins, suppression of arsenic toxicity, production of antioxidants, production of selenium, tellurium and bixbyite Mn_2O_3 nanoparticles which is detailed in the following chapter V. It was, therefore, pertinent to obtain a possible chemical profile of the culture. This chapter is the record of the restricted chemical profile data of cells of *Haloferax alexandrinus* GUSF-1 (KF796625) obtained through Reverse Phase-High Performance Liquid Chromatography coupled with High Resolution Mass Spectroscopy analysis and their interpretation using appropriate software and database assistance leading to identification of the biomolecules.

4.1 METHODOLOGY

4.1.1 GROWTH AND PRODUCTION OF LARGE QUANTITIES OF CELL MASS OF *Haloferax alexandrinus* GUSF-1 (KF796625)

Large quantities (3 litres) of cell mass of *Haloferax alexandrinus* GUSF-1 (KF796625**)** was prepared by growing the culture on a large scale in NTYE at 42ºC, pH 7 and 150 rpm aeration for 5 days.

4.1.2 EXTRACTION OF CELLULAR CONTENTS FROM *Hfx*A

As per flow chart **Fig 4.1**, Methanolic extract with antioxidant capacity (*Hfx*A) from washed wet cells was prepared in dim light and stored at 4°C. Further the polar and non-polar components from *Hfx*A were separated according to a method of Asker *et al*. (2002) by adding hexane and distilled water. The non-polar lipids were recovered in the hexane layer, which was then washed several times with distilled water and dried over anhydrous sodium sulfate. The washed hexane layer was subjected to cold acetone precipitation to precipitate out the polar components, by addition of cold acetone in small volumes. The precipitate was separated out, re dissolved in methanol and stored at -20^{o}C till further use. This extract has been termed as Acetone

precipitated Material (APM). The non- polar components left in the hexane layer was termed as Hexane Extract (HE) and stored at -20^{o}C till further use.

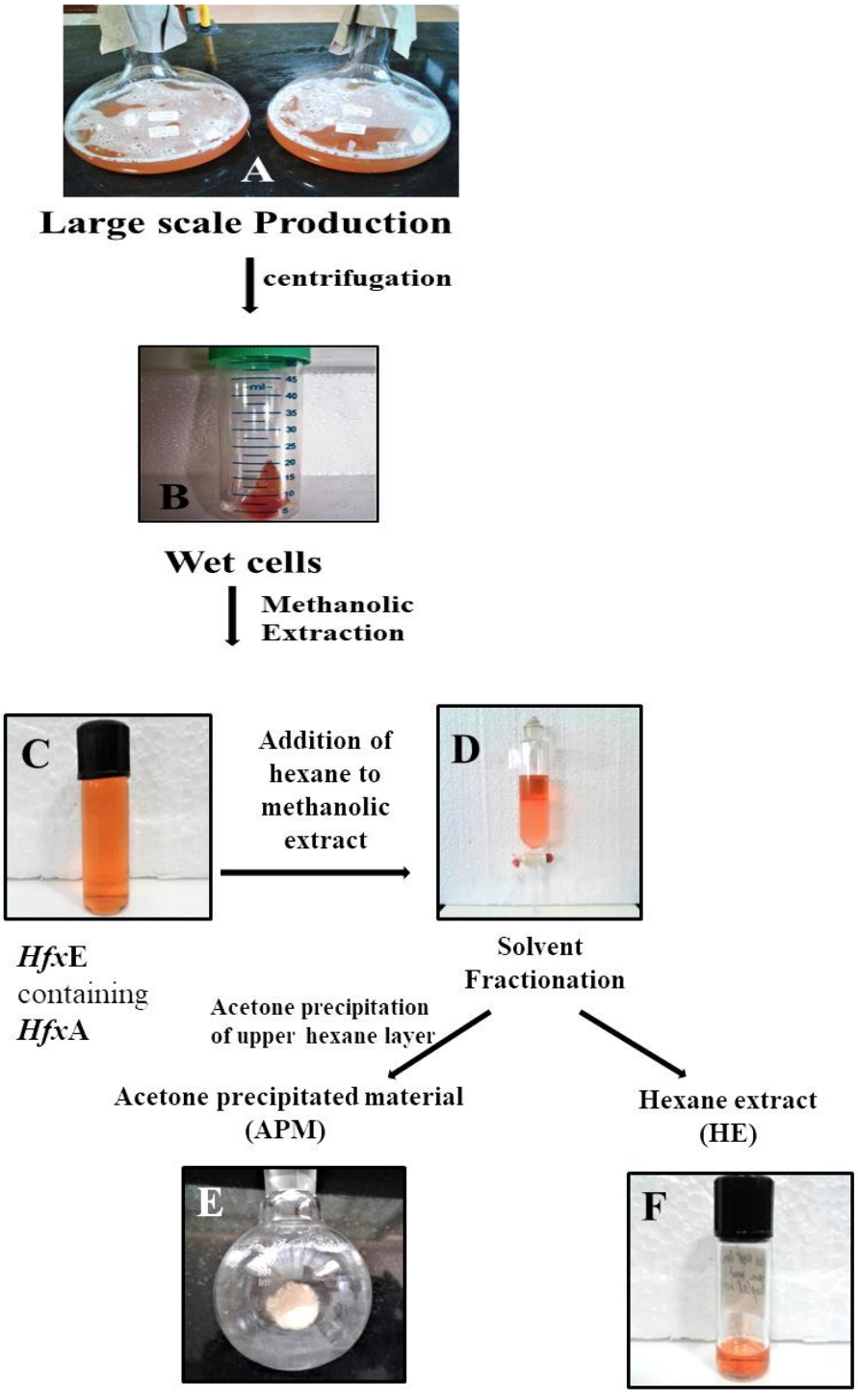

Fig. 4.1 Extraction steps followed for separation of free radical scavengers
A: Growth of *Haloferax alexandrinus* GUSF-1 (KF796625) under optimized conditions; **B:** Wet cells obtained on centrifuging the culture broth used for methanolic extraction; **C:** Methanolic extract from wet cell with antioxidant capacity; **D:** Solvent fractionation with hexane; **E:** Acetone Precipitated Material (APM) and **F:** Hexane Extract

4.1.3 CONCENTRATION OF HEXANE EXTRACT AND ACETONE PRECIPITATED MATERIAL

The hexane extract (HE) and the acetone precipitated material (APM) obtained after solvent fractionation of the methanolic extract from cells of *Haloferax alexandrinus* GUSF-1 (KF796625) was first concentrated under liquid N_2 gas and chemically profiled as detailed in **4.1.4**

4.1.4 CHEMICAL PROFILING OF CONCENTRATED HE AND APM USING HRLC-MS/MS

Chemical profiling of concentrated HE was carried out on HRLC-MS/MS instrument; Agilent 1290 Infinity UHPLC System, 1260 infinity Nano HPLC with Chipcube series (Agilent Technologies, USA) with ESI interface and consisting of a binary pump, an autosampler and 6550 i funnel QTOF-LC/MS. The LC-MS operating parameters were as follows: Each sample was analyzed in both positive and negative modes in the range of m/z = 130–3200, scan rate 1.00 spectra/ sec, gas temperature 250°C, gas flow 13 l/ min, nebulizer 35 psig, sheath gas temperature 250°C, capillary voltage 2500 V, and fragmentor 175 V. The solvent composition was 0.1% formic acid in water (A) and 70% acetonitrile + 30% methanol (B). The chromatographic separation was achieved using a Hypersil gold 3 micron 100 x 2.1 mm C - 18 reverse phase column from Agilent Technologies, at a flow rate of 0.3 ml/ min, with gradient program as follows: 0-2 min ; A: 95.00% & B: 5.00%, 2-30min; A: 5.00% & B:95%, 30-35 min; A: 5.00% & B:95%, 35-38 min; A: 95.00% & B: 5.00%, 38-45 min; A: 95.00% & B: 5.00%. The column temperature was operated at 25℃ and injection volume was 3 µl. All the operations, acquisition and analysis of data were controlled by Agilent Mass Hunter Acquisition Software version A.05.00 and processed with Mass Hunter Qualitative Analysis Software version B.05.00. Tentative identification of the compounds was made using Pubchem database and the Agilent Mass Hunter software.

4.2 RESULTS

4.2.1 SEPARATION OF CELLULAR COMPONENTS IN *Haloferax alexandrinus* GUSF-1 (KF796625)

A total of 97.7007 g of wet weight of *Haloferax alexandrinus* GUSF-1 (KF796625) cells was obtained on 7 d of growth in NTYE under optimized conditions deduced in Chapter III **(Fig. 4.1A)**. The wet cells (**Fig. 4.1B)** yielded 850 ml of orange methanolic extract with antioxidant capacity (*Hfx*A) (**Fig. 4.1C**). The addition of hexane to *Hfx*A resulted in separation into two phases; upper hexane layer and lower methanol. The hexane layer was separated out and further the addition of cold acetone to this hexane layer resulted in precipitation (**Fig. 4.1D**). This precipitate which was insoluble in acetone and contained polar components was termed as Acetone Precipitated Material (APM) and hexane extract, containing non polar components, that was left behind was termed as Hexane soluble Extract (HE) (**Fig. 4.1E** & **F)**.

4.2.2 CHEMICAL PROFILING OF HEXANE EXTRACT (HE)

The chemical profiling of hexane extract showed the presence of 12 peaks which were labeled in the increasing order of their retention time (R_t) (**Fig. 4.2**) and are listed in **Table 4.1**. The EI-MS spectrum of compound 1eluted at R_t 1.121 with m/z of 202.17 , mass 201.17 and molecular formula of $C_{11}H_{23}NO_2$. The peak at R_t 4.528 showed m/z of 302.19, mass 301.18 and molecular formula of $C_{16}H_{23}N_5O$. The peak at R_t 6.823 showed m/z of 565.3, mass 564.3and molecular formula of $C_{40}H_{52}O$. The peak at R_t 9.801 showed m/z of 430.24, mass 429.23 and molecular formula of $C_{22}H_{31}N_5O_4$. The peak at R_t 20.523 showed m/z of 415.20, mass of 414.20 and molecular formula of $C_{30}H_{54}$. The peak at R_t 23.457 showed m/z of 301.13, mass 278 and molecular formula of $C_{18}H_{34}O_4$. There were four compounds that were eluted at R_t 25.471; m/z of 568.45 with mass of 567.45 and molecular formula of $C_{40}H_{56}O_2$, m/z of 595.38 with mass of 572.39 and molecular formula of $C_{40}H_{60}O_2$, m/z of 546.40 with mass of 545.39 and molecular formula of $C_{40}H_{64}$ and m/z of 597.4 with mass of 596.6 and molecular formula of $C_{40}H_{52}O_4$. The peak at R_t 27.226 showed m/z of 337.23 (mass 314.24 and molecular formula of $C_{18}H_{34}O_4$). The compounds eluted at R_t 29.943 showed m/z of 705.55 with mass of 704.55 and molecular formula of $C_{50}H_{72}O_2$, m/z

of 723.57 with mass of 722.55 and molecular formula of $C_{50}H_{74}O_3$ and m/z of 741.58 with mass of 740.57 and molecular formula of $C_{40}H_{76}O_4$. The peak at R_t 30.209 showed m/z of 537.4 with mass 536 and molecular formula of $C_{40}H_{56}$. The peak eluted at R_t 31.68 had m/z of 739.56 with mass of 738.55 and molecular formula of $C_{50}H_{74}O_4$. The peak eluted at R_t 35.658 showed m/z of 543.2 with mass of 542.2 and molecular formula of $C_{40}H_{62}$.

Fig. 4.3 reveals the Diode Array Detector (DAD) response of the hexane extract at 320 nm showed that the peak 1 at R_t 1.121, peak 8 at R_t 27.226, peaks 9 and 10 between R_t 29.943 and 31.68 showed absorption signal at 320 nm.

Fig. 4.4 and **Fig. 4.5** reveals the Diode Array Detector (DAD) response of the hexane extract at 447 nm and 490 nm showed that the peaks at 9 and 10 between R_t 29.943 and 31.68 were seen to show an absorption signal at both the wavelengths.

Fig. 4.2 HR-LCMS chromatogram of hexane extract of *Haloferax alexandrinus* GUSF-1 (KF796625) chromatographed on a C-18 reverse phase column; Hypersil gold 3micron 100 x 2.1 mm column. Peaks are labelled based on increasing retention times (R_t) (decreasing polarity)

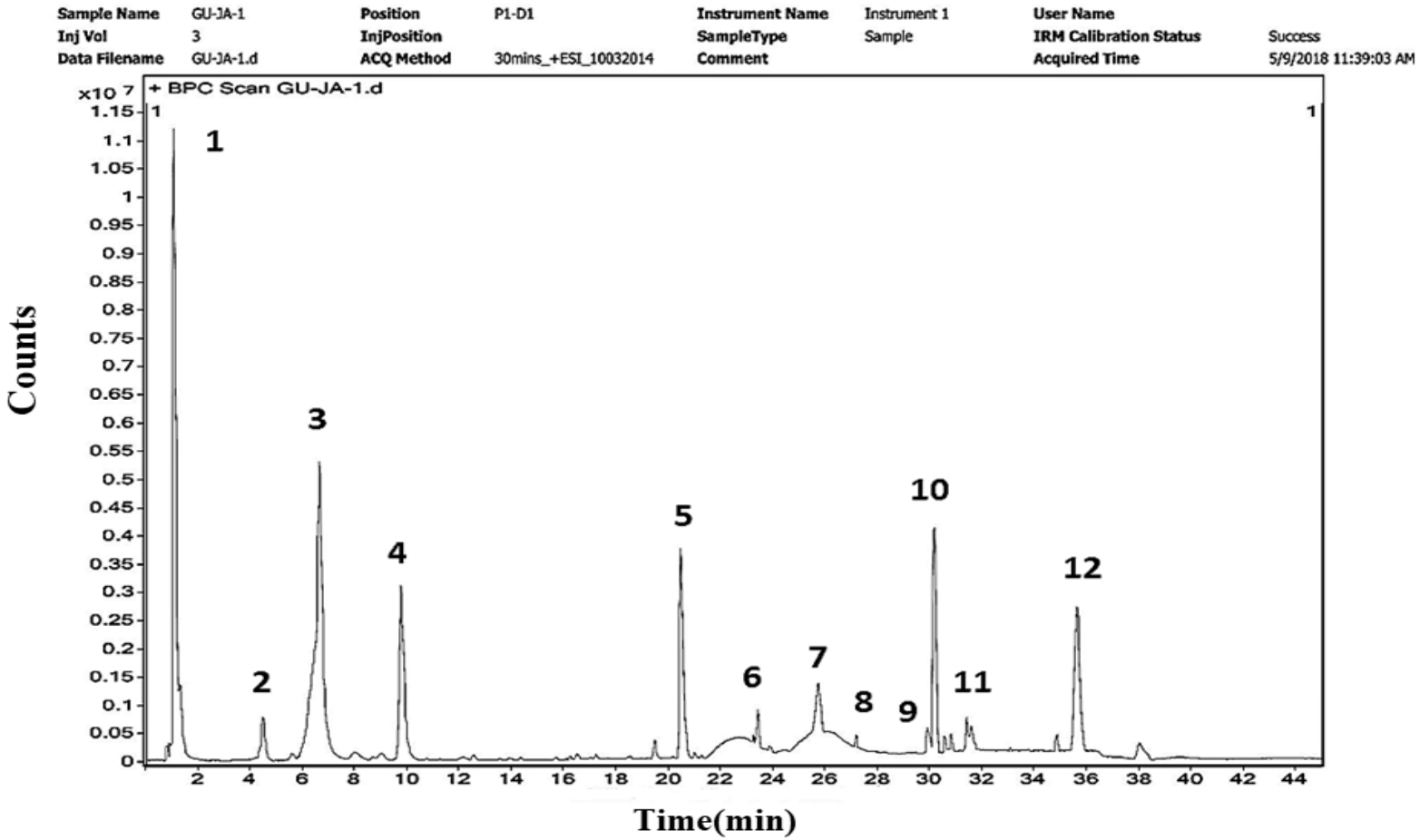

Table 4.1 Mass Spectra analysis of the hexane extract of *Haloferax alexandrinus* GUSF-1 (KF796625)

Peak No	Rt	**(m/z)**	z	**Ion**	Abundance (conc)	**Mass**	Molecular formula
1	1.121	**202.17**	1	(M+H)+	**1.12×10^{7}**	201.17	**$C_{11}H_{23}NO_2$**
2	4.528	**302.19**	1	(M+H)+	**0.07×10^{7}**	301.18	**$C_{16}H_{23}N_5O$**
3	6.823	**565.3**	1	(M+H)+	**0.51×10^{7}**	564.3	**$C_{40}H_{52}O_2$**
4	9.801	**430.24**	1	(M+H)+	**0.31×10^{7}**	429.23	**$C_{22}H_{31}N_5O_4$**
5	20.523	**415.20**	1	(M+H)+	**0.37×10^{7}**	414.20	**$C_{30}H_{54}$**
6	23.457	**301.13**	1	(M+ Na)+	**0.02×10^{7}**	278.15	**$C_{16}H_{22}O_4$**
7	25.471	**568.45**	1	(M+H)+	**0.03×10^{7}**	567.45	**$C_{40}H_{54}O_2$**
		595.38	1	(M+Na)+	**0.08×10^{7}**	572.39	**$C_{40}H_{60}O_2$**
		546.40	1	(M+H)+	**0.1×10^{7}**	545.39	**$C_{40}H_{64}$**
		597.4	1	(M+H)+	**2×10^{4}**	596.6	**$C_{40}H_{52}O_4$**
8	27.226	**337.23**	1	(M+ Na)+	**0.04×10^{7}**	314.24	**$C_{18}H_{34}O_4$**
9	29.943	**705.55**	1	(M+H)+	**0.3×10^{4}**	704.55	**$C_{50}H_{72}O_2$**
		723.57	1	(M+H)+	**0.9×10^{4}**	722.55	**$C_{50}H_{74}O_3$**
		741.58	1	(M+H)+	**0.03×10^{7}**	740.57	**$C_{50}H_{76}O_4$**
10	30.209	**537.4**	1	(M+H)+	**1×10^{3}**	536	**$C_{40}H_{56}$**
11	31.68	**739.56**	1	(M+H)+	**0.07×10^{7}**	738.55	**$C_{50}H_{74}O_4$**
12	35.658	**543.2**	1	(M+H)+	**2.1×10^{3}**	542.2	**$C_{40}H_{62}$**

Fig. 4.3 Diode Array Detector response at 320 nm of the hexane extract of *Haloferax alexandrinus* GUSF-1 (KF796625) showed that the peak 1, 8, 9 and 10, showed absorption signal at 320 nm

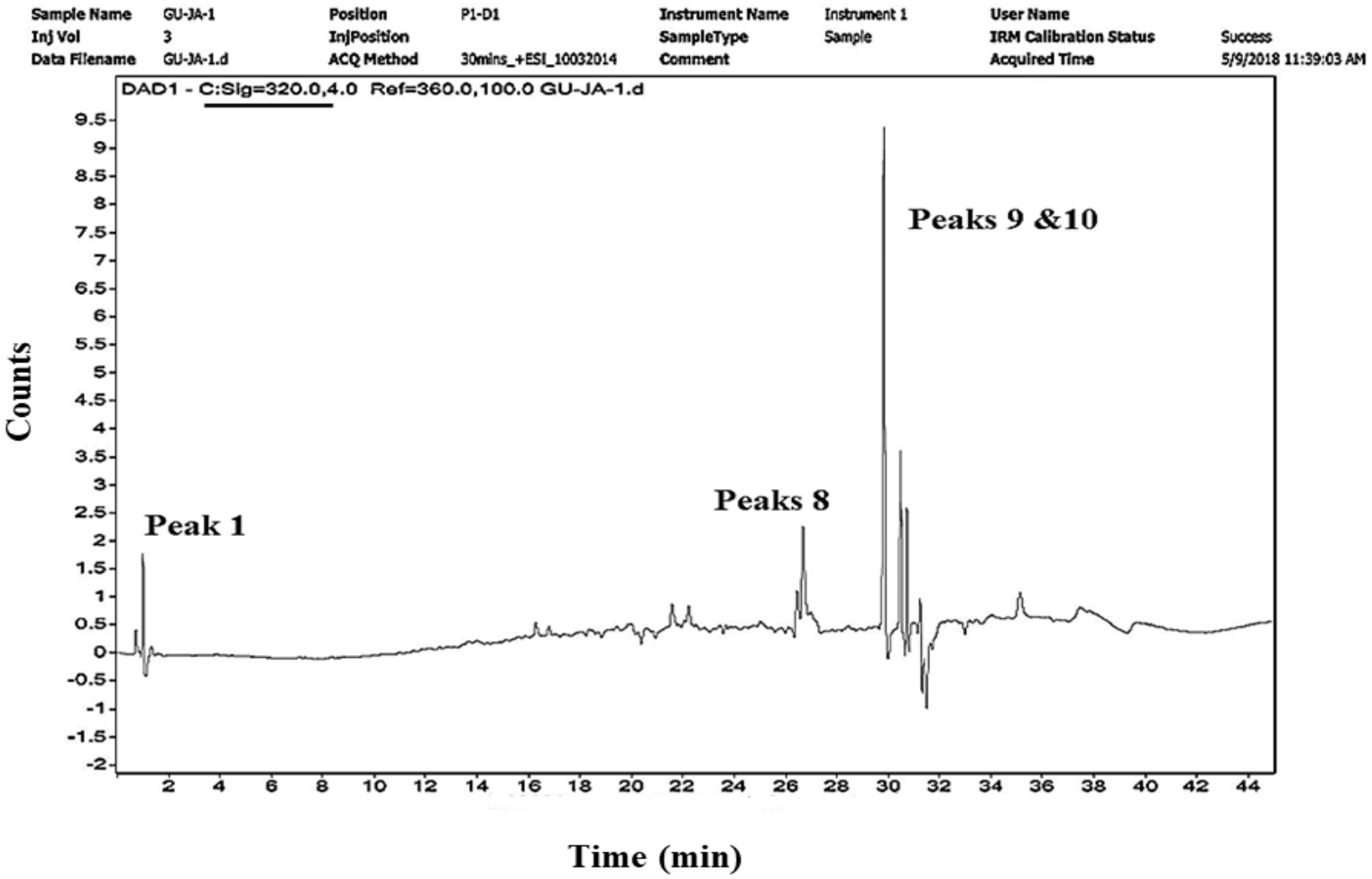

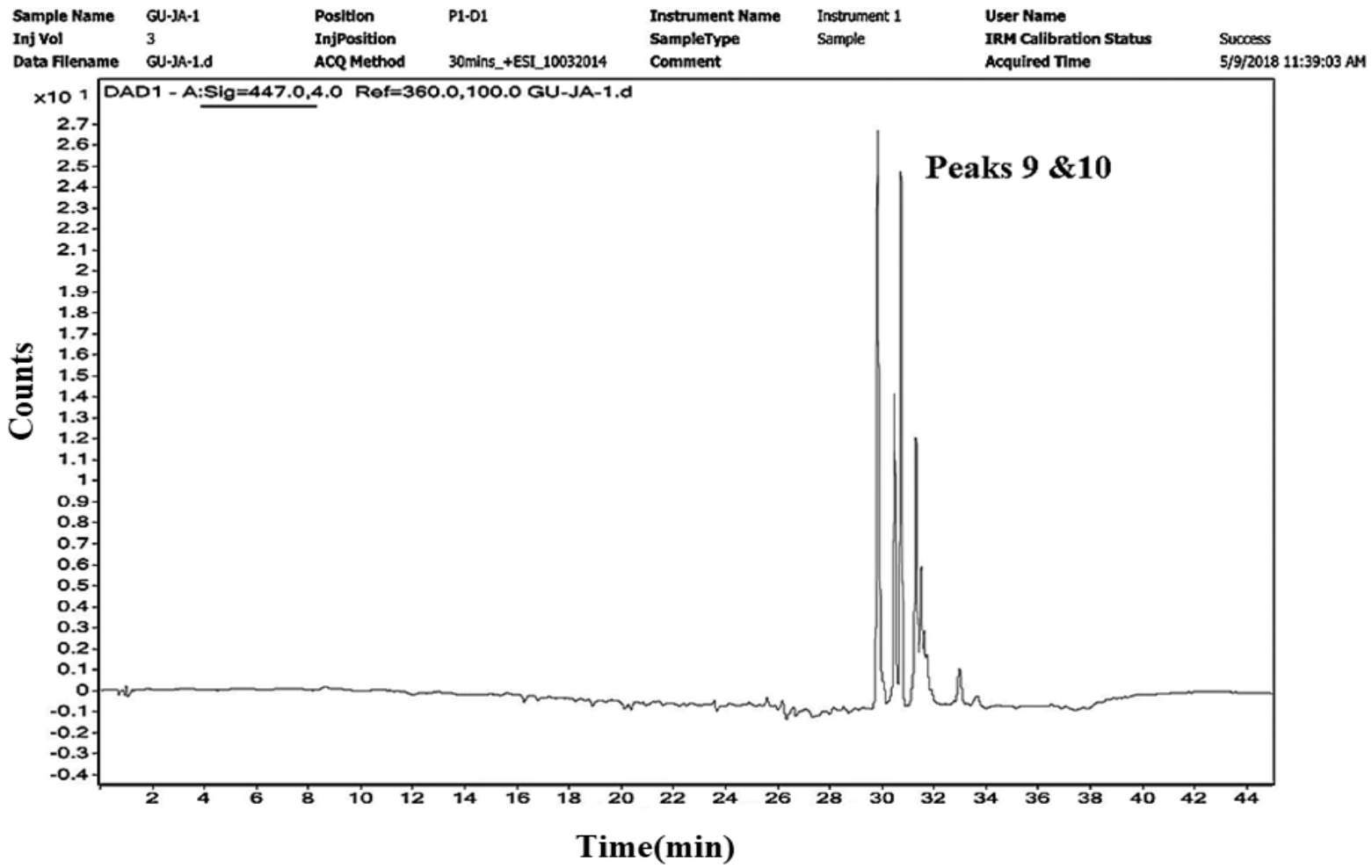

Fig. 4.4 Diode Array Detector response at 447 nm of the hexane extract of *Haloferax alexandrinus* GUSF-1 (KF796625) showed that the peaks 9 and 10, showed absorption signal at 447 nm

Fig. 4.5 Diode Array Detector response at 490 nm of the hexane extract of *Haloferax alexandrinus* GUSF-1 (KF796625) showed that the peaks 9 and 10, showed absorption signal at 490 nm

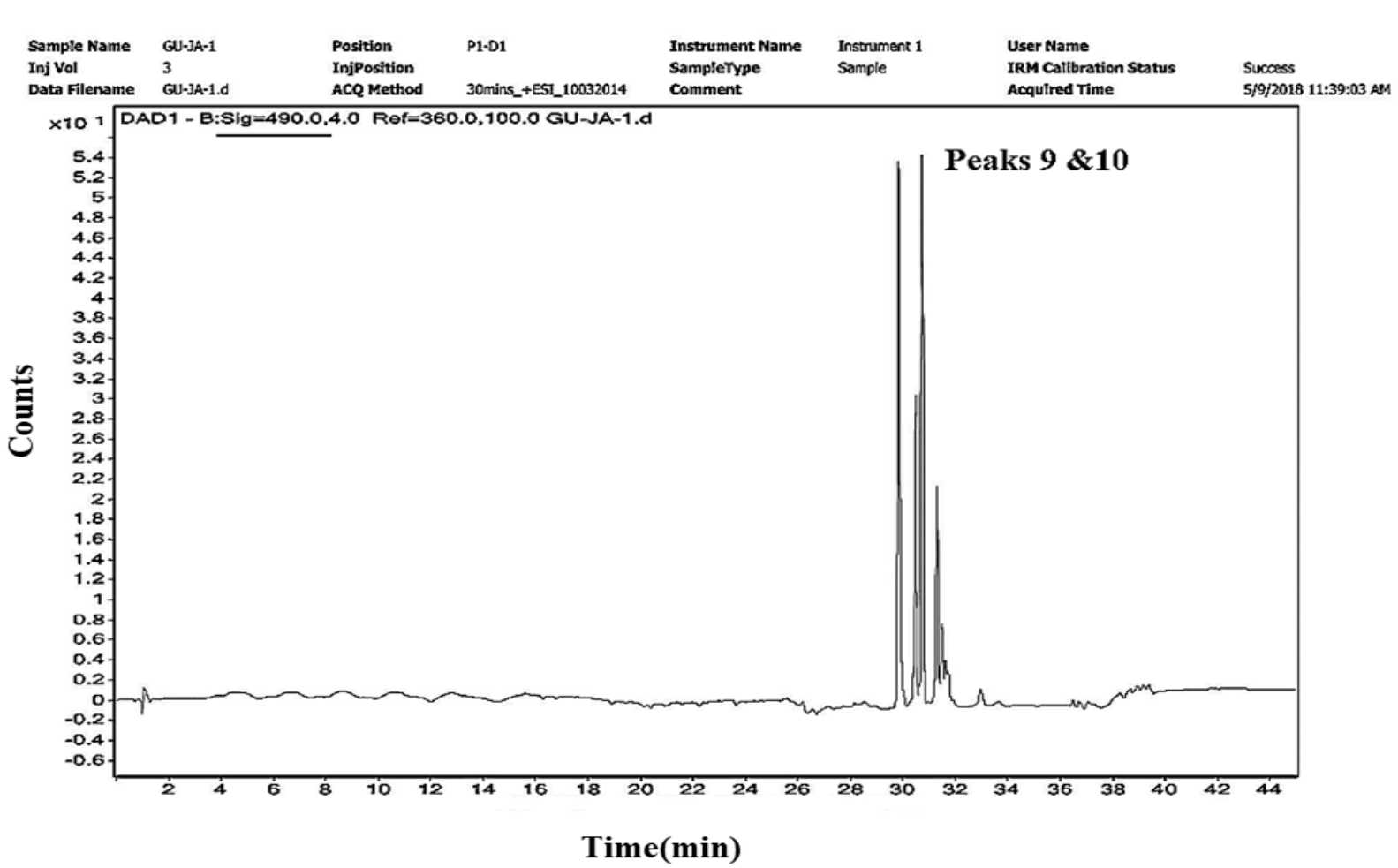

4.3.2 CHEMICAL PROFILING OF ACETONE PRECIPITATED MATERIAL (APM)

The chemical profiling of acetone precipitated material of *Haloferax alexandrinus* GUSF-1 (KF796625) showed the presence of 22 peaks which were labeled in the increasing order of their retention time (R_t) (**Fig. 4.6**). The mass spectra analysis and detailed identification is listed in **Table 4.2**.

The EI-MS spectrum of compound 1 eluted at R_t 0.847 was identical at m/z 185.06 showing mass of 162.07 and molecular formula $C_9H_{10}N_2O$. The compound eluted at R_t 1.02 had a m/z of 140.06 showing mass of 117.07 and molecular formula $C_5H_{11}NO_2$. The peak at R_t 6.097 showed a m/z of 307.1746, showing mass of 306.1 and molecular formula $C_5H_{11}NO_2$. The compound that was eluted at R_t 7.959 with m/z of 183.09 showing mass of 160.1and molecular formula of $C_5H_{11}NO_2$ .The compound eluted at R_t 8.944 showed m/z of 430.24 showing mass of 429.2 and molecular formula $C_{22}H_{31}N_5O_4$. The peak eluted at R_t 9.338 had a mass of m/z of 245.12, with mass of 244.1 and molecular formula $C_{10}H_{14}NO_6$. The peak eluted at R_t 9.837 had a mass of m/z of 379.18 with mass of 378.1 and molecular formula $C_{13}H_{26}N_6O_5S$. The compound that was eluted at Rt 10.809 showed m/z of 171.14 and mass of 170.1; R_t 11.313 with m/z of 219.05 and mass of 218.0; compounds at Rt 13.9 had m/z of 835.36 and 418.18 showed a mass of 834.3 and 417.1. There were 2 compounds eluted at R_t 15.4 showing m/z of 573.25 and 432.2 had mass of 572.2 and 431.1. At R_t 16.438, compound with m/z 343.11 and mass 342.1 with molecular formula of $C_{12}H_{22}O_{11}$. The compound that was eluted at R_t 17.013 showed m/z of 969.0, 977.7 and 955, the compound with m/z 977.7 showed a mass of 976.7. The compound with R_t 18.061 showed a m/z of 875.1. The compound at R_t 19.261 had a m/z of 773.6 and mass of 772.6.The two compounds eluted at R_t 20.069 had m/z of 432.23 and 460.26, mass of 431.2 and 459.2 and molecular formula of $C_{20}H_{29}N_7O_4$ and $C_{22}H_{33}N_7O_4$.The three compounds eluted at R_t 22.074 had m/z of 646.34, 669.42 and 697.45, showed mass of 623.3, 668.4 and 696.4 respectively. The two compounds that were eluted at R_t 25.5 min showed m/z of 921 and m/z of 899.6, mass of 920.1 and 898.6. The compound at R_t 30.05 had a m/z of 353.26, 381.29 and 393.29, mass of 330.2, 358.3 and 370.3 respectively, $C_{19}H_{38}O_4$, $C_{21}H_{42}O_4$ and $C_{22}H_{42}O_4$. The compound at R_t 32.05 had a m/z of 449.35 and mass of 426.36 with

molecular formula $C_{26}H_{50}O_4$. The compound at R_t 35.716, showed m/z of 685.43 and 736.54 and mass of 662.4452 and 735.5342.

Fig. 4.7 reveals the Diode Array Detector response of APM of *Haloferax alexandrinus* GUSF-1 (KF796625) which showed that the peak labelled as 1, 2, 3, 4, 5, 6, 11, 12, 16, 17, 19 and 22 at R_t 0.847, 1.02, 6.097, 7.959, 8.944, 9.338, 15.4, 16.43, 20.06, 22.068, 22.076 and 27.0 showed absorption signal at 320 nm.

Fig. 4.8 and **Fig. 4.9** is the Diode Array Detector response of APM of *Haloferax alexandrinus* GUSF-1 (KF796625) at 490 nm and 447 nm showed no absorption.

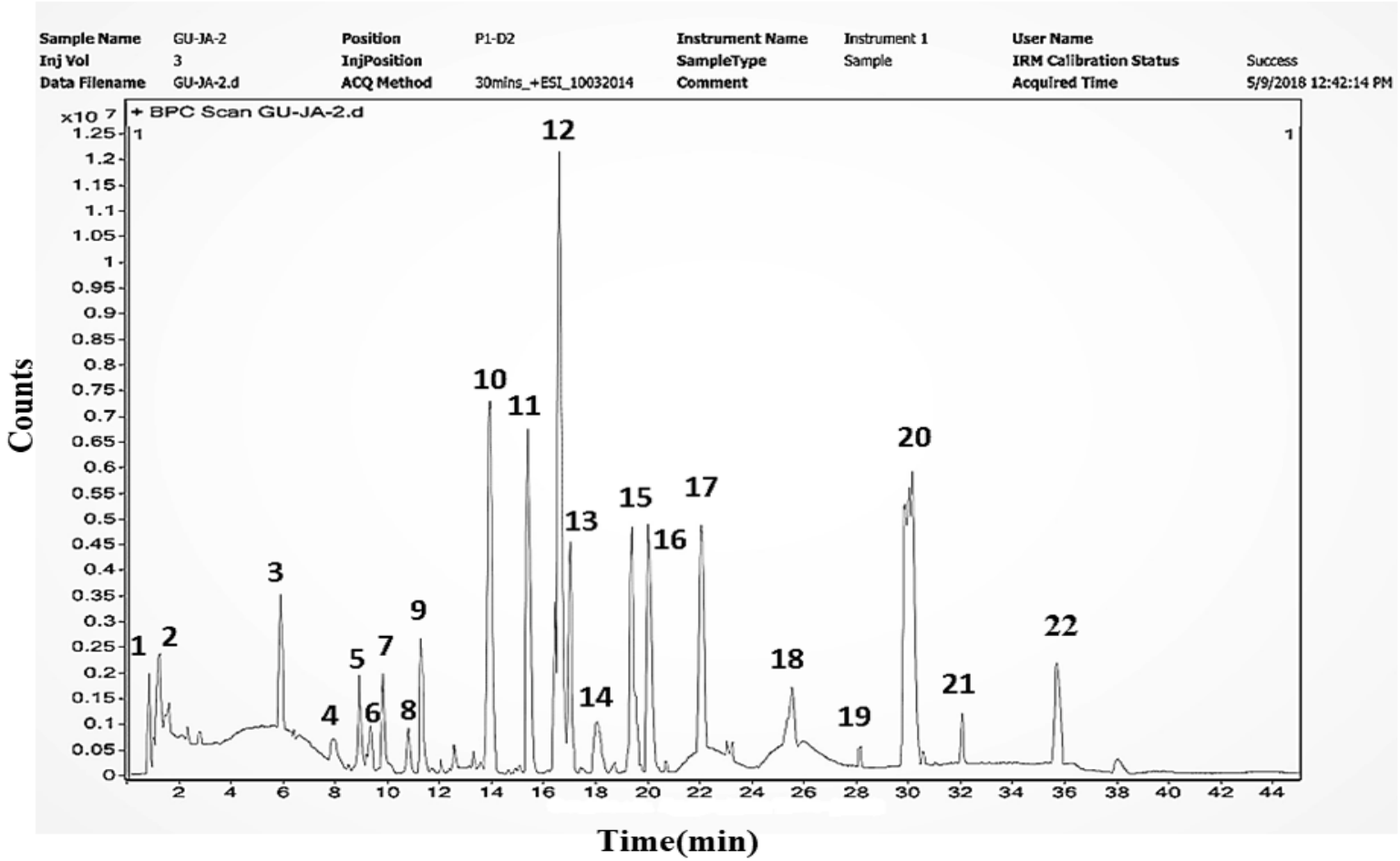

Fig. 4.6 HR – LCMS chromatogram of APM of *Haloferax alexandrinus* GUSF-1 (KF796625) chromatographed on a C-18 reverse phase Hypersil gold 3micron 100 x 2.1 mm column. Peaks are labelled based on increasing retention times (R_t) (decreasing polarity)

Table 4.2 Mass Spectra analysis of the Acetone Precipitated Material of *Haloferax alexandrinus* GUSF-1 (KF796625)

Peak No	R_t	**(m/z)**	z	**Ion**	Abundance (Conc)	**Mass**	Molecular formula
1	0.847	**185.06**	1	**(M+Na)+**	1.9×10^6	**162.07**	$C_9H_{10}N_2O$
2	1.02	**140.06**	1	**(M+Na)+**	6.5×10^5	**117.07**	$C_5H_{11}NO_2$
3	6.097	**307.17**	1	**(M+H)+**	3.3×10^5	**306.1**	-
4	7.959	**183.09**	1	**(M+Na)+**	7.1×10^5	**160.1**	$C_{10}H_{12}N_2$
5	8.944	**430.24**	1	**(M+H)+**	1.9×10^6	**429.2**	$C_{22}H_{31}N_5O_4$
6	9.338	**245.12**	1	**(M+H)+**	9.6×10^5	**244.1**	$C_{10}H_{14}NO_6$
7	9.837	**379.18**	1	**(M+H)+**	1.9×10^6	**378.1**	$C_{13}H_{26}N_6O_5S$
8	10.809	**171.14**	1	**(M+H)+**	9.2×10^5	**170.1**	-
9	11.313	**219.05**	1	**(M+ Na)+**	2.6×10^6	**218.0**	-
10	13.9	**835.36**	1	**(M+H)+**	5.7×10^6	**834.3**	-
		418.18	1	**(M+H)+**	7.2×10^6	**417.1**	-
11	15.4	**573.25**	1	**(M+Na)+**	3.1×10^5	**572.2**	-
		432.20			6.7×10^6	**431.1**	-
12	16.438	**343.11**	1	**(M+H)+**	7.2×10^5	**342.1**	$C_{12}H_{22}O_{11}$
		969.0	1	**(M+H)+**	0.25×10^4	**-**	-
13	17.013	**977.7**	1	**(M+H)+**	1.4×10^5	**976.7**	-
		955.7	1	**(M+H)+**	1.4×10^4	**-**	-
14	18.061	**875.1**	1	**(M+H)+**	0.4×10^5	**-**	-
15	19.261	**773.6**	1	**(M+H)+**	3.5×10^5	**772.6**	-

Peak No	R_t	**(m/z)**	z	**Ion**	Abundance (conc)	**mass**	Molecular formula
16	20.069	432.23	1	(M+H)+	1.2×10^6	431.2	$C_{20} H_{29} N_7 O_4$
		460.26			3.1×10^5	459.2	$C_{22} H_{33} N_7 O_4$
		646.34	1	**(M+Na)+**	1.5×10^6	**623.3**	-
17	22.074	**669.42**	1	**(M+H)+**	3.8×10^5	**668.4**	-
		697.45	1	**(M+H)+**	8.0×10^5	**696.4**	-
18	25.5	**921.1**	1	**(M+H)+**	0.3×10^5	**920.1**	-
		899.6	1	**(M+H)+**	1.7×10^5	**898.6**	-
19	27.0	**429.31**	1	**(M+H)+**	313638	**406.3**	-
		353.26	1	**(M+Na)+**	5.6×10^5	**330.2**	$C_{19}H_{38}O_4$
20	30.05	**381.29**	1	**(M+Na)+**	3.2×10^5	**358.3**	$C_{21}H_{42}O_4$
		393.29	1	**(M+Na)+**	4.4×10^5	**370.3**	$C_{22}H_{42}O_4$
21	32.05	**449.35**	1	**(M+ Na)+**	1.2×10^6	**426.3694**	$C_{26}H_{50}O_4$
22	35.716	**685.43**	1	**(M+ Na)+**	8.8×10^5	**662.4452**	-
		736.54	1	**(M+H)+**	2.2×10^6	**735.5342**	-

Fig. 4.7 Diode Array Detector response at 320 nm of APM of *Haloferax alexandrinus* GUSF-1 (KF796625) showed that the peaks 1, 2, 3, 4, 5, 6, 11, 12, 16, 17, 19 and 22 showed an absorption signal at 320 nm

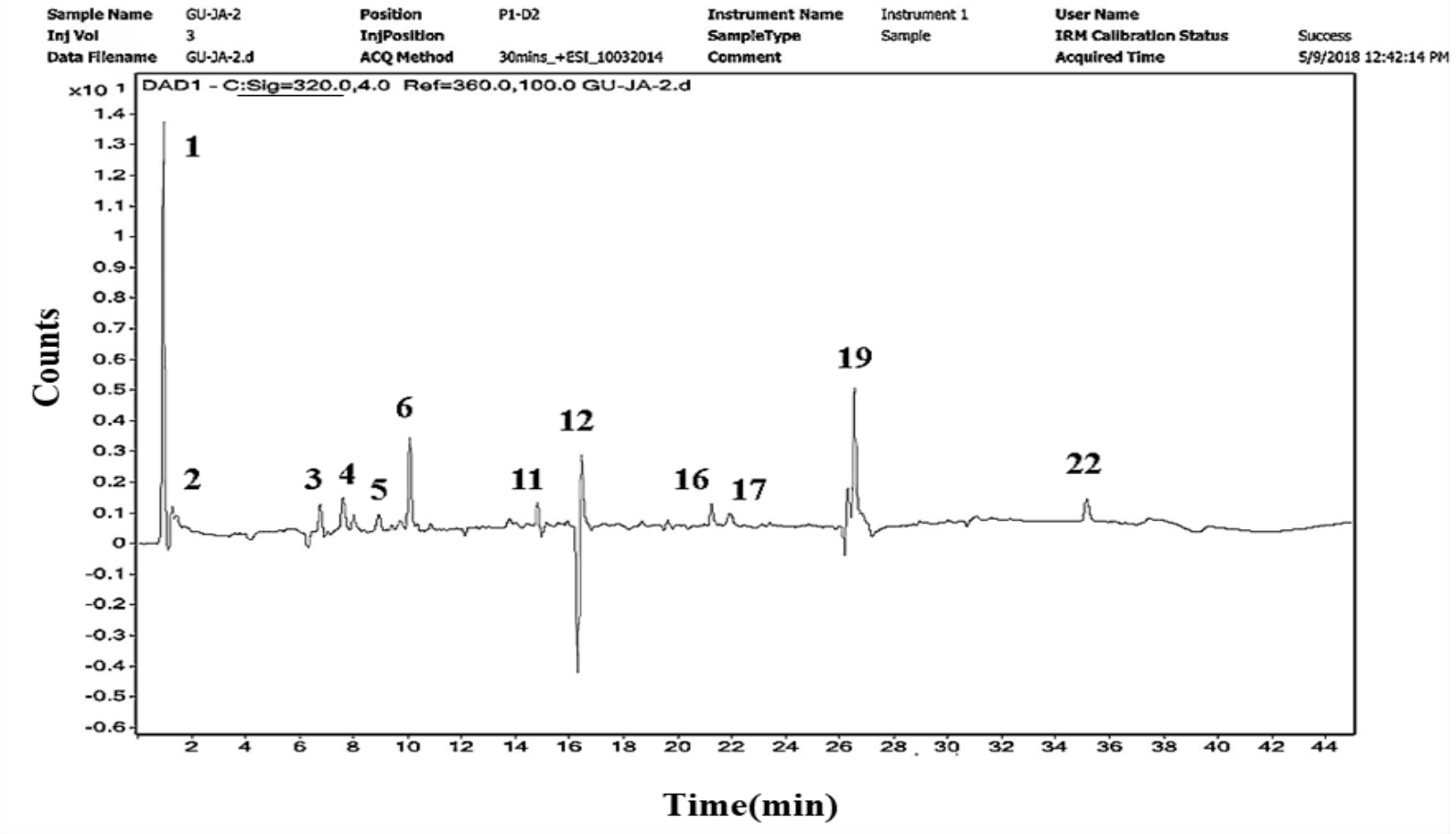

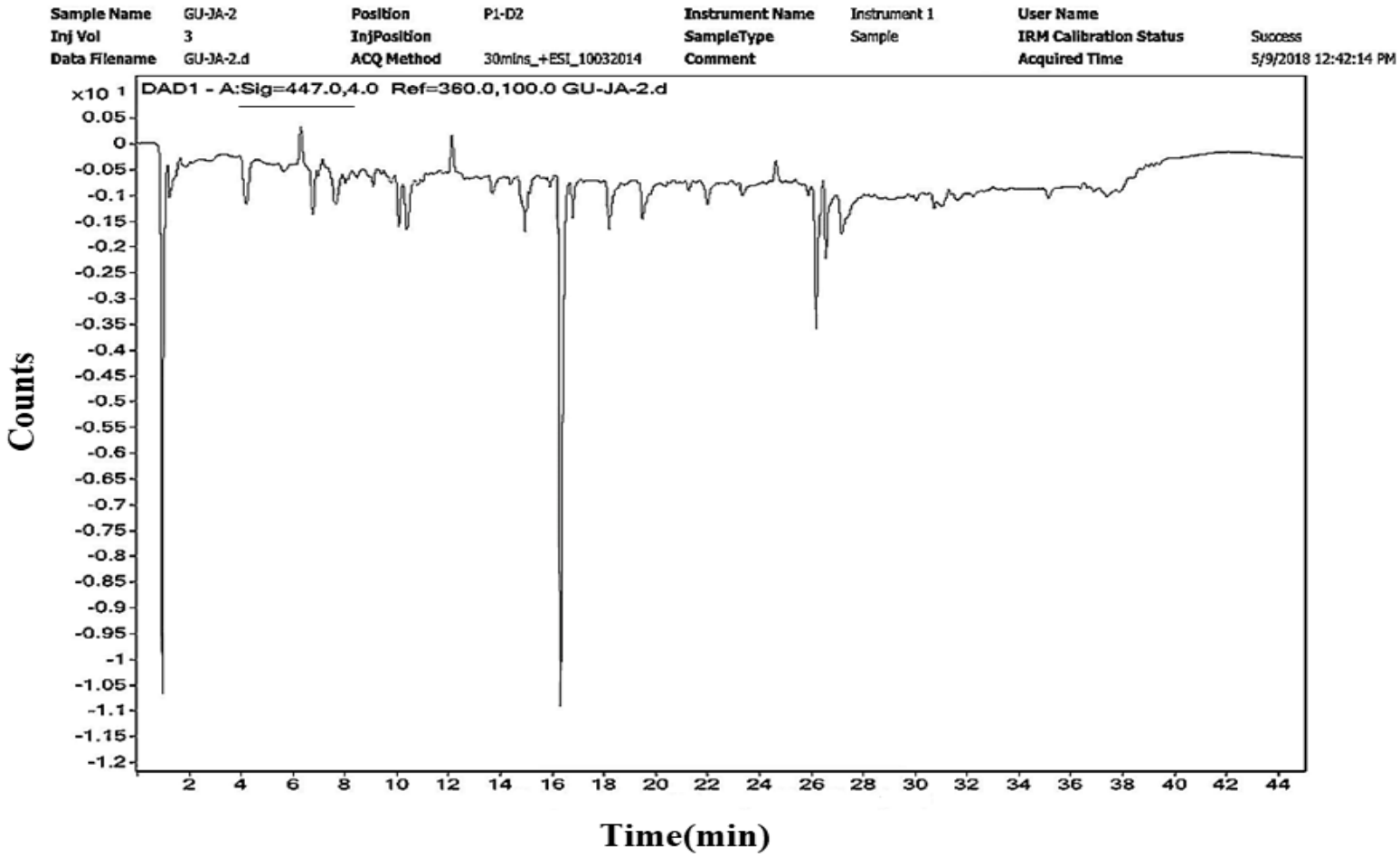

Fig. 4.8 Diode Array Detector response at 447 nm of APM of *Haloferax alexandrinus* GUSF-1 (KF796625) showed that the peaks 9 and 10, showed an absorption signal at 447 nm

Fig. 4.9 Diode Array Detector response at 490 nm of APM of *Haloferax alexandrinus* GUSF-1 (KF796625) showed that the peaks 9 and 10, showed absorption signal at 490 nm

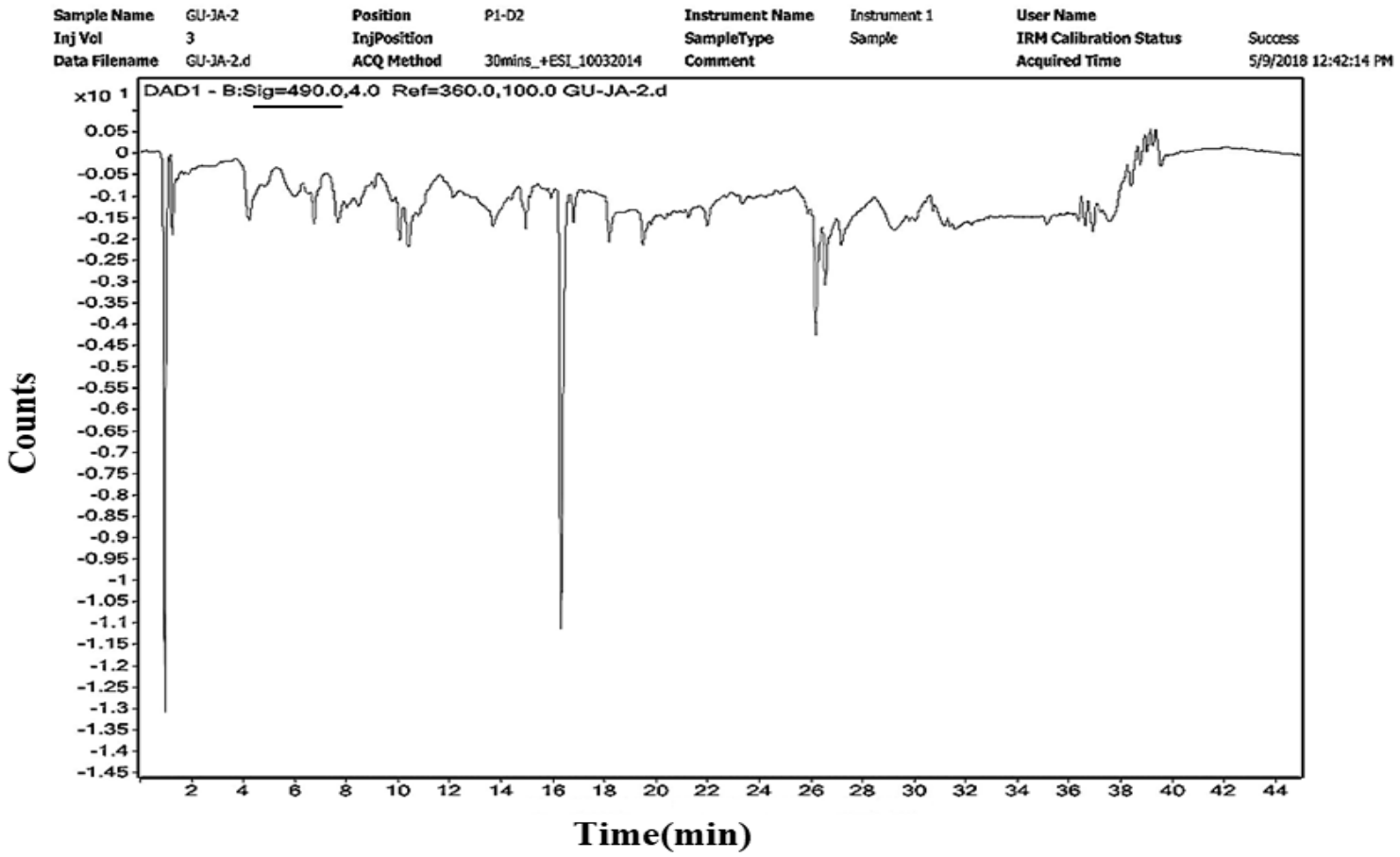

4.3 DISCUSSION

Cellular components that are largely in hydrophobically associated form may be extracted with relatively non-polar solvents such as ethyl ether, chloroform or benzene. However, membrane-associated polar lipids require polar solvents such as ethanol or methanol to disrupt the hydrogen bonding or electrostatic forces between the lipids and the protein and facilitate extraction. The additions of methanol to wet cells resulted in an orange red coloured extract. Addition of hexane to methanolic extract led to a phase separation of an upper hexane layer which was coloured and the lower off white methanol layer. The simplest and often the most efficient procedure for separating polar lipids (phosphatides and glycolipids) from neutral lipids (including pigments) is the procedure of acetone precipitation (Kates and Kushwaha, 1995). The method depends on the general insolubility in cold acetone of most glycolipids and phosphatides and the fact that glycerides and other neutral lipids are soluble in cold acetone. In general, the acetone-insoluble material is expected to contain 95% or more of the polar lipids and only traces of neutral lipids material largely pigments, whereas the acetone-soluble fraction is expected to contain all of the neutral lipids and only traces of phosphatides. The upper hexane layer was separated and subjected to cold acetone precipitation to separate polar lipids from the hexane layer. The red coloured layer containing red neutral lipid fraction now referred to as hexane extract (HE) and tan coloured acetone precipitated material (APM) containing precipitated polar lipids were used for further analysis.

The **chemical profiling of hexane extract** showed the **presence of 12 peaks** and a **total of 22 compounds** were eluted in the increasing order of their retention time. The different m/z and mass obtained were identified using the software Agilent Mass Hunter; the Japanese carotenoid database and PubChem. The compounds that were identified were as follows; the peak at R_t 1.121 identified as **11-amino-undecanoic acid**; the peak at R_t 4.528 was unidentified. The peak at R_t 6.823 was identified as **canthaxanthin**. The peak at R_t 9.801 was unidentified. The peak at R_t 20.523 was identified as **tetrahydrosqualene**. The peak at R_t was unidentified. There were four compounds that were eluted at R_t 25.471 was **3-hydroxyechinone**, **dihydroxylycopene, phytoene and asthaxanthin**. The peak at R_t 27.226 was unidentified. The compounds eluted at R_t 29.943 were identified as

bisanhydrobacterioruberin (BABR), monoanhydrobacterioruberin (MABR) and bacterioruberin (BR). The peak at R_t 30.209 was identified as **lycopene**. The peak eluted at R_t 31.68 was identified as **haloxanthin**. The peak eluted at R_t 35.658 was identified as **phytofluene**. The diode array detector revealed that peaks at R_t 1.121 and 27.226 absorbed at 320 nm, whereas peaks at R_t 29.943 and 31.68 absorbed at 320, 447 and 490 nm which is the visible range and further confirms that the compounds eluted at this R_t are carotenoids. The information provided by DAD analyses further aids in identification. Many recent works dealing with carotenoid identification, couple UV–Vis, MS detection and DAD analysis techniques.

The neutral lipids of haloarchaea account for about 10% by weight of the total lipids and consist virtually exclusively of isoprenoid derived compounds (Tornabene *et al*., 1969; Kushwaha *et al*., 1972). The neutral lipids can be grouped into four classes according to the chain length as follows i) C_{20} isoprenoids (geranylgeraniol) ii) C_{30} isoprenoids (squalenes) iii) C_{40} isoprenoids (carotenes) and iv) C_{50} isoprenoids (bacterioruberins). Geranylgeraniol is the main C_{20} isoprenoid and accounts for 11% of the total neutral lipids. The glycerol diether moiety is present in free form as part of the neutral lipids and accounts for about' 8%. It is similar to 2, 3-di-o-phytanyl-sn-glycerol present in polar lipids (Mullakhanbhai and Francis, 1972; Kates, 1978). The C_{30} isoprenoids squalenes form the major component comprising about 36% of the neutral lipids. They consist of squalene, dihydrosqualene, tetrahydrosqualene and dihydrosqualene. They occur as all-trans-squalenes (Tornabene *et al*., 1969). The C_{40} isoprenoids exist as lycoserene, cis and trans - phytoene, cis and trans - phytofluene, lycopene, alpha and ß-carotenes in most of the extreme halophiles. The C_{50} isoprenoids, the main red pigment, isolated first from *Halobacterium cutirubrum*, was named bacterioruberin (Petter, 1931). It is a tetrahydroxy C_{50} - noncyclic carotenoid (Kelly and Liaaen-Jensen, 1967; Kelly *et al*., 1970; Mullakhanbhai and Francis, 1972). All pigmented extreme halophiles contain bacterioruberin, monoanhydrobacterioruberin and bisanhydrobacterioruberin in decreasing concentrations (Kushwaha *et al*., 1974). Similarly pigments extracted from *Halorubrum* sp. an isolate from the solar salterns of Mumbai, was found to have antioxidant activity, assessed by the $DPPH^{\bullet}$ assay, equivalent to astaxanthin and lutein, and spectrophotometric analysis of the pigment extract revealed it to be of the bacterioruberin type of carotenoid (Pathak and Sardar, 2012). In a study aimed to

investigate the biological properties of carotenoids extracted from halophilic Archaea, *Halobacterium halobium* isolated from a Tunisian solar saltern, carotenoids showed free significant antiproliferative activity against HepG2 human cancer cell lines (Abbes *et al*., 2013). LC-MS analytical results revealed that carotenoids produced in *Halorubrum* sp., TBZ126, an extremely halophilic archaeon was isolated from Urmia Lake in Iran are bacterioruberin, lycopene and β-carotene with bacterioruberin was found to be the predominant produced carotenoid (Naziri *et al*., 2014). The carotenoids produced by extremely halophilic archaeon *Haloarcula japonica* were extracted and identified by their chemical, chromatographic and spectroscopic characteristics (UV-Vis and mass spectrometry). The composition of carotenoids varied, it was maximum for bacterioruberin, followed by monoanhydrobacterioruberin, isopentenyldehydrorhodopin, and trace amounts of lycopene and phytoene. The invitro scavenging capacity of a carotenoid, bacterioruberin, extracted from *Haloarcula japonica* cells against 1, 1-diphenyl-2-picrylhydrazyl ($DPPH^{\bullet}$) radicals was evaluated. The antioxidant capacity of bacterioruberin was much higher than that of β-carotene (Yatsunami *et al*., 2014). Carotenoids from *Htg. turkmenica* (DSM-5511) were extracted with methanol, separated by RP-HPLC, and identified by mass spectrometry and UV/ Vis spectra were reported. C_{50} carotenoids for bacterioruberin, monoanhydrobacterioruberin and bisanhydrobacterioruberin were the main pigments. C_{30} carotenoids like squlaene and dihydrosqualene were present in the cells. C_{40} carotenoids like lycopene, phytoene and lycopersene were among the minor carotenoids further identified (Squillaci *et al*., 2017). Carotenoid produced by halophilic archaeal strains *Halogeometricum rufum, Halogeometricum limi, Haladaptatus litoreus, Haloplanus vescus, Halopelagius inordinatus, Halogranum rubrum, and Haloferax volcanii* have been reported for their antioxidant activity assessed by the $DPPH^{\bullet}$ assay. The antioxidant capacities of the carotenoids from these strains were significantly higher than β-carotene as determined by $DPPH^{\bullet}$ radical scavenging assay (Hou and Cui, 2018).

The carotenoid **phytoene** has been identified **in very low concentrations in our analysis** as compared to the abundance of other compounds, a similar report of very low concentrations of phytoene in other halophilic Archaea has been reported (Rodrigo-Baños *et al*., 2015). Some haloarchaea like *Haloferax alexandrinus* are able to produce canthaxanthin and astaxanthin (Asker *et al*., 2002). The neutral lipids

particularly squalenes appear to aid in the stabilization of the membrane structure by facilitating interaction of divalent ions such as Mg^{2+} or Ca^{2+} with the acidic groups in the polar lipids. Bacterioruberin also plays an equal important role in maintaining membrane fluidity, including its function as a water barrier and for the permeability of oxygen and other molecules, thus enhancing bacterial survival in hypersaline and low-temperature environments (Strand *et al*., 1997).

The **chemical profiling of APM** showed the **presence of 22 peaks** and a **total of 46 compounds** eluted with m/z varying from 117.07 to 977.7. The compound eluted at R_t 1.02 which was identified as **glycine betaine**, at R_t 16.438, the compound with m/z 343.11 and mass 342.1 was identified as **trehalose**. To survive in high salinity environments, members of halophilic archaea maintain an intracellular osmotic pressure that is equal to or higher than that of the surrounding environment (Oren, 2013). In general, maintenance of high intracellular osmotic pressure by extreme halophilic eubacteria and Haloarchaea is achieved either by the uptake and accumulation of high concentrations of inorganic ions such as K^+ (salting-in strategy) or by synthesis and/ or uptake of highly soluble organic solutes that do not interfere with intracellular enzymatic activities and cellular processes (compatible solute strategy) (Grant, 2004). However, the permanently high levels of intracellular K^+ trigger multiple structural and metabolic adaptations that limit the metabolic flexibility and ecological range of microorganisms utilizing this strategy for osmoadaptation (Oren, 2013). Besides some members of halophilic archaea such as those belonging to genus *Haloferax* have been reported to be constituent of the microbial population in low salinity environments including sea water (Ventosa *et al*., 1998) and low salinity salterns (Mani *et al*., 2012). Therefore, in such habitats, members of halophilic archaea must cope with extended periods of low salinities and/ or constant fluctuations in salinity levels, conditions that are not conducive to microorganisms solely dependent on a salting-in strategy for osmoadaptation. Hence the production and uptake of compatible solutes represent a common mechanism of osmoadaptation in haloarchaea of which trehalose or 2-sulfotrehalose biosynthesis and glycine-betaine uptake are widely spread reported mechanisms for osmoadaptation in the haloarchaea (Youssef *et al*., 2014). Glycine betaine is known as a universal solute has also been implicated in reducing lipid peroxidation in plants reviewed in Cushman, 2001. The synthesis of glycine betaine is common in

phototrophic bacteria and in archaea, which exhibit moderate to high salt tolerance (Empadinhas and da Coata, 2008).

The peak eluted at R_t 9.338 was identified as **mycosporine glycine**. Mycosporines and mycosporines like amino acids (MAA) secondary metabolites of marine origin. These metabolites are composed of cyclohexenone and cycloheximine ring structures conjugated to an amino acid subunit and, in some instances, linked to various carbohydrates. Due to the conjugated double bonds in their structure they absorb radiation with a maximum between 310 and 360 nm and thus can act as photoprotective UV-B and UV-B filters in microbes exposed to sunlight (Karsten *et al*., 1998). Some MAAs may protect the cell not only against UV radiation by absorbing the high-energy photons and dissipating the energy as heat but also by scavenging reactive oxygen species such as singlet oxygen, superoxide anions, hydroperoxyl radicals and hydroxyl radicals. The antioxidant activity of mycosporine-glycine has been demonstrated in vitro by measuring the chemically initiated free radical hydroperoxidation of phosphatidylcholine; mycosporine-glycine is thus a biological antioxidant in coral tissue and zooxanthellae (Dunlap and Yamamoto, 1995; Yakovleva *et al*., 2004).

The compound with m/z of 977.7 showed a mass of 976.7 and identified as **DGD-1**. The compound at R_t 19.261 had an m/z of 773.6 and mass of 772.6 identified as **PG C_{20}-C_{20}.** The compound at R_t 20.069 were identified as **tripeptides**. The two compounds that were eluted at 25.5 min showed m/z of 921 and m/z of 899.6, mass of 920.1 and 898.6, was identified as **PGP-Me C_{20}-C_{20} + Na** and **PGP-Me C_{20}-C_{20}** respectively. The compound at R_t 30.05 with m/z of 353.26, 381.29 and 393.29, mass of 330.2, 358.3 and 370.3 respectively was identified as 1-hexadecanoyl-sn-glycerol, 1-octadecanoyl-rac-glycerol and docosanedioic acid. The compound at R_t 32.05 had a m/z of 449.35 was identified as hexacosanedioic acid $C_{26}H_{50}O_4$. The Diode Array Detector response of the APM of *Haloferax alexandrinus* GUSF-1 (KF796625) showed that the peak labelled as 1, 2, 3, 4, 5, 6, 11, 12, 16, 17, 19 and 22 at R_t 0.847, 1.02, 6.097, 7.959, 8.944, 9.338, 15.4, 16.43, 20.06, 22.068, 22.076, 27.0 showed absorption signal at 320 nm.There was no DAD response at 490 nm and 447 nm indicating the absence of any compounds that absorbs light maximally in the visible light such as carotenoids.

The diether core lipid that forms the basis for most polar lipid structures present in the family *Halobacteriaceae* is 2,3-di-O-phytanyl-snglycerol (C_{20}-C_{20}), also called as archaeol (Kates, 1978). In some haloalkaliphile and *Halococcus* species, C_{20}-C_{25} and C_{25}- C_{25} diether variants of the diphytanylglycerol diether lipid core were also identified (Kates, 1993).The diphytanylglycerol diether lipid core is considered as one of the most useful chemotaxonomic markers of the Archaea domain. A great variety of polar lipids is encountered in the different representatives of the *Halobacteriaceae*, including phospholipids, sulfolipids and glycolipids. The phospholipid structures have been shown to be archaeol analogs of: Phosphatidylethanolamine (PE), phosphatidylglycerol (PG), methyl ester of phosphatidylglycerophosphate (PGP-Me), phosphatidylglycerosulfate (PGS) and phosphatidic acid (PA). PGP-Me is the major phospholipid in all extreme halophiles and extreme haloalkaliphiles, having been identified by FAB-MS and TLC in several genera of extreme halophiles including *Halobacterium*, *Haloarcula*, *Haloferax*, *Halococcus*, *Natronobacterium* and *Natronococcus* (Kates, 1993). The structures of the glycolipids appear to be derived from a basic diglycosyl archaeol, mannosylglucosyl-diphytanylglycerol (DGD), by substitution of sugar or sulfate groups at the 3 or 6 position of the mannose residue. The crude methanolic extract which was positive for presence of glycosides and saponins confirms the presence of sugar moieties in the polar lipids of *Haloferax alexandrinus* GUSF-1 (KF796625).The sulfated diglycosyl archaeol S-DGD-1 (1-*O* [alpha-D-mannose- (6´-SO_3H)-(1´ $\rightarrow$ 2´) – alpha -D-glucose]-2,3-di-*O*-phytanyl-sn-glycerol) is the major glycolipid in the genus *Haloferax* (Kushwaha *et al*., 1982). As ether lipids cannot be degraded easily, they are thermally and mechanically resistant, and highly salt tolerant, they are considered an ideal biomaterial to prepare lipid matrix for membrane protein reconstitution. In particular, membranes of halophiles are stable over a wide range of salt concentrations and at elevated pH values and are well adapted to the halophilic conditions (Corcelli, 2006).

Chemical profiling is a frontline technique employing upfront tools and collated databases which find use in identification and characterization of bioactive molecules. With the help of the HR-LCMS and different databases, we were able to identify most of the separated biomolecules from *Haloferax alexandrinus* GUSF-1 (KF796625) which would have been otherwise impossible using the conventional methods routinely employed.

Chapter V

Biosynthesis of Nanoparticles by Extremely Halophilic *Chromohalobacter salexegines* GUVFFM-3 (JF330126) and Haloarchaeon *Haloferax alexandrinus* GUSF-1 (KF796625)

The haloarchaeon *Haloferax alexandrinus* GUSF-1 (KF796625) is known to biosynthesize silver nanoparticles with broad spectrum antimicrobial activity against human and lower mammalian pathogens (Patil *et al*., 2014). Nanoparticles have great use in biotechnological systems due to their novel physicochemical, magnetic and optoelectronic properties that are governed by their size, shape and size distribution. Owing to relatively very sparse reports on the use of *Chromohalobacter* and *Haloferax* for nanoparticle synthesis, this chapter accounts the further use of *Haloferax alexandrinus* GUSF-1 (KF796625) for the biogenic production of selenium, tellurium and manganese oxide nanoparticles and compares the nanomaterial with that biosynthesized using *Chromohalobacter salexegines* GUVFFM-3 (JF330126).

5.1 METHODOLOGY

5.1.1 SCREENING OF EXTREME HALOPHILES FOR THE ABILITY TO GROW IN THE PRESENCE OF SILVER, SELENIUM AND TELLURIUM

The ability of seven cultures to biosynthesise nanomaterial was studied in terms of growth and colour change in the presence of final concentration of 0.05 mM Ag^{1+} **(**$AgNO_3$**)** or 0.2 mM SeO_3^{2-} **(**sodium selenite) or 0.1mM TeO_3^{2-} (potassium tellurite). A loopful of each of the haloarchaeal cultures; *Haloferax* sp. $GUBF_3$ (ATCC BAA 646), *Halobacterium* sp. $GUBF_{11}$ (ATCC BAA 654), *Haloferax alexandrinus* GUSF-1 (KF796625), *Haloferax* sp. GUIF2 (MH169338), *Haloferax* sp. GUIF3, *Haloferax* sp. GUIF4 (MG199078) and *Chromohalobacter salexegines* GUVFFM-3 (JF330126) was streaked onto sterile NTYE agar plates incorporated with the respective salts and incubated at 37ºC.

5.1.2 TOLERANCE STUDIES OF GUVFFM-3 AND GUSF-1 TO Ag^{1+}, SELENITE SeO_3^{2-} AND TELLURITE TeO_3^{2-}

The response of these cultures to varying concentrations of the salt was studied by inoculating 5% v/v of GUVFFM-3 and GUSF-1 at A_{480} = 1/ A_{600} = 1 into tubes containing 15% TYE or NTYE having 0.2 to 2mM of Ag^{1+} or 0.05 to 2mM of TeO_3^{2-}

or 1 to 150 mM of SeO_3^{2-}increasing by 0.2/ 10 units respectively. The tubes were incubated at 37ºC and growth and colour change monitored visually.

5.1.3 USE OF CELL LYSATE FOR BIOGENIC SYNTHESIS OF SILVER NANOPARTICLES (AgNPs)

Five cultures $GUBF_{11}$, GUIF2, GUIF3, GUIF4 and GUVFFM-3 were grown individually in NTYE for six days to $A_{/600}$ =2/ A_{480}= 2. Cells of each haloarchaeon were individually harvested by centrifuging at 10,000 rpm at 4^{o}C and cell lysate was prepared as mentioned in **5.1.7.** 1 ml of cell lysate of each of the cultures was incubated with 1 ml of 0.01% aqueous silver nitrate separately in dark and light conditions. A control consisting only of silver nitrate solution was also maintained individually. The reaction mixture was scanned from 300 to 600 nm using an UV-Visible dual beam spectrophotometer (Shimadzu UV- 1800, Japan) after 5 min.

5.1.4 BIOSYNTHESIS OF Se^0 NANOPARTICLES (SeNPs) AND Te^0 NANOPARTICLES (TeNPs) DURING GROWTH OF GUVFFM-3 AND GUSF-1

5% v/v inoculum (A_{480}/ A_{600} = 1) of GUVFFM-3 or GUSF-1 pre grown in 15% TYE/ NTYE at 37ºC added respectively to separate flasks containing 100 ml of 15% TYE or NTYE containing 5 mM SeO_3^{2-} or 0.1 mM TeO_3^{2-}, respectively. The flasks were incubated at 37ºC, at 150 rpm for 7 d. Positive control of the medium with culture and negative control of the medium with only the salt solution was also maintained. The typical biosynthesis of SeNPs was followed by monitoring the colour change in the medium to brick-red. Similarly for TeNPs, the synthesis was monitored by formation of black colouration in the medium. Cells growing in the presence of selenite was aseptically withdrawn at regular intervals and analyzed for growth in terms of colony forming units (CFU). Formation of SeNPs and residual selenite SeO_3^{2-} was also quantified.

5.1.5 ESTIMATION OF RESIDUAL SELENITE USING THE ASCORBIC ACID METHOD AND SODIUM SULPHIDE SOLUBILISATION

5.1.5.1 Ascorbic acid reduction method

Residual selenite was first reduced to Se^0 using the procedure of Malhotra *et al*. (2014). 5 mM SeO_3^{2-} and 50 mM ascorbic acid was prepared in sterile distilled water. 1 ml of 50 mM ascorbic acid was added drop wise to the sodium selenite solution under shaker conditions (50 rpm) at room temperature (28 ± 2ºC). The mixture was allowed to react with each other for 30 min under shaker conditions, till the colour changed was observed from colourless to light orange. With time of incubation the reaction mixture started to agglomerate and hence interfered with the spectroscopic estimation of SeNPs at 390 nm.

5.1.5.2 Sodium sulphide solubilisation of SeNPs

SeNPs that was formed from the chemical reduction by ascorbic acid was spectroscopically estimated using the procedure of sodium sulphide solubilisation as described by Biswas *et al*. (2014). SeNPs formed was dissolved in 1 ml of 1M Na_2S and was centrifuged to remove bacterial cells. The absorption of the red-brown solution formed was monitored at 475 nm against 1 M Na_2S as blank.

5.1.5.3 Intracellular selenite reduction in GUVFFM-3 and GUSF-1

100 µl of cells of GUVFFM-3 and GUSF-1 were spread plated on 15% TYE or NTYE plates and allowed to grow till well isolated colonies were seen. After that 5 mM SeO_3^{2-} was gently sprayed on the plates around the colonies and incubated further.

5.1.5.4 Pigmentation of GUSF-1 during growth in 5 mM SeO_3^{2-}

Cells grown in the presence of 5 mM SeO_3^{2-} were harvested by centrifuging at the end of 6 days of incubation, at 10000 rpm, 4ºC for 10 min and washed with 15% NaCl. The pigment was extracted with acetone. 1 ml of acetone was added to the cell pellet and kept standing for 5 min; the supernatant was recovered by centrifuging at 10000 rpm, for 10 min with minimum exposure to light. The acetone extract was analyzed by scanning the extract in the wavelength region of 190-800 nm using the UV-Vis

spectrophotometer (Shimadzu-UV 2450).

5.1.6 BIOSYNTHESIS OF SeNPs AND TeNPs BY WHOLE CELLS OF GUVFFM-3 AND GUSF-1

5% v/v (A_{480}/ A_{600} =1) GUVFFM-3 or GUSF-1 pre grown in 15% TYE/ NTYE at 37ºC inoculum was added respectively to separate flasks containing 100 ml of 15% TYE or NTYE allowed to grow at 150 rpm till the absorbance of culture broth reached A_{480} = 2 for GUVFFM-3 and A_{600} = 2 for GUSF-1. The cells were harvested by centrifuging at 10,000 rpm at 4ºC for 10 min. Cell pellet (50 mg) of GUVFFM-3 and GUSF-1 were washed separately three times with distilled water/ 15% NaCl and suspended in fresh distilled water / 15% NaCl. 5 mM SeO_3^{2-} or 0.1 mM TeO_3^{2-} was added separately to the cell pellets and the reaction mixture was incubated at ambient room temperature (28 ± 2ºC). Control of cells with distilled water/ 15% NaCl and salt solutions alone were maintained. All the test flask and controls were periodically monitored for colour change.

5.1.7 BIOSYNTHESIS OF SeNPs AND TeNPs BY CELL LYSATE OF GUVFFM-3 AND GUSF-1

Cell lysate of GUVFFM-3 and GUSF-1 was prepared from fully grown cells. The cell pellets were individually washed three times with distilled water/ 15% NaCl. Wet weight of 100 mg of GUSF-1 was suspended in 5 ml of distilled water and shaken vigorously for 30 min. The pellet of GUVFFM-3 was sonicated (8 pulses of 15 sec duration, with 15 sec cooling time using the Labsonic M,B.Braun biotech International, Germany) for 5 min to ensure lysis of cells. Cell debris from each of the mixtures was individually separated by centrifuging at 10,000 rpm at 4^{o}C for 10 min. One ml of cell lysate was added to 1 ml of 5 mM SeO_3^{2-} or 0.1 mM TeO_3^{2-} and the reaction mixture was incubated at ambient room temperature. All the test flask tubes and controls were periodically monitored for colour change. Control of cell lysate with distilled water/ 15% NaCl and salt solutions alone were also maintained.

5.1.8 LOCALISATION OF SELENITE REDUCING ACTIVITY AND POSSIBLE MECHANISM OF SELENITE REDUCTION TO SeNPs

To deduce the cell component and understand where selenite reduction occurs, intracellular fractions (soluble proteins and membrane fractions), extracellular polymeric substance (EPS) and spent medium of GUVFFM-3 and GUSF-1 were tested for their involvement in reduction of selenite using the selenite reducing enzyme assay described in **5.1.8.4**.

5.1.8.1 Extraction of intracellular fractions

Cell lysate of GUVFFM-3 and GUSF-1 was prepared as detailed in **5.1.7**. The cell lysate was centrifuged at 8,000 rpm for 40 min to separate the soluble and membrane fractions. The membrane fraction was dispersed in 15% sterile NaCl. Total protein content of soluble and membrane fraction was estimated by Folin Lowry method (*Appendix I*).

5.1.8.2 Extraction of EPS

For extraction of EPS, the protocol of Del Gallo and Haegi, (1990) was used with some modifications. Five-day old cultures of GUVFFM-3 and GUSF-1 were centrifuged separately at centrifuged at 8000 rpm for 40 min at 4°C. The supernatants were passed through a 0.2 μm filter and filtrates were precipitated overnight with the equal volume of cold ethanol at -20°C. Pellets containing EPS of both cultures were centrifuged at 10000 for 30 min at 4°C and dispersed in distilled water for EPS and in 15% NaCl for GUSF-1.

5.1.8.3 Cell free culture supernatant (spent medium)

Spent medium obtained on centrifuging culture broth as mentioned above were filtered through 0.2 μm nitrocellulose paper and tested for selenite reducing activity using the selenite reducing enzyme assay **(5.8.1.4)**.

5.1.8.4 Selenite reducing enzyme assay

The assay was performed according to a method by Lampis *et al*. (2014) in a 96 well micro titre plate. Each well of a 96-well plate was filled with the following mixture: 100 µl of either soluble protein/ membrane fraction/ EPS. 10 µl of 5 mM SeO_3^{2-} and 100 µl of McIlvaine buffer pH values (6-7) (***Appendix I***). Distilled water was added to a final volume of 200 µl in each well. Wells with no selenite, no NADH and without soluble protein/ membrane fraction/ EPS or supernatant were maintained as negative controls. Plate was incubated at room temperature and monitored for formation of red colour after 24 h.

5.1.8.5 Involvement of enzymes in selenite reduction

The selenite reducing enzyme assay to check involvement of enzymes in reduction of selenite to SeNPs was performed using specific enzyme inhibitors. Different concentrations of enzyme inhibitors; sodium arsenite (0.01 mM, 0.05 mM and 0.1 mM) for glutathionine reductase and sodium azide (5 mM and 10 mM) for nitrate reductase were added to the wells. Distilled water was added to a final volume of 200 µl in each well. One positive control containing either soluble protein or membrane fraction and no inhibitor was maintained. The selenite reducing assay was carried out as detailed in **5.1.8.4.** Plates were incubated at room temperature for 24-48 h to check for colour change.

5.1.9 FTIR ANALYSIS

Growing cells and cell lysate of GUVFFM-3 and GUSF-1 used for biosynthesis of nanomaterial was dried at 80ºC and ground in an agate mortar and pestle separately. IR analysis of dried sample was obtained with a Fourier Transform Infrared Spectrometer (FT- IR) (IRPrestige-21 Shimadzu) by mixing the sample with KBr powder in 1:10 ratio (w/w). The KBr pellet was analyzed in the range of 4000–400 cm^{-1} at a resolution of 4 cm^{-1}. The FT-IR spectrum was analyzed for functional groups.

5.1.10 CHARACTERIZATION OF Se AND Te NANOPARTICLES

5.1.10.1 Preparation of samples for characterization and release of nanomaterial from cells

The cell pellet containing selenium and tellurium nanomaterial was first washed by incubating in sterile ultra pure water for the product of GUVFFM-3 and sterile 15% NaCl for the product of GUSF-1. The flask was then kept on the orbital shaker at 150 rpm overnight for washing. The procedure was repeated for another 3 cycles.To release the nanomaterial from the washed cell pellet of GUVFFM-3, the pellet was sonicated with ultrapure water, the nanomaterial was pelleted out by centrifuging at 10000 rpm for 40 min and then dried in the oven at 80ºC with constant stirring. For GUSF-1, the cells were lysed in sterile distilled water. The nanomaterial obtained after centrifuging for 40 min at 10,000 rpm was dried in the oven at 80ºC with constant stirring. The dried sample was scrapped and pulverized using an agate mortar and pestle and stored in a clean vial at room temperature until used for characterization and further studies.

5.1.10.2 UV-Visible spectrophotometric analysis

The powdered nanomaterial (1mg) was suspended in methanol and sonicated using a sonicator (model Labsonic M, B. Braun Biotech International, Germany) for 2 min. The optical characterization of the obtained nanomaterial was measured using UV-Visible dual beam spectrophotometer (Shimadzu UV-1800, Japan) using methanol as reference solution.

5.1.10.3 Raman spectroscopy

The confocal Raman spectrum was recorded with STR 500 Confocal Micro Raman Spectrometer (Airix Corp. Japan 20X) at Malaviya National Institute of Technology, Jaipur. A laser power of 2.5 mW was used for excitation in the range of 3000 and 100 cm^{-1} and spectral resolution of 4 cm^{-1}.

5.1.10.4 X-ray Diffraction analysis

The thin film of dried nanoparticles was scanned from 30 to 80ºC by Rigaku Miniflex X-ray diffractometer operated at a voltage of 40 kV and current 20 mA with Cu Ka radiation of 1.541 ºA. The data obtained from XRD machine was plotted using Origin 8 software and FWHM value was obtained. The crystallite size of the nanoparticles was calculated using Scherrer's equation $D = K \lambda / \beta Cos \theta$ where D is the grain size, K is a constant taken to be 0.94, λ is the wavelength of the x-ray radiation, β is the full width at half maximum and θ is the angle of diffraction.

5.1.10.5 Scanning Electron Microscopy (SEM) and Energy dispersive X-ray Spectroscopy (EDX)

The sample powders were deposited on carbon and coated with gold using a high vacuum evaporator tapes before mounting on a sample holder. It was then analyzed by SEM EDX (JEOL JSM-5800LV). The elemental composition of the nanomaterial was determined by energy disruptive analysis of X-ray (EDX).

5.1.10.6 Transmission Electron Microscopy and Selected Area Electron Diffraction

Samples for transmission electron microscope (TEM) analysis were prepared by drop-coating of colloidal solution of selenium, tellurium and manganese oxide nanoparticles on carbon-coated copper TEM grids. The TEM images were obtained using Philips (Model-CM200) TEM with resolution of 2.4 °A, operated at an accelerating voltage of 200 keV. Selected area electron diffraction (SAED) was also carried out for the above prepared TEM samples.

5.1.11 USE OF SeNPs BIOSYNTHESIZED BY GUSF-1 IN MODULATING SIZE AND SHAPE OF CALCIUM OXALATE CRYSTALS

Supersaturated CaC_2O_4 was prepared from stock solutions of three salts: sodium chloride (100 mM), calcium chloride (100 mM) and sodium oxalate (100 mM). All stock solutions were filtered through a 0.22 µm nitrocellulose filter before use. Thoroughly cleaned glass coverslips were rinsed with double distilled water and kept

in three 10 ml sterile beakers containing 30 mM for Ca^{2+} and $C_2O_4^{2-}$. This method induces the formation of the calcium oxalate monohydrate (COM) crystals. 50 µg ml^{-1} and 100 µg ml^{-1} of SeNPs was added to the 1st and 2nd beaker, the 3rd beaker without SeNPs was the control. All beakers were allowed to stand at 37°C for 3 d. The glass coverslips with deposits of CaC_2O_4 crystals + SeNPs and CaC_2O_4 crystals were transferred carefully to petri plates and allowed to dry. The glass coverslips with deposited material were analyzed by scanning electron microscopy (SEM) and Energy-Dispersive X-ray analysis (EDX), the protocol of which is detailed in **5.1.10.5.**

5.1.12 ANTI-BIOFILM ACTIVITY OF TeNPs BIOSYNTHESIZED BY GUSF-1

5.1.12.1 Growing of biofilms of *Ps. aeruginosa* ATCC 9027

A loopful of *Ps*. *aeruginosa* ATCC 9027 was aseptically inoculated into Luria Bertani (LB) broth and incubated overnight at 37ºC. The overnight grown culture was diluted 1:100 into fresh LB medium to which 2% glucose was added to initiate biofilm production. The anti-biofilm assay was carried out in 96 well microtitre plate in a final volume of 100 µl. 50 µl of the culture was added per well. Different volumes of TeNPs were prepared in sterile milli Q water and was added to 6 different wells to give a final concentration of 10, 20, 30, 40 50, 60 µg ml^{-1}. The microtiter plate was incubated overnight at 37°C. The 96 microtitre plate was incubated at 37ºC for 18 h. Control of *Ps*. *aeruginosa* ATCC 9027 and *Ps*. *aeruginosa* ATCC 9027 with 60 µg ml^{-1} of the antiobiotic ciprofloxacin was also maintained.

5.1.12.2 Staining of the biofilm formed

Free cells that were not attached to the micro titre plate and the spent medium was discarded by turning the plate over and shaking out the liquid into a beaker and later decontaminated and disposed off. The plate was gently submerged in a small tub of water for washing in order to remove unattached cells and extra components of media. To each well of the microtiter plate, 125 µl of a 0.1% aqueous solution of crystal violet (***Appendix I***) was added. The plate was further incubated at room temperature for 10-15 min and then rinsed for 3-4 times with water by submerging in a tub of

water and finally, the micro titer plate was turned upside down and left to dry overnight.

5.1.12.3 Quantification of the biofilm

To each well of the microtiter plate, 125 µl of 30% acetic acid in water was added to solubilize the crystal violet and incubated at room temperature for 10-15 min. The 125 µl of the solubilized crystal violet was quantified at 550 nm using 30% acetic acid prepared in water as the blank. The experiment was carried out in duplicates. The % inhibition was calculated =A_{550} of preformed biofilm - A_{550} test sample/ A_{550} of preformed biofilm × 100. Appropriate controls were maintained. All the experiments were carried out in triplicates and statistical analysis was performed by using IBM-SPSS 23 statistical software. A one-way analysis of variance (ANOVA) was used to assess the variation between all the treatment groups. A level of probability of $p < 0.05$ was considered as statistically significant data.

5.1.13 DETERMINATION OF THE ABILITY OF CELL LYSATE OF GUSF- 1 TO BIOSYNTHESIZE MANGANESE OXIDE NANOPARTICLES

5.1.13.1 Synthesis of manganese oxide nanoparticles

The potential of cell lysate of GUSF-1 to biosynthesize manganese oxide nanoparticles (MnO NPs) was evaluated. Cell lysate of GUSF-1 was prepared as mentioned in **5.1.6.** A set of three test tubes was used; first tube contained 1 ml of 10 mM $MnSO_4$. $2H_2O$, second tube contained 1 ml of cell lysate of the GUSF-1 and third tube contained the mixture of 10 mM $MnSO_4$. $2H_2O$ and cell lysate in 1:1 proportion. All the tubes were kept standing at room temperature for incubation, till a colour change to brown was observed.

5.1.13.2 FTIR analysis

The reaction mixture of the cell lysate and the nanomaterial formed was processed and analyzed as per procedure detailed in **5.1.8.**

5.1.13.3 Characterization of manganese oxide NPs

Characterization of manganese oxide NPs formed by cell lysate of GUSF-1 was carried out using SEM-EDS, XRD and TEM and SAED analysis as detailed in **5.1.10.**

5.1.14 EVALUATION THE ROLE OF BIXBYITE LIKE Mn_2O_3 NPs AS AN ALTERNATIVE MAGNETIC PROBE IN MEDICAL DIAGNOSTIC TOOLS

The magnetic property Mn_2O_3 NPs was determined as a function of external magnetic field using a Quantum Design-Versa Lab Vibrating sample magnetometer (VSM). The sample was prepared by weighing 5.6 mg of the powder, wrapping it in teflon tape and mounting on the sample holder. An external field up to 3 Tesla was used at room temperature. The magnetic moment (Oesterds) v/s magnetic field (emu/g) – Magnetic Hysteresis curves was obtained at room temperature.

5.2 RESULTS

5.2.1 SCREENING OF EXTREMELY HALOPHILIC CULTURES FOR THE ABILITY TO REDUCE SALTS OF SILVER, SELENIUM AND TELLURIUM

The ability to reduce salts of silver, selenium and tellurium was studied in 7 extremely halophilic cultures; $GUBF_3$, $GUBF_{11}$, GUSF-1, GUIF2, GUIF3, GUIF4 and GUVFFM-3 in terms of colour change of the colonies and growth was also noted. As seen in **Fig. 5.1 C and D**, cultures when grown on NTYE with 0.05 mM Ag^{1+} **(**silver nitrate**)**, were seen to develop varying hues of brownish black colouration as compared to the colonies on the control plates indicated in **Fig. 5.1 A, B**.

A colour change of the colonies from orange/ cream to a brick red colouration was seen in all the cultures growing on NTYE incorporated with 2 mM SeO_3^{2-} **(**sodium selenite) **(Fig. 5.1 E & F**). When grown in NTYE with 0.1 mM TeO_3^{2-} (potassium tellurite), all the seven cultures were seen to produce a black colour in their colonies (**Fig. 5.1 G)**. The haloarchaeal culture GUSF-1 and the extremely halophilic eubacterial biont GUVFFM-3 were selected for further studies of nanoparticle biosynthesis.

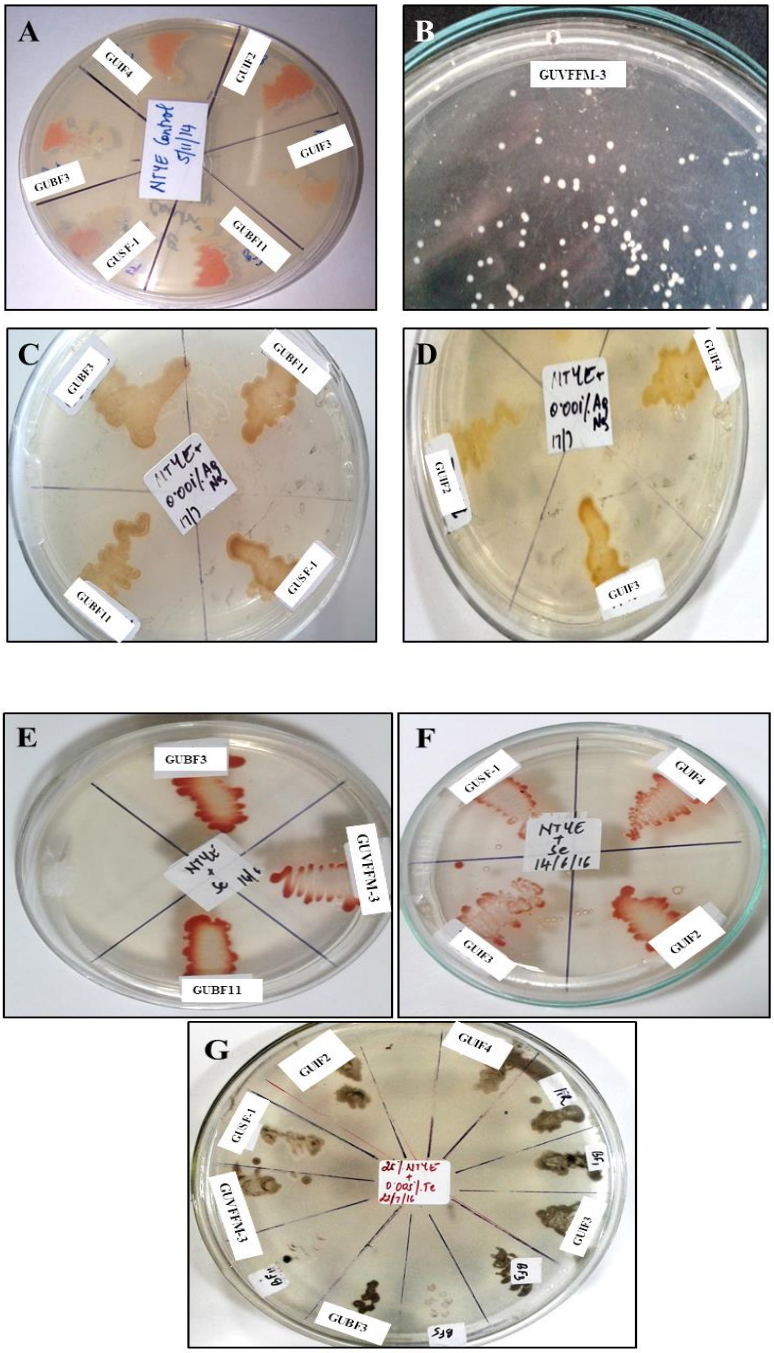

Fig. 5.1 **A & B:** Growth of extremely halophilic cultures on NTYE medium **C & D:** Reduction of Ag^{1+} indicated by formation of brown colour in the colonies; **E & F:** Reduction of selenite indicated by formation of brick red colour in the colonies; **G:** Reduction of tellurite indicated by formation of black colour in the colonies.

5.2.2 RESPONSE TO VARYING CONCENTRATION OF SALTS DURING GROWTH

Response of the cultures to each concentration of the salt was studied in terms of absence or presence of growth. Minimum Inhibitory Concentration (MIC) was determined as the concentration at which there was absence of growth. As seen in **Fig. 5.2**, GUVFFM-3 was inhibited by 1.2 mM Ag^{1+} while GUSF-1 failed to grow in the presence of 1.5 mM Ag^{1+}. Selenite SeO_3^{2-} at 120 mM and 90 mM inhibited growth of GUSF-1 and GUVFFM-3 while tellurite TeO_3^{2-} inhibited growth GUVFFM-3 and GUSF-1 at MIC of 0.6 mM and 0.55 mM respectively.

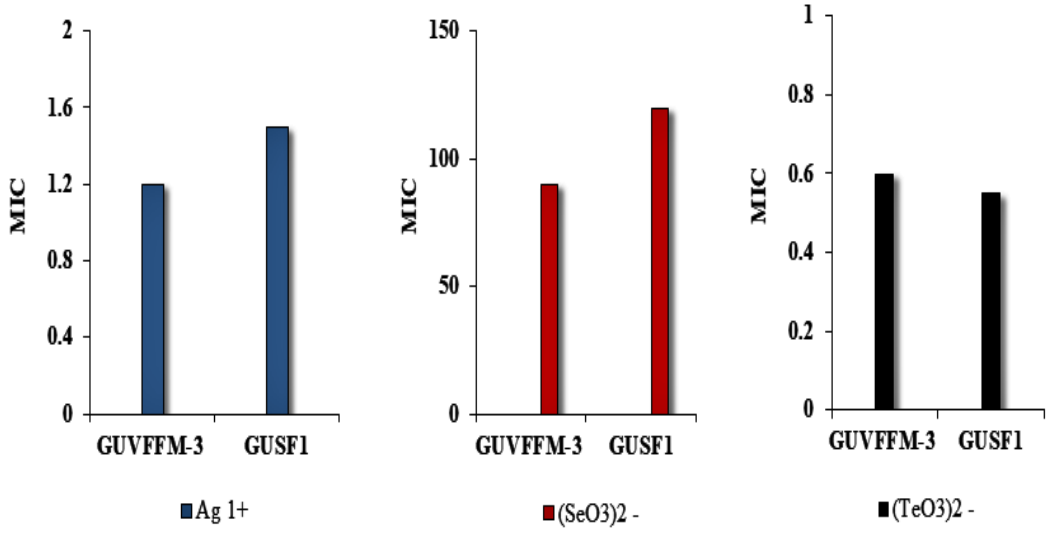

Fig. 5.2 The minimum concentration of $Ag^{1+,}$ SeO_3^{2-}, TeO_3^{2-} inhibiting growth of GUVFFM-3 and GUSF-1

5.2.3 BIOGENIC SYNTHESIS OF SeNPs AND TeNPs BY GROWING CELLS OF GUVFFM-3 AND GUSF-1

Both the cultures grew in nutrient rich medium in the presence of 5 mM SeO_3^{2-} or 0.1 mM TeO_3^{2-} as visually indicated by the increase in turbidity and by change in colour when compared to the control flasks. In the presence of 5 mM SeO_3^{2-}, the creamish colouration of GUVFFM-3 changed to brick red by 2 d (**Fig. 5.3 A)**. The

characteristic orange pigment of GUSF-1 turned to a reddish hue on day two and brick red by the end of 4 d (**Fig. 5.3 B**). The control flask with only SeO_3^{2-} showed no change in turbidity or colour.

In the presence of 0.1mM TeO_3^{2-}, the creamish colouration of GUVFFM-3 changed to black by day 2 (**Fig. 5.3 C)**. The otherwise characteristic orange pigment of GUSF-1 changed to black by the end of 4 d (**Fig. 5.3 D**). The control flask with only TeO_3^{2-} showed no change in turbidity or colour.

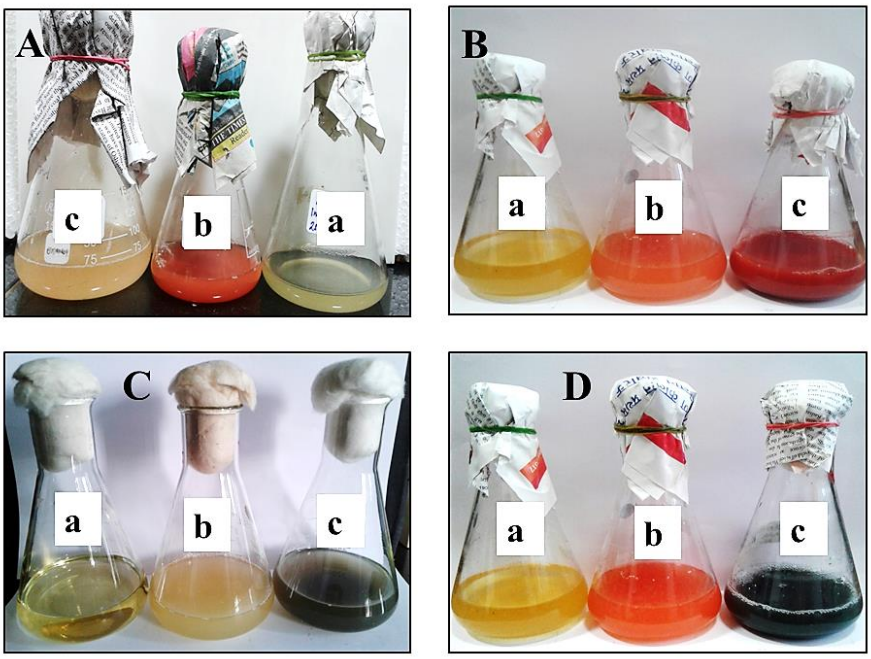

Fig. 5.3 Reduction of 5 mM SeO_3^{2-} as indicated by colour change to brick red by growing cells of **A:** GUVFFM-3 and **B:** GUSF-1; Reduction of 0.1mM TeO_3^{2-} as indicated by colour change to black by growing cells of **C:** GUVFFM-3 and **D:** GUSF- 1. All flask labelled '**a**' are media control: flask labelled '**b**' is growth of culture in 15% TYE/ NTYE; flask labelled '**c**' is growth of culture in 15% TYE/ NTYE + salt solution

5.2.4 GROWTH AND SELENITE REDUCTION IN GUVFFM-3 AND GUSF-1

The capability of GUVFFM-3 or GUSF-1 to transform selenite to SeNPs was evaluated by monitoring growth and conversion of selenite to SeNPs in 15% TYE or NTYE medium in the presence of 5 mM SeO_3^{2-}. 5 mM concentration of selenite was chosen as the concentration for selenite reduction tests under aerobic growth conditions. Three parameters that were measured every 4 h for GUVFFM-3 and every 8 h for GUSF-1 were (i) bacterial cell growth (CFU counts), (ii) residual selenite in the growth medium and (iii) SeNPs content were all measured.

Growth in 5 mM SeO_3^{2-} was accompanied brick-red particulate matter. The brick-red particulate matter formed was found to interfere with the absorbance measurements at 480/ 600 nm giving a false positive reading. Therefore, growth was evaluated by determining the colony forming units/ ml of culture broth. Residual selenite was chemically converted to SeNPs by reducing SeO_3^{2-} to Se^0 and the reaction mixture could be monitored at 390 nm, but the SeNPs that was formed started to agglomerate and hence an alternative to monitor the reduced product was required. Using a procedure of Biswas *et al*. (2014) the SeNPs was solubilized in 1 M Na_2S. The red brown solution obtained on solubilizing the SeNPs revealed absorption max at 475 nm as indicated in the visible scan instead of 500 nm that is mentioned in the procedure by Biswas *et al*. (2014) so A_{475} was used to monitor and quantify the SeNPs which was solubilized by 1 M Na_2S in our study (**Fig. 5.4)**. The SeNPs biosynthesized by the cultures was quantified using the procedure of Biswas *et al*. (2014).

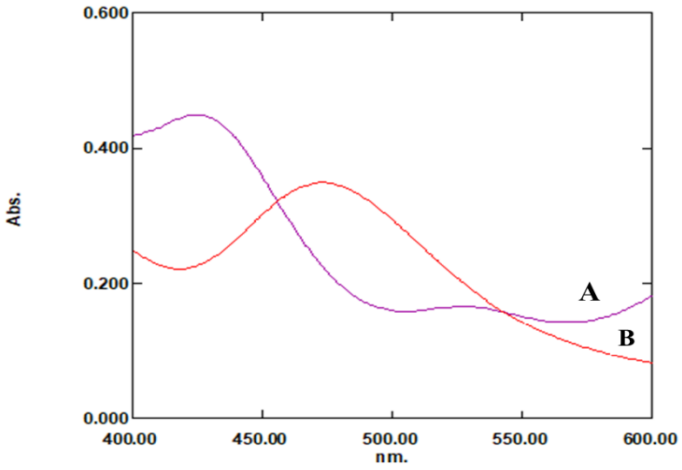

Fig. 5.4 Absorption spectra **A:** 1 M Na_2S solution **B:** Solubilized SeNPs

Selenite positively affected the growth dynamics and final cell yield of GUVFFM-3 and GUSF-1 (**Fig. 5.5 & 5.6**). In the case of GUVFFM-3 no significant differences were observed on cell concentrations at the beginning of the log phase between the selenite supplemented culture when compared with control culture. Nevertheless, the stationary phase was attained by GUVFFM-3 more rapidly without selenite in the medium than by the culture supplemented with selenite. In particular, for the culture growing with no selenite added, the stationary phase was reached after about 28 h, whereas in cultures growing in medium supplemented with SeO_3^{2-}, the stationary phase was attained after 32 h of growth. The stationary phase for the control culture and for the culture grown in media supplemented with selenite, was prolonged up to the 40^{th} h after which a decrease in cell growth was observed corresponding to a reduction of about 0.1 Log unit for the control culture and a reduction of about 1 log unit for the test culture. In culture spiked with 5 mM SeO_3^{2-}, an overall final cell yield (1 Log unit) was observed when compared to the control. In the case of GUSF-1, no lag phase was seen in the growth of the selenite supplemented culture as compared to the 8 h lag phase of the control. Growth increased steadily for the selenite supplemented culture and the control till 120 h, after which stationary phase was attained, but the overall final cell yield corresponding to about 2 log units in the selenite supplemented culture as compared to the control was observed.

Residual SeO_3^{2-} concentration revealed an opposite trend; decreasing concentration along with the rising of cell numbers for both the cultures studied. In the case of GUVFFM-3 an initial of 5 mM SeO_3^{2-} concentration in the medium was reduced to 0.55 of SeO_3^{2-} mM till 52 h of incubation indicating an overall of 91% reduction in the initial SeO_3^{2-} concentration. About 74% of SeO_3^{2-} exhaustion occurred up to the onset of the stationary phase (till 32 h of incubation). After the culture attained stationary phase, a further reduction of 17% of the initial concentration of SeO_3^{2-} selenite occurred leaving a 0.55 mM of SeO_3^{2-}unutilized. In the case of GUSF-1, reduction of SeO_3^{2-} in the medium occurred steadily till stationary phase at which 0.28 mM of SeO_3^{2-} was detected in the medium, indicating a reduction of 94% of the initial SeO_3^{2-} concentration. A further reduction of 4% (0.18 mM) of selenite occurred indicating an overall 97.4% utilization of selenite from the medium.

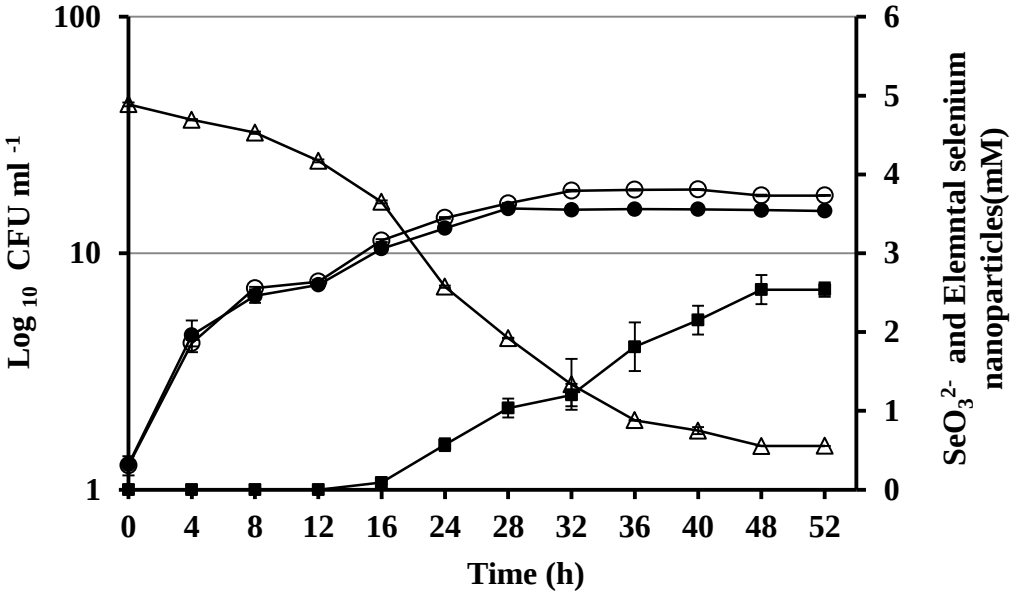

Fig. 5.5 Growth of GUVFFM-3 in 15 % TYE —●—,15 % TYE + SeO_3^{2-} —○— , Residual SeO_3^{2-} —△— , and selenium nanoparticle formation —■— by GUVFFM-3. Each curve shows means ± SD based on the results of three experiments

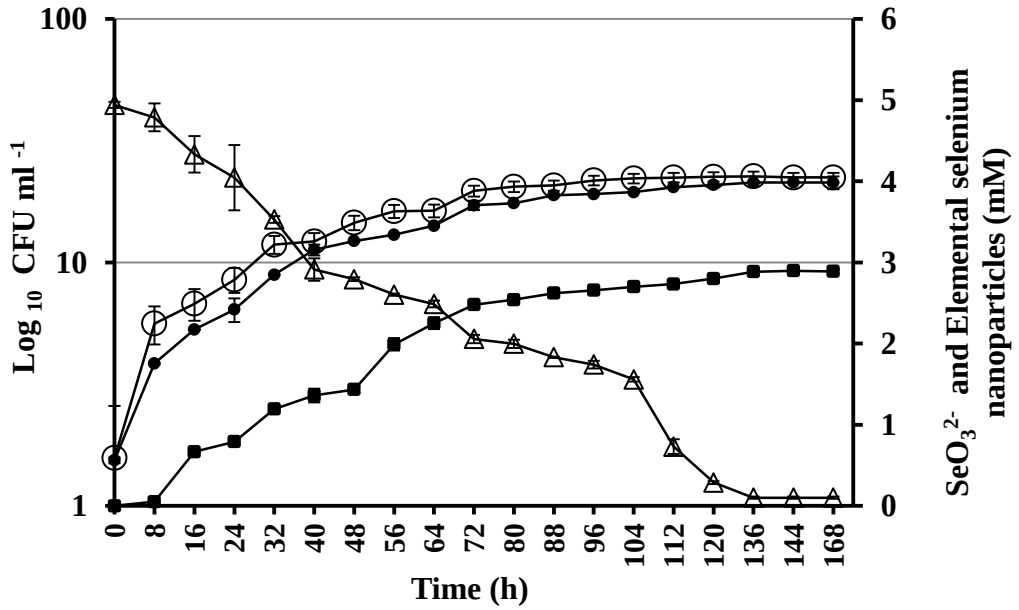

Fig. 5.6 Growth of GUSF-1 in 15% TYE —●— , 15% TYE + SeO_3^{2-} —○— , Residual SeO_3^{2-} —△— and selenium nanoparticle formation —■— by GUSF-1. Each curve shows means ± SD based on the results of three experiments.

Reduction and consequent depletion of sodium selenite were accompanied by the appearance of a bright red colour in the growth medium. Control flasks containing

medium with only selenite and medium with culture, did not exhibit the change of color, showing that the red color is of biological origin in the presence of selenite. Despite the reduction process running parallel to the microbial growth, red color in flask was visually noiticed only at 16 h of incubation from the start of growth accompanied by a garlic odour till 36 h after which it decreased in the case of GUVFFM-3. These results are in agreement with levels of SeNPs measured during the growth of GUVFFM-3 in the presence of 5 mM SeO_3^{2-}. Although 1.4 mM of initial SeO_3^{2-} (28%) was exhausted from the medium in 16 h of incubation, only 0.09 mM of SeNPs was detected. Moreover at 32 h and 52 h of incubation, only 1.2 mM and 2.53 mM of SeNPs was detected. While the 91% SeO_3^{2-} content was completely reduced within 52 h of growth, only about 84.33% of SeNPs were detected after 52 h. In the case of GUSF-1, a faint red colouration appeared in the flask with a concomitant garlic odour by end of 8 h of incubation. The garlic odour increased till 112 h of incubation after which it gradually decreased. The intensity of the red colour increased, visually observed, till about 136 h after which there was no change. SeNPs was detected within 8 h of incubation (0.05 mM), the concentration steadily increased till the end of the stationary phase, at which 4.9 mM of selenite was reduced, resulting in formation of 2.89 mM of SeNPs which was detected by the end of 168 h.

Table No 5.1: Comparison of selenite uptake studies between GUVFFM-3 and GUSF-1

	Growth in 5 mM Selenite	Selenite uptake	Biosynthesis of selenium nanoparticles
GUVFFM-3	• Stationary phase (SP); 32 h in TYE with Se_2O_3 v/s 28 h in TYE • Cell yield - 2 log unit	**91%** 74% - onset of SP, further 17%	**84.33%**
GUSF-1	• Stationary phase 120 h • Cell yield 2 log unit	**98%** 94% - onset of SP, further 4%	**96.33%**

5.2.5 INTRACELLULAR REDUCTION OF SELENITE IN GUVFFM-3 AND GUSF-1

As seen in the **Fig. 5.7 A & B**, pregrown colonies of GUVFFM-3 on 15% TYE and GUSF-1 on NTYE, labelled as **'a'** when carefully exposed to 5mM SeO_3^{2-} red colouration seen in the colonies labelled as **'b'.**

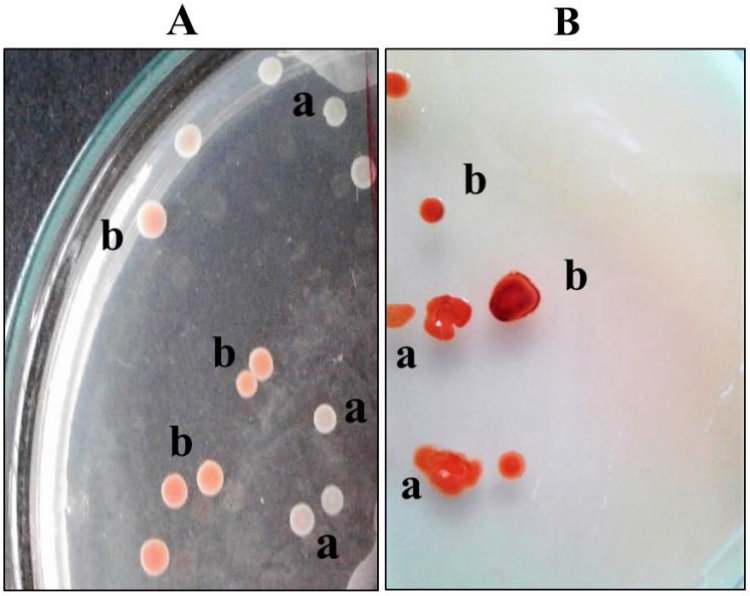

Fig. 5.7 Reduction of 5 mM SeO_3^{2-} is an intracellular feature in **A:** GUVFFM-3 **B:** GUSF-1

5.2.6 EFFECT OF SELENITE ON PIGMENTATION OF CELLS OF GUSF-1 DURING GROWTH

The pigment from wet cells grown in the presence of 5 mM SeO_3^{2-} was extracted with acetone and scanned between 300-600 nm using the spectrophotometer. The acetone extract showed characteristic absorptions of red carotenoids at 522, 489, a broad shoulder at 463 nm, two cis peaks at 386, 368 and peaks at 317 and 304 nm. The acetone extract of cells grown with 5 mM SeO_3^{2-} showed peaks only at 489 and 386 nm, while peaks at 522, 463, 368, 317 and 304 nm were not seen in the visible scan (**Fig. 5.8)**.

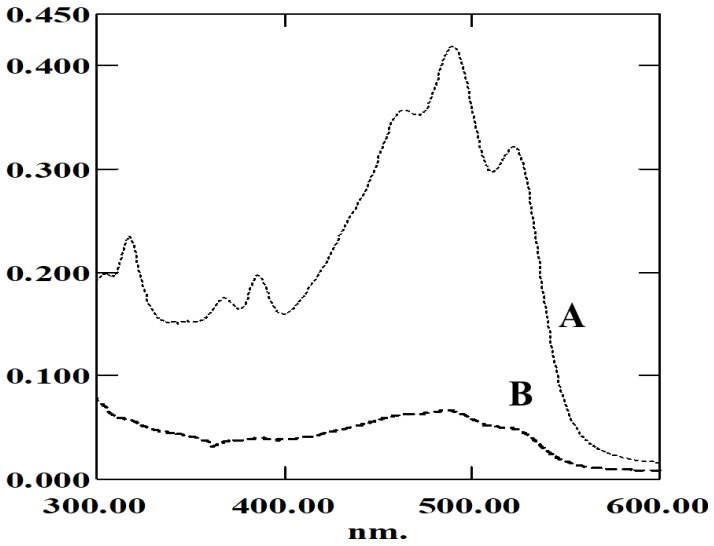

Fig. 5.8 Spectral scans of cells of GUSF-1 grown in **A:** NTYE and **B:** NTYE with 5 mM selenite

5.2.7 BIOGENIC SYNTHESIS OF SeNPs AND TeNPs BY WHOLE CELLS GUVFFM-3 AND GUSF-1

Washed cells of GUVFFM-3 and GUSF-1 were incubated with 5 mM SeO_3^{2-} and 0.1 mM TeO_3^{2-}. In the presence of 5 mM SeO_3^{2-}, the creamish colouration of whole cells of GUVFFM-3 changed to brick red indicating formation of SeNPs (**Fig. 5.9 A)**. Orange colored whole cells of GUSF-1 turned to a reddish hue on day three, and brick red by the end of 4 d, which also indicated the formation of SeNPs (**Fig. 5.9 B**). The control tubes showed no change in colour.

In the presence of 0.1 mM TeO_3^{2-}, the creamish colouration of whole cells of GUVFFM-3 changed to black by 2 d, indicating formation of TeNPs (**Fig. 5.9 C)**. Orange coloured cells of GUSF-1 changed to black by the end of 4 d, indicating the formation of TeNPs (**Fig. 5.9 D**). The control tubes showed no change in turbidity or colour.

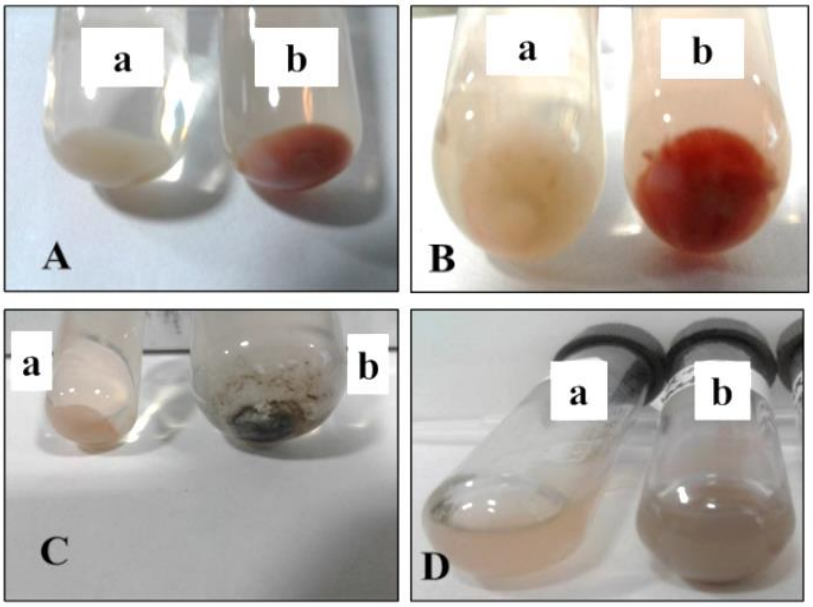

Fig. 5.9 Reduction of 5 mM SeO_3^{2-} as indicated by change in colour to brick red by whole cells of **A:** GUVFFM-3 and **B:** GUSF-1; Reduction of 0.1mM TeO_3^{2-} as indicated by change in colour to black by whole cells of **C:** GUVFFM-3 and **D:** GUSF-1. All tubes labelled '**a**' are control tubes of culture only, whereas tubes labelled '**b**' is culture + salt solution

5.2.8 BIOGENIC SYNTHESIS OF SeNPs AND TeNPs BY CELL LYSATE OF GUVFFM-3 AND GUSF-1

The cell lysates of both the cultures, when incubated, with 5 mM SeO_3^{2-} and 0.1 mM TeO_3^{2-} was seen to reduce the salt to its elemental form as indicated by formation red colour for Se^0 and black colour for Te^0 respectively (**Fig. 5.10**).

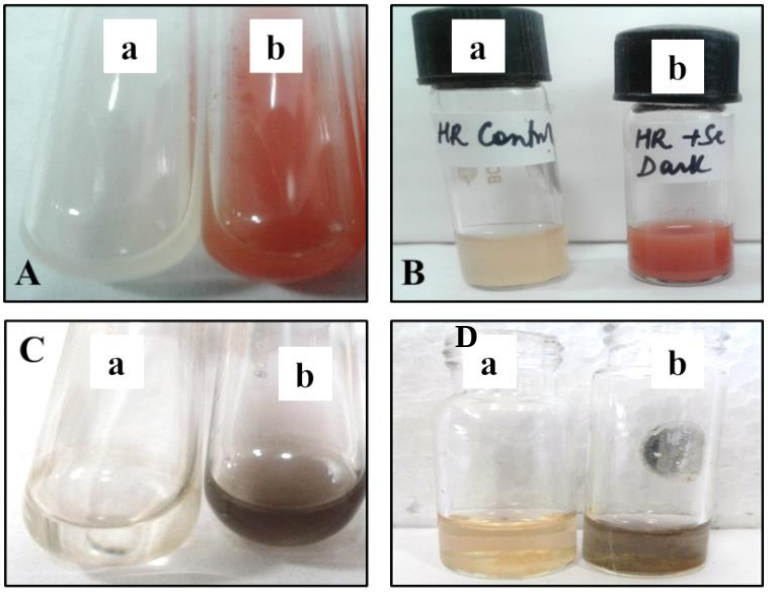

Fig. 5.10 Reduction of 5 mM selenite SeO_3^{2-} as indicated by change is colour to brick red by whole cells of **A:** GUVFFM-3 and **B:** GUSF-1; Reduction of 0.1mM TeO_3^{2-} as indicated by colour change to black by whole cells of **C:** GUVFFM-3 and **D:** GUSF-1. All tubes labelled '**a**' are control tubes, whereas tubes labelled '**b**' is the culture + salt solution

5.2.9 FT-IR ANALYSIS

5.2.9.1 FT-IR spectra of cells of GUVFFM-3 growing in the presence 5 mM SeO_3^{2-} and 0.1mM TeO_3^{2-}

Fig. 5.11 showed the FTIR spectrum of cells of GUVFFM-3 growing in the presence of 5 mM SeO_3^{2-} and 0.1mM TeO_3^{2-}. Growing control cells revealed bands at 3250 cm^{-1}, 1660 cm^{-1}, 1537 cm^{-1}, 1430 cm^{-1} and at 1020 cm^{-1} (**Fig. 5.11 A**). Cells growing in the presence of 0.1mM TeO_3^{2-} showed peaks at 3275 cm^{-1}, 1668 cm^{-1}, 1548 cm^{-1},

1471 cm^{-1} and 1058 cm^{-1} (**Fig. 5.11 B**). Cells growing in the presence of 5 mM SeO_3^{2-} showed peaks at 3307 cm^{-1}, 1672 cm^{-1}, 1548 cm^{-1}, 1431 cm^{-1} and 1089 cm^{-1} (**Fig. 5.11 C**).

As compared to the peaks obtained in the control cells at 3250/ 1660/ 1537/ 1430/ 1020 cm^{-1} , peaks of cells growing in the presence of 5 mM SeO_3^{2-} and 0.1mM TeO_3^{2-} was shifted to 3307/ 3275 cm^{-1}, 1672/ 1668 cm^{-1}, 1548 cm^{-1}, 1431/ 1471 and 1089/ 1058 cm^{-1} respectively.

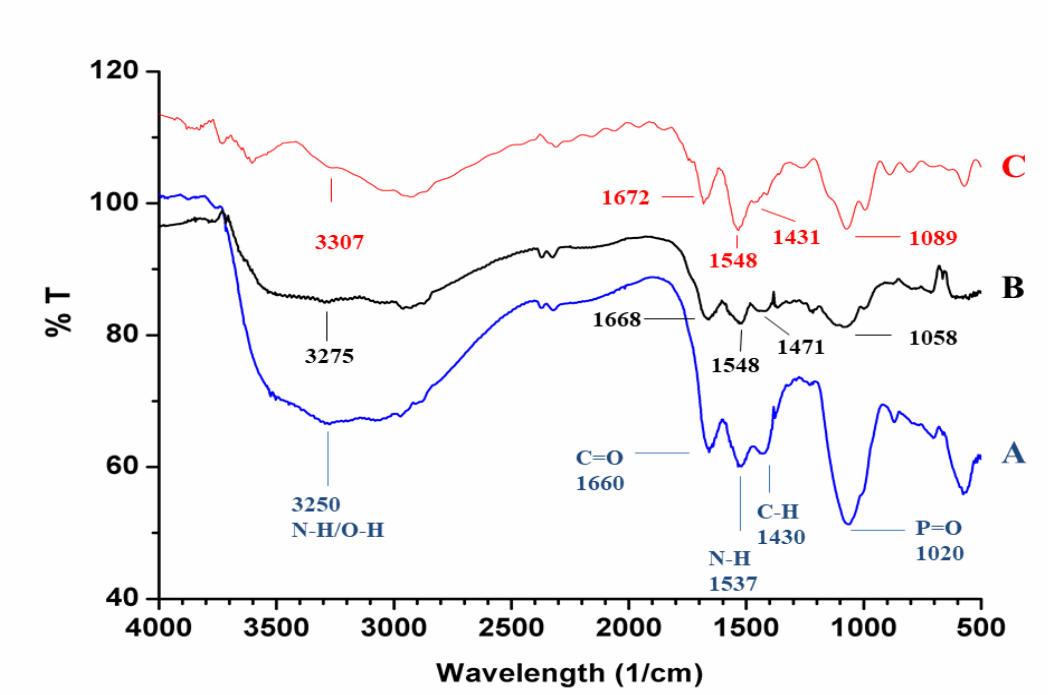

Fig. 5.11 A: FTIR spectrum of cells of GUVFFM-3 growing in 15% TYE; **B:** cells grown in the presence of 0.1 mM TeO_3^{2-} ; **C:** cells grown in the presence of 5 mM SeO_3^{2-}

5.2.9.2 FTIR spectra of cell lysate of GUVFFM-3 incubated with 5 mM SeO_3^{2-} and 0.1mM TeO_3^{2-}

Fig. 5.12 showed the FTIR spectrum of cell lysate of GUVFFM-3 incubated with 5 mM SeO_3^{2-} and 0.1mM TeO_3^{2-}. The cell lysate revealed peaks at 3410 cm^{-1}, 2926, 1629 cm^{-1}, 1402 cm^{-1} and 1134 cm^{-1} (**Fig. 5.12 A)**. The spectra of cell lysate incubated with 0.1mM TeO_3^{2-} showed peaks at 3489 cm^{-1}, 2910 cm^{-1}, 1735 cm^{-1},

1539 cm^{-1} and 1045 cm^{-1} (**Fig. 5.12 B**). The spectra of cell lysate incubated with 5 mM SeO_3^{2-} showed peaks at 3442 cm^{-1}, 2985 cm^{-1}, 1724 cm^{-1}, 1508 cm^{-1} and 1097 cm^{-1} (**Fig. 5.12 C)**. As compared to the peaks obtained in the control cells at 3410/ 2926/ 1629/ 1402 and 1134 cm^{-1}, peaks of cell lysate incubated with 5 mM SeO_3^{2-} and 0.1mM TeO_3^{2-} was shifted to 3442/ 3489 cm^{-1}, 2985/ 2910 cm^{-1}, 1724/ 1735 cm^{-1}, 1508/ 1539 cm^{-1} and 1097/ 1045 cm^{-1} respectively.

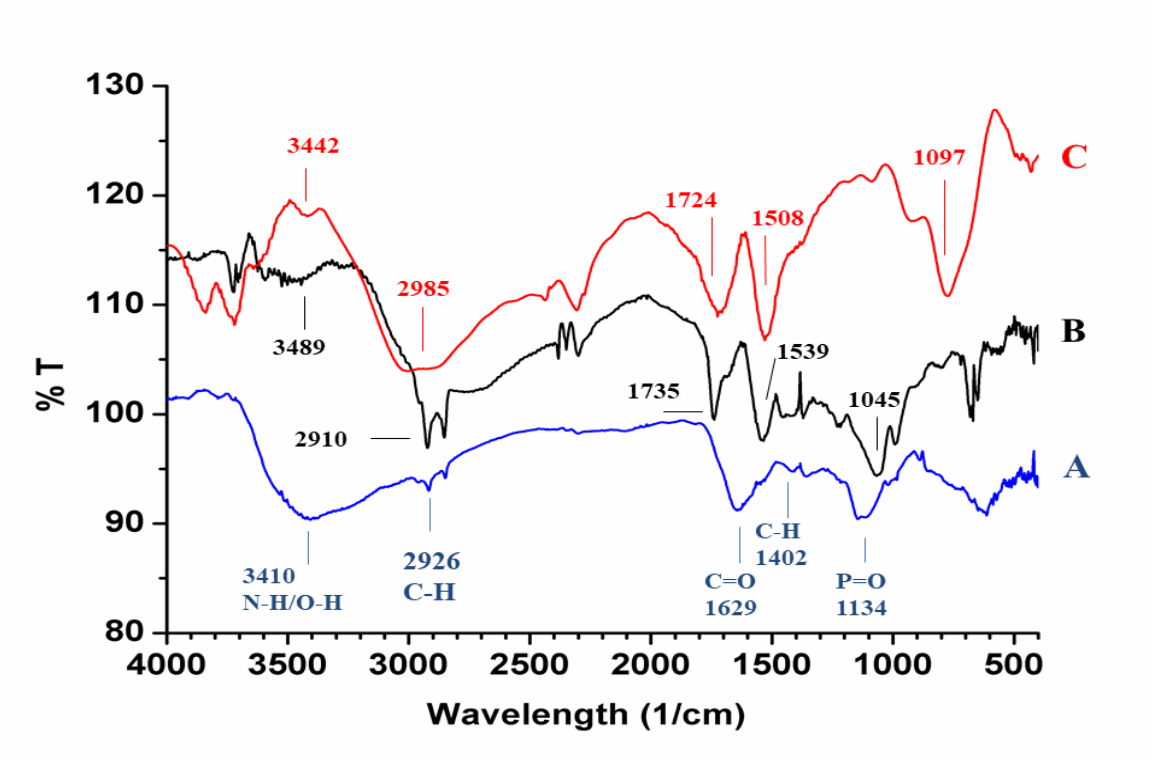

Fig. 5.12 A: FTIR spectrum of cell lysate of GUVFFM-3; **B:** cell lysate with 0.1mM TeO_3^{2-}; **C:** cell lysate with 5 mM SeO_3^{2-}

5.2.9.3 FTIR spectra of cells of GUSF-1 growing in the presence 5 mM SeO_3^{2-} and 0.1mM TeO_3^{2-}

In **Fig. 5.13 A** , the spectrum of cells of GUSF-1 growing in NTYE without 5 mM SeO_3^{2-} or 0.1mM TeO_3^{2-} showed peaks at 3332 cm^{-1}, 2960 cm^{-1} , 1627 cm^{-1} , 1509 cm^{-1} and 1118 cm^{-1}. Cells of GUSF-1 growing in the presence of 0.1mM TeO_3^{2-} showed peaks at 3284 cm^{-1}, 2939 cm^{-1}, 1647 cm^{-1},1531 cm^{-1} and 1083 cm^{-1} (**Fig. 5.13 B)**. Cells of GUSF-1 growing in the presence of 5 mM SeO_3^{2-} showed peaks at 3292 cm^{-1}, 2951 cm^{-1}, 1649 cm^{-1}, 1577 cm^{-1} and 1074 cm^{-1} (**Fig. 5.13 C)**. As compared to

the peaks obtained in the control cells at 3332/ 2960/ 1627/ 1409/ 1118 cm^{-1}, peaks of cells growing in the presence of 5 mM SeO_3^{2-} and 0.1mM TeO_3^{2-} was shifted to 3292/ 3284 cm^{-1}, 2951/ 2939 cm^{-1}, 1649/ 1647 cm^{-1}, 1377/ 1531, 1074/ 1083 cm^{-1} respectively.

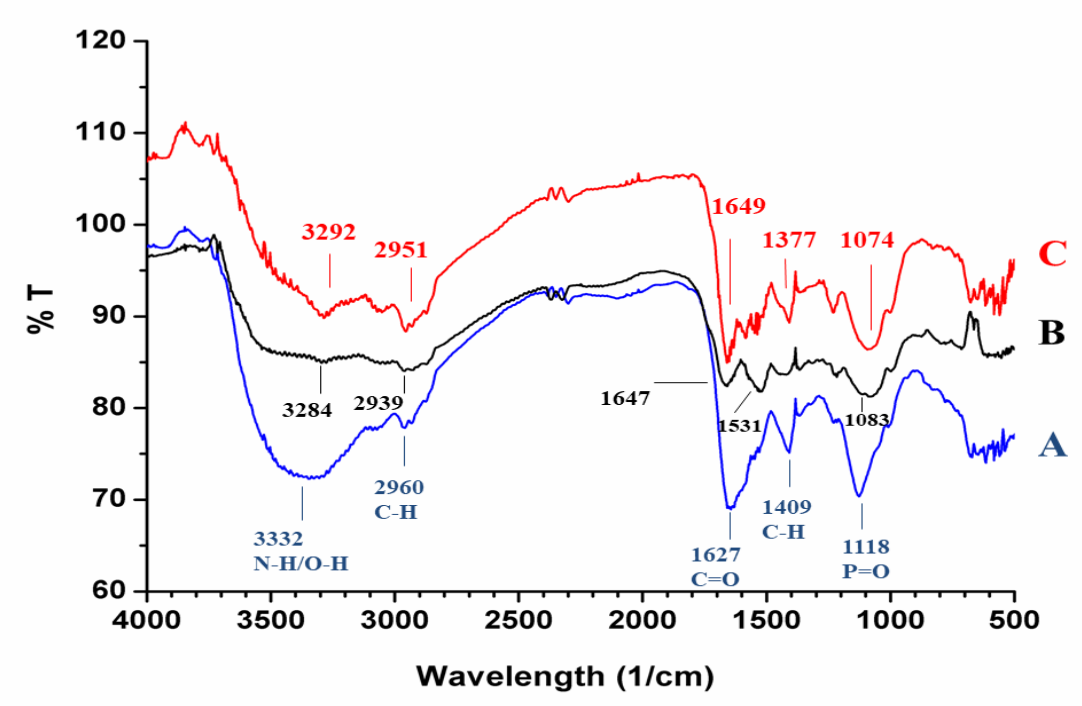

Fig. 5.13 A: FT-IR spectrum of cells of GUSF-1 grown in NTYE; **B:** cells grown in the presence of 0.1mM TeO_3^{2}; **C:** cells grown in the presence of 5 mM SeO_3^{2-}

5.2.9.4 FTIR spectra of the cell lysate of GUSF-1 incubated with 5 mM SeO_3^{2-} and 0.1mM TeO_3^{2-}

Cell lysate of GUSF-1 revealed the intense absorption bands at 3313 cm^{-1}, 2962 cm^{-1}, 1664 cm^{-1}, 1544 cm^{-1}, 1415 cm^{-1} and 1110 cm^{-1} (**Fig. 5.14 A**). The cell lysate of GUSF-1 incubated with 0.1mM TeO_3^{2-} showed peaks at 3280 cm^{-1}, 2952 cm^{-1}, 1639 cm^{-1}, 1539 cm^{-1}, 1408 cm^{-1}, and 1093 cm^{-1} (**Fig. 5.14 B**). The cell lysate of GUSF-1 incubated with 5 mM SeO_3^{2-} showed peaks at 3402 cm^{-1}, 2945 cm^{-1}, 1624 cm^{-1}, 1573 cm^{-1}, 1421 cm^{-1} and 1120 cm^{-1} (**Fig. 5.14 C**). As compared to the peaks obtained in the control cells at 3313/ 2962/ 1664/ 1544/ 1415/ 1110 cm^{-1}, peaks of cells growing in the presence of 5 mM SeO_3^{2-} and 0.1mM TeO_3^{2-} was shifted to 3402/ 3280 cm^{-1},

2945/ 2952 cm^{-1}, 1624/ 1639 cm^{-1}, 1573/ 1539, 1421/ 1408 and 1120/ 1093 cm^{-1} respectively.

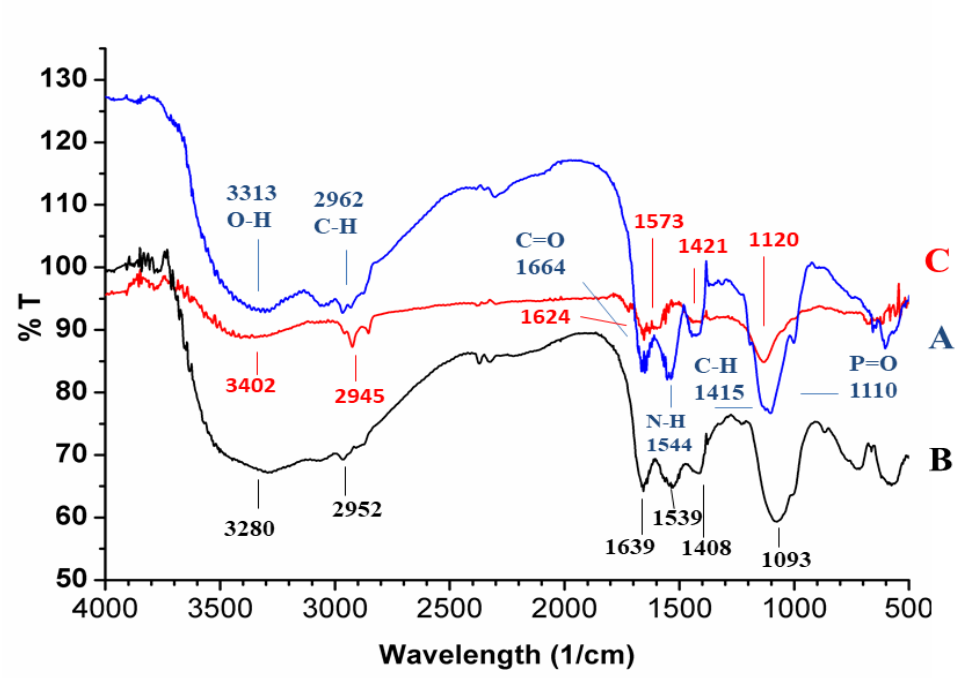

Fig. 5.14 A: FT-IR spectrum of cell lysate of GUSF-1; **B:** in the presence of 0.1mM TeO_3^{2-} ; **C:** in the presence of 5 mM SeO_3^{2-}

5.2.10 SELENITE REDUCING ASSAY AND IDENTIFICATION OF CELLULAR FRACTIONS INVOLVED IN SELENITE REDUCTION IN GUVFFM-3 AND GUSF-1

To localize selenite reduction in GUVFFM-3 and GUSF-1, in vitro assays were performed by testing intracellular fractions containing soluble proteins, membrane fractions, EPS and the extracellular growth medium i.e spent medium **(Fig. 5.15 A & B)**.

In the case of GUVFFM-3, supernatant and EPS showed no change in color to red both at pH 6 and 7, and thus no selenite reduction activity to SeNPs was detected. Soluble protein**,** membrane fractions evidenced selenite reduction through the production of red SeNPs.

In the case of GUSF-1, EPS showed no change in colour to red both at pH 6 and 7 and thus no selenite reduction activity to SeNPs was detected. Soluble protein, membrane fractions and spent medium showed selenite reduction through the production of red SeNPs.

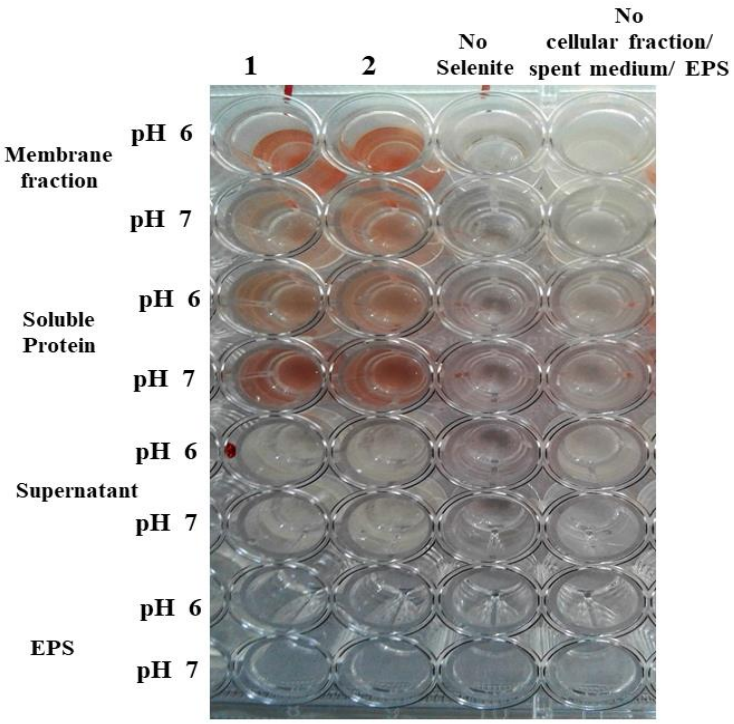

Fig. 5.15 A Selenite reduction assay on different fractions of GUVFFM-3 (two replicates) reacting with selenite

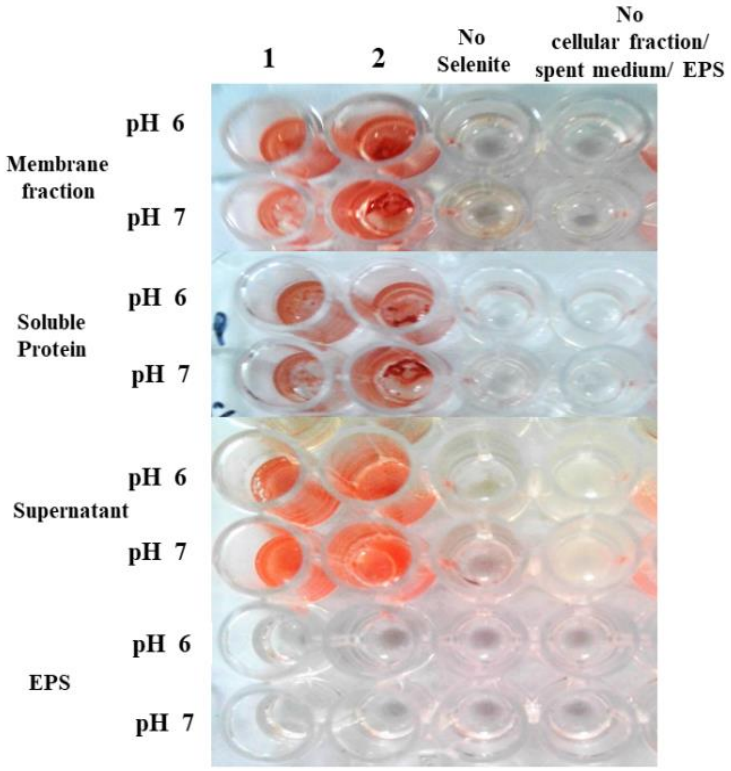

Fig. 5.15 B Selenite reduction assay on different fractions of GUSF-1 (two replicates) reacting with selenite

5.2.11 MECHANISM OF SELENITE REDUCTION IN GUVFFM-3 AND GUSF-1

Selenite reducing enzyme assay was carried out in the presence of known enzyme inhibitors, such as 0.01, 0.05 and 0.1 mM concentrations of sodium arsenite; and 5 and 10 mM of sodium azide. **Fig. 5.16 A & B** depicts inhibition of enzymes by enzyme inhibitors which are involved in selenite reduction in GUVFFM-3 and GUSF-1. In the case of GUVFFM-3, all the concentrations of sodium arsenite inhibited selenite reduction, both in soluble proteins and membrane fractions. Inhibition of selenite reduction in soluble protein and membrane fractions was also observed in the presence of 5 and 10 mM concentrations of sodium azide used. For GUSF-1, 5 and 10 mM concentrations of sodium azide inhibited selenite reduction in soluble proteins and membrane fractions, whereas only 10 mM sodium azide inhibited selenite reduction in the spent medium. Inhibition of selenite reduction capacity was also seen in soluble proteins, membrane fractions and spent medium in the presence of all three concentrations of sodium arsenite.

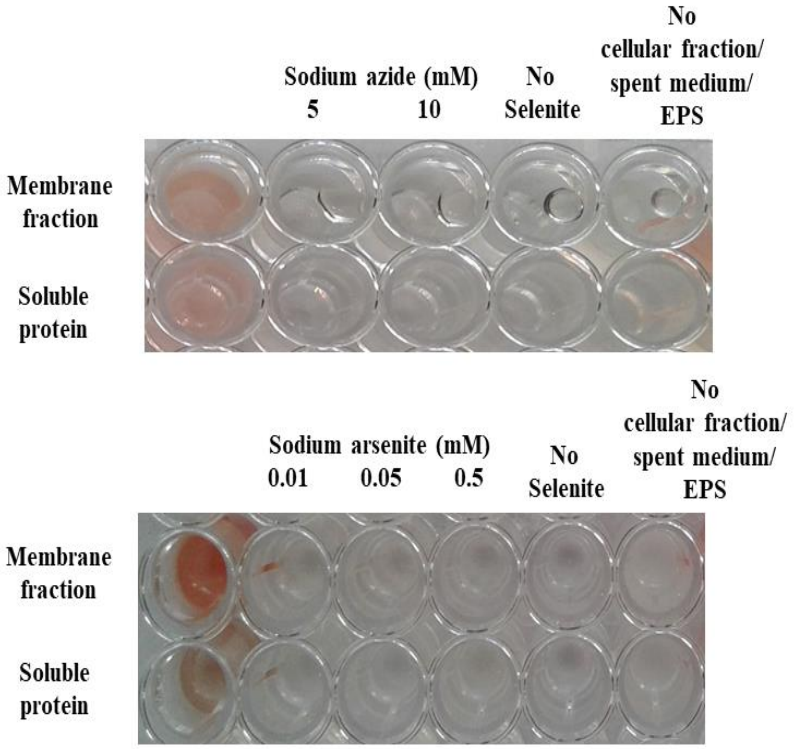

Fig. 5.16A: Evaluation of enzyme inhibitors on selenite assay reduction in GUVFFM-3 (two replicates)

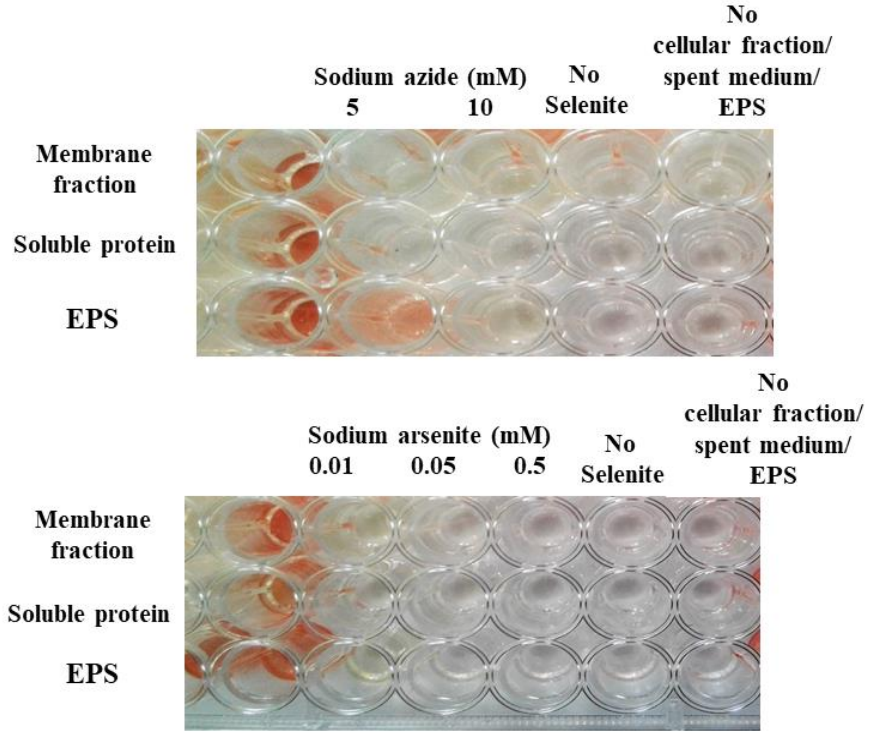

Fig. 5.16B: Evaluation of enzyme inhibitors on selenite reduction assay in GUSF-1 (two replicates)

5.2.12 POTENTIAL OF CELL LYSATES OF CULTURES FOR BIOGENIC SYNTHESIS OF SILVER NANOPARTICLE (AgNPs)

On incubation of each of the cell lysate of the 4 haloarchaeal cultures namely $GUBF_{11}$, GUIF2, GUIF3, GUIF4 and the extremely halophilic eubacterial biont GUVFFM-3 with 0.01% aqueous silver nitrate in sunlight, there was an instant colour change in the reaction mixture from pale yellow to brown to dark brown within a minute of incubation in sunlight (**Fig. 5.17)**. The intensity of the colour increased with increase in incubation time up to 5 min. There was no colour change in the tube with 0.01% aqueous silver nitrate when incubated in sunlight. Another set of tubes when incubated in the dark showed no change in colour. The reaction mixture of each of the cultures when scanned against distilled water showed absorption maximum between 400 - 450 nm (**Fig. 5.18**).

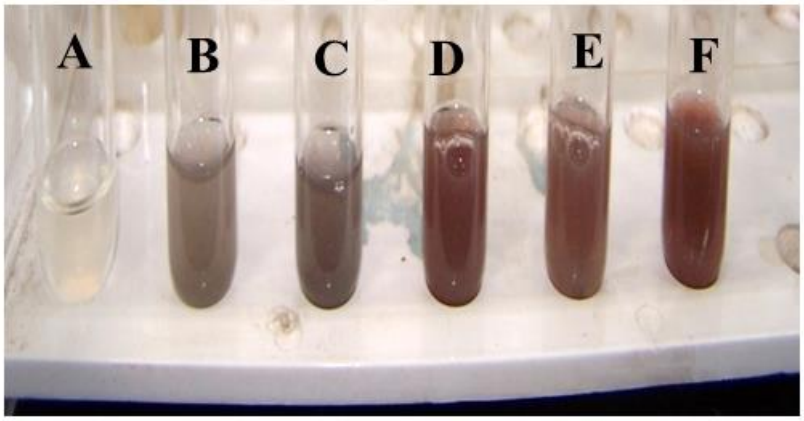

Fig. 5.17 A: Silver nitrate on incubation in the sun; **B-F:** Cell lysate of $GUBF_{11}$, GUIF2, GUIF3, GUIF4 and GUVFFM-3 with 0.01% aqueous silver nitrate on incubation in sunlight for 5 min

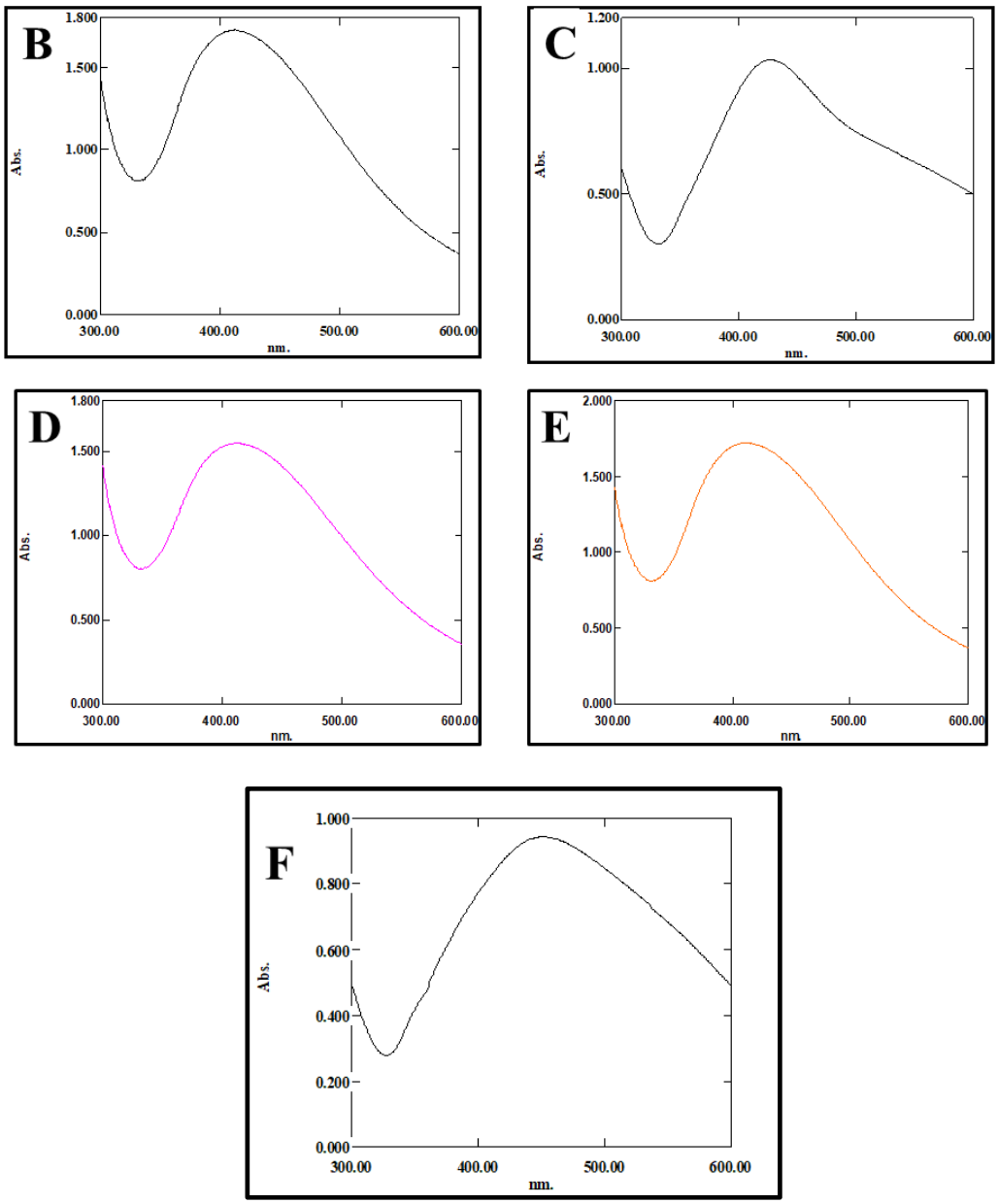

Fig. 5.18 Visible spectral scans of the reaction mixture of cell lysate of **B:** $GUBF_{11}$ **C:** GUIF2 **D:** GUIF3 **E:** GUIF4 and **F:** GUVFFM-3 with 0.01% aqueous silver nitrate on incubation in sunlight

5.2.13 CHARACTERIZATION OF THE SeNPs BIOSYNTHESIZED BY GUVFFM-3 AND GUSF-1

The UV absorption scan of the SeNPs biosynthesized by GUVFFM-3 and GUSF-1 in methanol showed a characteristic peak at 239 nm between 200-300 nm with absorption maxima at 240 nm (**Fig. 5.19**). An intensive peak at 254 cm^{-1} was observed in the Raman spectra of the SeNP biosynthesized by GUVFFM-3 and GUSF-1 (**Fig. 5.20)**.

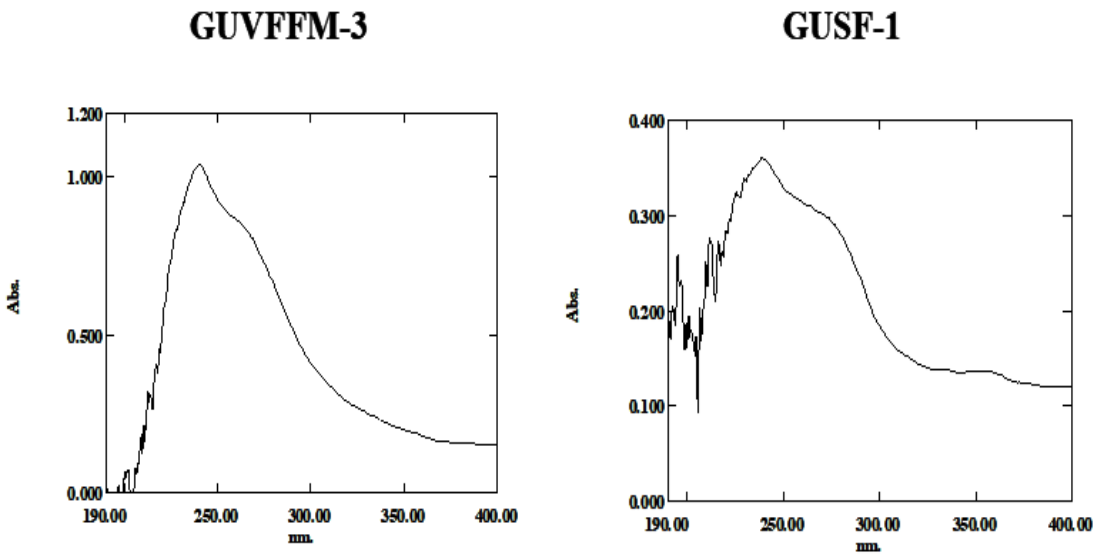

Fig. 5.19 UV Vis spectra of SeNPs biosynthesized by GUVFFM-3 and GUSF-1

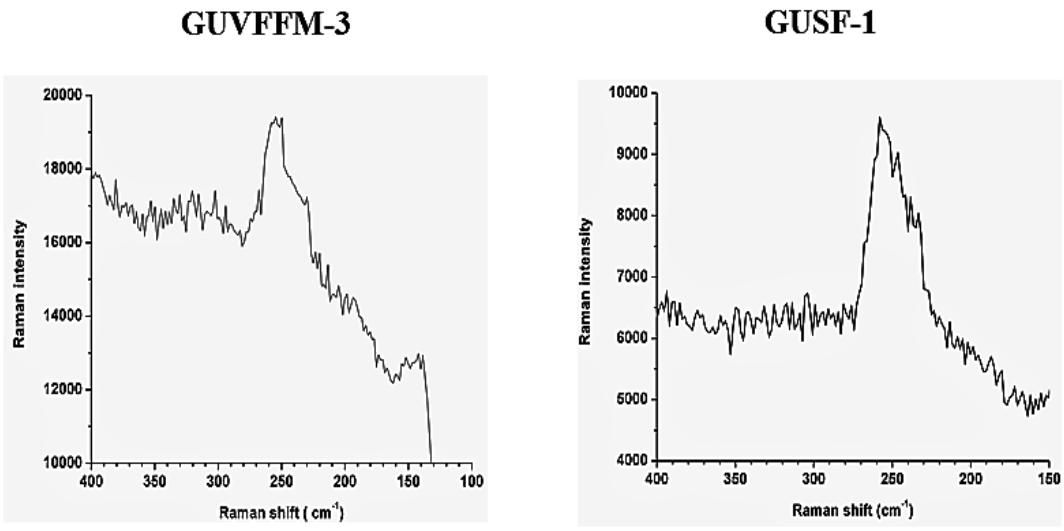

Fig. 5.20 Raman spectra of SeNPs biosynthesized by GUVFFM-3 and GUSF-1

Fig. 5.21 shows the X-ray diffraction pattern of the SeNPs biosynthesized by GUVFFM-3 and GUSF-1. The diffraction peaks present at 2θ (degrees) of 23.40°, 29.66°, 41.26°, 43.68°, 45.24°, 51.62°, 55.93°, 61.47° and 65.24° corresponds to (100), (101), (110), (012), (111), (201), (112), (022) and (210) planes of selenium and were in good agreement to JCPDS card no 073-0465. The average crystallite size of selenium was calculated using Scherrer's equation and was found to be 12 nm for the SeNPs biosynthesized by GUVFFM-3. The average crystallite size of selenium was calculated using Scherrer's equation was found to be 10 nm for the SeNPs biosynthesized during growth of GUSF-1.

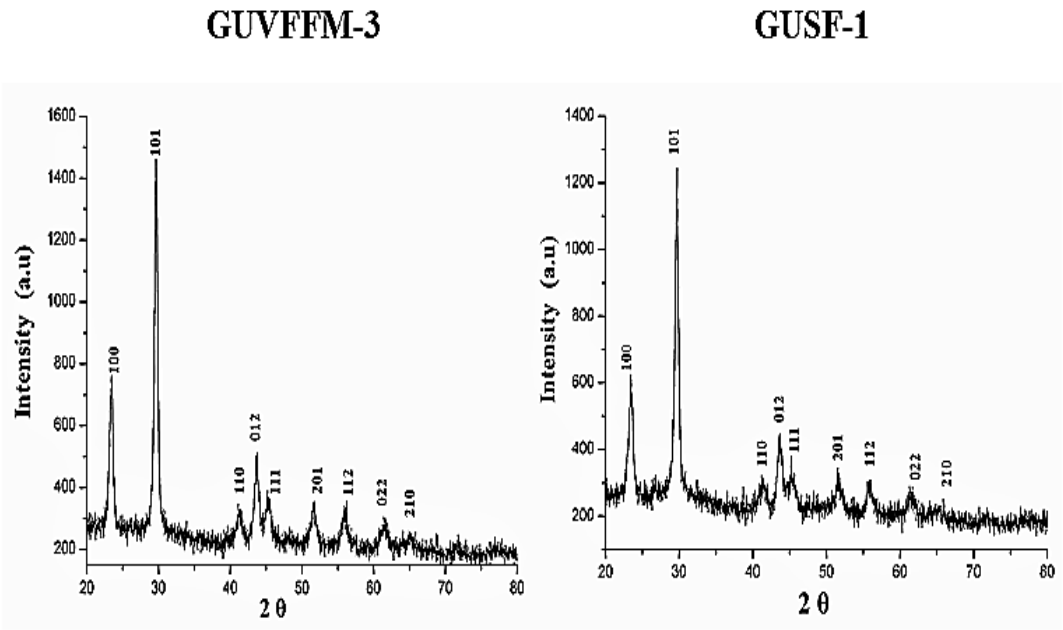

Fig. 5.21 XRD pattern of SeNPs biosynthesized by GUVFFM-3 and GUSF-1

The EDX pattern of the SeNPs biosynthesized by GUVFFM-3 is shown in **Fig. 5.22**. The elemental analysis by EDX exhibited absorption bands at 1.5, 11.2, and 12.5 KeV. The morphology of SeNPs observed during the morphological characterization by Transmission Electron Microscope (TEM) was nanocrystals with an average size of 32 nm (**Fig. 5.23 A**). The Selected Area Electron Diffraction (SAED) pattern of the nanocrystals biosynthesized by GUVFFM-3 is shown in **Fig. 5.23 B**. Selected area electron diffraction image exhibited diffraction rings corresponding to the (100), (101) and (012) directions of the hexagonal phase of selenium.

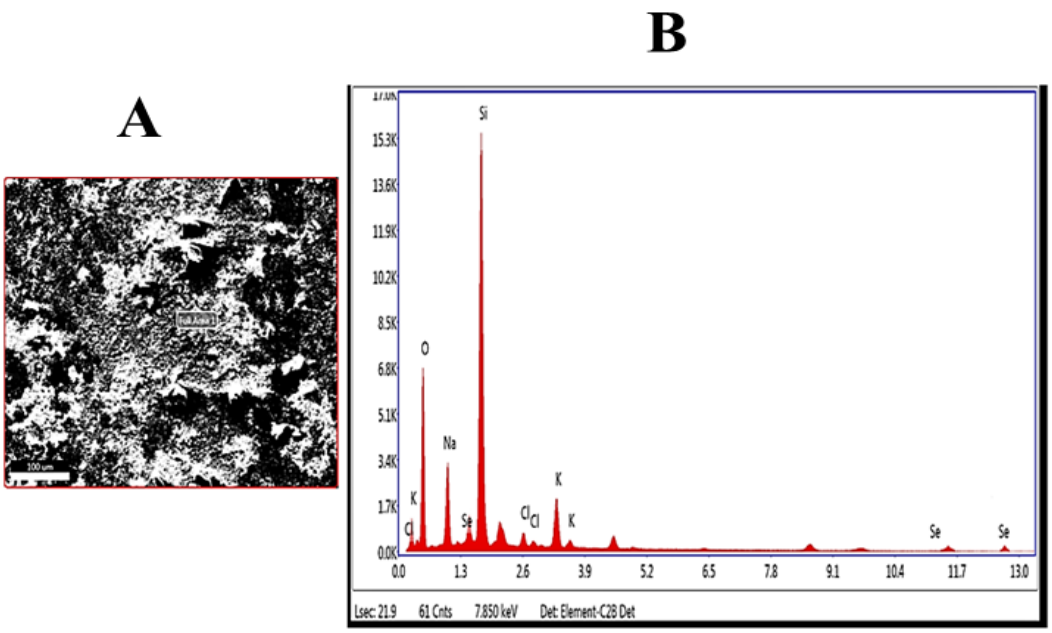

Fig. 5.22 Energy Dispersive X-ray micrograph of SeNPs biosynthesized by GUVFFM-3

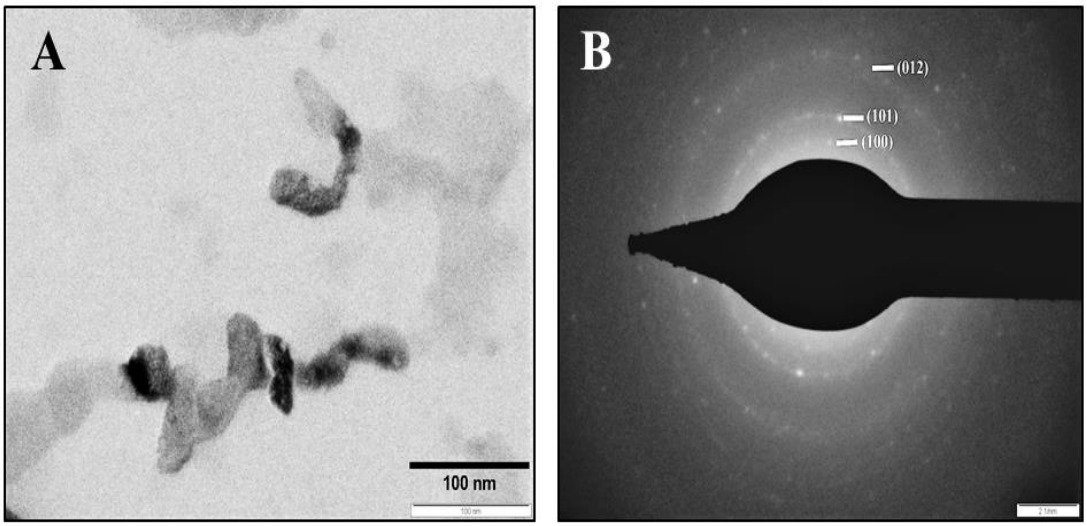

Fig. 5.23 A: TEM micrograph showing Se nanocrystals (average 32 nm) biosynthesized by GUVFFM-3 obtained by a drop coating of SeNPs onto copper stubs subjected to 200 keV; **B:** SAED of SeNPs biosynthesized by GUVFFM-3

Energy dispersive X-ray analysis was used to determine the composition of the selenium particles. EDX pattern of the SeNPs biosynthesized by GUSF-1 is shown in **Fig. 5.24**. The elemental analysis by EDX exhibited absorption bands at 1.5, 11.2, and 12.5 keV.

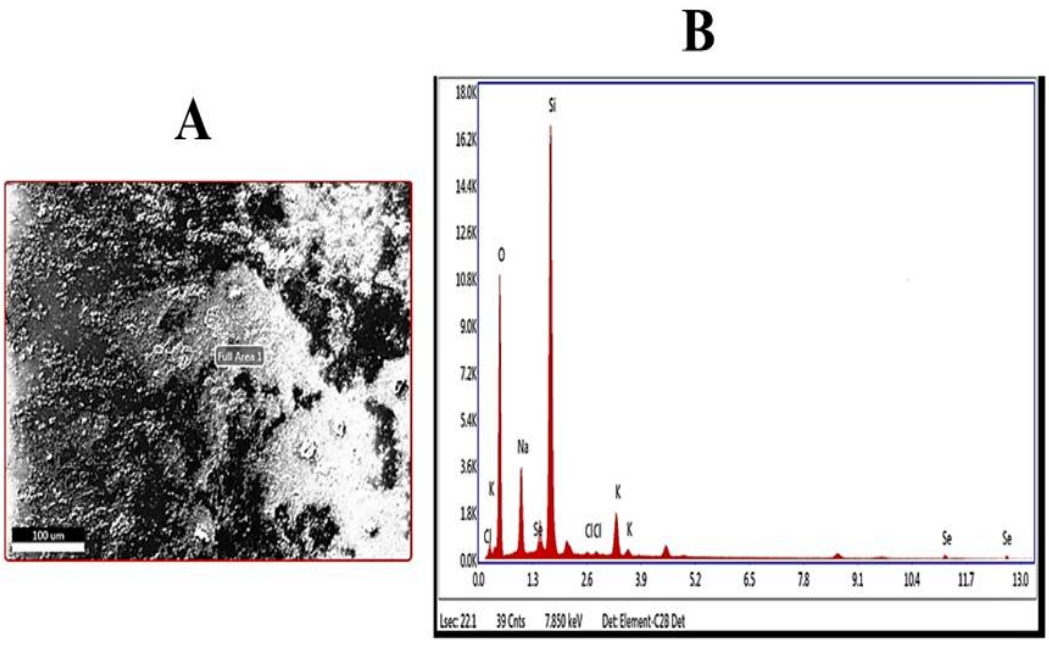

Fig. 5.24 Energy Dispersive X-ray micrograph of SeNPs biosynthesized by GUSF-1

Pentagonal shaped nanoparticles with and with an average diagonal length of 15nm and a height of 50 nm was observed during the morphological characterization of SeNPs biosynthesized by GUSF-1 by the Transmission Electron Microscope (TEM) (**Fig. 5.25 A & B**). The Selected Area Electron Diffraction (SAED) pattern of the SeNPs biosynthesized by GUSF-1 is shown in **Fig. 5.25 C**. Selected area electron diffraction image exhibited diffraction rings corresponding to the (100), (101) and (012) directions of the hexagonal phase of selenium.

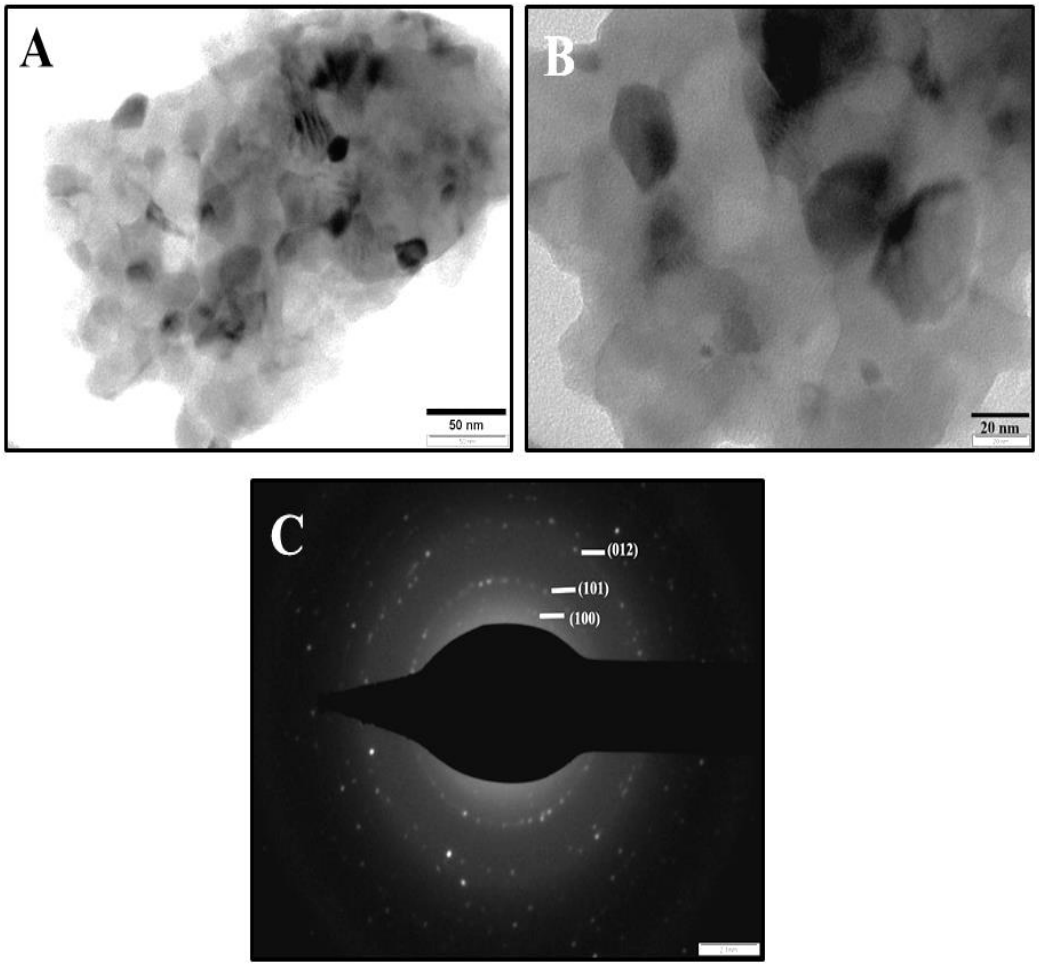

Fig. 5.25 A & B: TEM micrograph showing pentagonal shaped (with an average diagonal length of 15nm and a height of 50 nm) obtained by a drop coating of SeNPs biosynthesized by GUSF-1 onto copper stubs subjected to 200 keV **C:** SAED of SeNPs biosynthesized by GUSF-1

5.2.14 USE OF SeNPs BIOSYNTHESIZED BY GUSF-1 IN MODULATING SIZE AND SHAPE OF CALCIUM OXALATE CRYSTALS

Calcium oxalate monohydrate (COM) crystals formed from supersaturated solutions of sodium chloride, calcium chloride and sodium oxalate is shown in **Fig. 5.26 A**. Crystals synthesised here were the same as that formed in nature. The morphology seen is three-dimensional hexagonal crystals with a clear defined crystal borders with average area of 6.73 μm^2. According to the results of EDX spectrum analysis, the hexagonal COM crystals consisted only of Ca, C and O **(Fig. 5.26 B).** When 50 µg ml^{-1} of SeNPs was added to the mixture there was reduction in size of the crystals and the crystals now showed an irregular border with average area of 0.70 μm^2 **(Fig. 5.27 A)**. The elemental analysis by EDX exhibited absorption bands consistent with that of Ca, C, and O and also exhibited absorption bands at 1.5, 11.2, and 12.5 keV (**Fig. 5.27 B**). With the addition of 100 µg ml^{-1} of SeNPs the size of the crystal further decreased and the morphology changed to irregular spherical forms with average area of 0.46 μm^2 (**Fig. 5.28 A**). The elemental analysis by EDX exhibited absorption bands consistent with that of Ca, C, and O and also exhibited absorption bands at 1.5, 11.2 and 12.5 keV, confirming the presence of elemental selenium (**Fig. 5.28 B**)

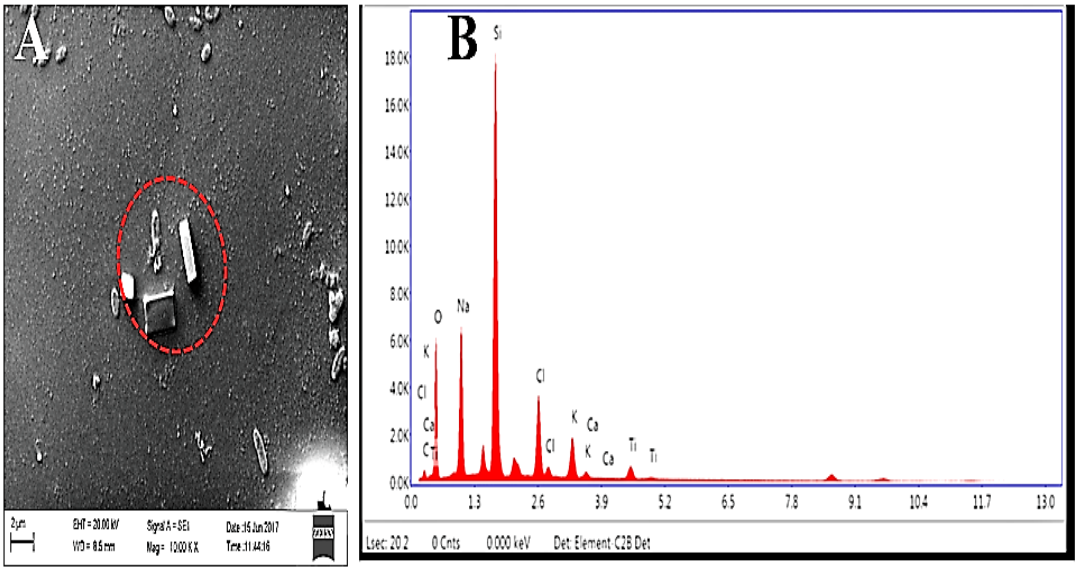

Fig. 5.26 A: SEM analysis and **B:** Energy Dispersive X-ray micrograph of calcium oxalate monohydrate (COM) crystals

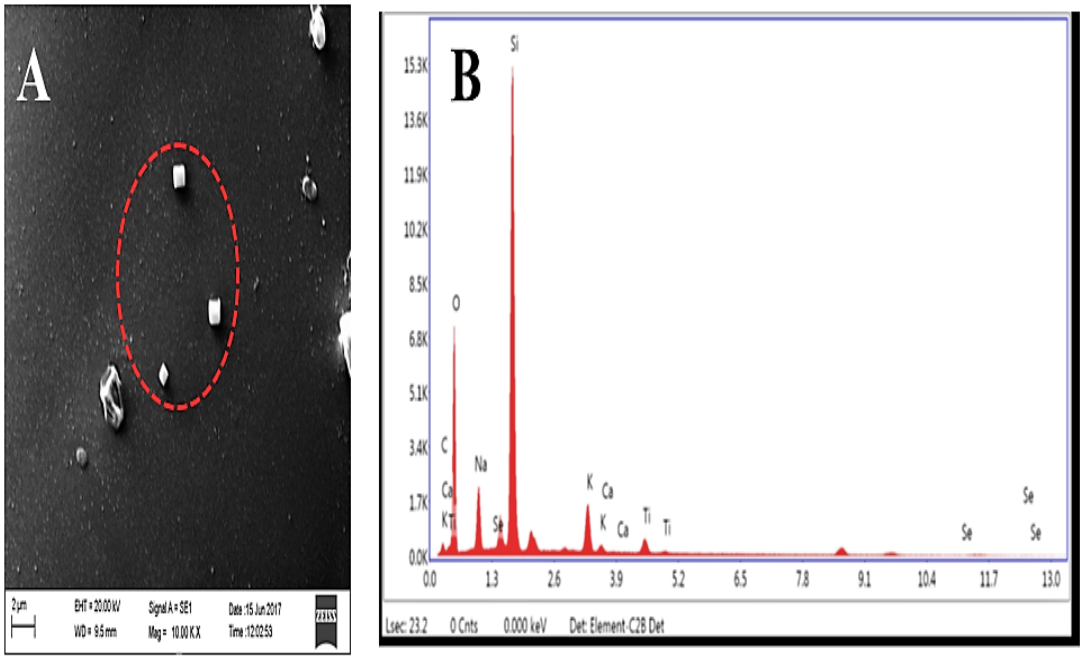

Fig. 5.27 A: SEM analysis and **B:** Energy Dispersive X-ray micrograph of calcium oxalate monohydrate (COM) crystals in the presence of 50 µg ml^{-1} of SeNPs

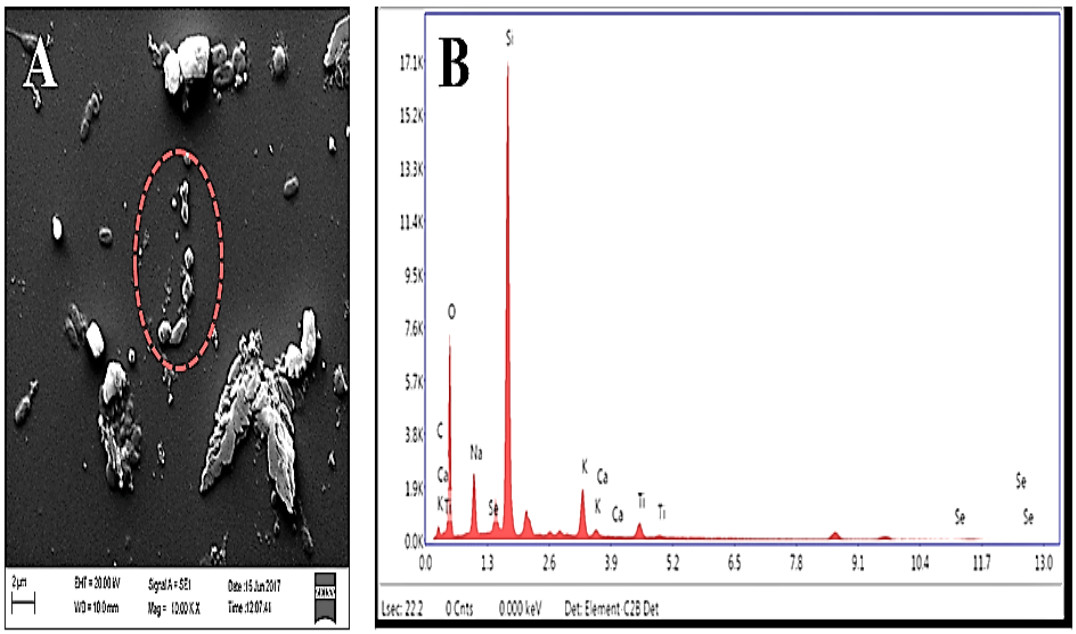

Fig. 5.28 A: SEM analysis and **B:** Energy Dispersive X-ray micrograph of calcium oxalate monohydrate (COM) crystals in the presence of 100 µg ml^{-1} of SeNPs

5.2.15 CHARACTERIZATION OF THE TeNPs BIOSYNTHESIZED DURING GROWTH BY GUSF-1

The UV absorption scan of the TeNPs in methanol showed a characteristic peak between 200 – 300 nm with absorption maxima at 204 nm (**Fig. 5.29**). The XRD pattern of the biosynthesised TeNPs is depicted in **Fig. 5.30**. The diffraction peaks at 2θ values 22.5°, 27.5°, 37.85°, 41.85° , 43.49° and 50.64° corresponds to the (100), (011), (102), (110), (111) and (201) planes of hexagonal structure of tellurium and corroborated with JCPDS card no No 065- 3370. The average crystallite size of tellurium was calculated using Scherrer's equation and was found to be 36.99 nm for the biosynthesised TeNPs by GUSF-1. Elemental analysis by EDAX exhibited a peak at 0.5 and 3.6 keV (**Fig. 5.31)**. TeNPs nanotubes with an average length size of 42 nm and an average width of 6 nm was observed during the morphological characterisation of TeNPs by the Transmission Electron Microscope (TEM) (**Fig. 5.32 A & B**). Selected area electron diffraction image exhibited diffraction rings corresponding to the (011) directions of the hexagonal phase of tellurium (**Fig. 5.32 C**).

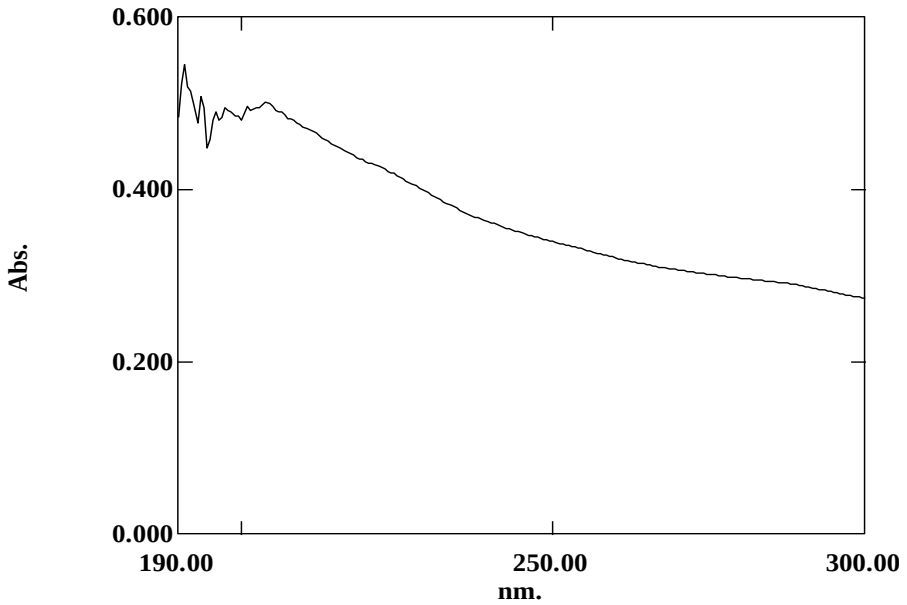

Fig. 5.29 UV Vis spectra of TeNPs biosynthesized by GUSF-1

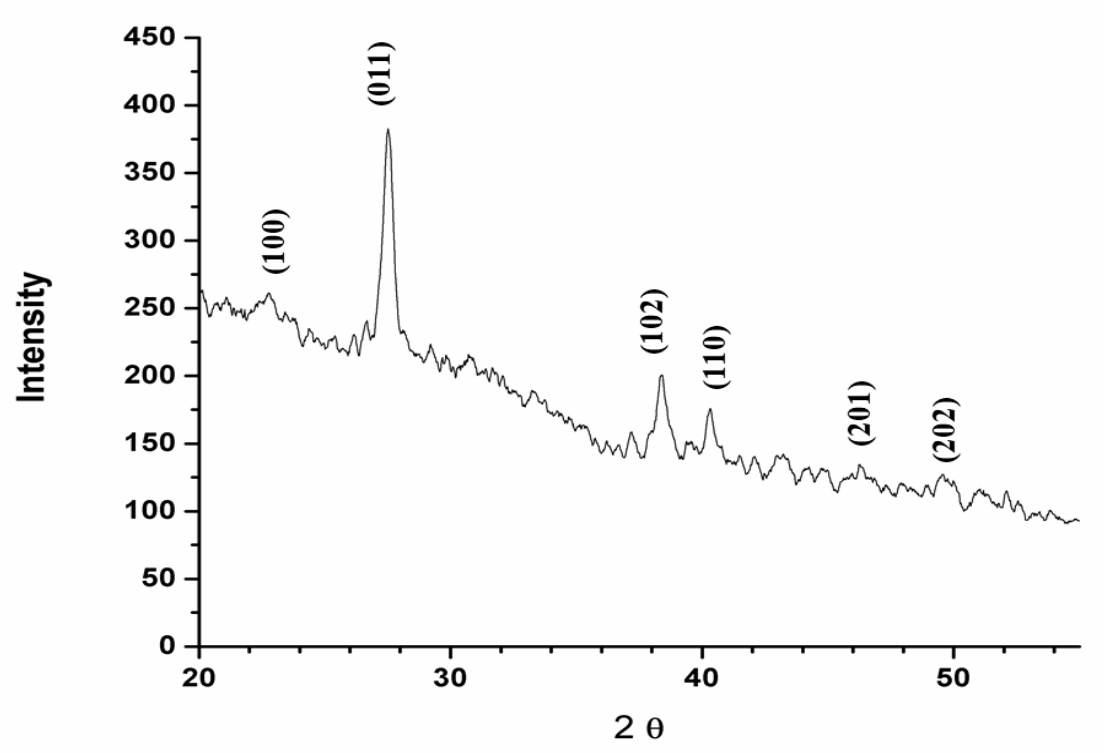

Fig. 5.30 XRD pattern of TeNPs biosynthesized during growth of GUSF-1

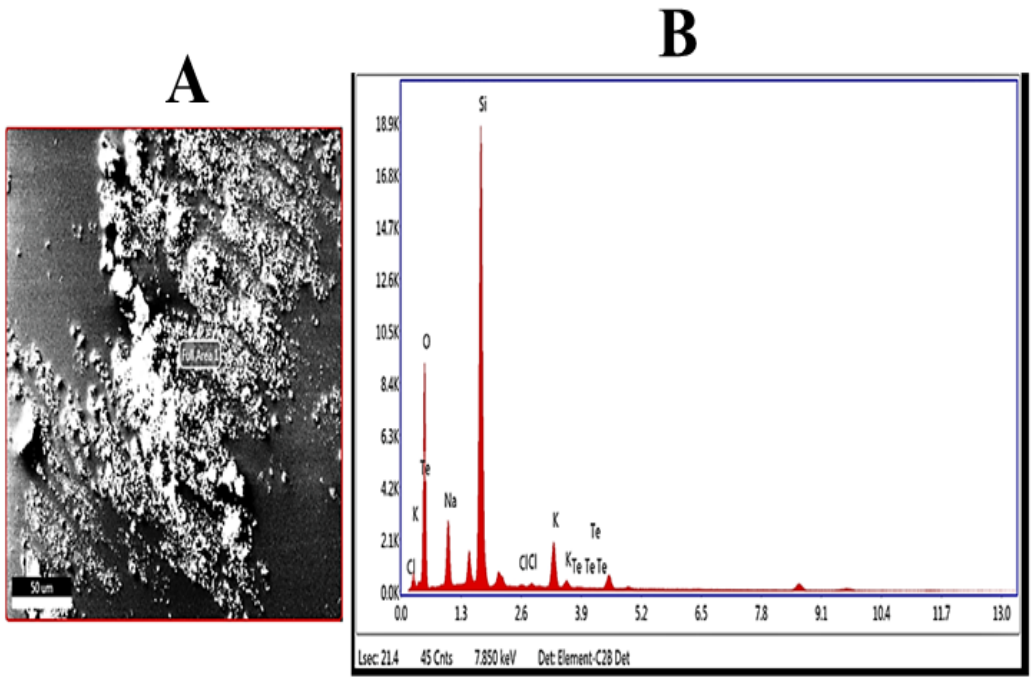

Fig. 5.31 Energy Dispersive X-ray micrograph of TeNPs biosynthesized by GUSF-1

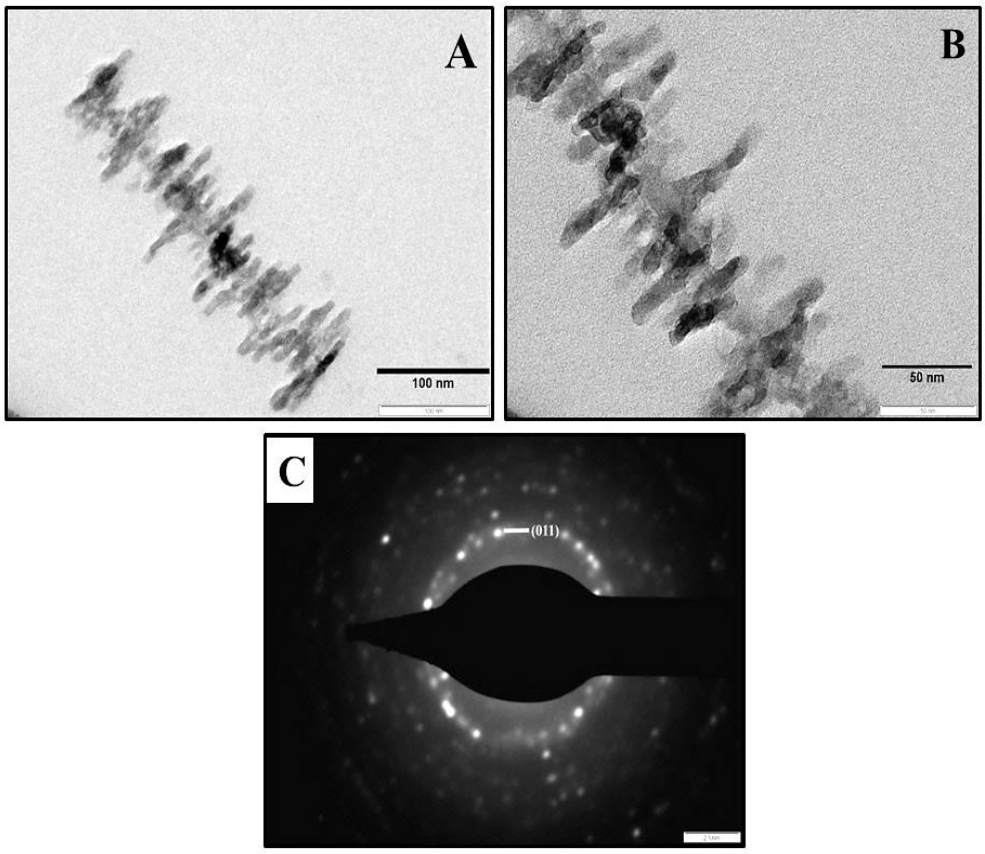

Fig. 5.32 A&B TEM micrograph showing nanorods biosynthesized by GUSF-1 obtained by a drop coating of TeNPs onto copper stubs subjected to 200 keV **C** SAED of TeNPs

5.2.16 ANTIBIOFILM POTENTIAL OF TeNPS BIOSYNTHESIZED BY GUSF-1

The ability of TeNPs biosynthesized by GUSF-1 to inhibit the formation of biofilms by *Ps. aeruginosa* ATCC 9027 was assessed. *Ps. aeruginosa* ATCC 9027 biofilms were developed in 96-well plates using Luria bertani medium supplemented with 0.2% glucose in the presence of different concentrations of TeNPs. As seen in **Fig. 5.33 A**, the control biofilm formed by *Ps. aeruginosa* ATCC 9027 is evident as seen by the crystal violet stained wells after overnight incubation of *Ps. aeruginosa* ATCC 9027 in LB broth supplemented with 0.2% glucose. **Fig. 5.34 B** depicts the

antibiofilm potential of ciprofloxacin and varying concentrations of TeNPs. A clear decrease in CV staining was observed with addition of 60 µg ml^{-1} of the antibiotic ciprofloxacin and with varying concentration of TeNPs as compared to the control biofilm formed. The biofilm formed was further quantified using the crystal violet quantification method by solubilising crystal violet with 30% acetic acid and monitoring the absorbance at 550 nm (**Fig. 5.35**). A significant 75.03% inhibition was observed with 60 µg ml^{-1} of TeNPs used whereas a 77.53% of inhibition was obtained with 60 µg ml^{-1} of the antibiotic ciprofloxacin used. One way ANOVA of the biofilm inhibition showed significant decrease in the attachment of the biofilm with increasing concentration of TeNPs used ($F= 520.856$; $p<0.001$). At the same concentration of the antibiotic and TeNPs used, the antibiofilm effect showed by the TeNPs was almost identical when compared to the effect of the antibiotic ciprofloxacin which served as the positive control.

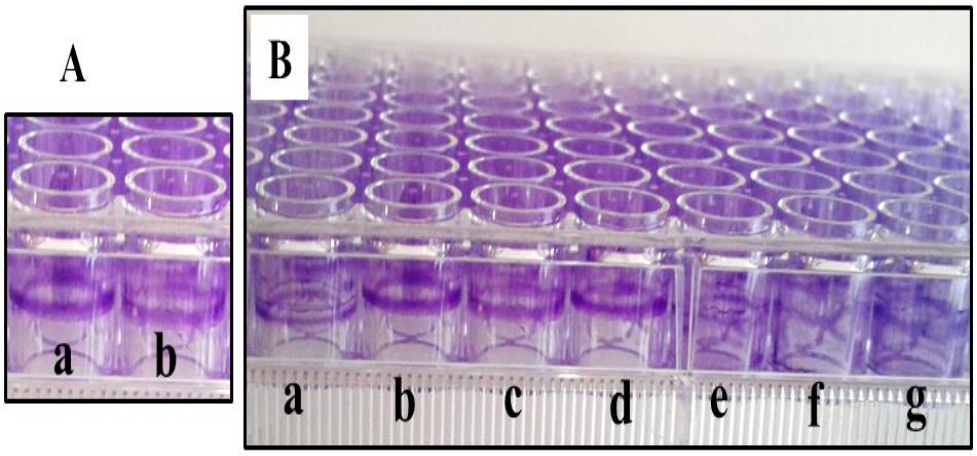

Fig. 5.33 A: Biofilm forming ability of *Ps. aeruginosa* ATCC 9027 seen by the crystal violet staining method; **Ba:** effect of ciprofloxacin for its anti biofilm activity
Bb-g: effect of different concentrations (10- 60 µg ml^{-1}) of TeNPs for its anti biofilm activity

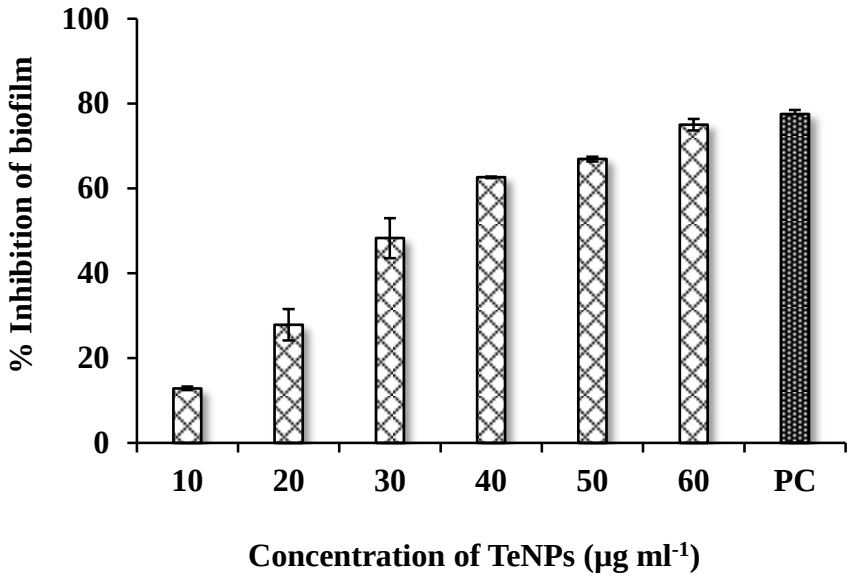

Fig. 5.34 Percent inhibition of the biofilm forming capacity with different concentrations (10 – 60 µg ml^{-1}) of TeNP and PC - positive control (antibiotic ciprofloxacin)

5.2.17 BIOGENIC SYNTHESIS OF MANGANESE OXIDE NANOPARTICLES (Mn_2O_3 NPs) BY GUSF-1

On incubation of cell lysate of GUSF-1 with an aqueous solution of 10 mM $MnSO_4.2H_2O$, at room temperature for 48 h, the reaction mixture turned brown. There was no colour change in the cell lysate or in the salt solution that were individually maintained as controls (**Fig. 5.35 A**). The reaction mixture was pelleted out, washed with sterile distilled water and the nanomaterial obtained was dried at 80°C in the oven. On drying the nanomaterial obtained was dark brown in colour (**Fig. 5.35 B**).

The FTIR spectrum of the cell lysate of GUSF-1 revealed peaks at 3400 cm^{-1}, 2966, 1668 cm^{-1}, 1537 cm^{-1}, 1436 cm^{-1} and 1100 cm^{-1}. The FTIR spectral analysis of cell lysate of GUSF-1 incubated with 10 mM $MnSO_4.2H_2O$ revealed intense absorption bands at 3220 cm^{-1}, 2960 cm^{-1}, 1666 cm^{-1}, 1550 cm^{-1}, 1369 cm^{-1},1118 cm^{-1} and a peak at 640 cm^{-1} (**Fig. 5.36**). The XRD pattern of the biosynthesized Mn_2O_3 NPs is depicted in **Fig. 5.37.** The diffraction peaks were found to be consistent with JCPDS card No 065-1123. The average crystallite size of the Mn_2O_3 NPs using Scherrer's formula of the Mn_2O_3 NPs was found to be 10 nm. The elemental analysis by EDX

exhibited absorption bands at 0.6, 5.8 and 6.4 keV (**Fig. 5.38**). The transmission electron microscopy revealed the morphology of Mn_2O_3 nanoparticles. Coin shaped Mn_2O_3 nanoparticles were observed with size ranging from 63 to 90 nm. The average size of Mn_2O_3 nanoparticles was found to be 77 nm (**Fig. 5.39 A &B**). The SAED analysis showed diffraction spots due to electron scattering (**Fig. 5.39C**).

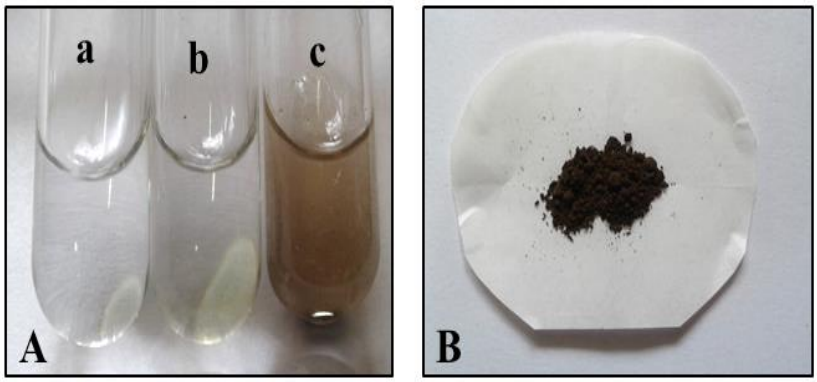

Fig. 5.35 Aa: Cell lysate **Ab:** 10 mM 10 mM $MnSO_4$. $2H_2O$ **Ac:** Incubation of the cell lysate of GUSF-1 with 10 mM $MnSO_4$. $2H_2O$ **B:** washed and dried manganese oxide nanoparticles

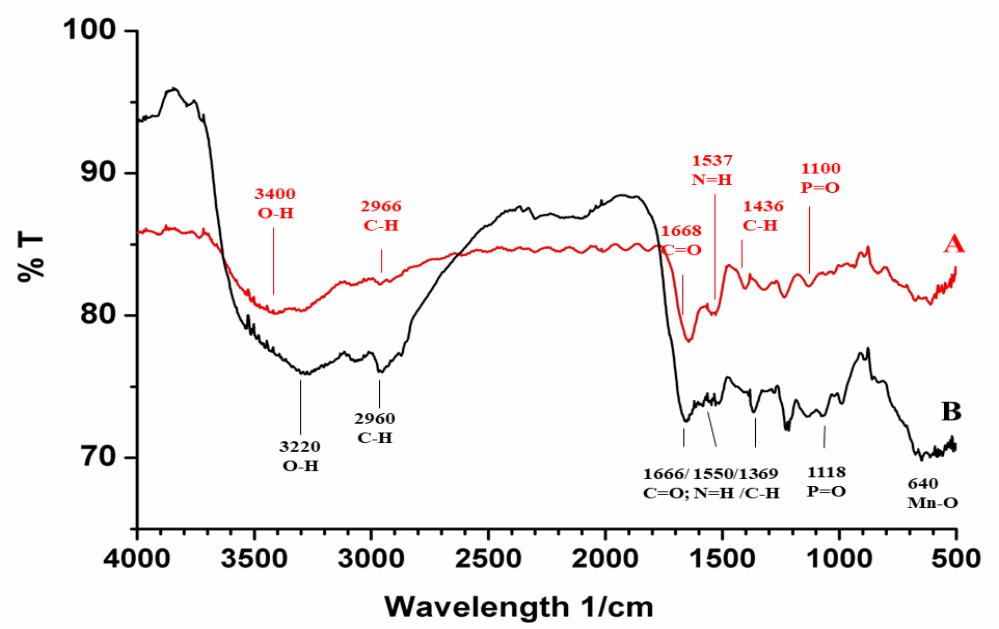

Fig. 5.36 A: FTIR spectrum of cell lysate of GUSF-1 and **B:** Cell lysate of GUSF-1 incubated with 10 mM $MnSO_4.2H_2O$

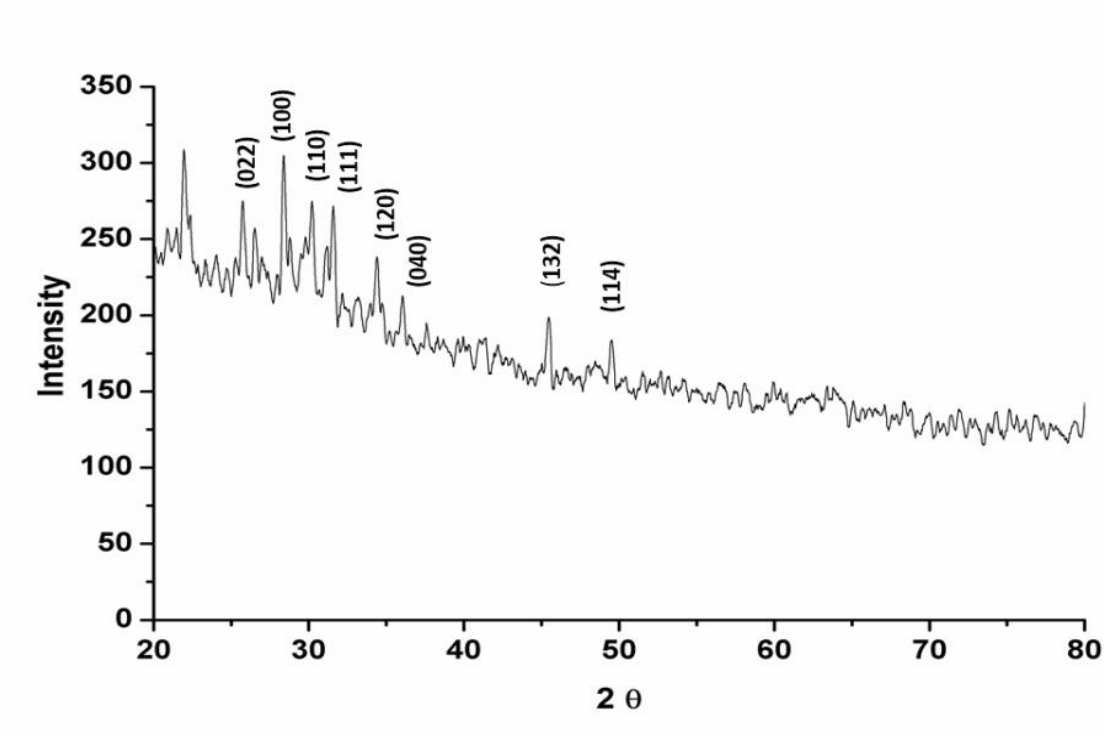

Fig. 5.37 XRD pattern of biosynthesized manganese oxide nanoparticles using cell lysate of GUSF-1

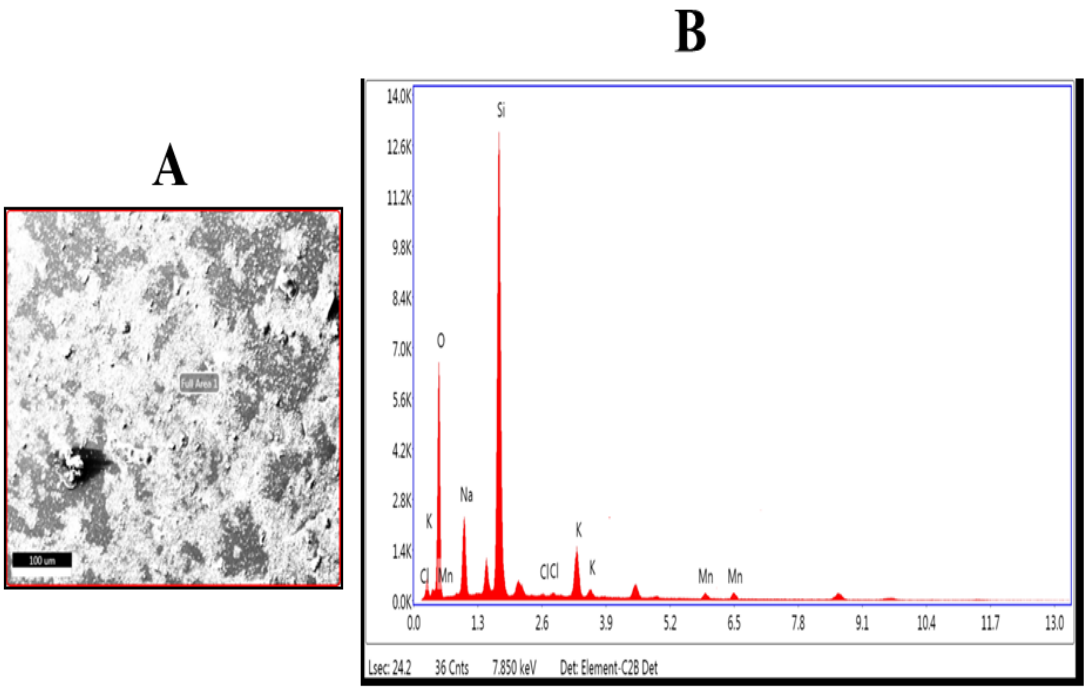

Fig. 5.38 Energy- dispersive X-ray profile of Mn_2O_3 (bixbyite) nanoparticles

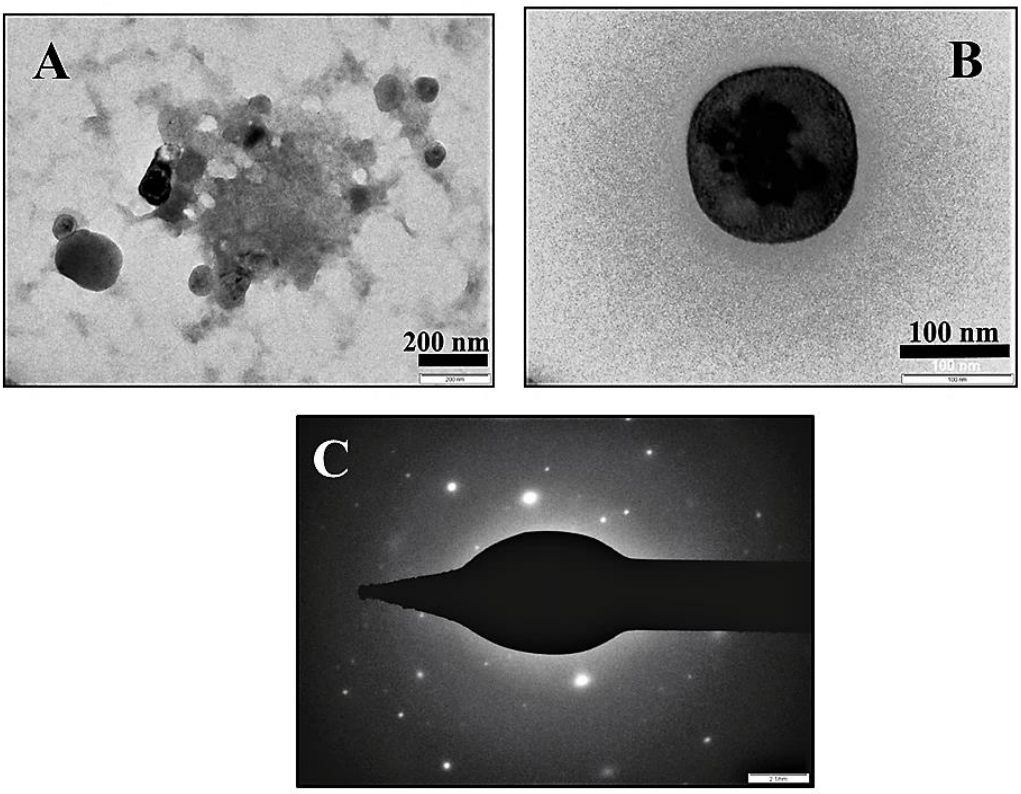

Fig. 5.39 A, B: TEM micrograph showing Mn_2O_3 nanocoins at various magnifications and **C:** SAED pattern of Mn_2O_3 nanoparticles

Table No 5.2: Comparative chart of characteristics of nanomaterial biosynthesized by GUVFFM-3 and GUSF-1

NPs	Culture	Cyrstallite domain size	Morphology	Average size
SeNPs	GUVFFM-3	12	Nanocrystals	32 nm
	GUSF-1	10	Pentagonal	Diagonal length =15nm Height of 50 nm
TeNPs	GUSF-1	36.99	Nanorods	Length = 42 nm Width = 6 nm
Bixbyite Mn_2O_3	Cell lysate of GUSF-1	10	Nanocoins	77 nm

5.2.18 EVALUATION THE ROLE OF BIXBYITE Mn_2O_3 NP AS AN ALTERNATIVE MAGNETIC PROBE IN MEDICAL DIAGNOSTIC TOOLS

The magnetic property of the sample was determined as a function of external magnetic field. The magnetic moment vs magnetic field (Magnetic Hysteresis) curve was obtained at room temperature. The curve shows a small hysteresis loop that does not saturate even at a high field typical of a super paramagnetic material. The curves (**Fig. 5.40**) show a small coercive force of 166 Oe and a remanent magnetization of 5mOe (milli Oesterds).

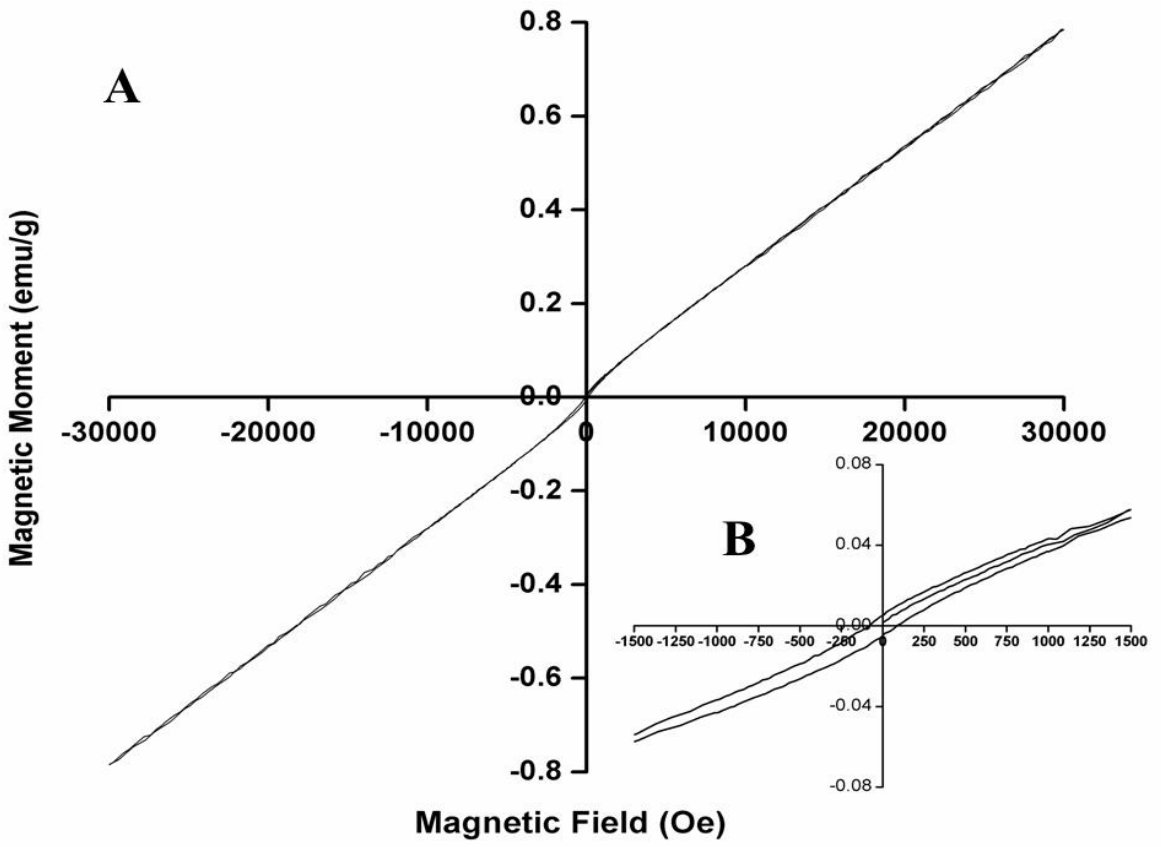

Fig. 5.40 Magnetic moment (Oesterds) vs magnetic field (emu/g) – Magnetic Hysteresis curve of Mn_2O_3 nanoparticles

5.3 DISCUSSION

Six haloarchaeal cultures *Haloferax* sp. $GUBF_3$ (ATCC BAA 646), *Halobacterium* sp. $GUBF_{11}$ (ATCC BAA 654), *Haloferax alexandrinus* GUSF-1 (KF796625), *Haloferax volcanii* GUIF2 (MH169338), *Haloferax* sp. GUIF3, *Haloferax gibonsii* GUIF4 (MG199078), *Halobacterium* sp. GUIF5 and the extremely eubacterial halophilic culture, *Chromohalobacter salexegines* GUVFFM-3 (JF330126) were screened for its ability to grow in the presence of salts of silver, selenium and tellurium. All the 7 extremely halophilic cultures grew on media incorporated with salts of silver, selenium, tellurium and growth was accompanied by colour change. Such colour change indicates reduction of salts to its zerovalent state (Saif *et al*., 2016). Various eubacterial cultures such as *Idiomarina* sp. PR 58-8, *Bacillus megaterium* BSB6 organisms have been shown to reduce silver nitrate ions, indicated by formation of brown-black coloration of the medium (Seshadri *et al*., 2012; Mishra *et al*., 2011), Similar reduction of Ag, Se and Te oxyanions accompanied by colour change to brown, red and black is reported using haloarchaeal cultures such as *Haloferax alexandrinus* (Patil and Furtado, 2014) and *Halococcus salifodinae* BK3 (Srivastava *et al*., 2013; 2014 and 2015).

Minimum Inhibitory Concentration (MIC) of metal for inhibiting growth was determined. The MIC of Ag^{1+} obtained for GUVFFM-3 and GUSF-1 was found to be 1.2 and 1.5 mM, respectively. **Both our cultures were resistant to concentrations 30 times more than the value reported** for *Chromobacterium marismortui* ATCC 17056 and *Halomonas elongata* ATCC 33173 which has MIC of 0.05 mM silver (Nieto *et al*., 1989). The **MIC of SeO_3^{2-} and TeO_3^{2-}** obtained **for GUVFFM-3 was found to be 90 mM amd 0.6mM while for GUSF-1 the MIC value was 120 mM and 0.55mM** respectively. Studies on MIC studies of sodium selenite and potassium tellurite with haloarcheaon *Halococcus salifodinae* BK3 reported a value of 6 mM and 5.5 mM respectively (Srivastava *et al*., 2014). Several bacteria belonging to ß-*Proteobacteria* and *Bacilli* isolated from soil and water samples collected from selenium-contaminated sites in India have seen to exhibit very high MIC values ranging from 300 to 600 mM for sodium selenite (Ghosh *et al*., 2006). In another study an isolate from the hypersaline selenite contaminated solar evaporation ponds;

Halomonas group was found to be tolerant of Se at concentrations up to 2 M (De Souza *et al*., 2001).

Four haloarchaeal cultures namely $GUBF_{11}$, GUIF2, GUIF3, GUIF4 and the eubacterial biont GUVFFM-3 was seen to biosynthesize AgNPs as evidenced by the formation of yellowish brown to brown colouration in the reaction mixture. This is indication of formation of silver nanoparticles (Eustis and El-Sayed, 2006). The absorption maxima of the reaction mixture ranged between 400-450 nm for the different cultures. This characteristic brownish colouration and the absorption maxima in the range between 400-450 nm is attributed to surface plasmon resonance which arises due to collective excitation of conduction electrons in metals. Similar observations are reported by Patil and Furtado, 2014. It was also interesting to observe that AgNPs synthesis by cell lysates of all the cultures occurred only in the presence of sunlight. No biosynthesis took place in the dark. Previous reports among eubacteria using culture supernatants of *Pseudomonas meridiana* (MTCC 4993), *Arthrobacter kerguelensis* (DSM 15797), *Arthrobacter gangotriensis (*MTCC 690), *Bacillus indicus* (MTCC 4374) and *Bacillus cecembensis* (MTCC 9127) in sunlight are also available (Shivaji *et al*., 2011). AgNPs synthesis in sunlight using growing cells is reported by Patil *et al*. (2014). In contrast to our result, Maduabuchi *et al*. (2018) reported the use of cell lysate for *Bacillus subtilis* for the biogenic formation of AgNPs in the dark. **The biogenic synthesis of AgNPs by the eubacterial genera *Chromohalobacter* is a first report**. It is important to note that the biosynthesis of AgNPs by this cultutre was also exclusively in the presence of sunlight.

The cultures GUVFFM-3 and GUSF-1 were also capable of biosynthesizing SeNPs and TeNPs during growth, using whole cells and cell lysate. The red colouring obtained in the reaction mixture, is characteristic of monoclinic colloidal selenium nanoparticles, which is due to surface plasmon excitation (Vieira *et al*., 2017). Studies on resistance to tellurites and formation of black precipitates, like in our case, is indicative of nano Te^0 and has been reported in eubacteria such as *Escherichia coli*, *Pseudomonas aeruginosa*, *Enterobacter* sp. YSU, *Roseococcus thiosulfatophilus*, *Erythrobacter litoralis* and *Erythromicrobium ramosum* (Turner *et al*., 1999; Summers and Jacoby, 1977; Jasenec *et al*., 2009; Yurkov *et al*., 1996). The eubacterial isolate *Pseudomonas pseudoalcaligenes* strain Te (number KF055346.1)

from the Sirch hot springs in Iran has been reported to biosynthesize Te nano rods. FT-IR analysis of growing cells and the cell lysate used for biogenic synthesis of SeNPs and TeNPs revealed the involvement of hydroxyl groups, protein moieties in reduction of selenite and tellurite.

In this study the reduction of selenite to Se^0 was investigated by two different cultures belonging to two different domains, extremely halophilic eubacterial *Chromohalobacter salexegines strain* GUVFFM-3 (JF330126) and haloarchaeon *Haloferax alexandrinus* GUSF-1 (KF796625). The study was carried out in the presence of 5mM SeO_3^{2-} was aimed at determining the efficiency of aerobic SeO_3^{2-} reduction to SeNPs within the two domains, to investigate the biofactors involved in the SeO_3^{2-} reduction and SeNPs formation, and to characterize the SeNPs. The brick-red particulate matter formed in the presence of SeO_3^{2-} interfered with the absorbance measurements at 480/ 600 nm giving a false positive result. Therefore, growth was evaluated by determining the colony forming units/ ml of culture broth. Growth studies determined by estimating colony forming units at regular time intervals showed an overall final cell yield of 1 log unit and about 2 log units for GUVFFM-3 and GUSF-1 respectively more than the control values. This could be attributed to the fact that selenium is a micronutrient and an essential trace element with importance in several physiological functions, such as biosynthesis of selenocysteine, coenzyme Q, glutathione peroxidase or thioredoxin reductase (Navarro-Alarcon and López-Martínez, 2000). The control flask containing only medium and SeO_3^{2-} but without either of the cultures did not exhibit the change of color, showing that the red colour is an indication of biogenic formation of SeNPs from SeO_3^{2-}.The participation of the cultures in the selenite reduction from selenite to elemental selenium is required.

Estimation of residual SeO_3^{2-} was first attempted by chemically reducing it with ascorbic acid using the method of Malhotra *et al*. (2014) but since the product started to agglomerate and interfered with the spectroscopic quantification, the SeNPs formed had to be converted to another form. We further employed the method of Biswas *et al*., 2014, and **solubilised the SeNPs using 1 M Na_2S which could be read at A_{475} instead of A_{500}.** GUVFFM-3 and GUSF-1 growing in the presence of 5mM SeO_3^{2-}, was able to reduce SeO_3^{2-} to SeNPs. Moreover, GUVFFM-3 in the presence 5 mM SeO_3^{2-} was able to reduce to 74% of SeO_3^{2-} during the exponential phase and the

remaining in the stationary phase, while, the same trend was observed for GUSF-1, growing in the presence of 5 mM SeO_3^{2-}, with 94% reduction occurred during the exponential growth and the remaining in the stationary phase. **Selenite reduction was seen to be growth associated**. The reduction occurred started at the beginning of the exponential phase and to the beginning of the stationary phase. Selenite reduction in the exponential phase has been reported in various eubacterial cultures; *Rhodobacter sphaeroides* and *Rhodospirillum rubrum* (Kessi *et al*., 1999) *Rhodopseudomonas palustris* strain N (Li *et al*., 2014), *Rhodobacter sphaeroides* (Bebien *et al*., 2001), *Burkholderia fungorum* strains (*B. fungorum* DBT1 and *B. fungorum* 95) (Khoei *et al*., 2017) similar to what was observed in our results. Our result of GUSF-1 can be also correlated with the results of growth and selenite reduction available on the haloarchaeon from genus *Halococcus*, which was seen to show similar behaviour (Srivastava *et al*., 2014). Despite the reduction process running parallel to the microbial growth, red colour in flask was visually noticed only at 16 hours of incubation for GUVFFM-3 and within 8 hours of incubation for GUSF-1. Besides this **a remarkable clear garlic acid-like smell was associated with growing cells of GUVFFM-3 and GUSF-1** cultured in the presence of selenite, thus suggesting that both these strains might be also able to produce/ generate organic volatile forms of selenium as an alternative resistance strategy. It has been described that some bacteria are able to methylate selenium oxyanions as part of their resistance mechanisms generating organic methylated forms, such dimethyl selenide or dimethyl diselenide, that share a garlic acid-like smell (Prigent-Combaret *et al*., 2012). Production of volatile selenium compounds by regulatory proteins has been previously suggested in other bacteria such *R. rubrum* (Kessi *et al*., 1999) and *Rhodopseudomonas palustris* strain N (Li *et al*., 2014). Delayed formation of elemental selenium with regard to selenite depletion had also been found in *Bacillus mycoides* SeITE01 attributing this delay to initial reactions transforming selenite into certain intermediates, such as selenodiglutathione or selenotrisulfides, before conversion to elemental selenium (Lampis *et al*., 2014). For instance, in *Rhodobacter sphaeroides* (Van Fleet-Stalder *et al*., 2000) and *Ralstonia metallidurans* CH_34 (Sarret *et al*., 2005) organic selenide (RSeR) is formed as intermediate.

Similar to the result on the pigment production in cultures belonging to the genus *Haloferax* discussed in Chapter II, the acetone extracts of the culture GUSF-1 also

showed the characteristic absorptions of red carotenoids at 463, 489 522, and two cis peaks at 386, 368 . There were peaks also noted at 304 and 317 nm respectively. **The presence of selenite in the medium during growth decreased the intensity of almost all the pigment peaks and also abolished some of them**. The decrease in carotenoid biosynthesis in the presence of Se treatment to a plant species, *Arabidopsis thaliana* was reported as a result of the downregulation of phytoene synthase by Se at the beginning of the carotenoid biosynthesis pathway (Sams *et al*., 2011). Similarly in the carotenoid biosynthetic pathway of haloarchaea, the enzyme phytoene synthase, encoded by the gene CrtB is reported to condense two geranylgeranyl pyrophosphate (GGPP) molecules, to yield the colourless carotenoid phytoene. Lycopene is than generated from phytoene via a series of desaturation reactions (Yang *et al*., 2015). Se NPs biosynthesized by GUSF-1 may also be involved in down regulating the gene CrtB hence interference in the carotenoid biosynthetic pathway of GUSF-1.

Elemental selenium can accumulate in the cytoplasm or outside the bacterial cells (Khoei *et al*., 2017). Different location for selenite reduction have been identified in different organism; namely cytoplasm in *E. coli* (Debieux *et al*., 2011), periplasm in *Thauera selenatis* (DeMoll-Decker *et al*., 1993) and *E. coli* (Debieux *et al*., 2011), cytoplasmic membrane in *Bacillus mycoides* SeITE01 (Lampis *et al*., 2014), extracellularly in *Rhodobacter* sp. strain NKPB030619 (Yamada *et al*., 1997) and *Bacillus mycoides* SeITE01 (Lampis *et al*., 2014) and associated to EPS (Jain *et al*., 2015). To **localize selenite reduction, *in vitro* selenite reduction enzyme assays were performed** by testing different intracellular fractions containing proteins, as well as EPS and extracellular growth spent medium (supernatant). Our results showed that in the case of GUVFFM-3, no selenite reduction activity to SeNPs was detected in the spent medium and EPS whereas soluble protein and membrane fractions evidenced selenite reduction through the production of red elemental selenium. Even in the absence of an electron donor, selenite reduction occurred. Whereas in the case of GUSF-1 even the spent medium was seen to reduce selenite to red Se^0. Using two enzyme inhibitors sodium arsenite; an inhibitor of glutathione synthesis and sodium azide; an inhibitor of nitrate reductase enzyme, we tried to implicate the role of these two enzymes in selenite reduction. Sodium azide and sodium arsenite was seen to inhibit selenite reduction in GUVFFM-3 and GUSF-1, confirming the involvement of nitrate reductase and glutathionine reductase in selenite reduction. Though no

inorganic nitrogen source was added to the medium in which these cultures were grown, tryptone yeast extract medium which is used for growth is a rich source of organic nitrogenous compounds, hence the presence of inducible nitrate reductase enzyme is confirmed. Presence of nitrate reductase activity is reported in *Chromohalobacter salexigens* DSM 3043 (Ates *et al*., 2011) and in *Halococcus salifonidae* BK18 (Srivastava *et al*., 2014). As *Chromohalobacter salexegines strain* GUVFFM-3 (JF330126) belongs to the gamma Proteobacteria group (Arahal *et al*., 2001), glutathione (GSH) is the most abundant thiol group present (Newton and Fahey, 1989). One of the general pathways of selenite reduction is through chemical reactions with thiol groups of proteins known as Painter-type reaction (Painter, 1941). The mechanism implies that selenite is transformed by glutathione reductase as main electron donors to hydrogen selenide (H_2Se) via selenodiglutathione (GS-Se-SG) and glutathionyl selenol intermediates. Initially unstable selenodiglutathione is produced that reacts with the residual GSH to form diglutathione (GSSG) and elemental selenium but since GSH is absent in Archaea, hence they would lack the glutathione-dependent reduction system for the dissimilatory reduction of selenite that is involved in gamma Proteobacteria group (Fahey, 2013), these glutathione deprived microrganisms contain high levels of other thiols, including coenzyme A, cysteine, lipoamide and pantetheine, with their corresponding thiol/disulfide oxidoreductases (Newton and Fahey, 1989). As selenite is highly reactive towards thiols (Painter, 1941; Ganther, 1971), such oxidoreductases are possibly involved in the reduction of selenite in these organisms. In halobacteria, γ-glutamyl-cysteine (γ-GC) is the predominant thiol, which is more stable in high salt concentrations than glutathione and they possess bis-γGC reductase activity **(**Newton and Javor, 1985; Fahey 2013; Sundquist and Fahey, 1989). Since on addition of sodium arsenite to soluble proteins, membrane fraction and the supernatant of GUSF-1 failed to produce the red colour, hence we speculate that sodium arsenite inhibited bis-γGC reductase activity involved in the reduction. To the best of our knowledge, this is the first report on the involvement of this enzyme in selenite reduction in Haloarchaea and is worth further investigating.

Taken together, these results reveal that GUVFFM-3 and GUSF-1 is the first example of a member of the genus *Chromohalobacterium* an eubacterial culture and GUSF-1 a culture belonging to *Haloferax* genus that is able to aerobically grow in the presence of selenite, hence opening new avenues for its application in bioremediation strategies. The ability of both the cultures to produce SeNPs, together with the fact that these can grow on sodium benzoate and GUSF-1 could also degrades different toxic aromatic hydrocarbons opens the bioprospect for the use for haloarchaea in general bioremediation strategies as well as in specific phytoremediation on selenium contaminated soils.

The nanomaterial obtained after biosynthesis was characterized using optical, crystallographic and microscopic techniques. The characteristic red colour of the SeNPs was due to the excitation of the surface plasmon vibrations of the monoclinic Se particles and provided a convenient spectroscopic signature of their formation. The UV absorption scan of the SeNP biosynthesized by GUVFFM-3 and GUSF-1 showed a characteristic peak at 240 nm and 239 nm indicating the formation of selenium nanoparticles. Fesharaki *et al*. (2010) showed that the Se NPs synthesised by *K. pneumonia* showed absorption at 248 nm whereas the SeNPs synthesized by *H. salifodinae* BK18 showed absorption maxima at 270 nm.

Raman scattering has been proven to be a versatile technique to characterize nanostructured materials. This technique provides information on the crystalline quality of samples and the Raman frequency is characteristics for material, structure and the mechanical forces of the crystals which have an effect on the sample. An intensive peak at 254 cm^{-1} was observed in the Raman spectra of the SeNP biosynthesized by GUVFFM-3 and GUSF-1 indicating the presence of monoclinic Se. Furthermore, the absence of any signals of the 264 cm^{-1} peak for amorphous selenium indicates that no amorphous selenium is present in the prepared sample biosynthesized by the two cultures. Characteristic Bragg's peaks confirmed the presence of well-prepared crystalline nanomaterial and corroborated with the standard JCPDS data, the EDX data confirmed the presence of elemental selenium for both the samples. TEM revealed nanocrystals biosynthesized by GUVFFM-3 and **pentagonal shaped nanoparticles biosynthesized by GUSF-1**. Reports of production of nano rods and nanospheres are available among *Halococcus* (Srivastava *et al*., 2014),

spherical and oblong produced by *Bacillus mycoides* SeITE01 (Lampis *et al*., 2014), spherical produced by *Burkholderia fungorum* strains (*B. fungorum* DBT1 and *B. fungorum* 95) (Khoei *et al*., 2017). The production of **pentagonal shaped nanomaterial** is not reported.

Urolithiasis, the formation of calcium oxalate (CaC_2O_4) urinary calculi, is one of the oldest documented diseases known to man (Grover *et al*., 1998). Calcium oxalate monohydrate (COM) crystals exhibit a greater degree of attachment to renal tubule cells compared with (Calcium oxalate dihydrate) COD crystals (Lieske *et al*., 1995) and theoretical calculations also suggest that COM crystals may have a stronger affinity to the cell membranes than COD crystals (Mandel *et al*., 1994). Crystal formation from a saturated solution may be prevented by small amount of chemicals which are known as crystallization inhibitor molecules. Some inhibitors are small biological molecules such as citrate, amino acids, while others are large biological molecules such as Tamm-Horsfall, uromodulim and osteopontin (Grohe *et al*., 2007) Similar to results obtained in a study carried out by Liang et al., 2009, **our results also proved that SeNPs synthesized by GUSF-1 was seen to play the role of crystallization inhibitor molecules and modulate the shape of calcium oxalate crystals from clear defined crystal borders to irregular spherical forms**. Elemental analysis by EDX further confirmed the presence of Ca, C, O and Se in the crystals that were formed. Reports that SeNPs exhibit low cytotoxicity compared with many other nanoparticles makes them apt in therapeutic activities for medical applications (Hatfield *et al*., 2014).

Synthesis of tellurium nano-rods and irregular nanospheres have been reported in bacteria such as *Bacillus selenitireducens*, *Bacillus* Sp. BZ and *Sulfurospirillum barnesii*, *Pseudomonas fluorescens* K27, *Rhodobacter capsulatus*, and *Shewanella oneidensis* (Baesman *et al*., 2007; Zare *et al*., 2012; Basnayake *et al*., 2001; Borghese *et al*., 2004; Klonowska *et al*., 2005). Studies on resistance to tellurates and tellurites and generation of black precipitates indicative of nano Te^0 have been reported in some bacteria such as *Escherichia coli*, *Pseudomonas aeruginosa*, *Enterobacter sp. YSU*, *Roseococcus thiosulfatophilus*, *Erythrobacter litoralis*, and *Erythromicrobium ramosum* (Turner *et al*., 1999; Summers and Jacoby, 1977; Jasenec *et al*., 2009; Yurkov *et al*., 1996). In the present study, an attempt was made to synthesise biogenic

TeNPs using the haloarchaeon *Haloferax alexandrinus* GUSF-1 (KF796625). Well crystallised Te nanorods (average length 42 nm and width of 6 nm) **forming rosette like structures was biosynthesized**. The occurrence of such rosettes composed of several Te nano rods by tellurium resistant bacterial strains such as *B. selenitireducens* was previously reported to be due to the adherence of Te nanorods to each other through electrostatic interaction (Baesman *et al*., 2007). Another report of an eubacterial culture *Bacillus selenitireducens* haloalkaliphile isolated from Mono Lake which initially form nanorods (32 nm in diameter × 260 nm in length) which cluster together, forming larger rosettes (Baesman *et al*., 2007). Among reports from the archaeal domain, Te needle-shaped nanoparticles biosynthesized by haloarcheaon *Halococcus salifodinae* BK3 is reported with an average diameter of 10 nm and length of 44 nm (Srivastava *et al*., 2014).

Biofilms are a consortium of microbes that attached to either a biotic or an abiotic surface and start growing on it (Srey *et al*., 2013). The bacteria in biofilms are highly persistent and have strong resistance mechanism towards antimicrobial treatment (Lewis, 2001). According to the Centre for Disease Control and Prevention (CDC), the bacterium is the fourth most common isolated nosocomial pathogen, accounting for 10% of all hospital-acquired infection, it is reported as an emerging opportunistic pathogen in the clinics owing to its increased antibiotic resistance and the ability to form biofilms and it is well established as a model organism for studying bacterial biofilm formation (Rasamiravaka *et al*., 2015). TeNP has been reported for its antibacterial activity (Srivastava *et al*., 2015). TeNPs are reported to be better anti-bacterial agents as compared to silver nanoparticles and sodium tellurite (Lin *et al*., 2012). Hence we evaluated the biofilm formation of *P. aeruginosa* ATCC 9027 and the anti- biofilm activity of TeNP against *P. aeruginosa* ATCC 9027 using the Crystal Violet (CV) Assay (O'Toole, 2011). The Luria Bertani medium was supplemented with 2% glucose which is reported to initiate biofilm formation (Srey *et al*., 2013). **Different concentrations of TeNPs ranging from 10 to 60 µg ml^{-1} was seen to eradicate the biofilm in a dose dependent manner** and the positive control was 60 µg ml^{-1} of the antiobiotic ciprofloxacin. The biofilms formed overnight were stained by the crystal violet and solubilised by acetic acid and spectrophotometrically quantified. Biogenic TeNPs have been investigated for their potential bactericidal activity. Zare *et al*. (2012) demonstrated antibacterial activity of TeNPs against

different clinical isolates (*S. aureus*, *P. aeruginosa*, *S. typhi* and *K. pneumonia*), with an MBC (minimum bactericidal concentration) between 125 and 500 mg L^{-1}. The concentration required to eradicate an already formed biofilm structure using TeNPs is over 150 mg L^{-2} (Radzig *et al*., 2013), which happens to be 15 times more than the minimum value reported in our case.

The coastline inundating the state of Goa is an active waterway for transporting of mining ores excavated from the mining areas of Goa. This process of transportation and anthropogenic human activities is responsible for run off waters to be released in the Arabian sea. Manganese-oxidizing micro-organisms are useful for treatment of Mn-contaminated water (Han *et al*., 2006). The haloarchaeon used in this study, *Haloferax alexandrinus* GUSF-1 (KF796625) is an inhabitant of solar salts from Siridao Goa-India and grows optimally at 42ºC in an aerobic environment, and is seen to tolerate NaCl concentration upto 35%. Among most of transition metal oxides, manganese oxides attract a broad interest, as they can exist in more than five easily exchangeable transition states with various structural forms over a wide range of temperatures, up 1200°C (Brock *et al*., 1998). Manganese oxides have various catalytic applications due to highly efficient redox properties, and the mixed valence has been confirmed to be important in redox catalysis as well as in energy and electron transfer (Tian *et al*., 1997). All oxidation states of manganese oxides (II, III, IV, and VII) have significant advantages over other oxidants in removing organic pollutants (Tu *et al*., 2015). In view of above, the potential of the culture to oxidise manganese was evaluated. The cell lysate obtained from lysis of the cells of GUSF-1 was incubated with manganese sulphate at ambient light and at room temperature. After 48 hours, **there was accumulation of dark brown precipitate in the reaction mixture which was seen to settle at the bottom of the tube, which was an indication that manganese oxide was formed**. A similar result has been reported in previous studies in a eubacteria *Ps. putida* strain MnB1 (Toner *et al*., 2005). The FTIR spectral analysis of cell lysate used for biogenic synthesis of manganese oxide revealed the involvement of hydroxyl groups, amide I (C=O) and amide II (N=H) groups, CH_2 and CH_3 groups. A weak peak due to the strectching of the Mn-O was also detected in the dried reaction mixture at 640 cm^{-1}. Similar peak is also reported by Parikh and Chorover, 2005. **The crystalline peaks of the XRD patterns at 0.6, 5.8 and 6.4 keV typically belong to bixbyite Mn_2O_3 NPs** as compared with position

and relative intensity of peaks closely resemble to the data reported by Toner *et al*. (2005). Energy dispersive X-ray analysis confirmed the presence of elemental manganese and oxygen and TEM analysis revealed the presence of **coin shaped Mn_2O_3 NPs.** Hosseinkhani and Emtiazi, 2011 have reported a gram-negative bacterium *Acinetobacter* isolated from Persian Gulf water could produce nanosized extracellular bixbyite-like Mn_2O_3. Magnetic resonance imaging (MRI) is a routine diagnostic tool in modern clinical medicine and majority of the MRI contrast probes are currently based on gadolinium (Gd^{3+}) in the form of paramagnetic chelates (Caravan, 2006). However their uses are mostly associated with nephrogenic system fibrosis (NSF), which suggests a need of finding alternatives (Langer *et al*., 2012). Recently, nanoparticles (NPs) have been extensively used in biomedical applications and among which Mn-based NPs are regarded as promising alternatives to MRI probes due to their lower intrinsic toxicity than that of Gd^{3+} is receiving attention. The magnetic property of the Mn_2O_3 NPs was determined as a function of external magnetic field. The **MH curve obtained had a small coercive force and remnant magnetization**. This easy reversibility of the curves **is typical of a soft magnetic material having a low anisotropy**. This makes them **ideally suited to be used as a magnetic probe**. No reports of synthesis of bixbyite Mn_2O_3 nanoparticles has been reported in the haloarchaeal domain.

This chapter conclusively records the involvement of **two representative cultures** belonging to **different domains** in the **biogenic formation of Selenium and Tellurium** nanoparticles. It also highlights the use of **selenium nanoparticles in the shape modulaton of calcium oxalate crystals** and **tellurium nanoparticles as antibiofilm material**. The formation of **bixbyite Mn_2O_3 nanoparticles by the haloarchaeaon is a novel report**.

Summary

The present thesis entitled **"Bioprospecting with Marine Halophilic Eubacteria and Haloarchaea for Bioactives"** details in five different chapters, the research effort directed at studying the bioprospects of marine extremely halophilic eubacterial and haloarchaeal cultures isolated from solar salts, estuarine sediments from estuarine and a euryhaline biont from a sponge for production of various bioactives such as extremozymes, aromatic oxgenases, antibacterial activity, halocins, antigenotoxic and antioxidant compounds, structural and functional biomolecules and biogenic synthesis of nanoparticles

Chapter I "**Biotechnological Potential of Marine Extremely Halophilic Eubacteria and Haloarchaea - Advancement in Bioprospecting**" points out the importance of the subject of bioprospecting with/ in marine cultures, which in the context of this study is restricted to extremes of salinity and hence marine extremely halophilic eubacteria and haloarchaea of Domain Archaea. It also brings out how such cultures exposed to industrial, chemical pollution and oxidative stress in their natural habitats, are expected to overcome various stressors and in turn could be a source of bioactives that could possibly be harnessed/ trapped. It also unveils how globally; studies on haloarchaea are taken up as front line research to harness their biomolecules, both active and structural, keeping in mind their industrial and biotechnological potential. Routine conventional methods as well as front line methods of bioprospecting such as (i) Sequence-based metagenomics (ii) Function-based metagenomics (iii) Chemical profiling using state of art instrumentation, used for characterization and identification of biomolecules are described. A brief on key features on the two extremely halophilic cultures representing the screened isolates from the domain eubacteria and archaea, namely; eubacterial *Chromohalobacter salexigenes* GUVFFM-3 (JF330126) and the haloarchaeon *Haloferax alexandrinus* GUSF-1 (KF796625) used for their bioprospective assessement and comparison are also added.

Chapter II "**Bioprospects of Extremely Halophilic Eubacteria and Haloarchaea as Producers of Bioactives**" records the production of hydrolytic extremozymes such as amylases, lipases by extremely halophilic eubacteria and haloarchaeal cultures from coastal solar salt-pans and estuarine sediments using the conventional plate

technique and observing either zones of decolourization on flooding with lugols iodine or precipitation around fully grown colonies. Amylolyitc and lipolytic producers constitute 28% of the total cultures screened. Extremely halophilic eubacterial amylase was produced by the genera *Alteromonas* and *Chromohalobacter* while the haloarchaeal amylase and lipase were produced by *Halobacterium, Haloferax, Haloarcula, Halorubrum* and *Halococcus* genera and also by *Natrialba* and *Natronomonas* repectively. The highest Shannon-Weiner Diversity Index 'H' for amylase and lipase producers was 1.71 and 1.86 and came from cultures from Ribandar for Agarwada salt pans respectively. *Chromohalobacter salexegines* strain GUVFFM-3 (JF330126) and GUIF4 were highest producers of amylase and lipase respectively. Screening the 117 cultures for presence of aromatic oxygenases was carried out using the ability of the cultures to grow on sodium benzoate as a sole source of carbon. Each of the cultures was grown in 20% NSM with 0.1% sodium benzoate. A total of 69 cultures were found to be positive from a total of 117 screened.Based on maximum growth obtained in 20% NSM with 0.1% sodium benzoate, GUIF2, a haloarchaea from the estuarine sediments of Betim Jetty was selected for further studies on sodium benzoate degradation.

Morphological, biochemical, chemotaxonomic and 16S ribosomal RNA analysis of GUIF2 was found to be related with 99% similarity to *Haloferax volcanii* strain DS2 and hence identified it as *Haloferax volcanii* and was deposited at GenBank with accession number MH169338. The culture GUIF4 was found to be related with 99% similarity to *Haloferax gibbonsii* strain ARA6 and hence was identified as *Haloferax gibbonsii* and was deposited at GenBank with accession number MG199078. *Haloferax volcanii* GUIF2 (MH169338) produced catechol from sodium benzoate and the benzene ring was cleaved via the ortho pathway with the involvement of catechol 1, 2 dioxygenase forming *cis-cis* muconic acid, the formation of which was monitored at 260 nm. The culture also grew in 0.1% petrol/ benzene / castrol oil and lindane as a sole source of carbon.

Antagonistic activity showed that only 6 haloarchaeal cultures from a total 30 screened, were positive against 4 human pathogens *S. aureus* ATCC 6538, *S. typhimurium* ATCC 14028, *S.* abony ATCC 6017 and *C. albicans* 10231 with zone sizes of inhibition ranging from 8 – 12 mm. The cultures positive for activity were

Halobacterium sp. GUIF5, *Natrinema* sp. $GUFF_{231}$, *Natrialba* sp. $GUFF_{82}$, *Haloferax volcanii* GUIF2 (MH169338), *Haloferax gibbonsii* GUIF4 (MG199078) and *Halobacterium* $GUBF_5$ (ATCC BAA 647). Screening for halocin production revealed a great diversity in production. Interactions within the *Haloferax* genera and *Halobacterium* were also observed. The study reports for the first time halocin production by *Natronococcus* sp. $GUFF_{233}$ from the solar salt sample of Siridao.

Protogonistic activity against human pathogens was evident by formation of zones of exhibition around the wells. Thin layer chromatography and spectral analysis showed that bacterioruberin, bisanhydrobacterioruberin and lycopene present in the methanolic extract prepared from whole cells of *Haloferax alexandrinus* GUSF-1 (KF796625) also showed protogonistic activity evaluated against arsenic induced DNA damage, detectable through the alkaline comet assay.

(Results on 'Supression of Arsenic(III) genotoxicty in human lymphocytes by bacterioruberin, bisanhydrobacterioruberin and lycopene of Haloferax alexandrinus GUSF-1(KF796625)' communicated for publication).

Chapter III "**Antioxidant Production in Extremely Halophilic Eubacteria and Haloarchaeal Cultures**" records results and observations on the free radical scavenging potential of Goan solar salt and associated microbial cultures together with extremely halophilic cultures from estuarine regions. It also reports the capability of growth paramaters and wide polarity range of solvents inducing maximum free radical scavenging activity. It also details antioxidant production kinetics and characterization using the 1, 1-diphenyl-2-picrylhydrazyl ($DPPH^{\bullet}$) scavenging in *Haloferax alexandrinus* GUSF-1 (KF796625). It reports for the first time the antioxidant potential of Goan solar salt and that extremely halophilic eubacteria and haloarchaea are responsible for this activity.The study also demonstrates for the first time the ability of $DPPH^{\bullet}$ to directly sort out colonies, while still on agar plate into free radical scavengers and non-scavengers. Three eubacterial genera namely *Alteromonas, Gluconobacter* and *Chromohalobacter* and eight different haloarchaeal genera namely *Halobacterium, Haloferax*, *Haloarcula*, *Halococcus*, *Halorubrum, Natrialba, Natrinema and Natronococcus* retrieved from solar salts produced in salt pans of Agarwada, Arambol, Arpora, Nerul, Ribandar and Siridao in Goa; estuarine

sediments from Bainguinim, Betim Jetty, Captain of Ports, Dona Paula, Panjim Jetty, Ribandar Patto Panjim and the sponge sample scavenged free radicals at varying degree. *Haloferax alexandrinus* GUSF-1 (KF796625) (% DPPH$^{\bullet}$ RSA 31.5 ± 0.43/ 252.2 ± 1.14 µg AAE g^{-1} cells), having phenolic moieties as antioxidant principle, offers a promise for antioxidant harnessing. Interestingly, this is also the first time *Alteromonas, Gluconobacter, Natrialba, Natrinema* and *Natronococcus* are reported with antioxidant capability. To our mind, this free radical scavenging potential of natural solar salts by microbes associated with it is possibly the thus far scientifically unknown reason for its traditional use in Goa, as soil conditioner possibly reflects its use, through chemo-reactive free radical scavenging bio-principles. Additionally, the phenolic antioxidant moieties of salt associated microbes is expected to ensure free radical scavenging of metals and hydrocarbon pollutants which are on increase in coastal soil. **Based on maximum % DPPH$^{\bullet}$ RSA activity, total antioxidant activity and total phenolic content, *Haloferax alexandrinus* GUSF-1 (KF796625) was further investigated.**

(Results published as 'Alvares, J.J., Furtado, I.J. (2018). Extremely halophilic Archaea and Eubacteria are responsible for free radical scavenging activity of solar salts of Goa – India. Global Journal of Bio-science and Biotechnology, 7 (2), 242-254').

Maximum production of free radical scavenging activity was induced in six days old cells growing in 25% NaCl TYE medium at pH 7, 42ºC, 150 rpm and ambient light and was optimally extracted in methanol and termed as '*Hfx*E'. The free radical scavenging activity of *Hfx*E and the component/ s responsible which was termed as *Hfx*A was monitored as DPPH$^{\bullet}$ decay at 517 nm, at fixed time and expressed as EC_{50} that related nearly to that obtained by kinetic observation.

The EC_{50} and stoichiometric values for *Hfx*A was three times more than that of ascorbic acid which was used for comparison studies. Further, the antioxidant activity index (AAI) was thrice, the antioxidant power (ARP) was 3.5 times and the antiradical efficieny (ARE) was five times more for *Hfx*A than that of ascorbic acid, respectively. DPPH$^{\bullet}$ scavenging reaction followed first order kinetics with rate constant k calculated at t = 1 and t = 15 min for all concentration tested and the EC_{50} concentration. The rate constant k at EC_{50} concentration was found to be 7×10^{-4} s^{-1}

for *Hfx*A and 4×10^{-4} s^{-1} for ascorbic acid which 1.75 faster with *Hfx*A. This is the first study reporting kinetics of $DPPH^{\bullet}$ scavenging reaction of antioxidants *Hfx*A from *Haloferax alexandrinus* GUSF-1(KF796625), a haloarchaeal member of the Domain Archaea.

(Results on 'Kinetics of antioxidant 'HfxA' of Haloferax sp. GUSF-1 (KF796625)' communicated for publication).

Separation into separate individual extracts was achieved by addition of hexane to methanolic extract from whole cells of *Haloferax alexandrinus* GUSF-1 (KF796625) to get the hexane extract. Further the addition of cold acetone to this hexane extract precipitated the polar lipids from non - polar lipids. Each of the individual extracts revealed peaks in the UV range and characteristics red carotenoid peaks between 300-600 nm in the visible region. Infrared spectroscopy confirmed presence of functional groups such as alcohol, alkanes, carbonyl groups and unsaturated double bonds. **Thin layer chromatographic separation technique** of each of the individual extract using different solvent system further separated out into individual components and were evaluated for $DPPH^{\bullet}$ decolourization by spraying the chromatogram. Each of the extract were able to individually abolish the two peaks of pure $DPPH^{\bullet}$ solution (at 517 nm and 327 nm) and reduce the original purple colour to very light purple to yellow. **Presence of 3–hydroxyechinenone, bacterioruberin, bisanhydrobacterioruberin monoanhydrobacterioruberin, canthaxanthin, haloxanthin and tetrahydrosqualene with $DPPH^{\bullet}$ scavenging property** (white bands against a purple stained background) were identified on thin layer chromatography using different solvent systems and comparable to R_f reported earlier.

Chapter IV '**Chemical Profiling of *Haloferax alexandrinus* GUSF-1 (KF796625)**' focuses on the haloarchaeon *Haloferax alexandrinus* GUSF-1 (KF796625) which holds a promise in biotechnology from results obtained during earlier studies as well as in this study. In this study, the culture was seen to produce lipase and aromatic oxygenase extremozymes, halocin production, suppression of arsenic toxicity, production of antioxidants and production of selenium, tellurium and Mn_2O_3 bixbite nanoparticles described in **chapter V**; therefore, it was pertinent to chemically profile the culture. Hence large quantities of culture was extracted in methanol, the extract

concentrated under vacuum using rotary evaporator (Buchi Rotavapor, R-201) and as before termed *Hfx*A since it had the antioxidant capacity. Separation and isolation of constituents was achieved using solvent fraction protocols of methanolic extraction (*Hfx*E), solvent fractionation into Hexane extract (HE) and acetone precipitation (APM).

Chemical profiling and characterization was achieved using Reverse Phase-High Resolution-Liquid Chromatography coupled with high resolution Mass Spectroscopy. The identification of the separated compounds was achieved using literature, online databases and the Mass Hunter software. Compounds in the Hexane Extract (HE) were 11-amino-undecanoic acid, 3´ Hydroxyechinenone, asthaxanthin, bisanhydrobacterioruberin, bacterioruberin, canthaxanthin, dihydroxylycopene, haloxanthin, lycopene, monoanhydrobacterioruberin, tetrahydrosqualene, phytoene, and phytofluene which were seen to absorb at 320, 447 and 490 nm, while compounds in the Acetone Precipitated Material (APM) were identified as (i) glycine betaine and trehalose (compatible solute); (ii) Mycosporine glycine (Mycosporine); (iii) polar lipids such as phosphatidylglycerol (PG) C_{20}-C_{20}, methyl ester of phosphatidylglycerophosphate (PGP-Me C_{20}-C_{20} and PGP-Me C_{20}-C_{20} + Na, and diglycosyl archaeol, mannosylglucosyl- diphytanylglycerol (DGD) which only absorb at 320 nm.

(Results on 'Characterization of multicomponent antioxidant '*HfxA*' *of Haloferax alexandrinus GUSF-1 (KF796625)' communicated for publication).*

Chapter V 'Biosynthesis of Nanoparticles by Extremely Halophilic *Chromohalobacter salexegines* GUVFFM-3 (JF330126) and Haloarchaeon *Haloferax alexandrinus* GUSF-1 (KF796625)' delves into the **biosynthesis of nanoparticles** by extremely halophilic *Chromohalobacter salexegines* GUVFFM-3 (JF330126) and by haloarchaeon *Haloferax alexandrinus* GUSF-1 (KF796625). Formation of selenium, tellurium and silver nanoparticles was demonstrated by the colour change from colourless to red, black and straw brown respectively by using growing cells, whole cells and cell lysate of *Chromohalobacter salexegines* GUVFFM-3 (JF330126) and/or *Haloferax alexandrinus* GUSF-1 (KF796625).

Growth studies of cultures *Chromohalobacter salexegines* GUVFFM-3 (JF330126) and *Haloferax alexandrinus* GUSF-1 (KF796625) with 5 mM selenite were investigated. Growth was monitored as biomass; residual selenite was estimated using the ascorbic acid reduction method to elemental selenium which was solubilized using 1 M Na_2S. Results revealed that 91% of selenite was reduced to 84.33% of Se^0 in the case of *Chromohalobacter salexegines* GUVFFM-3 (JF330126) and 98% of selenite was reduced to 96.33 % of Se^0 by *Haloferax alexandrinus* GUSF-1 (KF796625).

The involvement of biomolecules from growing cells/ whole cells and cell lysates of *Chromohalobacter salexegines* GUVFFM-3 (JF330126) and *Haloferax alexandrinus* GUSF-1 (KF796625) in the biosynthesis of nanomaterial was demonstrated by FT-IR. The **involvement of nitrate reductase, glutathionine reductase and and bis-γGC reductase activity** in the reduction of selenite to elemental selenium by cultures *Chromohalobacter salexegines* GUVFFM-3 (JF330126) and *Haloferax alexandrinus* GUSF-1 (KF796625) was elucidated using selenite reductase assay and enzyme specific inhibitors such as sodium arsenite and sodium azide.

(Results on 'Biosynthesis and comparison of selenium nanoparticles by Haloferax alexandrinus GUSF-1 (KF796625) and Chromohalobacter salexigenes (JF330126)' communicated for publication).

All the **nanoparticles were characterized** by UV-Vis and Raman spectroscopy, SEM- EDS, XRD, TEM and SAED. Shapes of selenium such as nanocrystals of 32 nm & pentagonal shaped nanoparticles with an average diagonal length of 15nm and a height of 50 nm were seen to be produced during growth of *Chromohalobacter salexegines* GUVFFM-3 (JF330126) and *Haloferax alexandrinus* GUSF-1 (KF796625) respectively. Te nano rods of 42 nm length and of 6 nm of width with rosette like pattern were seen to be produced during growth of *Haloferax alexandrinus* GUSF-1 (KF796625). Bixbyite Mn_2O_3 nano coins of 77 nm diameter were biosynthesized using cell lysate of *Haloferax alexandrinus* GUSF-1 (KF796625) evident by the formation of a brown colour on incubation with 10 mM $MnSO_4$. $2H_2O$.

The biosynthesized nanomaterials were investigated for their use as follows:

1. SeNPs biosynthesized during growth of *Haloferax alexandrinus* GUSF-1 (KF796625) were seen to modulate the size and shape of calcium oxalate crystals, thus implicating the use of SeNPs in treatment of renal caliculi which are responsible for urolithiasis.
2. TeNPs biosynthesized during growth of *Haloferax alexandrinus* GUSF-1 (KF796625) inhibited the biofilm formed by *Ps. aeruginosa* ATCC 9027 in a dose dependent manner. The antibiotic ciprofloxacin was used as a positive control. This ability of TeNPs can be harnessed in combating virulent nosocomial infections from *Ps. aeruginosa*.
3. The bixbyite Mn_2O_3 NPs biosynthesized using cell lysate of *Haloferax alexandrinus* GUSF-1 (KF796625) was subjected to vibrating sample magnetometer for studies on its magnetic property. The Magnetic Hysteresis curve obtained revealed MH curves typical of soft magnetic property ideally suited for use as nano probes.

(Results on 'Biosynthesis of tellurium nanoparticles produced by Haloferax alexandrinus GUSF-1 (KF796625)' communicated for publication).

(Results on 'Biogenic synthesis and characterization of manganese oxide nanocoins (bixbyite Mn_2O_3 NPs) by haloarchaeon Haloferax alexandrinus GUSF-1 (KF796625) showing soft magnetic property' communicated for publication)

CONCLUSION OF THE RESEARCH STUDY

The study highlights that

1. Most Extremely halophilic eubacteria and haloarchaea from Goan crude solar salt, estuarine sediments and from sponge tissue are producers of bioactives.
2. Several cellular components of *Haloferax alexandrinus* GUSF-1 (KF796625) are responsible for antioxidant activity
3. Green synthesis of nanoparticles (Silver AgNPs, Selenium SeNPs, Tellurium TeNPs and Manganese oxide Mn_2O_3 NPs) has been achieved using *Chromohalobacter salexegines* GUVFFM-3 (JF330126) and *Haloferax alexandrinus* GUSF-1 (KF796625).

OUTCOME OF THE RESEARCH STUDY

A. This study reports for the first time that:

1. Extremely halophilic archaea and eubacteria are responsible for the free radical scavenging activity of solar salts of Goa which possibly is the reason for its traditional use in Goa, as soil conditioner.
2. The Development of Agar-growth $DPPH^{\bullet}$ method directly detects free radical scavenging colonies while still on an agar plate.
3. The generas of *Alteromonas*, *Gluconobacter*, *Natrialba*, *Natrinema* and *Natronococcus* as free radical scavengers.
4. *Haloferax alexandrinus* GUSF-1(KF796625) is a rich source of antioxidants *Hfx*A extractable in methanol and follows 1st order reaction with rate constant of $7 \times 10^{-4} s^{-1}$.
5. Members of genera *Natronococcus* as producers of halocins.
6. Ability of haloarchaeal cultures to promote growth of human pathogens *E.coli* ATCC 8739 and *S.abony* ATCC 6017.
7. Antigenotoxicity of *Haloferax alexandrinus* GUSF-1(KF796625) against arsenic induced genotoxicity in human lymphocytes.
8. Role of Glycerol Dither Moieties, haloxanthin, tetrahydrosqualene and polar lipids as free radical scavengers.
9. Biosynthesis of SeNPs and TeNPs by members of the genus *Haloferax* and *Chromohalobacter*.
10. Biosynthesis of bixbyite Mn_2O_3 NPs in the haloarchaeal domain with soft magnetic properties making it suitable as nanoprobes in medical imaging technology.

B. 16S rRNA gene sequence of *Haloferax volcanii* GUIF2 (MH169338) and *Haloferax gibbonsii* GUIF4 (MG199078) deposited in Genbank

C. Research papers

FUTURE PROSPECTS

To develop technologies for:

1. Use of extremozymes in bioprocesses that employ high salts such as fermentation food processing units.
2. Use of halocins as preservatives during curing of hides in brine; an alternative to expensive antimicrobials which are inactivated in high salinity processes.
3. Use of antioxidant as preservatives in salty foods and in sun screen formulations as the antioxidant is active even in non-saline conditions.
4. Use of SeNPs in treatment/ prophylactic measures of urolithiasis.
5. Bixbyite Mn_2O_3 NPs as an alternative probe in medical imaging.

RESEARCH PUBLICATIONS

A. In Journals

1. Alvares, J.J., Furtado, I.J. (2018). Extremely halophilic Archaea and Eubacteria are responsible for free radical scavenging activity of solar salts of Goa – India. *Global Journal of Bio-science and Biotechnology*, 7 (2), 242-254.

B. Proceedings

1. Alvares, J.J., Gaonkar, S.K., Furtado, I.J. (2015). Diversity Enzymes and their potential applications. Proceedings of the State level Seminar, *Archaea: Microbes of the third domain of life*, at PES's college of Arts & Science Farmagudi Ponda Goa.
2. Alvares, J.J., Furtado, I.J. (2015). Antioxidant activity in Haloarchaea. Proceedings of the State level Seminar, *Archaea: Microbes of the third domain of life*, at PES's college of Arts & Science Farmagudi Ponda Goa.

C. Manuscripts Communicated

1. Alvares, J.J., D'Costa, A., Shyama, S.K., Furtado, I.J. (2018). Supression of arsenic (III) genotoxicty in human lymphocytes by bacterioruberin, bisanhydrobacterioruberin and lycopene of *Haloferax alexandrinus* GUSF-1(KF796625).
2. Alvares, J.J., Furtado, I.J. (2018). Kinetics of antioxidant *Hfx*A of *Haloferax* sp. GUSF-1 (KF796625).
3. Alvares, J.J., Furtado, I.J. (2018). Characterization of multicomponent antioxidant *Hfx*A of *Haloferax alexandrinus* GUSF-1 (KF796625).
4. Alvares, J.J., Furtado, I.J. (2018). Biosynthesis and comparison of selenium nanoparticles by *Haloferax alexandrinus* GUSF-1 (KF796625) and *Chromohalobacter salexigenes* (JF330126).
5. Alvares, J.J., Furtado, I.J. (2018). Biosynthesis of tellurium nanoparticles produced by *Haloferax alexandrinus* GUSF-1 (KF796625).
6. Biogenic synthesis and characterization of manganese oxide nanocoins (bixbyite Mn_2O_3) by haloarchaeon *Haloferax alexandrinus* GUSF-1 (KF796625) showing soft magnetic property.

D. Manuscript under preparation

1. Alvares, J.J., Furtado, I.J. (2018). Bioprospects of haloarchaeal cultures of Goa-India.
2. Alvares, J.J., Furtado, I.J. (2018). Antagonistic interactions among extreme halophiles from Goa.

Research findings presented as

A. Poster presentations

1. Alvares J and Furtado I (2014). "**Prospects of Extremely Halophilic Eubacteria and Haloarchaea of Marine Origin for Production of Antioxidants**". 55th National Conference of the Association of Microbiologists of India on Empowering Mankind with Microbial Technologies (AMI-EMMT-2014) organized by Tamil Nadu Agricultural University Coimbatore held from 12^{th} -14^{th} November 2014.
2. Alvares J and Furtado I (2015). "**Antagonistic interactions among extreme halophiles from salterns of Goa**". 4^{th} Bharatiya Vigyan Sammelan, held at the Kala Academy, Panaji, Goa from the 6^{th} - 8^{th} Febraury, 2015.
3. Alvares J, Gaonkar S. and Furtado I. (2015). "**Diversity and potential applications of haloarchaeal enzymes"** at state level Seminar on Archaea: Microbes of the third domain of life held on 28^{th} of September, 2015, at PES's college of Arts & Science Farmagudi Ponda Goa.
4. Malik A, Alvares J, Gaonkar S and Furtado I (2017). "**Haloarchaea of Goan origin as a source of biotechnologically important Archaeal enzyme**". National seminar in advances in sustainable biotechnology held on the 27^{th} and 28^{th} January 2017 at Department of Biotechnology, St Xavier's College, Mapusa, Goa, India.
5. Alvares J and Furtado I (2019). **"Biosynthesis of selenium nanoparticles by *Haloferax alexandrinus* GUSF-1 (KF796625) and their use in modulating the size and shape of calcium oxalate crystals".** Abstracted at STUDIA UNIVERSITATIS BABEŞ – BOLYAI, BIOLOGIA, 64, 1, 2019 (Halophiles 2019).

B. Oral presentation

1. Alvares J and Furtado I (2015). **"Antioxidants in Haloarchaea"**. State level seminar on Archaea: Microbes of the third domain of life, held on 28th of September, 2015, at PES's college of Arts & Science Farmagudi Ponda, Goa. (**Second Prize**).
2. Alvares J and Furtado I (2019). "**Antibiofilm property of tellurium nanoparticles synthesized by *Haloferax alexandrinus* GUSF-1 (KF796625)".** International Conference on Nanomaterial for Environmental Application (NEA 2019) held on 6th and 7th March 2019 at Dhempe College, Miramar, Goa.

C. Workshops and Seminars

1. Participated in the ASM virtual workshop on "**Art of Science Communication**" on the 6th of December, 2013 at Department of Biotechnology, Goa University, Goa.
2. Attended seminar on **"New perspectives in Biosciences"** held on 7th December 2017 at Department of Microbiology, Goa University.

Bibliography

Aakvik, T., Lale, R., Liles, M., Valla, S. (2011). Metagenomic libraries for functional screening. In: de Bruijn, F. J. (ed.), *Handbook of molecular microbial ecology*, Hoboken, Wiley-Blackwell, pp. 171-181.

Abbes M., Baati, H., Guermazi, S., Messina, C., Santulli, A., Gharsallah, N., Ammar, E. (2013). Biological properties of carotenoids extracted from *Halobacterium halobium* isolated from a Tunisian solar saltern. *BMC Complement Altern Med*., 13: 255.

Abed, R. M. M., Dobretsov, S., Al-Fori, M., Gunasekera S. P., Sudesh, K., Paul, V. J. (2013). Quorum-sensing inhibitory compounds from extremophilic microorganisms isolated from a hypersaline cyanobacterial mat. *J Ind Microbiol Biotechnol*., 40(7). DOI: 10.1007/s10295-013-1276-4.

Aebi, H. (1984). Catalase. *Methods Enzymol*., 105: 121-126.

Aguiar, R. (1994). Degradation of fractions of crude oil by *Halobacterium* strain R1. Msc Thesis, Goa University, Taleigao, Goa.

Aguiar, R., Furtado, I. (1996). Growth of *Halobacterium* strain R1 on sodium benzoate. In: Kahlon, R.S. (ed.), *Perspectives in Microbiology*, India: National Agricultural Technology Information Centre, pp. 78-79.

Alam M. N., Bristi N. J., Rafiquzzaman M. (2013). Review on in vivo and in vitro methods evaluation of antioxidant activity. *Saudi Pharm J*., 21: 143-152.

Alberola, A., Meseguer, I., Torreblanca, M., Moya, A., Sancho, S., Polo, B., Soria, B., Such, L. (1998). Halocin H7 decreases infarct size and ectopic beats after myocardial reperfusion in dogs. *J Physiol*., 509:108.

Albrecht, M., Takaichi, S., Steiger, S., Wang, Z., Sandmann, G. (2000). Novel hydroxycarotenoids with improved antioxidative properties produced by gene combination in *Escherichia coli*. *Nat Biotechnol.*, 18:843–846.

Al-Mailem, D. M., Sorkhoh, N. A., Al-Awadhi, H., Eliyas, M., Radwan, S. S. (2010). Biodegradation of crude oil and pure hydrocarbons by extreme halophilic archaea from hypersaline coasts of the Arabian Gulf. *Extremophiles*, 14: 321-328.

Altschul, S.F., Madden, T.L., Schäffer, A.A., Zhang, J., Zhang, Z., Miller, W., Lipman, D.J. (1997). Gapped BLAST and PSI-BLAST: a new generation of protein database search programs. *Nucleic Acids Res*., 25(17): 3389-402.

Alvarenga, P., Laneiro, C., Palma, P., de Varennes, A., Cunha-Queda, C. (2013). A study on As, Cu, Pb and Zn (bio)availability in an abandoned mine area (São Domingos, Portugal) using chemical and ecotoxicological tools. Environ Sci Pollut Res Int. 20(9):6539-50. doi: 10.1007/s11356-013-1649-2

Alvares, J.J., Furtado, I.J. (2018). Extremely halophilic Archaea and Eubacteria are responsible for free radical scavenging activity of solar salts of Goa – India, *Global J Biosci and Biotechnol.*, 7(2): 242-254.

Amoozegar, M. A.; Schumann, P.; Hajighasemi, M.; Fatemi, A. Z. (2008). *Salinivibrio proteolyticus* sp. nov. a moderately halophilic and proteolytic species from a hypersaline lake in Iran. *Int. J. Syst. Evol. Microbiol.*, 58(5): 1159-1163.

Anderson, P., Kedersha, N. (2009). Stress Granules. *Curr Biol*., 19(10): 397-398.

Antón, J., Meseguer, I., Rodríguez-Valera, F. (1988). Production of an extra-cellular polysaccharide by *Haloferax mediterranei*. Appl Environ Microbiol., 54(10):2381–2386.

Apak, R., Guclu, K., Ozyurek, M., Karademir, S.E. (2008). Mechanism of antioxidant capacity assays and the CUPRAC (cupric ion reducing antioxidant capacity) assay. *Microchim. Acta*, 160: 413-419.

Arahal, D.R., García, M.T., Vargas, C., Cánovas, D., Nieto, J.J., Ventosa, A. **(**2001). *Chromohalobacter salexigens* sp. nov., a moderately halophilic species that includes

Halomonas elongata DSM 3043 and ATCC 33174**.** *Int J Syst Evol Microbiol.*, 51(4): 1457-62.

Aral, H., Hill, B.D., Sparrow, G. J. (2004). Salts from saline waters and value added products from the salts. CSIRO Minerals Report DMR-2378C.

Arena, A., Gugliandolo, C., Stassi, G., Pavone, B., Iannello, D., Bisignano, G., Maugeri, T.L. (2009). An exopolysaccharide produced by Geobacillus thermodenitrificans strain B3-72: antiviral activity on immunocompetent cells. *Immunol Lett*., 123(2): 132-137.

Arena, A., Maugeri, T.L., Pavone, B., Jannello, D., Gugliandolo, C., Bisignano, G. (2006). Antiviral and immunoregulatory effect of a novel exopolysaccharide from a marine thermotolerant Bacillus licheniformis. *Int Immunopharmacol*., 6(1): 8-13.

Arnow, L. E. (1937). Colorimetric determination of the components of 3, 4-dihydroxy phenylalanine-tyrosine mixtures. *J Biol Chem*., 118: 531-537.

Arora, P.K., Kumar, M., Chauhan, A., Raghava, G.P., Jain, R. K. (2009). OxDBase: a database of oxygenases involved in biodegradation. *BMC Res Notes*, 2:67. DOI: 10.1186/1756-0500-2-67.

Asker, D., Awad, T., Ohta, Y. (2002). Lipids of *Haloferax alexandrinus* Strain TMT: an extremely halophilic canthaxanthin producing archaeon. *J Biosci Bioeng*., 93(1): 37-43.

Ates Ö., Oner, E., Kazim, T., Arga, Y. (2011). Genome-scale reconstruction of metabolic network for a halophilic extremophile, *Chromohalobacter salexigens* DSM 3043. *BMC Syst. Biol.*, 5:12. https://doi.org/10.1186/1752-0509-5-12

Ausubel, J.H., Langford, H.D. (1997). *Technological Trajectories and the Human Environment*, National Academy Press, Washington D.C.

Baesman, S.M., Bullen, T.D., Dewald, J., Zhang, D., Curran, S., Islam, F.S.,

Beveridge, T.J., Oremland, R.S. (2007). Formation of tellurium nanocrystals during anaerobic growth of bacteria that use Te oxyanions as respiratory electron acceptors. *Appl Environ Microbiol*., 73(3):2135-2143. DOI**:** 10.1128/AEM.02558-06

Bajpai, B., Chaudhary, M., Saxena, J. (2015). Production and Characterization of α-Amylase from an Extremely Halophilic Archaeon, *Haloferax* sp. HA10. *Food Technol Biotechnol.,* 53(1): 11-17. DOI: 10.17113/ftb.53.01.15.3824

Bakalyar, S. R., Mcllwrick, R., Roggendorf, E., (1977). Solvent selectivity in reversed- phase high-pressure liquid chromatography, J. *Chromatogr*., 142: 353.

Balasubramanian, S., Pal, S., Bagchi, B. (2002). Hydrogen-bond dynamics near a micellar surface: origin of the universal slow relaxation at complex aqueous interfaces. *Phys Rev Lett*., 89: 115-505.

Balch, W.E., Magrum, L.J., Fox, G.E., Wolfe R.S., Woese C.R. (1977). An ancient divergence among the bacteria. *J Mol Evol*., 9(4): 305-311.

Barns, S.M., Delwiche, C.F., Palmer, J.D., Pace, N.R. (1996). Perspectives on archaeal diversity, ther-mophily and monophyly from environmental rRNA sequences. *Proc Natl Acad Sci USA*. 93(17): 9188-9193.

Bansal, N., Furtado, I.J. (2004). Halocins in haloarchaeal isolates from marine and salt pan sediments of Goa- India. Abstracted at the The 7th International conference on Halophilic Microorganism, held at Ljubljana (Slovenia).

Bartilson, M., Shingler, V. (1989). Nucleotide sequence and expression of the catechol 2, 3-dioxygenase gene of phenol catabolizing *Pseudomonas* CF600. *Gene*, 85:233-238.

Barton, H., Grant, M. (2006). A health map for the local human habitat. *The Journal of the Royal Society for the Promotion of Health*, 126(6): 252-253.

Basnayake, R.S.T., Bius, J.H., Akpolat, O.M., Chasteen, T.G. (2001). Production of dimethyl telluride and elemental tellurium by bacteria amended with tellurite or tellurate. *Appl Organomet Chem*., 15: 499-510.

Bebien, M., Chauvin, J.P., Adriano, J.M., Grosse, S., Verméglio, A. (2001). Effect of selenite on growth and protein synthesis in the phototrophic bacterium *Rhodobacter sphaeroides*. *Appl Environ Microbiol*., 67: 4440-4447.

Behal, V. (2003). Alternative sources of biological active substancesia. *Folia Microbiol*., 48: 563-571.

Ben-Amotz A, Kay ZA, Avron M. (1982). Accumulation of β-carotene in halotolerant alge: purification and characterization of β-carotene-rich globules from *Dunaliella bardawil* (*Chlorophyceae*). *J Phycol*., 18: 529-537.

Benzie, I.F.F., Strain, J.J. (1999). Ferric reducing antioxidant power assay: direct measure of total antioxidant activity of biological fluids and modified version for simultaneous measurement of total antioxidant power and ascorbic acid concentration. *Methods Enzymol*., 299, 15-27.

Bernan, V.S., Greenstein, M., Maiese, W.M. (1997). Marine microorganisms as a source of new natural products. *Adv Appl Microbiol*., 43: 57-90.

Bertoldo, C., Antranikian, G. (2002). Starch-hydrolyzing enzymes from thermophilic archaea and bacteria. *Curr Opin Chem Biol*., 6: 151-160.

Bertrand, J.C., Almallah, M., Aequaviva, M., Mille, G. (1990). Biodegradation of hydrocarbons by an extremely halophilic archaebacterium. *Lett Appl Microbiol*., 11: 260-263.

Bhatnagar, T., Boutaiba, S., Hacene, H., Cayol, J-L., Fardeau, M-L., Ollivier, B., Baratti, J.C. (2005). Lipolytic activity from Halobacteria: Screening and hydrolase production. *FEMS Microbiol Lett*., 248: 133-140.

Bini E. (2010). Archaeal transformation of metals in the environment. *FEMS Microbiol Ecol*., 73(1): 1-16.

Birbir, M., Calli, B., Mertoglu, B., Bardavid, R., Oren, A., Ogmen, M., Ogan, A. (2007). Extremely halophilic Archaea from Tuz Lake, Turkey, and the adjacent Kaldirim and Kayacik salterns. *World J Microbiol Biotech*., 23(3): 309-316.

Birbir, M., Eryılmaz, S., and Ogan, A. (2004): Prevention of halophilic bacterial damage on brine cured hide with halocins. *J Soc Leather Technol Chem*., 88(3): 99-104.

Biswas, J., Haique, F. N., Paul, A.K. (2016). Carotenogenesis in *Haloferax* sp. strain BKW301, a halophilic archaeoan from Indian solar saltern. *J Advances in Microbiol*., 1(3): 1-11.

Biswas, K.C., Barton, L.L., Tsui, W.L., Shumana, K., Gillespie, J., Eze, C.S. (2011). A novel method for the measurement of elemental selenium produced by bacterial reduction of selenite. *J Microbiol Methods*., 86: 140-144.

Bonfá, M.R., Grossman, M.J., Mellado, E., Durrant, L.R. (2011). Biodegradation of aromatic hydrocarbons by Haloarchaea and their use for thereduction of the chemical oxygen demand of hypersaline petroleum produced water. *Chemosphere*, 84:1671-1676

Bonomini, F., Tengattini, S., Fabiano, A., et al. (2008). Atherosclerosis and oxidative stress. *Histology and Histopathology*, 23, 381-390.

Borghese, R., Borsetti, F., Foladori, P., Ziglio, G., Zannoni. D. (2004). Effects of the metalloid oxyanion tellurite (TeO_3^{2-}) on growth characteristics of the phototrophic bacterium *Rhodobacter capsulatus*. *Appl. Environ. Microbiol*., 70: 6595-6602.

Bornscheuer, U.T., Kaslauskas, R.J. (1999). *Hydrolases in organic synthesis: regional and stereoselective biotransformations,* Wiley-VCH, Weinheim.

Boutaiba, S., Bhatnagar, T., Hacene, H., Mitchell, D.A., Baratti, J.C. (2006). Preliminary characterization of a lipolytic activity from an extremely halophilic archaeon, *Natronococcus* sp. *J. Mol. Cat. B: Enzymatic*., 41: 21-26.

Bouwer, E.J., Zehnder. A.J.B. (1993). Bioremediation of organic compounds--putting microbial metabolism to work. *Trends Biotechnol*., 11(8): 360-7. DOI: 10.1016/0167-7799(93)90159-7.

Braganca, E.M., Furtado, I. (2004). Polyhydroxyalkanoate production by Haloarchaea from saltpans and fish - Jetty sediments of Goa - India. Abstracted at the The 7th International conference on Halophilic Microorganism, held at Ljubljana (Slovenia).

Braganca, J.M. (2002). Uptake of arsenic and cadmium by halophilic archaea. PhD Thesis. Goa University.

Braganca, J.M., Furtado, I. (2009). Isolation and characterisation of haloarchaea from low- salinity costal sediments and waters of Goa. *Curr Sci.*, 96: 1182-84.

Bragança, J.M., Furtado, I.J. (2017). Removal of cadmium by *Halobacterium* strain R1 MTCC 3265 from saline and non-saline econiches. *Ind J Geo-Mar Sci*., 46(11) 2215-2219.

Brand-Williams, W., Cuvelier, M.E., Berset, C. (1995). Use of a free radical method to evaluate antioxidant activity. *LWT-Food Sci Technol.*, 28: 25-30.

Brien, O., Colwell, R. (1987). A rapid test for chitinase activity that uses 4-methyl umbelliferyl-N-acetyl-P-D-glucosamine. *Appl Environ Microbiol*., 53: 1718-1720.

Britton, G. (1995). UV/Visible Spectroscopy. In: (Britton, G., Liaaen-Jensen, S., Pfander, H., Eds.), *Carotenoids*, Birkhäuser Verlag: Basel, Switzerland. Volume 1B, pp. 13-62.

Britton, K.L., Baker, P. J., Fisher, M., Ruzheinikov, S., Gilmour, D. J., Bonete, M. J., Ferrer, J., Pire, C., Esclapez, J., Rice, D.W. (2006). *Proc Natl Acad Sci USA.* 103: 4846-4851.

Brochier-Armanet, C., Boussau, B., Gribaldo, S., Forterre, P. (2008). Mesophilic Crenarchaeota: proposal for a third archaeal phylum, the Thaumarchaeota. *Nat Rev Microbiol*., 6(3): 245-252.

Brock, S.L., Duan, N., Tian, Z.R., Giraldo, O., Zhou, H., Suib, S.L. (1998). A review of porous manganese oxide materials. *Chem Mater*., 10: 2619-2628.

Brown, A., Simpson, J. (1972). Water relations of sugar-tolerant yeasts: the role of intracellular polyols. *J. Gen. Microbiol.*, 72: 589-591.

Brusa, T., Borin, S., Ferrari, F., Sorlini, C., Corselli, C., Daffonchio, D. (2001). Aromatic hydrocarbon degrading patterns and catechol 2, 3-dioxygenase genes in microbial cultures from deep anoxic hypersaline lakes in the eastern Mediterranean sea. *Microbiol Res*., 156: 49-58.

Buege, J.A., Aust, S.D. (1978). Microsomal lipid peroxidation. *Methods Enzymol*., 52: 302-310.

Burton, S.G. (2003). Oxidising enzymes as biocatalysts. *Trends Biotechnol*., 21: 543-549.

Caldwell, M.E., Suflita J. M. (2000). Detection of phenol and benzoate as intermediates of Anaerobic Benzene Biodegradation under Different Terminal Electron-Accepting Conditions. *Environ. Sci. Technol*., 34(7). DOI: 10.1021/es990849j.

Camacho, R. M., Mateos-Díaz, J. C., González-Reynoso, O., Prado L. A., Cordova J. (2009). Production and characterization of esterase and lipase from *Haloarcula marismortui. J Ind Microbiol Biotechnol*., 36(7): 901-909. DOI: 10.1007/s10295-009-0568-1.

Cao, B., Geng, A., & Chee, L. (2008). Induction of ortho- and meta- cleavage pathways in *Pseudomonas* in biodegrada-tion of high benzoat concentration: MS identification of catabolic enzymes, genomics and proteomics. *Appl Microbiol Biotechnol*., 81: 99-107.

Cao, B., Xu, H., Mao, C. (2011). Transmission electron microscopy as a tool to image bioinorganic nanohybrids: The case of phage-gold nanocomposites. *Microsc. Res. Tech*., 74: 627-635.

Caravan, P. (2006). Strategies for increasing the sensitivity of gadolinium based MRI contrast agents. *Chem Soc Rev*., 35: 512-523.

Castelle, C.J., Wrighton, K.C., Thomas, B.C., Hug, L.A., Brown, C.T., Wilkins, M.J., Frischkorn, K.R., Tringe, S.G., Singh, A., Markillie, L.M., Taylor, R.C., Williams, K.H., Banfield, J.F. (2015) Genomic expansion of domain archaea high-lights roles for organisms from new phyla in anaerobic carbon cycling. *Curr Biol*., 25(6): 690-701.

Cerniglia, C.E. (1984). Microbial metabolism of polycyclic aromatic hydrocarbons. *Adv Appl Microbiol*., 30: 31-71.

Chaga, G., Porath, J., Illéni. T. (1993). Isolation and purification of amyloglucosidase from *Halobacterium sodomense.* 7(5): 256-261.

Cheung, J., Danna, K.J., O'Connor, E.M., Price L.B., Shand, R.F. (1997). Isolation, sequence and expression of the gene encoding halocin H4, a bacteriocin from the halophilic archaeon *Haloferax mediterranei* R4. *J Bacteriol.*, 179: 548-551.

Chimileski, S., Franklin, M.J., Papke T. R. (2014). Biofilms formed by the archaeon *Haloferax volcanii* exhibit cellular differentiation and social motility and facilitate horizontal gene transfer *BMC Biol*., 12:65.

Corcelli, A., Lattanzio, V. M. T., Mascolo, G., Papadia, P., Fanizzi, F. P. (2002a). Lipid-protein stoichiometries in a crystalline biological membrane: NMR quantitative analysis of the lipid extract of the purple membrane. *J Lipid Res*., 43: 132-140.

Cuadros-Orellana, S., Pohlschro, M., Durrant, L. R. (2006). Isolation and characterization of halophilic archaea able to grow in aromatic compounds. *Int Biodeterior Biodegrad*., 57:151–154.

Cuadros-Orellana, S., Pohlschröder, M., Grossmanc, M. J., Durrant, L. R. (2012). Biodegradation of aromatic compounds by a halophilic archaeon isolated from the Dead Sea. *Chemical Engineering Transactions*. 27: 13-18.

Cushman, J.C. (2001). Osmoregulation in plants: Implications for agriculture. *Amer zool*. 41: 758-769.

Dagley, S. (1986). Biochemistry of aromatic hydrocarbon degradation in *Pseudomonas*. In: *The Bacteria, vol. X, The Biology of Pseudomonas*, (J. R. Sokatch, ed.), London: Academic Press. 527-556.

Danson, M. J., Hough, D. W. (1997). The structural basis of protein halophilicity. *Comp Biochem Physiol*., 117(3): 307-312.

Darmanyan, A.P., Gregory, D.D., Guo, Y., Jenks, W.S., Burel, L., Eloy, D., Jardon, P. (1998). Quenching of singlet oxygen by oxygen- and sulfur-centered radicals: Evidence for energy transfer to peroxyl radicals in solution. *J Am Chem Soc*., 120: 396-403.

DasSarma, S., Arora, P. (1997). Genetic analysis of the gas vesicle gene cluster in haloarchaea. *FEMS Microbiol Lett*., 153: 1-10.

DasSarma, S., Arora, P. (2001). Halophiles. In: *Encyclopedia of life sciences*, Nature Publishing Group, London. http://www.els.net

De Boer, J., Hoeijmakers, J.H. (2000). Nucleotide excision repair and human syndromes. *Carcinogenesis*. 21: 453-460.

de Pascale, D., De Santi, C., Fu, J., Landfald, B. (2012). The microbial diversity of Polar environments is a fertile ground for bioprospecting. *Mar Genomics*. 8: 15-22.

De Souza, M. P., Amini, A. Dojka, M. A., Pickering, I. J., Dawson, S. C., Pace, N. R. Terry. N. (2001). Identification and characterization of bacteria in a selenium contaminated hypersaline evaporation Pond. *Appl. Environ. Microbiol.*, 3785-3794.

Debieux, C.M., Dridge, E.J., Mueller, C.M., Splatt, P., Paszkiewicz, K., Knight, I., Florance, H., Love, J., Titball, R.W., Lewis, R.J., Richardson, D.J., Butler, C.S. (2011). A bacterial process for selenium nanosphere assembly, *Proc Natl Acad Sci USA.*, 108:13480-13485.

Del Gallo, M., Haegi, A. (1990). Characterization and quantification of exocellular poly-saccharides in *Azospirillum brasilense* and *Azospirillum lipoferum*. *Symbiosis*, 9:155-161.

Demain, A.L. Fang, A. (2000). The Natural Functions of Secondary Metabolites. In: (A., Fiechter, ed.) *History of Modern Biotechnology I, Advances in Biochemical Engineering/Biotechnology*, Springer, Berlin, 69: 1-39. DOI:org/10.1007/3-540-44964-7_1

DeMoll-Decker, H., Macy, J.M. (1993).The periplasmic nitrite reductase of Thauera selenatis may catalyze the reduction of selenite to elemental selenium, *Arch Microbiol.*, 160:241-247.

Dhawan, A., Mathur, N., Seth, P.K. (2001). The effect of smoking and eating habits on DNA damage in Indian population as measured in the comet assay. *Mutat Res*., 474:121-128.

Diaz, E. (2004). Bacterial degradation of aromatic pollutants: a paradigm of metabolic versatility. *Int. Microbiol.*, (7)3: 173-180.

Diaz, M.P., Boyd, K.G., Grigon, S.J.W., Burgess, J.G. (2002). Biodegradation of crude oil across a wide range of salinities by an extremely halotolerant bacterial consortium MPD-M, immobilized onto polyproylene fibers. *Biotechnol Bioeng*., 79: 145-153. DOI: 10.1016/j.materresbull.2012.06.034

Duncan, J.L. (2004). Haloarchaeal growth physiology, characterization of halocin A4 and cloning *tbp* and *tfb* genes. Masters of Science Thesis, Northern Arizona University, Flagstaff, AZ.

Dunlap, W.C., Yamamoto, Y. (1995) Small-molecule antioxidants in marine organisms: antioxidant activity of mycosporine glycine. *Comp Biochem Physiol*., B 112: 105-114.

Dussault, H.P. (1955). An improved technique for staining halophilic bacteria. *J Bacteriol*., 70: 484-485.

Dym, O., Mavaerech, M., Sussman, J.L. (1995). Structural features that stabilize halophilic malate dehydrogenase from an archaebacterium. *Science*. 267: 1344-1346.

Ehrlich, P. R., Raven, P. H. (1964). Butterflies and plants: A study in co-evolution. *Evolution*. 18: 586-608.

Ekkers, D.M., Cretoiu, M.S., Kielak, A.M., Elsas, J.D. (2012). The great screen anomaly—a new frontier in product discovery through functional metagenomics. *Appl Microbiol Biotechnol.*, 93: 1005-1020.

Elevi, R., Assa, P., Birbir, M., Ogan, A., Oren, A. (2004). Characterization of extremely halophilic Archaea isolated from the Ayvalik Saltern, Turkey. *World J Microbiol Biotech*. 20(7): 719-725.

Elsztein, C., Herrera Seitz, M.K., Sanchez, J.J., de Castro, R.E. (2001). Autoproteolytic activation of the haloalkaliphilic archaeon *Natronococcus occultus* extracellular serine protease. *J Basic Microbiol*., 41: 319-327.

Eme, L., Doolittle, W.F. (2015). Microbial diversity: a bonanza of phyla. *Curr Biol*., 25(6): R227-R230.

Emerson, D., Sadhana, C., Oriel, P., Breznak, J. A. (1994). *Haloferax sp*. D1227, a halophilic archaeon capable of growth on aromatic compounds. *Arch Microbiol.* 161: 445-452.

Empadinhas, N., da Costa, M. S. (2008). Osmoadaptation mechanisms in prokaryotes: distribution of compatible solutes. *Int. Microbiol*., 11: 151-161.

Erdoğmuş, S. F., Mutlu, M. B., Safiye, Korcan, S. E., Guven, K., Konuk, M. (2013). Aromatic Aromatic hydrocarbon degradation by halophilic Archaea isolated from Çamalt Saltern, Turkey. *Water Air Soil Pollut*., 224: 1449. DOI 10.1007/s11270-013-1449-9

Eustis, S., El-Sayed, M.A. (2006). Why gold nanoparticles are more precious than pretty gold: Noble metal surface plasmon resonance and its enhancement of the radiative and nonradiative properties of nanocrystals of different shapes. *Chem Soc Rev*., 35: 209-217.

Eyles, M. J., Warth, A.D. (1989). The response of *Gluconabacter oxydans* to sorbic and benzoic acids. *Int J Food Microbiol*., 8(4): 335-42. DOI: 10.1016/0168-1605(89)90004-4

Fairley, D.J., Boyd, D.R., Sharma, N.D., Allen, C.C.R., Morgan, P., Larkin, M.J. (2002). Aerobic metabolism of 4-hydroxybenzoic acid in Archaea via an unusual pathway involving an intramolecular migration shift (NIH shift). *Appl Environ Microbiol*., 68: 6246-6255.

Fathepure, B. Z., Nicholson, C. A. (2004). Biodegradation of benzene by halophilic and halotolerant bacteria under aerobic conditions. *Appl Environ Microbiol*., 1222-1225.

Feldheim, D.L., Foss, C.A. (2002). Metal Nanoparticles: Synthesis, Characterization, and Applications CRC Press: Boca Raton, FL, USA.

Felsenstein, J. (1985). Confidence limits on phylogenies: An approach using the bootstrap. *Evolution*. 39: 783-791.

Fernandes, A. (1999). Isolation of Amylolytic, Lipolytic, Proteolytic microorganisms from Salt pan and Fish Jetty and use in Fish Fermentation. Master of Science Dissertation thesis, Goa University, Department of Microbiology.

Fernandes, C.F.E. (2006). Salt pan ecology and its impact on community structure of Halophilic Archaea. Ph.D thesis, Goa University, Department of Microbiology

Fernandes, C., Furtado, I. (2005). Culturable haloarchaeal diversity of salt pans of Goa, India. Abstracted at *International Marine Biotechnology Conference* at St. John's New Foundland. 300 Canada.

Fesharaki, P.J., Nazari, P., Shakibaie, M., Rezaie, S., Banoee, M., Abdollahi, M., Shahverdi, A.R. (2010). Biosynthesis of selenium nanoparticles using *Klebsiella pneumoniae* and their recovery by a simple sterilization process. *Braz J Microbiol.*, 41: 461-466.

Fogliano, V., Verde, V., Randazzo, G., Ritieni, A. (1999). Method for measuring antioxidant activity and its application to monitoring antioxidant capacity of wines. *J. Agric. Food Chem*., 47: 1035-1040.

Fondekar, S. P., Reddy, C.V.G. (1976). Arsenate and arsenite levels in the coastal and estuarine waters of Goa. *Mahasagar-Bull National Institute of Oceanography*. 8: 157-163.

Fondekar, S.P., Reddy, C.V.G. (1974). Arsenic content in the coastal and estuarine waters around. Goa. *Mahasagar-Bull National Institute of Oceanography*. 7: 27-32.

Fox, G.E., Magrum, L.J., Balch, W.E., Wolfe, R.S., Woese, C.R. (1977). Classification of methanogenic bacteria by 16S ribo-somal RNA characterization. *Proc Natl Acad Sci USA*. 74(10): 453-454.

Fu, W., Oriel, P. (1999). Degradation of 3-phenylpropionic acid by *Haloferax* sp. D1227. *Extremophiles*, 3: 45-53.

Fuchs, G., Boll, M., Heider, J. (2011). Microbial degradation of aromatic compounds-from one strategy to four. *Nat Rev Microbiol.*, 9(11): 803-16. DOI: 10.1038/nrmicro2652

Fukushima, T.1., Mizuki, T., Echigo, A., Inoue, A., Usami, R. (2005). Organic solvent tolerance of halophilic alpha-amylase from a Haloarchaeon, *Haloarcula* sp. strain S-1. *Extremophiles*. 9(1): 85-9.

Fuller, R.A., Irvine, K.N., Devine-Wright, P., Warren, P.H., Gaston, K.J. (2007). Psychological benefits of greenspace increase with biodiversity. *Biol. Lett*., 3:390-394.

Furtado, I., Fernandes, C.F.E. (2009). Traditional salt production in Goa- India enriches diverse microbial resource. In 2009 9th international symposium on salt, Volume A. Gold Wall Press. 781-786.

Gandol, W. R., Marinelli, F., Lazzarini, A., Molinari, F. (2000). Cell bound and extracellular carboxylesterases from *Streptomyces*: hydrolytic and synthetic activities. *J Appl Microbiol*., 89:870-875.DOI:10.1046/j.1365-2672.2000.01194.x

Ganther, H.E. (1971). Reduction of the selenotrisulfide derivative of glutathione to a persulfide analog by gluthathione reductase, *Biochemistry*, 10: 4089-4098.

Garcia, M. T., Ventosa, A., Mellado, E. (2005). Catabolic versatility of aromatic compound degrading halophilic bac-teria. *FEMS Microbiol Ecol.*, 54: 97-109.

Garcia, M.T., Mellado, E., Ostos, J.C., Ventosa, A. (2004*). Halomonas organivorans* sp. nov., a moderate halophile able to degrade aromatic compounds. *Int J Syst Evol Microbiol*., 54: 1723-1728.

Ghiselli, A., Serafini, M., Maiani, G., Azzini, E., Ferro-Luzzi, A. (1995). A fluorescence-based method for measuring total plasma antioxidant capability. *Free Radic Biol Med*., 18: 29-36.

Ghosh, A., Mohod, A M., Paknikar, K.M., Jain, R.K. (2008). Isolation and characterization of selenite-and selenate-tolerant microorganisms from selenium-contaminated sites. *World J Microbiol Biotechnol*., 24:1607-1611. DOI 10.1007/s11274-007-9624-z

Gibson, D.T., Mahadevan, V., Jerina, D.M., Yogi, H., Yeh, H.J. (1975). Oxidation of the carcinogens benzo[a]pyrene and benzo[a]anthracene to dihydrodiols by a bacterium. *Science*, 189: 295-297.

Gibson, J., Harwood. C.S. (2002). Metabolic diversity inaromatic compound utilization by anaerobic microbes. *Annu Rev Microbiol*., 56: 345-369.

Gimenez, M.I., Studdert, C.A., Sanchez, J.J., De Castro, R.E. (2000). Extracellular protease of *Natrialba magadii*: purification and biochemical characterization. *Extremophiles*. 4:181-188.

Goankar, S., Furtado, I. (2018a). Isolation and culturing of protease- and lipase-producing *Halococcus agarilyticus* GUGFAWS-3 from marine *Haliclona* sp. inhabiting the rocky intertidal region of Anjuna in Goa, India. *Ann Microbiol.* 68(1). DOI: 10.1007/s13213-018-1391-6.

Gaonkar, S. K, Furtado, I. J., (2018b). Use of immobilized whole cells of *Haloferax* ATCC BAA 645 for treatment of dairy and fish waste effluents. International Journal of Pharmacy and Biological Sciences. 8:22-28.

Gonzalez, C., Gutierrez, C. (1970). Presence of lipase among species of extremely halophilic bacteria. *Can J Microbiol*., 16, 1165-1166.

Grant, W.D. (2004). Life at low water activity. *Philos Trans Roy Soc B.*, 359: 1249-1267.

Grant, W.D., Larsen, H. (1989). Group III. Extremely halophilic archaebacteria. Order Halobacteriales ord. nov. In: Stanley J.T., Bryant, M.P., Pfennig N., Holt J.G. (eds.), *Bergey's Manual of Systematic Bacteriology*, 3, Williams & Wilkins, Baltimore, pp: 2216-2233

Grohe, B., O'Young, J., Ionescu, D.A., Lajoie, G., Rogers, K.A., Karttunen, M., Goldberg, H.A., Hunter, G.K. (2007). Control of calcium oxalate crystal growth by face-specific adsorption of an osteopontin phosphopeptide. *J Am Chem Soc.,* 5; 129(48): 14946-51.

Grover, P.K. Moritz, R.L. Simpson, R.J. Ryall, R.L. (1998). Inhibition of growth and aggregation of calcium oxalate crystals in vitro; a comparison of four human proteins. *Eur. J. Biochem.,* 253: 637.

Guo, S., Mao, W., Han, Y., Zhang, X., Yang, C., Chen, Y., Xu, J., Li, H., Qi, X. (2010). Structural characteristics and antioxidant activities of the extracellular polysaccharides produced by marine bacterium *Edwardsiella tarda*. *Bioresour Technol*., 101(12): 4729-4732.

Gupta, R., Gigras, P., Mohapatra, H., Goswami, V.K., Chauhan, B. (2003). Microbial alpha-amylases: a biotechnological perspective. *Proc Biochem*., 38: 1599-1616.

Guy, L., Ettema, T.J. (2011). The archaeal 'TACK' superphylum and the origin of eukaryotes. *Trends Microbiol.*, 19(12): 580-587.

Halliwell, B. (1990). How to characterize a biological antioxidant. *Free Radic Res Commun.*, 9: 1-32.

Halliwell, B. (2007). Biochemistry of oxidative stress. *Biochem Soc Trans.,* 35: 1147-1150.

Halliwell, B., Chirico, S. (1993). Lipid peroxidation: Its mechanism, measurement, and significance. *Am J Cli Nutr*., 57: 715-724.

Halliwell, B., Gutteridge, J. M. (1995). The definition and measurement of antioxidants in biological systems. *Free Radic Biol Med.,* 18: 125-126.

Hampp, N., Popp, A., Miller, A., Brauchle, C., Oesterhelt, D. (1992). U.S. Pat., 5, 374, 492.

Hampp, N., Thoma, R., Oesterhelt, D., Brauchle, C. (1991). U.S. Pat., 5, 223, 355.

Hamzah, R.Y., Albaharna, B.S. (1994). Catechol ring-cleavage in *Pseudomonas cepacia*- the simultaneous induction of ortho and meta pathways. *Appl Microbiol Biotechnol*., 41: 250-256.

Han, R. P., Zou, W. H., Zhang, Z., Shi, J., Yang, J. (2006). Removal of copper (II) and lead (II) from aqueous solution by manganese oxide coated sand I. Characterization and kinetic study. *J Hazard Mater*., 137, 384-395.

Harborne, J. B. (1998). Phytochemical Methods: A guide to Modern Techniques of Plant Analysis. London, Chapman and Hall Ltd.

Harwood, C.S., Parales. R.E. (1996). The β-ketoadipate pathway and the biology of self identity. *Annu Rev Microbiol*., 50: 553-590.

Haseltine, C., Hill, T., Montalvo-Rodriguez, R., Kemper, S.K., Shand, R.F., Blum, P. (2001). Secreted euryarchaeal microhalocins kill hyperthermophilic crenarchaea. *J Bacteriol*., 183:287-291. DOI:10.1128/JB.183.1.287- 291

Hatfield, D.L., Tsuji, P.A., Carlson, B.A., Gladyshev, V.N. (2014). Selenium and selenocysteine roles in cancer, health, and development. *Trends Biochem Sci.*, 39:112-120. DOI: 10.1016/j.tibs.2013.12.007

Hayaishi, O., Katagiri, M., and Rothberg, S., (1957). Studies on oxygenases. Pyrocatechase, *J. Biol. Chem*., 229: 905-920.

Heim, K.E., Tagliaferro, A.R., Bobilya, D.J. (2002). Flavonoid antioxidants: Chemistry, metabolism and structure-activity relationships. *J Nutr Biochem.*, 13: 572-584.

Hezayen, F.F., Rehm, B.H.A., Tindall, B.J., Steinbuchel, A. (2001). Transfer of *Natrialba asiatica* B1T to *Natrialba taiwanensis* sp. nov. and description of *Natrialba aegyptiaca* sp. nov., a novel extremely halophilic, aerobic, non-pigmented member of the *Archaea* from Egypt that produces extracellular poly(glutamic acid). *Int J Syst Evol Microbiol*., 51: 1133-1142.

Holmes, M.L., Scopes, R.K., Moritz, R.L., Simpson, R.J., Englert, C., Pfeifer, F., Dyall-Smith, M.L. (1997). Purification and analysis of an extremely halophilic beta-galactosidase from *Haloferax alicantei*. *Biochim Biophys Acta.*, 1337:276–286.

Hosseinkhani, B., Emtiazi, G. (2011). Synthesis and characterization of a novel extracellular biogenic manganese oxide (Bixbyite-like Mn_2O_3) nanoparticle by isolated *Acinetobacter* sp. *Curr Microbiol.*, 63(3): 300-5.

Hou, J., Cui, H.L. (2018). In vitro antioxidant, antihemolytic, and anticancer activity of the carotenoids from halophilic archaea. *Curr microbiol*., 75: 266-271.

Huang, D., Ou, B., Prior R.L. (2005). The chemistry behind antioxidant capacity assays. *J Agr Food Chem.*, 53: 1841-56.

Hughes, M.F. (2002). Arsenic toxicity and potential mechanisms of action. *Toxicol Lett*., 133(1): 1-16.

Hume, R.I., Dingledine, R., Heinemann, S.F. (1991). Identification of a site in glutamate receptor subunits that controls calcium permeability. *Science*. 253: 1028-1031.

Hunter, C.I., Mitchell, A., Jones, P., McAnulla, C., Pesseat, S., Scheremetjew, M., Hunter, S. (2012). Metagenomic analysis: the challenge of the data bonanza. *Brief Bioinform*., 13:743-746.

Izotova, L.S., Strongin, A.Y., Chekulaeva, L.N., Sterkin, V.E., Ostoslavskaya, V.I., Lyublinskaya, L.A., Timokhina, E.A., Stepanov, V.M. (1983). Purification and properties of serine protease from *Halobacterium halobium*. *J Bacteriol.*, 155:826-830.

Jaeger, K.E., Eggert, T. (2002). Lipases for biotechnology. *Curr Opin Biotechnol*., 13:390–397. DOI:10.1016/S0958-1669(02)00341-5

Jain, R., Jordan, N., Weiss, S., Foerstendorf, H., Heim, K., Kacker, R., Hübner, R., Kramer, H., van Hullebusch, E. D., Farges, F., Lens P. N. L. (2015). Extracellular polymeric substances govern the surface charge of biogenic elemental selenium nanoparticles, *Environ Sci Technol*., 49: 1713-1720.

Jasenec, A., Barasa, N., Kulkarni, S., Shaik, N., Moparthi, S., Konda, V., Caguiat, J. (2009). Proteomic profiling of l-cysteine induced selenite resistance in *Enterobacter* sp. YSU. *Proteome Sci*., 7:30. DOI:10.1186/1477-5956-7-30

Jiang, J. Oberdörster, G. Biswas, P. (2009). Characterization of size, surface charge, and agglomeration state of nanoparticle dispersions for toxicological studies. *J. Nanopart. Res*., 11: 77-89.

Kabouche, A., Kabouche, Z., Ozturk, M., Kolal, U., Topcu, G. (2007). Antioxidant abietane diterpenoids from *Salvia barrelieri*. *Food. Chem.*, 102: 1281-1287.

Kakhki, A.M., Amoozegar, M.A., Khaledi, E.M. (2011). Diversity of hydrolytic enzymes in haloarchaeal strains isolated from salt lake. *Int J Environ Sci Technol*. 8(4): 705-714.

Kamekura, M., Kates, M. (1988). Lipids of halophilic archaeabacteria. In: Rodriguez-Valera, F. (ed.), *Halophilic bacteria II*, CRC Press. Boca Raton, FL, pp. 25-54.

Kamekura, M., Seno, Y. (1990). A halophilic extracellular protease from a halophilic archaebacterium strain 172 P1. *Biochem Cell Biol*., 68:352-359.

Kamekura, M., Seno, Y., Dyall-Smith, M. (1996). Halolysin R4, a serine proteinase from the halophilic archaeon *Haloferax mediterranei*; gene cloning, expression and structural studies. *Biochim Biophys Acta*., 1294: 159-167.

Kancheva, V.D. (2009). Phenolic antioxidants, radical scavenging and chain breaking activity: A comparative study. *Eur J Lipid Sci Technol.*, 111:1072-1089.

Karsten, U., Franklin, L.A., Luning, K., Wiencke, C. (1998). Natural ultraviolet radiation and photosynthetically active radiation induce formation of mycosporine-like amino acids in the marine macroalga *Chondrus crispus* (Rhodophyta). *Planta* 205: 257-262.

Karthikeyan, P., Bhat, S. G., Chandrasekaran, M. (2013). Halocin SH10 production by an extreme haloarchaeon *Natrinema* sp. BTSH10 isolated from salt pans of south India. *Saudi J Biol Sci*., 20: 205-212.

Kates, M. (1978). The phytanyl ether-linked polar lipids and isoprenoid neutral lipids of extremely halophilic bacteria. *Progress in the Chemistry of Fats and other Lipids*. 15(4): 301-42.

Kates, M. (1986). Techniques of Lipidology. Laboratory Techniques in Biochemistry and Molecular Biology, vol. 3, Part 2, 2nd edn., Elsevier, Amsterdam.

Kates, M. (1993). Membrane lipids of Archaea. In: Kates, M., Kushner D. J., Matheson, A. T. (eds.), *The Biochemistry of Archaea (Archaebacteria)*, Elsevier, Amsterdam, pp. 261-295.

Kates, M., Kushwaha, S. C. (1978). Biochemistry of lipids of extremely halophilic bacteria. In: Caplan S. R., Ginzburg, M. (eds.) Energetics and Structure of Halophilic Microrganisms, Elsiever, Amsterdam. pp. 461-480.

Kates, M., Kushwaha, S.C. (1995). Isoprenoids and polar lipids of extreme halophiles. In: DasSarma, S., Fleischman E. M. (eds.), *Archaea: A Laboratory Manual, Halophiles*. Cold Spring Harbor Laboratory Press, New York, NY, pp. 35-54.

Kavitha, P., Lipton, A.P., Sarika, A.R., Aishwarya. M.S. (2011). Growth characteristics and halocin production by a new isolate, *Haloferax volcanii* KPS1 from Kovalam solar Saltern (India). *Research Journal of biological sciences*, 6(5): 272-262.

Kelly, M., Liaaen-Jensen, S. (1967). Bacterial Carotenoids XXVI. C_{50}-Carotenoids 2. Bacterioruberin. *Acta Chem Scand.*, 21: 2576-2580.

Kelly, M., Norgard, S., Liaaen-Jensen, S. (1970). Bacterial Carotenoids XXXI. C_{50}-Carotenoids 5. Carotenoids of *Halobacterium salinarium*, especially bacterioruberin. *Acta Chem Scand.*. 24: 2169-2182.

Kessi J, Ramuz M, Wehrli E, Spycher M, Bachofen R. (1999). Reduction of selenite and detoxification of elemental selenium by the phototrophic bacterium *Rhodospirillum rubrum*. *Appl Environ Microbiol.*, 65: 4734-40.

Kessi, J., Hanselmann, K.W. (2004). Similarities between the abiotic reduction of selenite with glutathione and the dissimilatory reaction mediated by *Rhodospirillum rubrum* and *Escherichia coli*. *J Biol Chem.*, 279: 50662-9.

Khachik, F., Beecher G.R., Whittaker N. F. (1986). Separation, identification, and quantification of the major carotenoid and chlorophyll constituents in extracts of

several green vegetables by liquid chromatography. *J Agric Food Chem.*, 34(4). DOI: 10.1021/jf00070a006

Khandavilli, S., Sequeira, F. Furtado I. (1999). Metal tolerance of extremely halophilic bacteria isolated from estuaries of Goa. *India Ecol Env Cons.*, 5: 149-152.

Khlebnikov, A. I., Schepetkin, I. A., Domina, N. G., Kirpotina, L. N., Quinn, M. T. (2007). Improved quantitative structure-activity relationship models to predict antioxidant activity of flavonoids in chemical, enzymatic, and cellular systems. *Bioorg Med Chem.*, 15: 1749-1770.

Khoei, N.S., Lampis, S., Zonaro, E., Yrjälä, K., Bernardi, P., Vallini, G. (2017). Insights into selenite reduction and biogenesis of elemental selenium nanoparticles by two environmental isolates of *Burkholderia fungorum*. *New Biotechnol.,* 34:1–11. DOI: 10.1016/j.nbt.2016.10.002

Kikuzaki, H., Usuguchi, J., Nakatani, N. (1991). Constituents of Zingiberaceae I. Diarylheptanoid from the rhizomes of ginger (Zingiber officinale Roscoe). *Chem. Pharm. Bull.*, 39:120.

Kim, D., Kim, S.W., Choi, K.Y., Lee, J.S., Kim, E. (2008). Molecular cloning and functional characterization of the genes encoding benzoate and p-hydroxybenzoate degradation by the halophilic *Chromohalobacter* sp. strain HS-2. *FEMS Microbiol Lett*., 280: 235-24.

Kis-Papo, T., Oren, A. (2000). Halocins: are they involved in the competition between halobacteria in saltern ponds? *Extremophiles*. 4: 35-41.

Klaunig, J.E., Kamendulis, L.M. (2004). The role of oxidative stress in carcinogenesis. *Annu Rev Pharmacol Toxicol*., 44: 239-267.

Klonowska, A., Heulin, T., Vermeglio, A. (2005). Selenite and tellurite reduction by *Shewanella oneidensis*. *Appl Environ Microbiol.,* 71:5607-5609

Klug, H.P., Alexander, L.E. (1974). X-ray Diffraction procedures for polycrystallite and amorphous materials, 2nd ed, Wiley, New York, NY, USA.

Kobayashi, T., Kanai, H., Aono, R., Horikoshi, K., Kudo, T. (1994). Cloning, expression, and nucleotide sequence of the alpha-amylase gene from the haloalkaliphilic archaeon *Natronococcus* sp. strain Ah-36. *J Bacteriol*., 176: 5131-5134.

Konca, K., Lankoff, A., Lisowska, H., Kuszewski, T., Gozd, S., Koza, Z., Wojcik, A. (2003). Cross-platform public domain PC image-analysis program for the comet assay. *Mutat Res*., 534(1-2): 15-20.

Kooy, N.W., Royall, J.A., Ischiropoulos, H., Beckman, J.S. (1994). Peroxynitrite-mediated oxidation of dihydrorhodamine 123. *Free Radic. Biol. Med.*, 16:149-156.

Krebs, M.P., Khorana, H.G. (1993). Mechanism of light-dependent proton translocation by bacteriorhodopsin. *J Bacteriol*., 175: 1555-1560.

Krishnan, G., Altekar, W. (1991). An unusual class I (Schiff base) fructose-1, 6-bisphosphate aldolase from the halophilic archaebacterium *Haloarcula vallismortis*. *Eur J Biochem*., 195 (2): 343-50.

Kukor J.J., Olsen R. H. (1991). Genetic organization and regulation of a meta cleavage pathway for catechols produced from catabolism of toluene, benzene, phenol, and cresols by *Pseudomonas pickettii* PKO1. *J. Bacteriol.*, 173(15): 4587-4594.

Kumar, V., Saxena, J., Tiwari, S. K. (2016). Description of a halocin-producing *Haloferax larsenii* HA1 isolated from Pachpadra salt lake in Rajasthan. *Arch Microbiol*. DOI 10.1007/s00203-015-1175-3

Kumaravel, T.S., Vilhar, B., Faux, S.P., Jha, A.N. (2009). Comet Assay measurements: a perspective. *Cell Bio Toxicol*., 25(1): 53–64.

Kunchandy, E., Rao, M.N.A. (1990). Oxygen radical scavenging activity of curcumin. *Int. J. Pharm.* 58:237–240.

Kushner, D.J., Kamekura, M. (1988). Physiology of halophilic eubacteria. In: Rodríguez-Varela, F. (ed.), *Halophilic Bacteria*, CRC Press, Boca Raton, FL, USA, pp.109-138.

Kushwaha, S. C., Gochnauer, M. B., Kushner, D. J., Kates, M. (1974). Pigments and isoprenoid compounds in extremely and moderately halophilic bacteria. *Can J Microbiol*., 20: 241-245.

Kushwaha, S. C., Kates, M., Juez, G., Rodriguez-Valera, F., Kushner, D. J. (1982). Polar lipids of an extremely halophilic bacterial strain (R-4) isolated from salt ponds in Spain. *Biochim Biophys Acta*., 7(11): 19-25.

Kushwaha, S. C., Kramer, J.K.G., Kates, M. (1975). Isolation and characterization of C_{50} carotenoid pigments and other polar isoprenoids from *Halobacterium cutirubrum*. *Biochim et biophy acta*., 398: 303-314.

Kushwaha, S.C., Pugh, E.L., Kramer, J.K.G., Kates, M. (1972). Isolation and identification of dehydrosqualene and C_{40} carotenoid pigments in *Halobacterium cutirubrum*. *Biochim Biophys Acta*., 260: 492-506.

Lafferty, R.A., Korsatko, B., Korsatko, W., Rehm, H.J., Reed, G. (1988). Biotechnology. Volume 6b, Weinheim: VCH.135-176.

Lampis, S. Zonaro, E. Bertolini, C. Bernardi, P. Butler, C.S. Vallini, G. (2014). Delayed formation of zerovalent selenium nanoparticles by *Bacillus mycoides* SeITE01 as a consequence of selenite reduction under aerobic conditions. *Microb Cell Fact*., 13: 13-35.

Langer, R.D., Lorke, D.E., Neidl van Gorkom, K.F., Petroianu, G., Azimullah, S., Nurulain, S.M., Singh, S., Fuchsjäger, M. (2012). In an animal model nephrogenic systemic fibrosis cannot be induced by intraperitoneal injection of high-dose

gadolinium based contrast agents. *Eur J Radiol.*, 81(10): 2562-7. DOI: 10.1016/j.ejrad.2011.10.032

Laviano, A., Meguid, M.M., Preziosa, I., Fanelli, F.R. (2007). Oxidative stress and wasting in cancer. *Curr Opin Clin Nutr Metab Care*., 10: 449-456.

Lee, M.H., Lee, S.W. (2013). Bioprospecting potential of the soil metagenome: novel enzymes and bioactivities. *Genomics Inform*., 11: 114-120.

Lee, X., Weinfeld, M. (2004). *Cellular Response to Arsenic:DNA Damage and Defense Mechanisms*, London, UK: IWA Publishing.

Leveque, E., Janecek, S., Belarbi, A., Haye, B. (2000). Thermophilic archaeal amylolytic enzymes. *Enzyme Microb Technol*., 26: 2-13.

Lewis K. (2001). Riddle of Biofilm Resistance. *Antimicrob Agents Chemother.*, 45(4):999–1007. DOI:10.1128/AAC.45.4.999–1007.2001

Li, B., Liu, N., Li, Y., Jing, W., Fan, J., Li, D., Zhang, L., Zhang, X., Zhang, Z., Wang, L. (2014). Reduction of selenite to red elemental selenium by *Rhodopseudomonas palustris* strain N. PLoS ONE. 9:e95955.

Li, Y., Xiang, H., Liu, J., Zhou, M., Tan, H. (2003). Purification and biological characterization of halocin C8, a novel peptide antibiotic from *Halobacterium* strain AS7092. *Extremophiles*. 7:401–407. DOI:10.1007/s00792-003-0335-6

Liang, M., Bai, Y., Huang, L., Zheng W., Jie, L. (2009). Inhibition of the crystal growth and aggregation of calcium oxalate by elemental selenium nanoparticles. *Colloids Surf B Biointerfaces,* 74: 366–369.

Lieske, J.C., Leonard, R., Toback, F.G. (1995). Adhesion of calcium oxalate monohydrate crystals to renal epithelial cells is inhibited by specific anions. *Am J Physiol.,* 268(4 Pt 2):F604-12.

Lin, Z.-H., Lee, C.-H., Chang, H.-Y., Chang, H.-T. (2012). Antibacterial activities of tellurium nanomaterials. *Chemistry - An Asian Journal*, 7(5), 930-934. DOI:10.1002/asia.201101006

Lindsey, H., Petersen, N.O., Chan, S.I. (1979). Physicochemical characterization of 1, 2-diphytanoyl-sn-glycero-3-phosphocholine in model membrane systems. *Biochim Biophys Acta., BBA Biomembranes*, 555: 147-167.

Lizama, C., Monteoliva-Sánchez, M., Prado, B., Ramos-Cormenzana, A., Weckesser, J., Campos, V. (2001). Taxonomic study of extreme halophilic archaea isolated from the "Salar de Atacama". *Chile. Syst. Appl. Microbiol*., 24(3): 464-474.

Lobo, V., Phatak, A., Chandra, N. (2010). Free radicals and functional foods: Impact on human health. *Pharmacogn Rev.*, 4: 118-126.

Lowry, O.H., Rosebrough, N.J., Farr, A.L., Randall, R.J. (1951). Protein measurement with the Folin phenol reagent. *J Biol Chem.*, 193: 265-275.

Lü, J., Lin, P.H., Yao, Q., Chen, C. (2010). Chemical and molecular mechanisms of antioxidants: Experimental approaches and model systems. *J. Cell Mod Med.*, 14:840-860.

MacElroy, R. D. (1974). Some comments on the evolution of extremophiles. *Biosystems*, 6: 74-75.

Madern, D., Ebel, C., Zaccai, G. (2000). Halophilic adaptation of enzymes, *Extremophiles*, 4(2): 91-98.

Madigan, M. T., Marrs, B. L. (1997). Extremophiles. *Sci Am*., 276:66-71.

Maduabuchi, E. K., Noundou, X. S., Ejike, U. S., Atuzie, W. (2018). Biosynthesis, characterization and antimicrobial activity of silver nanoparticles using cell free lysate of *Bacillus Subtilis*: A Biotechnology Approach. *American Journal of Nanoscience and Nanotechnology Research,* 6: 18-27.

Magat, S.S. (2000). An effective and cheap fertilizer for high coconut productivity. *Technology Guide Sheet No. 5*, Philippine Coconut Authority.

Mahansaria, R., Dhara, A., Saha, A., Haldar, S., Mukherjee, J. (2018). Production enhancement and characterization of the polyhydroxyalkanoate produced by *Natrinema ajinwuensis* (as synonym) ≡ *Natrinema altunense* strain RM-G10. *Int J Biol Macromol.* 107(B): 1480-1490.

Mal, J., Veneman, W. J., Nancharaiah, Y. V., Van Hullebusch, E. D., Peijnenburg, W.J.G.M., Vijver, M.G. (2017). A comparison of fate and toxicity of selenite, biogenically, and chemically synthesized selenium nanoparticles to zebrafish (Danio rerio) embryogenesis. *Nanotoxicol*., (11)1: 87-97.

Malhotra, S., Jha, N., Desai, K. (2014). A superficial synthesis of selenium nanospheres using Wet chemical approach. International Journal of Nanotechnology and Application, 3(4):7-14.

Malik, A.D., Furtado, I.J. (2018). Clarification of saline textile dye waters using haloarchaeal aerobic sequential bioreactor system. *International Journal of Pharmacy and Biological Sciences*. 8:22-28.

Mandel, N. **(**1994). Crystal-membrane interaction in kidney stone disease. *J Am Soc Nephrol.,* 5(1): S37-45.

Mandelli, F., Miranda, V. S., Rodrigues, E., Mercadante, A. Z. (2012). Identification of carotenoids with high antioxidant capacity produced by extremophile microorganisms. *World J Microbiol Biotechnol.,* 28: 1781-1790.

Mani, K., Salgaonkar, B., Das, D., Bragança, J.M. (2012). Community solar salt production in Goa, India. *Aqua Biosyst*., 8: 30.

Margesin, R., Schinner, F. (2001). Biodegradation and bioremediation of hydrocarbons in extreme environments. *Appl Microbiol Biotechnol*., 56: 650-663.

Marhuenda-Egea, F. C., Bonete, M. J. (2002). Extreme halophilic enzymes in organic solvents. *Curr Opin biotech*., 13(4): 385-389.

Mateo, N., Nader, W., Tamayom, G. (2001). Bioprospecting. *Encyclopedia of Biodiversity.* 1: 471-487.

Matsumoto, T., Ito, M., Fukuda, H., Kondo, A. (2004). Enantioselective transesterification using lipase-displaying yeast whole-cell biocatalyst. *Appl Microbiol Biotechnol*., 64:481-485. DOI:10.1007/s00253-003-1486-1

Mayer, R.L., Sulzberger, M.B. (1931). Zur. Frug der yahreszeit lichen schwanKungen der Krannei ten. Der Einglus s der Kost auf. Experimental le sensipilisierungen. Archiv für Dermatologie und Syphilis. 163, 245.

McCord, J., Fridovich, I. (1969). Superoxide dismutase, an enzymic function for erythrocuprin. *J. Biol. Chem.* 244:6049-6055.

Meseguer, I. Rodriguez-Valera, F. (1985). Production and purification of halocin H4. FEMS *Microbiol Lett*., 28: 177-182.

Meseguer, I., Rodriguez-Valera F., Ventosa, A. (1986). Antagonistic interactions among halobacteria due to halocin production. *FEMS Microbiol. Lett*., 36:177-182.

Meyer, A.S., Isaksen, A. (1995). Application of enzymes as food antioxidants. *Trends Food Sci. Technol.*, 6: 300-304.

Mille, G., Almallah, M., Bianchi, M., Wambeke, F., Bertrand, J.C. (1991). Effect of salinity on petroleum biodegradation. *Fresenius J Anal Chem*., 339: 788-791.

Miller, N. J., Sampson, J., Candeias, L.P., Brameley, P.M., Rice-Evans, C.A. (1996). Antioxidant activities of carotenes and xanthophylls. *FEBS Lett* 384: 240–242. http://dx.doi.org/10.1016/0014-5793(96)00323-7.

Miltonprabu. S., Sumedha, N. C. (2014). Ameliorative effect of diallyl trisulphide on arsenic-induced oxidative stress in rat erythrocytes and DNA damage in lymphocytes. *J Basic Clin Physiol Pharmacol.*, 25(2): 181-197.

Min, D.B., Boff, J.M. (2002). Chemistry and reaction of singlet oxygen in foods. *Comp Rev Food Sci F.*, 1: 58-72.

Mirabet. V., Vaca. P., Carbonell-Uberos. F., Lequerica, J.L., Montero, J.A., Piquer, S., Dalmau, M.J., Hornero, F. (2002). Ischemic heart disease; searching for therapeutical solutions. In Phillips, G.O. (ed.), *Advances in Tissue Banking*, World Scientific Pusblishing, Singapore, Vol 6, Chapter 20, pp. 359-374.

Mishra, K., Ojha, H., Chaudhury, N.K. (2012). Estimation of antiradical properties of antioxidants using DPPH$^{\bullet}$ assay: A critical review and results, *Food Chem.*, 130:1036-1043.

Mishra, R.R., Prajapati, S., Das, J., Dangar, T.K., Das, N., Thatoi, H. (2011). Reduction of selenite to red elemental selenium by moderately halotolerant *Bacillus megaterium* strains isolated from Bhitarkanika mangrove soil and characterization of reduced product. *Chemosphere*, 84:1231-1237.

Montitsche L, Driller H, Galinski E. U.S. Pat. 060071. 2000.

Moshfegh, M., Reza, A., Gholamreza, S., Mohammad, Z., Faramarzi, A. (2013). Biochemical characterization of an extracellular polyextremophilic α-amylase from the halophilic archaeon *Halorubrum xinjiangense*. *Extremophiles*, 17(4): 677-687.

Mukherjee, S., Roy, M., Dey, S., Bhattacharya, R.K. (2007). A mechanistic approach for modulation of arsenic toxicity in human lymphocytes by curcumin, an active constituent of medicinal herb *Curcuma longa Linn*. *J Clin Biochem Nutr*., 41: 32-42.

Mullakhanbhai, M. F., Francis, G. W. (1972). *Halobacterium volcanii* spec. nov., a Dead Sea halobacterium with a moderate salt requirement. *Acta Chem. Scand*., 26: 1399-1410.

Nader, W. F., Hill, B. (1999). Der Schatz im Tropenwald-Biodiversita¨ t als Inspirations- und Innovationsquelle. Shaker Verlag, Aachen, Germany.

Naik S.S., Furtado, I. J. (2014). Equilibrium and Kinetics of Adsorption of Mn^{2+} by haloarchaeon *Halobacterium* sp. GUSF (MTCC3265). *Geomicrobiol*., 31(8).

Navarro-Alarcón, M., López-Martínez, M.C. (2000). Essentiality of selenium in the human body: relationship with different diseases. *Sci Total Environ*., 17; 249(1-3): 347-71.

Naziri, D., Hamidi, M., Hassanzadeh, S., Tarhriz, V., Zanjani, B. M., Nazemyieh, H., Hejazi, M. A., Hejazi, M.S. (2014). Analysis of carotenoid production by *Halorubrum* sp. TBZ126; an extremely halophilic Archeon from Urmia Lake. Adv Pharm Bull. 4(1):61-67. http://dx.doi.org/10.5681/apb.2014.010

Newton, G. L., Fahey. R. C. (1989). Glutathione in procaryotes,. In Vin˜a, J. (ed.), *Glutathione: metabolism and physiological functions*. CRC Press, Boca Raton, Florida, pp. 69-77.

Nieto, J.J., Fernandez-Castillo, R., Marquez, M.C., Ventosa, A., Quesada, E., Ruiz-Berraquero, F. (1989). Survey of metal tolerance in moderately halophilic Eubacteria. *Appl Environ Microb*., 55: 2385-90.

Nigra, A. E., Sanchez, T. R., Nachman, K.E., et al. (2017). The effect of the Environmental Protection Agency maximum contaminant level on arsenic exposure in the USA from 2003 to 2014: an analysis of the National Health and Nutrition Examination Survey (NHANES). *Lancet public health*. (2)11: PE513-E521.

Norberg, P., Hofsten, B.V. (1969). Proteolytic enzymes from extremely halophilic bacteria. *J Gen Micro.*, 55: 251-256.

Noro, T., Oda, Y., Miyase, T., Ueno, A., Fukushima, S. (1983). Inhibitors of xanthine oxidase from the flowers and buds of Daphne genkwa. *Chem. Pharm. Bull.*, 31: 3984-3987.

Nriagu, J., Bhattacharya, P., Mukherjee, A., Bundschuh, J., Zevenhoven, R., Loeppert, R. (2007). Arsenic in soil and groundwater: an overview. In: *Arsenic in Soil and Groundwater Environment,* (P. Bhattacharya, A. Mukherjee, J. Bundschuh, R. Zevenhoven, R. Loeppert eds.), Amsterdam, The Netherlands: Elsevier. 3-60.

Nunoura, T., Takaki, Y., Kakuta J et al (2010) Insights into the evolution of Archaea and eukaryotic protein modifier systems revealed by the genome of a novel archaeal group. *Nucleic Ac Res*. 1-20. DOI:10.1093/nar/gkq1228

O'Connor, E.M., Shand, R.F. (2002). Halocins and sulfolobicins: The emerging story of archaeal protein and peptide antibiotics. *J Ind Microbiol Biotechnol*., 28: 23-31.

O'Toole GA. (2011). Microtiter dish biofilm formation assay. *J Vis Exp.*, 47:e2437-e2437. DOI: 10.3791/2437

Oesterhelt, D., Stoeckenius, W. (1971). Rhodopsin-like protein from the purple membrane of *Halobacterium halobium*. *Nat New Biol*., 233: 149-152.

Ohkawa, H., Onishi, N., Yagi, K. (1979). Assay for lipid peroxidation in animal tissue by thiobarbituric acid reaction. *Anal. Biochem.*, 95: 351-358.

Olajire, A.A., Essien, J.P. (2014). Aerobic degradation of petroleum components by microbial consortia. *J Pet Environ Biotechnol*., 5: 195. DOI:10.4172/2157-7463.1000195

Onishi, H., Mori, T., Takeuchi, S., Tani, K., Kobayashi, T. (1983). Halophilic nuclease of a moderately halophilic *Bacillus* sp. Production purification and characteristics. *Appl. Environ. Microbiol.*, 45(1): 24-30.

Oren, A. (1983). *Halobacterium sodomense* sp. nov., a dead sea halobacterium with an extremely high magnesium requirement. *Int J Syst Bacteriol.*, 33: 381-386.

Oren, A. (2000). Life at high salt concentrations. In: The prokaryotes: an evolving electronic resource for the microbiological community, 3rd edn, Springer, New York. http://link. springer-ny.com/link/service/books/10125

Oren, A. (2002). Diversity of halophilic microorganisms: environments, phylogeny, physiology, and applications. *J Ind Microbiol Biotechnol*., 28:56-63.

Oren, A. (2013). Life at high salt concentrations, intracellular KCl concentrations, and acidic proteomes. *Front Microbiol.*, 4:315.

Oren, A., Gunde-Cimerman, N. (2007). Mycosporines and mycosporine-like amino acids: UV protectants or multipurpose secondary metabolites? *FEMS Microbiol Lett.*, 269: 1-10.

Oren, A., Gurevich, P., Azachi, M., Henis, Y. (1992). Microbial degradation of pollutants at high salt concentrations. *Biodegradation*. 3: 387-398.

Oren, A., Ventosa, A., Grant, W. D. (1997). Proposed minimal standards for description of new taxa in the order Halobacteriales. *Int J Syst Bacteriol*., 47: 233-238.

Ottolenghi, A. (1959). Interaction of ascorbic acid and mitochondria lipids. *Arch. Biochem. Biophys.*, 79: 355.

Ottow, J. C. G., Zolg, W. (1974). Improved procedure and colorimetrics test for the detection of ortho- and meta-cleavage of protocatechuate by *Pseudomonas* isolates. *Can J Microbiol.*, 20:1059-1061.

Ou, B.X., Huang, D.J., Hampsch-Woodill, M., Flanagan, J.A., Deemer, E.K. (2002). Analysis of antioxidant activities of common vegetables employing oxygen radical absorbance capacity (ORAC) and ferric reducing antioxidant power (FRAP) assays: a comparative study. *J Agric Food Chem.*, 50(11): 3122-3128.

Oyaizu, M. (1986). Studies on products of browning reactions: antioxidant activities of products of browning reaction prepared from glucosamine. *J. Nutrit.*, 44: 307-315.

Ozcan B., Ozcengiz, G., Coleri, A. Cokmus. C. (2007). Diversity of halophilic archaea from six distinct parts of Turkey. *J. Microbiol. Biotechnol.*, 17: 985–992.

Ozcan, B., Cokmus, C., Coleri, A., Caliskan, M. (2006). Characterization of extremely halophilic Archaea isolated from saline environment in different parts of Turkey. *Microbiol.*, 75: 739-746.

Ozcan, B., Ozyilmaz, G., Cokmus, C., Caliskan, M. (2009). Characterization of extracellular esterase and lipase activities from five halophilic archaeal strains. *J Ind Microbiol Biotechnol*., 36(1): 105-10. DOI: 10.1007/s10295-008-0477-8

Painter, E.P. (1941). The chemistry and toxicity of selenium compounds, with special reference to the selenium problem, *Chem Rev*: 28 179–213.

Parikh, S.J., Chorover, J. (2005). FTIR spectroscopic study of biogenic mn-oxide formation by *Pseudomonas putida* GB-1. *Geomicrbiol. J*., 22: 207-218.

Park, S., Lee, J., Lee, H. (2000). Purification and characterization of chitinase from a marine bacterium, *Vibrio* sp. 98CJ11027. *J. Microbiol*., 38(4): 224-229.

Pasic, L., Velikonja B.H., Ulrih, N.P. (2008). Optimization of the culture conditions for the production of a bacteriocin from halophilic archaeon Sech7a. *Prep Biochem Biotechnol*., 38: 229-245.

Pathak, A.P., Sardar, A.G. (2012). Isolation and characterization of carotenoid producing *Haloarchaea* from solar salterns of mulund, Mumbai, India. *Ind J Nat Prod Res*. 3: 483-88.

Patil, S., Fernandes, J., Tangsali, R.B., Furtado, I. (2014). Exploitation of *Haloferax alexandrinus* for biogenic synthesis of silver nanoparticles antagonistic to human and lower mammalian pathogens. *J Clust Sci*. 25: 423-433.

Pérez-Pomares, F., Bautista, V., Ferrer, J., Pire, C., Marhuenda-Egea, F. C., Bonete, M. J. (2003). α-Amylase activity from the halophilic archaeon *Haloferax mediterranei Extremophiles*, 7(4): 299-306.

Petter, H.F.M. (1931). On bacteria of salted fish. *Koninkl Akad Wetenschap* 34: 1417-1423.

Platas, G., Meseguer, I., Amils, R. (2002). Purification and biological characterization of halocin H1 from *Haloferax mediterranei* M2a. *Int Microbiol* 5:15–19. DOI: 10.1007/s10123-002-0053-4

Platas, G., Meseguer, I., Amils, R. (1996). Optimization of the production of a bacteriocin from *Haloferax mediterranei* Xia3. *Microbiologia*. 12(1):75-84.

Poinern, G.E.J.A. (2014). Laboratory Course in Nanoscience and Nanotechnology, 1st ed., CRC Press Taylor & Francis: Boca Raton, FL, USA.

Pokorny, J. (2007). Are natural antioxidants better and safer than synthetic antioxidants? *Eur J Lipid Sci Technol.*, 109: 629-642.

Prabhu, N. (2002). Impact of hydrocarbon pollution on the chemical status of soil and response of resting cells of *Halobacterium* strain R1 MTCC 3265 to sodium benzoate. MSc Thesis, Goa University, Taleigao, Goa.

Prasad, K.S., Selvaraj, K. (2014). Biogenic synthesis of selenium nanoparticles and their effect on As (III)-induced toxicity on human lymphocytes. *Biol Trace Elem Res*., 157: 275-283.

Price, L.B. Shand, R.F. (2000). Halocin S8: A 36-amino-acid microhalocin from the Haloarchaeal strain S8a. *J Bacteriol*., 182: 4951-4958.

Prieto, P., Pineda, M., Aguilar, M. (1999). Spectrophotometric quantitation of antioxidant capacity through the formation of a phosphomolybdenum complex: specific application to the determination of vitamin E. *Anal. Biochem.*, 269: 337-341.

Prigent-Combaret, C., Sanfuin, H., Champier, L., Bertrand, C., Monnez, C., Collnon, C., Blaha, D., Ghigo, J.M., Cournoyer, B. (2012). The bacterial thiopurine

methyltransferase tellurite resistance process is highly dependent upon aggregation properties and oxidative stress response. *Environ Microbiol.*, 14: 2645-60.

Prior, R.L., Hoang, H., Gu, L. (2003). Assays for hydrophilic and lipophilic antioxidant capacity (oxygen radical absorbance capacity (ORAC (FL)) of plasma and other biological and food samples. *J. Agric. Food Chem.,* 51: 3273-3279.

Purdy, K. J., Cresswell-Maynard, T. D., Nedwell, D. B., McGenity, T. J., Grant, W. D., Timmis, K. N., Embley, T. M. (2004). Isolation of haloarchaea that grow at low salinities. *Environ Microbiol*. 6: 591-595.

Racker, E., Stoeckenius, W. (1974). Reconstitution of purple membrane vesicles catalyzing light-drivenproton uptake and adenosine triphosphate formation. *J Biol Chem*., 249: 662-663.

Radzig, M. A., Nadtochenko, V. A., Koksharova, O. A., Kiwi, J., Lipasova, V. A., and Khmel, I. A. (2013). Antibacterial effects of silver nanoparticels on gram-negative bacteria: influence on the growth and biofilm formation, mechanisms of action. *Colloids Surf. B Biointerfaces* 102, 300-306. DOI: 10.1016/j.colsurfb.2012.07.039

Raghavan, T. M., Furtado, I. (2004). Occurrence of extremely halophilic Archaea in sediments from the continental shelf of west coast of India. *Curr. Sci.,* 86(8): 1065-1067.

Raghavan, T.M., Furtado, I. (2005). Expression of Carotenoid Pigments of Haloarchaeal Cultures Exposed to Aniline. *Environ. Toxicol*., 20, 165-169.

Rasamiravaka, T., Quentin, L., Pierre, D., Mondher, E. J. (2015). The Formation of Biofilms by *Pseudomonas aeruginosa*: A Review of the Natural and Synthetic Compounds Interfering with Control Mechanisms. *Biomed Res Int*. https://doi.org/10.1155/2015/759348

Rdest, U. Sturm, M. (1987). Bacteriocins from Halobacteria. In: *Protein Purification: Micro to Macro*, (R. Burgess, ed.). John Wiley and Sons Canada Limited, New York, USA, pp: 271-278.

Reardon, K.F., Mosteller D.C., Bull Rogers, J.D. (2000). Biodegradation kinetics of benzene, toluene and phenol as single and mixed substrates for *Pseudomonas putida* F1. *Biotechnol Bioeng*., 69: 385-400. DOI: 10.1002/1097-0290(20000820)69:43.0.CO;2-Q

Reeves, P. (1972). The bacteriocins. In: *Mol Biol. Biochem and Biophy*.,(A., Kleinzeller Springer, G.F. and Whitmann H.G. ed). Vol. 11.

Reid, W. V., Laird, S., Meyer, C. A., Ga´mez, R., Sittenfeld, A., Janzen, D. H., Gollin, M. A., and Juma, C. (1993). *Biodiversity Prospecting: Using Genetic Resources for Sustainable Development*. World Resources Institute, Washington, D.C.

Rhykerd, R.L., Weaver, R.W., McInnes, K.J. (1995). Influence of salinity on bioremediation of oil in soil. *Environ Pollut*., 90:127-130.

Rinke, C., Schwientek, P., Sczyrba, A., Ivanova, N. N., Anderson, I.J. (2013).Insights into the phylogeny and coding potential of microbial dark matter. *Nature*, 499: 431-437.

Rodrigo-Baños, M., Garbayo, I., Vílchez, C., Bonete, M.J., Martínez-Espinosa, R.M. (2015). Carotenoids from Haloarchaea and their potential in biotechnology. *Mar Drugs* 13:5508-5532.

Rodriguez-Amaya, D. B., Kimura, M. (2004). Harvestplus Handbook for Carotenoid Analysis. HarvestPlus Technical Monograph 2. Washington, DC and Cali: International Food Policy Research Institute (IFPRI) and International Center for Tropical Agriculture (CIAT).

Rodriguez-Valera, F., Juez, G., Kushner, D.J. (1982). Halocins: Salt dependent bacteriocins produced by extremely halophilic rods. *Can J Microbiol*., 28: 151-154.

Romero, M.C., Cazau, M.C., Giorgieri, S., Arambarri, A.M. (1998). Phenanthrene degradation by microorganisms isolated from a contaminated stream. *Environ Pollut*., 101: 355-359.

Ronnekleiv, M., Liaaen-Jensen, S. (1995). Bacterial carotenoids. 53, C50-carotenoids 23; Carotenoids of *Haloferax volcanii* versus other halophilic bacteria. *Biochem Syst Ecol*., 23: 627-734.

Ross, H.N.M., Grant, W.D., Harris, J. E. (1985). Lipids in archaebacterial taxonomy. In: *Chemical methods in bacterial systematics*, (M. Goodfellow and D.E. Minnikin ed.). Society for Appl Bacteriol.Technical Series 20, Academic Press, London. 289-300.

Ruben, D., Gonzalez, E., Arenas, C., Vilches, E. B., De Billerbeck, M. (1993). Selective procedure for isolating microorganisms producing pullulanase and isoamylase. *Biotech Tech.*, 7(6): 429-434.

Ruch, R.J., Cheng, S.J., Klaunig, J.E. (1989). Prevention of cytotoxicity and inhibition of intercellular communication by antioxidant catechins isolated from Chinese green tea. *Carcinogen*, 10:1003-1008.

Ryu, K., Dordick. J. S. (1994). Catalytic properties and potential of an extracellular protease from an extreme halophile. *Enzyme Microb Technol.*, 16: 266-275.

Saif, S., Tahir A., Chen Y. (2016). Green synthesis of iron nanoparticles and their environmental applications and implications. *Nanomaterials (Basel)*, 6(11): 209. DOI: 10.3390/nano6110209

Saito T., Miyabe Y., Ide, H., Osamu, Y. (1997). Hydroxyl radical scavenging ability of bacterioruberin. *Radiat Phys Chem.*, 50(3): 267-269. DOI: 10.1016/S0969-806X(97)00036-4

Saitou, N., Nei, M. (1987). The Neighbor-Joining method: A new method for reconstructing phylogenetic trees. *Mol Biol Evol*., 4: 406-425.

Salgaonkar B.B., Bragança J.M. (2017). Utilization of sugarcane bagasse by *Halogeometricum borinquense* strain E3 for biosynthesis of poly (3-hydroxybutyrate-co-3-hydroxyvalerate). *Bioengineering*. 4:50 DOI: 10.3390/bioengineering4020050.

Salgaonkar, B.B., Bragança, J.M. (2015a). Biosynthesis of poly (3-hydroxybutyrate-*co*-3-hydroxyvalerate) by *Halogeometricum borinquense* strain E3. *Int J Biol Macromol*. 78:339–346.

Salgaonkar, B.B., Bragança, J.M. (2015b). Synthesis of Polyalkanoates by Halophilic Archaea amd Bacteria and their osmoadaptation. PhD thesis, Birla Institute of Technology and Science, Pilani.

Salgaonkar, B.B., Kabilan, M., Nair, A., Gangadharan, S., Braganca, J.M. (2012). Interspecific interactions among members of family *Halobacteriaceae* from natural solar salterns. *Probiotics Antimicrob Proteins* 4(2):98–107.

Salgaonkar, B.B., Das, D., Bragança, J.M. (2016) Resistance of extremely halophilic archaea to zinc and zinc oxide nanoparticles**.** *Appl Nanosci* 6: 251–258**.** https://doi.org/10.1007/s13204-015-0424-8

Samad, M. Y. A., Razak, C. A. N., Salleh, A. B., Zinwan Yunus, W. M., Ampon, K., Basri, M. (1989). A plate assay for primary screening of lipase activity. *J Microbiol Meth.*, 9(1): 51-56.

Sams, C.E., Panthee, D.R., Charron, C. S., Kopsell, D.A., Yuan, J. S. (2011). Selenium regulates gene expression for glucosinolate and carotenoid biosynthesis in *Arabidopsis*. *J Am Soc Hortic Sci.*, 136(1). DOI: 10.21273/JASHS.136.1.23

Sanchez-Moreno, C., Larrauri, J. A., Saura-Calixto, F. (1998). A procedure to measure the antiradical efficiency of polyphenols. *J Sc Food Agr*., 76: 270-276.

Sand, F.E.M.J. (1975). *Gluconobacter* still drinks and plastic containers. *Soft Drinks Trade Journal*, 29: 371-373.

Sapakal, V.D., Shikalgar, T.S., Ghadge, R.V., Adnaik, R.S., Naikwade, N.S., Magdum, C.S. (2008). In vivo screening of antioxidant profile: a review. *J. Herbal Med. Toxicol.*, 2 (2):1-8.

Sarret, G., Avoscan, L., Carrière, M., Collins, R., Geoffroy, N., Carrot, F., Covès, J., Gouget, B. (2005). Chemical forms of selenium in the metal-resistant bacterium *Ralstonia metallidurans* CH34 exposed to selenite and selenite. *Appl Environ Microbiol.*, 71: 2331-2337.

Scherer, R., Godoy, H.T. (2009). Antioxidant activity index (AAI) by the 2, 2-diphenyl-1-picrylhydrazyl method. *Food Chem.*, 112: 654-658.

Schmid, R.D., Verger, R. (1998). Lipases: interfacial enzymes with attractive applications. *Angew Chem Int Ed Engl.*, 37: 1608-1633. DOI: 10.1002/(SICI)15213773(19980703)37:12\1608

Seeram, N.P., Henning, S.M., Lee, R., Niu, Y., Scheuller, H.S., Heber, D. (2006). Catechin and caffeine contents of green tea dietary supplements and correlation with antioxidant activity. *J. Agric. Food Chem.*, 54:1599-1603.

Sen, S., Chakraborty, R. (2017). Revival, modernization and integration of Indian traditional herbal medicine in clinical practice: Importance, challenges and future. *J Tradit Complement Med*., 7(2): 234-244. DOI:10.1016/j.jtcme.2016.05.006

Seo, J.Y., Masamune, A., Shimosegawa, T., Kim, H. (2009). Protective effect of lycopene on oxidative stress-induced cell death of pancreatic acinar cells. *Ann N Y Acad Sci*. 1171:570-575.

Sequeira, F. (1992). Microbiological study of salt pans of Goa. Master of Science dissertation. Goa University, India.

Serdakowski, A. L. Dordick, J. S. (2008). Enzyme activation for organic solvents made easy. *Trends Biotechol.,* 26(1): 48-54.

Seshadri, S., Prakash, A., and Kowshik, M. (2012). Biosynthesis of silver nanoparticles by marine bacterium, *Idiomarina* sp. PR58–8. *Bull. Mater. Sci.,* 35: 1201-1205.

Shahmohammadi, H. R., Asgarani, E., Terato, H., Saito, T., Ohyama, Y., Gekko, K., Yamamoto O., Ide H. (1998). Protective Roles of Bacterioruberin and Intracellular KCl in the resistance of *Halobacterium salinarium* against DNA-damaging Agents. *J Radiat.,* 39(4): 251-262. Doi: 10.1269/jrr.39.251

Shand R.F., Leyva K.J. (2007). Peptide and protein antibiotics from the domain Archaea: Halocins and Sulfolobicins. In: *Bacteriocins*, (M.A. Riley, M.A. Chavan eds), Springer, Berlin, Heidelberg.

Shand, R.F., Price, L.B., O'Connor, E.M. (1998). Halocins: protein antibiotics from hypersaline environments. In: *Microbiology and Biogeochemistry of Hypersaline Environments*, (A., Oren. ed.), CRC. press, Boca Raton, FL. 295-306.

Shannon, C. E., Weaver, W. (1949). The mathematical Theory of Communication, (The University of Illinois Press, Urbana, USA), 117.

Sharma, R., Chisti, Y., Banerjee, U.C. (2001). Production, purification, characterization and applications of lipases. *Biotechnol Adv*. 19: 627-662. DOI:10.1016/S0734-9750(01)00086-6.

Shivaji, S., Madhu, S., Singh, S. (2011). Extracellular synthesis of antibacterial silver nanoparticles using psychrophilic bacteria. *Process Biochem*., 46: 1800-1807.

Sikkandar, S., Murugan, K., Al-Sohaibani, S., Rayappan, F., Nair A., Tilton, F. (2013). Halophilic bacteria - a potent source of carotenoids with antioxidant and anticancer potentials. *J Pure Appl Microbiol.,* 7: 2825-2830.

Simeonova, P.P., Luster, M.I. (2000). Mechanisms of arsenic carcinogenicity: Genetic or epigenetic mechanisms? *J Environ Pathol Toxicol Oncol*., (19): 281-286.

Simon C., Daniel, R. (2011). Metagenomic analyses: past and future trends. *Appl Environ Microbiol.*, 77:1153-1161.

Singh, S., Rana, S.V.S. (2007). Amelioration of arsenic toxicity by L-Ascorbic acid in laboratory rat. *J Environ Biol*., 28(2): 377-384.

Singleton, V.L., Rossi, J.A. (1965). Colorimetry of total phenols with phosphomolybdic- phosphotungstic acid reagents. *Am J Enol Vitic.*, 16: 144-158.

Sittenfeld, A. (1996). Special article on issues and strategies for bioprospecting. *Genet Eng Biotechnol J.*, 4: 1-12.

Sittenfeld, A., Lovejoy, A. (1999). Managing bioprospecting and biotechnology for conservation and sustainable use of biological diversity. In: *Managing Agricultural Biotechnology-Addressing Research Program Needs and Policy Implications for Developing Countries* (J. Cohen, ed)), ISNAR/ CAB International, UK, pp: 92-101.

Sivaramakrishnan, S., Gangadharan, D., Nampoothiri, K.M., Soccol, C.R. (2006). α-Amylases from microbial sources - An overview on recent developments. *Food Technol Biotechnol*. 44:173-184

Smedley, P.L., Kinniburgh, D.G. (2002). A review of the source, behaviour and distribution of arsenic in natural waters. *Appl Geochem*. 17(5): 517–568.

Soares Marcia, M. C.N., De Silva, R., Gomez, E. (1999). Screening of bacterial strains for pectinolytic activity: characterization of the polygalacturonase produced by *Bacillus* sp. *Rev. Microbiol*. 30(4), 299–303.

Soppa, J., Oesterhelt, D. (1989). *Halobacterium* sp. GRB: a species to work with!? *Can J Microbiol*. 205–209.

Spudich, J.L. (1993). Color sensing in the archaea: a eukaryotic-like receptor coupled to a prokaryotic transducer. *J Bacteriol*., 175: 7755-7761.

Squillaci, G. & Finamore, R. & Diana, P. & Restaino O. F. & Schiraldi C. & Arbucci S. & Ionata E. & La Cara F. & Morana. A. (2016). Production and properties of an exopolysaccharide synthesized by the extreme halophilic archaeon *Haloterrigena turkmenica*. *Appl Microbiol Biotechnol*., 100: 613-623. DOI 10.1007/s00253-015-6991-5

Squillaci, G., Parrella, R., Carbone, V., Minasi, P., La Cara, F., Morana, A. (2017). Carotenoids from the extreme halophilic archaeon *Haloterrigena turkmenica*: identification and antioxidant activity. *Extremophiles*. 21:933–945.

Srey, S., Jahid, I.K. & Ha, S. (2013). Biofilm formation in food industries: A food safety concern. *Food Control*., 31(2): 572-585.

Srivastava, P., Bragança, J., Kowshik, M. (2014). *In vivo* synthesis of selenium nanoparticles by *Halococcus salifodinae* BK18 and their anti-proliferative properties against HeLa cell line. *Biotechnol Prog*., 30: 1480-1487.

Srivastava, P., Bragança, J., Ramanan, S.R., Kowshik, M. (2013). Synthesis of silver nanoparticles using haloarchaeal isolate *Halococcus salifodinae* BK3. Extremophiles 17: 821-831. DOI 10.1007/s00792-013-0563-3

Srivastava, P., Nikhil, R., Braganca, J. M., Kowshik, M. (2015). Anti-bacterial TeNPs biosynthesized by haloarcheaon *Halococcus salifodinae* BK3. *Extremophiles*, 19(4). DOI: 10.1007/s00792-015-0767-9

Stan-Lotter, H., Doppler, E., Jarosch, M., Radax, C., Gruber, C., Inatomi, K.I. (1999). Isolation of a chymotrypsinogen B-like enzyme from the archaeon *Natronomonas pharaonis* and other halobacteria. *Extremophiles*, 3:153-161.

Stepanov, V.M., Rudenskaya, G.N., Revina, L.P., Gryaznova, Y.B., Lysogorskaya, E.N., Filippova, I.Y., Ivanova, I.I. (1992). A serine proteinase of an archaebacterium, *Halobacterium mediterranei*. *Biochem J*., 285: 281-286.

Strand, A., Shivaji, S., Liaaen-Jensen, S. (1997). Bacterial carotenoids 55. C-50-carotenoids 25. Revised structures of carotenoids associated with membranes in psychrotrophic *Micrococcus roseus*. *Biochem Syst Ecol*., 25: 547-552.

Strober, W. (2015). Trypan Blue Exclusion Test of Cell Viability. *Curr Protoc Immunol*., 111(1): A3.B.1-A3.B.3

Studdert, C.A., De Castro, R.E., Seitz, K.H., Sanchez, J.J. (1997). Detection and preliminary characterization of extracellular proteolytic activities of the haloalkaliphilic archaeon *Natronococcus occultus*. *Arch Microbiol*., 168: 532-535.

Sujatha, J. Esther Jasmine, J. (2017). Halocin production from *Haloarcula hispanica*, a saltern extremophile. *World Journal of Pharmacy and Pharmaceutical Sciences*, (6)8: 1510-1525.

Summers, A.O., Jacoby, G.A. (1977). Plasmid-determined resistance to tellurium compounds. *J Bacteriol*., 129:276-281.

Sun, M.L., Liu, S.B., Qiao, L.P., Chen, X.L., Pang, X., Shi, M., Zhang, X.Y., Qin, Q.L., Zhou, B.C., Zhang, Y.Z., Xie, B.B. (2014). A novel exopolysaccharide from deep-sea bacterium Zunongwangia profunda SM-A87: low-cost fermentation, moisture retention, and antioxidant activities. *Appl Microbiol Biotechnol*., 98(17): 7437-7445.

Sutherland, I.W. (2001). Biofilm exopolysaccharides: a strong and sticky framework. *Microbiology*, 147(1): 3-9.

Takao, T., Kitatani, F., Watanabe, N., Yagi, A., Sakata. K. (1994). A simple screening method for antioxidants and isolation of several antioxidants produced by marine bacteria from fish and shellfish. *Biosci.Biotech.Biochem*., 58:1780-83.

Tamayo, G., Nader, W. F., and Sittenfeld, A. (1997). Biodiversity for bioindustries. In: *Biotechnology and Plant Genetic Resources* (J. A. Callow, B. V. Ford-Lloyd and H. J. Newbury, eds.), CAB International, Wallingford, United Kingdom. 255-280.

Tamerler, C.B., Martinez, A.T., Keshavarz, T. (2001). Production of lipolytic enzymes in batch cultures of *Ophiostoma piceae*. *J Chem Technol Biotechnol*., 76: 991-996. DOI:10.1002/jctb.473

Tamura, K. (1992). Estimation of the number of nucleotide substitutions when there are strong transition-transversion and G + C-content biases. *Mol Biol Evol*., 9: 678-687.

Tamura, K., Peterson, D., Peterson, N., Stecher, G., Nei, M., Kumar, S. (2011). MEGA5: Molecular evolutionary genetics analysis using maximum likelihood, evolutionary distance and maximum parsimony methods. *Mol Biol Evol*., 28(10): 2731-2739. DOI:10.1093/molbev/msr121

Tapilatu, Y.H., Grossi, V., Acquaviva, M., Cecile, M., Bertrand, J.C., Cuny, P. (2010). Isolation of hydrocarbon-degrading extremely halophilic archaea from an uncontaminated hypersaline pond (Camargue, France). *Extremophiles*, 14: 225-231.

Taupp, M., Mewis, K., Hallam, S.J. (2011). The art and design of functional metagenomic screens. *Curr Opin Biotechnol*., 22: 465-472.

Temperton, B., Giovannoni, S.J. (2012). Metagenomics: microbial diversity through a scratched lens. *Curr Opin Microbiol.,* 15: 605-612.

Tenover, F. C. (2006). Mechanisms of antimicrobial resistance in bacteria. *Am J Med.*, 119(6A): S3-S10.

Teo, J.W.P., Zhang, L.H., Poh, C.L. (2003). Cloning and characterization of a novel lipase from *Vibrio harveyi* strain AP6. *Gene* 312:181–188. DOI:10.1016/S0378-1119(03)00615-2

Tharanya, P., Vadakkan, K., Hemapriya, J., Kannan, V. R., Vijayanand, S. (2015). Biogenic approach for the synthesis of titanium dioxide nanoparticles using a halophilic bacterial isolate - *Chromohalobacter salexigens* Strain PMT-1. *International Journal of Current Research and Academic Review*, 3(10): 334-342.

Tian, B., Xu, Z., Sun, Z., Lin, J., Hua, Y. (2007). Evaluation of the antioxidant effects of carotenoids from *Deinococcus radiodurans* through targeted mutagenesis, chemiluminescence, and DNA damage analysis. *Biochim. Biophys. Acta*, 1770: 902–911. doi: 10.1016/j.bbagen.2007.01.016

Tian, Z-R., Tong, W., Wang, J-Y., Duan, N-G., Krishnan, V.V., Suib, S.L. (1997). Manganese oxide mesoporous structures: mixed valent semiconducting catalysts. *Science*, 276: 926-930.

Tindall, B. J. (1992). The family Halobacteriaceae. In: Balows, A., Trtiper, H.G., Dworkin, M., Harder, W., Schleifer, K-H. (eds), *The prokaryotes 2nd edn*, New York, Berlin, Heidelberg, Springer, pp 768-808.

Tommonaro G., Abbamondi G. R., Iodice, C., Tait, K., De Rosa, S. (2012). Diketopiperazines Produced by the Halophilic Archaeon, *Haloterrigena hispanica*, Activate AHL Bioreporters. *Microb Ecol.* (63)3: 490-495. DOI 10.1007/s00248-011-9980-y

Toner B, Fakra S, Villalobos M, Warwick T, Sposito, G. (2005). Spatially resolved characterization of biogenic manganese oxide production within a bacterial biofilm. *Appl Environ Microbiol.*, 71: 1300-1310.

Torbergsen, A.C., Collins, A.R. (2000). Recovery of human lymphocytes from oxidative DNA damage; the apparent enhancement of DNA repair by carotenoids is probably simply an antioxidant effect. *Eur J Nutr*., 39: 80-85.

Tornabene, T.G., Kates, M., Gelpi, E., Oro, J. (1969). Occurrence of squalene, di- and tetrahydrosqualenes, and vitamin MK8 in an extremely halophilic bacterium, *Halobacterium cutirubrum*. *J Lipid Res.*, 10: 294-303.

Torreblanca, M., Meseguer I. Rodriguez-Valera, F. (1989). Halocin H6, a bacteriocin from *Haloferax gibbonsii*. *J Gen Microbiol.*, 135: 2661-2665.

Torreblanca, M., Meseguer, I., Ventosa, A. (1994). Production of halocin is a practically universal feature of archaeal halophilic rods. *Lett Appl Microbiol*., 19: 201- 205.

Tu, Ju., Yang, Z., Hu, C. (2015). Efficient catalytic aerobic oxidation of chlorinated phenols with mixed-valent manganese oxide nanoparticles. *J Chem Technol Biotechnol.*, 90: 80-86.

Turner, R.J., Weiner, J.H., Taylor, D.E. (1999). Tellurite mediated thiol oxidation in *Escherichia coli*. *Microbiology*, 145: 2549-2557.

Ullrich, R., Hofrichter, M. (2005). The haloperoxidase of the agaric fungus *Agrocybe aegerita* hydroxylates toluene and naphthalene. *FEBS Lett*., 579: 6247-6250. DOI:10.1016/j.febslet.2005.10.014

Umesh, B. Jagtap, S.N. Panaskar, Bapat, V.A. (2010). Evaluation of antioxidant capacity and phenol content in jackfruit (*Artocarpus heterophyllus* Lam.) fruit pulp. *Plant Foods Hum. Nutr*., 65: 99-104.

Utkina, N.K., Makarchenko, A.E., Shchelokova, O.V., Virovaya, M.V. (2004). Antioxidant activity of phenolic metabolites from marine sponges. *Chem of Nat Comp.,* 403: 73-77.

Valko, M., Izakovic, M., Mazur, M., Rhodes, C.J., Telser, J. (2004). Role of oxygen radicals in DNA damage and cancer incidence. *Mol Cell Biochem*., 266: 37-56.

Van der Meer, J. R., de Vos, W. M., Harayama, S., Zehnder, A. J. (1992). Molecular mechanisms of genetic adaptation to xenobiotic compounds. *Microbiol Rev.*, 56(4): 677-694.

Van Fleet-Stalder, V., Chasteen, T.G., Pickering, I.J., George, G.N., Prince, R.C. (2000). Fate of selenate and selenite metabolized by *Rhodobacter sphaeroides*. *Appl Environ Microbiol.*, 66: 4849-4853.

Vargas, C., Jebbar, M., Carrasco, R., Blanco, C., Calderón, M.I., Iglesias-Guerra, F., Nieto J.J. (2006). Ectoines as compatible solutes and carbon and energy sources for the halophilic bacterium *Chromohalobacter salexigens*. *J. Appl. Microbiol.* 100(1):98-107. https://doi.org/10.1111/j.1365-2672.2005.02757.x

Vartoukian, S.R., Palmer, R.M., Wade, W.G. (2010). Strategies for culture of 'unculturable' bacteria. *FEMS Microbiol Lett*., 309: 1-7.

Velho-Pereira, S., Furtado, I. (2012). Antibacterial activity of halophilic bacterial bionts from marine invertebrates of Mandapam-India. *Indian J Pharm Sci*., 74(4): 331-8.

Velho-Pereira, S., Furtado, I. (2014). Retreival of eurylhaline eubacterial and haloarchaeal bionts from nine different benthic sponges: reflection of the bacteriological health of waters of Mandapam, Tamil Nadu. *Ind J Mar Sci.,* 43:773-83.

Velho-Pereira, S., Parvatkar, P., and Furtado, I. (2015). Evaluation of antioxidant producing potential of halophilic bacterial bionts from marine invertebrates. *Indian J. Pharm. Sci*., 77: 183-89.

Ventosa, A., Nieto, J.J., Oren, A. (1998). Biology of moderately halophilic aerobic bacteria, *Microbiol Mol Biol Rev.*, 62: 504-544.

Ventura-Lima, J., Bogo, M.R., Monserrat, J.M. (2011). Arsenic toxicity in mammals and aquatic animals: A comparative biochemical approach. *Ecotoxicol Environ Saf*., 74: 211-218.

Vieira, A. P., Stein, E.M., Andreguetti, D. X. Cebrián-Torrejón, G. Doménech-Carbó, A., Colepicolod, P., Ferreira Ana Maria D. C.(2017). Sweet Chemistry": a green way for obtaining selenium nanoparticles active against cancer cells. *J. Braz Chem Soc.*, 00: 00: 1-7.

Wackett, L.P. (2002). Expanding the map of microbial metabolism. *Environ. Microbiol*., 4: 12-13.

Ward, D.M., Brock, T.D. (1978). Hydrocarbon degradation in hypersaline environments. *Appl Environ Microbiol.*, 35: 353-359.

Wejse, P. L. Ingvorsen, K. (2003). Purification and characterization of two extremely halotolerant xylanase from a novel halophilic bacterium. *Extremophiles*, 7(5): 423-431.

Wiernsperger, N.F. (2003). Oxidative stress as a therapeutic target in diabetes: Revisiting the controversy. *Diabetes Metab*., 29: 579-585.

Wijaya, A., Rangaswamy, V. (1992). Degradation of endogenous fructose during catabolism of sucrose and maniitol in halphilic Archaebacteria. *Arch Microbiol.*, 153: 356-363.

Williams, T. A. Embley, T. M. (2014). Archaeal "Dark Matter" and the origin of eukaryotes genome. *Biol Evol Mar*., 6(3): 474-481. DOI:10.1093/gbe/evu031

Wink, M. (1993). Production and application of phytochemicals from an agricultural perspective. In: *Phytochemistry and Agriculture* (T. A. Beek and H. Breteler eds.), Clarendon Press, Oxford, United Kingdom. 171-213.

Witkiewicz-Kucharczyk, A., Bal, W. (2006). Damage of zinc fingers in DNA repair proteins, a novel molecular mechanism in carcinogenesis. *Toxicol Lett*., 162: 29-42.

Woese, C.R., Fox, G.E. (1977). Phylogenetic structure of the prokaryotic domain: the primary kingdoms. *Proc Natl Acad Sci USA*., 74(11): 5088-5090.

Woese, C.R., Kandler, O., Wheelis, M.L. (1990). Towards a natural system of organisms: proposal for the domains Archaea, Bacteria, and Eucarya. *Proc Natl Acad Sci USA.*, 87(12): 4576-4579.

Wood, J.L. (1970). In: Metabolic Conjugation and Metabolic Hydrolysis, (W.H. Fishman, ed.), vol. II. Academic Press, New York, 61-299.

Yakovleva, I., Bhagooli, R., Takemura, A. Hidaka, M. (2004). Differential susceptibility to oxidative stress of two scleractinian corals: antioxidant functioning of mycosporine-glycine. *Comp Biochem Physiol B.,* 139: 721-730.

Yamada, A., Miyashita, M., Inoue, K., Matsunaga, T. (1997). Extracellular reduction of selenite by a novel marine photosynthetic bacterium, *Appl Microbiol Biotechnol.,* 48: 367-372.

Yancey, P. H., Clark, M. E., Hand, S. C., Bowlus, R. D. Somero, G. N. (1982). Living with water stress: evolution of osmolyte systems. *Science*, 217: 1214-1222.

Yang, Y., Yatsunami, R., Ando, A., Miyoko, N., Fukui, T., Takaichi, S., Nakamura, S. (2015). Complete biosynthetic pathway of the C_{50} carotenoid bacterioruberin from lycopene in the extremely halophilic archaeon *Haloarcula japonica*. *J Bacteriol*., 197:1614-1623. DOI:10.1128/JB.02523-14

Yankov, D., Dobreva, E., Beschkov, V., Emanuilova, E. (1986). Study of optimum conditions and kinetics of starch hydrolysis by means of thermostable α-amylase. *Enzyme Microb Technol*., 8: 665-667.

Yatsunami, R., Ando, A., Yang, Y., Takaichi, S., Kohno, M., Matsumura, Y., Ikeda, H., Fukui, T., Nakasone, K., Fujita, N., Sekine, M., Takashina, T., Nakamura, S. (2014). Identification of carotenoids from the extremely halophilic archaeon *Haloarcula japonica*. *Front Microbiol*., 5:1-5.

Yevgenia, S., David, I., Yael, K., Zvy, D., Yaron, Y. (2013). Natural antioxidants: function and sources food and nutrition sciences. *Food Nutr Sci.,* 46: 43-649.

You, Y., Shim, J., Cho, C.H., Ryu M.H., Shea P.J., et al., (2013). Biodegradation of BTEX mixture by *Pseudomonas putida* YNS1 isolated from oil contaminated soil. *J Basic Microbiol.*, 53: 469-475. DOI: 10.1002/jobm.201200067

Youssef, N. H., Savage-Ashlock K. N., McCully, A. L., Luedtke, B. Shaw, E. I. Hoff, W. D., Elshahed, M. S. (2014). Trehalose/2-sulfotrehalose biosynthesis and glycine-betaine uptake are widely spread mechanisms for osmoadaptation in the Halobacteriales. *ISME J*., 8(3): 636-649. doi: 10.1038/ismej.2013.165

Yurkov, V., Jappe, J., Vermeglio, A. (1996). Tellurite resistance and reduction by obligately aerobic photosynthetic bacteria. *Appl Environ Microbiol*., 62: 4195-4198.

Zamanian, M., Mason, J. R. (1987). Benzene dioxygenase in *Pseudomonas putida*, Subunit composition and immuno-cross-reactivity with other aromatic dioxygenases. *Biochem J*., 244(3):611-616. DOI: 10.1042/bj2440611

Zare, B., Faramarzi, M. A., Sepehrizadeh, Z., Shakibaie, M., Rezaie, S., Shahverdi, A. R. (2012). Biosynthesis and recovery of rod-shaped tellurium nanoparticles and their bactericidal activities. *Mat. Res. Bull*., 47, 3719-3725.

Zhang, Y., Lu, X., Fu, Z., Wang, Z., & Zhang, J. (2011). Sulfated modification of a polysaccharide obtained from fresh persimmon (*Diospyros kaki* L.) fruit and antioxidant activities of the sulfated derivatives. *Food Chem*., 127:1084-1090.

Zhou, X. H., Li, Z. (2004). CMCase activity assay as a method for cellulose adsorption analysis. *Enzyme Microbiol. Tech*., 35(5): 455-459.

Zingde, M.D., Singbal, S.Y.S., Moraes, C.F., Reddy, C.V.G. (1976a). Arsenic, copper, zinc and manganese in the marine flora and fauna of coastal and estuarine waters around Goa. *Indian J Geomarine Sci.*, 5: 212-217.

Zingde, M.D., Singbal, S.Y.S., Moraes, C.F., Reddy, C.V.G. (1976b). Some observations on pollutants of Velsao bay (Goa). *Mahasagar-Bulletin National Institute* of *Oceanography*. 12(2): 69-74.

Appendices

NTYE (Tryptone-yeast extract medium containing 25% NaCl)

NaCl	250.0 g
$MgSO_4$	20 g
KC1	5.0 g
$CaC1_2$	0.2 g
Tryptone	5.0 g
Yeast Extract	3.0 g

Adjusted pH to 7 using 1N NaOH

For solid media: (Agar) 18.0 g

Digest for 30 min, sterilize at 121°C and 15 lbs pressure for 20 min.

NGSM (Mineral salt medium containing 20% NaCI and 0.2% Glucose)

NaC1	200.0 g
$MgSO_4.6\ H_2O$	20.0 g
KC1	4.0 g
$CaC1_2$	1.0 g
$MgC1_2$	13.0 g
NH_4C1	2.0 g
KH_2PO_4	0.5 g
$FeC1_3.H_20$	0.005 g

Adjusted pH to 7 using 1M KOH

For solid media: (Agar) 20.0 g

Digest for 30 min, sterilize at 121°C and 15 lbs pressure for 20 min.

Glucose stock solution

A stock solution of 20% glucose was prepared in distilled water, sterilized separately at 121°C for 10 min and kept under refrigerated conditions (4°C).

Glucose was added to 20% NSM so as to give a final concentration of 0.2% in the medium to give NGSM.

All other concentrations of glucose were prepared from 20% of stock using the formula $C_1V_1=C_2V_2$

Starch stock solution

A stock solution of 20% soluble starch was prepared in distilled water, sterilized separately at 121°C for 10 min. Soluble starch was added to 20% NSM so as to give a final concentration of 0.2% in the medium.

Lugol's Iodine

Potassium iodide	10 g
Iodine crystals	5 g
15% NaCl	15 g in 100 ml of DW

Dissolve Potassium iodide in 15% NaCl. Slowly add iodine crystals while shaking. Filter and store in a tightly stoppered amber coloured bottle.

0.2 mM DPPH$^{\bullet}$ reagent

DPPH$^{\bullet}$ reagent	0.0789g
Methanol	100 ml

The DPPH reagent was prepared by dissolving the chemical in methanol in the presence of minimal light and storing it in amber bottles at 4ºC.

Nitrite Molybdate Reagent

Sodium nitrite	10g
Sodium molybdate	l0g
Distilled Water	100 ml

Phosphomolybdenum reagent solution

0.6 M Sulphuric acid

33.33 mL of concentrated (18 N) sulphuric acid (Rankem) was added to distilled water to make up the final volume of the reagent to 1 L.

28 mM sodium phosphate

It was prepared by dissolving 3.35 g of sodium phosphate (SRL) in 1 L of distilled water.

4 mM ammonium molybdate

4.94 g of ammonium molybdate (S-d fine chemicals) was dissolved in 1 L of distilled water

Reagents for comet assay

Phosphate buffer saline (PBS); (0.1M), pH 7.4

1. NaCl	8.0 g
2. KCl	0.2 g
3. KH2PO4	0.2 g
4. Na2HPO4	0.92 g

Mix all the ingredients in small amount of water then makeup to 1 L

1 % Normal Melting Point Agarose (NMPA)

100 mg of normal agarose was mixed with 9 ml of DDW and heated till the agarose dissolves. 1 ml of 10X PBS was added and the final volume was made up to 10 ml with DDW.

0.5% Low Melting Point Agarose (LMPA)

0.5 % LMPA was prepared by mixing 50 mg of low melting agarose with 9 ml of DDW and heated until just boiling. 1 ml of 10X PBS was added and the solution was made up to a final volume of 10 ml with DDW.

Lysing solution

73.01 g of NaCl (2.5 M), 18.7 g of EDTA (100mM) and 0.6 g of Tris base (10 mM) were dissolved in about 350 ml DDW. About 4 g of NaOH pellets were added and the mixture was allowed to dissolve. The pH was adjusted to 10 by HCl q.s. to 445 with DDW. The remaining amount (55 ml) was adjusted by 10 % DMSO and 1% Triton X which was added fresh according to the required amount.

10% DMSO 10 parts in 90 ml of DDW, total volume adjust to 100ml

1% TritonX-100 1 part in 90 ml of DDW, total volume adjust to 100ml

Electrophoresis buffer (pH > 13)

10 N NaOH: 200 g of NaOH pellets were dissolved in 500 ml DDW. This solution was dispersed in 27 ml aliquots in tightly capped tubes and was stored at ambient temperature (28-34 °C).

200 mM EDTA: 14.89 g of EDTA was dissolved in 200 ml DDW, the pH was adjusted to 10 and stored at ambient temperature (28-34 °C). The working solution was prepared by mixing 27 ml of 10 N NaOH, 4.5 ml of 200 mM EDTA and 1 ml of DMSO.

The working solution was prepared fresh before each run.

Neutralization buffer (400 mM Tris, pH 7.5)

4.845 g of Tris base was added to 90 ml of DDW. The pH was adjusted to 7.5 and the volume was adjusted to 100 ml. the solution was stored at room temperature.

Stain

Ethidium bromide	15 µg
DW	1 ml

50mM Ascorbic acid

Ascorbic acid	8.806g
DW	1000 ml

McIlvaine buffer pH values (6–7)

A: 0.1 M solution of citric acid 19.21 g in 1000 ml

B: 0.2 M solution of dibasic sodium phosphate 53.65 g of Na_2HPO_4. $7H_2O$ or 71.7 g of Na_2HPO_4. 12H2O in 1000 ml

x ml of A	y ml of B,	diluted to a total of 100 ml
17.9	32.1	6.0
16.9	33.1	6.2
15.4	34.6	6.4
13.6	36.4	6.6
9.1	40.9	6.8
6.5	43.6	7.0

50 mM Tris-HCl buffer (pH 8.0)

To prepare a 1M stock solution of Tris-Cl: Dissolve 121 g Tris base in 800 ml H_2O. Adjust to desired pH with concentrated HCl. Approximately 70 ml HCl is needed to achieve a pH 7.4 solution and 42 ml for a pH 8.0 solution.

0.1% aqueous solution of Crystal Violet

Crystal violet	0.1 g
95% ethyl alcohol (95 ml of ethanol + 5 ml DW)	100 ml

2 mM Nicotinamide Adenine Dinucleotide (NADH)

Nicotinamide adenine dinucleotide (NADH)	1.32686g
DW	1000 ml

Fig. I Standard curve of Bovine Serum Albumin by Folin Lowry method

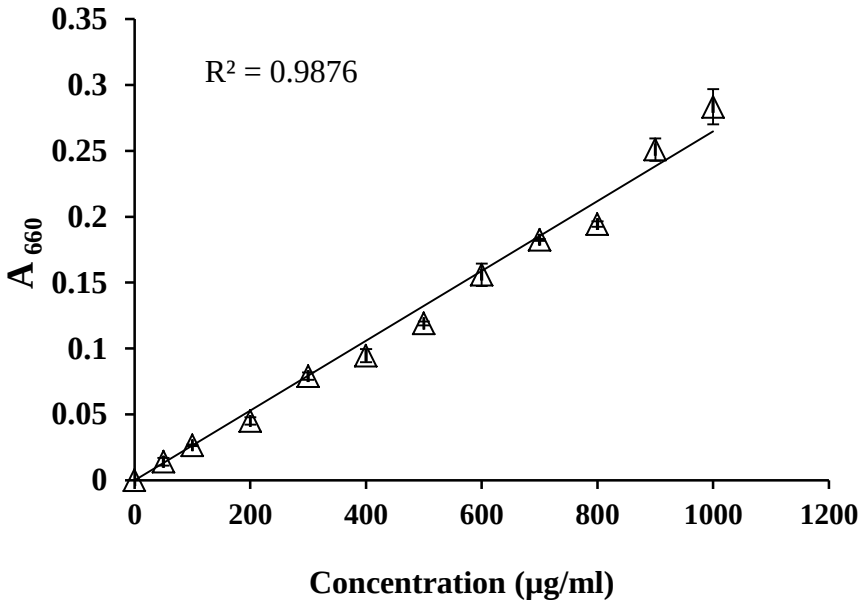

Fig. II Standard curve of Catechol by Arnow's method

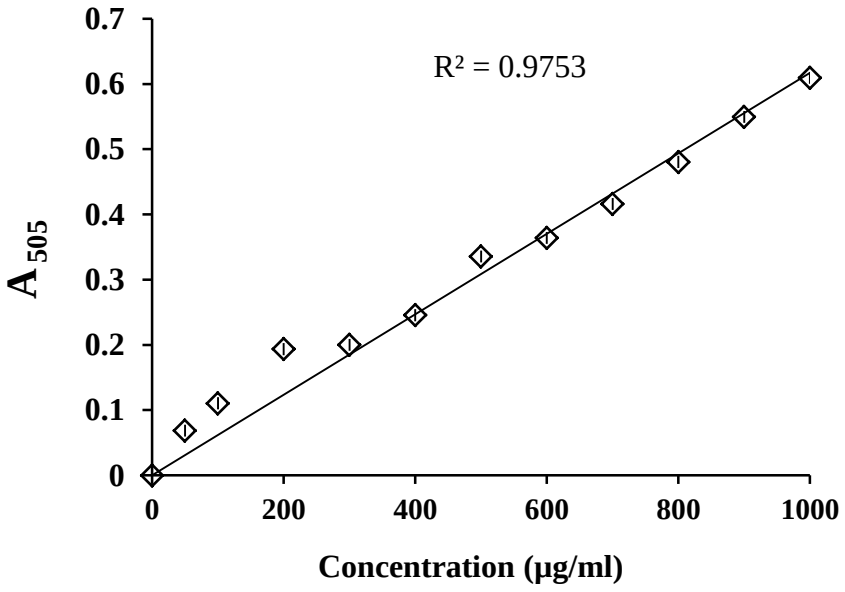

Fig. III Absorbance of different concentrations of DPPH$^{\bullet}$ at 517 nm

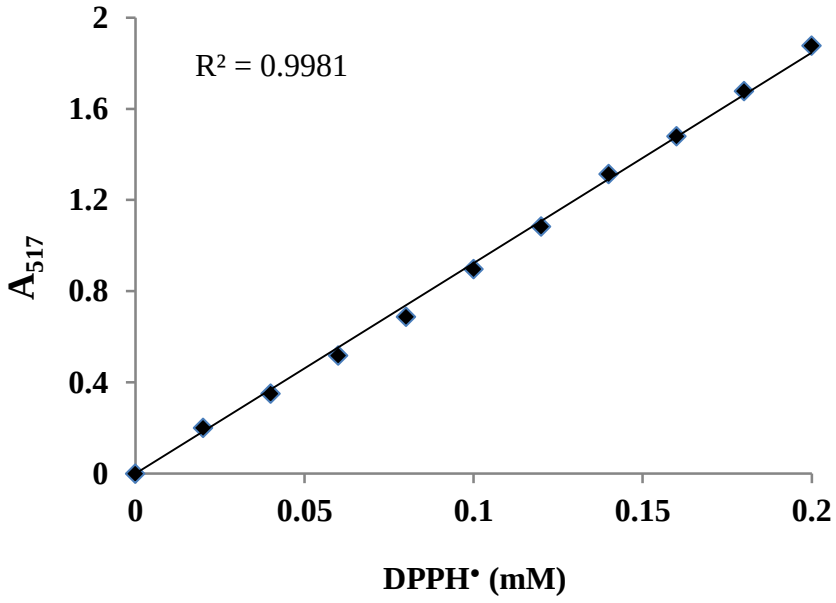

Fig. IV Standard curve of Ascorbic acid by the DPPH$^{\bullet}$ assay

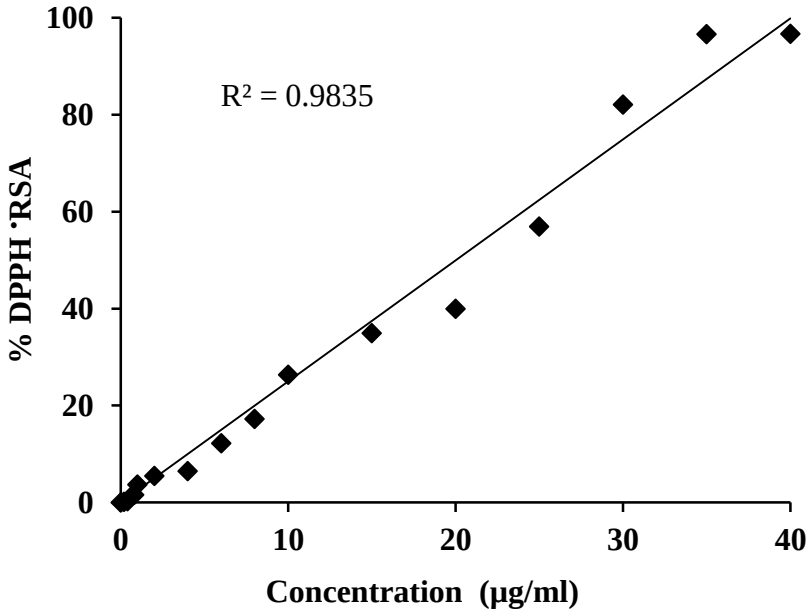

Fig. V Standard curve of Ascorbic acid (Total Antioxidant Activity)

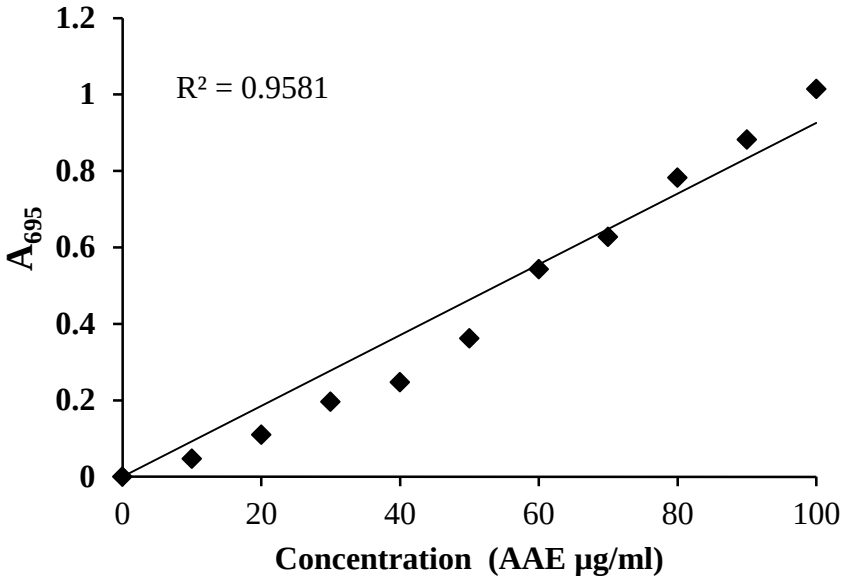

Fig. VI Standard curve of Gallic acid (Total Phenolic content)

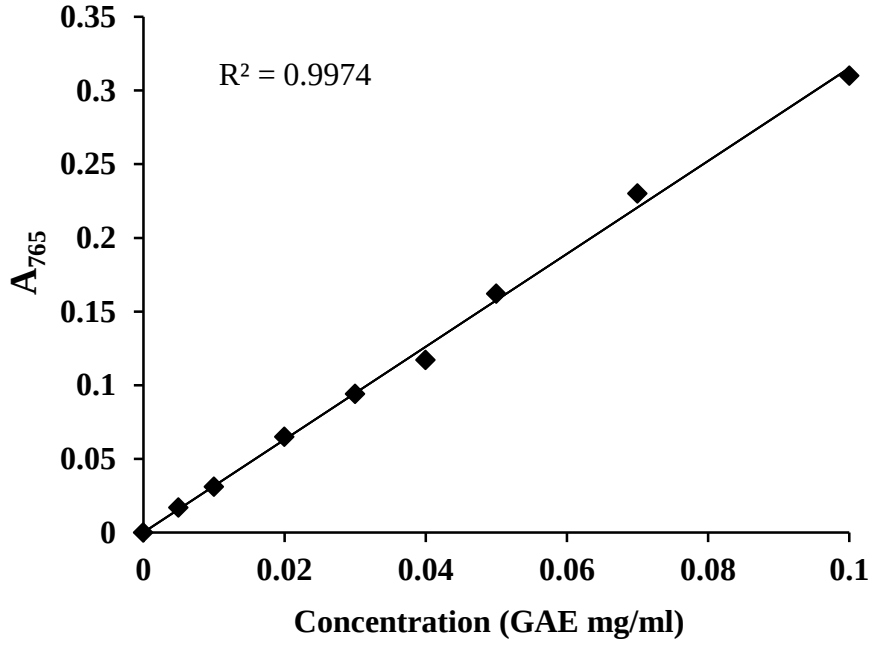

Fig. VII Standard curve for Selenite ($Se_2O_3^{2-}$)

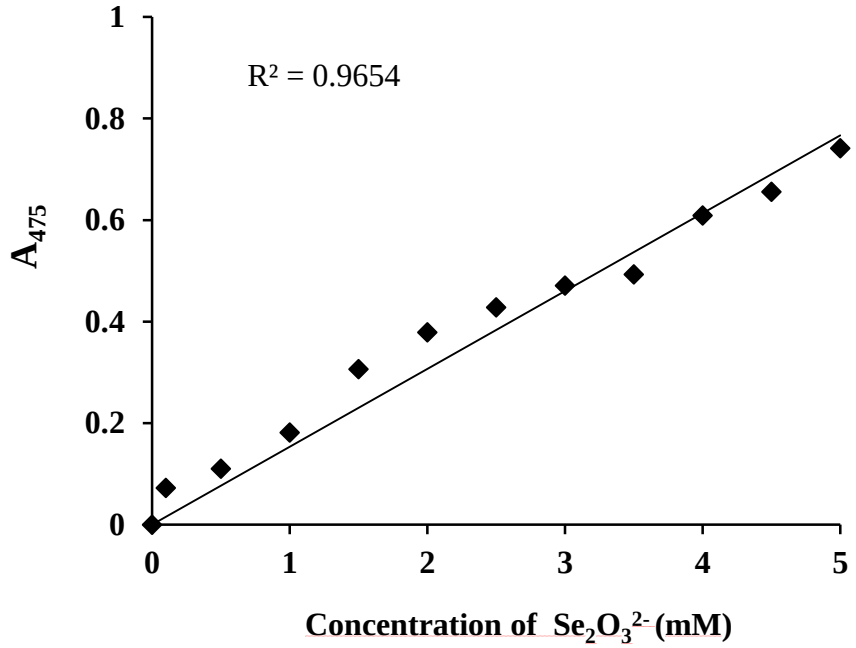

Fig VIII Standard chart for Estimation of Selenium

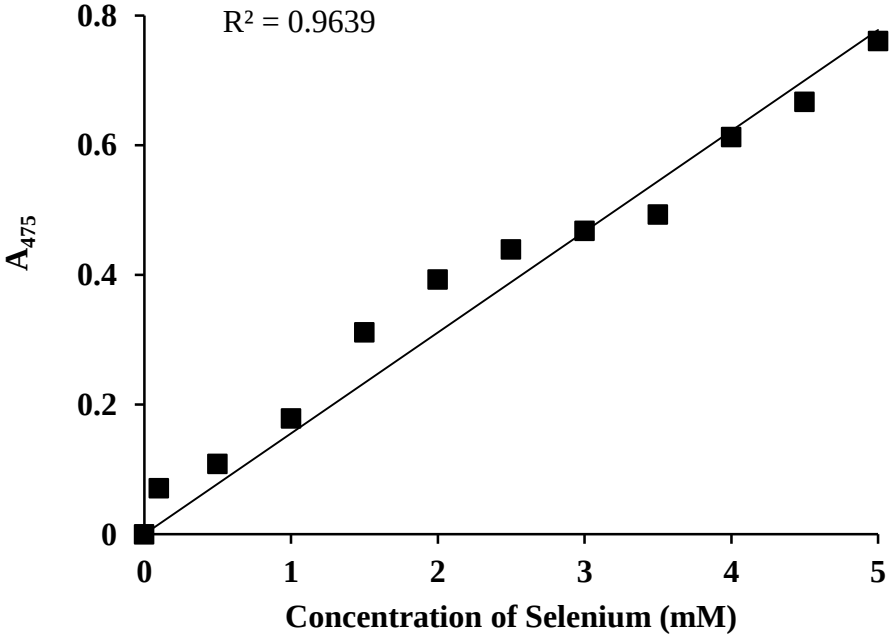

STUDIA UNIVERSITATIS BABEŞ – BOLYAI, BIOLOGIA, **64**, 1, 2019

Biosynthesis of selenium nanoparticles by *Haloferax alexandrinus* GUSF-1 (KF796625) and their use in modulating the size and shape of calcium oxalate crystals

Jyothi J. Alvares[1] and Irene J. Furtado[2]✉

*[1,] Goa University, Faculty of Life Sciences and Environment, Department of Microbiology, Taleigao Plateau, Goa- India, 403206ş [2,] ✉, **Corresponding author,** Goa University, Faculty of Life Sciences and EnvironmentDepartment of Microbiology, Taleigao Plateau, Goa- India, 403206.*
***E-mail:** ijfurtado@unigoa.ac.in*

Abstract

The ability to resist and biotransform toxic metalloids and chalcogens though widespread among prokaryotes is relativley less explored among the archaeal domain (Srivastava and Kowshik, 2013). In this study, a haloarchaeon, *Haloferax alexandrinus* GUSF-1 (KF796625) isolated from solar saltern of Goa – India grew optimally at 25% NaCl and was resistant to 120 mM concentration of toxic selenite (SeO_3^{2-}), with formation of deep red particulate matter in 4 days. Whole cells incubated with SeO_3^{2-} also gave the red particulate matter. SEM-EDX of the red material exhibited absorption peaks at 1.5, 11.2, and 12.5 keV thus indicating the presence of selenium. Further, the 8 diffraction peaks between 23 and 62 θ in XRD, corresponding to planes at (100), (101), (110), (012), (111), (201), (112) and (022) matched with those for selenium (Se^0) in JCPDS card No. 073-0465. TEM micrograph revealed rhombic shaped nanoparticles with capping material. The SeNPs at 100 µg/mL were able to substantially modulate the size and hexagonal shape of the calcium oxalate crystals to smooth spheres. Conclusively, this study gives an important lead for harnessing the potential of *Haloferax alexandrinus* GUSF-1 (KF796625) for biogenic synthesis of Se^0 from SeO_3^{2-} and for exploring the possible use of Se^0 in pharmaceutical application.

Keywords: calcium oxalate crystals, haloarchaeon, *Haloferax*, selenium nanoparticles

References:

Srivastava, P., Kowshik, M., (2013). Mechanisms of metal resistance and homeostasis in haloarchaea. *Archaea* 1–16.

GLOBAL JOURNAL OF BIO-SCIENCE AND BIOTECHNOLOGY

www.scienceandnature.org

EXTREMELY HALOPHILIC ARCHAEA AND EUBACTERIA ARE RESPONSIBLE FOR FREE RADICAL SCAVENGING ACTIVITY OF SOLAR SALTS OF GOA – INDIA

Jyothi J Alvares[1] and Irene J Furtado[2]*
[1,2] Department of Microbiology, Goa University, Taleigao Plateau, Goa- India. 403206.
*Corresponding author - ijfurtado@unigoa.ac.in

ABSTRACT
Free radical scavenging activity of natural solar salt of Goa was evaluated by the DPPH method. It ranged between 0.0793 µg AAE /g and 0.145 µg AAE/g. Our results showed that this antioxidant activity of salt was contributed by extremely halophilic *Alteromonas*, *Gluconobacter* and members of haloarcheal genera such as *Halobacterium, Haloferax*, *Haloarcula*, *Halococcus*, *Halorubrum, Natrialba, Natrinema and Natronococcus,* associated with it. This is the first record of *Alteromonas*, *Gluconobacter*, *Natrialba*, *Natrinema*, and *Natronococcus* as free radical scavengers. A positive correlation of R = 0.89, p< 0.001 between the total antioxidant capacity and the phenolic content was observed in five Haloarchaeal genera selected for studies. Among which, *Haloferax* sp. GUSF-1 (KF796625) exhibited % DPPH RSA of 31.5 ± 0.43, total antioxidant capacity of 1.176 ± 0.75 mg AAE/g and phenolic content of 0.784 ± 0.004 mg GAE /g cells. This free radical scavenging potential of solar salts due to presence of these microbes, possibly reflects its use in moderation, as soil conditioner and fertiliser for coastal fruit bearing trees such as C*ocos nucifera*, *Mangifera indica* and *Artocarpus heterophyllus* in Goa-India.

KEYWORDS – Antioxidant, DPPH, extreme halophiles, Haloarchaea, phenolic content.

INTRODUCTION

Globally, solar salt plays an important role in all forms of life (Aral *et al*., 2004). Goa situated on the west coast of India, is engaged in natural salt production through green process of salt farming for the past 1500 years (Furtado and Fernandes 2009). This solar salt is widely used in moderate quantities as fertiliser and soil conditioner in Goa and in South Asian countries (Mani *et al*., 2012; Magat 2000). Both in biota as well as in the environment, oxidation reactions produce free radicals which are atoms, molecules or ions with unpaired electrons that are highly unstable and charged (Lü *et al*., 2010). These free radicals react with the first available oxidisable substrate causing damage and in case of cells, death. This process is however, averted by antioxidant molecules which scavenge free radicals as- (i) preventers: by preventing formation of free radicals; (ii) scavengers: by removing radicals and halting further propagation of chain reactions and (iii) repairers: which ameliorate oxidative damage to a cell (Lü *et al*., 2010). In recent years, researchers are keen to unveil antioxidant substances from plants, animals, microbes and natural substances with an ability to fight oxidative stress (Yevgenia *et al*., 2013). In the present study, we screened and quantitatively assessed free radical scavenging activity of extremely halophilic microbes retrieved from solar salts of Goa- India (Braganca and Furtado 2009; Fernandes and Furtado 2005; Sequeira 1992).

MATERIALS & METHODS

Chemicals and reagents

All chemicals and reagents used were of analytical grade. 1, 1-diphenyl-2- picrylhydrazyl (DPPH), (Sigma, USA). Ascorbic acid, gallic acid, ammonium molybdate, sodium phosphate, sodium carbonate and Folin- Ciocalteu reagent, (Himedia laboratories, India). Solar salt recovered from salt farming facilities in Goa was used in this study. Methanol and other solvents, sulphuric acid (Sd-fine chemicals, India). Ultrafltration unit M Direct – Q3, Millipore- USA was used for pure water.

Free radical scavenging activity of solar salt

Saturated solutions of each variety of solar salt was prepared by gradually adding sterile ultrafiltered water such that at each addition of water to 40 g of solar salt a super saturation state was maintained throughout the preparation of the super saturated solution of solar salt. Each of the saturated solutions were individually filtered through Whatman No 1 filter paper, and analyzed separately for its ability to decolourize DPPH. $MgSO_2.7H_2O$, $MgCl_2$, NaCl, $CaCl_2.2H_2O$ were also individually analysed for DPPH decolourization. The DPPH decolourization was assayed by a method previously described (Brand-Williams *et al*., 1995). 0.5 ml of individual solutions of solar salt and other salts were added to 1 ml of 0.1 mM methanolic DPPH reagent, mixed vigorously with minimum light exposure, incubated in the dark at room temperature (28 ± 30 ºC), for 30 min and monitored at 517 nm, using the UV- vis spectrophotometer (UV–1601, Shimadzu, Kyoto,Japan) against methanol as blank. The stability of the DPPH solutions was also monitored separately by checking the

absorbance of 0.1 mM methanolic solution of DPPH, every 5 min, at 517 nm, for over an hour.

Demonstration of free radical scavenging microbes in solar salt

Extremely halophilic microbes in solar salt

An aliquote of 0.1 ml of the sediment free super saturated solution of solar salt was inoculated in a 50 ml Erlenmeyer flask containing 10 ml of NTYE broth (Braganca and Furtado 2009). The composition of the medium was as follows (g/liter): $MgSO_2.7H_2O$ 20, KCl 5, $CaCl_2.2H_2O$ 0.2, Tryptone 5, Yeast extract, 3; NaCl, 250 and pH adjusted to 7, using 1N NaOH. The flask was incubated at 42 ºC, 150 rpm using an incubator (REMI CIS-24 PLUS-India). After 7 days, an aliquote of 0.1 ml of this culture broth was then spread plated onto NTYE agar plates and incubated at 42 ºC in light, till well developed colonies were seen.

Development of Agar-growth-DPPH method

The fully formed colonies on NTYE agar were very carefully exposed to freshly prepared 0.1, 0.2 and 0.5 mM methanolic DPPH by layering the DPPH solution just to cover the surface of the agar and the colonies on it. Plates were incubated in the dark for 40 min at room temperature (28-30 ^{o}C), and those colonies surrounded by clear colourless/straw colour haloes against a purple background were scored and recorded as positive free radical scavengers.

Screening of free radical scavenging ability of extremely halophilic isolates retrieved from crude solar salt

A total of 101 extremely halophilic microbes isolated from crude solar salt produced in salt pans, located at Arambol (A), Agarwada (Ag), Arpora (Ar), Nerul (N), Ribandar (R) and Siridao (S) in Goa- India, maintained on NTYE agar at the Haloarchaeal repository, Department of Microbiology, Goa University, India (Braganca and Furtado 2009; Fernandes and Furtado 2005; Sequeira 1992). These were spot inoculated onto NTYE agar using a template, allowed to grow at 42 ºC for a period of 7 days and then subjected to Agar-growth-DPPH method.

Determination of free radical scavenging activity of extremely halophilic isolates retrieved from crude solar salt

Culturing and preparation of Methanolic Extract of Cells (MEC)

Each of the above 101 isolates on agar-slopes was inoculated, into a set of three large sterile tubes with 5 ml, of sterile NTYE broth. All tubes were incubated at 150 rpm on the orbital shaker (REMI CIS-24 PLUS- India) at 42 ºC. After 6 days, cells were harvested at 10000 rpm, 4 ºC for 10 min by using an Eppendorf centrifuge 5804 R. Cells washed with 15% NaCl and adjusted to a wet weight of 100 mg were treated with 1 ml of methanol and kept standing at 4 ºC in the dark, overnight and recovered by centrifuging at 10000 rpm, for 10 min and the resulting MEC stored in the dark at 4 °C.

Evaluation of free radical scavenging efficiency of MEC

Evaluation of free radical scavenging activity was carried out by a method of Brand-Williams *et al*., 1995. The degree of decolourization by cell extracts of individual isolates was monitored by measuring changes in the absorbance at 517 nm. Ascorbic acid (0.1%) was used as the positive control and also as the standard for the calibration curve. Experiments were carried out in triplicates. Results averaged and expressed as mean ± SD of ascorbic acid equivalent µg AAE/ g cells.

Computation of % DPPH RSA

% DPPH RSA was computed using the generalization;

% DPPH RSA = $(A_{control}–A_{test})/A_{control}$) x 100,

where $A_{control}$ is the absorbance of control and A_{test} is the absorbance of the crude MEC. Results were expressed as mean ± SD of % DPPH RSA.

Statistical analysis

The experimental data of DPPH RSA was analysed using IBM-SPSS 23 statistical software. Analysis of variance and significant differences among means of different isolates were performed with one-way analysis of variance (ANOVA).

Identification of extremely halophilic isolates retrieved from crude solar salt

Morphological characterization

Eighty four isolates from different solar salt samples, testing positive for free radical scavenging activity were individually subjected to various tests. Gram staining using acetic acid fixed smears was performed by a method previously reported (Khandavilli *et al* 1999).

Biochemical analysis

Isolated and purified cultures were pre-grown on NTYE agar slants for 6 days at 42 ^{o}C. l ml suspension of each of the isolates was made in sterile 20% NaCl. 3 ml of Norberg & Hofstein's media 1969, supplemented with 20% NaCl, containing 0.1% phenol red was distributed into test tubes and sterilized (Norberg and Hofstein 1969). Each of the sugars (10%) were sterilized separately and an aliquot of 0.5 ml was added to test tube containing the media just before inoculating 100 µl of the inoculum. Growth and colour change was observed visually. The change in colour from yellow to red was recorded as indicative of acid production.

Chemotaxonomic analysis

Pigment analysis of cells

All eighty four isolates were individually grown at 42 °C, in NTYE broth shake culture. Cultures were centrifuged at 10000 rpm using a cooling centrifuge (Eppendorf centrifuge 5804 R), at 4 °C, for 20 min. Pellet was washed twice with 20% NaC1 solution. Cellular pigment was extracted in methanol using sonicator (B. Braun Biotech International, USA) at 0.7cycles/sec and the methanolic extract were scanned between 190- 800 nm.

Evaluation of the presence of glycerol diether moieties (GDEM) in cells

Glycerol diether linked lipids (GDEM) were extracted from cells by the method previously described (Ross *et al*., 1985). Inorder to reflect the phenotypic relationship between the retrieved isolates, dendograms were generated using the individual characteristics of every isolate recorded and computed to attain a hierarchical rearrangement of cultures through paired UPGMA, based on Jaccard distance using the software PAST3 v.1 and

expressed as a phenogram.

Total antioxidant capacity of select haloarchaeal genera

Five isolates namely, GUSF-1 *Haloferax* sp. (KF796625), $GUFF_{188}$ *Haloarcula* sp. $GUFF_{179}$ *Halococcus* sp. $GUFF_{72}$ *Halorubrum* sp. and $GUFF_{233}$ *Natronocccus* sp. were selected assessment of total antioxidant capacity by the method previously described (Prieto *et al*., 1999). Ascorbic acid was used as a positive control and also as the standard. Experiments were carried out in triplicates, results averaged and expressed as ascorbic acid equivalent (mg AAE/g cells).

Total phenolic content of select haloarchaeal genera

The total phenolic content was determined spectrophotometrically as previously described (Singleton and Rossi 1965). Gallic acid was used as a positive control also as the standard for the calibration curve Experiment was carried out in triplicates, results averaged and the content of phenolics in the extracts was expressed in terms of gallic acid equivalent (mg GAE/g).

Statistical analysis

The correlation between antioxidant activity and phenolic content for five promising cultures was analysed using Pearson's correlation test (Pearson 1900).

Diversity studies

The generic level occurrence and diversity of extremely halophilic eubacteria and haloarchaea associated with solar salts from different locations of Goa were calculated as:

a) Simpson's Index of Diversity D' (Simpson 1949).

The index of extremely halophilic eubacteria and haloarchaea was calculated by applying the generalization:

$D' = N(N-1)/\Sigma n(n-1)$

D' = Diversity index

n = number of individuals of each genera found in solar salt of a salt pan

N = Total number of individual of all genera found in solar salt of a salt pan

b) The generic diversity in community was carried out by Shannon-Weiner's Diversity Index H' by using the generalization (Shannon *et al*.,1949);

$H' = \Sigma [(n/N)\ln(n/N)]$;

Where n=number of individual isolates; N= total number of all isolates.

RESULTS & DISCUSSION

Antioxidant activity of solar salt

Solar salts from six different salt pans, namely Arambol (A), Agarwada (Ag), Arpora (Ar), Nerul (N), Ribandar (R) and Siridao (S) could be categorized visually by the naked eye into: white with greyish tinge and the other white with brownish tinge. The tinge of colours was merely due to the colour of the soil of evaporation pans, wherein sea water is allowed to stagnate during solar salt crystallization stage. The conventional, well tested and highly employed method of DPPH was used to quantify the antioxidant ability of solar salt and of the extremely halophilic microbes retrieved from it. Saturated solutions of brownish solar salt and the greyish solar salt with a methanolic solution of DPPH resulted in decolourization of the purple colour of DPPH with a corresponding drop in absorbance at 517 nm. A drop in absorbance at 517 nm observed for the solar salt with the greyish tinge was 0.063 nm corresponding to 0.0793µg AAE / g, whereas for the solar salt with a brownish tinge was 0.083 nm corresponding 0.145µg AAE / g when compared to the DPPH solution whose absorbance did not decline over a period of 1 hour. This clearly indicated that solar salt had ability to scavenge free radicals and hence possessed antioxidant activity. This is the first time that free radical scavenging activity is checked and reported directly using solar salt. As the Goan crude solar salt is prepared through natural fractional crystallisation it essentially consists of NaCl with traces of $MgCl_2$ (Mani *et al*., 2012). Individual solutions of $MgSO_2.7H_2O$, $MgCl_2$, NaCl and $CaCl_2.2H_2O$ however failed to decolourize DPPH reagent.

Demonstration of free radical scavenging microbes in solar salt

Retrieval of extremely halophilic microbes from solar salt

Aliquots of saturated solutions of solar salt when spread out onto nutrient rich agar with 25% NaCl and incubated at 42 ^{o}C, developed into colonies in 8 days. As recorded in figure (1A) a variety of colonies grew ranging from pin heads to 1-1.5 mm in size, butyrous to dry, with even and uneven margins, colourless and others having yellow, orange and red pigmentation, grew within a week on NTYE, but none on TYE agar which did not have any NaCl. The absolute requirement of high concentration of NaCl for growth suggested that growth was either of members of heterotrophic halobacteria or of extremely halophilic eubacteria, known to dominate hypersaline econiches having salts upto saturation concentration (Grant and Larsen 1989). Such microbial growth has been reported from solar salts of Goa (Aguiar and Furtado 1996; Braganca and Furtado 2009; Fernandes and Furtado 2005; Khandavilli *et al*., 1999; Sequeira 1992).

Scoring of growing colonies as free radical scavenger

Careful exposure of these bacterial colonies to methanolic DPPH directly, while still on agar resulted in some of the colonies exhibiting a light yellow halo around themselves, against a purple colour of DPPH retained by the agar (Fig. 1B) thus indicating the ability of some colonies to decolourize DPPH and others not. Such DPPH decolourization by microbial cultures has been conventionally evaluated in cultures, by spraying with DPPH, a Whatman filter paper, having the replicate of growth on agar plate (Velho-Pereira *et al*., 2015). The decolourization of DPPH, herein observed by us of colonies on agar is taken as an indicator of free radical scavenging potential and a measure of antioxidant activity of the corresponding colony, similar to that observed with the filter paper replicates. This method, herein referred by us as 'Agar-growth-DPPH method', is direct, easy and gives easy reproducible antioxidant scoring efficiency. Hence, the antioxidant potential of solar salt was not an attribute of its chemical constituents, but of the microbes associated with it (Fig. 1A and 1B). These results support and confirm our presumption that tons of locally produced Goan solar salt, used as soil conditioner and fertilizer carried the free radical scavenging potential.

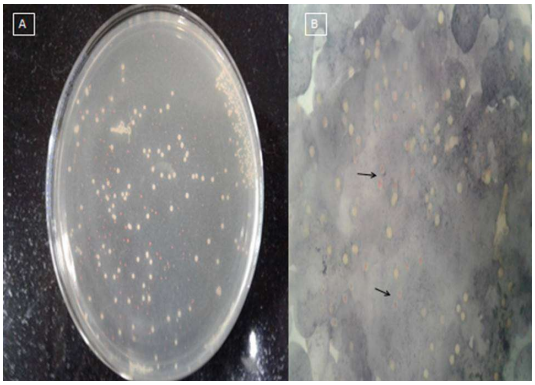

FIGURE 1A: Growth on NTYE agar on plating aliquot of saturated solution of solar salt.

FIGURE 1B: Arrows indicating colonies showing free radical scavenging activity with a halo around it, against a purple stained NTYE plate.

Screening for free radical scavenging activity among extremely halophilic isolates from solar salt/ brine isolates of Goa

Having established that the free radical scavenging ability of solar salt is associated with microbes growing in nutrient rich medium with 25% NaCl, we screened out 101 extremely halophilic microbes retrieved during earlier studies for their ability to scavenge free radicals. Eighty four of these isolates gave white-yellow zones around their colonies, by the 'Agar- growth – DPPH' method and were recorded as free radical scavengers. Analysis of MEC of each of these 84 extremely halophilic isolates further confirmed their ability to decolourize the purple coloured solution of DPPH to varying shades of purple, with a corresponding decrease in absorbance at 517 nm. As recorded in figure (2), the degree of DPPH decolourization, varied in isolates retrieved from different solar salts. Further as recorded in figure (2) the % DPPH RSA ranged from a minimum of 6.06 ± 0.19 exhibited by the isolate coded as $GUFF_3$ to a maximum of 31.5 ± 0.43 shown by GUSF-1. The isolate GUSF-1 from Siridao salt gave the highest activity and was followed by $GUFF_{188}$, $GUFF_{179}$, $GUFF_{66}$, and $GUFF_{72}$ of Arambol, Arpora, Siridao, Ribandar respectively. A low activity of less than 10% was shown by 7 ($GUFF_{20,35,88,90,146,148\ 187}$), 1 ($GUFF_{95}$), 3 ($GUFF_{26,98,51}$), 4 ($GUFF_{28,56,82,83}$), 5 ($GUBF_{2,3}$, $GUFF_{3,61,168}$) and 2($GUFF_{36,76}$) obtained from Arambol, Agarwada, Arpora, Nerul, Ribandar and Siridao respectively. A highly significant variation ($F = 563.627$; $p<0.001$) of antioxidant values was observed within the free radical scavengers from different salt samples as per the one-way ANOVA obtained using the IBM SPSS software.

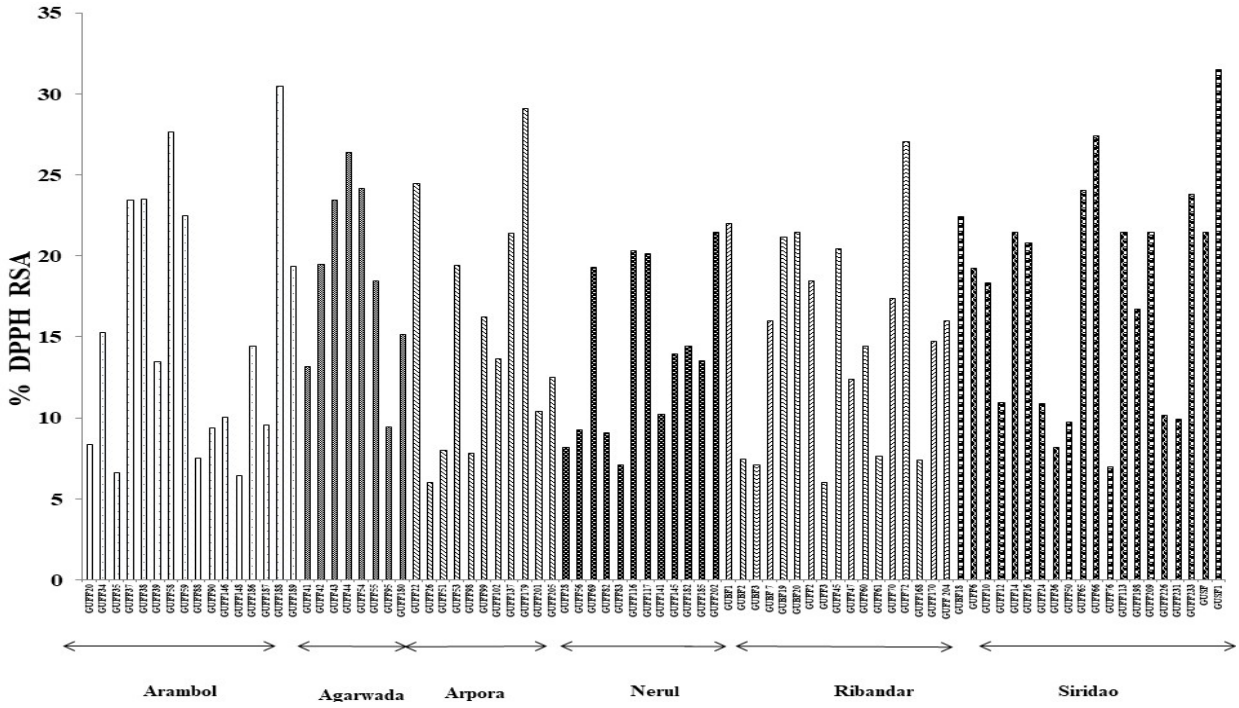

FIGURE 2: Decolourization of DPPH by methanolic extracts of individual extremely halophile isolates retrieved from different solar salts of Goa.
Isolate code: GUB/F/SF (Goa University/ Braganca/Fernandes/Sequeira Furtado).

Genera level identification of free radical scavengers retrieved from solar salts.

Eighty four extremely halophilic microbial isolates capable of scavenging free radical were assigned to their taxonomic domains and genera. Chromatograms of hexane extracts of methanolysates of cells of 78 (93%) isolates gave distinct spot at Rf 0.2, corresponding to that of GDEM's, a characteristic of cellular core lipid in cells of Archaea (Fig. 3). Additionally, these 78 isolates were resistant to penicillin G, erythromycin and cyclohexamide,

known to inhibit bacteria and eubacteria, but not archaea. Halobacteria are also known for its resistance towards many antibiotics especially those of cell wall and protein synthesis (Purdy et al., 2004). Further the absolute requirements of high salt concentration of NaCl for growth and extreme sensitivity to bile salts affirmed the 78 isolates belonged to haloarchaea of Domain Archaea (Purdy et al., 2004). Bile salts has been known to cause lysis of halobacteria due to it's presence of high concentration of taurine conjugates of cholic acid (Purdy et al., 2004). Core lipids are completely absent in eubacteria and eukarya (Purdy et al., 2004). The remaining 6 isolates did not posess GDEM's, grew on 0-25% NaCl and showed resistance to bile salts. As GDEM is the main key for assigning affiliation of domains to isolates (Purdy et al., 2004). The former group of 78 isolates were assigned to the domain Archaea**,** and the latter group of six isolates were assigned to domain Eubacteria.

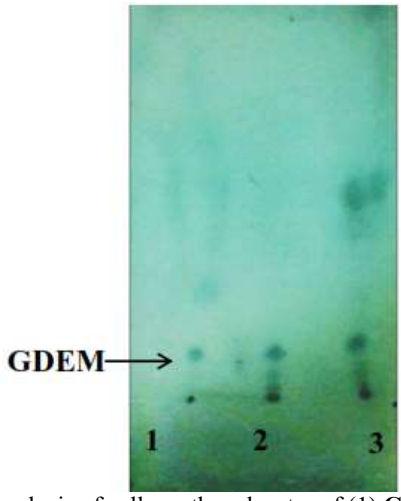

FIGURE 3: Thin-layer chromatographic analysis of cells methanolysates of (1) **GUSF-1** (2) **$GUFF_{233}$** (3) **$GUFF_{72}$**

These six eubacterial isolates, were gram negative and they were all classified to belong to Phylum Proteobacteria (Holt *et al*., 1994). Based on their biochemical characteristics, (Table 1), $GUFF_{76,83,95}$, were assigned to the class *Alphaproteobacteria*, order *Rhodospirillales*, family *Acetobacteraceae* and genera *Gluconobacter*. Because $GUFF_{141,145,146}$ did not grow on pyruvate and arginine hence referred to class *Gamaproteobacteria,* order *Alteromonadales*, family *Alteromonadaceae* and genus *Alteromonas*. The statistical software PAST3 v.1 also confirmed the biochemical differences as represented in the phenogram (Fig. 4) and sorted them as *Alteromonas* and *Gluconobacter* respectively. As yet there are no reports available on free radical scavenging activity within these two genera (*Alteromonas* and *Gluconobacter*). Hence, this is the first time free radical scavenging activity is reported in these two genera by us. However, such activity has been reported in *B. cereus* isolate from salt pan soil samples (Venkatajalapathi *et al*., 2016).

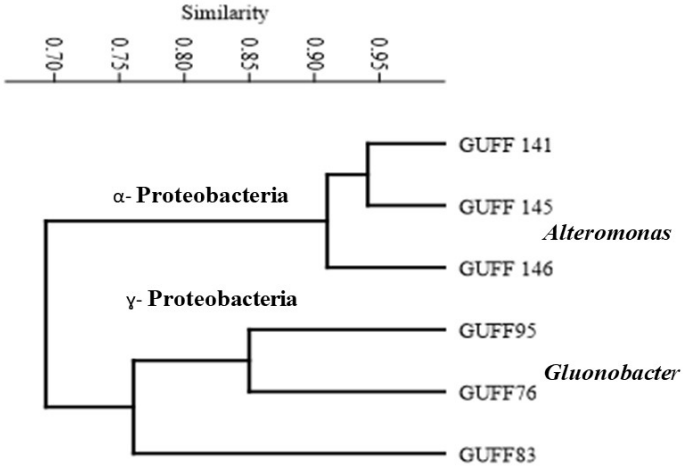

FIGURE 4: Phenogram depicting the sorting of eubacterial isolates to their respective genera based on biochemical characteristics using keys of Bergey's Systematic Bacteriology and the software **PAST3 v.1.**

TABLE 1. Free radical scavenging activity and biochemical potentials of extremely halophilic free radical scavengers from different solar salt samples

Solar Salt sample	Extreme halophilic isolates (GU)	Free radical scavenging activity	GDEM	Pigmentation	Gram character	Morphology					pH		Mg^{+2}		Biochemical potentials																		Genera
		µg AAE g^{-1} cells				Cocci (Co)	Cups (C)	Rods (R)	Triangles (T)	Pleomorphic (P)	Squares (S)	7	10	10 mM	790mM	Gelatinase	Protease	Lipase	Amylase	Mannitol	Glucose	Sucrose	Fructose	Galactose	Lactose	Arabinose	Citrate	Acetate	Malate	Pyruvate	Succinate	Lactate	Formate	Arginine	
A	FF_{41}	105.8 ± 0.18	+	R	+	-	C	-	-	P	-	+	-	+	-	+	+	+	+	+	+	+	+	+	+	+	+	-	-	+	-	-	-	+	*Haloferax* sp.1
	FF_{42}	156.0 ± 0.24	+	O	+	-	C	-	-	P	-	+	-	+	-	+	+	+	+	+	+	+	+	+	+	+	+	-	-	+	-	-	-	+	*Haloferax* sp.2
	FF_{43}	188.1 ± 0.3	+	O	+	-	C	-	-	P	-	+	-	+	-	+	+	-	+	+	+	+	+	+	+	+	+	-	+	+	+	-	-	+	*Haloferax* sp.3
	FF_{44}	211.6 ± 0.28	+	R	+	-	C	-	-	P	-	+	-	+	-	+	+	-	+	+	+	+	+	+	+	+	+	-	-	+	-	+	-	+	*Haloferax* sp.4
	FF_{54}	193.8 ± 0.2	+	P	-	Co	-	-	-	-	-	+	-	+	-	+	+	+	+	+	+	+	+	+	+	+	+	+	+	+	+	+	+	+	*Halococcus* sp.1
	FF_{55}	148.0 ± 0.48	+	O	-	-	-	R	-	-	-	+	-	+	-	+	+	-	+	+	+	+	+	+	+	+	+	+	+	+	+	+	+	+	*Halobacterium* sp.1
	FF_{95}	76 ± 0.008	-	P	-	Co	-	-	-	-	-	+	-	+	-	+	+	-	+	+	+	+	+	+	+	+	-	-	+	+	-	+	-		*Gluconobacter* sp.1
	FF_{180}	121.8 ± 0.16	+	O	-	Co	-	-	-	-	-	+	-	+	-	+	+	+	+	+	+	+	+	+	+	+	+	+	+	+	+	+	+	+	*Halococcus* sp.2
	FF_{20}	64.2 ± 0.64	+	Y	-	-	C	-	-	P	-	+	-	+	-	+	-	+	+	+	+	+	+	+	+	+	+	+	+	+	+	-	+		*Haloferax* sp.5
	FF_{14}	122 ± 0.04	+	O	-	-		-	Tr	P	-	+	-	+	-	+	+	+	+	+	+	+	+	+	-	-	-	-	-	-	-	-	-		*Haloarcula* sp.1
	FF_{35}	52.8 ± 0.016	+	Y	-	-	-	R	-	-	-	+	-	+	-	+	-	-	+	+	+	+	+	+	+	+	+	-	-	+	-	-	-	-	*Halobacterium* sp.2
Ag	FF_{37}	187.5 ± 0.36	+	O	-	-	-	R	-	P	-	-	+	+	+	+	+	+	+	+	+	+	+	+	+	+	+	-	-	+	-	-	-	+	*Natrialba* sp.1
	FF_{38}	188 ± 0.56	+	O	-	-	-	C	-	P	-	+	-	+	-	-	+	+	+	+	+	+	+	+	+	+	+	-	-	+	-	-	+	+	*Haloferax* sp.6
	FF_{39}	107.6 ± 0.2	+	R	-	Co	-	-	-	-	-	+	-	+	-	+	+	-	+	+	+	+	+	+	+	+	+	-	-	+	-	-	+	+	*Halococcus* sp.3
	FF_{58}	221.2 ± 0.5	+	O	-	Co	-	-	-	-	-	+	-	+	-	+	+	-	+	*	+	+	+	+	+	+	+	+	+	+	+	+	+	+	*Halococcus* sp.4
	FF_{59}	180 ± 1.2	+	O	+	Co	-	-	-	-	-	+	-	+	-	+	+	-	+	+	+	+	+	+	+	+	+	+	+	+	+	+	+	+	*Halococcus* sp.5
	FF_{88}	60 ± 0.14	+	O	-	-	-	R	-	-	-	+	-	+	-	+	+	+	-	+	+	+	+	+	+	+	+	+	+	+	+	+	+	+	*Halobacterium* sp.3
	FF_{90}	74.4 ± 0.28	+	O	-	-	-	-	-	P	-	+	-	+	-	+	+	-	+	+	+	+	+	+	+	+	+	+	+	+	+	+	+	+	*Halorubrum* sp.1
	FF_{146}	80.4 ± 0.62	-	R	-	Co	-	-	-	-	-	+	-	+	-	+	+	-	+	+	+	+	+	+	+	-	-	-	-	-	-	-	-	-	*Alteromonas* sp.1
	FF_{148}	51.6 ± 0.02	+	P	-	-	-	R	-	-	-	+	-	+	-	+	+	+	-	+	+	+	+	+	+	+	+	+	+	+	+	+	+	+	*Halobacterium* sp.4
	FF_{186}	115.4 ± 0.42	+	P	-	-	-	-	Tr	-	-	+	-	+	-	+	+	+	+	+	+	+	+	+	+	+	-	-	-	-	-	-	-	-	*Haloarcula* sp.2
	FF_{187}	76.4 ± 0.18	+	O	-	-	-	-	Tr	-	-	+	-	+	-	+	+	+	+	+	+	+	+	+	+	+	-	-	-	-	-	-	-	-	*Haloarcula* sp.3
	FF_{188}	243.8 ± 0.4	+	O	-	-	-	-	Tr	-	-	+	-	+	-	+	+	+	+	+	+	+	+	+	+	+	-	-	-	-	-	-	-	-	*Haloarcula* sp.4
	FF_{189}	155 ± 0.14	+	C	-	-	-	-	Tr	-	-	+	-	+	-	+	+	+	+	+	+	+	+	+	+	+	-	-	-	-	-	-	-	-	*Haloarcula* sp.5
	FF_{22}	196 ± 0.36	+	O	-	-	C	-	-	-	-	+	-	+	-	-	+	-	+	+	+	+	+	+	+	+	+	-	-	+	+	+	+	+	*Haloferax* sp.7
	FF_{26}	48.5 ± 0.04	+	Y	+	Co	-	-	-	-	-	+	-	+	-	+	+	-	+	+	+	+	+	+	+	+	+	+	+	+	+	+	+	+	*Halococcus* sp.6
	FF_{51}	64.3 ± 0.1	+	P	-	Co	-	-	-	-	-	+	-	+	-	+	+	-	+	+	+	+	+	+	+	+	+	+	+	+	+	+	+	+	*Halococcus* sp.7
	FF_{53}	155.5 ± 0.16	+	P	-	Co	-	-	-	-	-	+	-	+	-	+	+	-	-	+	+	+	+	+	+	+	+	+	+	+	+	+	+	+	*Halococcus* sp.8
	FF_{98}	62.8 ± 0.2	+	O	-	Co	-	-	-	-	-	+	-	+	-	+	+	-	+	+	+	+	+	+	+	+	-	-	+	+	+	+	+	+	*Halococcus* sp.9
Ar	FF_{99}	130.1 ± 0.36	+	P	-	Co	-	-	-	-	-	+	-	+	-	+	+	+	+	+	+	+	+	+	+	+	+	+	+	+	+	+	+	+	*Halococcus* sp.10
	FF_{102}	109.5 ± 0.12	+	O	-	Co	-	-	-	-	-	+	-	+	-	-	-	-	-	+	+	+	+	+	+	+	+	+	+	+	+	+	+	+	*Halococcus* sp.11
	FF_{137}	171.5 ± 0.24	+	O	-	-	-	-	Tr	-	-	+	-	+	-	+	+	+	+	+	+	+	+	+	+	+	-	-	-	-	+	+	+	+	+	*Haloarcula* sp.6
	FF_{179}	233.4 ± 0.52	+	C	-	Co	-	-	-	-	-	+	-	+	-	-	-	-	-	+	+	+	+	+	+	+	+	+	+	-	+	+	+	+	*Halococcus* sp.12
	FF_{201}	83.3 ± 0.5	+	C	-	Co	-	-	-	-	-	+	-	+	-	-	-	-	-	+	+	+	+	+	+	+	+	+	+	-	+	+	+	+	*Halococcus* sp.13
	FF_{205}	100.5 ± 0.2	+	O	-	Co	-	-	-	-	-	+	-	+	-	-	-	-	-	+	+	+	+	+	+	+	+	+	+	-	+	+	+	+	*Halococcus* sp.14
	FF_{28}	65.6 ± 0.26	+	Y	-	Co	-	-	-	-	-	+	-	+	-	-	-	-	+	+	+	+	+	+	+	+	+	-	+	-	-	-	-	-	*Halococcus* sp.15
N	F_{56}	74.3 ± 0.09	+	O	-	Co	-	-	-	-	-	+	-	+	-	+	-	+	+	+	+	+	+	+	+	+	+	+	+	+	+	+	+	+	*Halococcus* sp.16
	FF_{69}	156 ± 0.6	+	O	-	-	-	-	Tr	-	-	+	-	+	-	+	+	+	+	+	+	+	+	+	+	+	+	+	+	+	+	+	+	+	+	*Halococcus* sp.17
	FF_{82}	36.5 ± 0.02	+	C	-	-	R	-	-	-	-	-	+	+	+	-	-	-	+	+	+	+	+	-	+	+	+	+	+	+	+	+	+	+	*Natrinema* sp.1

	FF_{83}	57 ± 0.02	-	P	-	Co	-	-	-	-	-	+	-	+	-	+	+	-	+	+	+	+	+	+	+	+	+	+	+	+	+	+	-	*Gluconobacter* sp.1
	FF_{116}	183.5 ± 0.14	+	R	-	Co	-	-	-	-	-	+	-	+	-	+	-	+	+	+	+	+	+	+	+	+	+	+	+	+	+	+	+	*Halococcus* sp.18
	FF_{117}	161.5 ± 0.06	+	R	-	Co	-	-	-	-	-	+	-	+	-	+	-	+	+	+	+	+	+	+	+	+	+	+	+	+	+	+	+	*Halococcus* sp.19
	FF_{141}	82.3 ± 0.24	-	P	-	Co	-	-	-	-	-	+	-	+	-	+	+	-	+	+	+	+	+	+	+	-	-	-	-	-	-	-	+	*Alteronomonas* sp.2
	FF_{145}	111.9 ± 0.19	-	P	-	Co	-	-	-	-	-	+	-	+	-	+	+	+	+	+	+	+	+	+	+	-	-	-	-	-	-	-	-	*Alteronomonas* sp.3
	FF_{182}	115.9 ± 0.16	+	P	-	Co	-	-	-	-	-	+	-	+	-	+	-	+	+	+	+	+	+	+	+	+	+	+	+	+	+	+	+	*Halococcus* sp.20
	FF_{185}	108.7 ± 0.15	+	P	-	-	-	-	Tr	-	-	+	-	+	-	+	+	+	+	+	+	+	+	+	+	-	-	-	-	-	-	-	-	*Haloarcula* sp.7
	FF_{202}	182.5 ± 0.64	+	O	-	Co	-	-	-	-	-	+	-	+	-	+	-	+	+	+	+	+	+	+	+	+	+	+	+	+	+	+	+	*Halococcus* sp.21
	BF_1	176.5 ± 0.16	+	RO	-	Co	-	-	-	-	-	+	-	+	-	+	+	+	+	+	+	+	+	+	+	-	-	+	-	+	+	-		*Haloferax* ATCC BAA 644
	BF_2	59.6 ± 0.1	+	O	-	Co	-	-	-	-	-	+	-	+	-	+	+	-	-	+	+	+	+	+	+	-	-	+	+	+	+	+		*Haloferax* ATCC BAA 645
	BF_3	56.8 ± 0.02	+	O	-	Co	-	-	-	-	-	+	-	+	-	+	+	+	-	+	+	+	+	+	+	-	-	+	+	+	+	-		*Haloferax* ATCC BAA 646
	BF_7	130.3 ± 0.12	+	O	-	-	-	R	-	-	-	+	-	+	-	+	+	+	+	+	+	+	+	+	+	+	+	+	+	+	+	+	+	*Haloarcula* sp.8
	BF_{19}	193.4 ± 0.08	+	RO	-	-	-	R	-	-	-	+	-	+	-	+	+	+	+	-	+	+	+	+	+	-	-	+	-	+	+	+		*Halobacterium* sp.5
R	BF_{20}	172 ± 0.82	+	RO	-	-	-	R	-	-	-	+	-	+	-	+	+	+	+	-	+	+	+	+	+	-	-	-	-	+	+	+		*Halobacterium* sp.6
	FF_2	148 ± 0.16	+	O	+	C	-	-	-	-	-	+	-	+	-	+	-	-	-	+	+	+	+	+	+	+	+	+	+	+	+	+	+	*Halococcus* sp.22
	FF_3	48.5 ± 0.08	+	Y	-	-	-	-	Tr	-	-	+	-	+	-	+	-	-	+	+	+	+	+	+	+	+	+	+	+	+	+	+	+	*Haloarcula* sp.9
	FF_{45}	164 ± 0.08	+	O	-	Co	-	-	-	-	-	+	-	+	-	+	+	+	+	+	+	+	+	+	+	+	+	+	+	+	+	-	+	*Halococcus* sp.23
	FF_{47}	99.6 ± 0.06	+	P	-	Co	-	-	-	-	-	+	-	+	-	+	+	-	+	+	+	+	+	+	+	+	+	+	+	+	+	+	+	*Halococcus* sp.24
	FF_{60}	115.9 ± 0.34	+	P	-	-	-	R	-	-	-	+	-	+	-	+	+	-	+	+	+	+	+	+	+	+	+	+	+	+	+	+	+	*Halobacterium* sp.7
	FF_{81}	61.2 ± 0.074	+	O	-	-	-	R	-	-	-	+	-	+	-	-	+	-	-	+	+	+	+	+	+	+	+	+	+	+	+	+	+	*Halobacterium* sp.8
	FF_{70}	139.5 ± 1.32	+	SP	-	Co	-	-	-	-	-	+	-	+	-	-	+	-	+	+	+	+	+	+	+	+	+	+	+	+	+	+	+	*Halococcus* sp.25
	FF_{72}	56.4 ± 0.12	+	R	-	Co	-	-	-	-	-	+	-	+	-	+	-	+	-	+	+	+	+	+	+	+	+	+	+	+	+	+	+	*Halorubrum* sp.2
	FF_{168}	59.4 ± 1.3	+	C	-	Co	-	-	-	-	-	+	-	+	-	+	+	+	+	+	+	+	+	+	+	+	+	+	+	+	+	-	+	*Halococcus* sp.26
	FF_{170}	118 ± 0.02	+	O	-	Co	-	-	-	-	-	+	-	+	-	+	+	+	+	+	+	+	+	+	+	+	+	+	+	+	+	-	+	*Halococcus* sp.27
	FF_{204}	111.8 ± 0.08	+	C	-	Co	-	-	-	-	-	+	-	+	-	+	+	+	+	+	+	+	+	+	+	+	+	+	+	+	+	-	+	*Halococcus* sp.28
	BF_{18}	211.8 ± 1.24	+	O	-	-	-	R	-	-	-	+	-	+	-	+	+	+	+	-	+	+	+	+	+	-	-	+	-	+	+	+		*Halobacterium* sp.9
	FF_6	154.2 ± 0.14	+	O	+	C	-	-	-	-	-	+	-	+	-	+	-	-	+	+	+	+	+	+	+	+	+	+	+	+	+	+	+	*Halococcus* sp.29
	FF_{10}	147 ± 0.14	+	P	-	-	C	-	-	-	-	+	-	+	-	+	+	-	+	+	+	+	+	+	+	+	+	+	+	+	+	+	+	*Haloferax* sp.8
	FF_{12}	88.2 ± 0.57	+	C	-	-	-	R	-	-	-	-	+	+	-	+	+	+	+	+	+	+	+	+	+	+	+	+	+	-	+	+		*Natrialba* sp. 2
	FF_{14}	172 ± 0.3	+	O	+	Co	-	-	-	-	-	+	-	+	-	+	+	+	+	+	+	+	+	+	+	+	+	+	+	+	+	+	+	*Halococcus* sp.30
	FF_{16}	166.6 ± 0.6	+	O	-	-	-	-	Tr	-	-	+	-	+		+	+	+	+	+	+	+	+	+	+	+	+	+	+	+	+	+	-	*Halorcula* sp.10
	FF_{24}	87.2 ± 0.4	+	O	-	-	C	-	-	-	-	+	-	+	-	-	+	+	+	+	+	+	+	+	+	+	+	+	+	-	+	+	+	*Haloferax* sp.9
	FF_{36}	65.8 ± 0.52	+	O	-	-	-	-	Tr	-	-	+	-	+	-	+	+	-	+	+	+	+	+	+	+	+	-	-	-	-	-	+	+	*Halorcula* sp.11
	FF_{50}	78 ± 0.54	+	P	-	Co	-	-	-	-	-	+	-	+	-	+	+	-	+	+	+	+	+	+	+	+	+	+	+	+	+	+	+	*Halococcus* sp.31
	FF_{65}	192.6 ± 0.34	+	O	+	Co	-	-	-	-	-	+	-	+	-	+	+	-	-	+	+	+	+	+	+	+	+	+	+	+	+	+	+	*Halococcus* sp.32
S	FF_{66}	219.8 ± 0.016	+	O	+	Co	-	-	-	-	-	+	-	+	-	+	+	-	-	+	+	+	+	+	+	+	+	+	+	-	+	+	+	*Halococcus* sp.33
	FF_{76}	56.16 ± 0.16	-	C	-	Co	-	-	-	-	-	+	-	+	-	-	-	-	-	+	+	+	+	+	+	-	-	-	+	-	-	-	+	*Gluconobacter* sp.3
	FF_{113}	172 ± 0.52	+	O	+	Co	-	-	-	-	-	+	-	+	-	+	-	-	+	+	+	+	+	+	+	+	+	+	+	+	+	+	+	*Halococcus* sp.34
	FF_{198}	133.9 ± 0.26	+	P	+	Co	-	-	-	-	-	+	-	+	-	+	-	-	+	+	+	+	+	+	+	+	+	+	+	+	+	+	+	*Halococcus* sp.35
	FF_{209}	171.8 ± 0.22	+	W	+	Co	-	-	-	-	-	+	+	+	+	+	-	-	+	+	+	+	+	+	+	+	+	+	+	+	+	+	+	*Halococcus* sp.36
	FF_{226}	81.5 ± 0.08	+	C	-	-	-	R	-	-	-	+	-	+	-	+	+	+	+	+	+	+	+	+	+	+	+	+	+	+	-	+	+	*Natrialba* sp.3
	FF_{231}	79.6 ± 0.12	+	C	-	-	-	R	-	-	-	+	+	+	+	+	+	+	+	+	+	+	+	+	+	+	+	+	+	+	-	+	+	*Natrialba* sp.4
	FF_{233}	191 ± 0.12	+	R	-	Co	-	-	-	-	-	+	+	+	+	+	+	-	+	+	+	+	+	+	+	+	+	+	+	+	+	+	+	*Natronococcus* sp.1
	SF	180 ± 0.36	+	O	-	-	-	R	-	-	-	+	-	+	-	+	+	-	+	+	+	+	+	+	+	+	+	+	+	+	+	+	+	*Halobacterium* sp.10
	SF-1	252.2 ± 1.14	+	O	-	-	C	-	-	-	-	+	-	+	-	+	+	-	+	+	+	+	+	+	+	+	+	+	+	+	+	+	+	*Haloferax sp.* (KF796625)

- Isolate GU ; Goa University
- Solar salt samples; A- Arambol, Ag- Agarwada, Ar- Arpora, N- Nerul, R-Ribandar, S- Siridao.
- GDEM + present, - absent
- Colony pigmentation; C- cream, O- orange, R – red, RO- red orange, P – peach, SP- salmon pink, W- white, Y- yellow ;
- Gram character (+) positive (purple), (-) negative (pink).
- Morphology; Co- cocci,, C-cups, R- rods, P – pleomorphic, Tr- triangles, S –squares.
- Biochemical trait; + positive , - negative

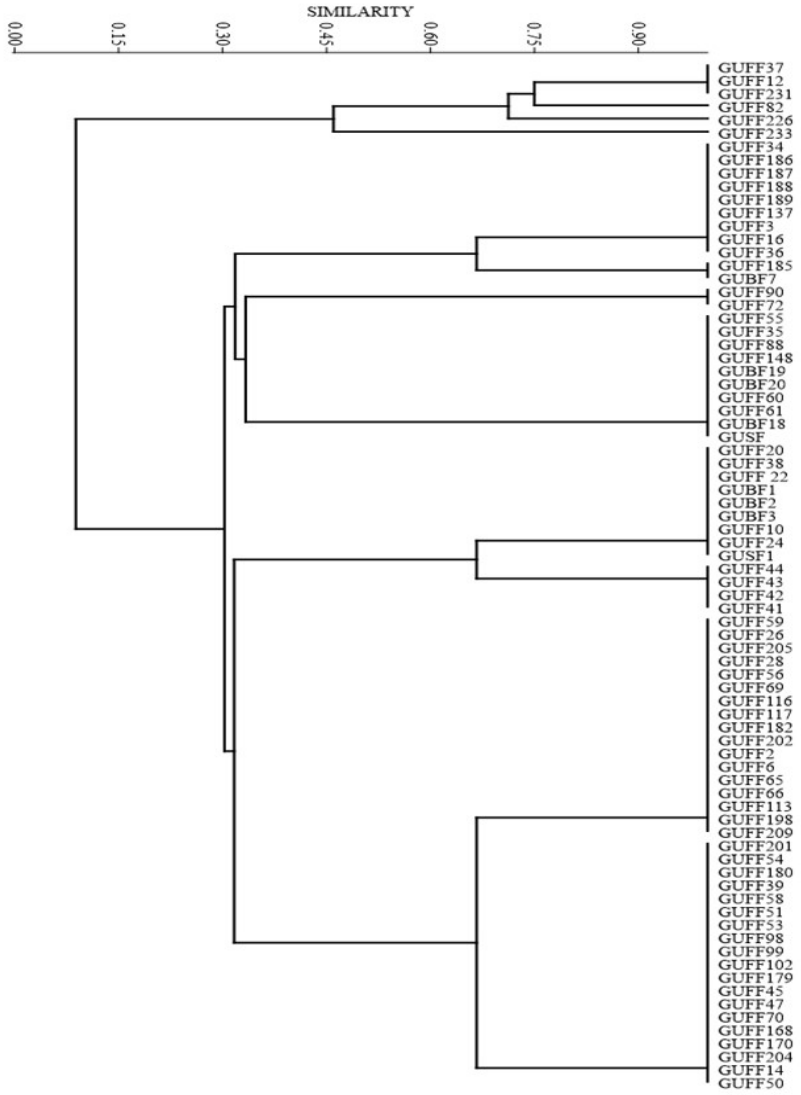

FIGURE 5: Phenogram depicting the sorting of Haloarchaeal isolates to their respective genera based on morphology, pH and Mg^{+2} ion requirements using the software **PAST 3.v.1**.

The 78 isolates belonging to the domain Archaea had a salt requirement above 15% wt/vol for growth and 25% for optimum growth. These were considered as extreme halophiles and hence were referred to Phylum Euryarchaeata, class *Halobacteria*, order *Halobacteriales*. Based on phenotypic test used were in accordance to minimal standards proposed for describing and assigning taxa in the order *Halobacteriales* (Oren *et al*., 1997). Based on gram character, cellular morphology, requirement of pH and Mg^{+2} ions (Table.1), the isolates from different salt samples were sorted out into eight genera; *Halobacterium*, *Haloferax*, *Haloarcula*, *Halococcus*, *Halorubrum*, *Natrialba*, *Natrinema*, *Natronococus* as in (Fig. 5) (Oren, A. 2012),. **$GUFF_{233}$** genus *Natronococcus*: Cells were non motile, cocci, arranged in irregular clusters, cells did not lyse in distilled water, utilized sucrose, fructose, glucose, acetate and lactose as sole source of carbon, had phosphatidyl glycerol and phosphatidyl glycerol phosphate methyl esters as polar lipids, grew at pH 10.5. The strain utilised citrate and resembled *Natronococcus* reported from Soda Lake (Roh *et al*., 2007). **$GUFF_{82}$** genus *Natrinema*: Colonies orange red, smooth circular, cells rod shaped, turned pleomorphic cells lysed at 1.5 M NaCl, Liquefied gelatin and did not hydrolyse starch. The isolate grew in the pH range of 6.0-8 (McGenity et al., 1998). **$GUFF_{12,\ 37,\ 231,\ 233}$** genus *Natrialba*: colonies were weakly cream to peach. Cells gram positive rods grew on media with NaCl upto 25% and pH 10.5 (Xu *et al*., 2001). **$GUFF_{72,\ 90}$** genus *Halorubrum*: Colonies orange red cells gram negative rods. Some cultures pleomorphic. Growth in medium containing 15-30% NaCl, pH 5-9 with optimum growth at pH 7. Starch, gelatin and casein were not hydrolysed. Arginine was not used as a sole source of carbon, nitrogen or energy, susceptible to bacitracin and novobiocin and hence resembled the *Halorubrum* isolated from saline soils (Ventosa *et al*., 2004). **$GUBF_{1,\ 2,\ 3,}$ $GUFF_{10,\ 20,\ 22,\ 24,\ 38,\ 41,\ 42,\ 43,\ 44}$ GUSF-1** genus *Haloferax*: cells gram-negative and

cup shaped. Cells lyse immediately in distilled water, isolates could tolerate salt as low as 1.0 M NaCl and high as 5.2 M NaCl, optimum pH for growth 7, resistant to rifampicin (Elshahed *et al*., 2004). **GUBF$_{18,19,20,}$ GUFF$_{35,55,60,61,88,148}$ GUSF** genus *Halobacterium*: cells gram negative and slender rods Colonies on agar plates containing 25% (w/v) total salts were red, elevated and round. pH for growth was 5.5–8.5, salt tolerance was from 2.7 to 5.2 M NaCl (Yang *et al*., 2006).

GUFF$_{2,6,14,26,28,39,45,47,50,51,53,54,56,58,59,,65,66,69,70,98,99,102,113,116,117,168,170,179,180,182,198,201,202,204,205,209}$ genus *Halococcus*: Cells were gram negative and coccoid. Colonies smooth-surfaced with clear edges. Susceptible to rifampicin and bacitracin (Wang *et al*., 2007). **GUBF$_7$, GUFF$_{3, 16, 34, 36, 137, 185, 186, 187, 188, 189}$** genus *Haloarcula*: cells were flat disk-shaped, round or triangular grew on simple carbon sources (glucose, fructose, sucrose, glycerol, acetate, succinate, and malate).Susceptible to bacitracin and novobiocin. These isolates resembled those isolated from the Dead Sea (Oren *et al*., 1990).

Diversity studies

Occurrence of free radical scavenging haloarchaea belonging to different genera differed from solar salt to solar salt (Fig. 6). A maximum of 6 genera were found in Agarwada, while a minimum of three haloarchaeal genera were found in Arambol, Arpora and Nerul. None of the solar salts had isolates belonging to all the 8 retrieved genera. Members of genus *Natrialba* were found in Agarwada and Siridao solar salts while *Natrinema* in Nerul and *Natronococcus* in Siridao. The frequency of ocurrence of free radical scavenging members was: *Halococcus* > *Haloarcula* = *Haloferax* > *Halobacterium* > *Halorubrum* = *Natrialba* > *Natrinema* = *Natronococcus*. Eubacteria retrieved although extremely halophilic was 10 times less than that of haloarchaea and was restricted to genus *Gluconobacter* and *Alteromonas*. Further, as accounted in (Fig. 6), the distribution of the two genera in Goan solar salts was very unequal. In Nerul members of *Gluconobacter* was 50% of *Alteromonas*. Siridao and Arambol had only *Gluconobacter*, whereas Agarwada had only *Alteromonas*. Antioxidation activity is widely distributed among members of eubacterial and archaeal domain retrieved from solar salt of Goa.

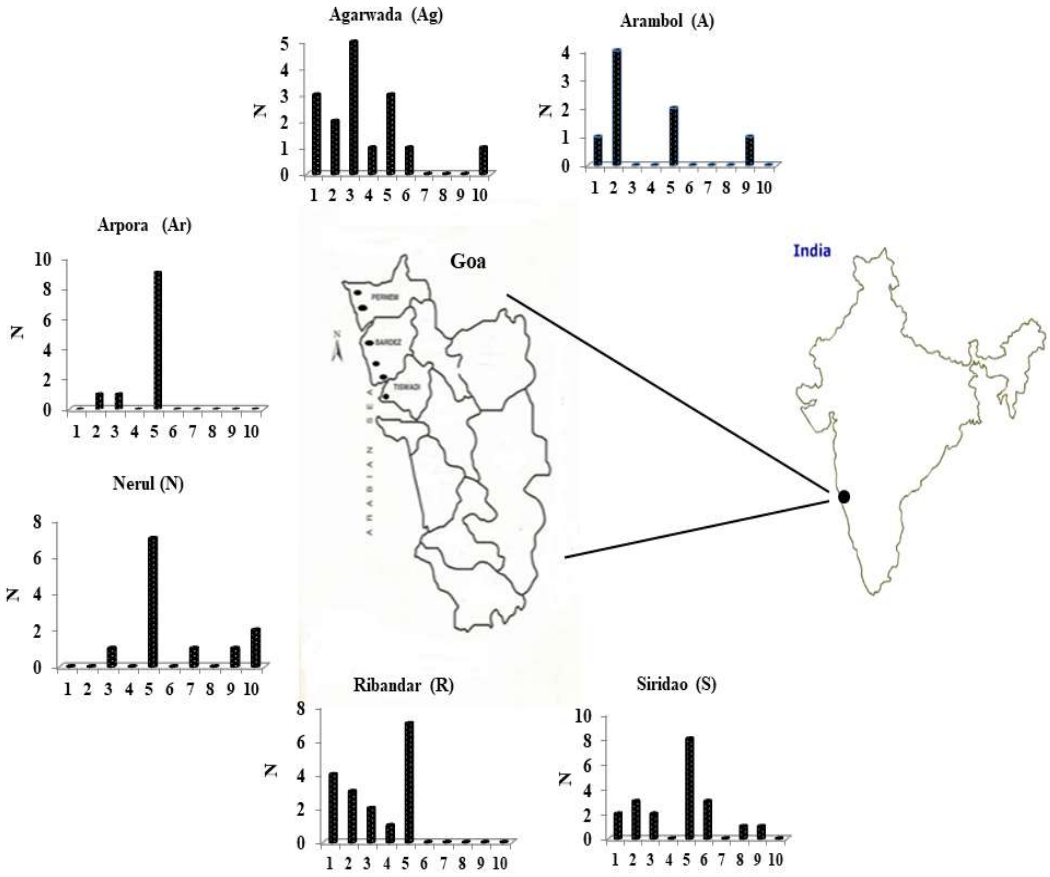

FIGURE 6: Number of free radical Haloarchaeal scavengers retrieved from solar salts of Goa:
A- Arambol; Ag- Agarwada; Ar -Arpora; N- Nerul; R- Ribandar; S- Siridao obtained from different geographical location of Goa- India.
X axis values indicate different retrieved genera; **1.** *Halobacterium*, **2.** *Haloferax*, **3.** *Haloarcula*, **4.** *Halorubrum*, **5.** *Halococcus*, **6.** *Natrialba*, **7.** *Natrinema*, **8.** *Natronocccus*, **9.** *Alteromonas*, **10.** *Gluconobacter.*
Y –axis indicate number of isolates present **(N)**.

Members of *Alteromonas* and *Gluconobacter* engaged in free radical scavenging as seen in Nerul (Fig. 7A) as per Simpson's Index of diversity whereas the diversity of haloarchaea associated with solar salts is Siridao> Agarwada= Ribandar>Arambol > Arpora >Nerul. The distribution of as per Shannon- Weiner's diversity index H' was Nerul > Arambol = Agarwada = Siridao. The diversity of haloarchaea (Fig. 7B) associated with solar salts as per Shannon-Weiner's Diversity Index H' was Agarwada > Ribandar > Siridao > Arpora> Arambol> Nerul. Only in the case of Ribandar, Shannon-Weiner's Diversity Index H' and Simpson's Index of Diversity, D' were nearly equal indicating that the dominance was in the following order; Siridao > Agarwada > Ribandar > Arambol > Arpora > Nerul. The antioxidant potential of eubacteria and haloarchaea associated with Goan solar salt is a reflection of constant exposure of these cultures to sunlight and radiations which is reported to trigger the formation of free radicals and reactive oxygen species (Abbes *et al*.,2013; Mandelli *et al*., 2012; Rodrigo-Baños *et al*., 2015; Sikkandar *et al*., 2013). (Pathak and Sardar 2012) have reported the antioxidant activity from *Halorubrum* sp. isolated from brine samples of solar salterns of Mumbai also evaluated through the DPPH assay.

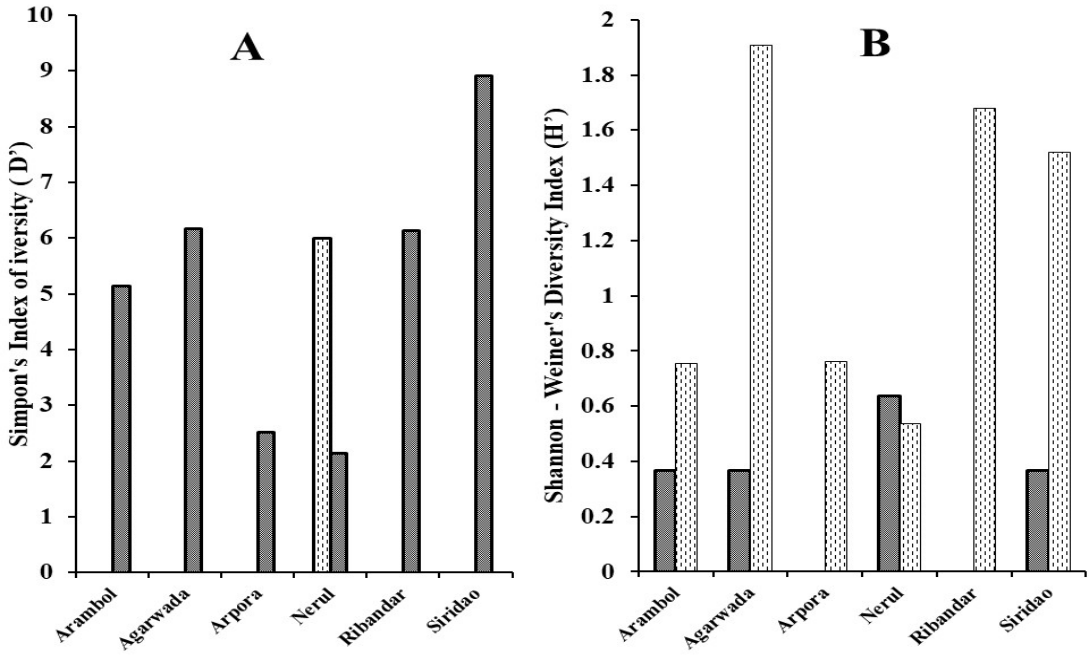

FIGURE 7: Diversity index, **A-** Simpson's Index of Diversity 'D' : Eubacteria ▨, Haloarchaea ■
B - Shannon- Weiner's Diversity Index 'H': Eubacteria , Haloarchaea ▨

Total antioxidant capacity and Total phenolic content.
GUSF-1 *Haloferax* sp. (KF796625), $GUFF_{188}$ *Haloarcula* sp. $GUFF_{179}$ *Halococcus* sp. $GUFF_{72}$ *Halorubrum* sp. and $GUFF_{233}$ *Natronocccus* sp. were assessed for further analysis of total antioxidant capacity and total phenolic content. Addition of MEC (with absorption peaks between 300-600 nm) of each of the five cultures to phosphomolybdenum reagent, resulted in development of a bluish greenish colouration readable at 695 nm and was accompanied by the disappearance of MEC absorption peaks between 300-600 nm, thus confirming the involvement of MEC in free radical scavenging through reduction of Mo (VI) – Mo (V) to the bluish green phosphate complex, under acidic conditions (Huang *et al*., 2005). As recorded in (Fig.8) total antioxidant capacity varied from haloarchaea to haloarchaea. *Haloferax* sp. GUSF-1 (KF796625) gave the maximum of 1.176 ± 0.75 mg AAE/ g cells, whereas *Halorubrum* sp. $GUFF_{72}$ gave minimum of 0.167 ± 0.001 mg AAE/ g cells, which was nearly 10 times less. Addition of FC reagent to the MEC developed blue colour which gave an absorption maximum at 765 nm. The formation of blue colour is attributed to an oxido- reduction reaction occurring between MEC and FC reagent, wherein phenolic moieties of the MEC are oxidised with simultaneous reduction of the alkaline FC. The extract of each of the 5 cultures showed presence of phenolic content capable of reacting with the alkaline FC. *Haloferax* sp. GUSF-1 (KF796625) gave highest value of phenolic content of 0.784 ± 0.004 mg GAE/g cells (Fig.8). This was followed by *Halococcus* sp. $GUFF_{179}$ > *Haloarcula* sp. $GUFF_{188}$ > *Natronococcus* sp. $GUFF_{233}$. The MEC of *Halorubrum* sp. $GUFF_{72}$ showed the minimum content of 0.135 ± 0.001 mg GAE/g cells. A positive correlation was also observed between phenolic content and total antioxidant capacity ($R = 0.89$, $p < 0.001$). The extracts which gave absorption between 300-600 nm was involved in the FC reaction as these peaks are seen to be abolished during the reaction. The occurrence of non- pathogenic haloarchaea and extremely halophilic eubacteria in Goan solar salts with an ability to scavenge free radicals adds value and promotes the traditional use of natural solar salt, in moderation, as conditioner and fertiliser to soils bearing trees such as *Cocos nucifera*, *Mangifera indica*, *Artocarpus*

heterophyllus and others. The presence of phenolic moieties in these cells ensure their involvement in free radical scavenging of metals and hydrocarbons which are on increase as pollutants in coastal soils (Utkina *et al*., 2004).

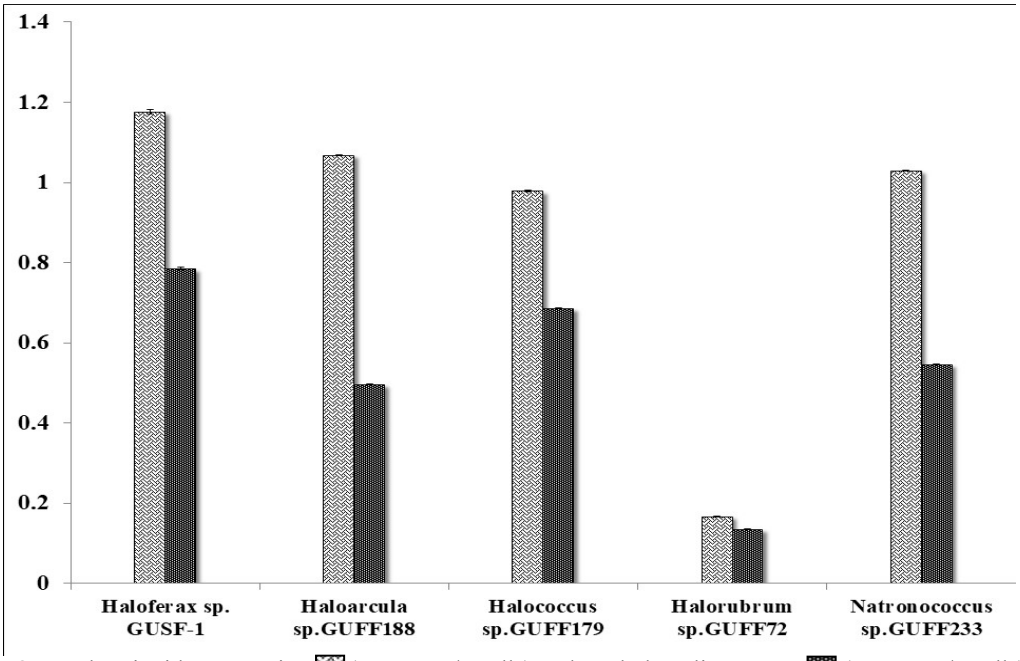

FIGURE 8; Total antioxidant capacity (mg AAE /g cells) and total phenolic content (mg GAE /g cells) of select isolates belonging to different genera

CONCLUSION

In conclusion, our study records that extremely halophilic eubacteria and haloarchaea are responsible for free radical scavenging activity exhibited by natural solar salt produced in salt pans of Agarwada, Arambol, Arpora, Nerul, Ribandar and Siridao in Goa - India. The study demonstrates for the first time the ability of DPPH to directly sort out colonies, while still on agar plate into free radical scavengers and non-scavengers. Two eubacterial genera namely *Alteromonas* and *Gluconobacter* and eight different haloarchaeal genera namely *Halobacterium, Haloferax*, *Haloarcula*, *Halococcus*, *Halorubrum, Natrialba, Natrinema and Natronococcus* retrieved from solar salts scavenge free radicals at varying degree. *Haloferax* sp. GUSF-1 (KF796625) (% DPPH RSA 31.5 ±0.43 / 252.2 ±1.14 µg AAE/g cell), having phenolic moieties as antioxidant principle, offers a promise for antioxidant harnessing. Interestingly, this is the first time *Alteromonas*, *Gluconobacter, Natrialba*, *Natrinema* and *Natronococcus* are reported with antioxidant capability. To our mind, this free radical scavenging potential of natural solar salts by microbes associated with it.

The bio-principles of these microbes make the crude solar salts chemo- reactive free radical scavengers. And possibly contributes to thus for scientifically unknown reason for traditional of solar salt Additionally, the phenolic antioxidant moieties of salt associated microbes is expected to ensure free radical scavenging of metals and hydrocarbon pollutants which are on increase in coastal soil.

REFERENCES

Abbes M., Baati, H., Guermazi, S., Messina, C., Santulli, A., Gharsallah, N. and Ammar, E. (2013) Biological properties of carotenoids extracted from *Halobacterium halobium* isolated from a Tunisian solar saltern. *BMC Complementary and Alternative Medicine* **13**, 255.

Aguiar, R. and Furtado, I. (1996) Growth of *Halobacterium* strain R1 on sodium benzoate. In *Perspectives in Microbiology*. Kahlon RS (ed.), pp 78–79, India: National Agricultural Technology Information Centre.

Aral, H., Hill, B.D. and Sparrow, G. J. (2004) Salts from saline waters and value added products from the salts. CSIRO Minerals Report DMR-2378C.

Braganca, J.M. and Furtado, I. (2009) Isolation and characterisation of haloarchaea from low- salinity costal sediments and waters of Goa. *Curr. Sci.* **96**, 1182-84.

Brand-Williams, W. Cuvelier, M.E. and Berset, C. (1995) Use of a free radical method to evaluate antioxidant activity. *LWT-Food Sci. Technol*. **28**, 25–30.

Elshahed M.S., Savage, K.N., Oren, A., Gutierrez, M.C. Ventosa, A. and Krumholz, L.R. (2004) *Haloferax sulfurifontis* sp. nov., a halophilic archaeon isolated from a sulfide- and sulfur-rich spring. *Int. J. Syst. Evol. Microbiol*. **54**, 2275–2279.

Fernandes, C. and Furtado, I. (2005) Culturable haloarchaeal diversity of salt pans of Goa, India. Abstracted at *International Marine Biotechnology Conference* at St. John's New Foundland, pp 300 Canada.

Furtado, I and Fernandes, C.F.E. (2009) Traditional salt production in Goa- India enriches diverse microbial resource. In 2009 *9th international symposium on salt*, pp 781–786, Volume A. Gold Wall Press.

Grant, W.D. and Larsen, H. (1989) Group III. Extremely halophilic archaebacteria. Order *Halobacteriales* ord. nov. In *Bergey's Manual of Systematic Bacteriology*, **3**, pp 2216 – 2233,Stanley J.T., M.P. Bryant, N. Pfennig and J.G. Holt (eds.), Williams & Wilkins, Baltimore.

Holt, J.G., Krieg, G.N.R., Sneath, P.H.A., Staley, J.T. and Williams S.T. (1994) *Bergeys Manual of Determinative Bacteriology*, Williams and Wilkins, Baltimore, 787.

Huang, D., Ou B. and Prior, R.L. (2005) The chemistry behind antioxidant capacity assays. *J Agr Food Chem* **53**, 1841-56

Khandavilli, S., Sequeira, F. and Furtado, I. (1999) Metal tolerance of extremely halophilic bacteria isolated from estuaries of Goa. India. *Ecol. Env. Cons*. **5**,149–152.

Lü, J., P.H. Lin, Q. Yao and Chen, C. (2010) Chemical and molecular mechanisms of antioxidants: Experimental approaches and model systems. *J. Cell Mod. Med*. **14**, 840-860.

Magat, S.S (2000) An effective and cheap fertilizer for high coconut productivity, Technology Guide Sheet No. 5, Philippine Coconut Authority.

Mani, K., Salgaonkar, B., Das, D. and Bragança, J.M. (2012) Community solar salt production in Goa, India. *Aquatic Biosystems* **8**, 30.

Mandelli, F., Miranda, V.S., Rodrigues, E. and Mercadante, A.Z. (2012) Identification of carotenoids with high antioxidant capacity produced by extremophile microorganisms. *World J Microbiol Biotechnol*. **28**, 1781–1790.

McGenity, T.J., Gemmell, R.T. and Grant, W.D. (1998) Proposal of a new halobacterial genus *Natrinema* gen. nov., with two species *Natrinema pellirubrum* nom. nov., and *Natrinema pallidum* norn. nov. *Int J Syst Evol Microbiol*.**48**,1187-1196.

Norberg, P. and Hofsten, B.V. (1969) Proteolytic enzymes from extremely halophilic bacteria. *J. Gen. Micro*. **55**, 251-256.

Oren, A., Ginzburg, M., Ginzburg, B.Z., Hochstein, L.I. and Volcani, B.E. (1990) *Haloarcula marismortui* (Volcani) sp. nov. nom. rev. an Extremely Halophilic Bacterium from the Dead Sea. *Int. J. Syst. Evol. Bacteriol*. 209-210.

ren, A., Ventosa, A. and Grant, W.D. (1997) Proposed minimal standards for description of new taxa in the order *Halobacteriales*. *Int. J. Syst. Bacteriol*. **47**, 233 – 238.

Oren, A. (2012) Taxonomy of the family Halobacteriaceae: a paradigm for changing concepts in prokaryote systematics. *Int J Syst Evol Microbiol.* **62**, 263–271.

Pathak, A.P. and Sardar, A.G. (2012) Isolation and characterization of carotenoid producing Haloarchaea from solar salterns of mulund, Mumbai, India. *Ind. J. Nat. Prod. Res*. **3**, 483-88.

Pearson, K. (1900) Mathematical contributions to the theory of evolution.VII. On the correlation of characters not quantitatively measurable. Philosophical Transactions of the Royal Soc. Ser. A.**195**, pp 1–47.

Prieto, P., Pineda, M. and Aguilar, M. (1999) Spectrophotometric quantitation of antioxidant capacity through the formation of a phosphomolybdenum complex: specific application to the determination of vitamin E. *Anal. Biochem* **269**, 337-41.

Purdy, K.J., Cresswell-Maynard, T.D., Nedwell, D.B., McGenity, T.J., Grant, W.D., Timmis, K.N. and Embley T.M. (2004) Isolation of haloarchaea that grow at low salinities. *Env. Micro*. **6**, 591–595.

Rodrigo-Baños, M., Garbayo, I., Vílchez, C., Bonete, M.J. and Martínez-Espinosa, R.M. (2015) Carotenoids from Haloarchaea and Their Potential in Biotechnology. *Mar. Drugs*. **13**, 5508-5532.

Roh, S.W., Nam, Y., Chang, H., Sung, Y., Kim, Y., H. Lee, H. Oh and Bae, J. (2007) *Natronococcus jeotgali* sp. nov., a halophilic archaeon isolated from shrimp jeotgal, a traditional fermented seafood from Korea. *Int J Syst Evol Microbiol* **57**, 2129–2131.

Ross, H.N.M.,. Grant W.D. and Harris, J.E. (1985) Lipids in archaebacterial taxonomy. In: *Chemical methods in bacterial systematics*. pp 289-300, M. Goodfellow and D.E. Minnikin (ed), Society for Appl Bacteriol.Technical Series 20, Academic Press, London.

Simpson, H.E (1949) Measurement of Diversity. *Nature* **163**, 688-688.

Shannon, C. E. and Weaver, W. (1949) The mathematical theory of communication. pp 117, The University of Illinois Press, Urbana, USA.

Sequeira, F. (1992) Microbiological study of salt pans of Goa. Master of Science dissertation. Goa University, India.

Sikkandar, S., Murugan, K., Al-Sohaibani, S., Rayappan, F. Nair, A. and Tilton, F. (2013) Halophilic bacteria- A potent source of carotenoids with antioxidant and anticancer potentials. *J. Pure Appl. Microbiol*. **7**, 2825–2830.

Singleton, V.L. and Rossi, J.A. (1965) Colorimetry of total phenols with phosphomolybdic- phosphotungstic acid reagents. *Am. J. Enol. Vitic*. **16**, 144-158.

Utkina, N.K., Makarchenko, A.E., Shchelokova, O.V and Virovaya, M.V. (2004) Antioxidant Activity of Phenolic Metabolites from Marine Sponges. *Chem. of Nat. Comp*. **40**, 373-77.

Velho-Pereira, S., Parvatkar, P. and Furtado, I. (2015) Evaluation of antioxidant producing potential of halophilic bacterial bionts from marine invertebrates. *Indian J. Pharm. Sci*. **77**, 183–89.

Venkatajalapathi, P., Baskar, M., Rajesh, V., Sharmal, K.M., Saraswathi, K., Arumugam, P. and Ravi, K.M. (2016) Studies on production of antioxidant and anti-proliferative secondary metabolites from halophilic *Bacillus cereus* isolated from open solar salt pans. *World J Pharm and Pharma Sci*. **5 (11)** 1235-1247.

Ventosa, A., Gutie´rrez, M.C., Kamekura, M., Zvyagintseva, I.S. and Oren, A. (2004) Taxonomic study of *Halorubrum distributum* and proposal of *Halorubrum terrestre* sp. nov. *Int. J. Syst. Evol. Microbiol*. **54**, 389–392.

Wang, Q., W. Li, H. Yang, Y. Liu, H. Cao, M. Dornmayr-Pfaffenhuemer, Stan-Lotter, H. and Guo, G. (2007) *Halococcus qingdaonensis* sp. nov., a halophilic archaeon isolated from a crude sea-salt sample *Int. J. Syst. Evol. Bacteriol*. **57**, 600–604.

Xu, Y., Z. Wang, Y. Xue, P. Zhou, Y. Ma, A. Ventosa and W.D. Grant (2001) *Natrialba hulunbeirensis* sp. nov. and *Natrialba chahannaoensis* sp. nov., novel haloalkaliphilic archaea from soda lakes in Inner Mongolia Autonomous Region, China. *Int. J. Syst. Evol. Microbiol*. **51,**1693–1698.

Yang, Y., Cui, H.L., Zhou, P.J. and Liu, S.J. (2006) *Halobacterium jilantaiense* sp. nov., a halophilic archaeon isolated from a saline lake in Inner Mongolia, China. *Int. J. Syst. Evol. Microbiol*. **56**, 2353–2355.

Yevgenia, S., David, I., Yael, K., Zvy, D. and Yaron, Y. (2013) Natural Antioxidants: Function and Sources Food and Nutrition Sciences. *Food and Nutr. Sci.* **4**, 643-649.